

City Research Online

City St George's, University of London

Citation: Barnes, M.R. (1977). Form finding and analysis of tension space structures by dynamic relaxation. (Unpublished Doctoral thesis, City University London)

This is the accepted version of the paper.

This version of the publication may differ from the final published version. To cite this item please consult the publisher's version.

Permanent repository link: https://city-ref-test.eprints-hosting.org/id/eprint/11887/

Copyright and Reuse: Copyright and Moral Rights remain with the author(s) and/or copyright holders. Copies of full items can be used for personal research or study, educational, or not-for-profit purposes without prior permission or charge, unless otherwise indicated, provided that the authors, title and full bibliographic details are credited, a hyperlink and/or URL is given for the original metadata page and the content is not changed in any way. For full details of reuse please refer to City Research Online policy.

City Research Online: http://openaccess.city.ac.uk/ publications@citystgeorges.ac.uk

FOREWORD

The thesis is submitted on the basis of papers published between April, 1974 and July, 1976 (chapters 2-8). Minor editing of the papers has been carried out for the sake of continuity of the thesis as a whole. Since each of the papers was written to be largely self-contained, however, a certain amount of repetition, particularly of introductory remarks, is unavoidable. For this reason the "contents" lists only those sections which introduce new material. Chapter appendices have been placed immediately following the papers to which they refer. In the majority of cases these were not included with the original texts, but have been added here to expand on points mentioned in the papers or dealt with during presentation.

The report supporting the submission is given in two sections: an introduction reviewing the behaviour and analytical requirements of tension structures which relates subsequent chapters to other publications, and a conclusion correlating the papers into an overall context of interactive design and analysis. For the sake of completeness as a thesis, main appendices A-D have been included at the end of the thesis to give comprehensive reviews of published work relating respectively to static analysis, form-finding, dynamic analysis, and the development and mathematical basis of dynamic relaxation. References in these appendices and the introduction (chapter 1) are contained in the main bibliography, appendix E.

CONTENTS

(Referencing also the papers forming the chapters)

		PAGE NO.
CHAPTER 1	INTRODUCTION - THE CHARACTERISTICS AND BEHAVIOUR OF TENSION STRUCTURES	14 - 46
	Static Behaviour	15
	Analytical Requirements	20
	Determination and Influence of Form	25
	Dynamic Behaviour	37
CHAPTER 2	"DYNAMIC RELAXATION ANALYSIS OF TENSION NETWORKS" (Int.Conf. on Tension Structures, London, April 1974)	47 - 92
	Dynamic relaxation	48
	Initial conditions	52
	Cladding	52
	Damping constant	55
	Time interval	56
	Application to geodesic network	58
	Model network test	60
	Results: Pretension geometry	64
	Behaviour under load	65
Appendix 2.1	Modal decomposition of an explicit dynamic response analysis	69
	Fourier analysis of D.R. output	70
	Plane prestressed net	73
	Cable edged spatial network	78
Appendix 2.2	Link extensions	82
Appendix 2.3	Comparison of D.R. and matrix iteration scheme	83
	Computer storage and operation requirements for dynamic relaxation	83
	Storage and operation requirements for matrix iteration	84
	Comparison of D.R. and Newton Raphson iteration schemes (plane truss and network)	89

		PAGE NO.
CHAPTER 3	"APPLICATIONS OF DYNAMIC RELAXATION TO THE FORM-FINDING AND ANALYSIS OF CABLE, MEMBRANE AND PNEUMATIC STRUCTURES" (2nd Int.Conf. on Space structures, Guildford, Sept. 1975)	93-145
	Factors affecting the rate of convergence	97
	Fictitious masses	99
	Form-finding applications:	99
	Geodesic networks	100
	Uniform mesh networks	102
	Momentless compression boundaries	103
	Minimum surface membranes	108
	Pneumatic structures	110
	Principal stress trajectories	112
	Membrane buckling and slackening of cables	114
	Force transfer process for stiff members	120
Appendix 3.1	Analytical model properties	125
Appendix 3.2	Accuracy and stability of central difference analysis involving recurrent dynamic buckling	127
	Basis for analytical tests	127
	Cable structure	128
	Membrane structure	138
	Mass components	141
	Composite cable and membrane structure	142
CHAPTER 4	"FORM-FINDING OF MINIMUM SURFACE MEMBRANES" (World Congress on Structures for Space Enclosure, Montreal, July 1976)	146-174
	Plane uniform stress membranes	150
	Non-circular boundaries (traction forces)	157
	Minimum surface spatial membranes	160
	Pneumatic structures	168
	Conclusions concerning quasi-instability	170

		PAGE NO.
Appendix 4.1	Disturbance of plane membrane nodes	171
	Alteration of topology	171
CHAPTER 5	"EXPLICIT DYNAMIC ANALYSIS OF TENSION STRUCTURES" (Int.Symposium on Wide-Span Surface Structures, Stuttgart, April 1976)	175-203
	Dynamic iteration scheme	177
	Link and nodal forces	179
	Incremental procedure allowing for creep and buckling	182
	Computation scheme	186
	Calibration of visco-elastic constants	187
	Dynamic, static and form-finding analyses	189
Appendix 5.1	Normal Pressure Vector	193
Appendix 5.2	Constant Moment homogeneous or sandwich plate element	195
CHAPTER 6	"AN INVESTIGATION OF VIBRATION DECAY IN A MODEL PNEUMATIC DOME" (Int.Symp. on Wide-Span Surface Structures, Stuttgart, April 1976)	204-224
	Model dome construction and testing	205
	Calibration of material constants	209
	Analysis of the dome	214
Appendix 6.1	Calibration analysis for single visco-elastic element	221
CHAPTER 7	"INTERACTIVE GRAPHICAL DESIGN OF TENSION SURFACE STRUCTURES" (Int.Symp. on Wide-Span Surface Structures, Stuttgart, April 1976)	225-249
	Basis for interactive form-finding by dynamic relaxation	226
	Uniform stress membranes	228
	Cable networks	231
	Variable stress membranes	234

		PAGE NO.
Appendix 7.1	Structure properties	243
Appendix 7.2	Collapse states	244
CHAPTER 8	"OPTIMIZATION OF SPACE TRUSS FORM" (Lecture at W.C.O.S.E., Montreal, July 1976. Subsequently incorporated in a paper for Int.Conf. on Slender Structures, London, Sept. 1977, reference 20)	250-282
	Approaches to structural optimization	251
	Theory of Michell structures	255
	Optimum modular space trusses	258
	Optimization by dynamic relaxation	259
	Test cases	264
	A policy for interactive form-finding and analysis	272
CHAPTER 9	CONCLUSIONS	283-288
APPENDIX A	REVIEW OF METHODS FOR THE STATIC ANALYSIS OF TENSION STRUCTURES	289-325
	Continuum analysis of tension systems	290
	Discrete analysis	291
	Element tangent stiffness relations	292
	Summation form of equilibrium equations	295
	Implicit Analyses:	
	Iterative methods (stiffening and softening systems; Newton Raphson method; Modified Newton Raphson; Secant stiffness method; Combined methods; Alpha-constant accelerated method)	298
	Incremental methods (Euler method; self-correcting methods; extrapolation methods; iteration; mid-slope stiffness)	307

PAGE NO.

Explicit Analyses:

Minimization methods (steepest descent; relaxed steepest descent; conjugate gradient method; scaling of energy surface) 312

Relaxation methods (point-Jacobi; Gauss-Seidel;S.O.R.) 320

APPENDIX B REVIEW OF METHODS FOR FORM-FINDING OF NETS AND MEMBRANES 326-343

Linear solutions:

Orthogonal nets 327

General nets 329

Non-linear form-finding:

Constrained force densitites method 331

Newton Raphson iteration 334

Optimization techniques 337

APPENDIX C NON-LINEAR DYNAMIC ANALYSES 344-370

Modal superposition analyses 346

Implicit Numerical integration methods 351

Hubolt method 352

Non-linear effects 353

Newmark β methods 354

Wilson θ method 356

Central difference method 356

Finite elements in time 357

Loading and co-efficient matrices 359

Explicit direct integration

Central difference method 360

Higher order methods 361

Euler methods 363

Comparative studies of integration methods 365

Computational efficiency 367

Artificial viscosity and structural idealization 369

PAGE NO.

APPENDIX D REVIEW OF DYNAMIC RELAXATION AS AN ITERATIVE METHOD AND THE CHOICE OF OPTIMUM ITERATION PARAMETERS 371-403

Assessment of DR as an iterative method 374

Choice of optimum parameters by comparison with the Frankel iteration 380

Convergence rate 383

Automatic adjustment of mass and damping parameters 388

Appendix D.1 Form-finding of a lattice shell dome 393

Viscous damping solution 395

Kinetic damping 401

APPENDIX E BIBLIOGRAPHY CONCERNING THE DESIGN AND ANALYSIS OF TENSION STRUCTURES 404-431

ABSTRACT

Chapter 1 reviews the behaviour and characteristics of tension-structures and the consequent analytical requirements for form-finding, static and dynamic analysis. Various published techniques, together with the work outlined in subsequent chapters, are considered with respect to their compliance with these requirements; particular emphasis being placed on the needs in form-finding to cope with inaccurate topology and geometrical data, the occurrence under static loading of buckling and zero stiffness situations and, during dynamic response, the interaction of the structure with the surrounding environment.

Chapter 2 examines the application of Dynamic Relaxation to the analysis of cable networks. Numerical and experimental results for a cable edged geodesic network subject to static loading are compared, and recorded natural frequencies are correlated with those obtained as a bye-product of the D.R. analysis. The stability of the analytical process is considered and an expression governing the critical time interval is derived. Appendices to the chapter consider in more detail the extraction of natural frequencies from static analyses for various load cases, and compare the computational efficiency of the DR process with a Modified Newton Raphson analysis. In chapter 3 the method is extended to form-finding and static analysis of networks with momentless compression boundaries, and to membrane and pneumatic structures. The derivation and accuracy of principal

stress trajectories in prestressed anticlastic membranes idealized as an assemblage of constant stress elements is illustrated for normal load and for higher loads sufficient to cause buckling. For dealing with structures employing very stiff elements compared with cable links, thus creating a high condition number, a force transfer procedure is derived and applied. An appendix to the chapter considers the accuracy and stability of the central difference integration scheme for cable and membrane structures with very low damping which are subject to recurrent dynamic buckling.

Problems with form-finding of uniform stress membranes, in particular the occurrence of quasi stable or unstable states due to inadequate transfer of concentrated support loads into the membrane, are examined in chapter 4. States which appear to be similar are also shown to occur due to inadequate idealization of the surfaces. The derivation of momentless contours for such structures is extended to include boundary traction forces, and these are shown to extend greatly the variety of possible forms. The above considerations are extended in chapter 7 to the case of variable stress membrane and pneumatic structures and geodesic networks; emphasis being placed on the value of DR when used interactively to simulate physical behaviour, particularly for examining impending collapse states or physically untenable specified stress distributions for trial forms.

A computational procedure for the explicit dynamic analysis of tension structures, accounting for pneumatic stiffening and air and visco-elastic material damping, is outlined in chapter 5; combined creep and buckling effects being accounted for by means of an

incremental stain formulation. A simplified basis for deriving series model visco-elastic constants by curve-fitting material test results is also suggested. The validity of the procedures is examined in chapter 6 by comparison with experimental results obtained from vibration decay tests on a model pneumatic dome subject to suddenly applied loading.

Chapter 8 considers the application of DR for optimizing the form of modular space truss systems subject to a dominant design loading. In contrast to mathematical programming techniques the method is shown to yield a graded preference of members in hyperstatic layouts which is ideally suited to interactive design procedures allowing architectural design freedom. A basis for such a procedure allowing for load variations and deflection limits is also suggested. The final chapter summarises the advantanges of DR for the design and analysis of tension space structures and indicates lines of current research.

ACKNOWLEDGEMENTS

I would like to thank the technicians in the department of Civil Engineering for constructing and gauging the model test structures referred to in this thesis (chapters 2 and 6), and also for their work in connection with other tension structures which have been tested in the laboratories. I am particularly grateful to Mr. Tony Jones, who has co-ordinated the fabrication of models, and to Mr. M. Gregory, Mr. J. Rose, Mr. A. Towells, and Mr. M. Saytch.

The work referred to has all been carried out at The City University and I would like to thank Professor P.O. Wolf and Professor J.E. Gibson for their continuous support.

The typing of the thesis report and appendices was done very efficiently by Mrs. Judith Northfield, and the majority of the papers by Mrs. Janet Prange as extra and willing help for which I am very grateful.

I am grateful also to my present Ph.D. students, Barry Topping, David Wakefield, and Manolis Papadrakakis, for lively discussions which have been of benefit to all of us as a group.

Finally, I thank my parents and my wife, Nicole, for their unselfish care.

CHAPTER I

INTRODUCTION

THE CHARACTERISTICS AND BEHAVIOUR OF TENSION STRUCTURES

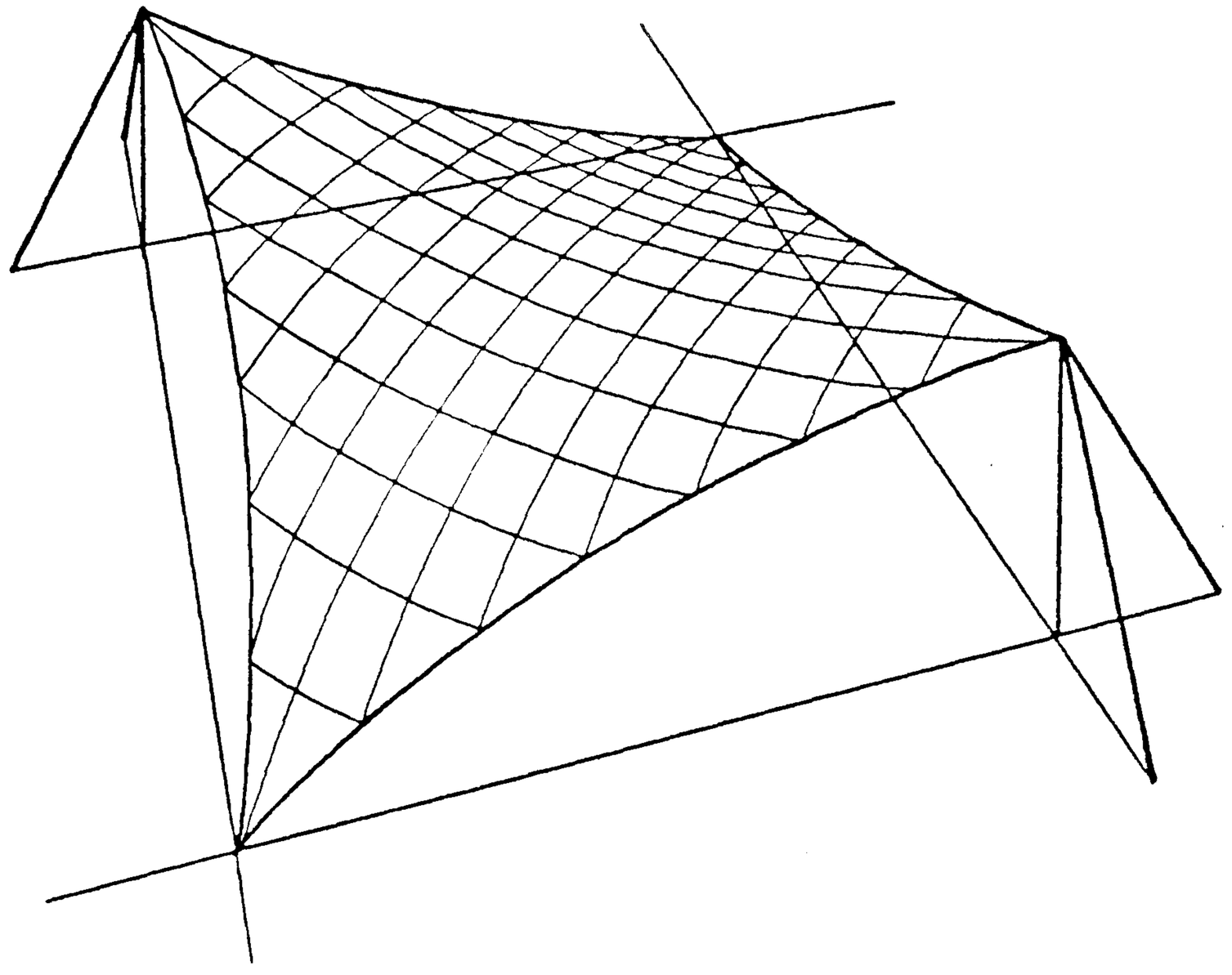
The chapter reviews the characteristics of tension systems which have a major influence on the requirements for form-finding and static and dynamic analyses. A detailed review of methods of analysis which are appropriate for tension structures is given in appendices A - C (pages 289-370). References in these appendices and the present chapter are contained in the main bibliography (appendix E p. 404).

The primary characteristic of tension structures is that main structural elements transmitting applied loads to bearing structures consist of high strength flexible cables or membranes sustaining only tensile forces. The cross section of these members may thus be fully utilized with permissible stresses not limited by instability effects. The use of high tensile components results in lightweight structures which, in comparison with conventional structures, become more economic with increasing spans. Major cost factors, however, for all tension systems are the bearing support structures, which may be subject to bending or compressive stresses, and the means of anchoring the high tensions resulting from long spans and shallow curvatures (113,185).

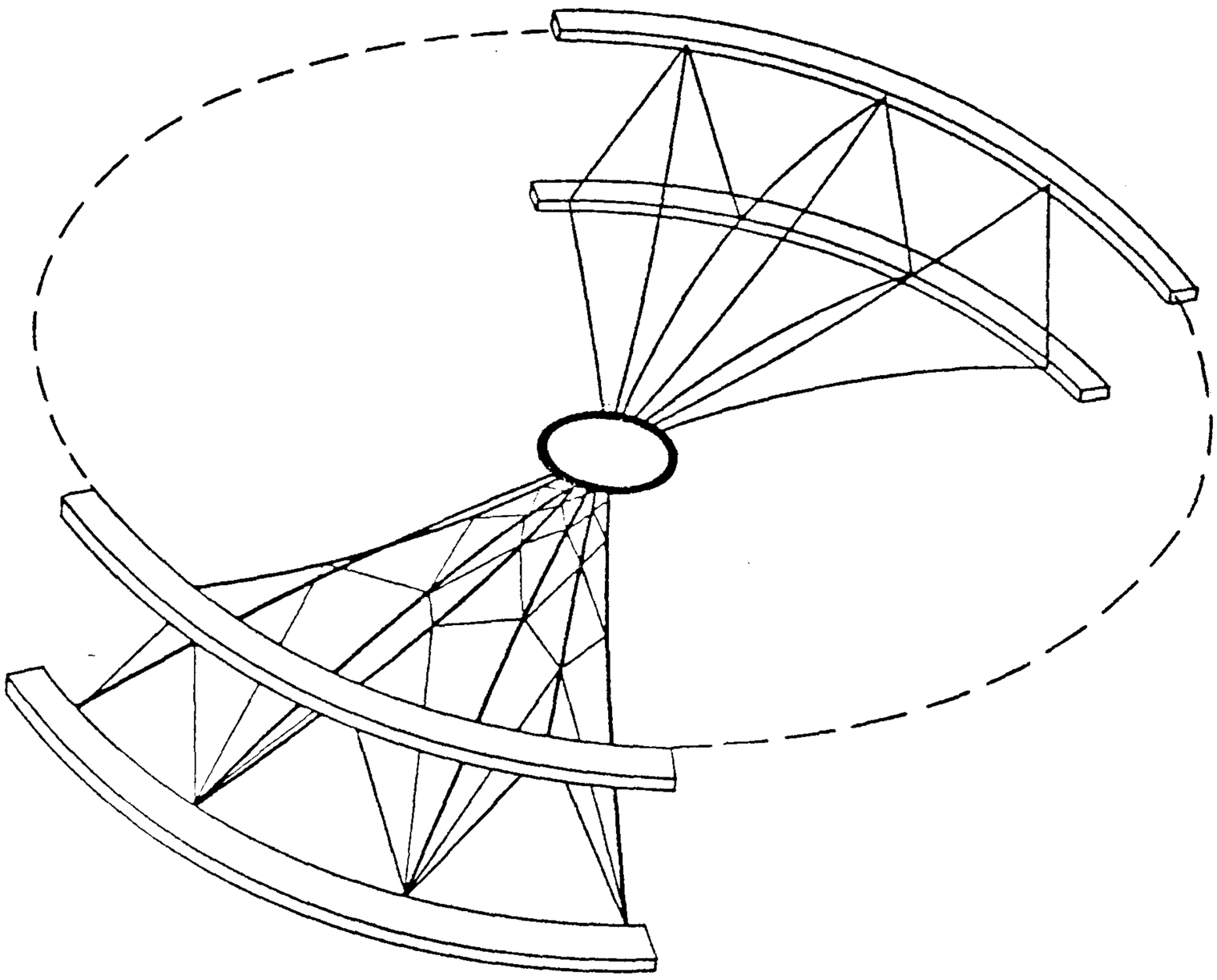
Architecturally, tension structures may be aesthetically pleasing, with structural function clearly expressed, primarily because the internal force distribution and surface and boundary forms are interdependent. Thus prestress ratios govern surface form and preferred boundary shapes, and changes in stresses due to applied loads, which depend on form, govern the required magnitudes of prestress. As a consequence, efficient design and subsequent economy of construction demand the closest collaboration between Architects and Engineers at all stages through repeated form-finding and analysis to detail design. Whilst this is desirable for the design of any structure, for tension structures it becomes essential because of the more direct inter-relation between form, internal forces and behaviour in service. A comprehensive discussion of these concepts for a large variety of tension systems has been given by Frei Otto (144-146).

STATIC BEHAVIOUR

For the purpose of reviewing the general behaviour and analytical



Structural Mechanism



Triangulated System

Figure 1 Pretensioned Cable Structures

requirements of tension systems it is convenient to group them in two broad classes:

(1) Properly triangulated structural systems

(2) Structural mechanisms possessing degrees of mechanical freedom.

Examples of the first group, provided elements remain tensioned, are triply threaded nets, prestressed suspended shells, and cable trusses; whilst two way cable nets, cable girders, deadweight systems, and stressed membranes without shear rigidity are all structural mechanisms (figure 1). For continuous structures the degree of mechanical freedom, or conversely the redundancy, cannot be quantified, but for discrete pin-jointed assemblies it may be expressed as (37):

$$DMF = f - m + p$$

where f is the number of degrees of freedom of the joints, m is the number of members, and p is the number of linearly independent force systems which can be superimposed without disturbing the equilibrium configuration. Normally, for a properly designed tension system p is zero unless the system is regarded as weightless in which case p = 1. In the pretension condition the equation of equilibrium in the x direction at a joint j, connected by links to adjacent nodes k, is given by:

$$\sum_k \left\{ \frac{T}{l} . Dx \right\}^{jk} = P^{o}_{xj} \qquad (1)$$

where T is the tension and l the length of link jk, P^{o}_{xj} is the component of self weight at node j in the x direction, and $Dx = (xj - xk)$. After the application of live loads, P, the equilibrium condition becomes:

$$\sum_k \left\{ \frac{(T+\Delta T)}{(l+\Delta l)} \cdot (Dx + D\delta_x) \right\}^{jk} = P^{o}_{xj} + P_{xj} = P^{`}_{xj} \qquad (2)$$

where ΔT and Δl are tension and length increments of link jk, and $D\delta_x = (\delta_{xj} - \delta_{xk})$, the difference in x displacements.

In matrix notation equations type (1) can be arranged in three sets of independent linear equations:

$$[H]\{X\} = \{P_x^o\};\ [H]\{Y\} = \{P_y^o\};\ [H]\{Z\} = \{P_z^o\} \qquad (3a\text{-}c)$$

where, if n is the number of active nodes (excluding fixed boundary nodes), $\{X\}$, $\{Y\}$, $\{Z\}$ are vectors of the unknown co-ordinates, each of order n x 1, $\{P_x^o\}$, $\{P_y^o\}$, $\{P_z^o\}$ are self weight loading vectors modified to incorporate the known boundary constraints, and $[H]$ is a matrix, n x n, dependent solely on the tension coefficients. If these are specified the geometry of the system can be found directly for any self weight vectors and boundary conditions (169, 123, 162).

Equations type (1) could alternatively be arranged in the form:

$$[G]\{T\} = \{P^o\}$$

where $\{T\}$ is an m x 1 vector of unknown tensions, and $[G]$ is a matrix (f x m) dependent solely on geometry. But for a structural mechanism $m<f$, and therefore the geometry cannot be arbitrarily specified but depends on $\{T\}$ and $\{P^o\}$.

For a properly triangulated structure, if members are assumed inextensible no deformation would take place under loading and equations (2) could be written in the form:

$$[G]\{T+\Delta T\} = \{P`\}$$

with only changes in tensions required to accommodate the loading.

For structural mechanism with m<f, however, $\{P\}$ cannot be arbitrary unless $[G]$ also changes with the loading. Thus even when members are assumed to be rigid, finite deformations of such systems must take place.

The major difference in behaviour between triangulated systems and structural mechanisms is that the latter are subject to much greater deformations under asymmetric loading, and dominant natural frequencies are closely grouped and tend to be much lower than the range for triangulated systems (13, 172). This is because the variations in elastic strain energy of structural mechanisms undergoing non-symmetric deformations are much lower. At one extreme, deadweight systems sustain asymmetric live loads, which must be small in comparison with the dead load in order to limit deformations, largely through geometric deformation; equilibrium being achieved through changes in shape with only small variations in cable tension. In lightweight prestressed systems the tie-down or prestressing cables do not merely serve to pre-load the main hanging cables but become elastically active in resisting deformations. Thus maximum tensions in the main cables and the consequent costs of support structures and anchorages may be lower than for deadweight systems; the essential feature of prestressed systems being that they are designed on the basis of maximum live load variations.

Under working loads, no links in prestressed cable structures should be allowed to slacken, otherwise the system may become too sensitive to dynamic loads with high local deformations. Elastically triangulated structures, whilst stiffer under non-symmetric loads

because they are braced against shearing deformations, attract greater tension changes in individual links, and the bracing cables in particular may slacken if the system is not sufficiently prestressed. In structural mechanisms tension changes tend to be smoother and they are less prone to cable slackening. On the other hand the geometric stiffness is a large proportion of the total stiffness and, for a given shape, is directly dependent on the level of prestress. In practice, the distinction between the two systems may be imprecise. In steeply curved two way cable nets, for example, following deformation by applied loads, the cladding may provide some measure of bracing across the tension diagonals of the mesh; being allowed to buckle in the compressive directions. In this case however, the cladding and jointing would have to be designed to accommodate the deformations of the composite structure. Usual practice is to make the jointing system very flexible in order to avoid distress in the roofing surface which is then assumed only to transmit applied loads to the structural net.

Analytical Requirements

Well conditioned triangulated cable structures may be approximately investigated under working loads by means of linear elastic analysis. For structural mechanisms, however, an analysis which accounts for geometric non-linearity at all stages of loading must be used. Near ultimate load conditions both systems may additionally require account to be taken of either discontinuous or continuous material non-linearities such as cable slackening and slip at the joints (164) or the true stress/strain curve of the material. The latter factors may enable a significant increase in

the ultimate load carrying capacity of the structure through redistribution of forces from highly strained links to those with lower strains. Greenberg (72) for example, using a continuous exponential function to represent the inelastic portion of the stress/strain curve for steel cables, has shown that for practical two way cable networks the ultimate load capacity may be increased by more than 50% compared with an analysis assuming a linear stress/strain relation throughout the range with the same ultimate stress. This is due partly to the redistribution of stresses and partly to the larger deflections and curvatures resulting from increased strains. A similar effect occurs during material softening under fire loading (88, 54) and, combined with the lack of instability problems, results in prolonged fire resistance of tension systems.

The combination of geometrical and material non-linearities, particularly where on/off non.linearities are involved, creates in general a path dependent problem which should be solved by means of an incremental solution technique in which loads are applied in small steps to obtain a unique solution. Many methods of analysis, (discussed fully in Appendix A,p.289), such as iterative Newton-Raphson, modified Newton-Raphson, or minimization methods, in fact may assume that a unique solution exists which is not path dependent. For the most part, however, these analyses have been applied to tension systems and verified assuming only geometrical non-linearity. For such cases, proofs of uniqueness have been given by Buchholdt et al.(39) and Mollmann (123). Assuming the strain energy of a link is a strictly convex function of its extension, they show that the total potential energy of a pin-jointed

assemblage is a convex function of the joint displacements for all configurations in which members are in tension and that the equilibrium state is therefore stable and unique. Mollmann further shows that for a two-way anticlastic cable net subject to loads which are constant in magnitude and direction the solution is unique provided all links in one family of cable lines remain in tension. For a completely general case, however, in which some compression elements may be employed, cable links may slacken, and loading, for example normal pressure loading, is deformation dependent, uniqueness of solution may not be theoretically guaranteed unless a path dependent solution is used.

Published information concerning the performance of methods of analysis in the presence of cable slackening is scarce. This is perhaps attributable to the normally accepted design requirement that slackening should not be allowed to occur in practise, yet final analyses for ultimate loads should reliably account for this. Moreover, for membrane and pneumatic structures wrinkling in a direction of zero principal strain will often occur under working loads, particularly in regions where the flexible membrane adjoins a rigid boundary or inclusion. The author (15) (Chapter 3 and appendix 3.2) has examined the problems of convergence and stability of a membrane analysis with buckling induced under both static and dynamic loads. For static analysis of an anticlastic membrane subject to normal pressure loads it was found that a unique solution was obtained provided buckling in any membrane element occurred in only one principal direction. When buckling occurred in both directions, however, convergence to a unique solution was not obtained.

This was perhaps due to the type of elements and idealization used, though other researchers at a recent conference (48) also reported convergence difficulties with buckled membranes.

The poorly conditioned geometrical forms of many tension systems may also give rise to numerical problems, particularly in matrix solution methods involving a large number of unknowns. If equations (1) are subtracted from (2), and the result is expressed in linearised and incremental form, the tangent stiffness relations corresponding to the current load level may be obtained:

$$\left[K_t\right]\left\{\Delta\delta\right\} = \left\{\Delta P\right\}$$

where $\left[K_t\right]$ is composed of two parts: the elastic and the geometric stiffness, $\left[K_e\right] + \left[K_g\right]$.

In the stiffness matrix of a linear elastic structure the elements of the ith column, k_{1i}, k_{2i}, k_{3i}.....k_{ii}.....k_{ni}, represent the nodal forces which would be required to maintain an imposed displacement increment of $\Delta\delta_i = 1$ with all other displacements zero. For a well triangulated structure k_{ii} would be greater than the off-diagonal components k_{ji}. For a shallow non-linear network structure, however, the leading diagonal terms corresponding to deflection normal to the surface may be very much less than the related off-diagonal terms. Referring to figure 2, for example, the horizontal node forces required to sustain an imposed vertical displacement of $\delta u_7 = 1$ at node 3 will be considerably larger than the direct vertical component of force at node 3. Thus $k_{7,7} \ll k_{3,7}$; $k_{5,7}$; $k_{12,7}$; $k_{14,7}$

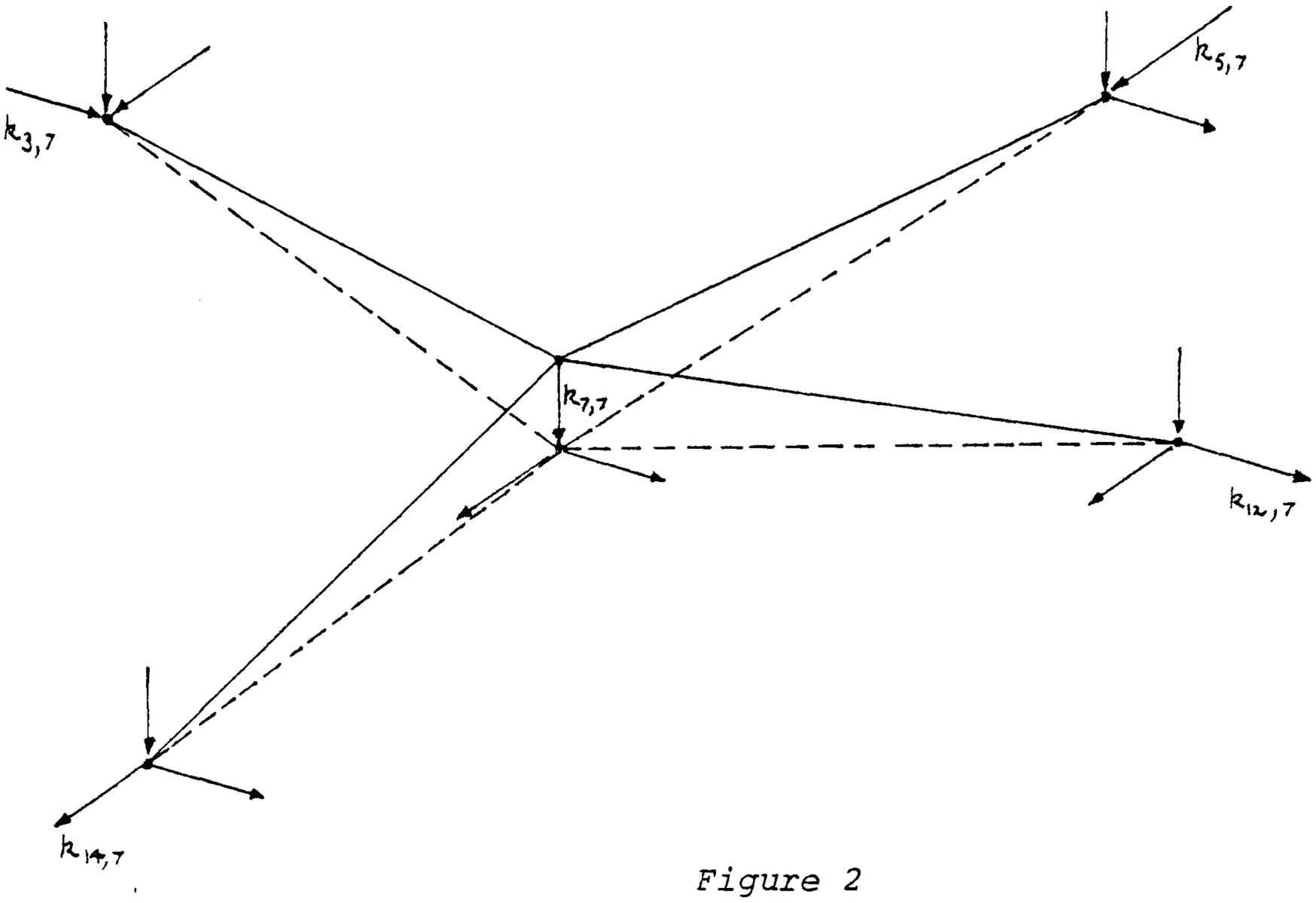


Figure 2

The non-dominance of some main diagonal terms, coupled with the greatly differing stiffness components along the leading diagonal, is a characteristic of poorly conditioned equations and is thus an inherent problem in the matrix analysis of tension structures (72). A further problem with either iterative or incremental matrix analyses is that for certain states of load and displacement the matrix may at some stage in the solution process become singular, with one or more direct stiffness components zero, necessitating conditional deflection controls (78).

Other than the characteristics discussed above, the analysis of tension systems involves a special consideration of two major aspects. The first is form-finding which, as already mentioned, is

directly coupled to the prestress distribution and consequent stresses under loading. And the second is dynamic behaviour; the lightweight and flexibility of tension structures making them particularly sensitive to dynamic loads.

DETERMINATION AND INFLUENCE OF FORM

Until 1969 model studies were the only practical basis for the form-finding of cable nets and membranes, and thin fabric models still provide a useful visual and experimental tool at preliminary design stages (145, 146, 112). During the design of the Munich Olympic games stadium, however, it was concluded that the determination of geometrical properties from wire models was dangerous owing to the error sensitivity of the structure; inaccuracies of jointing being liable to induce considerable discrepancies in the desired cable network forces, particularly in those links close to the edge cables (76, 164). Prior to this, the model design of cable networks, such as the German pavillion at the Montreal Expo' 67, had been based on a three phase form-finding procedure. The first phase was the study of soap films to simulate minimum surfaces with uniform stress distribution. From this an approximate form was obtained on which was based the pattern for constructing an orthotropic fabric model without shear stiffness. The fabric model provided a tactile means for investigating in more detail the architectural form with adjustment of supports and network/edge cable tension ratios, and also simulated a uniform mesh network more closely than the uniform stress soap film; curvatures and stress

distributions differing significantly because of distortion of the fabric mesh angles. The final phase of form-finding was based on an accurate uniform mesh wire model with geometric and elastic similarity to the real structure. This wire model permitted further small adjustments, following investigation of deflections and stresses under load, after which final measurements were taken to provide the scaled pattern for the real structure.

For the Munich Stadium Argyris, Scharpf and Angelopoulos developed a computer form-finding analysis to replace the wire model stage (6, 3). This was initially based on an iterative Newton-Raphson matrix method using as starting geometry and tensions data obtained from previous wire models of the structure. The prestress and link lengths were correlated at each stage so as to ensure uniform slack lengths throughout the interior of the cable mesh, together with control links at the ends of each cable of the network in which the slack length could be adjusted to ensure the design level of prestress. It was found, however, that convergence was either too slow or could not be obtained due to the inaccuracies of the scaled model data.

For this reason a mathematical model had to be constructed which consisted of smoothing the architectural data by quartic interpolation in separate regions of the network. On this mathematical surface a uniform mesh network was developed with the initial prestress values in links calculated assuming a constant projected component of tension throughout the length of each cable. The non-linear form-finding analysis was then applied to the resulting data with the tension at one end of each cable of the mesh held constant and edge cable nodes adjusted at each stage of iteration to minimise distortion

of the network at the boundaries and maintain close compliance with the required edge cable curves.

The above account indicates briefly some of the problems associated with analytical form-finding, detailed descriptions of which are given in Appendix B, p. 326. The analysis for the Munich Stadium was made more complex by the need to comply as closely as possible to a previously described surface obtained from approximate modelling, and by the fact that foundations for the main masts had already been placed before the analytical form-finding was commenced. Thus, whilst the engineering design required checks on stress levels and consequent adjustments to prestress distribution, it was at the same time necessary to fit rather precise specifications of shape and support points which in turn depended on the prestress yet were derived independently.

Since the construction of the Munich Stadium more formalised methods of correlating proposed architectural form and engineering design requirements have been developed by Knudson, Linkwitz, Schek and others (97, 110, 132). The form-finding process may be posed in the form of an optimisation problem such that, given a preferred architectural shape (Xd) and, independently, a preferred force distribution (Td), an exact figure of equilibrium is sought (satisfying equations 3a-c) which minimises:

$$\Sigma \left\{ x-x_d \right\}^T \cdot P_A \cdot \left\{ x-x_d \right\} + \Sigma \left\{ T-T_d \right\}^T \cdot P_E \cdot \left\{ T-T_d \right\} \qquad (4)$$

where $\{x\}$ and $\{T\}$ are the true equilibrium shape and force distribution, and P_A and P_E are respectively weighting factors given

to the architectural and engineering design preferences.

From the point of view of construction, cable networks are generally formed either from a pre-jointed uniform mesh with identical link lengths in the slack state, or as geodesic nets in which each cable takes a path of minimum length over the surface, with constant tension throughout its length, and nodes are jointed after prestressing. Thus, whilst the minimum to expression (4) is sought, constraints must simultaneously be applied to ensure uniformity of either mesh lengths or tensions. The former type of net is constructionally simpler and more appropriate for large structures. But because of the constraints on node positions, and hence also the cable trajectories, the network may contain areas in which the cables lie along lines of very shallow curvature. Coupled with the effects of distortion of the mesh angles, inducing significant variations in tension throughout cable lengths, this may necessitate higher levels of pretension than for geodesic nets in order to avoid areas which are too flexible and sensitive to gust loading.

Other classifications of two-way nets, which to a large extent are purely analytical, are:

a) Orthogonal nets, in which cables are assumed to lie in vertical planes with known spacing, derived by solving only the linear equations (3c) with specified horizontal tension components (170,123).

b) Uniform force-densities net derived by solving the three sets of linear equations (3a-c) assuming constant tension coefficients (162).

c) Isostatic nets in which cables follow the lines of principal stress trajectories which would result from the application of a uniform normal loading to a previously derived minimum surface membrane (13). Each of these nets may be useful at preliminary design stages. The first two enable a rapid search of feasible forms with differing specified supports and, for the chosen form, can provide initial data for a subsequent non-linear analysis with constraints on mesh lengths or tensions (162). Alternatively, if possible forms are investigated by means of a minimum surface membrane analysis, simulating soap film experiments, and the chosen form is analysed for normal loading, the stress trajectories derived give an indication of the preferred orientation of cables for a network (13,19). Since these trajectories follow lines of principal curvature they give a net which, in an overall sense, is stiffest to normal loading for the chosen surface shape. This may be a useful guide for the design of geodesic nets with complex curvature and support conditions. Similar comments relate to the design of membrane structures. Ideally the directions of the weave should coincide as closely as possible with lines of principal curvature, though this may conflict with the need for simplicity and economy in the cutting and jointing pattern. The most practical alternative, which does not entail distortion of the weave, is to base fabric cutting patterns on geodesic lines over the surface (87).

For triangulated systems statical constraints do not govern possible design forms to the same extent as for two-way networks or membranes without shear resistance. Reinforcement of pneumatic structures with a triply threaded grid of cables, for example, enables greater freedom of design since effective stress distributions may be more radically varied than those in an orthogonal fabric membreane. Again, however, the need for constructional simplicity may curtail this freedom.

Approaches to form-finding characterised by the minimisation of expression (4) imply the need for an architectural specification of shape which is initially independent of statical equilibrium and constructional constraints, except to the extent that the modelling material and process may qualitatively simulate such physical constraints. The model simulation, however, is not sufficiently accurate to provide an estimate of design prestress levels and distributions which take into account maximum and minimum tension changes under various conditions of loading. In consequence, approximate analytical modelling is desirable before the commencement of the non-linear optimisation process. Moreover, if the shape specification is based purely on crude physical modelling it may be very difficult to assign realistic values to the weighting factors P_A and P_E. In this case it would seem more appropriate to use an alternative approach to form-finding in which preliminary architectural sketches or physical models are used only to provide the conceptual topology of the structure. Feasible geometrical arrangements are then searched using interactive computer graphics

based on analytical techniques which satisfy engineering constraints at each stage of the search and also permit the behaviour in service of trial designs to be rapidly checked.

Two procedures for interactive design of tension systems have been described which may be classified as either discrete search or dynamic search methods. The first method, by Grieger (73), uses the interactive console to call and display the results of various separate programs, developed at the I.S.D. in Stuttgart, for approximate or exact form-finding, static and dynamic analyses. For the non-linear form-finding problem, with constraints accounting for mesh type, complete matrix iteration analyses to achieve or closely approximate static equilibrium are required for each change in support and prestress conditions. The system may thus make heavy demands on computing time, core store and backing facilities, but a large range of program and element types can be incorporated. An alternative approach to interactive form-finding, proposed by the author (17,19) (Chapters 5,7), is to treat the search as a physically dynamic problem in which the alterations of support and prestress conditions, and consequent changes in form, may be continuous. The analysis, based on a procedure termed Dynamic Relaxation, allows constructional constraints to be accounted for at both approximate and exact stages of form-finding; the distinction between these stages being merely a matter of degree of convergence, which initially is rapid (figure 3).

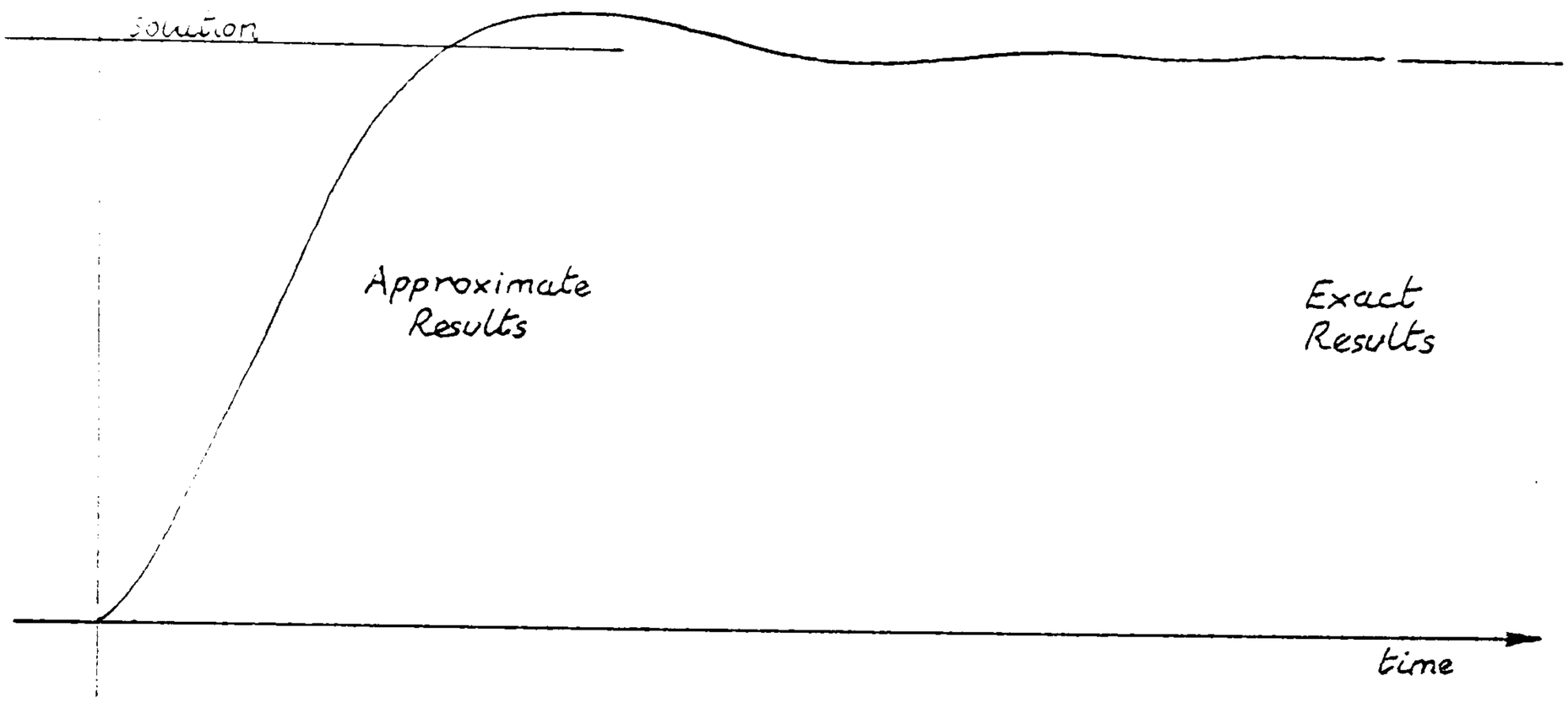


Figure 3

The same program may also be used to examine both static and dynamic behaviour under design loads, and it is thus theoretically possible to treat the entire design as a continuous process. A useful feature of the method is that the overall stiffness matrix need not be formed and thus the topology of the structure may be altered, for example by refining the idealisation or deleting certain links when edge curves are amended, during the form-finding process without having to reformulate the analysis. Another advantage of a direct rather than matrix formulation is that core store is considerably reduced, but a disadvantage is that, for efficiency, it is restricted to simple element types such as bar or cable links, constant moment beam elements, and triangular membrane or constant moment panel elements (Chapter 5, Appendex 2).

One problem at present with the concept of interactive form-finding is that surface shape and wind loading are interdependent, and this is a particularly important aspect in the case of light-weight tension structures. For any surface shape the pressure coefficients must usually be determined from wind tunnel tests and, without these tests, only very crude estimates of mean or fluctuating components of wind loads are possible. It is, however, necessary to qualitatively assess the effects of shape and other design parameters on the behaviour and efficiency of a structural system before embarking on wind tunnel testing. Critical wind speeds, for example, may be estimated from the lowest natural frequencies and mode shapes, and these in turn depend on surface curvatures, prestress levels and the elastic stiffnesses of the cables, membrane cover and support structures (43). Also the degree of pneumatic damping, dependent on permeability of the structure, and anelastic material damping, particularly from visco-elastic cladding elements, may be assessed (195,18) (Chapter 6). Nearly all of these factors are in turn governed by the static load carrying requirements and, because of the light self weight, the distribution of applied static loads may significantly affect dynamic response. Thus for each such distribution the static and dynamic behaviour should preferably be assessed together.

Since major cost items are the bearing structures, form-finding procedures should account for their efficient design and shape determination simultaneously with that of the surface structure. In the case of tension boundaries, assuming that when

necessary the topology of adjacent surface elements may be conveniently expanded or contracted, furnicular edge curves may be generated and amended automatically as tension elements in the overall analysis. The generation of momentless compression boundaries for structures of irregular shape, however, requires special treatment in order that the analysis does not become unstable. In a direct step-by-step procedure this entails simply the reversal of force *and* stiffness components at edge nodes at each stage of the form-finding process which is carried out simultaneously with the surface shape determination (15,16) (Chapters 3,4). In contrast, matrix methods require that the analyses for funicular compression boundaries and surface shape be de-coupled and this considerably increases the number of iterations compared with tension bounded structures in order to obtain convergence.

For orthotropically stressed membranes and networks with symmetric plan forms it is possible to derive analytically the required stress distributions in the suspension and prestress directions to ensure that a specified compression bearing contour with continuous curvature is approximately momentless (113). Alternatively the saddle surface curvatures and hence prestress ratios can be specified and thence the required momentless boundary may be derived. In practice some compromise between preferred boundary and surface forms may be required, and for the general case of irregularly shaped structures

numerical interactive form-finding is well suited to achieve a satisfactory overall design. From the point of view of static and dynamic behaviour in service, fairly uniform surface curvatures should be sought and this restricts the possible momentless boundary forms. An exception to this is the case when the surface boundary is connected also to a continuous support wall or network which is capable of transmitting shear forces to the ground. By varying the magnitudes of these shear forces, together with vertical loads acting along the bearing contour, it is possible to generate a considerable variety of regular or irregular boundary forms even for the support of uniformly stressed surface membranes or networks (Chapter 4).

Internally balanced tension systems using continuous compression boundaries to absorb cable forces from either double layer or network systems are generally more economic than open systems involving support masts and tension anchorages (113,185). The derivation of momentless boundaries, however, applies only to one condition of load and prestress and compression boundaries must be capable of supporting the moments induced by all variations of load and cable tensions. These become more severe as boundary shapes depart from circular or elliptical, but in considering the bending stresses induced in compression boundaries under various conditions of loading the structure must be analysed as an integral unit, accounting for the beneficial effect of non-linear interaction between the tension cable system and the bearing structure. This is

particularly important in respect of bearing contour stability since the cables not only transmit loads but also constitute an elastic support which may stiffen with increase of external load and provoke a simultaneous increase in the critical load of the compression boundary as this deflects. In circular saddle roofs subject to distributed loading, for example, deflection of the elastic boundary may induce an increase in tension in both the suspension and prestress cables; the stabilising effect of these cables, and consequent limitation of bending moments, being dependent on surface curvature and prestress levels. Shallow curvatures with high pretension may favour the use of slender ring beams and result in overall economy (43, 126).

The foregoing discussion of form-finding has primarily concerned tensioned structural mechanisms for which the form may be regarded as a spatial funicular of the link or element forces under prestress conditions. Another approach to structural form-finding, which has been applied to truss and space structures, is concerned with determining the arrangement of elements to achieve a minimum weight design whilst complying with various limits on deflections and stresses under differing loads. The majority of mathematical optimization techniques appropriate to this problem place severe constraints on freedom of architectural design and, for multiple loading conditions, may result in highly irregular structures. In contrast, the form of structural mechanisms which

are prestressed to ensure stability under live load variations reflect clearly their structural function because the prestress dominates.

When the problem of minimum weight design of triangulated space systems can alternatively be posed as finding the most efficient structural arrangement to support a maximum average design load, together with variations from this loading, the forms which result from optimization may also clearly reflect their structural function. This approach has been considered in Chapter 8 which outlines an optimisation process, based on Dynamic Relaxation, applicable to modular space structures which are complex in function and form. The procedure permits full emphasis to be placed on freedom of architectural design which may be carried out interactively. Thus, for each functional modification, applied and dead load conditions alter the preferred structural policy, determined by an analysis which continuously modifies member areas and allows topological changes to be made in the direction of currently greatest efficiency.

DYNAMIC BEHAVIOUR

The characteristics of tension systems which make them attractive for spanning large areas, that is, their light weight and the efficient use of tension members without flexural rigidity, also contribute to the drawback of sensitivity to

dynamic loading. This is particularly so in the case of prestressed structural mechanisms, such as networks, for which very low natural frequencies may possibly give rise to the danger of flutter at high wind speeds (171), or may place these frequencies in the high energy range of the gust frequency spectrum (42). Furthermore, the close grouping of natural frequencies in mechanisms can result in the occurrence of interference or beating phenomena, with dynamic response to buffeting wind loads involving the participation of many modes (96). Greater demands are thus placed on techniques of analysis which may be further complicated by the need to account for non-linear response, with stiffnesses, damping effects and effective masses being partially dependent on nodal deformations, velocities and accelerations (90,1,81). Wind tunnel tests are essential for the determination of pressure coefficients and also for the examination of frequencies of vortex shedding from bluff edges which may influence detailed design. In the case of the Munich Stadium, for example, following wind tunnel testing the edge rim was shaped to avoid dynamic excitation of the structure by buffeting vortices (109). For very flexible surfaces, such as pneumatic structures, the wind pressure coefficients, together with the internal volume and pressure, may also change significantly with deformations (25, 155); fully aeroelastic model tests may not, however, be practicable.

The low natural frequencies of tension networks can be increased by increasing the pretension, surface curvatures, or

the stiffness of support structures (38). Increasing the sectional area of cables has comparatively little effect on frequencies since the stiffening is offset by the additional dead weight. For steeply curved surfaces, however, the cladding may provide stiffening and triangulation across mesh diagonals and thus increase and disperse the range of natural frequencies (180). With shallow curvatures these effects are likely to be less significant because the dominant stiffness is geometric, and much larger deflections would be necessary to ensure the effective participation of initially unstressed cladding.

Following deformations by wind loading, in addition to the possible alteration of pressure coefficients, the high flexibility of many tension systems can also give rise to secondary interactions between the structure and the surrounding or enclosed air which should be accounted for in dynamic analyses. The inertial reaction of surrounding air to accelerations of the roof surface may need to be included as an "added mass" term with the mass components of the structure (90, 1). The effect can be significant for very light open-sided structures without superimposed loads (which otherwise may form the dominant mass components), and results in a further reduction of already low frequencies. For surface structures with closed sides, however, variations of internal pressure as the structure deforms may give rise to a stiffening effect which increases the natural frequencies. The magnitude of this effect will depend upon the mode of vibration. The first half-wave symmetric

mode is the main volume displacing mode and this will entail pressure changes which can have a considerable effect on internal pressure and air stiffness resisting deformation. To a lesser extent the same may apply to some higher symmetric modes, but anti-symmetric modes tend not to be volume displacing and are consequently little affected by additional air stiffness (1, 171, 195).

As a result of pressure stiffening the fundamental modes and frequencies of fully or partially enclosed structures may differ radically from those predicted by theory which does not account for variations in internal pressure, though this will depend on the type of structure and the cable curvatures employed (1). For triangulated truss and radial systems the first half-wave mode tends to be dominant for the unclad structure but is replaced by the first anti-symmetric mode as the fundamental when the roof surface and sides are clad. For cable girders with vertical struts or steeply curved networks the fundamental mode may be anti-symmetric whether or not the structure is clad since this entails smaller changes in strain energy than the first half-wave mode. For very shallow networks, however, the first unclad mode may again be symmetric and consequently volume displacing when the structure is clad.

In all tension systems the degree of damping is of major importance. It is impossible to ensure that vibrations will not occur but, with significant damping, amplitudes may be kept within acceptable limits. The mechanisms of damping which can occur in tension structures are:

a) Rheological material damping: due to visco-elastic behaviour of membrane cladding panels, and anelastic behaviour of the cables

b) Friction damping: due to the mechanical construction of cables and cladding and cable joints

c) Air damping: due to the kinetic energy of air resistance to structural vibrations

d) Pneumatic damping: due to the decay of internal air pressure changes lagging deformations of roof structures with permeable sides

e) Rheological and friction damping in support structures and foundations

f) Incorporation of damping elements in the design: for example, dashpots at the junction of cladding and cable nodes and in cable links or stays.

In tests on network and membrane structures with open sides Jensen (90) found that the logarithmic decrement associated with cladding or membrane damping ranged between 4-20% depending on the type of material and jointing. For cables the range was 0.5-3% depending on the level of prestress, with the higher values corresponding to low prestress. And air damping was found to be significant only for very light structures. Zingali (195), reporting on the design of the Palasport in Milan, showed by means of a simplified single degree of freedom analysis that pneumatic

damping, and the associated increase in stiffness due to changes in internal pressure, was sufficient to eliminate the first half-wave mode of vibration which otherwise would have been critical. He assumed an exponential decay of the pressure changes which depended on the permeability of the structure sides. The author (18) (Chapter 6), in vibration tests on a closed pneumatic dome subject to suddenly applied central ring loads, isolated the effects of material damping, air damping and pressure stiffness changes. The decay of vibrations was recorded and found to correlate fairly closely with an explicit numerical integration analysis which included all of these effects. The membrane was represented as a series of elements with visco-elastic properties which approximately simulated material damping; the visco-elastic constants having been obtained by means of a simple calibration test.

The inclusion of damping terms in matrix methods of dynamic analysis has traditionally had to be founded on previous experience or vibration tests on similar large scale structures which, in fact, have been comparatively rare. In modal superposition methods the percentage of critical damping for each normal mode and frequency is required. For implicit integration schemes, which are more suited to non-linear structural behaviour, a complete damping matrix is required which, for the purpose of obtaining a solution, is normally taken as a linear combination of the stiffness and mass matrices (K and M):

$$[M]\{\ddot{\delta}\} + [C_1[M] + C_2[K]]\{\dot{\delta}\} + [K]\{\delta\} = \{P(t)\}$$

Neither procedure can truly represent the physical mechanisms of damping and the coefficients can at best only be estimated. The latter procedure, however, has the merit of qualitatively being able to represent separate categories of damping. Thus, for example, air damping is dependent on nodal velocities and can be accounted for with an appropriate choice of C_1; whereas material damping is dependent on relative nodal velocities and is best incorporated by adjusting the coefficient C_2. A further difficulty with matrix methods of solution for structures which interact non-linearly with their environments is that the linearised mass, damping and stiffness matrices may be unsymmetric, consequently entailing increased computing effort (81). This results, for example, from the inclusion of added mass terms, directional drag and pneumatic damping and stiffness. The latter effects are most conveniently allowed for in the forcing function $\{P(t)\}$ and the solution is then greatly simplified by the use of explicit integration methods which do not require the formation of the various coefficient matrices.

Another problem concerning the coupling of structure deformations and loading, which may arise for very wide span flexible systems, is the danger of flutter. Classical flutter is generally regarded as a self-excited oscillation, with a sustained or divergent amplitude, which may occur when the structure is subject to sufficiently high laminar wind speeds (71). The basic cause is the extraction of energy from the flow by elastic deformation of the structure, and feeding of this energy into some particular mode of oscillation in such a way that the work done by the air balances or exceeds the energy

that is dissipated by damping. The small deflection eigenvalue problem for the natural modes and frequencies, w, of a structure not subject to excitation may be expressed as:

$$\left|\left[K\right] - w^2\left[M\right]\right| = 0$$

In the case of flutter, the modes and frequencies of motion are determined through the interaction of the inertial, elastic and aerodynamic forces:

$$\left|\left[K\right] - w^2\left[M\right] - \frac{\rho_o U}{2}\left[Q\right]\right| = 0$$

where ρ_o and U are the air density and free stream speed, and $\left[Q\right]$ is a matrix of aerodynamic influence coefficients. The latter, however, are not readily available except in the simplest cases.

The only analytical assessment of flutter relating to tension roofs which is known to the author is that given by Sofronie (173), who considered a very simplified structure consisting of parallel cable girders on a long rectangular plan with open sides or flexible column supports. Expressions for critical wind velocities were obtained in a similar manner to analyses for aeroelastic stability of rigid wing structures with coupling of bending and torsional degrees of freedom. These simplifying conditions would, however, not generally apply even for most rectangular truss or girder structures. It has been suggested (193) that the possibility of flutter may be precluded in cable girders by ensuring differing tensions and load distributions in the upper and lower cables. In fact, however, the system merely

prevents mechanical vibrations without straining, since corresponding natural modes and frequencies of the main cables considered in isolation must always differ.

Siev (171) has examined the occurrence of flutter in small scale wind tunnel tests of a stressed hypar membrane and concluded that for membranes or cable networks of daring design the possibility of flutter in practice does exist. A result of interest relating to pneumatic stiffening was the elimination of the lowest flutter frequency when the volume of the structure was enclosed. Tsuboi (180), for the design of the Tokyo olympic swimming pool roof, estimated critical wind speeds by regarding a disturbed air stream moving across the structure as a system of air blocks having various densities. By this analogy the critical velocity for any normal mode is given by the product of the wave length and frequency of vibration of the mode. A check on Siev's results for frequencies and critical velocities shows that the latter could have been adequately predicted using the air-block analogy, both for the fundamental and higher modes. Thus, although accurate analyses or aeroelastic model investigations for flutter may not in general be feasible, it appears that, for shallow roof surfaces, useful information in this respect may be gained from a knowledge of natural modes and frequencies under the various conditions of static load.

The discussions in the preceding sections concerning the characteristics of tension systems in relation to static behaviour, form-finding and dynamic behaviour have indicated, in a broad sense, the needs of analytical techniques. The various techniques appropriate to these problems are reviewed in Appendices A, B and C respectively. Appendix D gives a more complete review of the technique of dynamic relaxation than is contained in the papers which form the following chapters.

CHAPTER 2

DYNAMIC RELAXATION ANALYSIS OF TENSION NETWORKS

SUMMARY

The paper describes a general analysis based on the method of Dynamic Relaxation proposed by A.S. Day[1,2]*. A computational arrangement is outlined in a form applicable to tensioned cable structures and space frames with cladding or panel elements. The procedure reduces considerably the core storage required compared with matrix iteration schemes and enables zero stiffness situations to be coped with. The analysis may be used to determine pretension geometry and behaviour under static or dynamic loading with account being taken of slackening of cables. A general expression for deriving close bounds to the critical time interval is also given which avoids the need for trial runs or the determination of eigenvalues. The paper concludes by illustrating the use of the method to determine the initial geometry and subsequent behaviour under loading of a cable edged geodesic network model.*

The paper was presented at the Int. Conference on Tension Structures, London, April 1974.

DYNAMIC RELAXATION

The basis of the method is to trace step by step, for small time increments Δt, the dynamic behaviour of a structure from the time when it is initially loaded. For dynamic analyses with time dependent, impulse or transient loading the trace is terminated when the vibration characteristics and the maximum stresses and deflections have been obtained. For static loading, a high fictitious damping is imposed and the trace is terminated when the structure reaches a steady equilibrium state. The computational arrangement is similar for both cases though the term "Dynamic relaxation" strictly applies only to the case of static analysis. For dynamic analysis the real, usually light, structural damping would be used and smaller time integration steps may be necessary. In addition, the damping may not be applied as 'far-coupled' at the nodes but as 'close-coupled' within the structural members. This aspect is considered in Chapters 5 and 6. The present application concerns essentially the analysis of cable networks under static loading, though as a by-product an indication of the dominant natural frequencies is obtained.

The masses of the structure are assumed to be concentrated at the node points. It is also assumed in the following that these nodes are jointed; sliding nodes associated with geodesic networks being accounted for later by means of a simple modification.

The governing equation of motion in the x direction of any node i at time t is:

$$R_{xi}^{t} = M_i . \dot{V}_{xi}^{t} + K_i . V_{xi}^{t} \qquad (1)$$

where R_{xi}^{t} is the residual force at node i in direction x at time t.

M_i is the mass at node i.

K_i is the damping constant at node i.

V_{xi}^{t}, $\dot{V}_{xi}^{t}$ are respectively the velocity and acceleration of node i in direction x at time t.

Similar equations can be written for the y and z directions.

In finite difference form equation (1) is:

$$R_{xi}^{t} = \frac{M_i}{\Delta t}\left(V_{xi}^{t+\Delta t/2} - V_{xi}^{t-\Delta t/2}\right) + \frac{K_i}{2}\left(V_{xi}^{t+\Delta t/2} + V_{xi}^{t-\Delta t/2}\right) \qquad (2)$$

Note that as the trace is followed for successive time intervals, the residual forces are determined for times 0, Δt, $2\Delta t$ ..... $t-\Delta t$, t, $t+\Delta t$ ..... etc. whilst the average velocities are determined at the mid-points of these time intervals.

From (2) the velocity at time $t+\Delta t/2$ may be expressed as:

$$V_{xi}^{t+\Delta t/2} = R_{xi}^{t}\left[\frac{1}{Mi/\Delta t + Ki/2}\right] + V_{xi}^{t-\Delta t/2}\left[\frac{Mi/\Delta t - Ki/2}{Mi/\Delta t + Ki/2}\right] \qquad (3)$$

The damping factor K_i may be defined as a constant for the structure, or more conveniently may be defined as $K_i = M_i.(K'/\Delta t)$.

The damping/unit mass, $(K'/\Delta t)$, may be taken as constant for the structure but the actual damping will then be greatest for the most heavily loaded nodes. This will be preferable to uniform damping if, in addition to static deflections and member forces, the analysis is required to give some estimate of the range of dominant natural frequencies.

Equation (3) thus becomes:

$$V_{xi}^{t+\Delta t/2} = A_i' \cdot R_{xi}^{t} + B' \cdot V_{xi}^{t-\Delta t/2} \qquad (3a)$$

where $A_i' = \left[\frac{\Delta t}{M_i(1 + K'/2)}\right]$ a constant for each node

$B' = \left[\frac{1 - K'/2}{1 + K'/2}\right]$ a constant for the complete structure

The total x deflection of node i at time $t+\Delta t$ is:

$$\delta_{xi}^{t+\Delta t} = \delta_{xi}^{t} + \Delta t\, V_{xi}^{t+\Delta t/2} \qquad (4)$$

Similarly the velocities and deflections in the y and z directions may be determined.

These calculations are carried out simultaneously for each node of the structure to give the complete displaced form at $t+\Delta t$. The current force in each bar or cable link m is then given by:

$$T_m^{t+\Delta t} = T_m^{o} + \left(\frac{EA}{L_o}\right)_m \cdot e_m^{t+\Delta t} = T_m' + \left(\frac{EA'}{L}\right)_m \cdot e_m^{t+\Delta t} \qquad (5)$$

where, for links which have not slackened, $T_m' = T_m^{o}$ the specified pretension, $EA_m' = (EA_m + T_m^{o})$, and L_m and $e_m^{t+\Delta t}$ are respectively

the link length under pretension and the extension from that state. The current extension may be determined by a square root operation in the program, or more efficiently by means of an expression which makes use of the previously calculated extension e_m^t (appendix 2.2).

If the link connects nodes i and k then the force which it exerts in the x direction at i is:

$$\Delta R_{xim}^{t+\Delta t} = \frac{T_m^{t+\Delta t}}{L_m^{t+\Delta t}} \left[\left(X_k + \delta_{xk}^{t+\Delta t} \right) - \left(X_i + \delta_{xi}^{t+\Delta t} \right) \right] = -R_{xkm}^{t+\Delta t} \qquad (6)$$

where X_i, X_k are the co-ordinates in the pretension condition and $L_m^{t+\Delta t}$ is the current link length.

The contributions of all links connected to i are summed, with the applied load of P_{xi}, to give the current residual force:

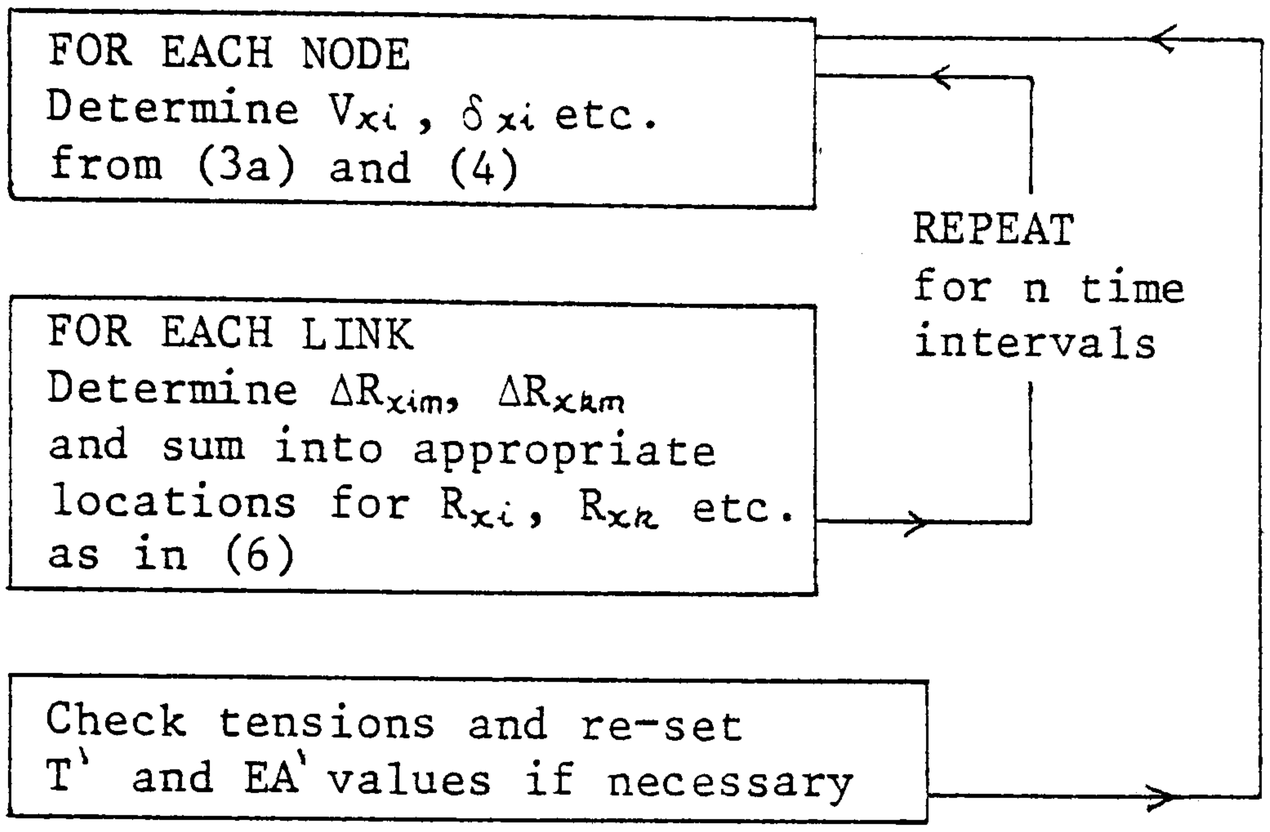
$$R_{xi}^{t+\Delta t} = P_{xi}^{t+\Delta t} + \sum \Delta R_{xim}^{t+\Delta t} \qquad (7)$$

The residual forces in the y and z directions may similarly be derived.

The effect of cable slackening may be accounted for by checking tensions at regular stages in the analysis (every n time intervals), and setting to zero T' and EA' in slack links until the next check. If a previously slack link is then found to be taut, the original T' $(=T^o)$ and EA' values in equation (5) are restored. Gradual changes in elastic modulus dependent on stress level can be accounted for in a similar

manner. For static analyses, with high viscous damping, the checks may be made at infrequent intervals ($n \gg 1$).

The complete cycle of calculations takes the form:



A summary of computer storage and operation requirements is given in appendix 2.3, and this is compared in addition with the computational efficiency of a matrix iteration scheme.

Initial Conditions:

It is assumed in the analysis that the velocity changes linearly over any time increment. Thus to satisfy the initial conditions ($V_{xi}^{o} = 0$, $R_{xi}^{o} = P_{xi}^{o}$),

$$V_{xi}^{\Delta t/2} = \frac{A_i'}{(1 + B')} \cdot P_{xi}^{o} \qquad (8)$$

CLADDING

Cladding membranes may be accounted for in the analysis as a finite system of "constant strain" triangular panel elements.

In order to keep computer storage requirements to a minimum the displacements $\{\delta^e\}$ of a typical element (fig.1) are defined as the extensions, Δ, of the edges[4]. This reduces the stiffness matrix for an element to (3x3) compared with the usual (6x6) associated with two displacements per node. It also complies with the programming procedure previously outlined for cable links. The transformation into (9x9) element stiffnesses required for procedures in which an overall stiffness matrix is assembled is thus avoided.

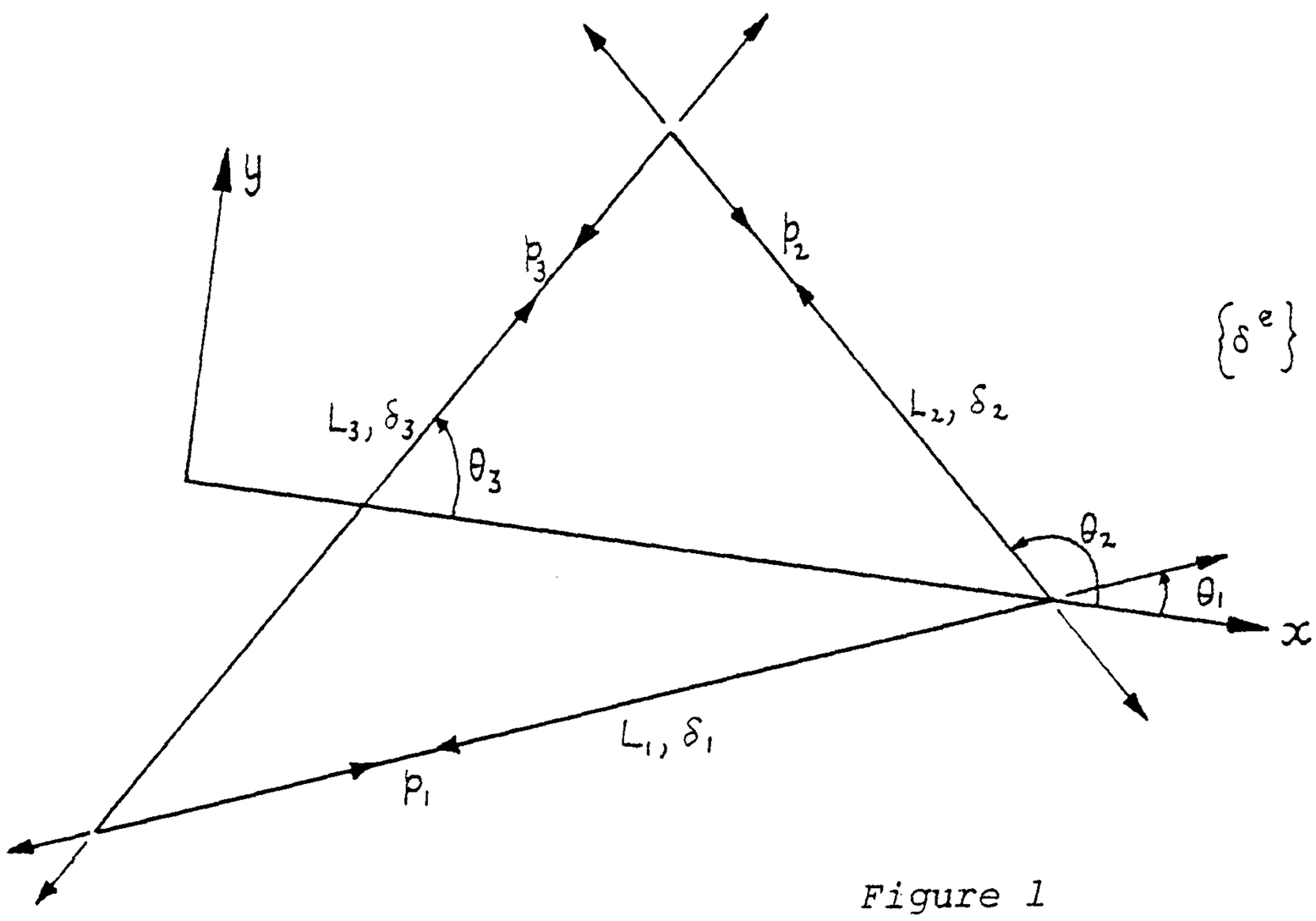


Figure 1

Corresponding element forces are the tensions along each edge:

$$\{p^e\} = \begin{Bmatrix} p_1 \\ p_2 \\ p_3 \end{Bmatrix}$$

The strains are assumed constant along each edge and throughout the panel and may be expressed in terms of $\{\delta^e\}$:

$$\{\varepsilon\} = \begin{Bmatrix} \varepsilon_x \\ \varepsilon_y \\ \gamma_{xy} \end{Bmatrix} = [G] \begin{Bmatrix} \delta_1 \\ \delta_2 \\ \delta_3 \end{Bmatrix} \tag{9a}$$

where x and y are convenient element axes.

The terms in the matrix $[G]$ are given by the equations:

$$\frac{\varepsilon_x}{\begin{vmatrix} b_1 & c_1 & \varepsilon_1 \\ b_2 & c_2 & \varepsilon_2 \\ b_3 & c_3 & \varepsilon_3 \end{vmatrix}} = \frac{-\varepsilon_y}{\begin{vmatrix} a_1 & c_1 & \varepsilon_1 \\ a_2 & c_2 & \varepsilon_2 \\ a_3 & c_3 & \varepsilon_3 \end{vmatrix}} = \frac{\gamma_{xy}}{\begin{vmatrix} a_1 & b_1 & \varepsilon_1 \\ a_2 & b_2 & \varepsilon_2 \\ a_3 & b_3 & \varepsilon_3 \end{vmatrix}} = \frac{1}{\begin{vmatrix} a_1 & b_1 & c_1 \\ a_2 & b_2 & c_2 \\ a_3 & b_3 & c_3 \end{vmatrix}} \tag{9b}$$

where $\varepsilon_i = \Delta_i / L_i$, $a_i = \text{Cos}^2\theta_i$, $b_i = \text{Sin}^2\theta_i$, $c_i = \text{Sin}\,\theta_i \text{Cos}\,\theta_i$

and θ_i = inclination of edge i to the x axis.

The stresses in an element are:

$$\{\sigma\} = \begin{Bmatrix} \sigma_x \\ \sigma_y \\ \tau_{xy} \end{Bmatrix} = \begin{bmatrix} d_{11} & d_{12} & 0 \\ d_{21} & d_{22} & 0 \\ 0 & 0 & d_{33} \end{bmatrix} \begin{Bmatrix} \varepsilon_x \\ \varepsilon_y \\ \gamma_{xy} \end{Bmatrix} = [D][G]\{\delta^e\} \tag{10}$$

In general, the orthotropic elastic constants, d_{ij}, must correspond with the element x,y axes. But for the particular case of an isotropic plane stress element which has not buckled:

$$d_{11} = d_{12} = \frac{E}{(1-\nu^2)} \quad ; \quad d_{12} = d_{21} = \nu d_{11} \quad ; \quad d_{33} = \frac{E}{2(1+\nu)}$$

and for convenience θ_1 may be set to zero.

Having obtained the $[G]$ and $[D]$ matrices the element stiffness relations are given by:

$$\{p^e\} = \left[[G]^T [D] [G] \, t.A \right] \{\delta^e\} \tag{11}$$

where t.A = volume of the element.

With triangular element stiffness relations in this form, panel elements can be incorporated without transformations in the basic program for cable or bar structures; the effect of panel edge forces being included in the same way as cable link forces. The effect of compressive buckling and consequent alteration of the [D] matrix is considered in Chapter 3.

To account for in plane distortion of very flexible membrane elements it may be necessary to reset the [G] matrix at infrequent intervals. Distortion will alter the values of θ_i in equation 9b, but lengths L_i remain the unstressed lengths upon which strains must be based. Similarly the volume of the element, tA, in equation (11) will remain unchanged.

DAMPING CONSTANT

For static load analysis a high fictitious damping constant must be used; the trace being terminated when the structure and loads are sufficiently close to a steady equilibrium state. To obtain bounds to the true equilibrium state a sub-critical damping constant should be used (fig. 2). Provided the damping is near the critical value, convergence in the early stages is rapid. Over-damping should generally be avoided, except in cases of static load failure analyses, such as the ultimate load of structures involving progressive buckling or cracking, when collapse should be approached from one side.

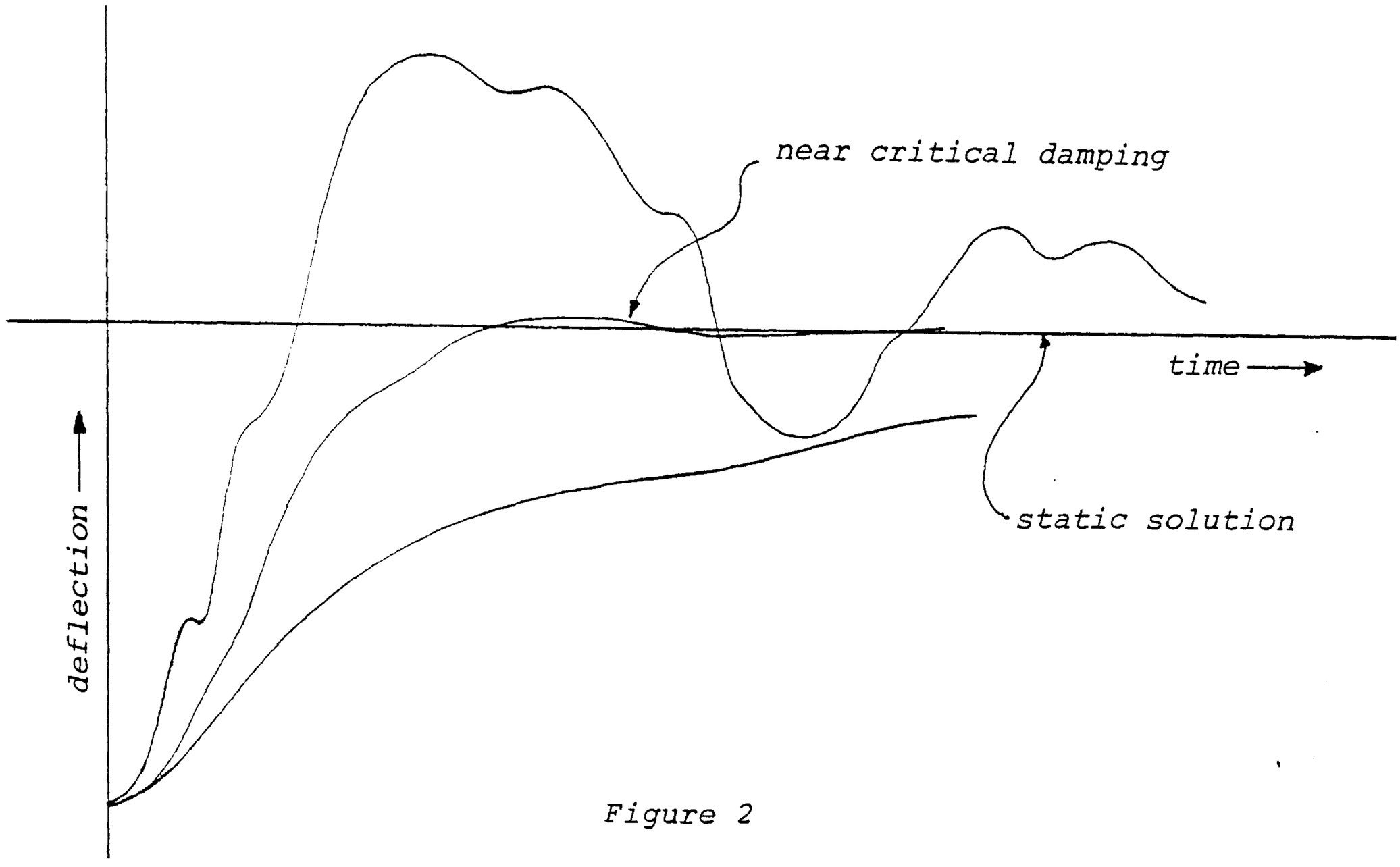


Figure 2

TIME INTERVAL

When the time interval exceeds a certain critical value, numerical instability of the calculations will occur. Considering only the x axis component of vibrations of a node i with structural connections to adjacent nodes k:

From (3a) $$V_{xi}^{t+\Delta t/2} = B_i \cdot V_{xi}^{t-\Delta t/2} + A_i \cdot R_{xi}^{t} \qquad (12)$$

For the next interval, assuming that the motions of nodes k and i are parallel to the x axis:

$$V_{xi}^{t+3\Delta t/2} = B_i \cdot V_{xi}^{t+\Delta t/2} + A_i \cdot \Big(R_{xi}^{t} - \sum_{\text{all links at } i} S_{xik}^{t+\Delta t} \cdot \Delta\delta_{xik}^{t+\Delta t}\Big) \qquad (13)$$

where $S_{xik}^{t+\Delta t}$ is the x axis direct stiffness of node i relative to adjacent nodes k due to the structural element connecting nodes i and k.

$\Delta\delta_{xik}^{t+\Delta t} = V_{xik}^{t+\Delta t/2} \cdot \Delta t$ is the increment of x deflection of node i relative to adjacent nodes k during the time interval $t \rightarrow t+\Delta t$.

Thus if the time interval is large when the stiffness/mass ratio (S_{xik}/M_i) is large, instability in the form of successive reversal and build up in the amplitude of velocities and deflections may result.

Bounds to Δt may be obtained by considering adjacent nodes I and K of a part of the structure at which the S/M ratio of the nodes, or one of the nodes is highest. The most critical structural configuration and state of motion will be such that all nodes k adjacent to I are different from all nodes i adjacent to K, with the relative vibrations of nodes i and k exactly out of phase.

Substituting R^{t}_{xi} from (12) into (13) - For node I:

$$V_{xI}^{t+3\Delta t/2} - (B' + 1)V_{xI}^{t+\Delta t/2} + B'.V_{xI}^{t-\Delta t/2} = -A'_I \sum_{all\ k} (S_{xIk}(\Delta\delta_{xI} - \Delta\delta_{xk}))^{t+\Delta t} \qquad (14)$$

Similarly for node K:

$$V_{xK}^{t+3\Delta t/2} - (B' + 1)V_{xK}^{t+\Delta t/2} + B'.V_{xK}^{t-\Delta t/2} = -A'_K \sum_{all\ i} (S_{xKi}(\Delta\delta_{xK} - \Delta\delta_{xi}))^{t+\Delta t} \qquad (15)$$

For the most critical condition assume that the direct stiffness/mass ratios of all nodes i and k are equal and for oscillations which are just stable: all $\Delta\delta_{xi} = \Delta\delta_{xI}$ and all $\Delta\delta_{xk} = \Delta\delta_{xK}$.

Hence subtracting (15) from (14):

$$V_{xIK}^{t+3\Delta t/2} - (B' + 1)V_{xIK}^{t+\Delta t/2} + B'.V_{xIK}^{t-\Delta t/2} = -A'_I (S_{xI}\ 2\Delta\delta_{xIK})^{t+\Delta t} \qquad (16)$$

where V_{xIK} is the velocity of I relative to K

S_{xI} is the direct stiffness of node I relative to all adjacent nodes (assumed highest in the x direction).

The limiting case of stability is when V_{xIK} during one time increment produces relative deflection changes $\Delta\delta_{xIK}$ such that V_{xIK} in the next time increment is equal and opposite to the previous value.

$$\text{Hence} \qquad -2(B' + 1)V_{xIK}^{t+\Delta t/2} = -A_I' \cdot S_{xI} \cdot 2\Delta\delta_{xIK}^{t+\Delta t}$$

$$\therefore \quad \frac{(B' + 1)}{A_I'} = S_{xI} \cdot \Delta t$$

$$\therefore \quad \Delta t_{critical} = \sqrt{\frac{2M_I}{S_{xI}}} \qquad (17a)$$

Assuming alternatively (when subtracting (15) from (14))

$S_{xK}/M_K \ll S_{xI}/M_I$

$$\Delta t_{critical} = \sqrt{\frac{4M_I}{S_{xI}}} \qquad (17b)$$

In calculating a permissible value for Δt, constant throughout the analysis for the whole structure, the highest ratio of S/M at any node in any co-ordinate direction must be considered. In practice the true critical time interval has been found to lie within the limits given above for all cable and space structures so far analysed.

APPLICATION TO A GEODESIC NETWORK

Pretension Geometry:

The initial geometry of geodesic networks is such that each cable takes a path of minimum length over the network surface and has a uniform tension throughout its length . The

geometry of a network with fixed boundary nodes can be determined from the analysis simply by holding the tension constant throughout each cable. Thus in equation (6) $T_m = T_m^{\circ}$, the specified pretension. At the start of the analysis any nodal co-ordinates may be assumed. It has been found in trials that rapid convergence to the correct geometry is obtained even when the assumed initial geometry is extremely inaccurate. The reason for this is that the stiffness of any node relative to adjacent nodes is very low; being controlled only by changes in geometry and not by the elastic properties of the cables. Therefore the critical time interval is comparatively large.

For geodesic networks in which the surface cables are jointed to edge cables the geometry is determined in the same way for surface cables, but for edge cables the tension in only one link of each cable is held constant at the required value whilst the other edge links are assumed to start from a slack state for which their lengths are specified; the tensions in them being controlled elastically.

Behaviour in Service:

After erection the nodes of a geodesic network would be jointed at least at the points of attachment of the cladding membrane. When all nodes are jointed the analysis follows the standard form. When only some of the nodes are jointed, with the rest being free to slide, tensions will be uniform over certain segments of each cable containing several links. The

analysis for nodes within these segments takes the same form but with the tensions being changed after each iteration due to elastic deformation of the segments in an overall sense. In the analysis of the model network under imposed loading all nodes were jointed, and the network was tested and analysed in an unclad condition.

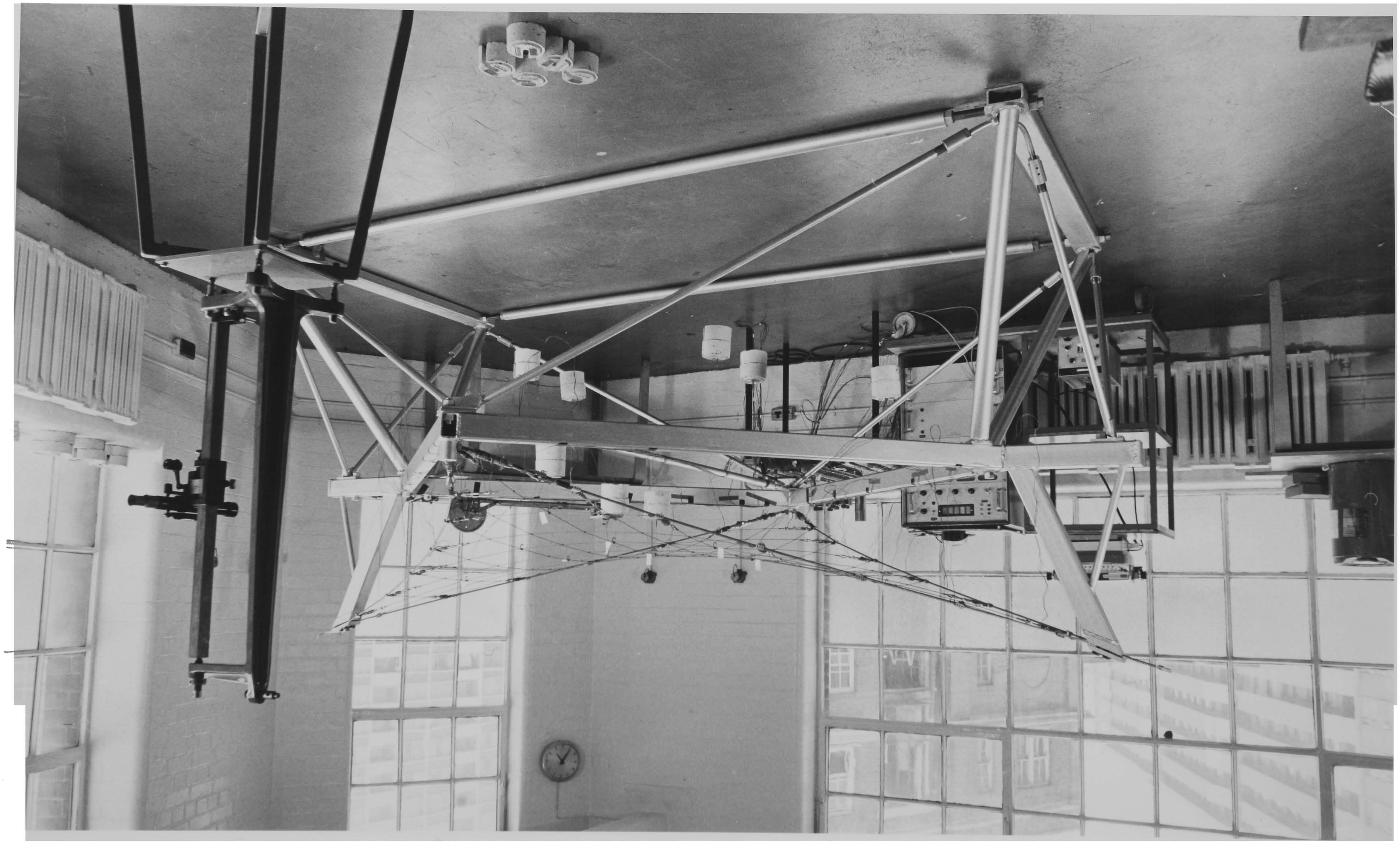
MODEL NETWORK TEST

The model network (figs. 3 & 4), measuring 2.6m across low points, 3.2m across high points, with a height difference of 560mm was constructed from 12 concave or sagging cables, 11 convex cables and four edge cables. The cables were of stainless steel and had EA values of 421 kN, 316 kN and 2740 kN respectively. The total number of nodes was 100, four of which were fixed anchorages corresponding to the high and low points at the ends of the edge cables.

The network was pretensioned by means of stainless steel turnbuckles at one end of all cables; tensions being recorded by means of two strain gauges in series on each turnbuckle. The applied cable tensions and the lengths between the edge nodes were such that the network was as nearly as possible symmetrical. The approximate tensions were 9000 N in edge cables and 450 N in all surface cables except the three central convex cables in which the tension was 670 N.

After tensioning the network, the nodes were jointed with wire clips and 13 N loads were applied at eight of the surface

Figure 3



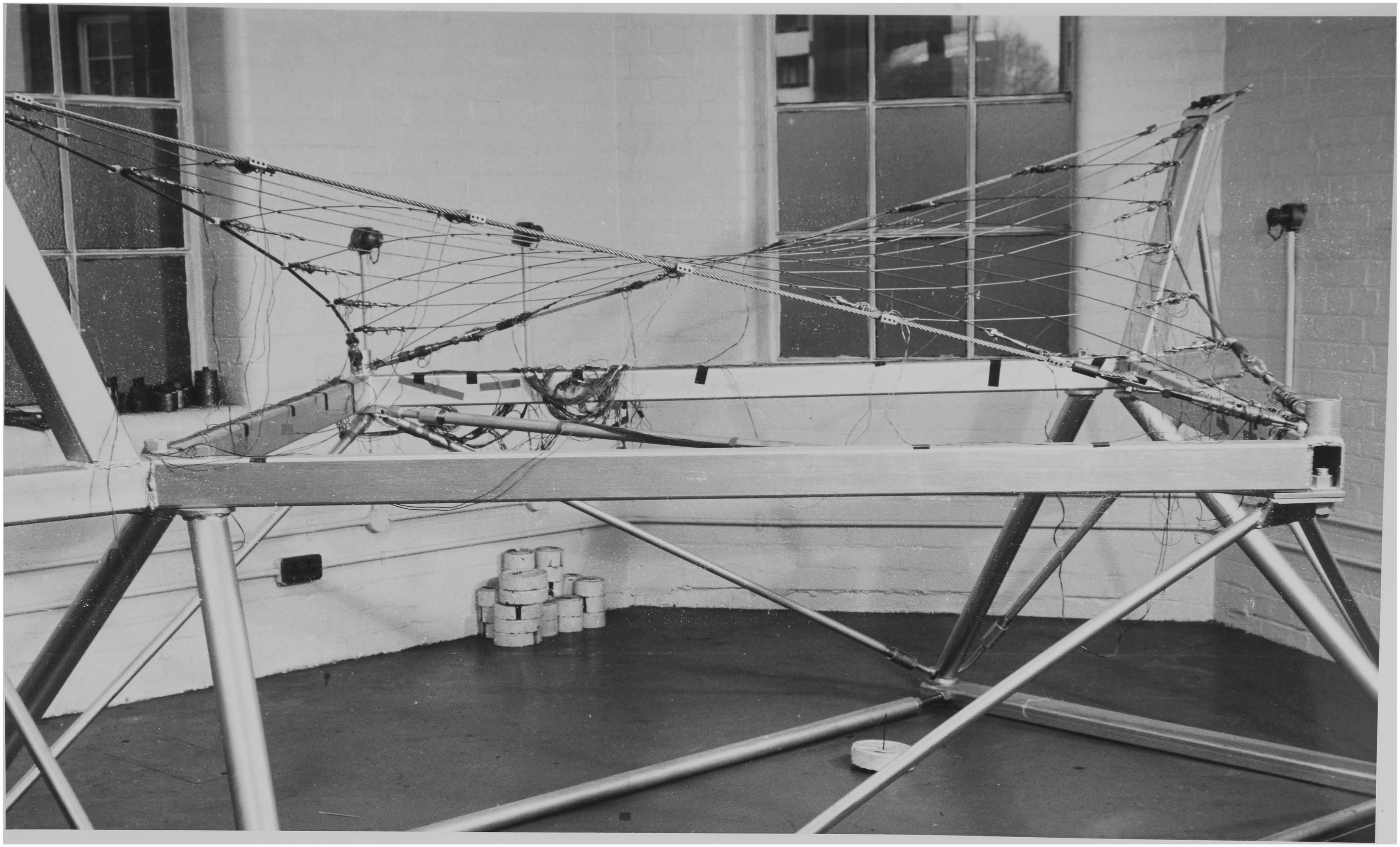


Figure 4

nodes as shown in fig.5. Deflections at these nodes could be recorded by means of a cathetometer. In addition to these static deflections, the lowest resonant frequencies of each loaded node and the central edge cable nodes were determined; resonance being induced and recorded with a small electronic vibrator. The comparatively small loads used in these tests were chosen to enable precise recording of the dynamic response. Equally good results have been obtained for much higher loads involving considerable distortion of the network.

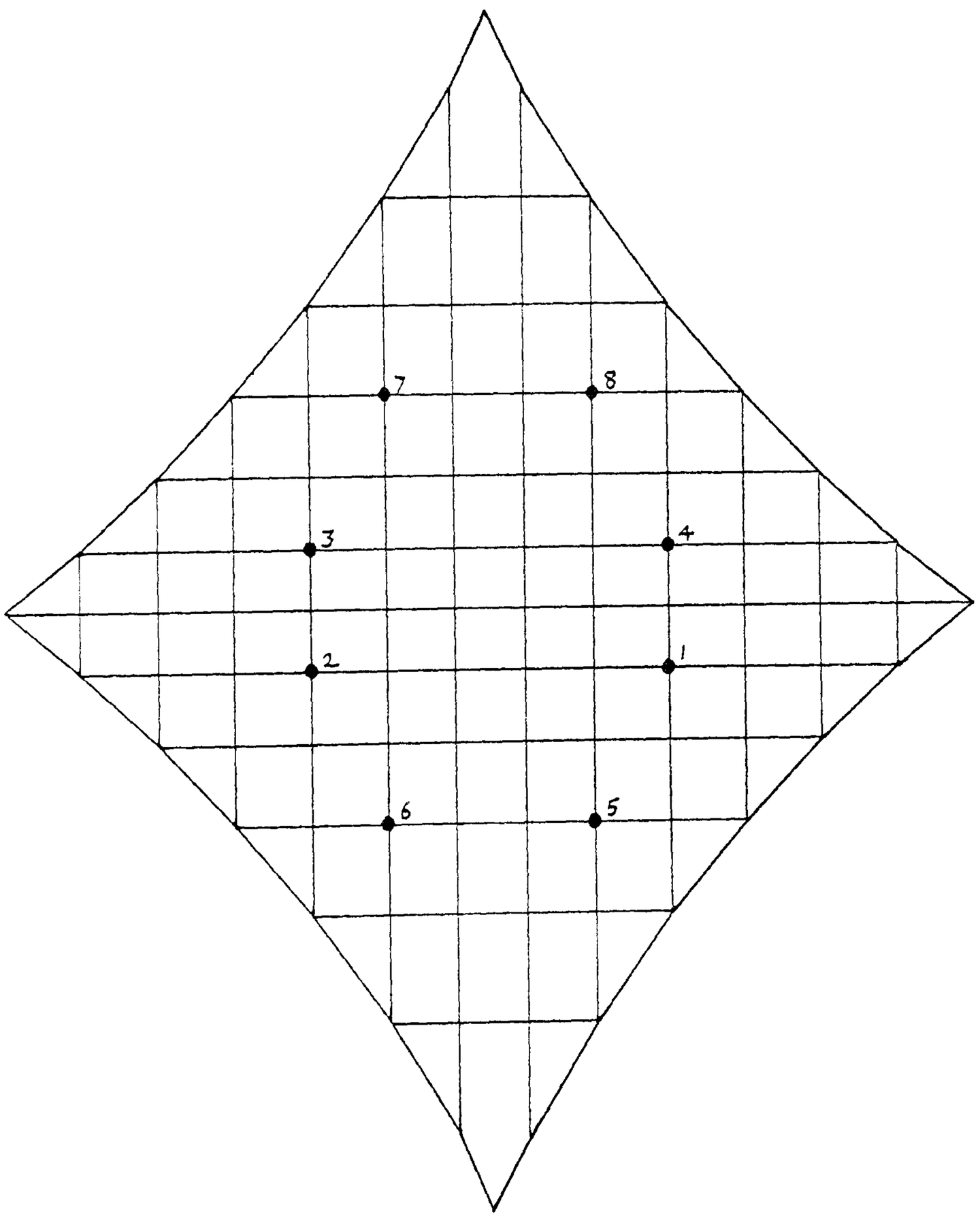


Figure 5

RESULTS

Pretension Geometry:

For the calculations of the geodesic geometry the time increment was $\Delta t = 0.00012$ sec and the damping constant per unit mass was $0.03/\Delta t$. A print-out was obtained for every 30 iterations (i.e. at time intervals of 0.0036 sec). The starting positions of the nodes in the calculation were based on the assumption that the surface was a diamond shaped hyperbolic parabaloid with straight boundaries. In spite of large deflections the analysis had converged after 10 print-outs, (300 iterations). It can be seen from the plot for a typical surface node (fig.6) that the motion was nearly critically damped.

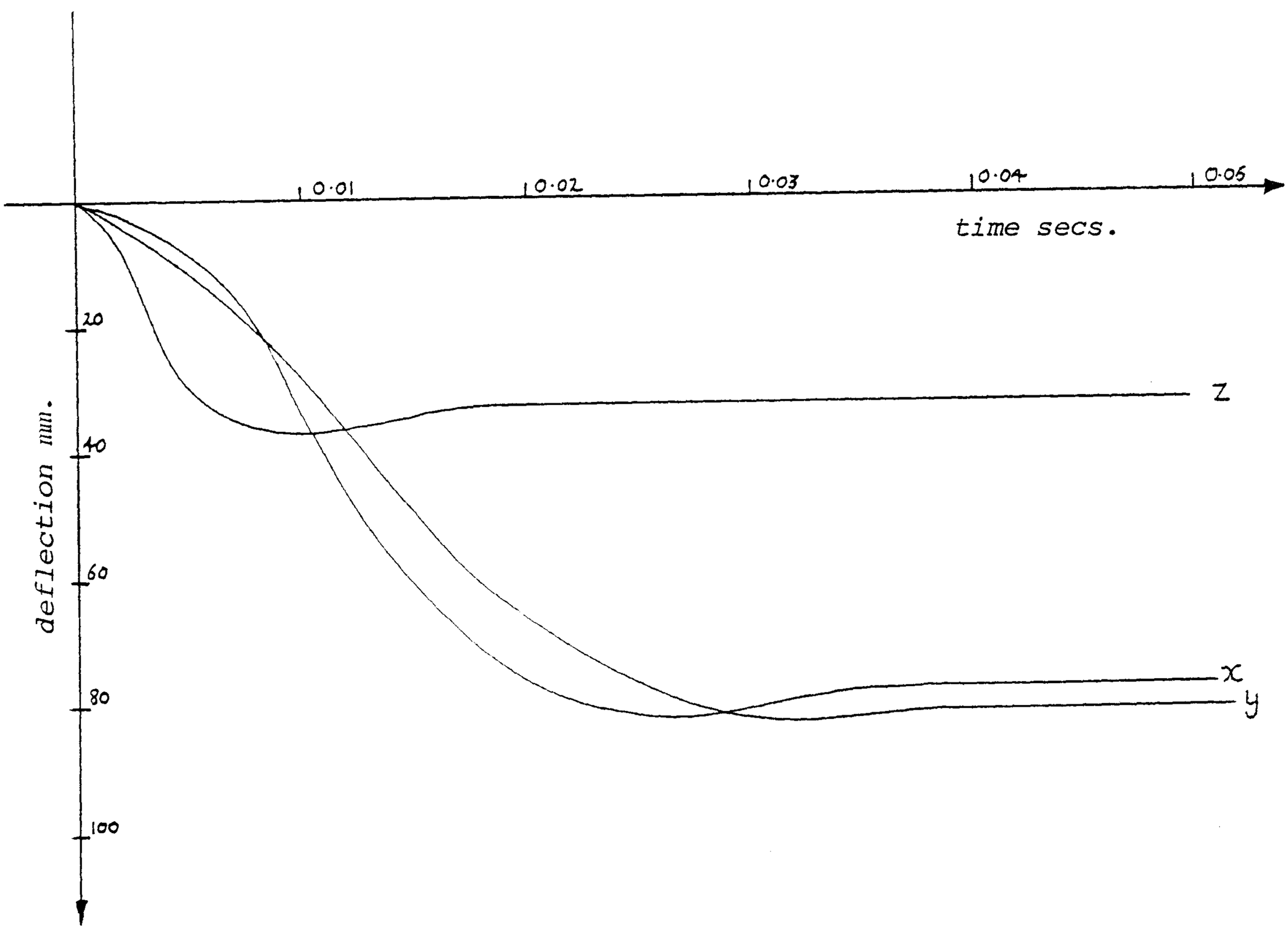


Figure 6

Behaviour Under Applied Loading:

With all nodes jointed the stiffness/mass ratios in some areas of the network were higher, but the most critical points were at nodes adjoining links which contained a turnbuckle since the EA values were considerably higher than the values for typical cable links. As a result, and because no use was made of fictitious masses, the analysis took longer to converge than the pretension analysis. Bounds to the critical time interval given by equations (17) were:

$$0.000038 < \Delta t_{crit} < 0.000054$$

The time interval used was 0.000045 sec, and the damping constant per unit mass was $0.005/\Delta t$. A subsequent analysis using a time interval of 0.000049 proved to be unstable. A total of 40 print-outs at time intervals of 0.0018 sec (or every 40 iterations) was required to obtain sufficient accuracy.

Fig.7 shows a plot of the dominant vertical motion of one of the four central loaded nodes. The final deflection of 0.0345" (0.876 mm) compares with a measured value of 0.036" (0.914mm). Results of similar accuracy were obtained for the other observed deflections. The analysis gave a damped frequency for load points 1→4 of about 13 Hz, and for nodes 5→8 about 9 Hz. These results compare respectively with observed values in the regions 14.5 and 11 Hz ($\pm\frac{1}{2}$ Hz). As would be expected the theoretical values are low because of the high fictitious damping at the loaded nodes in the analysis. A subsequent analysis with no damping gave frequencies of 15.5 and 12.5 respectively.

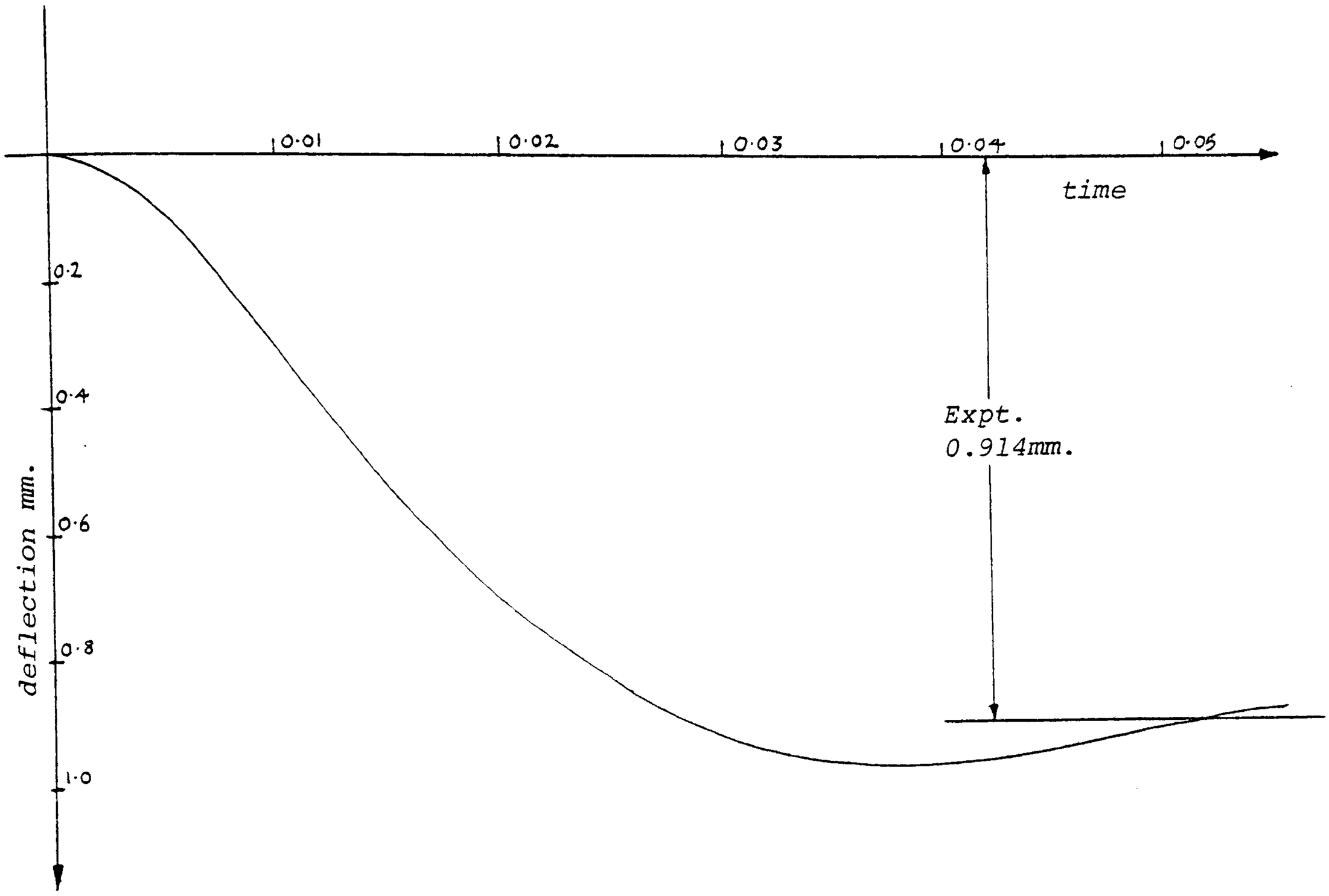


Figure 7

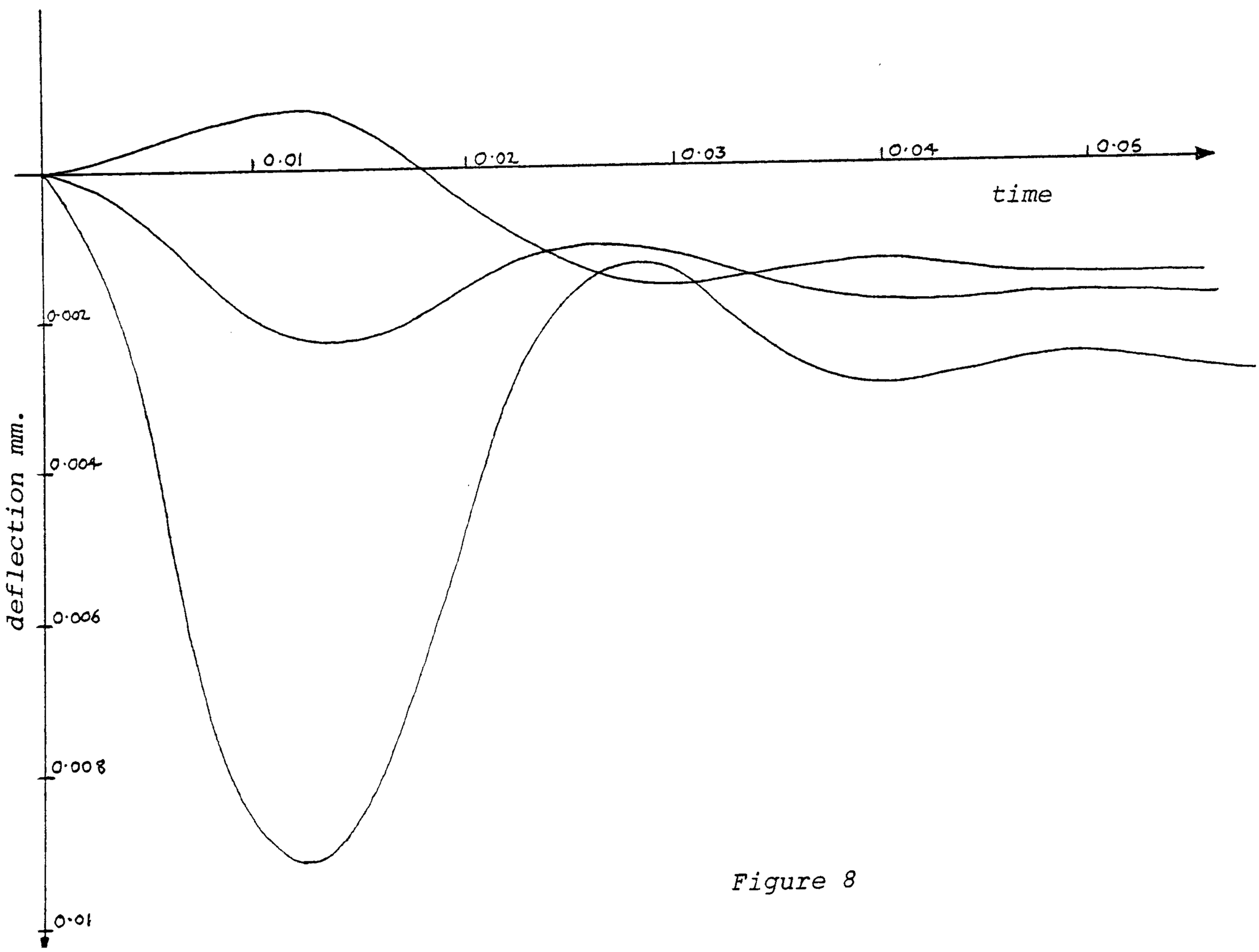


Figure 8

Fig.8 shows a plot of the damped motion of a node in the centre of one edge cable. The observed frequency agreed to within 1 Hz of the calculated frequency of 42 Hz; the difference between the values obtained from the damped and undamped analyses being negligible owing to the comparatively light damping at edge nodes.

Comments:

It can be seen from the rapid convergence of the calculations for the geodesic geometry that a Dynamic Relaxation analysis is particularly suited to this type of network when nodes are not jointed. For determining the static deflections of the jointed network under applied loads the analysis converged more slowly, which in large measure is due to the limitation of the critical time interval due to the turnbuckles. However, by using increased (fictitious) masses at the end nodes of edge cables the number of iterations for the loaded state analysis reduced to 800, and this had negligible effect on the frequency response of surface nodes. Since the dynamic relaxation process when used for static loading gives only an indication of frequency response, this reduction is very worthwhile. A further reduction in computing time could be obtained by using a higher damping constant and fictitious masses throughout the entire structure (considered in chapter3) but no indication of frequencies would be obtained.

For lightweight network roofs, estimates of the range ofdominant natural frequencies for each of various distributions of snow or other static load are required. Dynamic Relaxation may

provide such estimates as a bye-product of the static analyses. For the model test structure the dominant frequencies were obtained merely by inspection of the output. This was justified by the fact that the loads were released on the structure simultaneously and thus the damped dynamic trace contained components of only the lowest modes. Contributions from higher modes might be induced by staggering the application of the loads or imposing, on one or more unloaded nodes, initial displacements not compatible with any normal mode shape. After propogation and decay of these displacements, coupled with the effect of the applied loading, Fourier analysis of the output at any node should yield an estimate of the range of natural frequencies. A brief consideration is given to this in Appendix 2.1.

REFERENCES

(1) Day, A.S., 'An introduction to Dynamic Relaxation', Engineer, 219, 1965

(2) Day, A.S., Bunce, J., 'The analysis of hanging roofs', Arup Journal, Sept. 1969.

(3) Barnes, M.R., 'Pretensioned cable networks', CONRAD, April, 1971.

(4) Argyris, J.H., 'Recent advances in matrix methods of structural analysis', Progress in Aeronautical Sciences, London, 1963.

N.B. A list of references concerning dynamic relaxation, discussion relating to the development of the method, and consideration of the optimum convergence rate are given in appendix D (page 371).

APPENDIX 2.1

MODAL DE-COMPOSITION OF AN EXPLICIT DYNAMIC RESPONSE ANALYSIS

The results of a damped or undamped dynamic relaxation (or central difference) analysis of a linear elastic structure, in which one or more nodes are displaced from their equilibrium positions and suddenly released, can be de-composed to obtain an estimate of the natural frequencies of the structure. When the initial displacements are proportional to one of the normal modes the resulting vibration will consist entirely of this normal mode. If the initial displacements are not proportional to a normal mode then the response will consist of a superposition of vibrations in all the normal modes. The frequency content of the recorded motion can be determined from methods based on Fourier series if the motion can be treated as periodic, or from methods that utilize the Fourier integral when the motion is non-periodic [5].

If a damped analysis is used (D.R.), the damping should be light in order that frequencies (particularly the lower ones) are not attenuated. For this reason it may be uneconomic to attempt, by Fourier de-composition, to obtain the dominant natural frequencies from a dynamic relaxation analysis which is intended primarily to yield a solution to the static load behaviour of a cable structure. In practice, however, it is probable that a lightly damped trial run would be carried out to obtain a value for the critical damping (see Chapter 3). In such cases a Fourier analysis, incorporated as a simple routine within the program, may be useful in yielding an estimate of the range of dominant frequencies for each static mass distribution considered.

Fourier Analysis of D.R. output

The resultant displacement y of any particle in a wave represented by a complex periodic vibration is:

$$y = f(t) = A_o + a_1.\mathrm{Cos}(wt+\eta_1) + a_2.\mathrm{Cos}(2wt+\eta_2) + \ldots + a_n.\mathrm{Cos}(\eta wt+\eta_n)$$

$$\text{or } y = A_o + \sum_{r=1:n} A_r \mathrm{Cos}(rwt) + \sum_{r=1:n} B_r \mathrm{Sin}(rwt) \qquad (1)$$

where η_1 etc. are phase angles and A_1, B_1 etc. represent the amplitudes of the various fundamental and harmonic terms, the fundamental frequency being given by $w/2\pi$. A_o is a constant term representing the mean level of the ordinates since, by integrating both sides of (1) with respect to t over a complete vibration of period $T = 2\pi/w$ it follows that all the terms on the right-hand side are zero except A_o. Hence:

$$\int_o^T f(t)dt = \int_o^T A_o dt = A_o T$$

$$\therefore \quad A_o = \frac{1}{T}\int_o^T f(t)dt = \text{Average value of } f(T) \text{ over one cycle.}$$

To evaluate the amplitude coefficients use is made of the orthogonality of sines and cosines - if the product of two sinusoids of different frequencies is integrated over a complete cycle the integral will be zero:

$$\int_o^T \mathrm{Sin}(mwt)\mathrm{Sin}(nwt).dt = 0 \qquad m \neq n$$

$$\int_o^T \mathrm{Cos}(mwt)\mathrm{Cos}(nwt).dt = 0 \qquad m \neq n$$

$$\int_o^T \mathrm{Sin}(mwt)\mathrm{Cos}(nwt).dt = 0 \qquad m = n \text{ or } m \neq n$$

But $\int_o^T \text{Sin}^2(\text{mwt}).dt = \int_o^T \text{Cos}^2(\text{mwt}).dt = \frac{T}{2}$

Hence, by multiplying (1) by Cos(rwt) and integrating for a complete cycle:

$$\int_o^T f(t)\text{Cos}(\text{rwt}).dt = A_r.\frac{T}{2}$$

or $$A_r = \frac{2}{T}\int_o^T f(t)\text{Cos}(\text{rwt}).dt$$

Similarly the coefficients of the Sine series may be determined by multiplying by Sin(rwt) and integrating:

$$B_r = \frac{2}{T}\int_o^T f(t)\text{Sin}(\text{rwt}).dt$$

The above theory applies to periodic vibrations. The output from a damped central difference analysis may be treated as such in the following way:

The full line in figure 1 represents a trace of the damped or undamped displacements or velocities of any node of the structure:

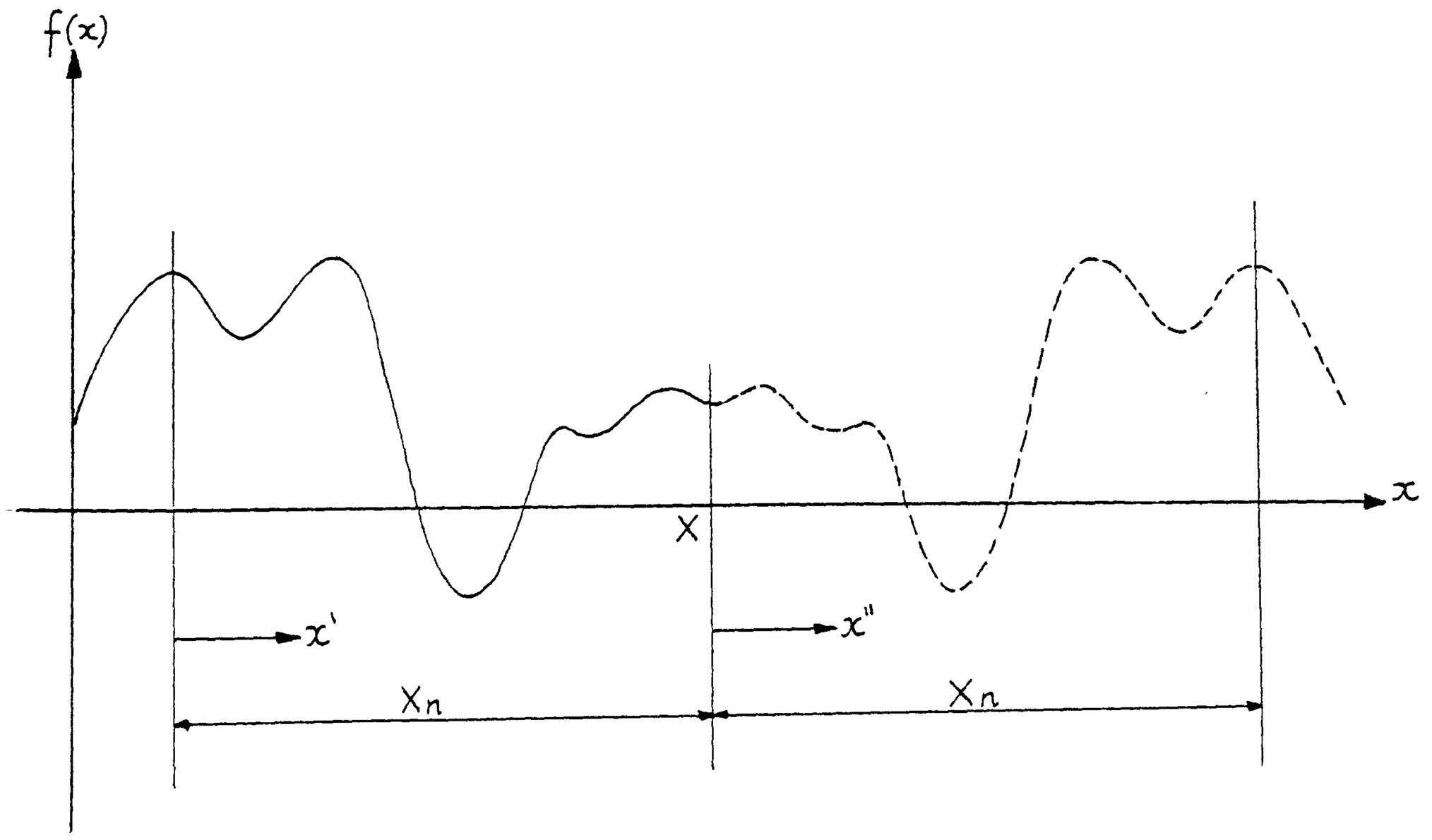


Figure 1

The dashed line represents the reflected image of the trace from X to $X+X_n$, where X is the last maximum or minimum of the trace and $X-X_n$ is the first. Associating $2X_n$ with the period:

$$A_o = \frac{1}{X_n}\int_{x-x_n}^{X} f(x)\,dx$$

hence, assuming n intervals (of length $\delta x = X_n/n$) from $X-X_n$ to X , and $f(x) = \alpha_m$ at the mid-point of interval m then by discrete summation:

$$A_o = \frac{1}{n}\sum_{m=1}^{m=n} \alpha_m$$

$$A_r = \frac{2}{2X_n}\int_{X-X_n}^{X} f(x)\mathrm{Cos}(rwx).dx + \frac{2}{2X_n}\int_{X}^{X+X_n} f(x)\mathrm{Cos}(rwx).dx$$

or, redefining origins for x' and x'':

$$A = \frac{1}{X_n}\int_{o}^{X_n} f(x')\mathrm{Cos}(rwx')dx' + \frac{1}{X_n}\int_{o}^{X_n} f(x'')\mathrm{Cos}(rwx'').dx''$$

and, since $f(x') = f(x'') = \alpha_m$ at $x' = \frac{(2m-1)}{2}\delta x = \frac{(2m-1)}{2n}X_n$

$$\text{and } x'' = X_n - \frac{(2m-1)}{2}\delta x$$

$$A_r = \sum_{m=1}^{m=n} \frac{\alpha_m}{X_n}(\mathrm{Cos}(rwx')\delta x + \mathrm{Cos}(rwX_n - rwx')\delta x)$$

hence, since $w = \pi/X_n$:

$$A_r = \sum_{m=1}^{m=n} \frac{\alpha_m}{n}\mathrm{Cos}(\frac{r\pi x'}{X_n})(1+\mathrm{Cos}r\pi) = 0 \text{ for all odd integers r}$$

$$A_r = \frac{2}{n}\sum_{m=1}^{m=n} \alpha_m \mathrm{Cos}(\frac{r\pi}{2n}(2m-1)) \text{ or all even integers r}$$

Similarly for the Sine coefficients:

$$B_r = \sum_{m=1}^{m=n} \frac{\alpha_m}{n}(\mathrm{Sin}(rwx') + \mathrm{Sin}(rwX_n - rwx'))$$

$$= \sum_{m=1}^{m=n} \frac{\alpha_m}{n}\mathrm{Sin}(rwx')(1 - \mathrm{Cos}r\pi) = 0 \text{ for all even integers } r$$

$$B_r = \frac{2}{n}\sum_{m=1}^{m=n} \alpha_m.\mathrm{Sin}\left(\frac{r\pi}{2n}(2m-1)\right) \quad \text{for all odd integers } r$$

The application and accuracy of the above de-composition method is compared in the following sections with eigenvalue and model test analyses for a plane prestressed net and a cable edged spatial network.

PLANE PRESTRESSED NET

The plane network shown in figure 2, when subject to constant prestress in each set of cables (S and T) and identical nodal masses, is amenable to a simple natural frequency analysis given by Grigorian [6].

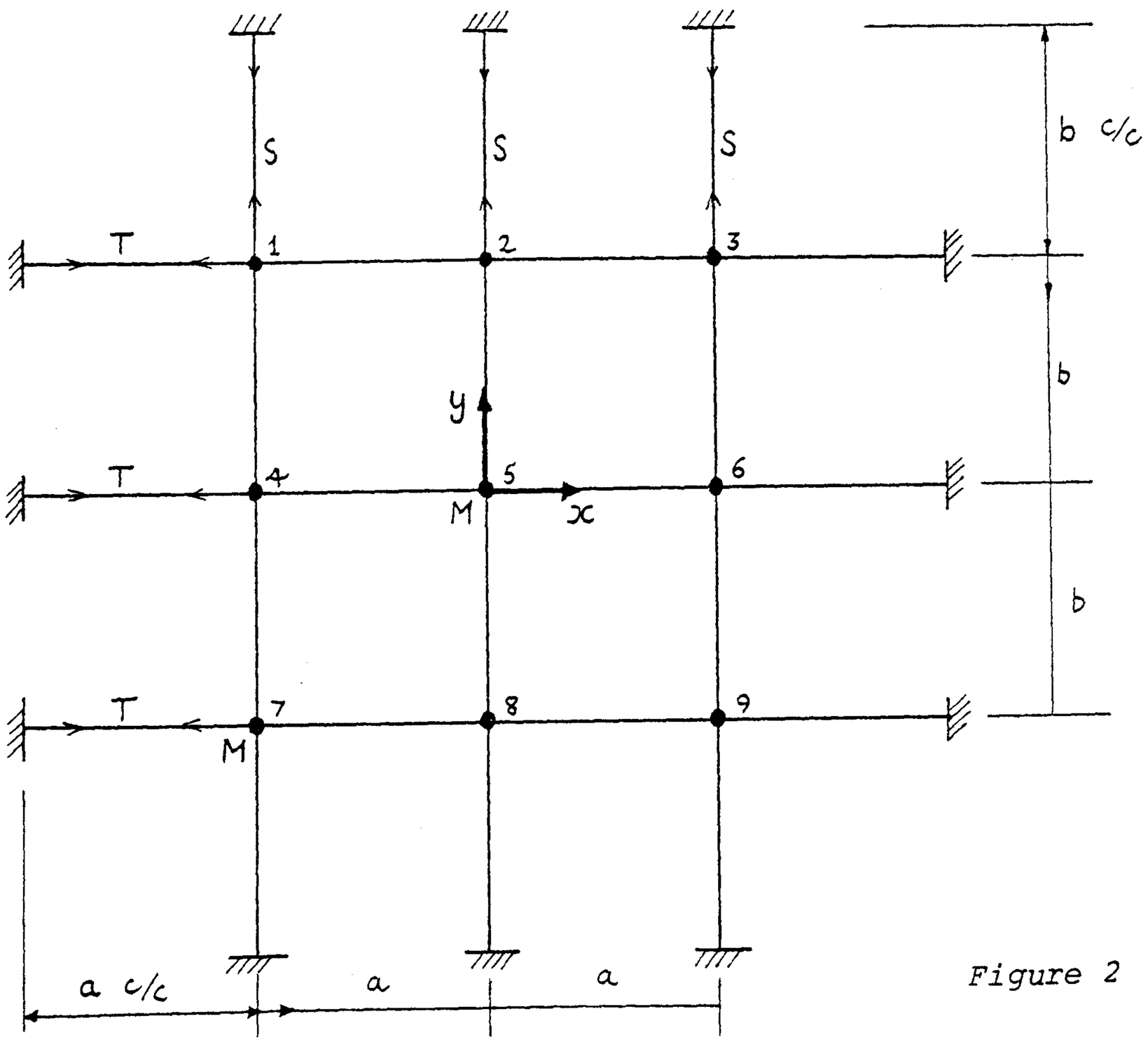


Figure 2

If the normal displacement of any intersection (x,y) in time (t) is given by a function $\Delta(x,y,t)$, then the equation of equilibrium at the intersection may be expressed as:

$$\left[-M\frac{d^2}{dt^2} + \frac{T}{a}\left(E_x - 2 + E_x^{-1}\right) + \frac{S}{b}\left(E_y - 2 + E_y^{-1}\right)\right]\Delta(x,y,t) = 0 \qquad (2)$$

where the mathematical operators carry out the functions:

$$E_x\Delta(x,y,t) = \Delta((x+1),y,t); \quad E_x^{-1}.\Delta(x,y,t) = \Delta((x-1),y,t)$$

A function $\Delta(x,y,t)$ which satisfies the boundary conditions of a completely supported net is:

$$\Delta(x,y,t) = \sum_{i=1,(m-1)} \sum_{j=1,(n-1)} D_{ij}.\ \mathrm{Sin}\left(\frac{i\pi x}{m}\right).\ \mathrm{Sin}\left(\frac{j\pi y}{n}\right).\ \mathrm{Sin}\omega t \qquad (3)$$

where D_{ij} is an arbitrary term.

Substituting the function (3) into the governing difference equation (2) gives:

$$\omega_{ij} = 2\sqrt{\left[\frac{T.}{M.a}\ \mathrm{Sin}^2\left(\frac{i\pi}{2m}\right) + \frac{S.}{M.b}\ \mathrm{Sin}^2\left(\frac{i\pi}{2n}\right)\right]} \qquad (4)$$

Assuming the following parameters in equation (4):

S = 20N; T = 60N; M = 0.123 kg; a=b=0.353m.

the natural frequencies $f_{ij} = \omega_{ij}/2\pi$ are as follows:

f = 5.2 Hz	f = 8.65 Hz	f = 11.2 Hz
f = 6.6 Hz	f = 9.6 Hz	f = 11.9 Hz
f = 7.8 Hz	f = 10.4 Hz	f = 12.6 Hz

Typical modes f_{12} and f_{23} are shown in figure 3

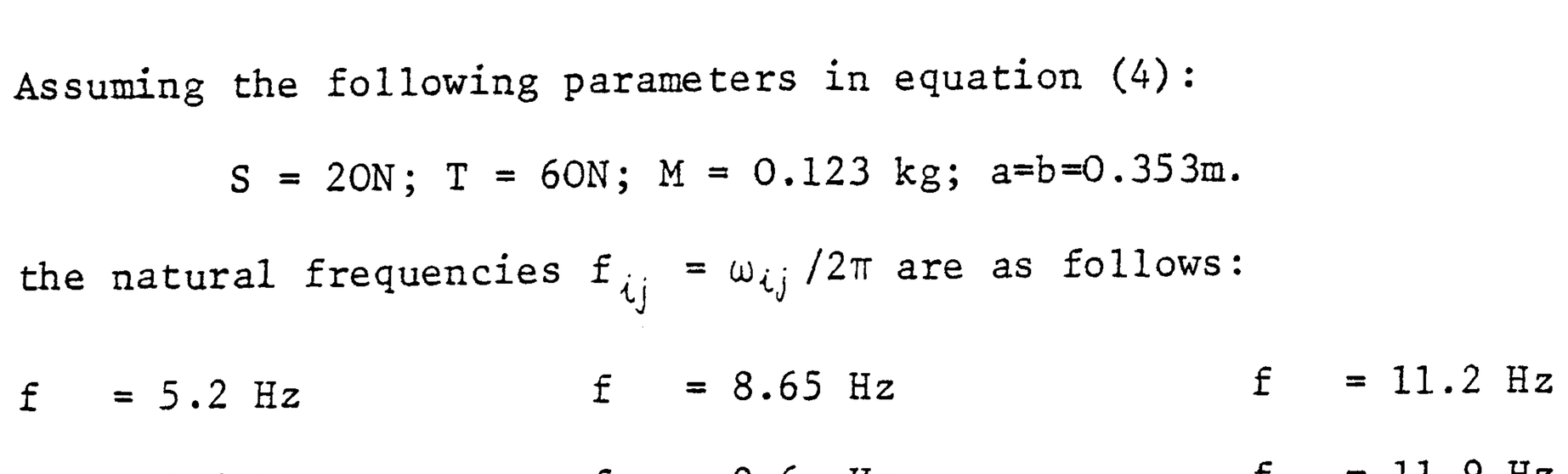


Figure 3

Dynamic Relaxation and Fourier Analyses

The stiffness of the network normal to the surface is given approximately by:

$$S = \frac{P}{\delta} = \sum \frac{H}{a} = 2\left(\frac{60}{0.353} + \frac{20}{0.353}\right) = 453 \text{ N/m}$$

This assumes deflections are sufficiently small not to increase tensions significantly. Since the same assumption is made in Grigorian's theory the tensions in the DR analysis were held constant.

Hence: $\Delta t_{crit} = \sqrt{\frac{2M}{S}} = 0.0233$ sec.

Based on the lowest frequency of 5.2 Hz, the critical damping per unit mass is given approximately by:

$$K_{crit} = 4\pi f \simeq 65$$

For the DR analyses of the net, node 1 was initially displaced 5mm normal to the surface with all other nodes held at their equilibrium positions. The nodes were then suddenly released and the vertical deflection of node 2 was traced to provide input for the Fourier analysis. Two cases were considered:

a) $\Delta t = 88\%\ \Delta t_{crit}$, $K = 40\%\ K_{crit}$, - traced for 0.52 sec.

b) $\Delta t = 22\%\ \Delta t_{crit}$, $K = 0$, - traced for 0.9 sec.

In each case the beginning and end points of the trace corresponded to minima or maxima.

For case (a) the deflection trace is shown in figure 4 and the result of the fourier analysis for the coefficients A_r and B_r is shown in figure 5. This suggests frequencies approximately in the range 4→11 Hz. The spectrum of coefficients is however very diffuse. For case (b) the

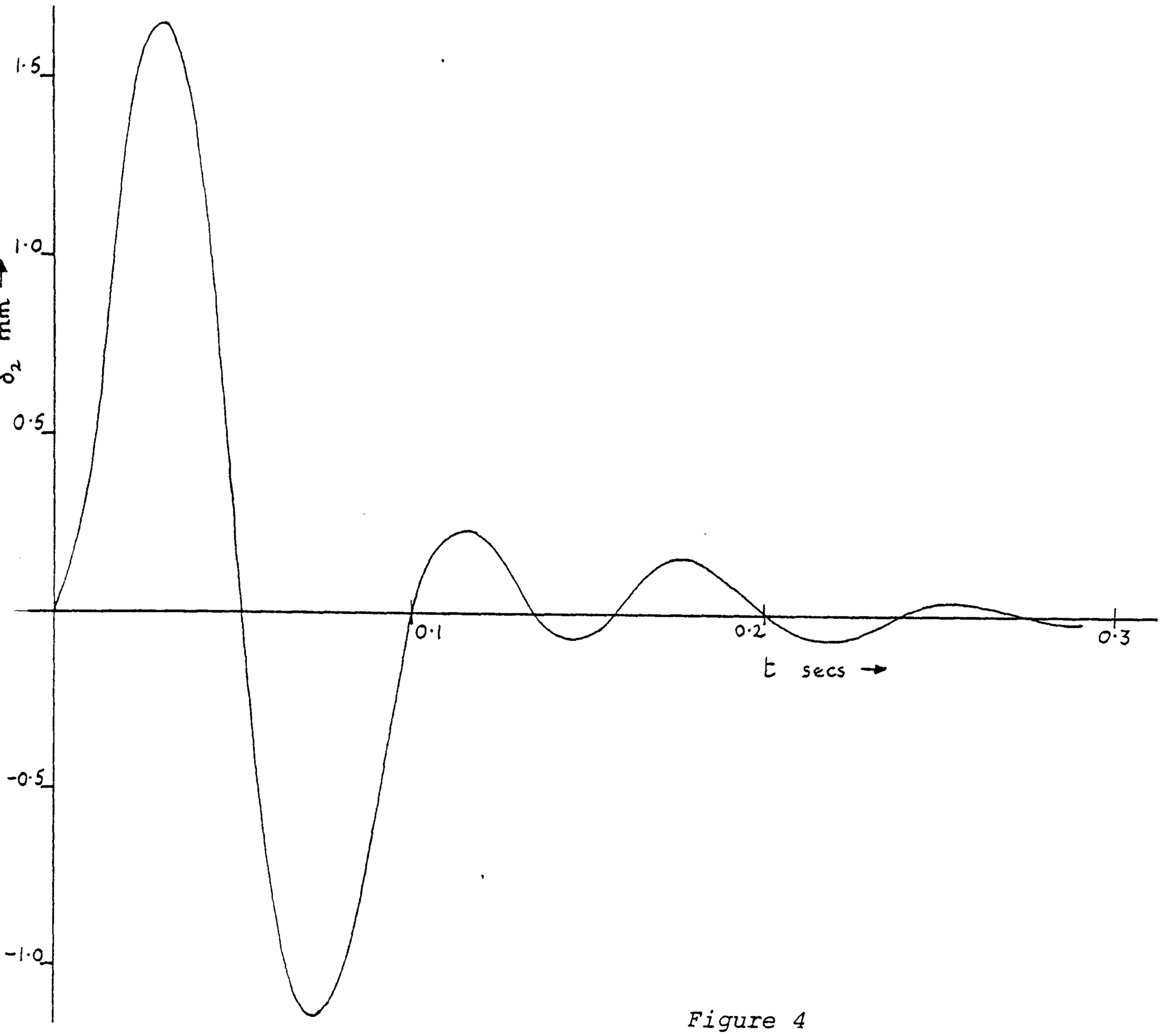


Figure 4

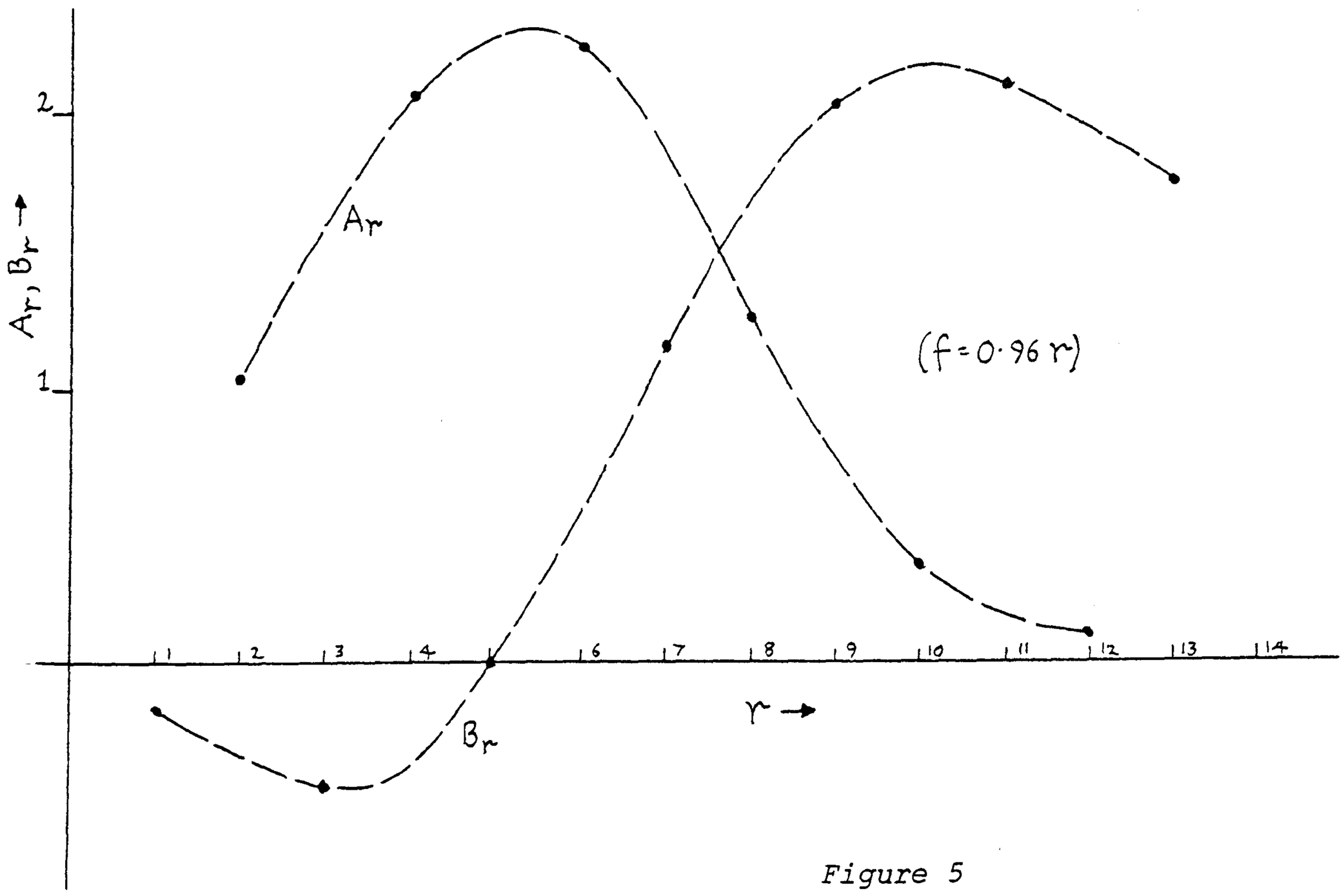


Figure 5

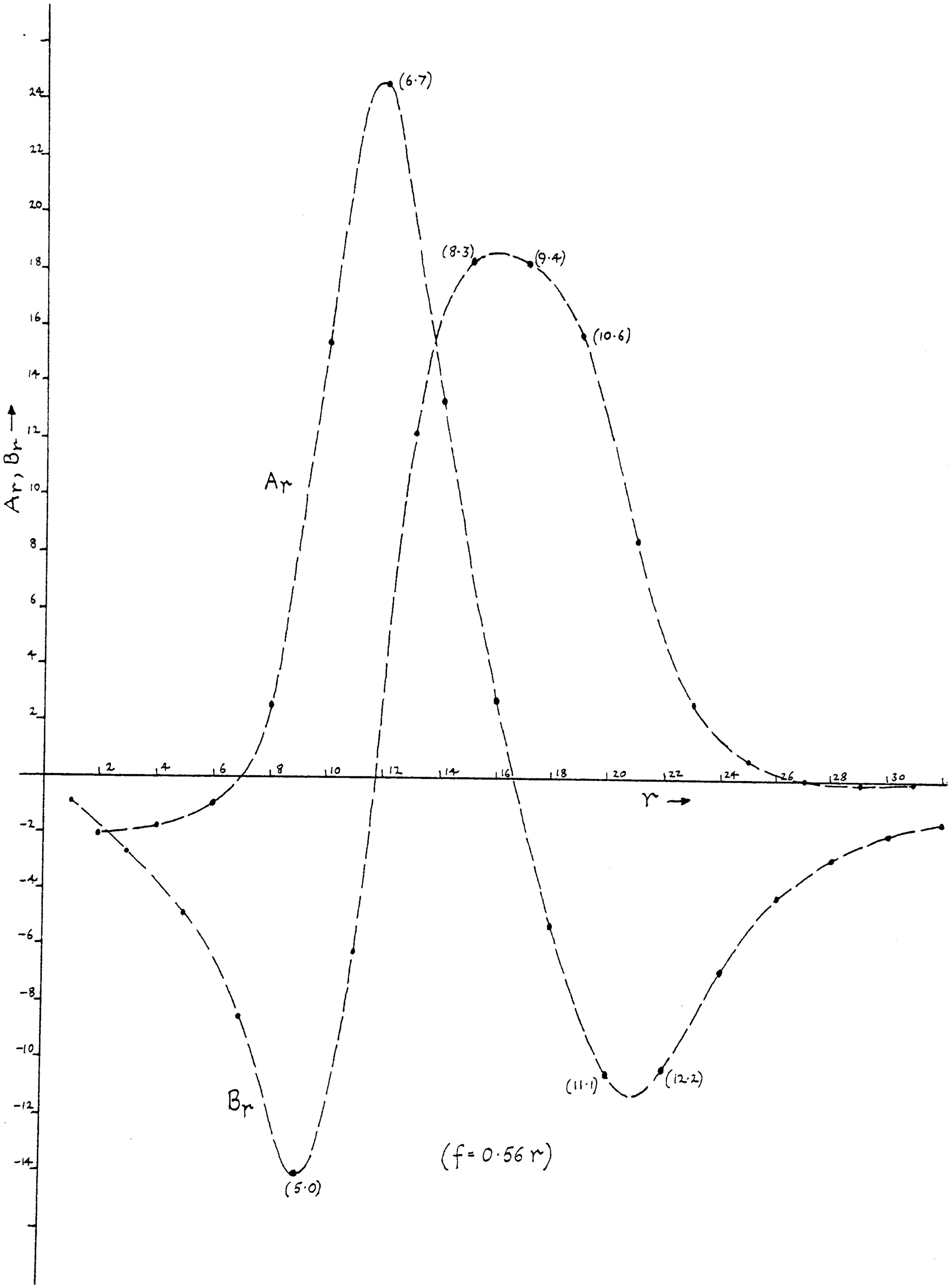


Figure 6

fourier analysis is shown in figure 6. The predicted frequencies lie in the range 5.0→12.2 Hz, corresponding reasonably with the theoretical range of 5.2→12.6 Hz.

CABLE EDGED SPATIAL NETWORK

A model network with the same overall dimensions as the structure in the main text, but with a reduced number of surface cables, was tested for dominant natural frequencies by means of a vibrator placed at each of the loaded nodes 1→6 in turn and at the centre of each edge cable. A plan of the network indicating the applied load points and the tensions in each cable is shown in figure 7. The masses of the loaded, unloaded, and edge nodes were respectively 1.33 kg, 0.05 kg and 0.3 kg, and the EA values of the cables were as given in the text.

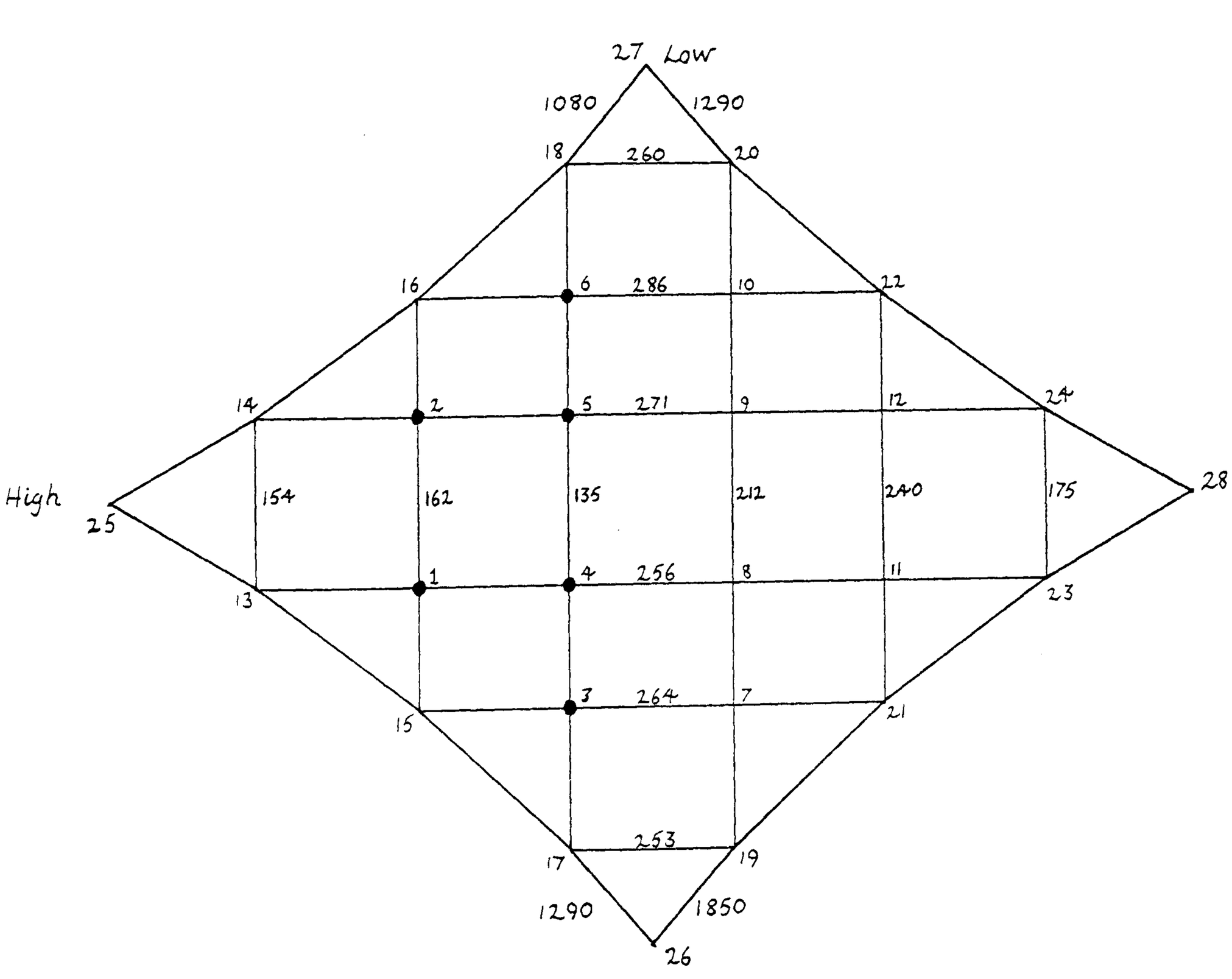


Figure 7 *Tension indicated* 253 N.

Table 1 shows the frequencies recorded in the test compared with the first ten natural frequencies obtained from a linearized eigenvalue analysis (see first term eq.2, Appendix 2.3). The full set of 72 eigenvalues so determined ranged from 6.4 Hz→1271 Hz, but the first ten, given in table 1, correspond to the six dominant surface modes involving vibration of the loaded nodes normal to the surface together with the four fundamental modes of the edge cables. The highest eigenvalues correspond to modes involving vibration of the unloaded nodes tangential to the surface or along edge cables.

Experimental	6.2	6.7	6.9	7.7	8.2	11.7	15.0	17.3	17.4	18.5
Eigenvalue analysis	6.4	7.3	7.4	7.5	8.3	11.3	15.4	16.2	16.5	17.4

Table 1: Dominant Frequencies

Coefficient r	3	4	5	6	9
Amplitude Ar,Br	0.160	-0.291	-0.239	0.070	-0.032
Frequency = 2.15r	6.4	8.6	10.7	12.9	19.3

Table 2: Fourier De-composition - dominant frequency components

An undamped central difference analysis was carried out using a time interval of 95% of the critical value. Node 4 was displaced 10mm in the z direction (approximately normal to the network surface) and suddenly released. The z displacement of node 1 was then recorded at each time interval for a total time, between initial and final minima, equal to 1.5 times the lowest period of vibration. A fourier

de-composition of this record yielded frequencies ranging from 6.4Hz to 215 Hz, with dominant components up to 19.3 Hz as shown in table 2. The amplitudes of the remaining frequency components were as follows:

Frequencies between	19.3→47.2 Hz:	Ar, Br < ±0.008
	47.3→70.78Hz:	Ar, Br < ±0.003
	70.9→215 Hz:	Ar, Br < ±0.001

A short undamped analysis using 60% of the critical time interval with the unloaded node 8 initially displaced 10mm in the x direction, and the recorded y deflection of node 11 de-composed by fourier analysis, yielded frequencies up to a maximum of 1140 Hz. In practice, however, it would be unnecessary to use a fourier analysis to estimate an upper bound to the range of natural frequencies since this can be obtained directly from the critical time interval ($f_{max} \rightarrow 1/(\pi \Delta t_{crit})$).

Comments on Results

For the plane net, natural frequencies were closely grouped because tensions were held constant in the analysis and thus all modes were dominant and involved only motions normal to the surface. For this reason it proved necessary to use a time interval less than 50% of the critical value in order to obtain reasonable results. For the spatial net, however, in which cable intersections were treated as jointed and thus tensions varied with deformation, the critical time interval was limited by motion tangential to the surface. Since the stiffness normal to the surface, which governs the dominant frequencies, was very much less than the tangential stiffness, a short trial run using a time interval almost equal to the critical value yielded a reasonable design estimate of the range of dominant frequencies.

REFERENCES

(5) Crandall, S.H., 'Random Vibration', J. Wiley, 1958.

(6) Grigorian, M., 'Free Vibrations of supported cable nets' Synopsis 7257, Proc. I.C.E., Feb. 1970.

APPENDIX 2.2

LINK EXTENSIONS

The extensions of links may be calculated either by means of square root operations at each stage or by making use of previously calculated extensions:

let L = Initial length, and e = current extension of a link

D_x = X(2)-X(1) = difference in the initial X co-ordinates of the two ends of the link

$D\delta_x = \delta_x(2) - \delta_x(1)$ = difference in current X displacements

similarly for D_y, D_z and $D\delta_y$, $D\delta_z$

$$\text{then } (L+e)^2 = \sum_{x,y,z}(D_x + D\delta_x)^2 = L^2 + \sum(2D_x.D\delta_x + D\delta_x^2)$$

$$\therefore \quad e = \sum \frac{D\delta_x(2D_x + D\delta_x)}{(2L + e)} \qquad (1)$$

When iterative analysis such as dynamic relaxation is used equation (1) may be applied in a modified form:

$$e_c \doteq \sum \frac{D\delta_x(2D_x + D\delta_x)}{(2L + e_p)} = \frac{Q}{(2L+e_p)} \qquad (2)$$

where e_c = current extension; e_p = previously calculated extension

Provided oscillations damp to a steady equilibrium state equation (2) precludes the possibility of accumulated errors since at each stage the total extension is calculated. When the time interval approaches the critical value, however, a form of instability can develop which is due to the fact that $|e_c|$ as calculated from (2) may be larger than the true value. This can be overcome by taking two "terms" in the expression for e_c, thus:

$$e_c \rightarrow \frac{Q}{(2L+\frac{Q}{2L+e_p})} \qquad (3)$$

APPENDIX 2.3

COMPARISON OF D.R. AND MATRIX ITERATION SCHEME

COMPUTER STORAGE AND OPERATION REQUIREMENTS FOR DYNAMIC RELAXATION

The total storage required and the number of numerical operations per iteration of the DR process may be assessed as follows for a structure employing only cable or bar-elements.

The recurrence equations for the iteration scheme (given in the text and appendix 2.2) are:

For each node (in direction x and similarly for y and z):

$$V_x^{t+\Delta t/2} = \dot{B}.V_x^{t-\Delta t/2} + \dot{A}.R_x^t \quad ; \quad \delta_x^{t+\Delta t} = \delta_x^t + \Delta t.V_x^{t+\Delta t/2}$$

$$(\text{Set} \quad R_x^{t+\Delta t} = P_x^{t+\Delta t})$$

For each member (joining nodes i and k):

$$e^{t+\Delta t} = \frac{Q}{(2L + Q/(2L+e^t))} \quad ; \quad \Delta R_x^{t+\Delta t} = \frac{(D_x+D\delta_x)}{(L+e^{t+\Delta t})}\left[T^\circ + \frac{(EA+T^\circ)}{L} e^{t+\Delta t}\right]$$

$$\text{where } Q = \sum_{x,y,z} D\delta_x(2D_x + D\delta_x) \quad \text{and } D\delta_x = \delta x_k^{t+\Delta t} - \delta x_i^{t+\Delta t}$$

$$(\text{Set } R_{xi}^{t+\Delta t} = R_{xi}^{t+\Delta t} + \Delta R_x^{t+\Delta t} \quad ; \quad R_{xk}^{t+\Delta t} = R_{xk}^{t+\Delta t} - \Delta R_x^{t+\Delta t})$$

Core Store:

For each member storage is required (or convenient) for e, L, T°, EA, $\dot{T}$, $(\dot{EA}/L)$, D_c (c=x,y,z), and N(1), N(2), where N are the node numbers at ends 1 and 2. For each node storage is

required for co-ordinates, velocities, deflections, applied loads, residual forces and A^{1}; in each case the number of components being equal to the number of degrees of freedom. Thus for a system with n nodes, m members, and DF degrees of freedom the total storage requirement, excluding the program and control parameters, is approximately:

$$m(8 + DF) + 6n.DF$$

Operations:

The number of sum ($\pm$) and product ($\times \div$) operations required per iteration is as follows:

For each node: 2 DF sums; 3DF products

For each member: (4+6DF) sums; (5+3DF) products.

STORAGE AND OPERATION REQUIREMENTS FOR MATRIX ITERATION

A Modified Newton Raphson iteration scheme equivalent to those given by Mollmann [7], Siev [8] and Eras and Else [9] is a widely used procedure which provides a suitable basis for comparison with dynamic relaxation. The procedure summarised below is set out fully in ref. [10] in a form which caters for slackening of cables by the use of "equivalent" sectional stiffnesses (EA') which ensure equilibrium of forces and compatibility of strains and deformations throughout the analysis.

(See Appendix A, page 298).

Procedure

The changed geometry of the deformed structure is taken into account by means of a non-linear load/displacement relationship of the form:

$$[K]\{\delta\} + \{W\} + \{CL\} = 0 \qquad (1)$$

where: $\{W\}$ is the vector of applied nodal loads

$\{CL\}$ is a correction vector, the elements of which are non-linear in displacements

$[K]$ is the stiffness matrix

$\{\delta\}$ is the vector of nodal displacements

The cycle of computations is as shown in figure 1.

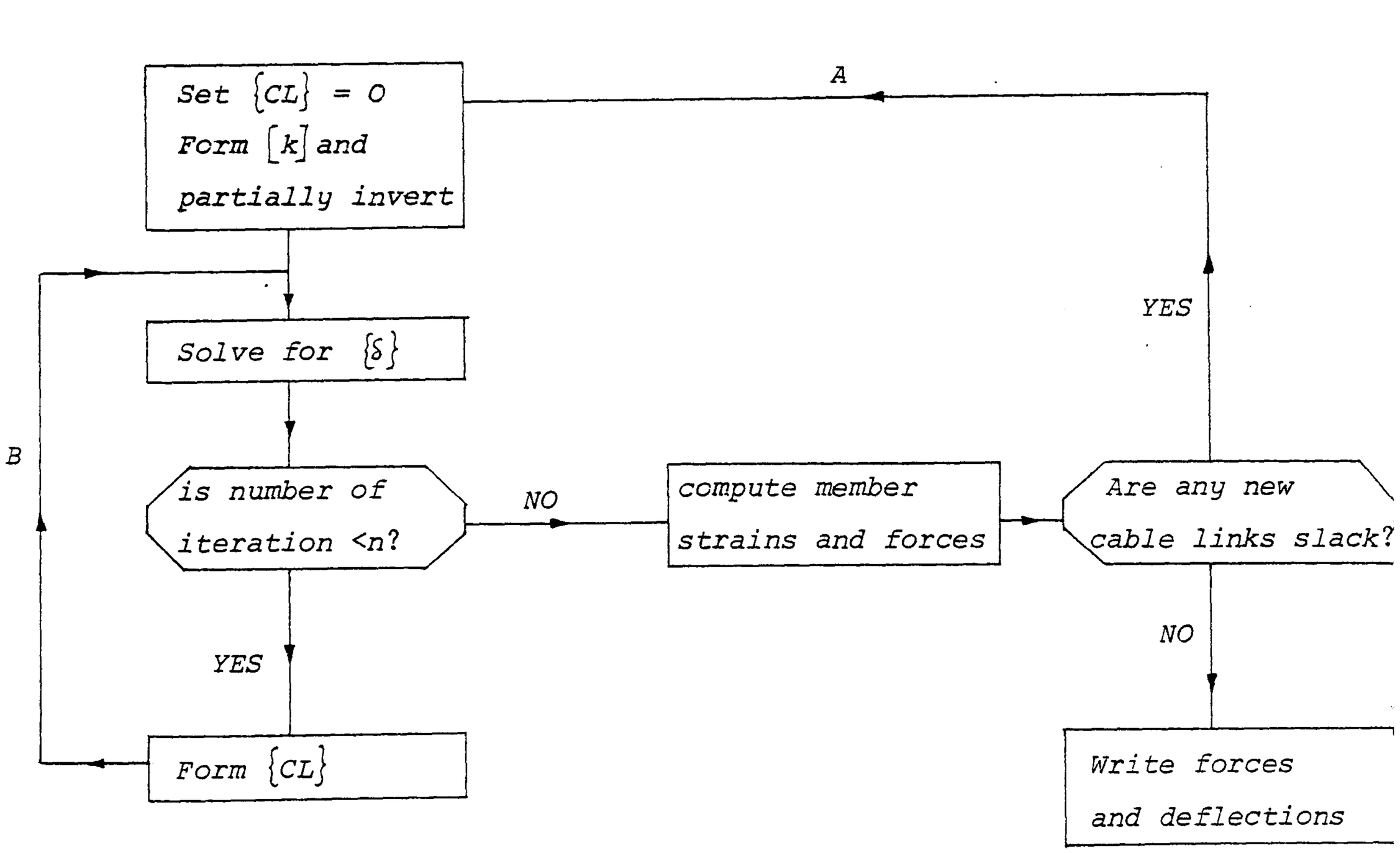


Figure 1

In explicit terms, assuming three degrees of freedom per node, a typical equation in the matrix set (1) expressing equilibrium in the x direction at a node i, with member connections to adjacent nodes k, is given by:

$$\sum_{ik} \left\{ (T+\Delta T_o)\ \frac{U}{L} + (\frac{P}{L}).\frac{EA}{L}.(pU + q\ V + rW) \right\} + W_{xi}$$

$$+ \sum_{ik} \left\{ (\frac{P}{L}).\left[EA.C\right]^{*} + \frac{U'}{L}\left[EA(B+C') - \Delta T_o\right]^{**} \right\} = 0 \qquad (2)$$

The notation is as follows:

T, ΔT_o - Initial tension and estimated tension change in link ik

L, EA - Length and sectional stiffness of link ik

P,q,r - Projections of initial length of ik on x,y,z axes

U,V,W - Projections of extension of ik on x,y,z axes

U',V',W' - Values of U,V,W determined in preceding iteration

The correction factors, based on previously calculated displacements are given by:

$$B = \frac{pU' + qV' + rW'}{L}; \qquad C = \frac{U' + V' + W'}{2L}$$

and C' is the previous value of C

Similar equations may be written for equilibrium in the y and z directions.

Core Store

The storage vectors required (or computationally convenient) for each member are: T, ΔT_o, L, C, D, E, S where D and E are working stores for * and **, and S is the 'strain' based on nodal displacements (required to be stored in connection with the checking and re-setting of EA values for slack cables [10]. Additionally, arrays will be required

for EA and EA', node numbers at ends 1 and 2 of each member, and preferably for p, q, (& r). The member storage requirements are thus m(11+DF) array elements, where m is the number of members and DF the number of degrees of freedom per node.

For each node, co-ordinates, displacements, applied loads and correcting loads must be stored and updated, requiring a total of 4.n.DF array locations, where n is the number of nodes.

In solving the set of simultaneous equations, if slack cables are allowed for and encountered, Gaussian reduction and elimination, in a form suitable for dealing with subsequently changed loading vectors, may be more efficient than matrix inversion (furthermore, for large structures Gaussian reduction entails considerably less storage). For such a solution process, unless backing store is utilized, the matrix storage required will be approximately $n.DF^2.(B+1)$, where B is the maximum difference in the node numbers of any member. With disc or tape backing storage and the use of a frontal solution technique, the minimum core store required would be $DF^2.(B+1)^2$. The use of backing store may be essential for large structures, but should preferably be avoided in iterative analysis of non-linear systems.

Summarising, the total convenient storage requirements (excluding the program) are:

$$m(11+DF) + 4\ n.DF + n.DF\ (B+1)$$

Operations

The number of operations (sums and products) required for each iteration is approximately as follows:

Correction term (line 2 of equation (2)) for each member:

(2+6DF) Sums; (9+6DF) products

Strains, forces and resetting EA for each member:

2 sums; 2 products

Setting the stiffness matrix, above the leading diagonal, by summation for each member:

$(1+2DF+2DF^2)$ sums; $(4+DF+DF^2)$ products

Gaussian reduction of stiffness matrix (outer loop A in figure 1) - approximate number of operations per node:

$DF^3.(B+1)^2/2$ sums; $DF^3.(B+1)^2/2$ products

Reduction of new force vector (inner loop B in figure 1):

$DF^2.(B+1)$ sums; $2DF^2.(B+1)$ products - per node

Back-substitution (or elimination) of a reduced stiffness matrix and force vector (inner loop B):

$DF^2.(B+1)$ sums; $DF^2.(B+1)$ products-per node

The maximum and minimum bounds to the total number of operations required per iteration are thus :

$$m.M + 5N < \text{Sums} + \text{Products} < m.M + N(5+DF(B+1))$$

where $M = (20 + 15DF + 3DF)$; $N = n.DF\,(B+1)$

The lower bound will give the closest estimate for systems in which slack cables do not occur (with the stiffness matrix reduced once only).

COMPARISON OF D.R. AND NEWTON RAPHSON ITERATION SCHEMES

When using time sharing facilities the operational cost of a program might be taken as approximately proportional to the product of core store and the number of operations. On this basis the relative costs per iteration of DR and Newton Raphson schemes are summarised in table 1 for systems with 2 and 3 degrees of freedom per node. For the Newton Raphson matrix analysis it is assumed that the number of iterations of loop B to the number of loops A is in the ratio 8:3.

	Dynamic Relaxation	Newton Raphson
$2^{o}F$	(27m + 10n) x (10m + 12n)	(62m + n ($3B^2$ + 26B + 23)) x (13m + n(4B + 12))
$3^{o}F$	(36m + 15n) x (11m + 18n)	(92m + n ($10B^2$ + 65B + 55)) x (14m + n(9B + 21))

Table 1

Examples:

(1) Plane Cable Truss

For the truss system shown in figure 2, B = 2 and m = (2n+3), where n = number of active nodes. The approximate cost ratios of Newton Raphson: DR per iteration are:

for n = 10: C_r = 4.54

for n = 20: C_r = 4.63

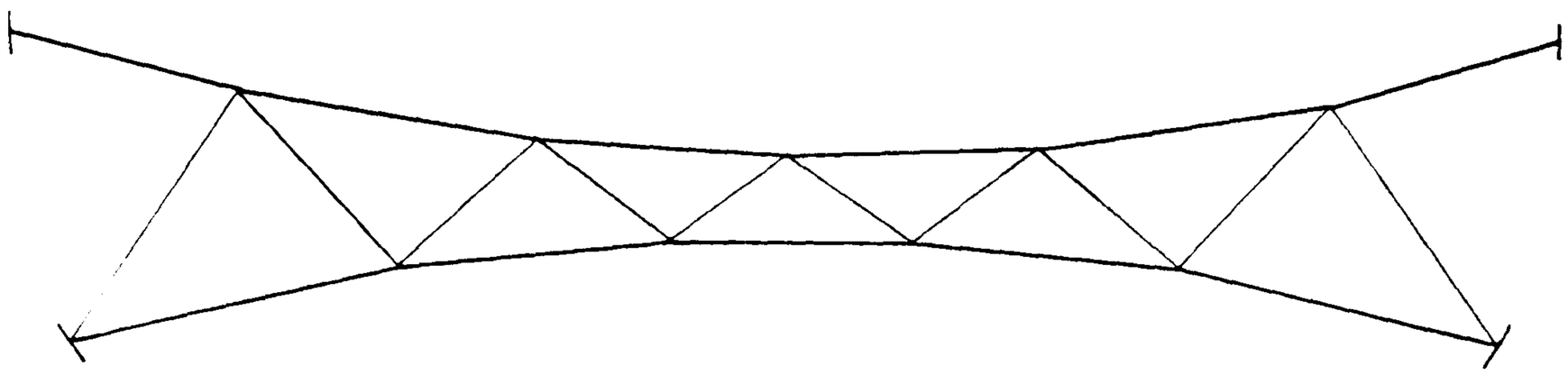


Figure 2

(2) Cable Network

For a single layer spatial network, square in plan, of the type shown in figure 3, $B = \sqrt{n}$ and $m = 2(n + B)$. Approximate cost ratios of NR : DR per iteration are:

for B = 10: $C_r = 68$

for B = 20: $C_r = 343$

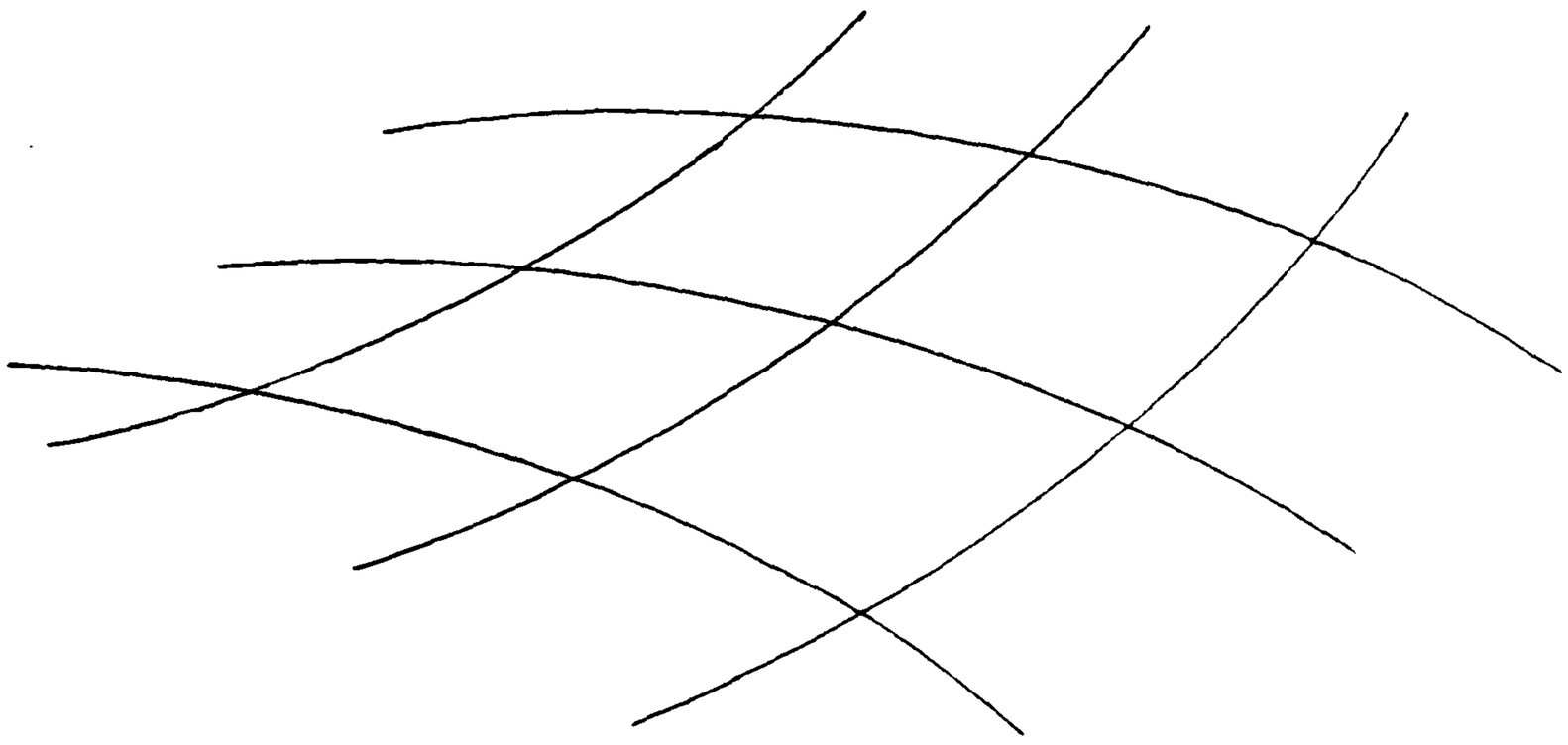


Figure 3

In general, to achieve sufficient accuracy, Newton Raphson analyses of cable systems have been reported to require from 3 to 17 iterations depending on the degree of non-linearity [7,10,11,12]. For plane systems involving no slackening of cables the lower figure is more

realistic, whilst the upper figure is more appropriate for form-finding of networks or the analysis of systems involving slack cables or other combined geometric and material non-linearities. The network system considered in the text of Chapter 2 required 300 iterations by dynamic relaxation for convergence of the form-finding, and a similar figure would be appropriate for a purely static analysis using fictitious mass components. For a similar efficiency a Newton Raphson analysis would need to converge at the second iteration. Dynamic relaxation thus shows to good advantage for the analysis of such a structure. For plane cable systems, however, Newton Raphson analysis has proved generally more efficient.

The crude comparison given above has assumed a Modified Newton-Raphson iteration with infrequent resetting of the stiffness matrix. For highly non-linear problems, however, a full Newton-Raphson procedure, or alternatively an incremental method with equilibrium iterations or load extrapolation (Appendix A, p.307), may be necessary; both cases requiring the stiffness to be reset at every stage. In such cases the dynamic relaxation process (assessed above on the basis of a test case with gross deformation) would show to even greater advantage. Haug (13), for example, quotes between 15 and 33 cycles of Newton-Raphson iteration for the form-finding of networks with inaccurate specifications of geometry at the start of the process. And for the cases quoted, to avoid singularity of the overall system equations, the use of conditional deflection controls or gradually relaxed fictitious stiffnesses were necessary (see also Appendix B, p.334).

REFERENCES

(7) Mollmann, H., Lundhus Mortensen, "The analysis of prestressed suspended roofs", Int. Conf. on Space Structures, Guildford 19

(8) Eras, G., Elze, H., "Sur erechnung und statisch vorteilhaften formgebung von seilnetzwerken", IASS Colloquium Hanging Roofs, Paris, 1962

(9) Siev, A., "A general analysis of prestressed nets", Publs. Int. Assoc. Bridge Struct., 1963, pp 283-292

(10) Beak, W.R.J., "Triangulated cable trusses", M.Sc. Thesis, The City University, 1972

(11) Barnes, M.R., "Prestressed cable networks", M.Sc. Thesis, University of Manchester, 1966

(12) Saafan, A.S., "Theoretical analysis of suspension roofs", J.Struct. Div., ASCE, V.96, n.ST2, Feb., 1970

(13) Haug, E., Powell, G.H., "Analytical shape finding of cable nets", IASS Symp. on Tension Structures and Space Frames, Tokyo and Kyoto, 1971

CHAPTER 3

APPLICATIONS OF DYNAMIC RELAXATION TO THE FORM-FINDING AND ANALYSIS OF CABLE, MEMBRANE AND PNEUMATIC STRUCTURES

SUMMARY

Design applications of dynamic relaxation are considered for the determination of various pretension geometries of uniform mesh or geodesic cable networks, minimum surface stressed membranes and pneumatic structures. For cable networks with complex curvature and boundaries the determination of stress trajectories due to uniform normal pressure on a minimum surface membrane can facilitate the choice of efficient cable trajectories. The pretension analyses can incorporate the derivation of tension cable boundaries or momentless compression contours.

The analysis of tension structures under static loading, and techniques to improve efficiency are considered. The method is shown to be useful when dealing with slackening of cables and buckling of membrane cladding.

The chapter is based on a paper given at the 2nd. Int. Conference on Space Structures (Guildford, Sept. 1975). The text has, however, been edited for continuity with chapter 2 and an error concerning buckling analysis, which occurred in the original paper, has been corrected.

DYNAMIC RELAXATION

The method of Dynamic Relaxation was conceived by Day [1] and developed by Otter [2]. In his original paper Day presented the application of dynamic relaxation (DR) to solutions based on both stiffness matrix and finite difference procedures. The majority of subsequent papers [2 - 9] have applied or examined the method in the latter form. For the case of linear finite difference problems it has been shown that the convergence rate of successive over-relaxation may be about twice that of DR [8,9], though this should be considered relative to the simplicity of DR, particularly when dealing with complex problems or boundary conditions. For problems involving geometrical and material non-linearity theoretical comparisons have not been made, though Brew and Brotton [10] suggest that compared with over-relaxation methods DR gives greater control over the path to solution and hence on stability of the iteration. It is this advantage which makes the method particularly appropriate for both the design and analysis of tension structures [11 - 13]. The procedure also has a rapid initial convergence rate which can be of special value in form-finding applications.

The main advantages of DR stem from the fact that equilibrium and compatibility conditions can be separated. Thus in differential form one high order equation is replaced by two lower-order equations. And in finite element form only the 'natural' stiffnesses of elements are required (chapter 2), as opposed to transformed stiffnesses assembled into an overall matrix. This results in a saving in storage and, for non-linear

tension network and membrane problems, a probable reduction in computing compared with procedures based on iterative solution of an overall, yet changing, stiffness matrix. Also, because of the degrees of mechanical freedom which may occur in tension structures, it is possible that iterative displacement solutions whether based on an overall stiffness matrix or nodal relaxation may become singular or unstable. Whilst this situation will not occur provided the tension or geometric stiffness is accounted for (in addition to the elastic stiffness) and the surface structure remains in tension, it may do so if buckling of membrane cladding or slackening of cables is allowed for and occurs. Alternatively, to avoid this situation, conditional controls may have to be incorporated in the analysis. In contrast, because of the separation of equilibrium and compatibility, DR copes naturally with zero stiffness situations.

The dynamic relaxation procedure based on a finite element structural idealization was set out in chapter 2 in a form most suitable for the form-finding and subsequent gross deformation analysis of cable structures. A summary of the recurrence equations is given below for completeness of the present account which is concerned with more varied applications.

The velocity of any node, i, at the mid-point of a time step ($t \rightarrow t + \Delta t$) is given by:

$$V_{xi}^{t+\Delta t/2} = V_{xi}^{t-\Delta t/2} \left[\frac{1 - K.\Delta t/2}{1 + K.\Delta t/2}\right] + R_{xi}^{t}.\frac{\Delta t}{M_i}\left[\frac{1}{1 + K.\Delta t/2}\right] \qquad (1)$$

where R_{xi} , V_{xi} are respectively the residual force and velocity at node i in the x direction

K is the viscous damping per unit mass (a constant for the complete structure)

M_i is the concentrated mass at node i (in form-finding or static load applications this may be replaced by a fictitious mass component M_{xi}, different from the y and z components, to speed convergence).

The x co-ordinate of node i at the end of the time interval is:

$$x_i^{t+\Delta t} = x_i^t + \Delta t . V_{xi}^{t+\Delta t/2} \qquad (2)$$

Similarly the new y and z co-ordinates may be determined.

These calculations are carried out (simultaneously) for each node of the structure to give the complete displaced form at time $t + \Delta t$, and hence also the extension $e^{t+\Delta t}$, from the initial state and the force, $T^{t+\Delta t}$, in each of the structural links (cable segments and/or sides of membrane elements.)

The current force in any cable is:

$$T^{t+\Delta t} = T^o + \left(\frac{EA}{L_o}\right) . e^{t+\Delta t} \qquad (3a)$$

And the side forces in a triangular membrane element are:

$$\begin{Bmatrix} T_1 \\ T_2 \\ T_3 \end{Bmatrix}^{t+\Delta t} = \begin{Bmatrix} T_1 \\ T_2 \\ T_3 \end{Bmatrix}^{o} + \begin{bmatrix} \quad k^e \quad \end{bmatrix} \begin{Bmatrix} e_1 \\ e_2 \\ e_3 \end{Bmatrix}^{t+\Delta t} \qquad (3b)$$

where link forces T^o are due to prestress and $[K^e]$ is the 3x3 natural stiffness matrix relating side tensions to side extensions.

Since an overall stiffness matrix is not formed it is unnecessary to transform relations 3a and 3b to a common global co-ordinate system. The use of natural stiffnesses for both cable and membrane elements, in addition to reducing core storage, eliminates more simply the possibility of accumulated errors due to gross changes in position.

Having obtained the current link tensions, and overall geometry, the residual nodal forces can be set:

$$R_{xi}^{t+\Delta t} = P_{xi} + \sum \left[\frac{(x_k - x_i)}{L_m} T_m \right]^{t+\Delta t} \qquad (4)$$

where P_{xi} is the applied load in direction x at node i, and the summation is taken for all links m connecting i to adjacent nodes k; all terms in the square brackets being current values at time $t+\Delta t$. Residual forces in the y and z directions are similarly derived. Whence the cycle of computations is repeated.

FACTORS AFFECTING THE RATE OF CONVERGENCE

Damping

For static load analyses, to obtain bounds to the true equilibrium state a slightly sub-critical damping factor is desirable. If the lowest frequency f of the structure has been approximately determined from a short undamped trial run, the critical damping factor per unit mass is given by:

$$K \triangleq 4\Pi.f$$

Rushton [5] determines the critical damping automatically by following the curve of total kinetic energy for the initally undamped system to its first true maximum (1/4 fundamental period). For properly triangulated or plate structures with distributed loading the technique has proved useful, but for cable networks, with many degrees of mechanical freedom, subject to non-uniform or concentrated loading it has been found difficult to locate this maximum.

Time Interval

When the time interval exceeds a certain critical value, instability of the calculations will occur. It may be shown [13 or chapter 2] that bounds to the critical time interval can be derived by considering only the node(s) of the structure at which the direct stiffness/mass ratio is highest. The limits are given by:

$$\sqrt{\frac{2M}{S}} < \Delta t_{crit} < \sqrt{\frac{4M}{S}}$$

where S is the greatest direct stiffness of the node relative to adjacent nodes (considered fixed).

This simple expression eliminates the need for trial runs or the determination of eigen-values and has been found to be equally valid for situations, such as the determination of geodesic or minimum surface geometry, where the elastic stiffness is zero, and S depends solely on the specified constant pre-tension or stress and relative node positions.

Fictitious Masses

Computing time can usually be considerably reduced by the use of fictitious masses [6,7,10] to ensure that the stiffness/mass ratios, and thus the critical time intervals, are in the same range for all nodes in each co-ordinate direction. This is particularly appropriate for cable networks and membranes in which the stiffness in the plane of the surface is very much greater than the normal stiffness. Thus in shallow areas (approximately parallel to the global x-y plane) fictitious mass components Mx and My should be much greater than Mz. And in general, the masses may be proportioned according to the direct stiffnesses in each co-ordinate direction; though a potentially more efficient procedure for such structures is to vary the co-ordinate system so that the z axis is always normal to the surface. For other types of cable structure, such as cable girders, the use of fictitious masses may be of little value. This problem is considered in a later section.

FORM-FINDING APPLICATIONS

For simplicity in illustrating the principles involved, the network and membrane structures considered in this section are all based on the same four point support system with either tension or compression momentless boundaries. The dimensions and properties, and example calculations for time interval, fictitious masses and damping constant are given in appendix 3.1.

Geodesic Networks

The initial geometry of geodesic networks is such that each cable takes a path of minimum length over the network surface and has a uniform tension throughout its length. The geometry of a network with fixed boundary nodes can be determined from the analysis simply by holding the tension constant. Thus in equation (3) $T = T^{o}$ at all stages, with the EA values set to zero. At the start of the analysis it is necessary merely to specify correct topological connections for the links of the structure; the geometry, apart from specified support points, can be arbitrary.

For geodesic networks in which the surface cables are jointed to edge cables the geometry is determined in the same way, but for edge cables the tension in only one link of each cable is held constant, whilst the other edge links are assumed to start from a slack state for which their lengths and EA values must be specified.

Because motion of the edge nodes is elastically controlled, the critical time interval may be much smaller than for the geodesic surface nodes. In contrast to analytical applications however, both fictitious EA values and nodal masses may be chosen in order to optimise the calculations. For the example structure in figs. 2a and b in which the edge cables intersect each global co-ordinate axis at about 45°, to increase the time interval the edge masses may be increased until their period of vibration is the same as that for the surface nodes. Beyond this there is no advantage to be gained unless a variable co-ordinate system is

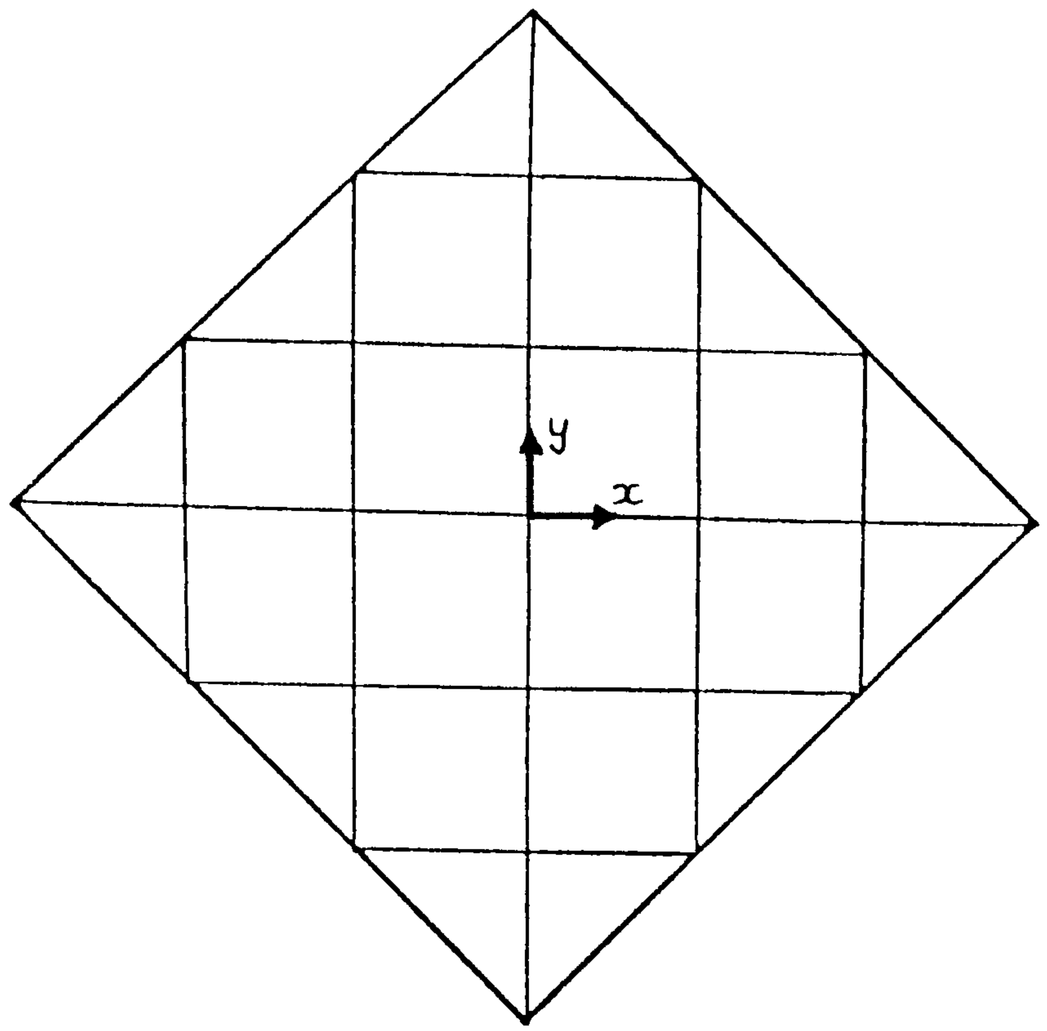
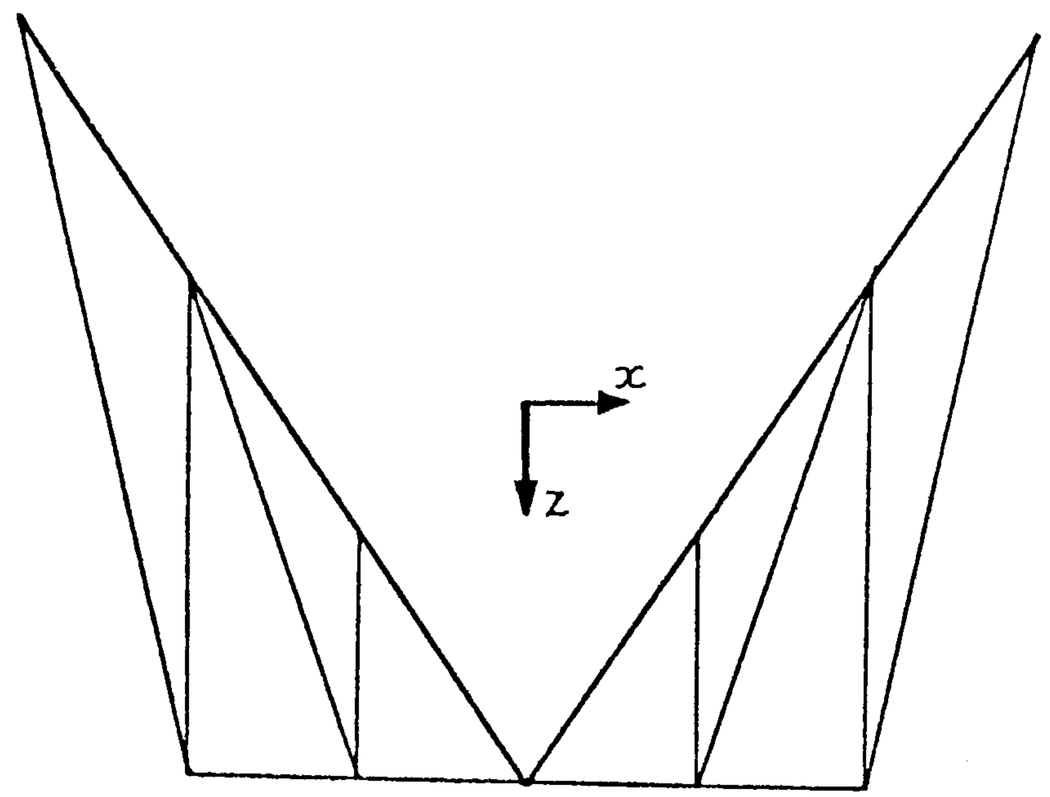


Fig. 1a



(1b)

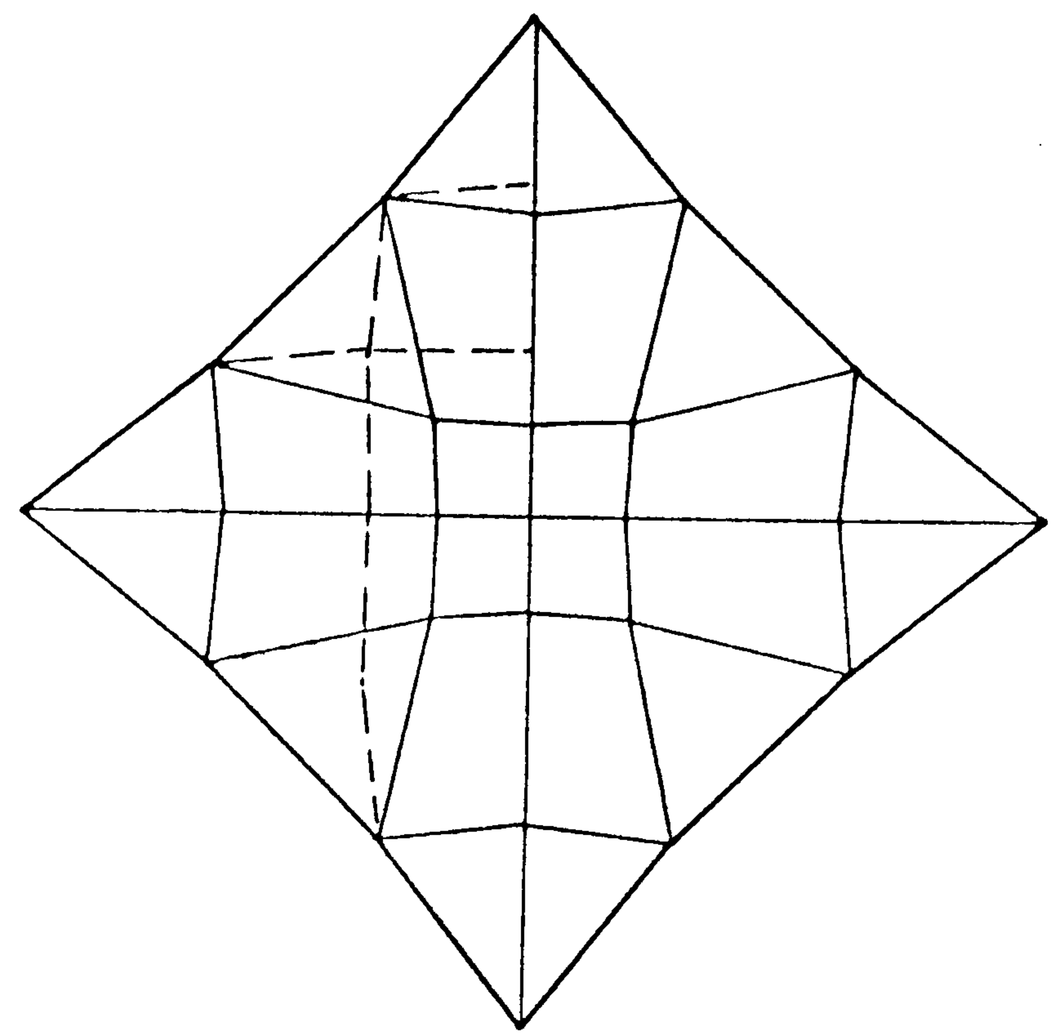
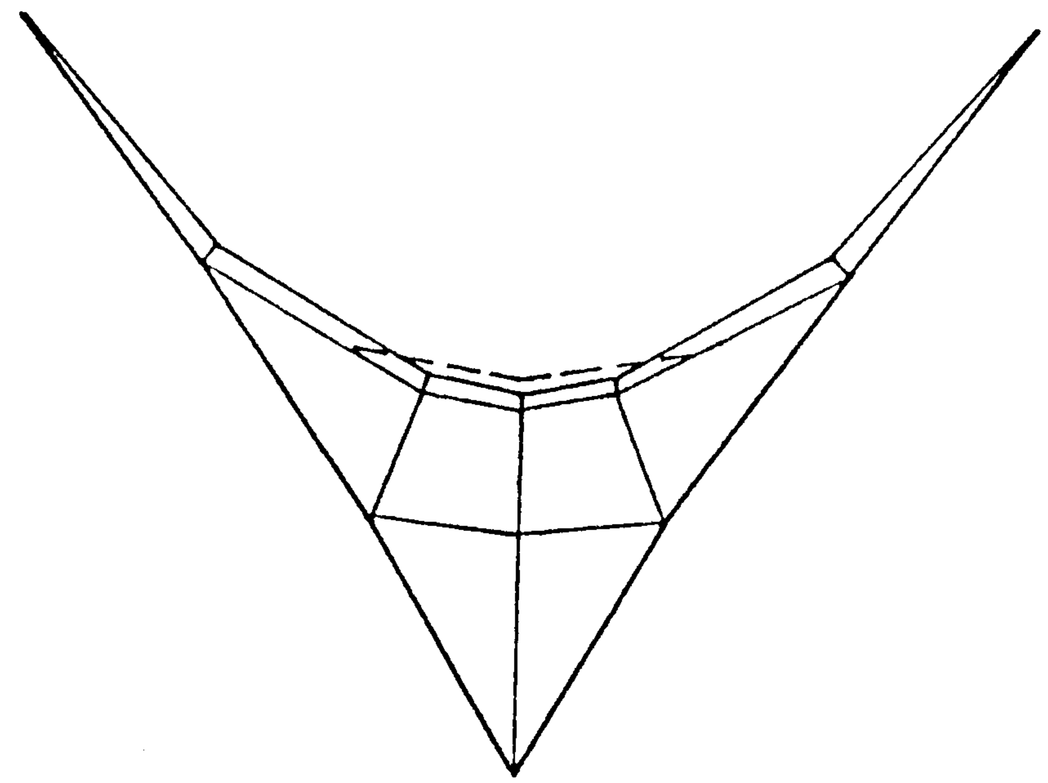


Fig. 2a



(2b)

used such that each edge cable is aligned with a co-ordinate axis. If however the EA values of the edge links are reduced, the time interval can be further increased to correspond with the critical value for surface nodes without appreciably increasing the period of vibration of edge cables; the main determinant of this being the specified tension in the control link. Starting from the very inaccurate geometry shown in figs. 1a and b, convergence to an accuracy of 0.01% of the grid spacing was obtained in less than 40 iterations. The geometry shown is for a surface to edge tension ratio of 1:20.

Uniform Mesh Networks

In contrast to geodesic networks in which cable intersections may be jointed only after pretensioning, the uniform mesh is pre-jointed so that, apart from cable segments adjacent to boundaries, the length between surface segments is constant in the slack state. For the example structure the initial tensions in such segments and two segments of each edge cable were set to zero, and deformations were controlled by specifying their EA values. For other segments the procedure was reversed; the tensions adjacent to boundaries being held constant. The resulting geometry is shown by the dashed line in figs. 2a and b.

The uniform mesh is shallower in central areas; and whereas the tensions throughout the geodesic net were held constant, resulting in approximately uniform curvatures and consequently greater stability under live loading, the ratio of max. to min. tensions in the uniform mesh was 1.43. For real structures with a much

finer mesh and complex boundaries this ratio and the non-uniformity of curvatures may be much greater, and ideally the tensions in some inner segments of the mesh should be held constant. Physically this corresponds to the use of turnbuckles in the real structure since the initial slack length of single segments cannot be adjusted with sufficient accuracy.

Momentless Compression Boundaries

Irrespective of starting geometry, if the force in edge cable segments is specified as a constant compression the system must always become unstable. Momentless contours can however be determined by the simple device of reversing all surface cable force components when applying equation (4) to the edge nodes, and calculating the edge contour as a tension boundary.

Starting from the initial geometry in figs. 1a and b, the resulting geometry for a surface to edge force ratio of -1:5 is shown in figs. 3a and b. To obtain symmetry the force in both end segments of each boundary was held constant; with only the centre segments j→m being elastically controlled. If the surface system had been entirely geodesic the structure would have become unstable. By assigning some elastic stiffnesses ($EA \gg 0$) to the surface segments a→h however, a stable system can be determined with the remaining tensions held constant. The surface is thus part geodesic and part elastically controlled.

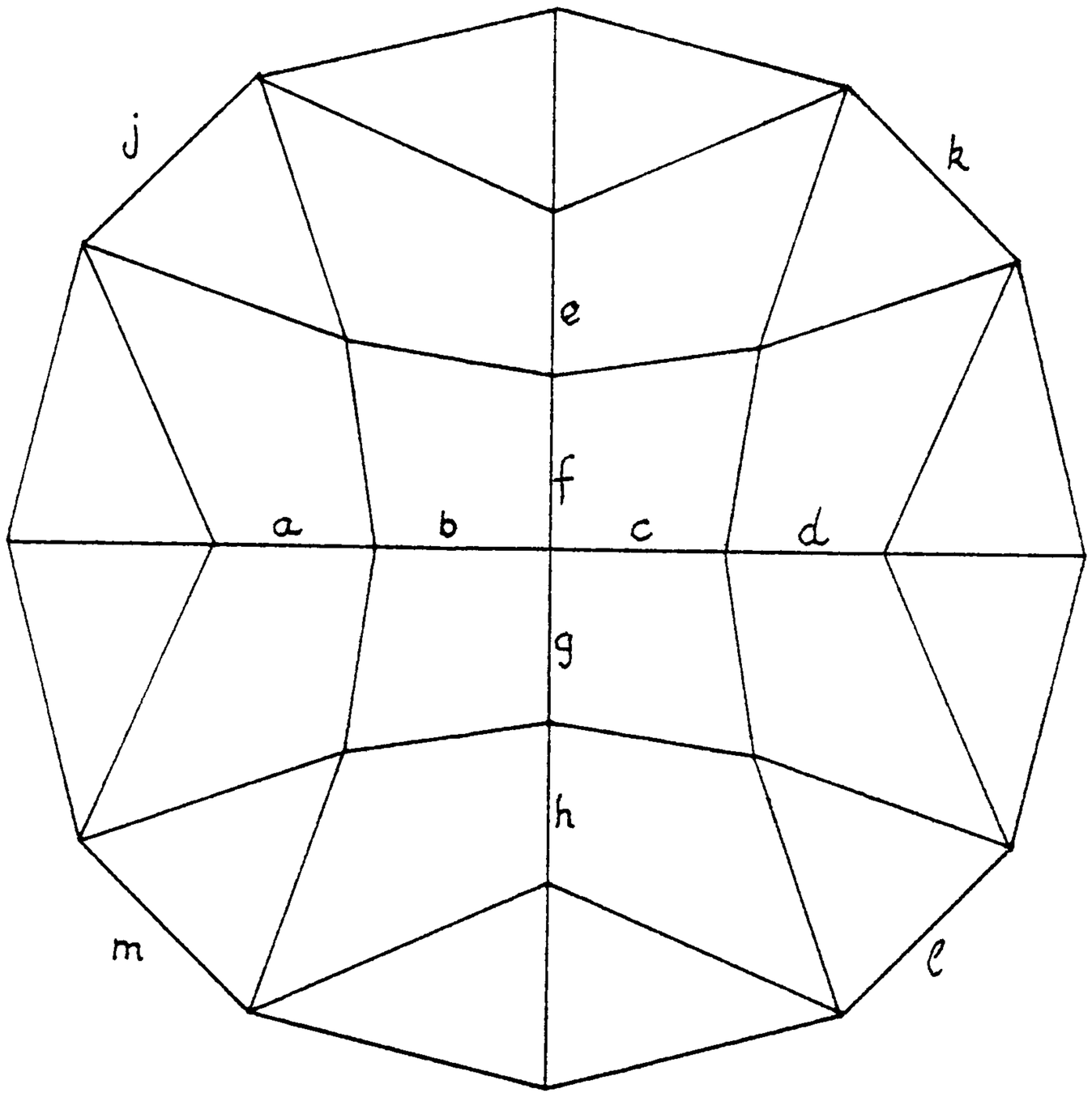
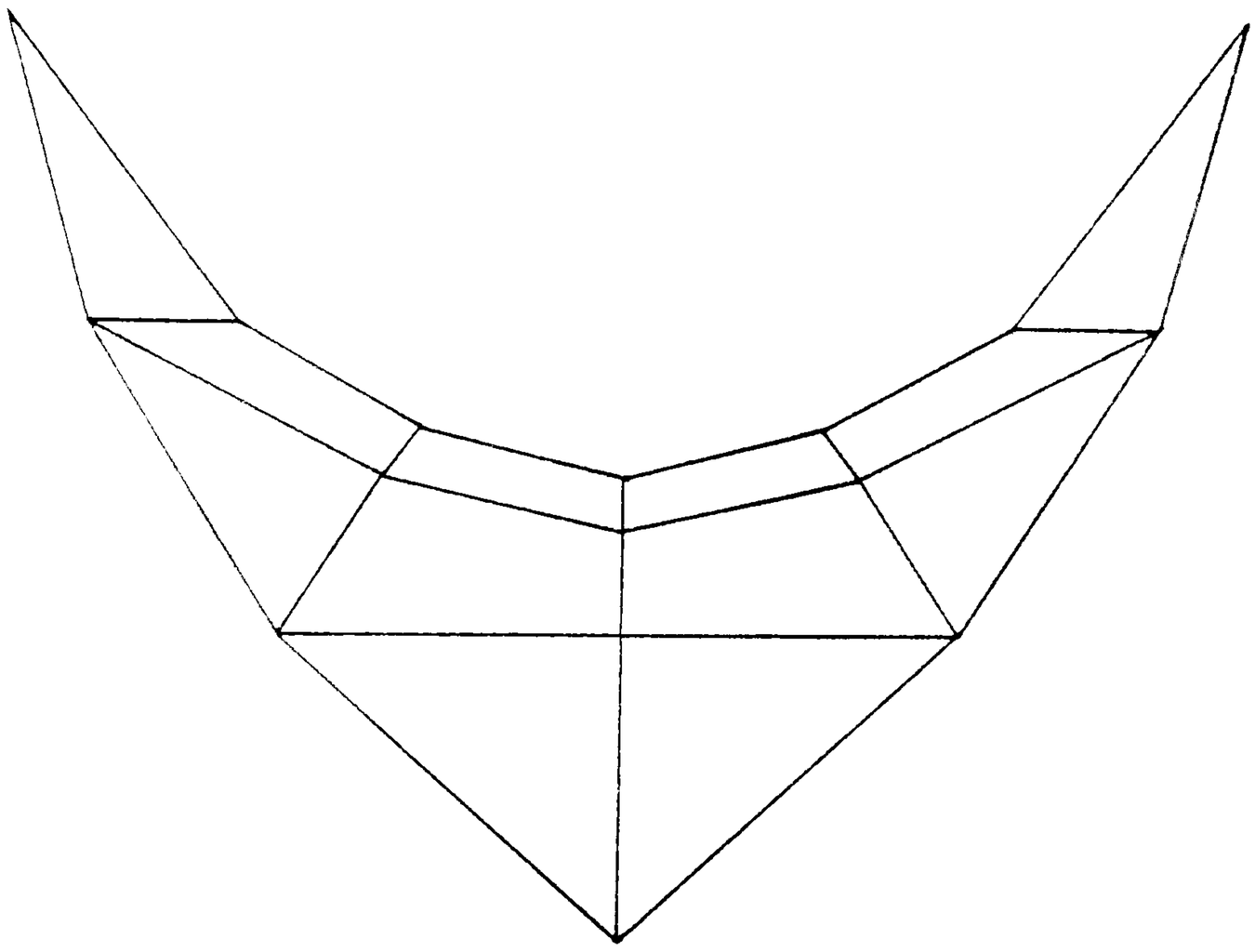


Fig. 3a



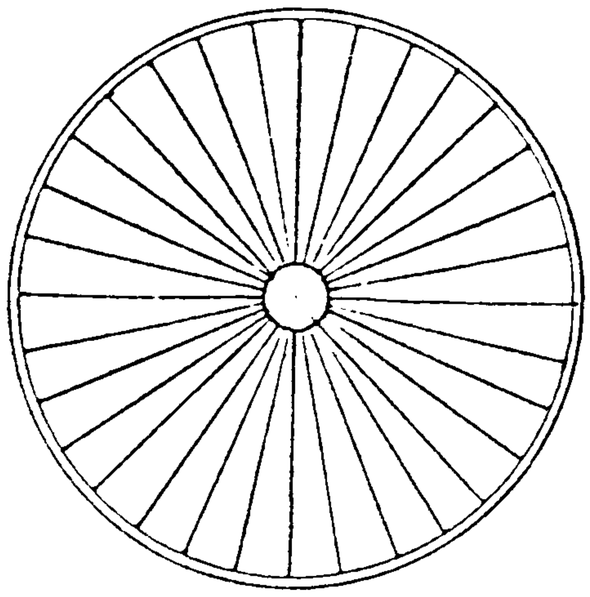
(3b)

For the same surface:edge force ratio, the geometry can be adjusted by altering the EA values of the segments a→h and j→m. For complex structures it is particularly useful to adjust the boundary values since this can enable additional control on the variation of curvatures and hence of the moments induced in the boundaries by live loading.

Similar design techniques can be used for the structure in fig. 4 which shows one unit of an articulating buoyant pipeline system [14]. The ½m dia. central pipe is given stability and resistance to bending by spiral cable bracing bearing on compression hoops connected to the pipe core by radial ties. Circular hoops (fig. 4a) would be appropriate for the conditions of neutral pipe bouyancy and live loading which may be of the same magnitude laterally and vertically. But to transmit positive buoyancy to the end chambers and provide sufficient lateral resistance, a more efficient hoop shape is shown in fig. 4b.

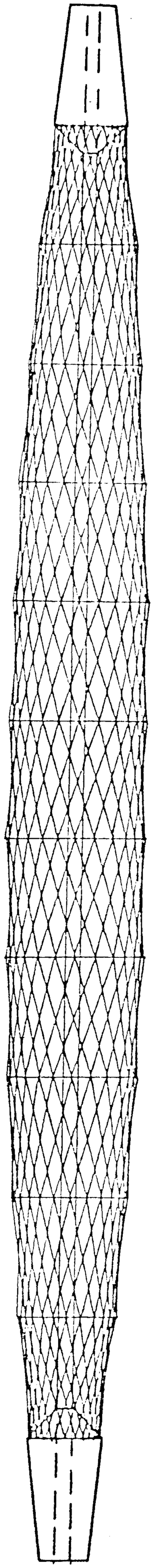
A more complex study for a bridging structure employing a spiral bracing network supported by momentless bearing contours is illustrated in fig. 5.

(4b)



(4a)

Fig. 4



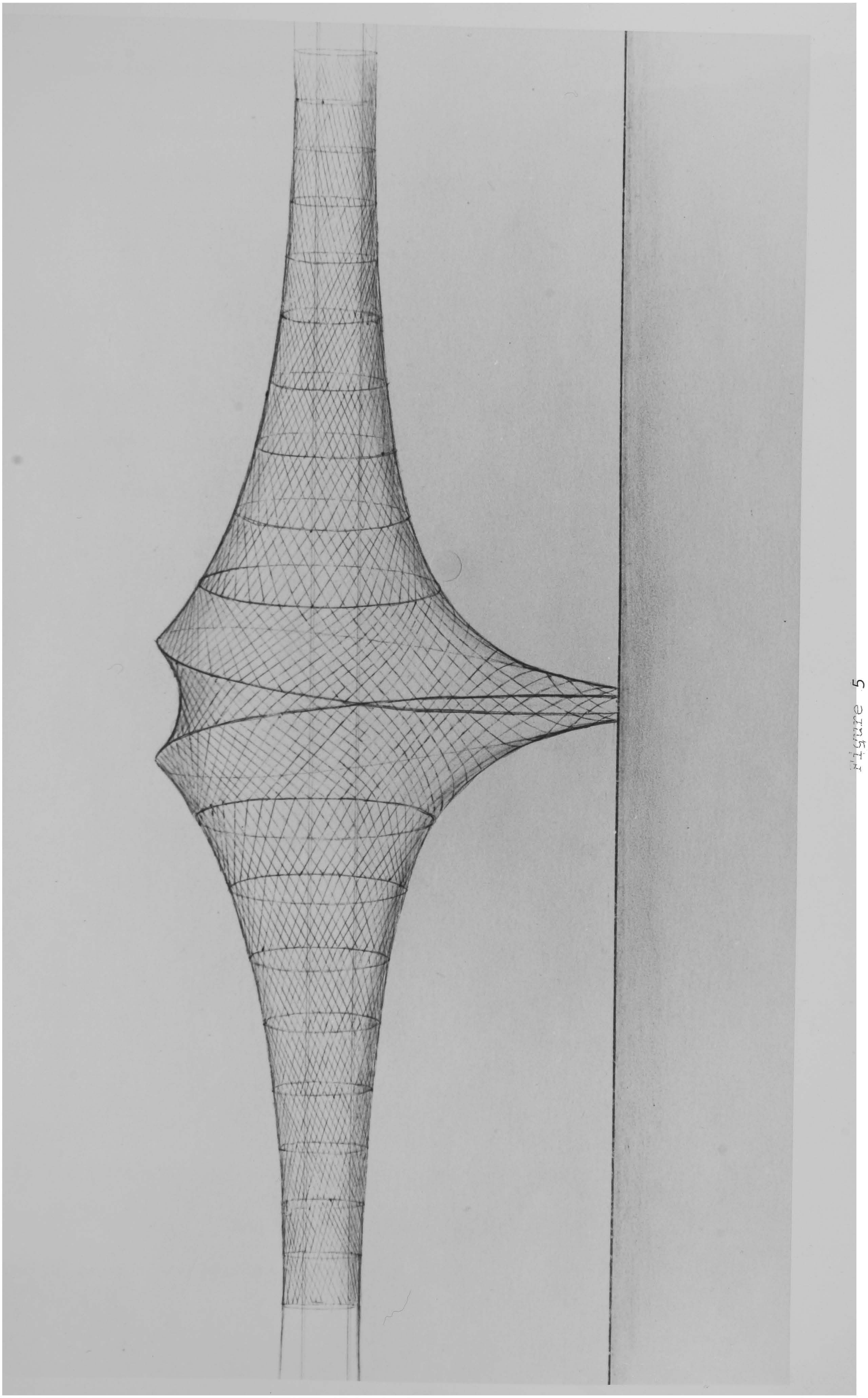


Figure 5

Minimum Surface Membranes

For a triangular element (fig. 6) subject to uniform tensile membrane stress, σ, the edge forces are given by:

$$\begin{Bmatrix} T_1 \\ T_2 \\ T_3 \end{Bmatrix}^{o} = \left[G \right] \begin{Bmatrix} \sigma \\ \sigma \\ o \end{Bmatrix} t.A$$

where t.A is the volume of the element and $\left[G \right]$ is the 3x3 matrix relating strains ε_x, ε_y, γ_{xy} to the side extensions. Substituting for $\left[G \right]$ (from equations 9a & b in chapter 2) gives:

$$T_i^{o} = \frac{\sigma.t.\ell_i}{2 \tan \alpha_i} \qquad (5)$$

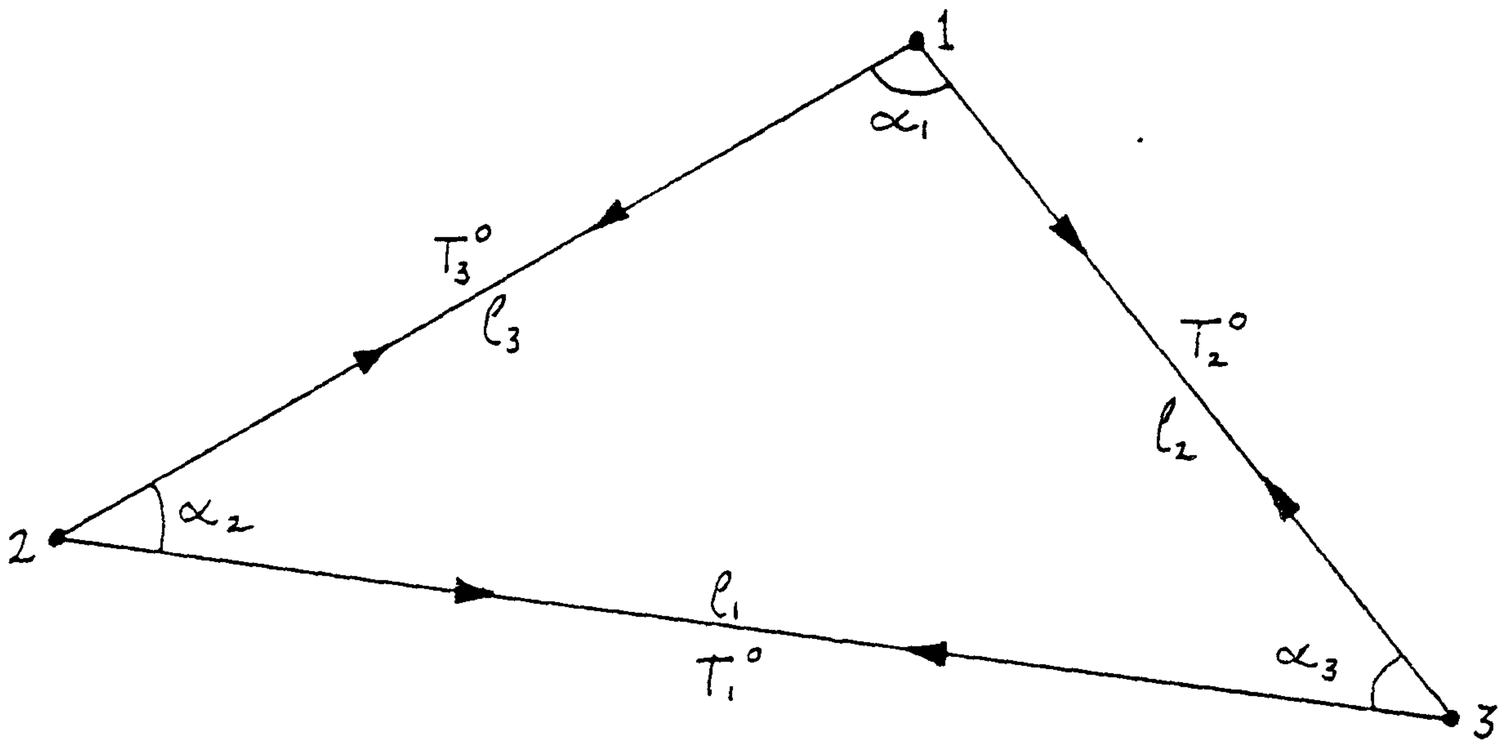


Figure 6

It may be noted that edge forces given by equation (5) are not always tensile. Thus uniform stress membranes cannot be accurately simulated by line elements.

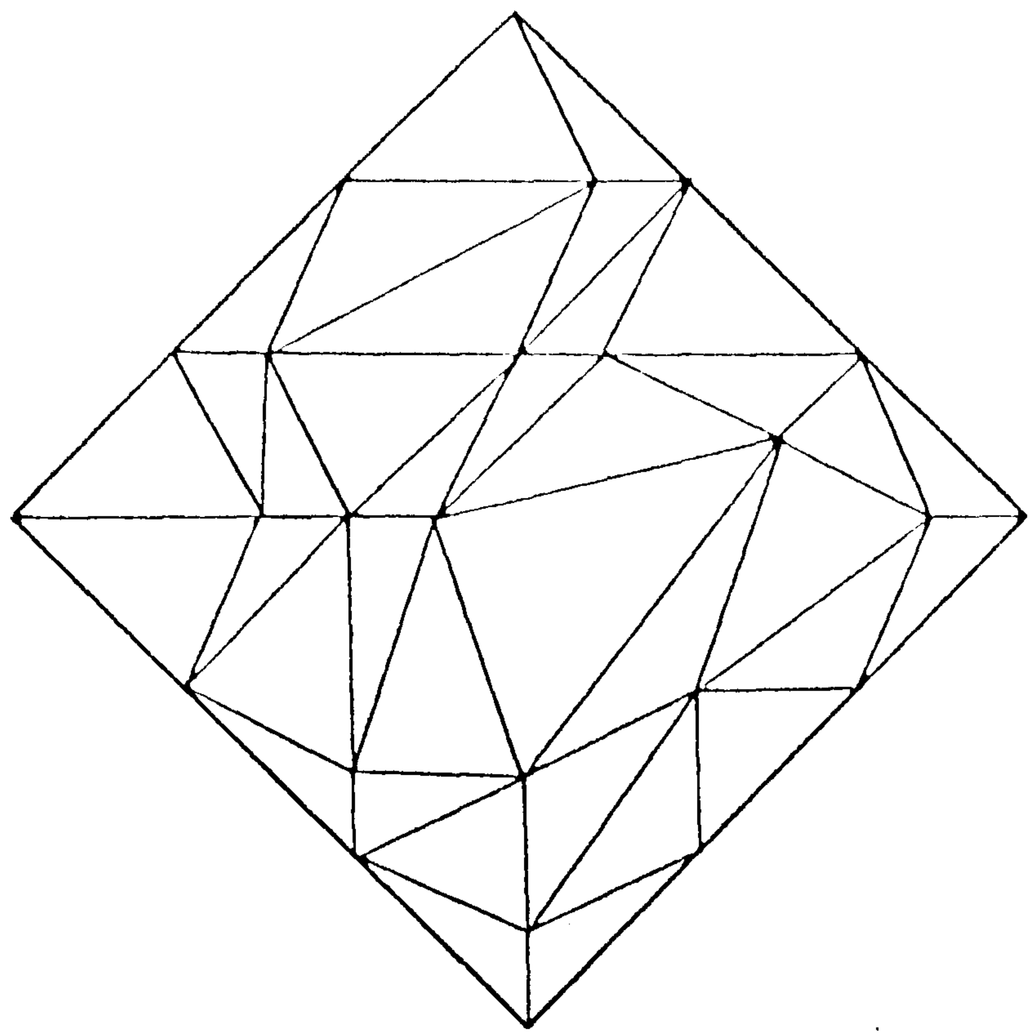
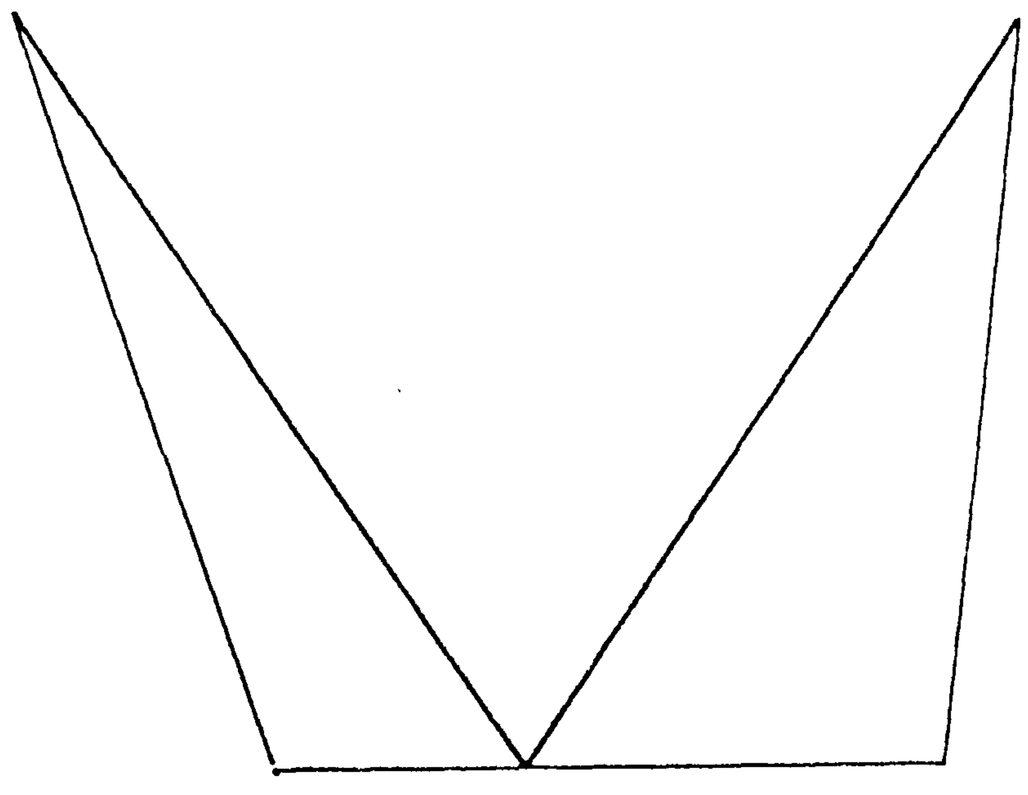


Figure 7a



(7b)

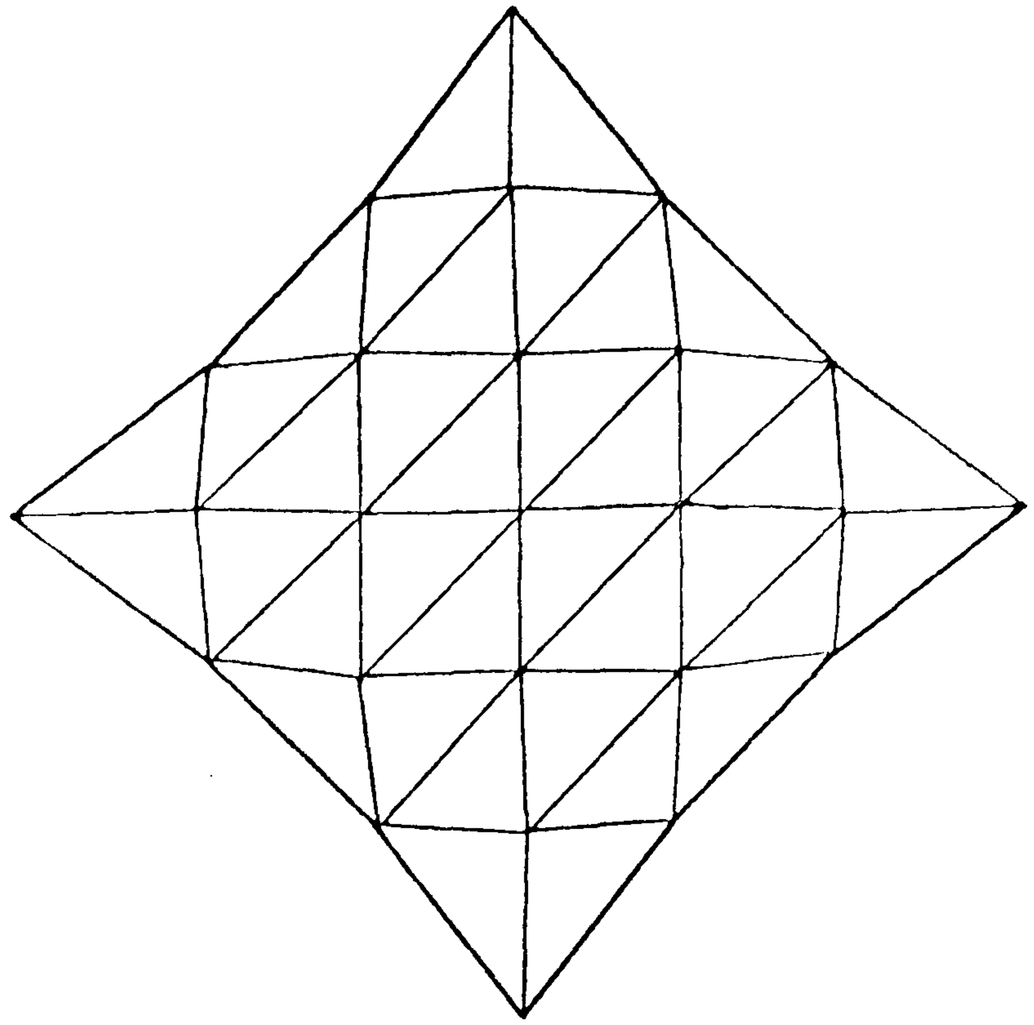
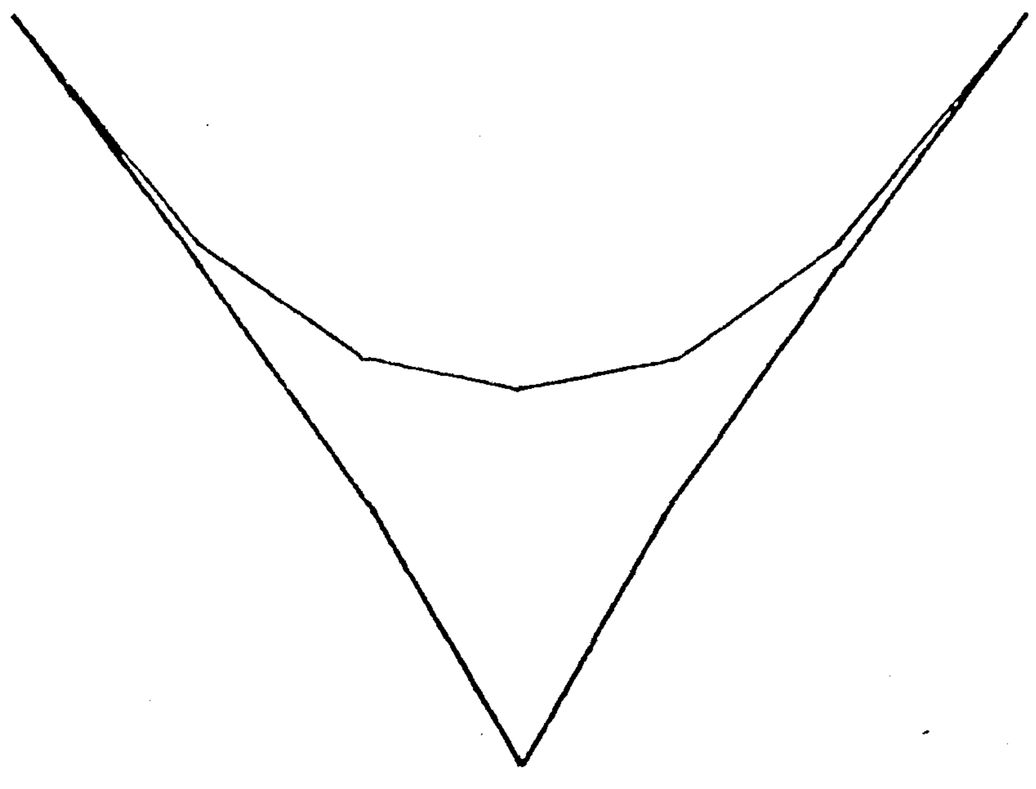


Figure 8a



(8b)

For the determination of minimum surface membranes the elastic stiffness $[k^e]$ in equation (3b) is set to zero and, as with geodesic networks, the motion of surface nodes is controlled by the geometric stiffness. For the example structure, starting with the coarse and irregular subdivision shown in figs. 7a and b, convergence to the cable edge membrane geometry (figs. 8a and b) was obtained in less than 50 iterations.

Pneumatic Structures

The geometry of uniformly stressed pneumatic structures can be derived by including in equation (4) for the membrane analysis, normal nodal forces proportional to the current area of elements as they change in shape throughout the analysis. The resolved load components can be expressed in terms of side vectors used in Eq. (4) without determining element areas, and little additional programming is required. For a right-handed global co-ordinate system and element nodes numbered anti-clockwise, the normal vector is out of plane and the resolved components at each node due to the internal pressure, p, are:

$$\begin{Bmatrix} P_x \\ P_y \\ P_z \end{Bmatrix} = \frac{P}{6} \begin{Bmatrix} y_{21} \cdot z_{32} - y_{32} \cdot z_{21} \\ z_{21} \cdot x_{32} - z_{32} \cdot x_{21} \\ x_{21} \cdot y_{32} - x_{32} \cdot y_{21} \end{Bmatrix} \quad \text{where } x_{21} = x_2 - x_1 \text{ etc.}$$

Figures 9 and 10 show the geometries of membranes, with a uniform tension of 2.5 kN/m, subject to normal pressure of 4 kPa and 10 kPa respectively. In both cases the minimum surface membrane (fig.8) was used as the starting geometry. For the lower pressure

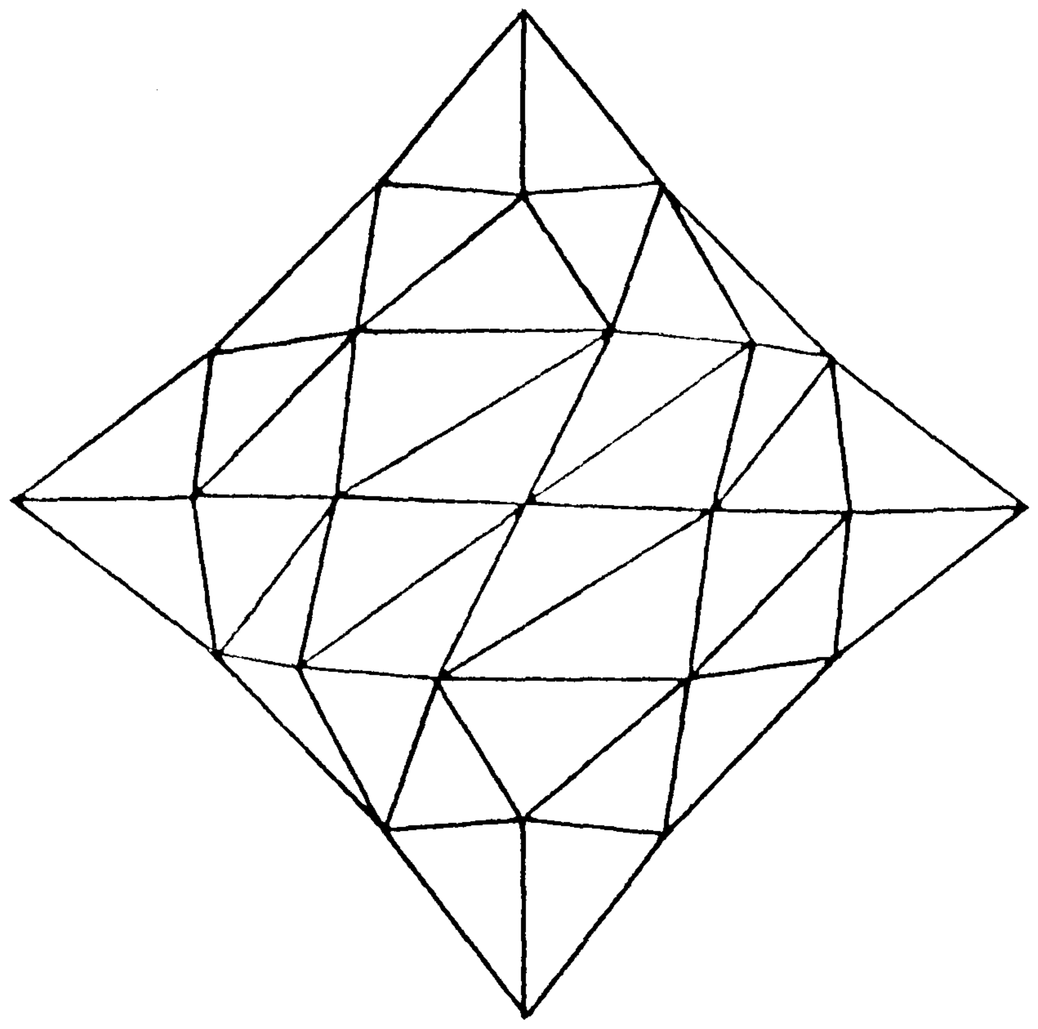
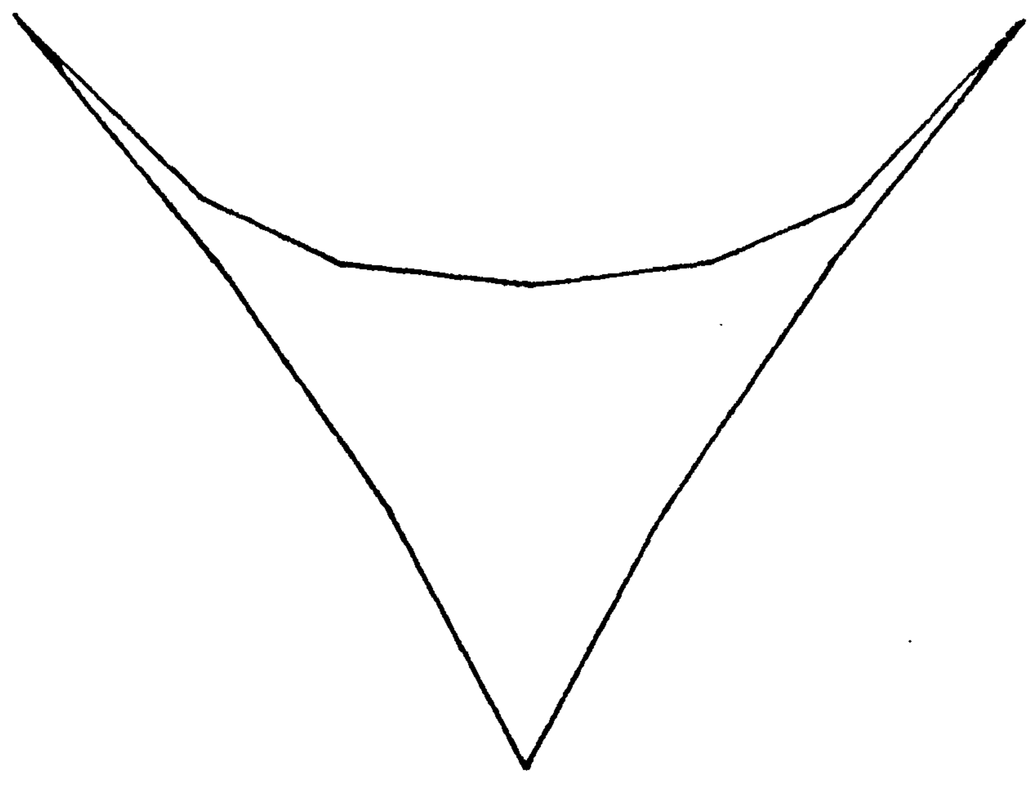


Figure 9a



(9b)

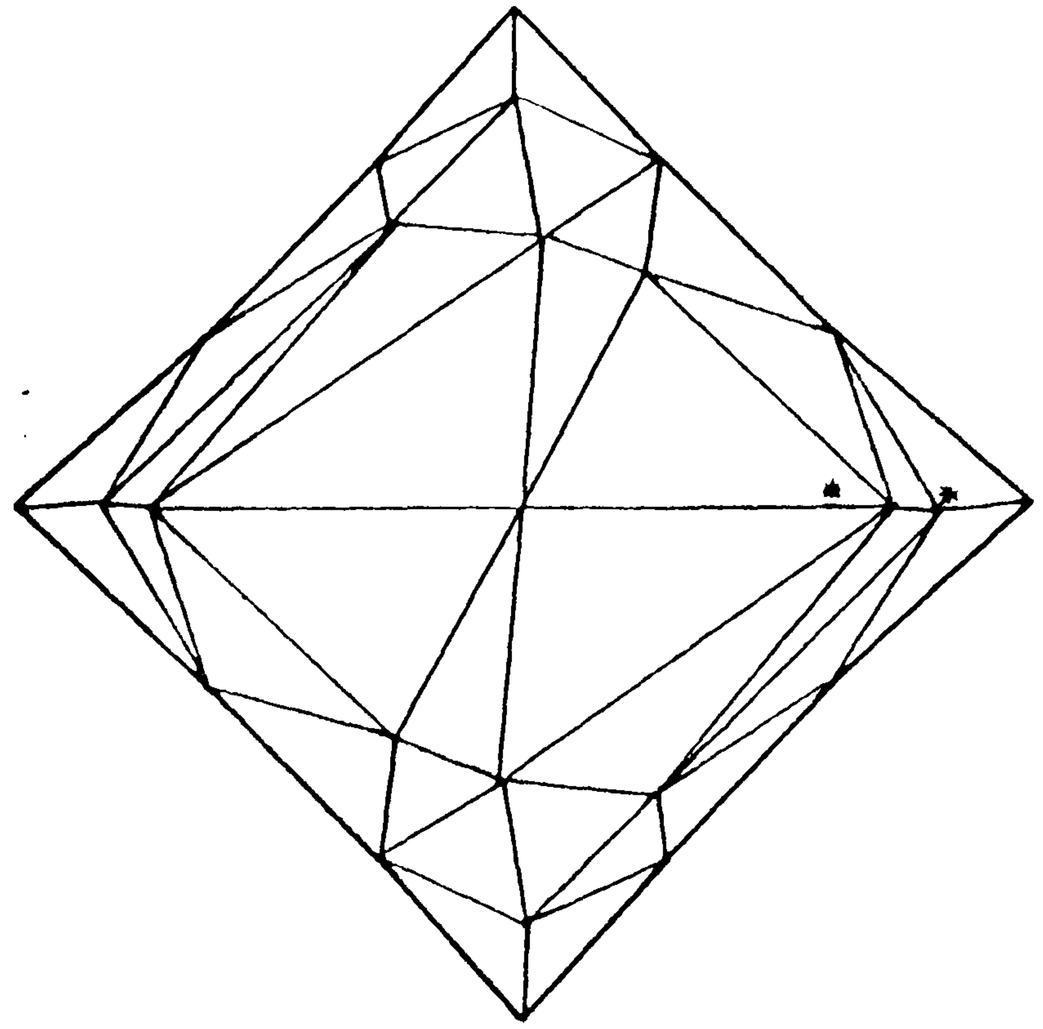
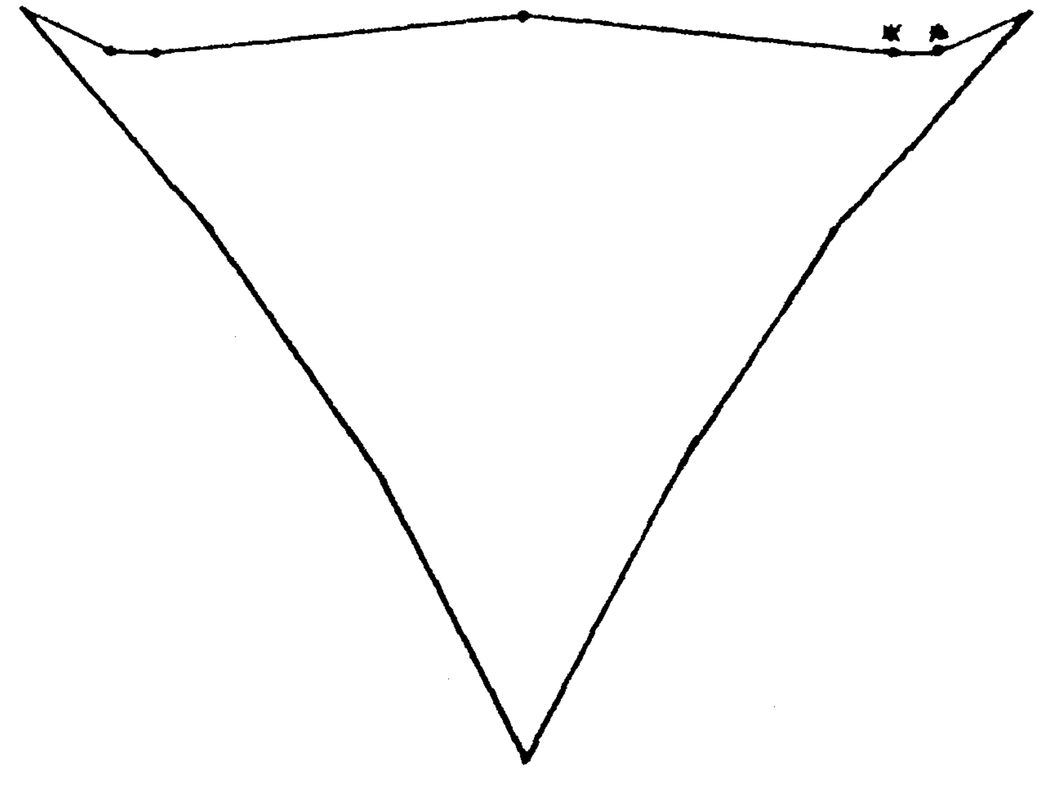


Figure 10a



(10b)

the geometry shown is converged, though the convergence rate was only 1/3 of that for the unloaded membrane. For the higher pressure, fig.10 represents the geometry after 50 iterations. At 60 iterations the nodes marked * were almost coincident. When the nodes cross they are immediately restored to correct topological positions, and continue to meet and part as the analysis progresses. The system is neither convergent nor completely unstable; the other nodes undergoing comparatively small changes in position. Solutions for finer sub-divisions, though not suffering from the same quasi-instability, converge very slowly. The results, after 400 iterations, for a sub-division using four times the number of elements are shown in figs. 11c & d. The apparently grossly distorted elements near the boundaries are lying in almost vertical planes, and if the pressure is increased by 20% the system diverges because the membrane tension is too low. Results for the 4 kPa pressure on the finer mesh are shown in figs. 11a and b.

Principal Stress Trajectories

The determination of minimum surface geometry is useful in the initial stages of design of cable networks with complex curvature and boundary conditions. The ideal membrane may be subsequently approximated by a distorted uniform mesh network. But the shallow curvature and light tensioning which can occur in areas of such networks increases the hazard of vibration, and the remedies of incorporating turnbuckles in the network surface or increasing the overall tensions increase the complexity of construction or the size and cost of boundary cables, tension anchorages and foundations.

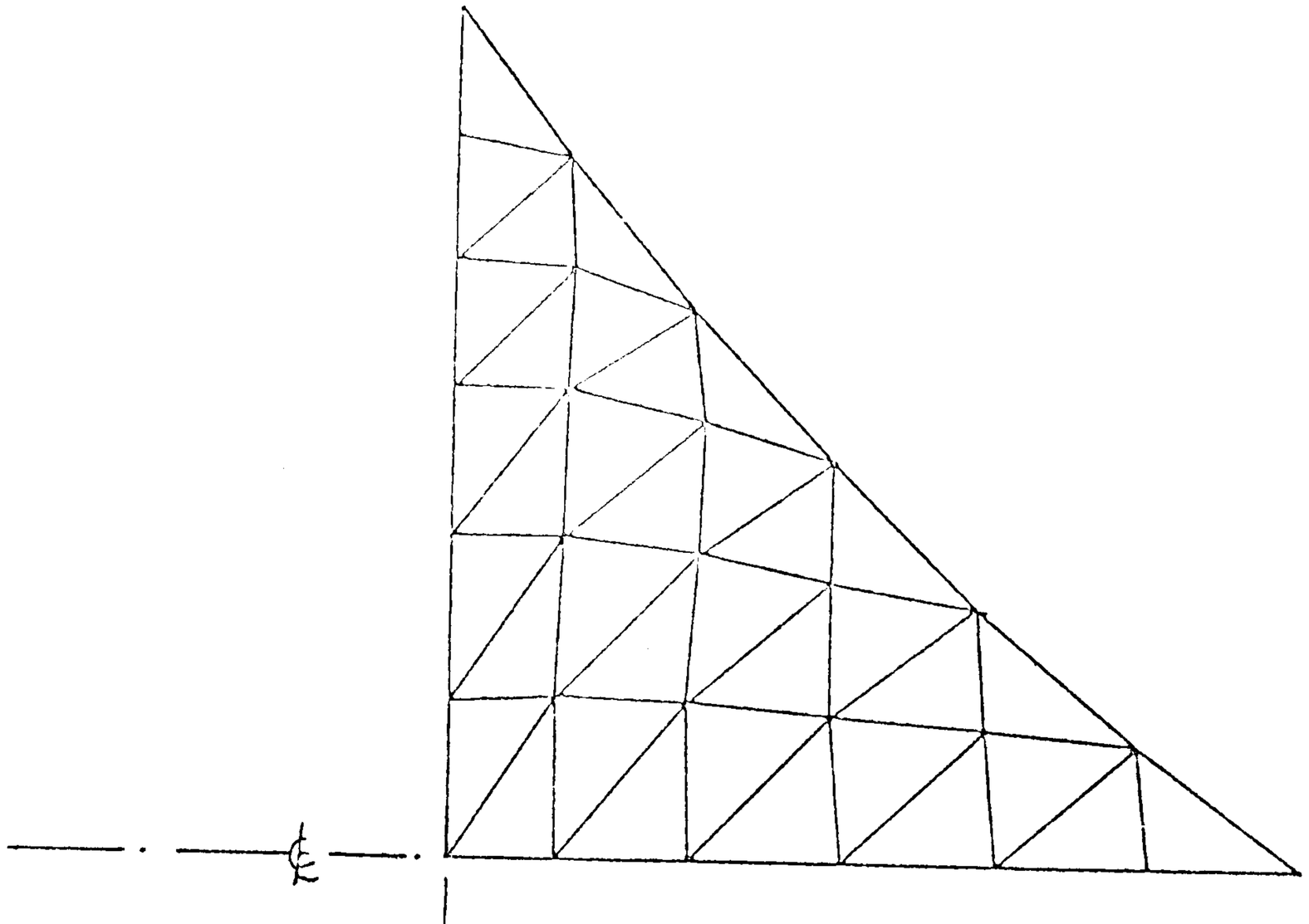
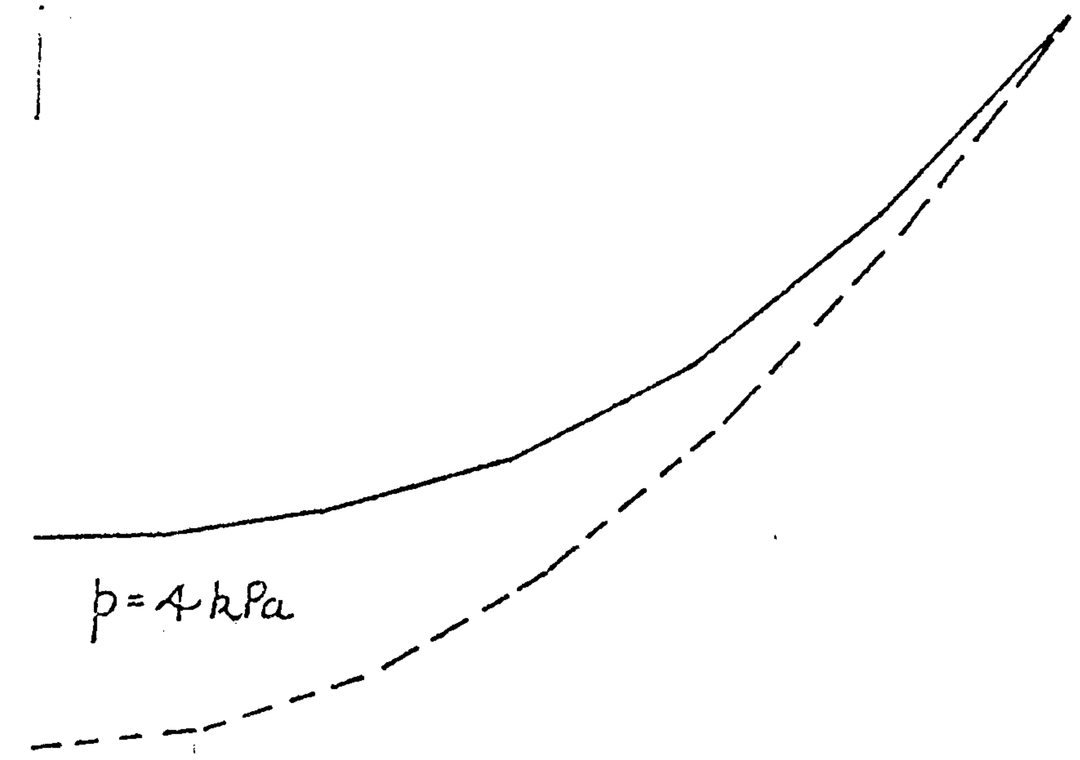


Fig 11a



(11b)

1/4 PLAN

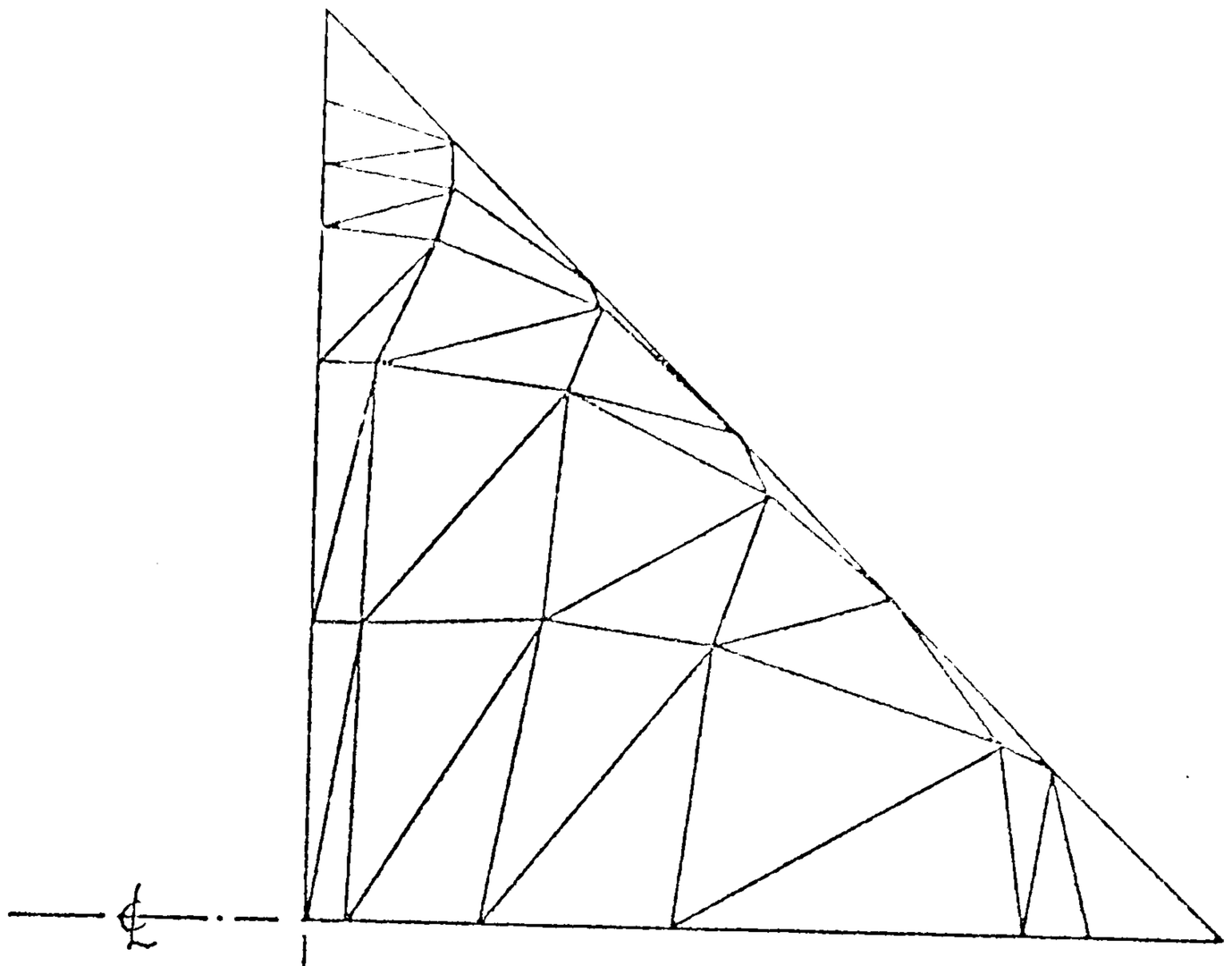
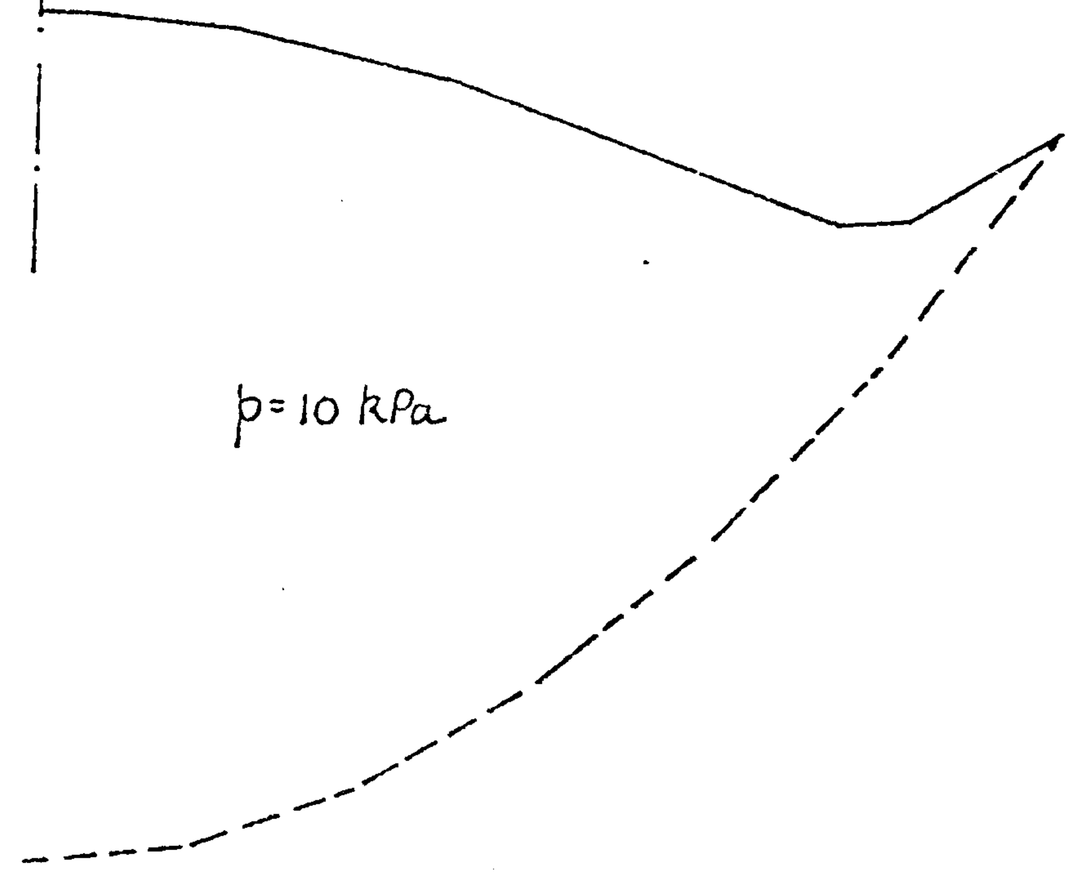


Fig. 11c



SECTION

(11d)

The alternative to a uniform mesh is a geodesic network in which cables follow approximately the trajectories of principal radii of curvature between boundaries. For simple structures, such as the one previously considered, the required boundary connections for the surface cables will be evident. For complex structures however this may not be so, and for such cases a simple initial design procedure is to determine the minimum surface and, having assigned elastic stiffness to the elements, to subsequently determine the principal stress trajectories due to light uniform loading. The best arrangement for the geodesic network system, determined entirely by the various end connection points, can then be found by following the stress trajectories between the boundaries. A fairly coarse element idealization can be used, and because loading is uniformly applied the trajectories can be adequately predicted with comparatively few iterations. The directions of principal stress developed in the minimum surface membrane due to a uniform normal pressure of 4 kPa are shown in fig. 12a. Bearing in mind the simplicity and number of elements the results are good; probably because of low stress gradients.

ANALYSIS OF TENSION STRUCTURES

This section considers briefly aspects of dynamic relaxation which are particularly relevant to the analysis of tension systems.

Membrane Buckling and Slackening of Cables

The convergence of DR, when dealing with non-linearities such as buckling might be questioned in view of the oscillating path to solution with sub-critical damping.

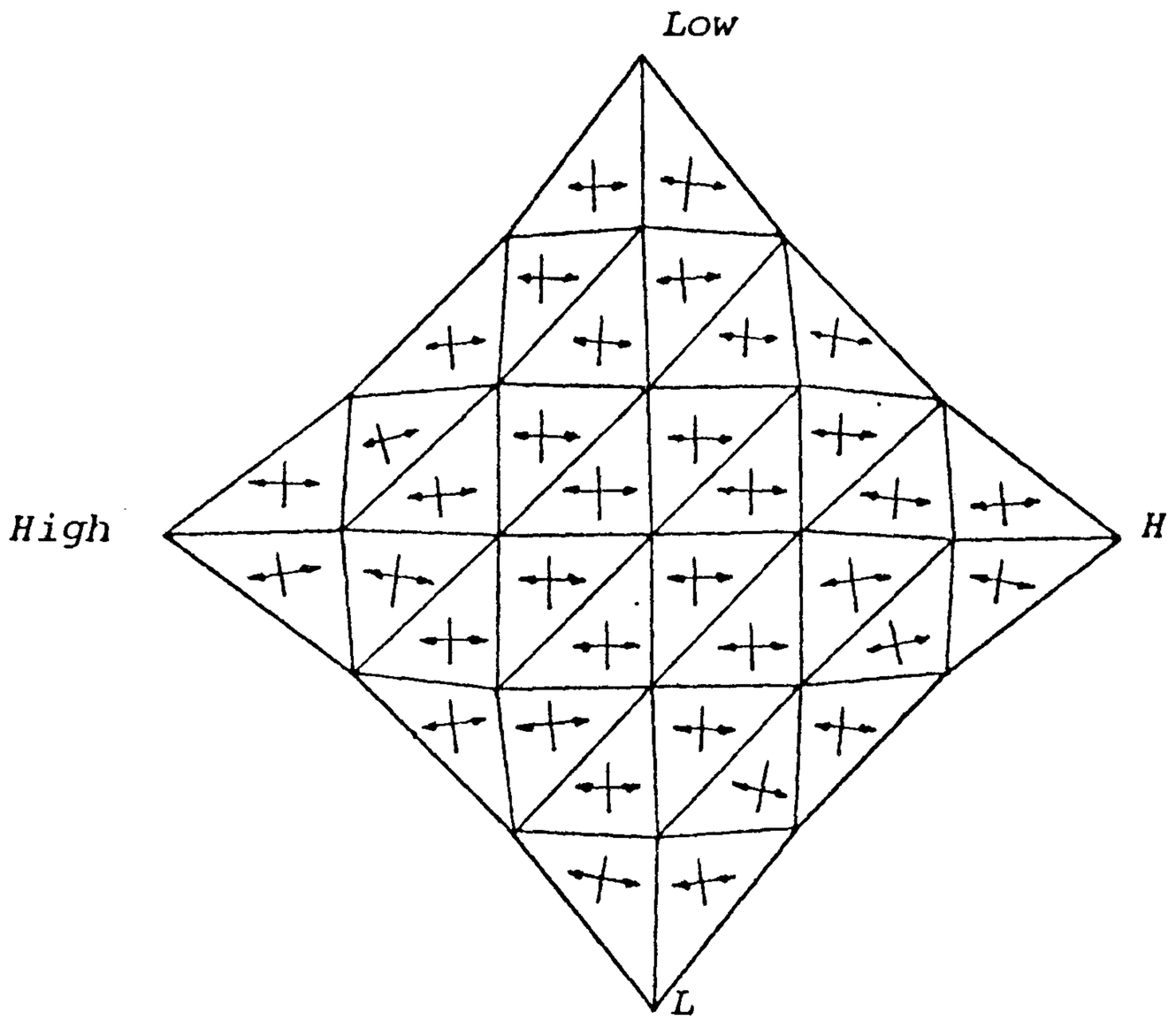


Figure 12a

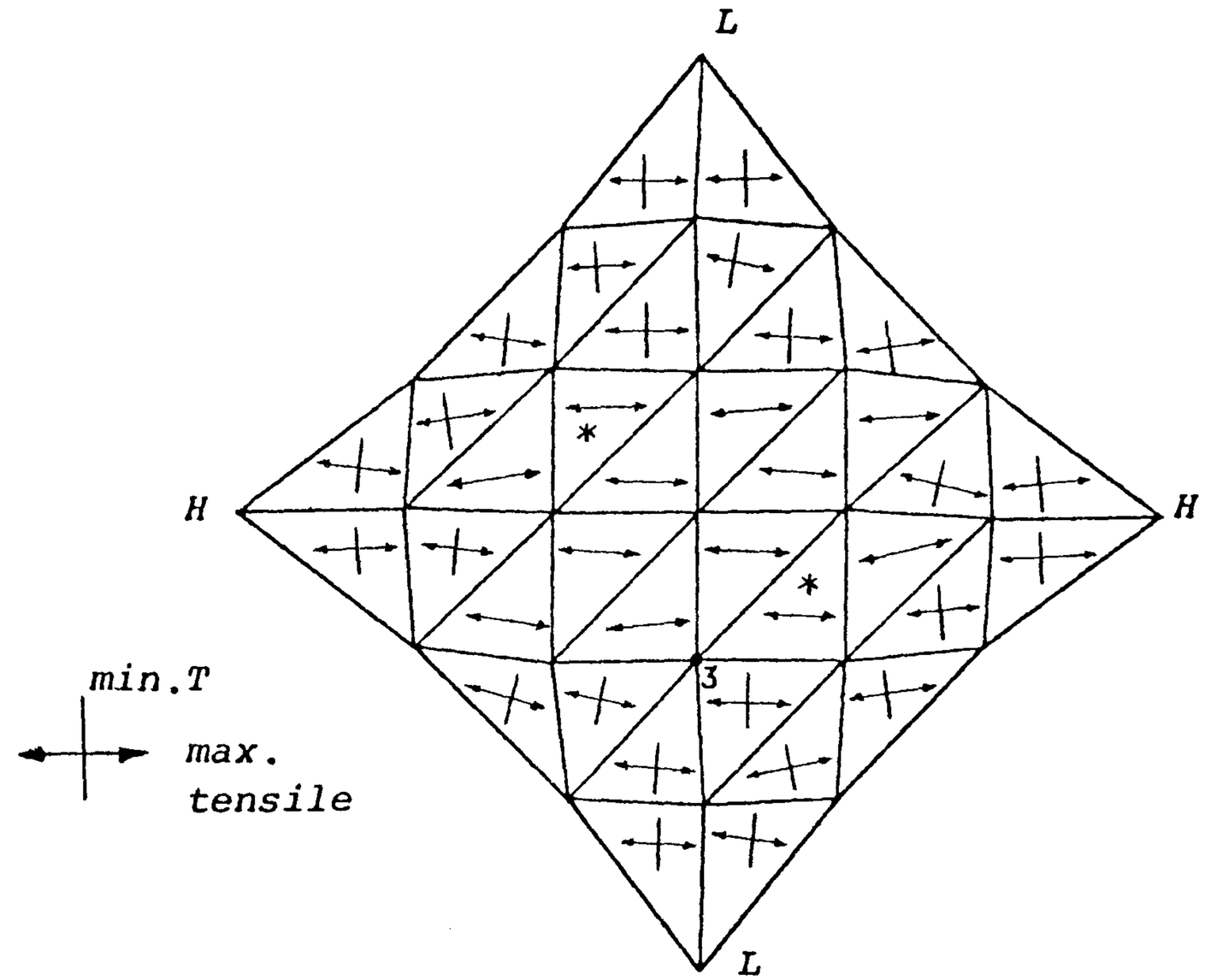


Figure 12b

To account for buckling of membranes or clad networks the stresses must be checked at certain stages:

$$\begin{Bmatrix} \sigma_x \\ \sigma_y \\ \tau_{xy} \end{Bmatrix} = [D][G]\{e\}$$

where $\{e\}$ is the vector of side extensions and $[D]$ and $[G]$ are respectively the stress and strain matrices related to the element x, y axes.

The directions and values of the principal stresses are then determined and, if buckling has occurred, the $[D]$ matrix is altered by setting to zero poisson's ratio and the elastic moduli corresponding to the direction(s) of principal compressive stress which exceed the limiting value. The matrix is then transformed (D') to relate to the element axes (fig. 13) and the stiffness is reset:

$$[k^e] = [G^T][D'][G]\ t.A$$

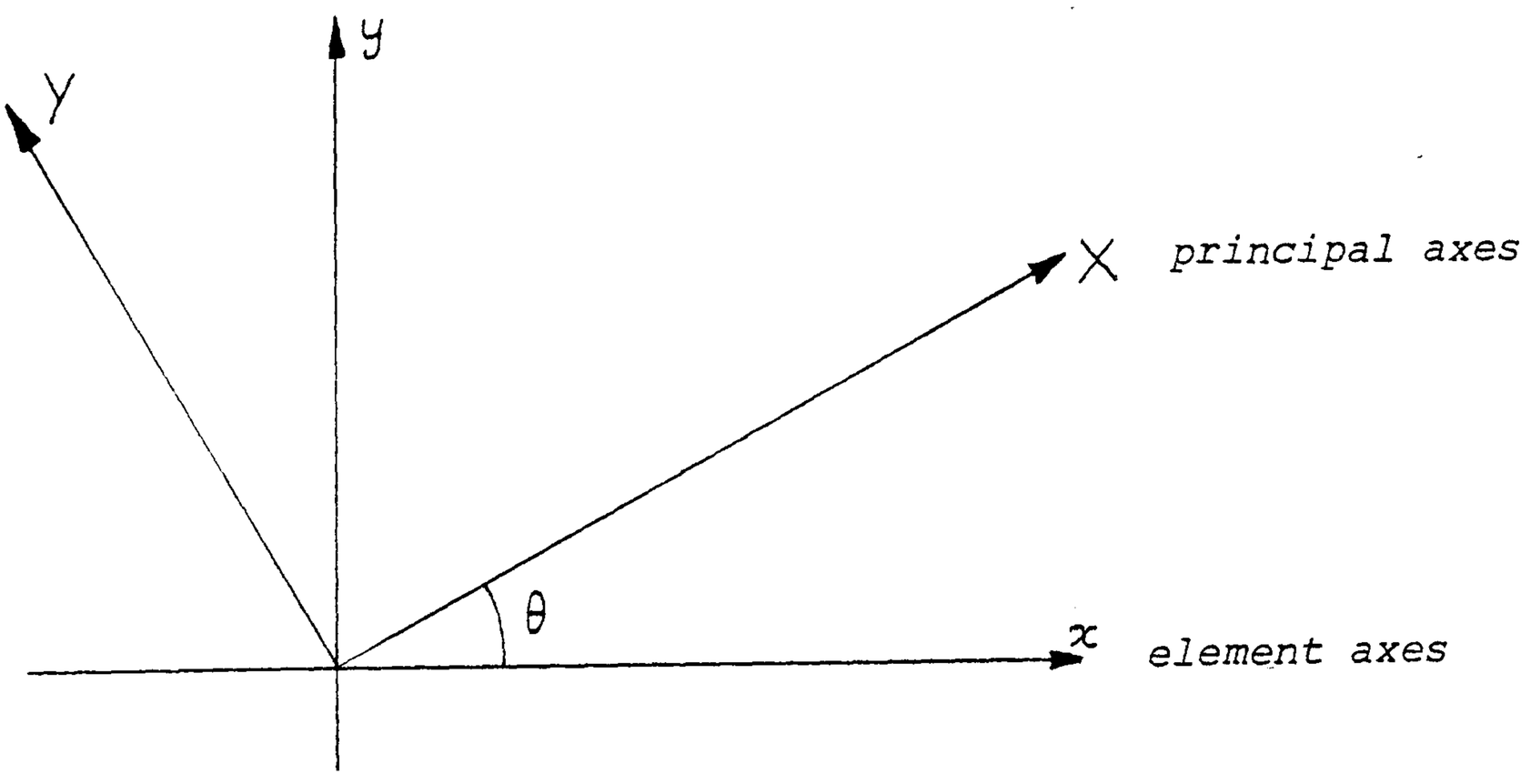


Figure 13

The relation between principal strains and the strains related to orthotropic or convenient axes of an element is:

$$\begin{Bmatrix} \varepsilon_x \\ \varepsilon_y \\ \gamma_{xy} \end{Bmatrix} = \begin{bmatrix} \text{Cos}^2\Theta & \text{Sin}^2\Theta & \text{Sin}\Theta\,\text{Cos}\Theta \\ \text{Sin}^2\Theta & \text{Cos}^2\Theta & -\text{Sin}\Theta\,\text{Cos}\Theta \\ -2\text{Sin}\Theta\,\text{Cos}\Theta & 2\text{Sin}\Theta\,\text{Cos}\Theta & \text{Cos}^2\Theta - \text{Sin}^2\Theta \end{bmatrix} \begin{Bmatrix} \varepsilon_x \\ \varepsilon_y \\ \gamma_{xy} \end{Bmatrix}$$

or $$\{\varepsilon_{xy}\} = [C]\{\varepsilon_{xy}\}$$

By equality of virtual work:

$$\{\varepsilon_{xy}\}^T \{\sigma_{xy}\} = \{\varepsilon_{xy}\}^T \{\sigma_{xy}\}$$

$$\therefore \quad \{\varepsilon_{xy}\}^T [D'] \{\varepsilon_{xy}\} = \{\varepsilon_{xy}\}^T [D_p] \{\varepsilon_{xy}\}$$

Hence $$[D'] = [C]^T [D_p] [C]$$

where $[D_p]$ is the stress matrix related to the principal axes and accounts for the changes in elastic constants due to buckling.

The prestress may be included as initial side extensions; thus in Eq.(3b) extensions e may be measured from the slack state and pretensions T^o deleted. A similar procedure can be used to account for slackening of cable links (in contrast to that outlined in chapter 2), but for common links account must be taken of the fact that the slack lengths of the cable and adjacent membrane elements are different. Extensions from the slack state must also be calculated by means of a square root operation rather than the expression in appendix 2.2.

The membrane previously analysed for a distributed load of 4 kPa was re-analysed with the load increased to 10 kPa with the limiting buckling stress assumed to be zero. The results, in figure 12b, show principal stresses which are tensile; elements in the central zone having buckled.

For the increased loading three analyses were carried out, each with a time interval of 99% of the critical value:

a) with damping $K = 90\% K_{crit}$

b) $K = 45\% K_{crit}$

c) $K = 45\% K_{crit}$, but surface mass components m_x and m_y doubled so that motion normal to the surface was underdamped but motion in the surface plane was less responsive.

Traces of the vertical (z) deflection of node 3 are shown for the three cases in figure 14. In case (a) the analysis converged to a unique solution in which, allowing for the antisymmetrical idealization, stresses and deflections in corresponding areas of the structure were consistent. The final solution contained no elements in which both principal stresses were zero and, because of the high damping, at no stage during the path to this solution did double buckling occur. In case (b) the stress changes were greater, and double buckling occurred alternately in elements marked *. Although the analysis closely approached the previous solution, complete convergence was not obtained. Deflections and stresses tended either to oscillate with small amplitudes about this solution or nodes of the membrane became unsymmetrically displaced from their correct positions and not in stable equilibrium. The maximum discrepancy in displacement occurred at node3 as shown in figure 14. For case (c), since the

damping was proportional to mass components, the relative motions, tangential to the surface, of adjacent groups of nodes in the central zone of the membrane were damped to the same degree as for case (a). Stress changes were thus less severe than in case (b) and, although the vertical motion of nodes was underdamped, the analysis eventually converged to the correct solution. For higher loads, which entail double buckling in several elements to achieve static equilibrium, all of the analyses failed to converge even when damping was further increased and the time interval reduced. This is probably due to an inadequate representation of stress because of the use of simple elements and a coarse idealization of the structure.

An examination of the problems of numerical stability and accuracy of analyses involving intermittent dynamic buckling with light damping is contained in Appendix 3.2.

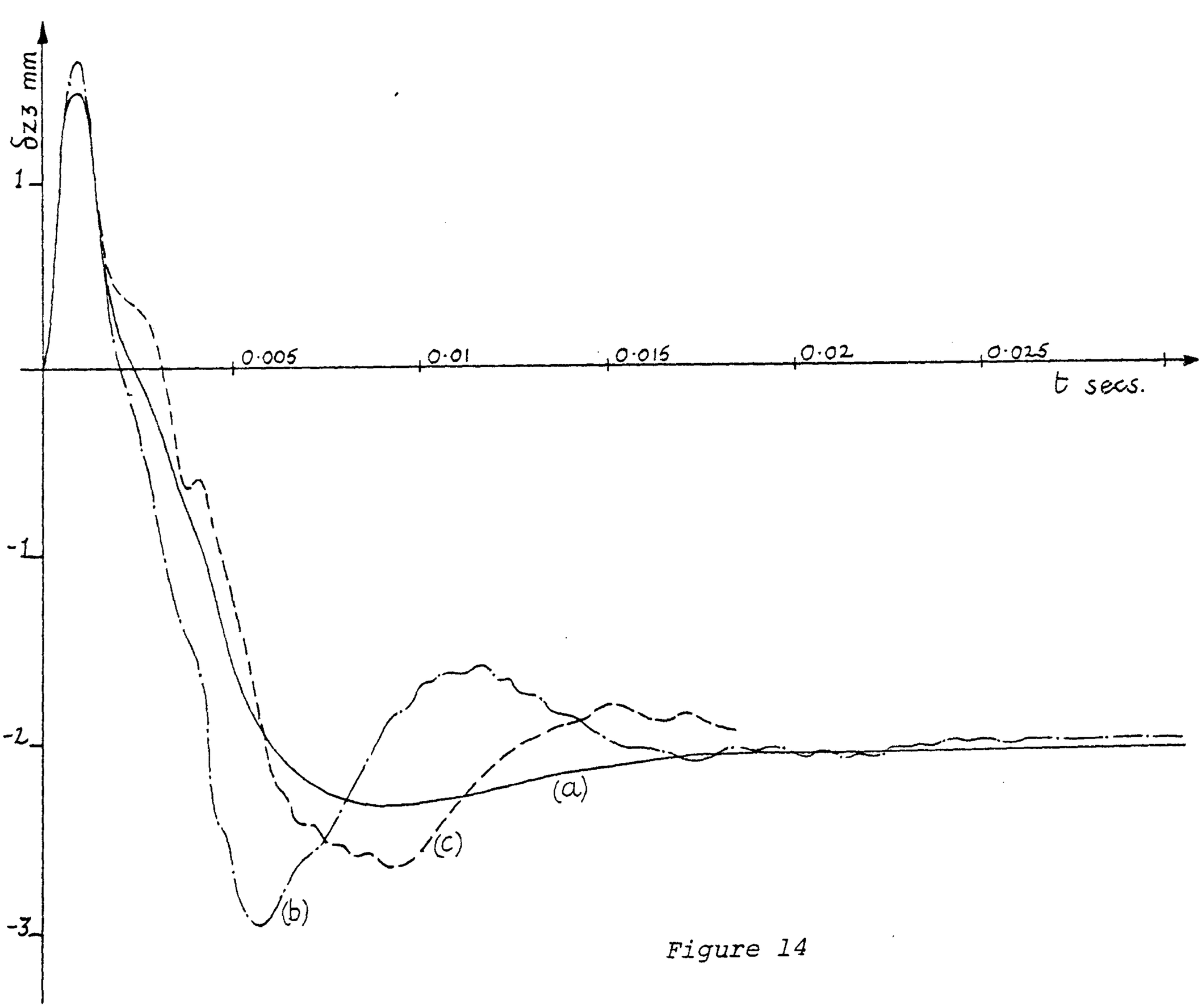


Figure 14

Force Transfer Procedure for Stiff Members

A characteristic of tension structures is their low stiffness. Some elements may, however, be short and very stiff; for example, spreaders in double layer systems. For structures of this type, the time interval and efficiency of DR may be restricted by these elements and, beyond a certain point, no advantage can be gained by the use of fictitious masses.

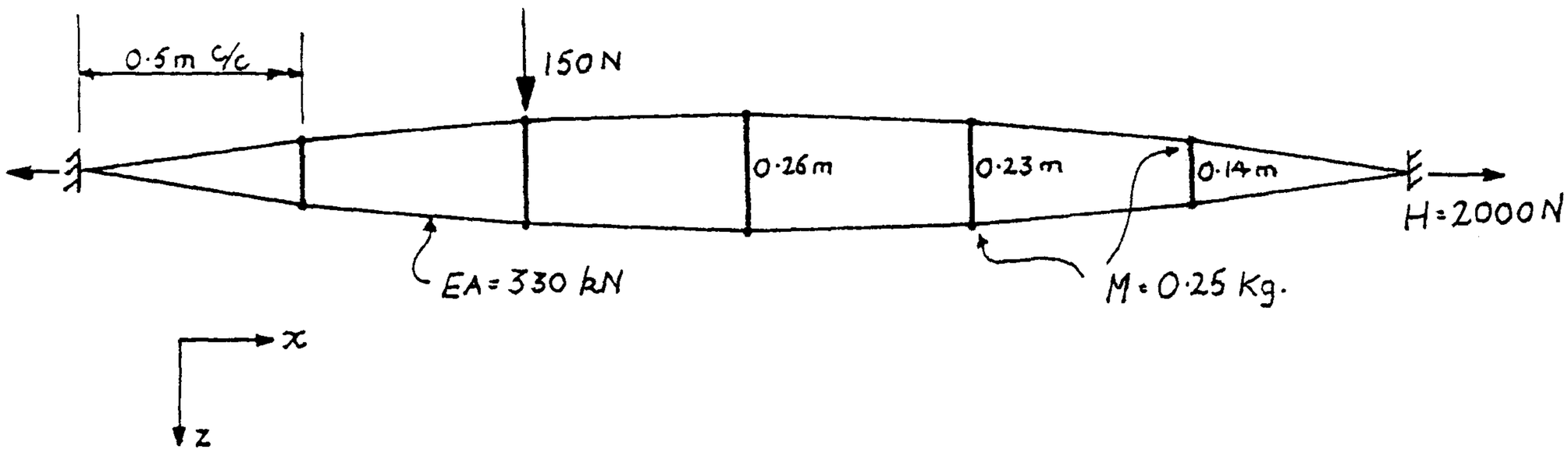


Figure 15

For the cable girder in fig. 15 the direct stiffness of the nodes (relative to adjacent nodes considered fixed) may be much greater in the vertical direction than horizontally. Increasing the fictitious masses M_z will have no effect on convergence since both the critical time interval and the period of vibration are approximately proportional to $\sqrt{M_z}$. The problem can be avoided by considering the motion of the upper and lower nodes in the direction of the strut axis simultaneously, and treating the relative motion as an additional variable. But the transformations involved add to the complexity and time of solution.

A simple alternative procedure is to use fictitious reduced axial stiffnesses S' for the struts. If the system is then analysed, a first estimate of the out of balance forces in struts is: $e_1 (S - S')$ where e is the extension and S is the real stiffness of a strut.

The system may then be re-analysed with applied constant correcting forces in the struts given by:

$$C_1 = e_1 (S - S') \; S'/S.$$

The second estimate for out of balance forces is: $(e_2 (S - S') - C_1)$ and the correcting loads are:

$$C_2 = C_1 + (e_2 (S - S') - C_1) \; S'/S.$$

Generally, for the nth correction analysis:

$$C_n = (e_{n-1} \cdot S' + C_{n-1})(1 - \frac{S'}{S})$$

The correction forces are stationary when: $C = e(S - S')$

and the true member forces are: $F = e.S' + C = e.S$

It would evidently be inefficient to reach convergence of the DR analysis at each stage before applying correction forces. Yet the force transfer process must converge from one side. It is therefore necessary that damping should be over-critical if corrections are applied gradually during a single DR analysis.

The cable girder in fig. 15 was analysed by this process assuming that the spreaders had infinite stiffness. From a short trial run, without force transfer but using fictitious stiffnesses for spreaders, the critical damping was found to be 0.03. The structure was then analysed, using the force transfer process, with damping of 0.04, and subsequently with damping of 0.02. The vertical deflection/time curves for the two cases are shown in fig. 16.

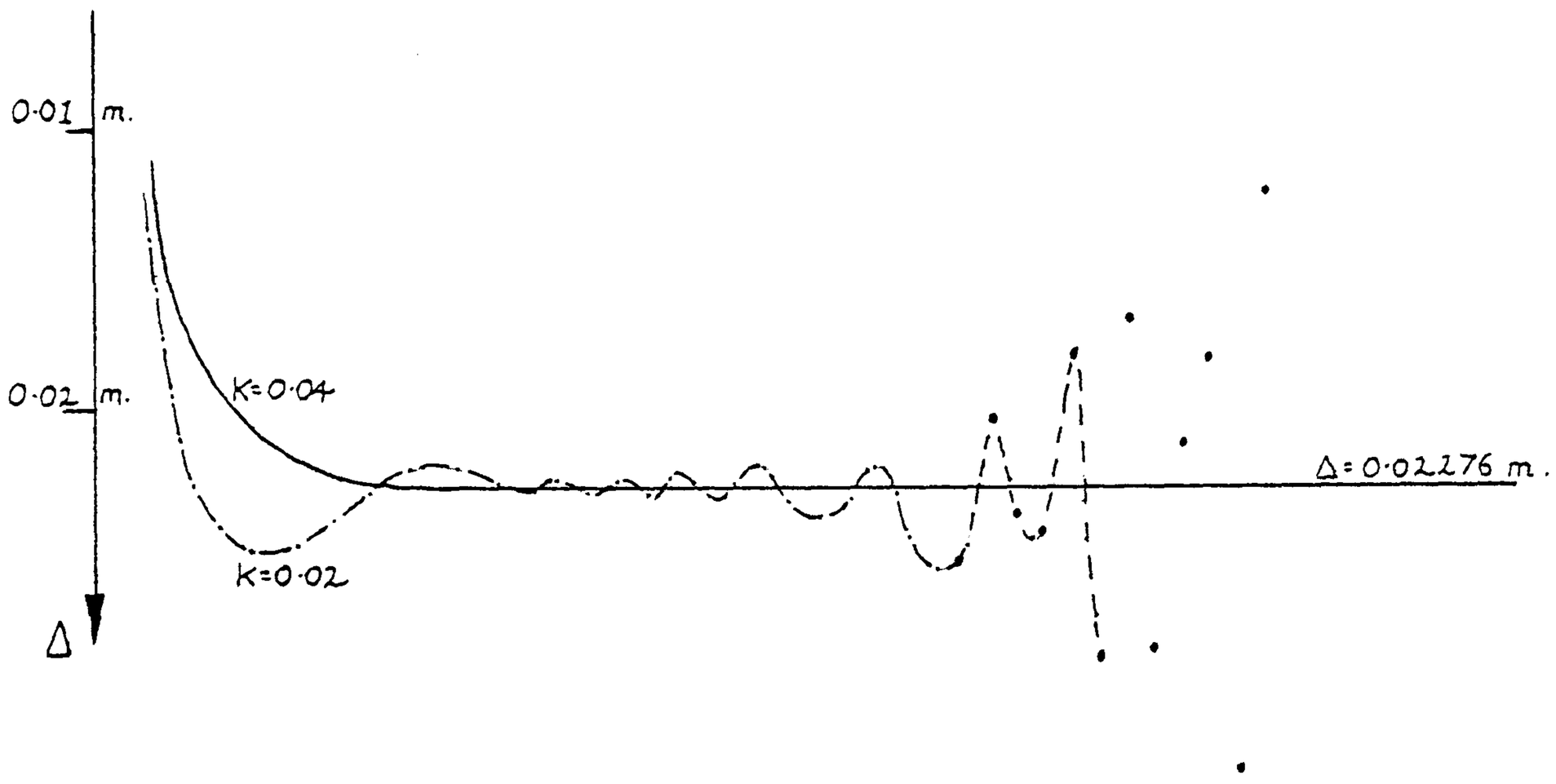


Figure 16

The method is not ideal since the solution is unbounded. It can however enable an efficient DR analysis of certain structures which would otherwise require a very small time interval, and it is not restricted to particular geometrical configurations (e.g. vertical struts). The example chosen, with struts of infinite stiffness, could only have been analysed in this way since for an ordinary DR analysis the critical time interval would have been zero.

CONCLUSIONS

The particular advantage of dynamic relaxation when applied to tension structures is its ability to cope with the degrees of mechanical freedom in these structures, both during the design determination of pretension geometry and momentless boundary structures, and during the analysis of the structures under live loading when, apart from inherent geometrical non-linearity, additional degrees of mechanical freedom may be induced by buckling of cladding or cables.

A further advantage of DR is that it can, with lighter damping and real masses, be used to obtain a good indication of dominant frequencies of free vibration. This also is especially relevant to the design of tension structures.

REFERENCES

(1) Day, A.S. 'An introduction to dynamic relaxation', Engineer, 219, (1965), pp 218-221.

(2) Otter, J.R.H., 'Computations for pre-stressed concrete reactor pressure vessels using dynamic relaxation', Mech.Engng. Des., 3, (1966), pp 183-185.

(3) Day, A.S., 'Analysis of plates by dynamic relaxation with special references to boundary conditions', Proc. Int. Symp. Digital Computers Struct. Analysis, Newcastle upon Tyne (1965)

(4) Otter, J.R.H, Cassel, A.C. and Hobbs, R.E., 'Dynamic Relaxtion', Proc. Inst. Civ. Engrs., 35, (1966), pp 633-656.

(5) Rushton, K.R., 'Dynamic relaxation solutions of elastic-plate problems', J. of Strain Anal., V.3.n.1, (1968), pp 23-32.

(6) Rushton, K.R., 'Large deflections of variable thickness plates', Int. J. Mech. Sci., 10, (1968), pp 723-735.

(7) Cassell, A.C. 'Shells of revolution under arbitrary loading and the use of fictitious densities in dynamic relaxation', Proc. Inst. Civ. Engrs., 40, (1970), pp 65-78.

(8) Otter, J.R.H., 'Dynamic relaxation compared with other iterative finite difference methods', Nucl. Engng. and Des., 3, (1966) pp 183-185.

(9) Wood, W.L. 'Comparison of dynamic relaxation with three other iterative methods', Engineer, (Nov. 1967), pp 683-687.

(10) Brew, J.S. and Brotton, D.M. 'Non-linear structural analyses by dynamic relaxation', Int. J. Num. Meth. Engng., 3, (1971) pp 463-483.

(11) Day, A.S. and Bunce, J. 'The analysis of hanging roofs', Arup Journal, (Sept. 1969), pp 30-31.

(12) Barnes, M.R., 'Pretensioned cable networks', J. of Constr. R. and D., V.3.n.1, (1971) pp 17-22.

(13) Barnes, M.R., 'Dynamic relaxation analysis of cable networks', Int. Conf. on Tension Structures, London (April 1974). Chapter 2.

(14) Barnes, M.R., 'An articulating buoyant pipeline', Proc. Int. Conf. on Underwater Construction Technology, Cardiff (April, 1975)

APPENDIX 3.1

ANALYTICAL MODEL PROPERTIES

H-P Model Structure dimensions:

Across High and Low point diagonals: 1.2m

Difference in height between High and Low points: 0.9m

$\therefore$ Length of each edge cable segment = 0.38m

EA values of edge cables initially assumed = 2.5 MN

All edge node masses initially assumed = 0.2 Kg

All surface node masses initially assumed = 0.02 Kg

Geodesic Analysis:

Constant tension in surface cables = 500 N

Constant tension in one end segment of each edge cable = 10,000 N

With assumed properties, the critical time interval is governed by motion of the edge nodes; surface node stiffness being very low.

Direct stiffness of an edge node relative to adjacent nodes is highest along the cable axis: $S = \frac{2 \times 2.5 \times 10^6}{0.38} \triangleq 13 \times 10^6$ N/m

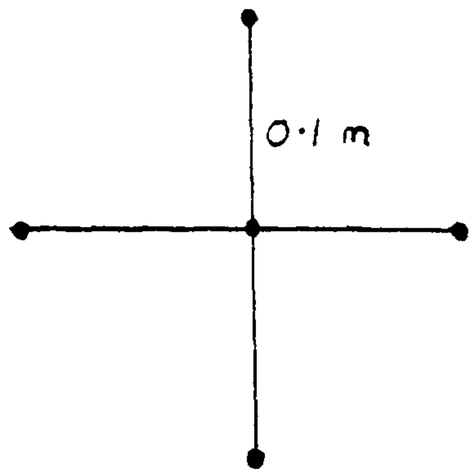
$$\Delta t_{crit} > \sqrt{\frac{2M}{S}} = \sqrt{\frac{0.4}{13 \times 10^6}} = 0.00017 \text{ sec.}$$

A short trial run gave frequencies of:

Edge nodes $\triangleq$ 150 Hz

Surface nodes $\triangleq$ 30 Hz $\therefore$ Increase edge masses to 1.0 Kg.

The surface grid spacing is initially 0.2m, but assuming a maximum reduction to 0.1m for the central areas of the geodesic net:



Geometric direct stiffness in the z direction:

$$S_z \leqslant \frac{P_z}{\Delta_z} \triangleq \frac{4 \times 500}{0.1} = 2 \times 10^4 \text{ N/m}$$

$$\Delta t_{crit} \text{ for surface node} > \sqrt{\frac{2m_z}{S_z}} = \sqrt{\frac{0.04}{2\times10^4}} \triangleq 0.0014 \text{ sec.}$$

Critical damping factor per unit mass, $K \triangleq 4\Pi.f = 0.53/\Delta t$

Geometric stiffness in xy plane $\triangleq S_z/2$

$\therefore m_x = m_y = 0.01$ Kg for surface nodes

To obtain same Δt_{crit} for edge nodes, required axial stiffness

$$= \frac{2.0}{(0.0014)^2} = 1 \times 10^6 \text{ N/m}$$

$\therefore$ Fictitious EA values for edge cables $\triangleq$ 0.2 MN

APPENDIX 3.2

ACCURACY AND STABILITY OF CENTRAL DIFFERENCE ANALYSIS INVOLVING RECURRENT DYNAMIC BUCKLING

When carrying out a dynamic analysis with light damping for structures which are subject to on-off slackening of cables or buckling of membrane elements, the use of a time interval which is small compared with the critical value may be necessary in order to avoid various forms of numerical instability. Alternatively it may be necessary to check stresses or tensions, and if necessary modify the elastic constants, at each time increment or at very frequent intervals. Structural shape and size, type of loading, and the degree of triangulation are all factors affecting numerical stability. Thus for each type of structure in which dynamic buckling is to be investigated it may be necessary to carry out short trial runs to determine an acceptable time increment and the frequency of checks on material properties.

BASIS FOR ANALYTICAL TESTS

To illustrate the types of instability which may occur during dynamic buckling of even the simplest structures, one cable and one membrane structure, each with only four elements and one active node, were investigated with a range of values for time interval (Δt), damping factor (K), and number of time intervals between buckling checks and modification of material properties (NBI).

All real systems will involve some, usually light, structural damping and, when a load is suddenly applied and then either released or held constant, vibrations of the system should gradually decay to a unique static solution. The trace of this behaviour, involving alternate buckling of different elements, thus provides a check on the stability of an analysis for dynamic buckling, and this is the basis for the following numerical tests. Consideration is also given to the hypothetical case of zero damping, with vibrations of the cable structure being traced for large numbers of iterations at different time intervals below the elastic critical interval. A similar test is also carried out on a third trial structure, with several active nodes, employing both cable and membrane elements. This structure, though more complex, remains properly triangulated when buckling occurs and it is shown that the dynamic analysis is thus more stable for time intervals approaching the critical value.

CABLE STRUCTURE

The four element cable structure shown in figure 17 is square in plan with node 1 equidistant from the fixed high and low points (2, 4 and 3,5). The pretension and EA values of the cables were taken as 50N and 50kN respectively, and node 1 was assigned mass components of 1.0 kg in the x and y directions and 0.05 kg in the z direction. The reason for the assumption of differing mass components, which would not of course correspond with a real physical situation, is discussed later. It does not, however, alter the concepts to be illustrated.

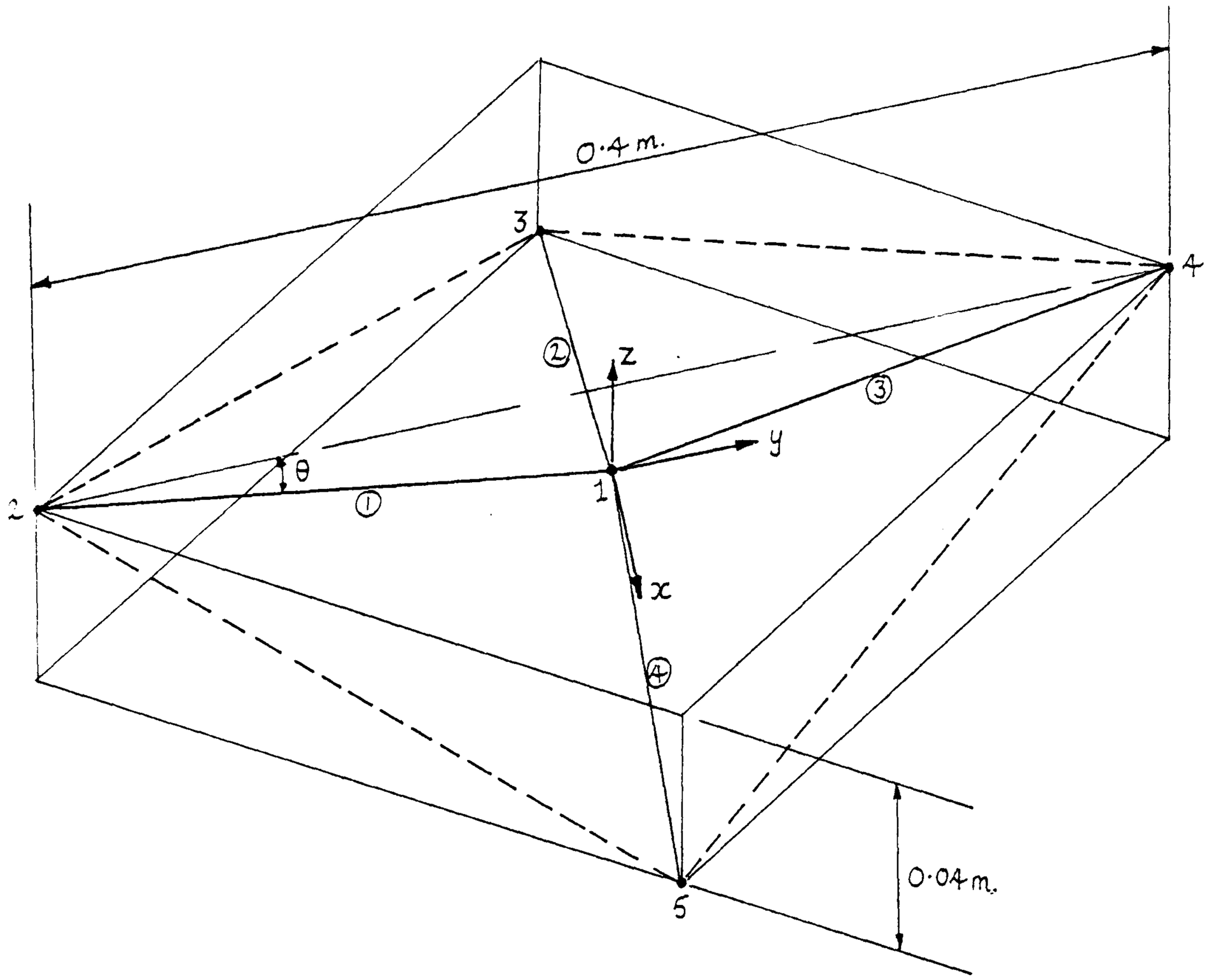


Figure 17

Critical Time Interval:

Based on the assumption that all cables are taut (eleastic),

the stiffness in the x or y directions = $\frac{2EA}{L}\cos\theta = \frac{100}{0.2}\cos^2\theta \simeq 500\text{kN/m}$

Stiffness in the z direction = $\frac{4EA}{L}\sin^2\theta \simeq 10\ \text{kN/m}$

Critical time interval for lateral motion
(with adjacent nodes fixed) $= \sqrt{\frac{4M}{S}} = \sqrt{\frac{4}{500000}} = 0.0028\text{sec.}$

Critical time interval for vertical motion = 0.0045sec.

A trial analysis without damping, using a time interval of 0.0005 sec. and checking for buckling at every iteration (NBI=1), indicated a natural frequency of 83.5 Hz based on tension peaks; the analysis being initiated with small lateral and vertical displacements of node 1, sufficient to cause alternate slackening of each of the cable links. For the study of dynamic buckling tension variations are of particular interest and thus the critical damping factor per unit mass was estimated using this frequency:

$$k_{crit} \simeq 4\pi f = 1050$$

Test Cases:

(a) Initial Displacement:

A series of analyses of the structure was carried out using time intervals ranging linearly from 0.00025→0.003 sec., and damping factors ranging exponentially from 5%→80% of the critical value. For each combination the number of time intervals between buckling checks and modification of properties was varied from 1 to 16. At the start of every analysis node 1 was displaced 5mm in each co-ordinate direction and then suddenly released. Table 1 shows the results obtained for the entire series. The figures in the table, e.g: 1312 in row 1 and column 1, denote the number of iterations to reach convergence to within 0.1% of the 50N static tensions. In all cases, when using a sufficiently small time interval with frequent alteration of material properties (either zero modulus or the real modulus), convergence is obtained. With higher time intervals and/or values of NBI, however, various forms of instability can occur. The notation in the table is as follows:

Δt ↓ / NBI →	5% K_{crit}					10% K_{crit}					20% K_{crit}					40% K_{crit}					80% K_{crit}				
	1	2	4	8	16	1	2	4	8	16	1	2	4	8	16	1	2	4	8	16	1	2	4	8	16
0.00025	1312	1312	1408	R	DIV	658	656	676	1040	R	332	332	332	376	416	168	156	168	176	176	91	90	88	88	112
0.0005	672	712	Q/S*	DIV		328	354	456*	Q/S	DIV	166	166	180	192	Q/S	84	84	84	88	80	46	44	44	56	64
0.00075	480	Q/S	Q/S			224	Q/S	Q/S	Q/S		112	118	Q/S	Q/S	C	56	60	60	Q/S	112	31	28	36	40	C_{nb}
0.001	420	Q/S	DIV			176	Q/S	R*	DIV		82	100	C	Q/S	C	42	44	48	C	C_{nb}	23	22	28	32	
0.00125	Q/S	DIV				148	R	DIV			68	Q/S	C	C	Q/S	34	42	32	Q/S		19	16	20	C_{nb}	
0.0015	Q/S					Q/S	Q/S				68	Q/S	Q/S	Q/S	C	26	36	Q/S	C		16	16	20		
0.00175	R					Q/S	Q/S				66	Q/S	DIV	C	C_{nb}	28	28	Q/S	C		14	16	20		
0.002	DIV					Q/S	DIV				Q/S	C		C_{nb}		30	26	C	C_{nb}		13	14	C_{nb}		
0.00225						R					Q/S	Q/S		Q/S		Q/S	26	Q/S			11	14	C_{nb}		
0.0025						R					Q/S	Q/S		Q/S		Q/S	Q/S	C			16	18	24		
0.00275						DIV					Q/S	Q/S		C		Q/S	Q/S	C			60	60	64	Q/S	Q/S
0.003											DIV	DIV		DIV	DIV	Q/S	Q/S	R	DIV	DIV	R	Q/S	Q/S	Q/S	DIV

Table 1 - Cable Structure Node Displaced

Q/S - Quasi-instability. The amplitude of variations in tensions and deflections decays in the early stages but subsequently approaches a constant value with no further decay. Thereafter the trace continues, with periodic oscillation about an incorrect mean position, never attaining convergence.

R - Random behaviour possibly leading eventually to periodic oscillation (Q/S).

DIV - The solution diverges with deflections and tensions becoming infinite (or numerically ill-conditioned)

C - Chance convergence at values of Δt or NBI which are above those at which quasi-instability first occurred.

C - Convergence without buckling after the first change in properties.

The last row in the table corresponds to a time interval which exceeds the critical value based on taut cables and thus in no case is convergence obtained.

For the purpose of illustrating typical behaviour patterns, full traces of the variations of tension in cable ④ are plotted in figure 18 for the analyses marked * in the table. Also plotted for comparison is the case of zero damping with $\Delta t = 0.0005$ which is shown to diverge. For each of the analyses plotted, the number of time intervals between buckling checks (NBI) was 4. With $\Delta t = 0.0005$ sec. and $k = 10\% \, k_{crit}$, convergence was obtained at 456 iterations though, as can be seen from the figure, a reasonably stable system was obtained after 300 iterations. Prior to this 78 changes in material properties had taken place (approx. 20 in each cable). With the time interval

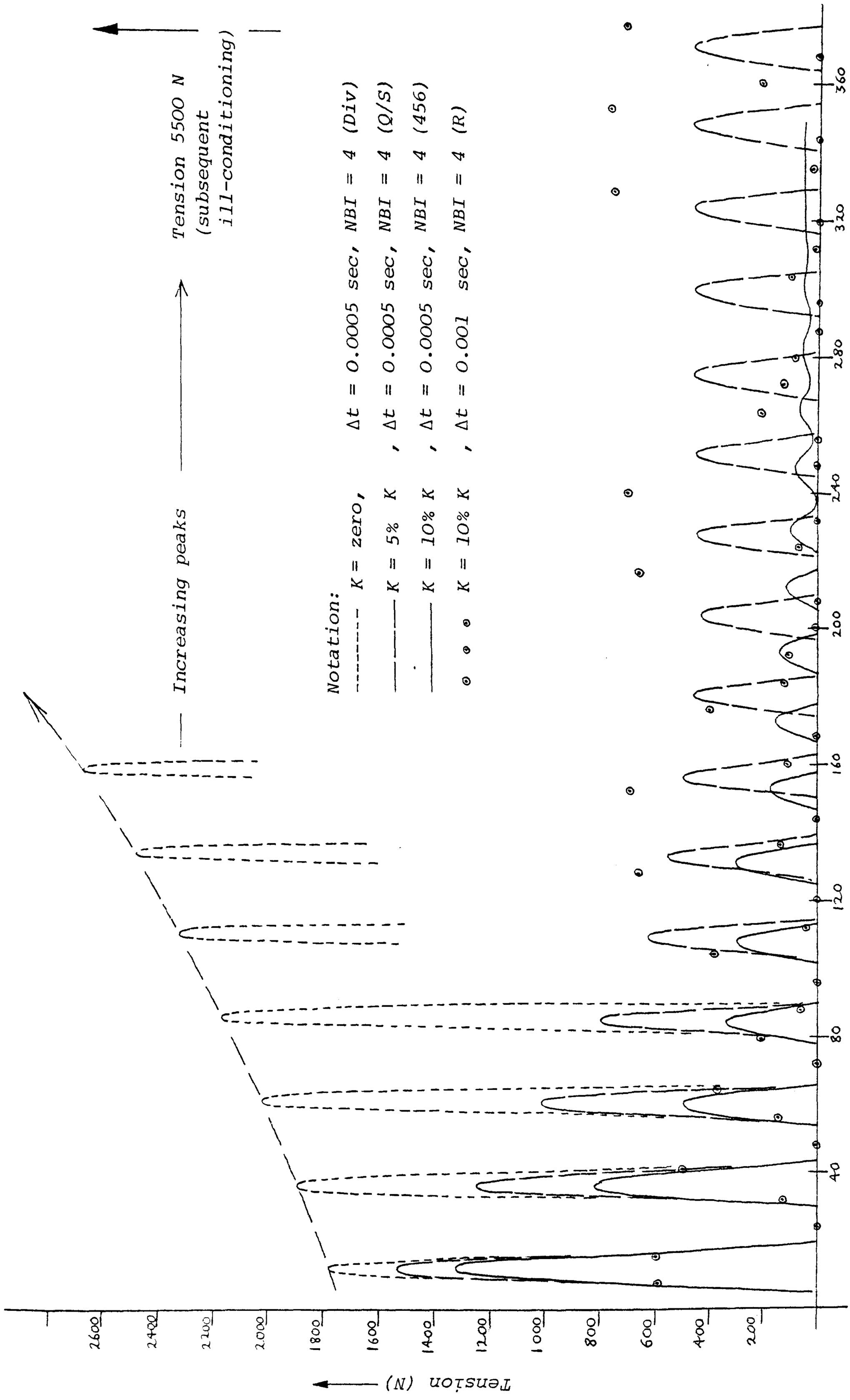

Tension 5500 N
(subsequent
ill-conditioning)
Increasing peaks
Notation:
K = zero, Δt = 0.0005 sec, NBI = 4 (Div)
K = 5% K , Δt = 0.0005 sec, NBI = 4 (Q/S)
K = 10% K , Δt = 0.0005 sec, NBI = 4 (456)
K = 10% K , Δt = 0.001 sec, NBI = 4 (R)
Iterations
Tension (N)

Figure 18

increased to 0.001 sec or damping reduced to 5% k_{crit} the trace does not converge. Similarly with higher values of NBI the solution becomes unstable or diverges. It can be seen from table 1 that when damping is below 50% k_{crit} convergence with Δt approaching the critical value cannot be obtained even when changing material properties at every iteration. On the other hand, with 80% damping convergence is obtained using Δt = 98% Δt_{crit} and checking for buckling at every four iterations. In this case however, a total of only 12 changes in EA values occurred.

(b) Zero Damping; long term trace:

Figure 19 shows the maximum tension variations in cable ④ with the system entirely undamped, following release of initial displacements, for the three cases: Δt = 0.00025, 0.0005, and 0.001 sec, with NBI = 1 in each case. The curves represent only the locus of peak tensions. Zero tensions (slackening) occurred at the intervals marked on the time axis.

For the lowest time interval the locus of peak tensions is fairly smooth. The curve shown, involving a total of approximately 600 property changes in the system, is terminated at 3500 iterations. At this point the tension in cable ④ was 1200N. After a further 7000 iterations the tension is also approximately 1200N, and between 3500 and 10500 iterations the maximum and minimum peak tensions which occurred were 1500N and 1050N respectively. With the time interval increased to 0.0005 sec. the peak tensions vary over a wider range. The tension at the end point of the curve shown, corresponding to 1750 iterations, is T(4) = 2200N. At 3500 iterations cable 4 is subject to the same tension, but between these limits the maximum and minimum peak tensions were 2700N and 1700N respectively. Moreover, for Δt = 0.0005 sec., whilst the average peak tension upto 0.7 sec. of

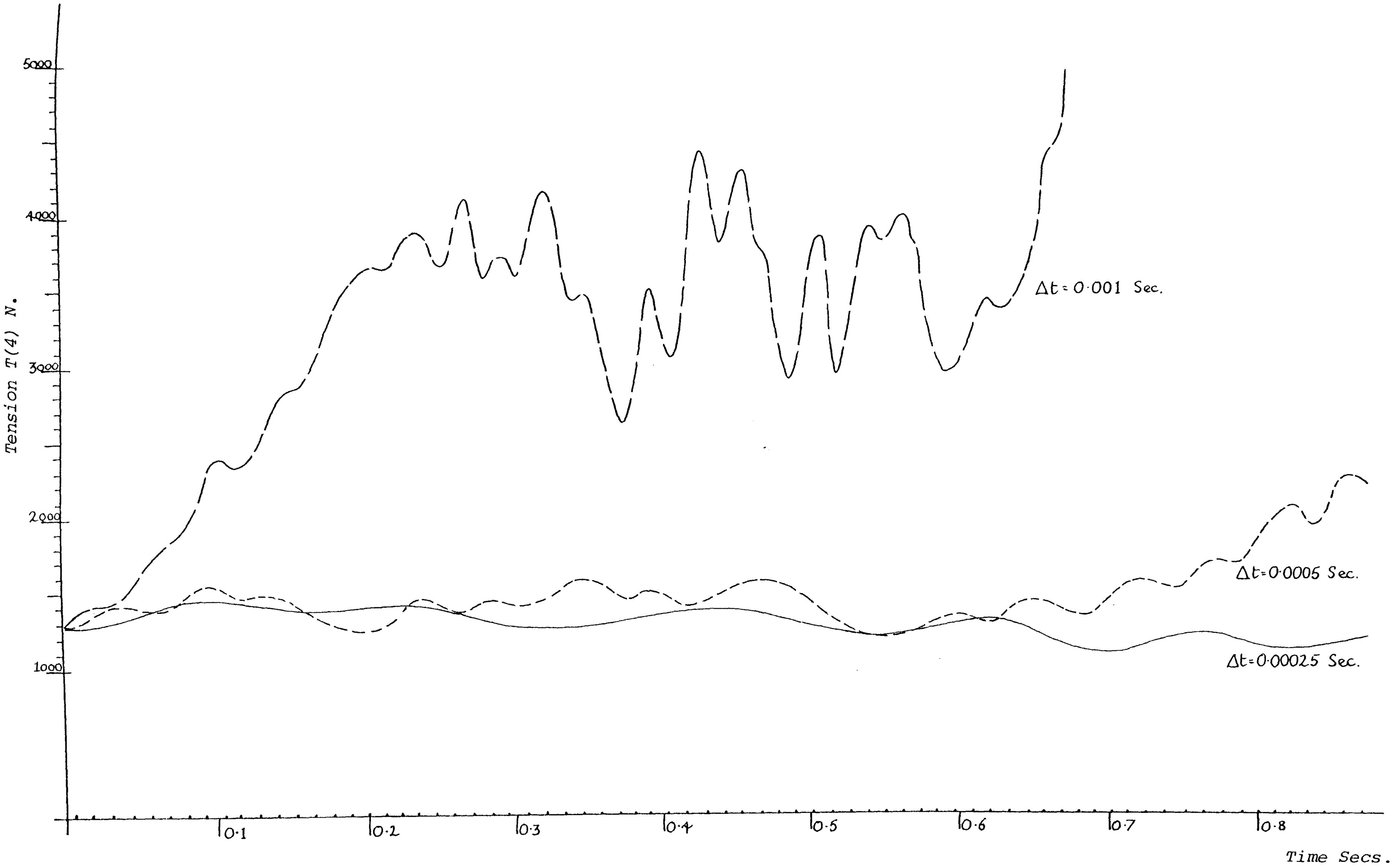


Figure 19 - Locus of Peak Tensions T(4) with Zero Damping

the trace was approximately 1400N, the average between 0.9 and 1.8 sec. was slightly in excess of 2200N. In contrast, for Δt = 0.00025 sec., the average peak tension was approximately 1300N throughout the entire trace up to 2.7 sec. Subsequent checks using much smaller time intervals showed that the latter value was realistic. Thus it appears that in this particular example the maximum time interval that can be used if stress variations are to be followed in the presence of dynamic buckling is less than 1/10 of the elastic critical value.

(c) Applied Loads:

To examine the effect of suddenly applied loads, as opposed to initial displacements, the cable system was subsequently analysed for the same range of time intervals and values of NBI, but with a reduced range of damping factors from 10→40% k_{crit}.

The loads applied at node 1 were:

$$P_x = 500N; \quad P_y = 5N; \quad P_z = 50N$$

The prestress and EA values were the same as for case (a), but under these applied loads the system, when convergent, requires the cable tensions to take the following static values:

$$T(1) = 19.6N; \; T(2) = 502.5N; \; T(4) = 14.6N; \; T(4) = 0$$

Thus it should converge to a buckled state.

Table 2 shows the results for the series of analyses. The convergence pattern is similar to table 1 with permissible values of Δt and NBI increasing with the magnitude of damping.

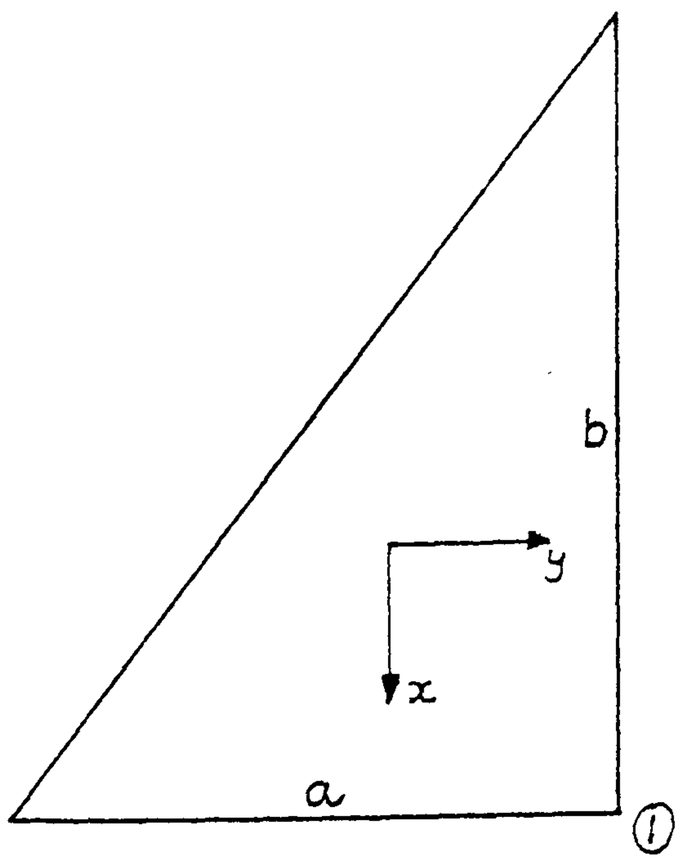
Δt ↓ / NBI →	10% K_{crit}					20% K_{crit}					40% K_{crit}				
	1	2	4	8	16	1	2	4	8	16	1	2	4	8	16
0.00025	620	620	616	624	656	312	312	312	296	304	144	144	144	152	176
0.0005	308	308	308	Q/S	Q/S	156	156	148	152	Q/S	72	72	72	88	Q/S
0.00075	206	198	Q/S	Q/S	Q/S	104	104	108	112	C	48	50	52	64	C
0.001	152	162	Q/S	Q/S	Q/S	78	74	76	Q/S		36	42	44	Q/S	
0.00125	126	122	C	C	C	62	62	56	C		28	30	40	C	
0.0015	104	100	Q/S	Q/S	C	52	52	56	C		24	24	32		
0.00175	88	Q/S	DIV	Q/S	Q/S	44	44	Q/S	Q/S		20	20	32		
0.002	Q/S	C		Q/S	C	36	40	Q/S	Q/S		20	20	Q/S		
0.00225	Q/S	Q/S		Q/S	C	Q/S	42	C	Q/S		19	20	C		
0.0025	Q/S	Q/S		C	C	Q/S	Q/S	C	C		18	20	C		
0.00275	DIV	DIV		C	C	Q/S	Q/S	Q/S	C		31	Q/S	Q/S		
0.003				DIV	DIV	DIV	DIV	Q/S	DIV	DIV	Q/S	Q/S	Q/S	Q/S	DIV

Table 2 - Cable Structure Node Loaded

MEMBRANE STRUCTURE

The membrane structure, the material of which was assumed isotropic when unbuckled, had the same overall geometry as the cable structure in figure 17 except that four triangular elements were used, as shown by the full and dashed lines. The analyses were carried out in the manner described in Chapter 3, with the stress matrix [D] being re-set every NBI time intervals to account for buckling in either of the current principal stress directions. To account for distortion of the elements, matrices [G] were also re-set at the same time stages. This was, in fact, a secondary effect which had little influence on numerical stability, and normally matrices [G] would either remain unchanged or be re-set at very infrequent intervals.

For the single triangular element in figure 20, the in plane direct stiffness of node 1 in the x direction is:



$$S_x = \frac{E.t}{2ab(1-\nu^2)} \left[b^2 \frac{(1-\nu)}{2} + a^2 \right]$$

where ν = Poisson's ratio

For $a = b = 0.2$ and $\nu = 0.3$:

$$S_x = 0.00371\,E \quad N/m$$

Figure 20

Since four similar triangles meet at node 1 in the membrane structure then, neglecting second order terms due to the small element inclinations, the lateral direct stiffness is 0.01484E N/m. Equating this to the lateral stiffness of the cable structure:

$$E = \frac{500000}{0.01484} = 3.37 \times 10^{7} \text{ N/m}^{2}$$

With the above structural properties, the membrane structure was analysed for the same series (a) tests as the cable structure, but with a reduced range of damping factors. The results are shown in table 3. In this structure, provided buckling is checked at every interval, convergence is more readily achieved with higher time intervals although the number of property changes, accounting for buckling in either of the variable principal directions of each element, considerably exceeded the number of changes with equivalent parameters for the cable analyses. In contrast to the cable system, the amount of damping for the range considered had relatively little effect on the magnitude of the time interval at which instability first occurred. For a value of NBI = 4, for example, the maximum stable time interval was 0.001sec. for each value of damping in the range 10→40% k_{crit}. (When, however, the damping was increased to 80% the system was found to converge with Δt = 0.0025 sec.). The generally greater stability of the membrane system may be due to more effective structural triangulation.

Δt ↓ / NBI →	10% K_{crit}					20% K_{crit}					40% K_{crit}				
	1	2	4	8	16	1	2	4	8	16	1	2	4	8	16
0.00025	808	808	816	1120	Q/S	400	400	400	416	512	204	204	204	208	208
0.0005	376	376	384	Q/S	DIV	188	188	188	224	224	92	92	92	104	Q/S
0.00075	244	244	448	Q/S		122	116	128	Q/S	144	60	60	60	Q/S	C
0.001	176	176	216	DIV		86	86	92	C	Q/S	44	44	44	C	C
0.00125	144	148	Q/S			68	66	Q/S	C	C	32	34	Q/S	C	C_{nb}
0.0015	112	144	Q/S			56	58	Q/S	C	C	26	28	Q/S	C	
0.00175	100	136	R			44	52	Q/S	C	C_{nb}	24	20	C	C_{nb}	
0.002	76	124	C			42	36	C_{nb}	C_{nb}		20	16	C_{nb}		
0.00225	76	Q/S	C			38	Q/S	C	C		16	16			
0.0025	72	Q/S	C			36	Q/S	C	C		16	Q/S			
0.00275	60	Q/S	DIV			28	Q/S	C	C_{nb}		30	Q/S	C	C	
0.003	K	DIV				Q/S	R	R	DIV	DIV	Q/S	Q/S	Q/S	R	DIV

Table 3 - Membrane Structure Node Displaced

MASS COMPONENTS

For the previous examples, the mass components were assigned values such that the frequencies of vibration in each co-ordinate direction, and consequently the critical damping, would be of the same order of magnitude. In a real dynamic analysis, however, lateral masses, and the corresponding proportional damping, could not be artificially increased in order to reduce the critical damping and frequency of lateral motion which governs the rate and number of property changes. If the actual nodal mass had been equal to the smaller vertical component, and the same damping factor was applied to each component of motion, the critical time interval and the degree of lateral damping would have been very much less.

Real damping in clad tension structures may be due to a number of factors[15]:

(1) Air damping (usually very light but perhaps significant for wide-span surface structures[16])

(2) Friction effects at joints and in steel cables or ropes.

(3) Strain-rate dependent damping in cables and cladding due to creep and visco-elastic effects.

Factors (1) and (3) are considered in Chapter 6 which concerns the decay of vibrations in a pneumatic dome subject to a suddenly applied dynamic load, the structural material being idealized as a "standard anelastic model"[15]. The numerical procedure, described in Chapter 5,

accounts automatically for close-coupled (material) damping dependent on relative velocities of adjacent nodes, and far-coupled (air) damping dependent on absolute nodal velocities normal to the surface. If visco-elastic sandwich or membrane cladding is chosen to provide high damping of unwanted vibrations, the damping of motions tangential to the surface of a structure should be very much greater than damping normal to the surface. The possible problems of numerical instability in transient dynamic analyses involving intermittent buckling of elements might thus be alleviated in real physical situations.

COMPOSITE CABLE AND MEMBRANE STRUCTURE

The two previous examples, particularly the cable structure, were severe tests of numerical stability since buckling of the elements, particularly in combination, created unrestrained degrees of mechanical freedom. In more complex arrangements involving a combination of cladding and cable elements, the structure (even though buckling of several components may occur at any stage) has a greater chance of being properly triangulated throughout a dynamic trace. Also, with a greater number of nodes, the higher frequency components might not be induced by most loading conditions.

The structure shown in figure 20 has 12 cable elements and 14 membrane elements. Nodes 1→4 are active and nodes 5→12 are fixed support points. Although again a simple structure, it illustrates the greater numerical stability which results from composite action.

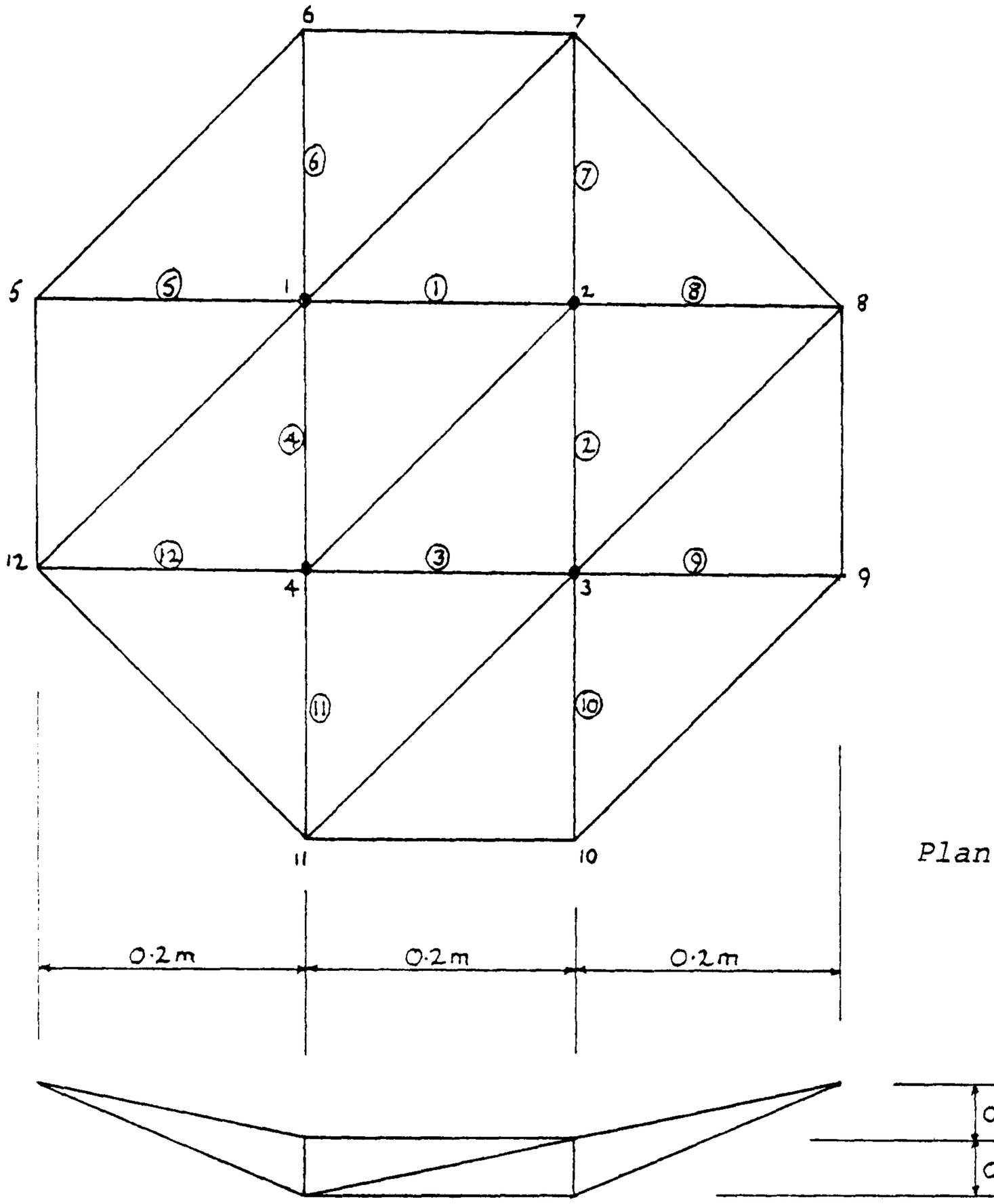


Figure 20

Under the condition of no applied loads, the pretension in all cables was 50N, and the stress in membrane elements was zero. The active nodes were assigned mass components of 1.0kg for each co-ordinate direction, and the values of EA for the cables and $Et/(1-\nu^2)$ for the membrane were the same as those used in the previous examples; giving a critical time interval, assuming elastic behaviour, of 0.00168 sec.

Loads of + 50N and -50N were suddenly applied at nodes 1 and 3 respectively and the behaviour of the structure, with no damping, was

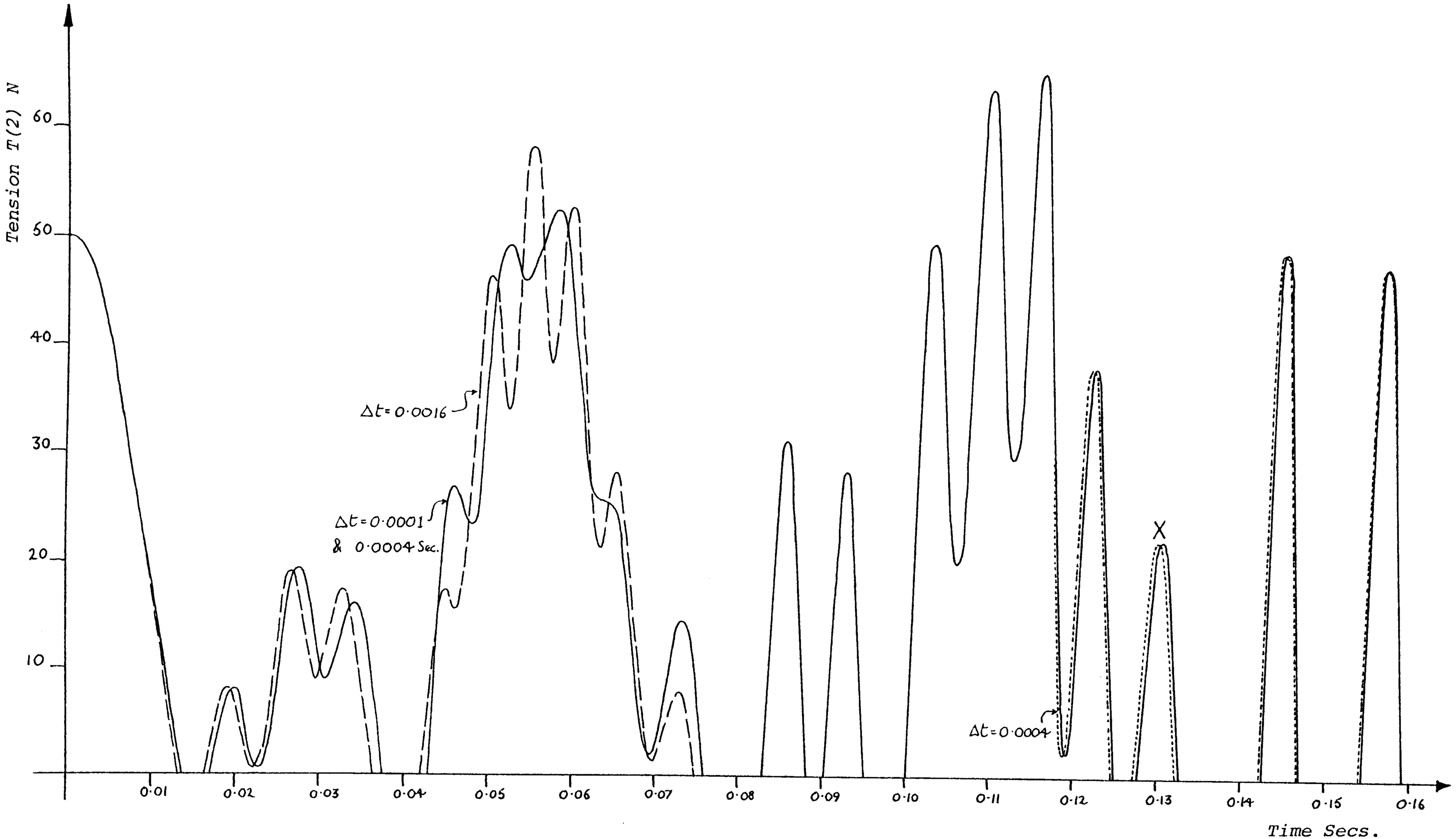

Tension T(2) N
60
50
40
30
20
10
Δt = 0·0016
Δt = 0·0001
& 0·0004 Sec.
Δt = 0·0004
X
0·01
0·02
0·03
0·04
0·05
0·06
0·07
0·08
0·09
0·10
0·11
0·12
0·13
0·14
0·15
0·16
Time Secs.

Figure 21

traced for time intervals ranging from 0.0001 to 0.0016 sec., with buckling checks at each time step. Figure 21 shows the variation with time of the tension in cable link ② for three of the cases considered. The differences between the traces for $\Delta t = 0.0001$ and $\Delta t = 0.0004$ sec. were insignificant up to approximately 0.11 sec. Thereafter the maximum recorded difference occurred at point x (0.13 sec.), by which time 226 membrane property changes and 48 cable property changes had taken place. Results of similar accuracy were obtained for time intervals up to 50% of the critical value. In view of the fact that no damping was applied, and the loads were sufficient to cause buckling in both the cables and the membrane, the system has far greater numerical stability than the previous examples.

A review and comparison of the central difference method and other explicit and implicit methods for non-linear dynamic analysis is given in appendix C (pp 344-370).

REFERENCES

(15) Lazan, B.J., "Damping of Materials and Members in Structural Mechanics", Pergamon Press, 1968

(16) Jensen, J.J., "Dynamics of tension roof structures", Int. Conf. on Tension Roof structures, London 1974.

(see also review and references in Chapter 1)

CHAPTER 4

FORM-FINDING OF MINIMUM SURFACE MEMBRANES

SUMMARY

The application of Dynamic Relaxation to the form-finding of minimum surface membranes with tensile or compressive funicular boundaries is illustrated; particular attention being given to sensitive problems involving neutral equilibrium or quasi-instability. For simplicity in examining concepts, a series of plane membranes and subsequently spatially curved uniform stress membrane and pneumatic structures are considered; most of which are generated from the same initial topology.

The chapter was presented as a paper at the IASS Congress on Structures for Space Enclosure at Montreal in July 1976.

THE BASIS OF DYNAMIC RELAXATION

The physical basis of DR is essentially the step by step solution, for small time increments, of Newton's second law of motion for each node of a structure with an imposed viscous damping; the motion of the structure being traced from a specified initial (or unloaded) condition to its position of static equilibrium. The equation governing this motion at any node in each co-ordinate direction is thus:

Residual Force = Nodal mass x Acceleration

where the residual force is the sum of the resolved components of member forces, applied load and damping force. Equations of this type, expressed in interlacing finite difference form, are followed simultaneously for all nodes; displacements and member forces being determined at the end of each time interval and velocities at mid-intervals until steady equilibrium of the entire structure is obtained. Typical traces for deflection components are shown in figure 1. The rate of convergence is governed by the choice of time step and damping factor. Ideally deflection components should be nearly critically damped, and in order to achieve this, fictitious masses which vary from node to node and each co-ordinate direction may be used. For tension structures the selection of these factors is considered in ref. 3 together with a more detailed account of computational procedures.

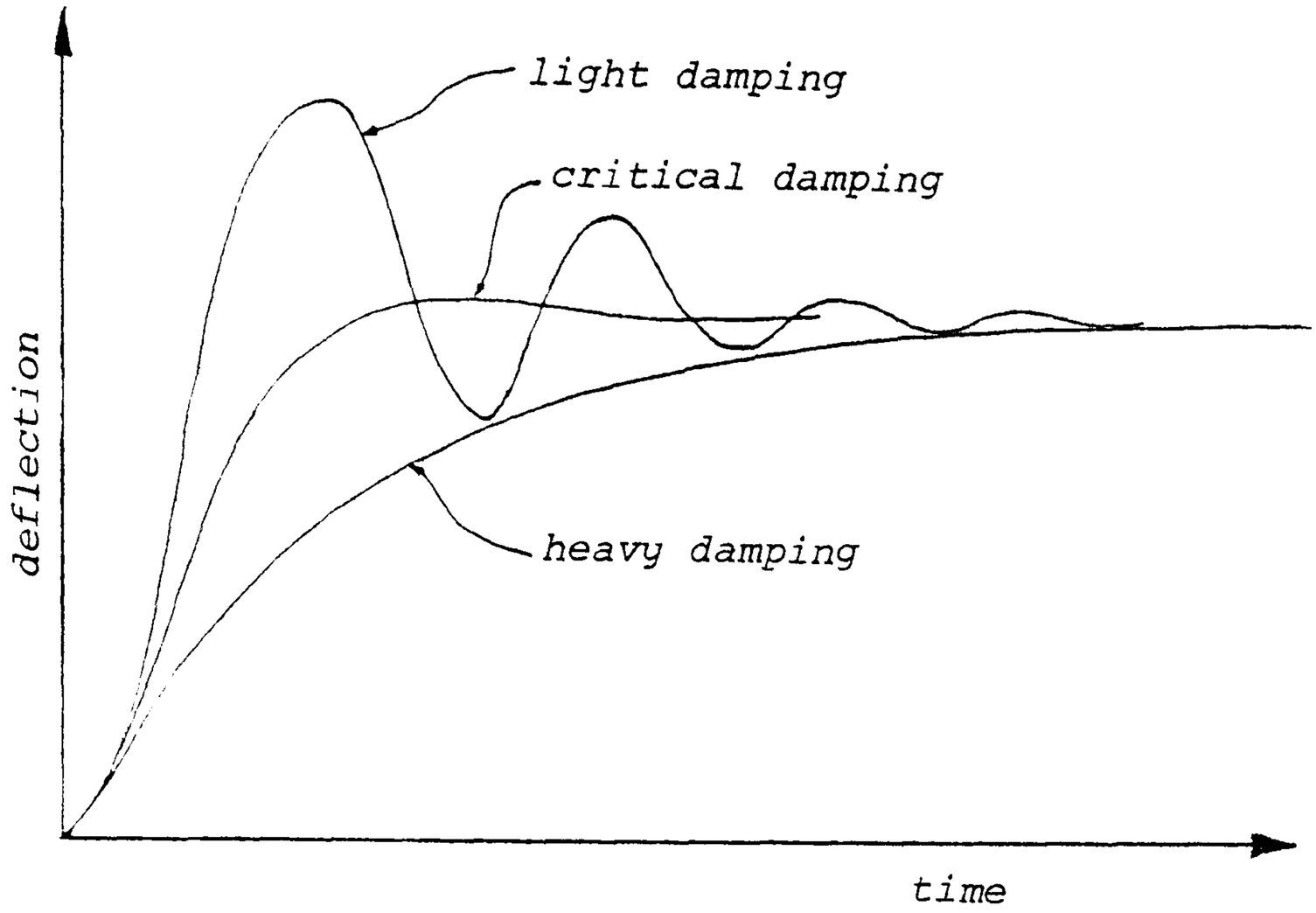


Figure 1

APPLICATION TO FORM FINDING

The basic topology of a structure or family of structures to be investigated may be idealized as a series of nodes interconnected by links. For open panel space or net structures the links are bar or cable elements and for membrane surface structures the links form edges of panels. In this chapter triangular elements with straight edges are used in order to reduce core store to a minimum and eliminate complex transformation in the iterative analysis. The use of such elements is also appropriate when dealing with a uniform state of stress.

At any stage of the analysis the tensions acting along triangular element edges are given by:

$$\{T\} = \{T^o\} + [K^e] \cdot \{e\}$$

where $\{T^o\}$ is the vector of side tensions statically equivalent to the specified prestress in the element.

$\{e\}$ is the vector of current side extensions.

$[k^e]$ is the current natural 3 x 3 elastic stiffness of the element.

In form-finding applications geometry may either be controlled elastically, with $\{T^o\}$ zero and $[k^e]$ non-zero, or by holding the prestress at a specified value with $[k^e]$ set to zero; the latter control being used for the generation of minimum surface membranes.

The tension in a cable link is given at any stage by: $T = T^o + S.e$ where T^o is the pretension, S the stiffness (=EA/L) and e the current extension. Again, the development of the geometry is controlled either elastically ($S \neq 0$) or by specified constant tensions ($S = 0$). In form-finding by elastic control it is not necessary that the real stiffness be used, and in fact the use of fictitious EA values greatly extends the possible family of structures which may be generated from the same initial topology. The determination of uniformly stressed membranes with boundaries which are either tension cable or funicular compression curves presents no problems of compatibility irrespective of the type of control used for the edge links. In order to derive compression boundaries, edge links are given either negative stiffness or negative T^o values and residual forces at edge nodes are reversed at each stage in the analysis; such boundaries are thus effectively determined as tension funiculars to the reflected image of the membrane surface.

PLANE UNIFORM STRESS MEMBRANES

The examples considered in this section may all be verified analytically but, though trivial, they illustrate the stability of the numerical analysis in dealing with problems of neutral equilibrium with non-unique solutions.

If the element shown in figure 2 is subject to a uniform stress, σ, the forces at the apex nodes required to equilibrate the stress on side i are $\sigma t \ell_i/2$ where t is the membrane thickness. The resultant of the membrane stress at any node j acting perpendicular to the opposite side is thus $Q.\ell_j$ (where $Q = \sigma t/2$). Alternatively, and more conveniently for programming purposes, the equivalent tension along any side j is given by $T_j^\circ = Q.\ell_j/\tan\alpha_j$.

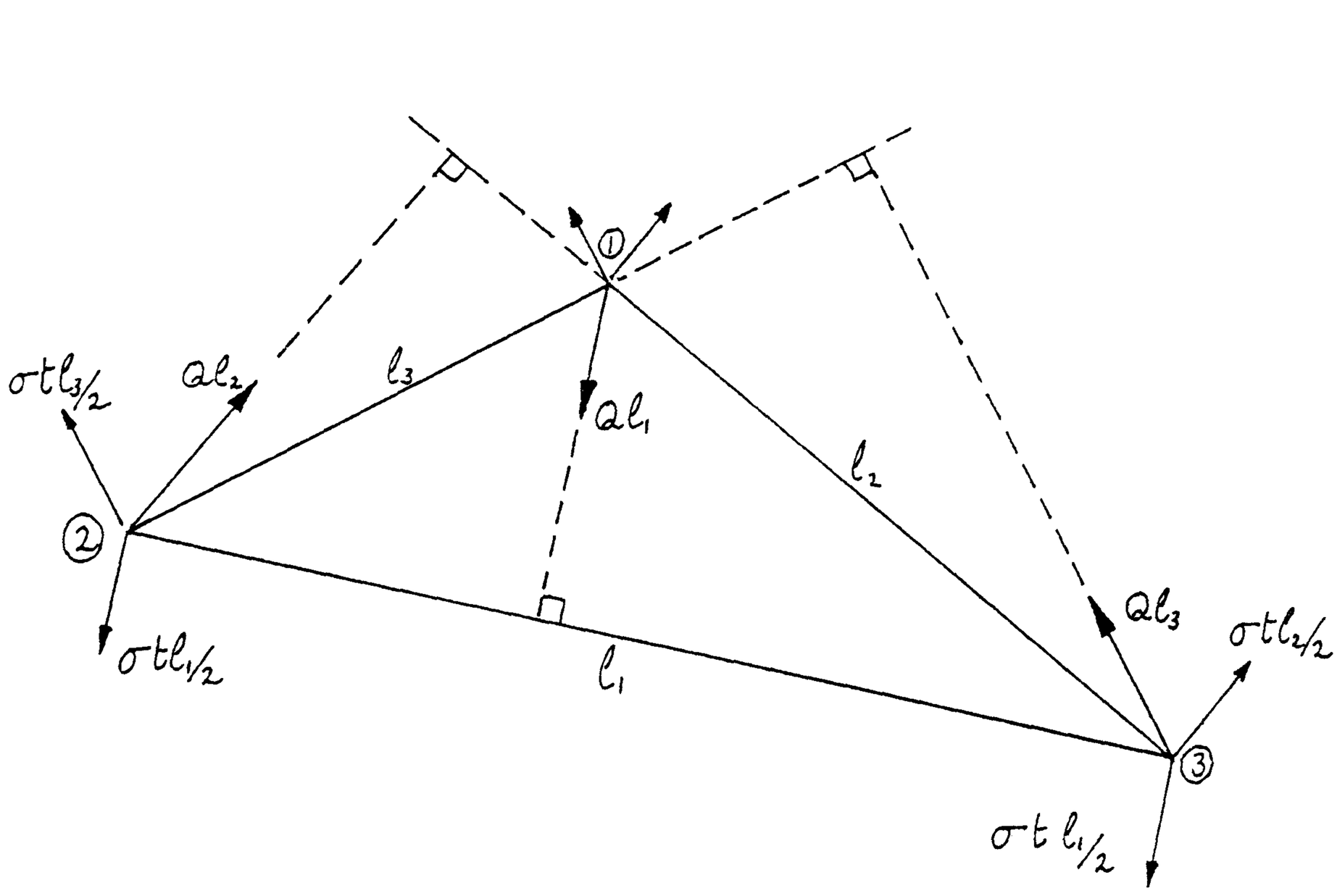


Figure 2

Considering a plane subdivision of such elements (fig.3a) the closed polygon of external edges of a connected group represents a reciprocal diagram of forces [1] for the equilibrium of the interior node I; the node, if static, being in equilibrium whatever its position within the polygon. If one of the edges (length b) belongs to a boundary structure not in equilibrium with the membrane and the motion of this boundary causes collapse and inversion of the adjacent triangle (fig. 3b) the node I is immediately subject to an out of balance force (2Qb') which restores the correct topology of the subdivision. Depending on the fineness of the subdivision and the magnitude of the viscous damping of node I, other nodes (J,K,L etc.) may also become disturbed; the process propogating throughout the surface subdivision if damping is light by successive collapse and expansion of the triangular elements until static equilibrium of the entire membrane and boundary is achieved.

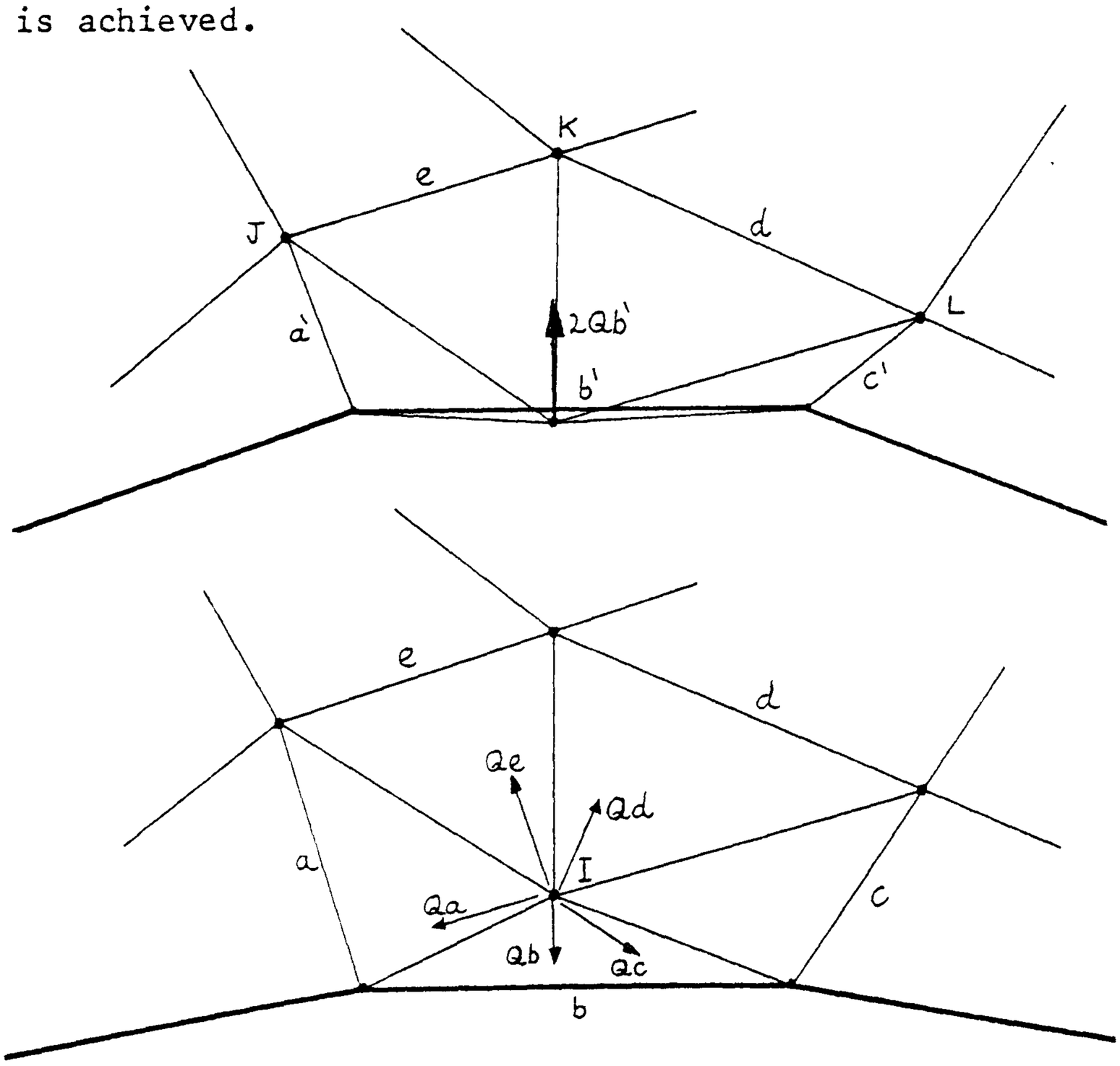


Figure 3b

Figure 3a

Figure 4 shows the initial subdivision of a perforated plane membrane with internal and external cable boundaries. For specified cable forces or stiffnesses and membrane tension, the radii of curvature of the edge cables and inner cable loop have a particular solution but the loop may take any position within the membrane. The state of the membrane at 20 and 160 iterations is shown in Figs. 5a and 5b respectively; the latter being fully converged; (the limits used for all examples are: tensions accurate to ±0.001% of true values; deflections ±0.001% of average link length). The following parameters were used in the analysis, and unless otherwise stated have been used for all subsequent structures considered:

Uniform membrane tension 2500 N/m

Edge node masses M = 0.2 kg } for motion in each
Surface node masses 0.02 kg } co-ordinate direction

Time interval Δt = 0.0008 sec

Viscous damping at any node i = M .K'/Δt

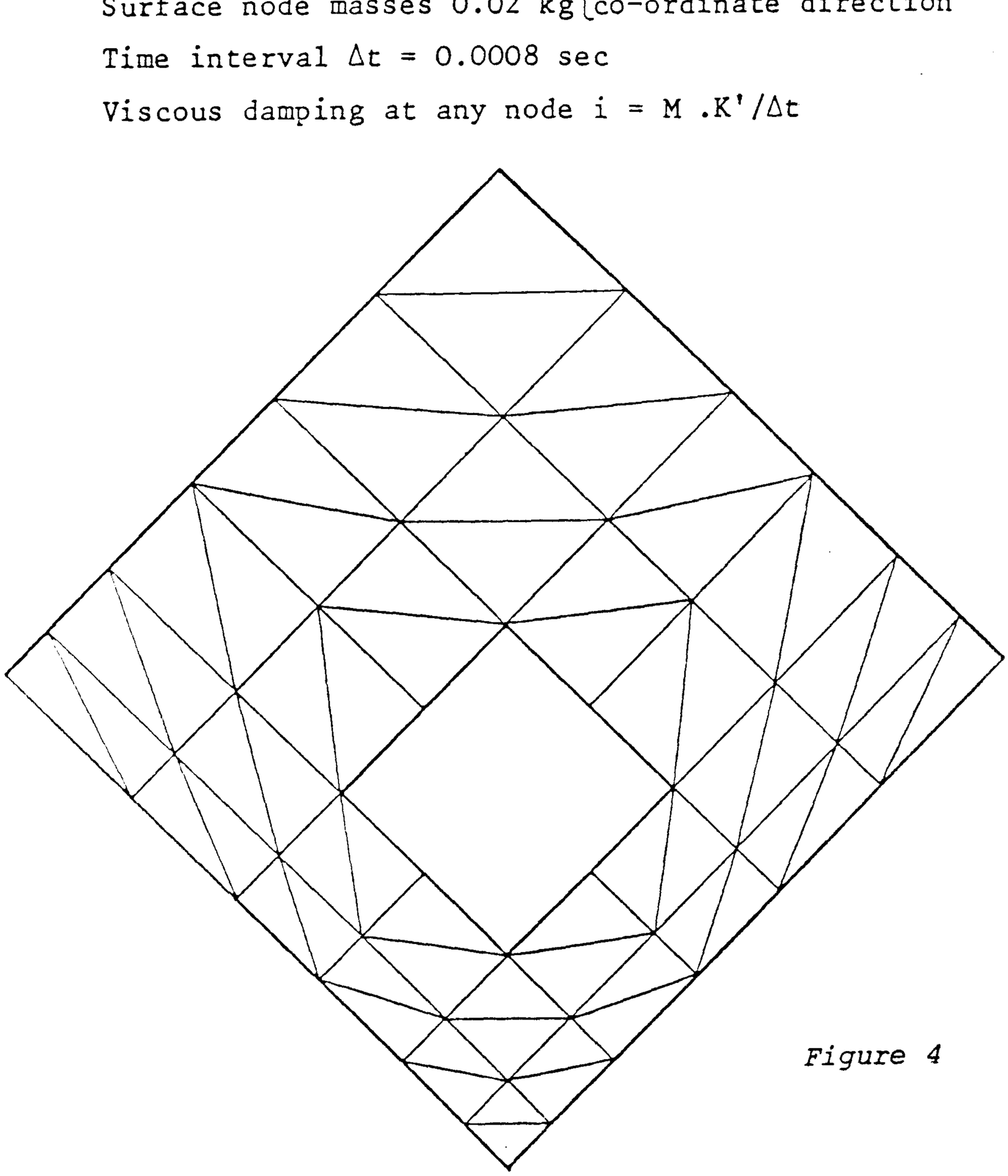


Figure 4

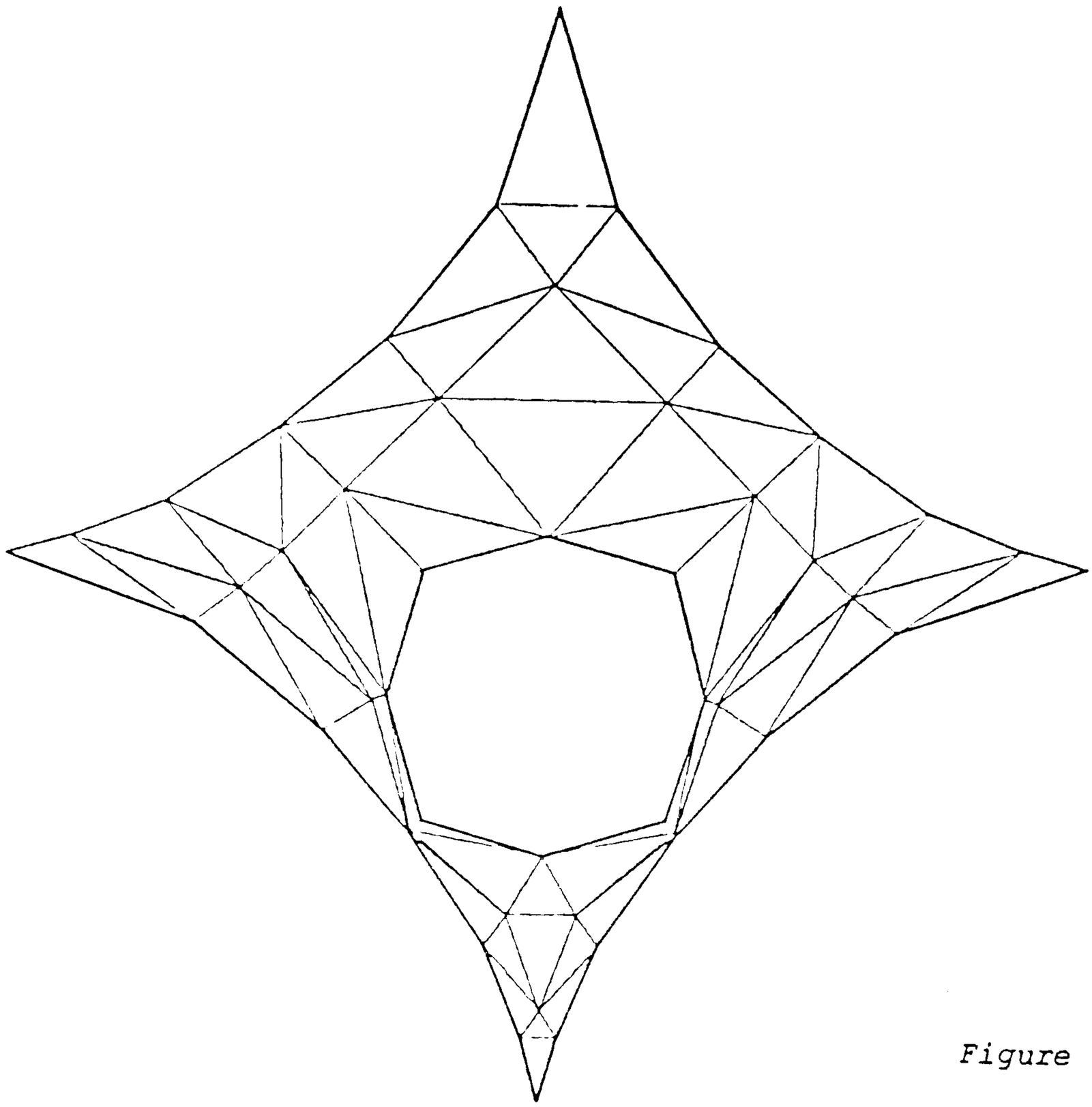


Figure 5a

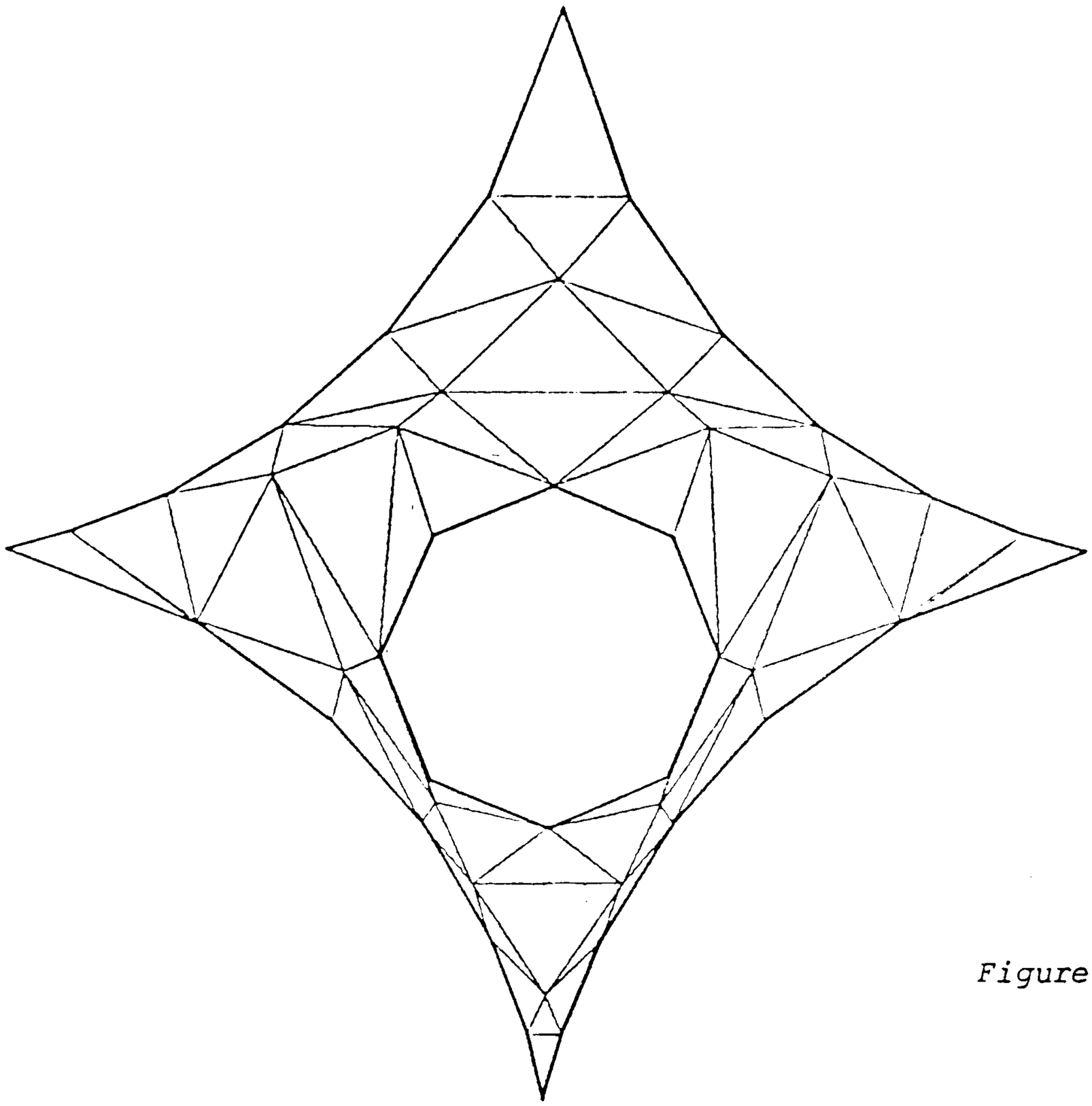


Figure 5b

Boundaries were elastically controlled with assumed EA values of 100 kN for all cables, and the overall damping factor, K', was 0.12. It can be seen that collapse of most of the triangles has taken place, with only three nodes (marked *) remaining undisturbed; the converged solution is, however, symmetric about the y axis. For lower damping factors this may not be so: figure 6 shows the result using a damping factor of 0.10. Prior states of this structure, showing gross disturbance of the geometry are shown in appendix 4.1

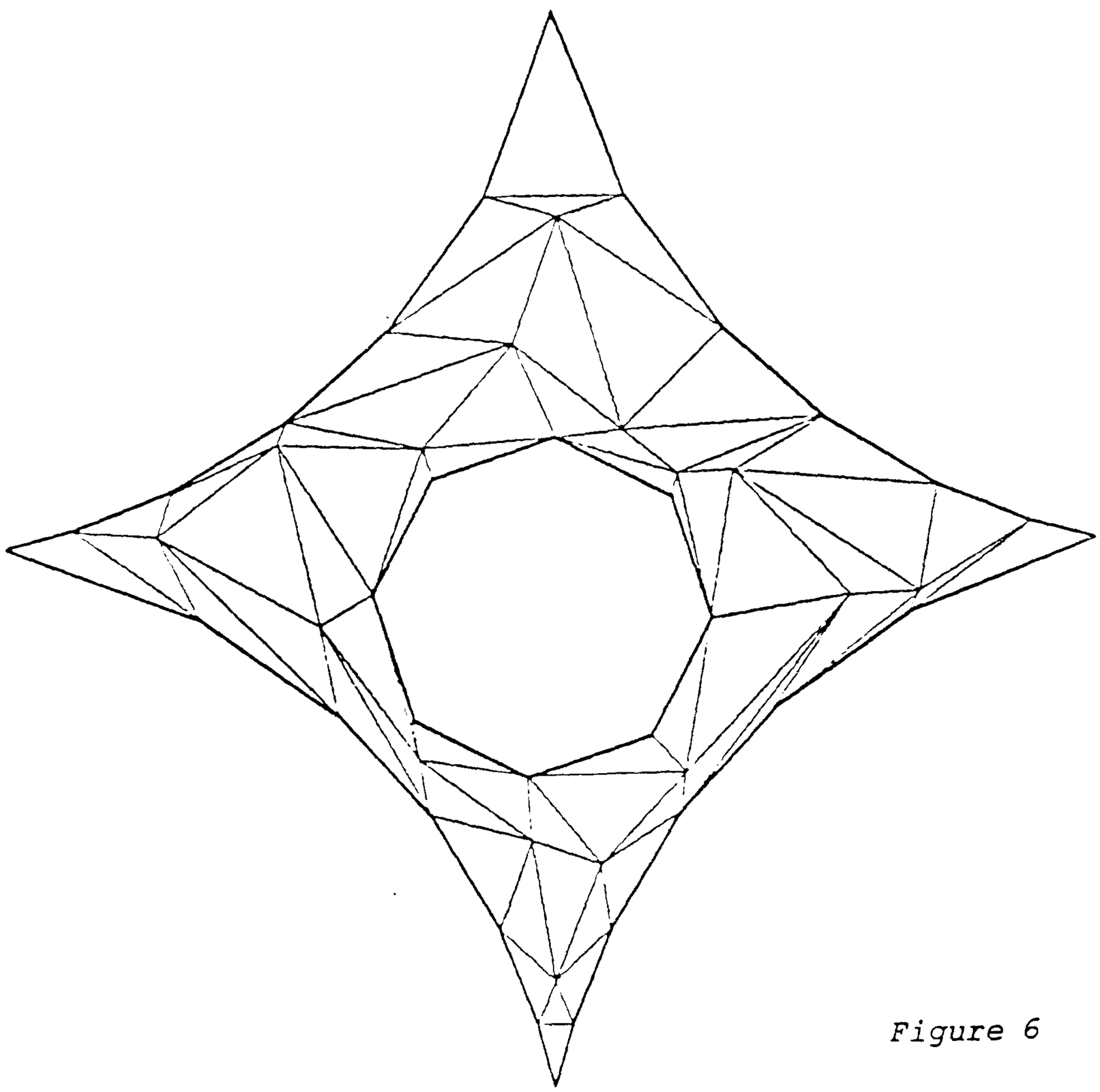


Figure 6

Although the iteration process is simultaneous and should, if calculations are precise, lead to symmetric solutions, computer round-off errors are sufficient to induce lack of symmetry. This

happens when a triangular element is just at the stage of inverting; the expression used for the side lengths ($T_i^o = Q.\ell_i/\tan\alpha_i$) being ill-conditioned when one of the apex angles is very small. In rare cases this could lead to divergence of the analysis and to avoid this a conditioning process is used. A satisfactory procedure is to adjust the side lengths of any triangle containing a very small apex angle according to:

$$L_i = L_i + 0.00001 \times (ASL - L_i)$$

where ASL is the average side length.

The membrane results discussed above give identical edge geometry and cable tensions, and all cable nodes lie precisely on circular arcs with a maximum variation in link tensions along any side of $\pm\frac{1}{2}\%$. If instead of controlling boundaries elastically, the external cable tensions are held constant throughout, the solutions obtained are similar except that the cable links become identical in length. It is not possible to use specified constant tensions to control the internal cable since, unless at least two of the cable nodes are rigidly or elastically constrained, the loop would either contract to a point or expand to the outer boundaries.

The membrane shown in figure 7 has a funicular compression boundary, derived in the manner previously outlined using EA values of -75 kN, a damping factor of 0.2, and starting from the same initial geometry (fig.4). Both boundaries are 'free' and in neutral equilibrium in the sense that no point was fixed with respect to any datum. Convergence was more rapid than the cable edged membrane since there was no disturbance of surface nodes between the boundaries.

As in the case of the tension loop, the compression outer boundary can only be controlled by initially specified link compressions if some parts of the boundary are elastically controlled.

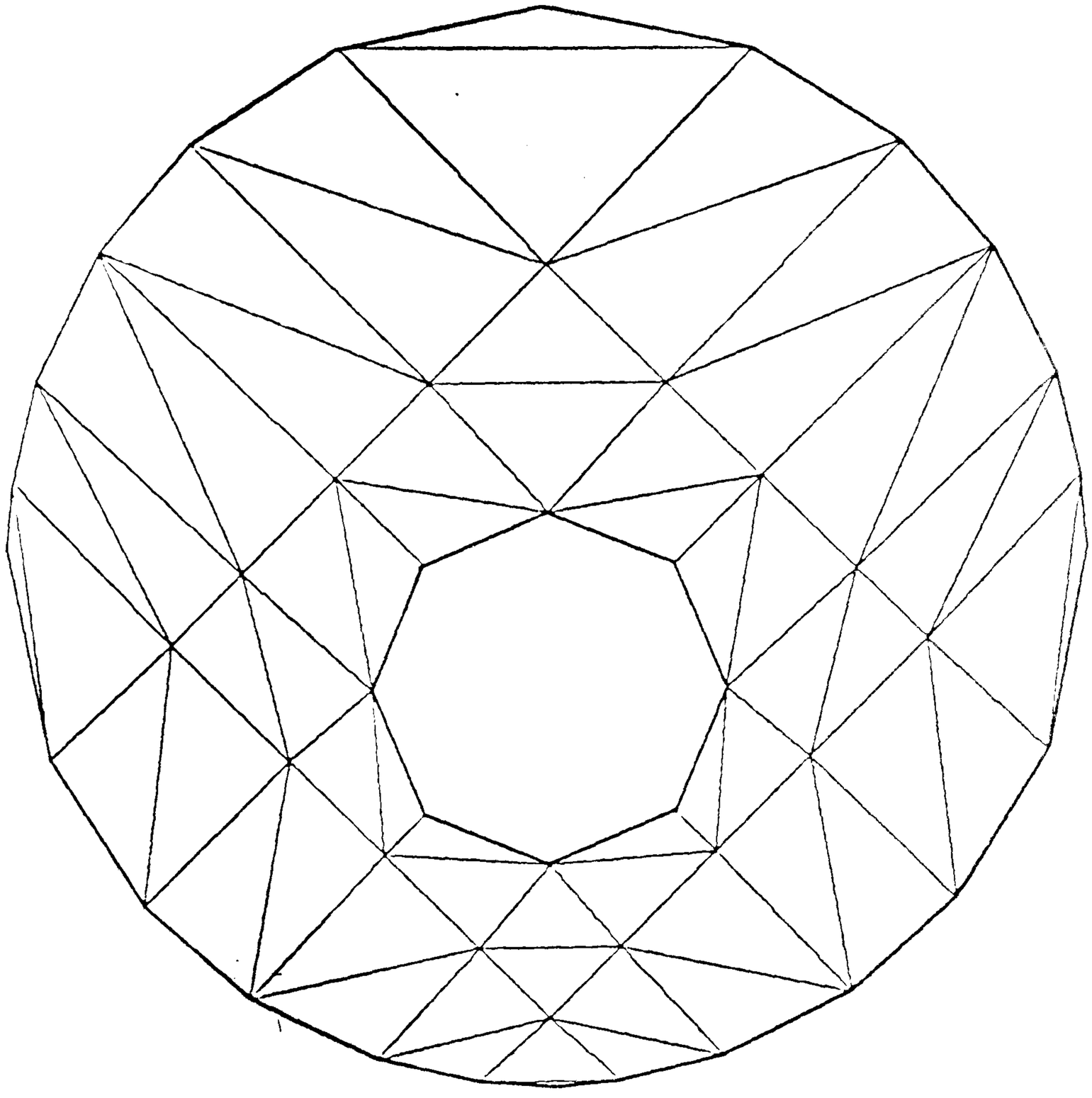


Figure 7

NON-CIRCULAR BOUNDARIES

Figure 8 represents a uniformly stressed membrane in equilibrium with tension boundary links AB, BC, CD, etc.

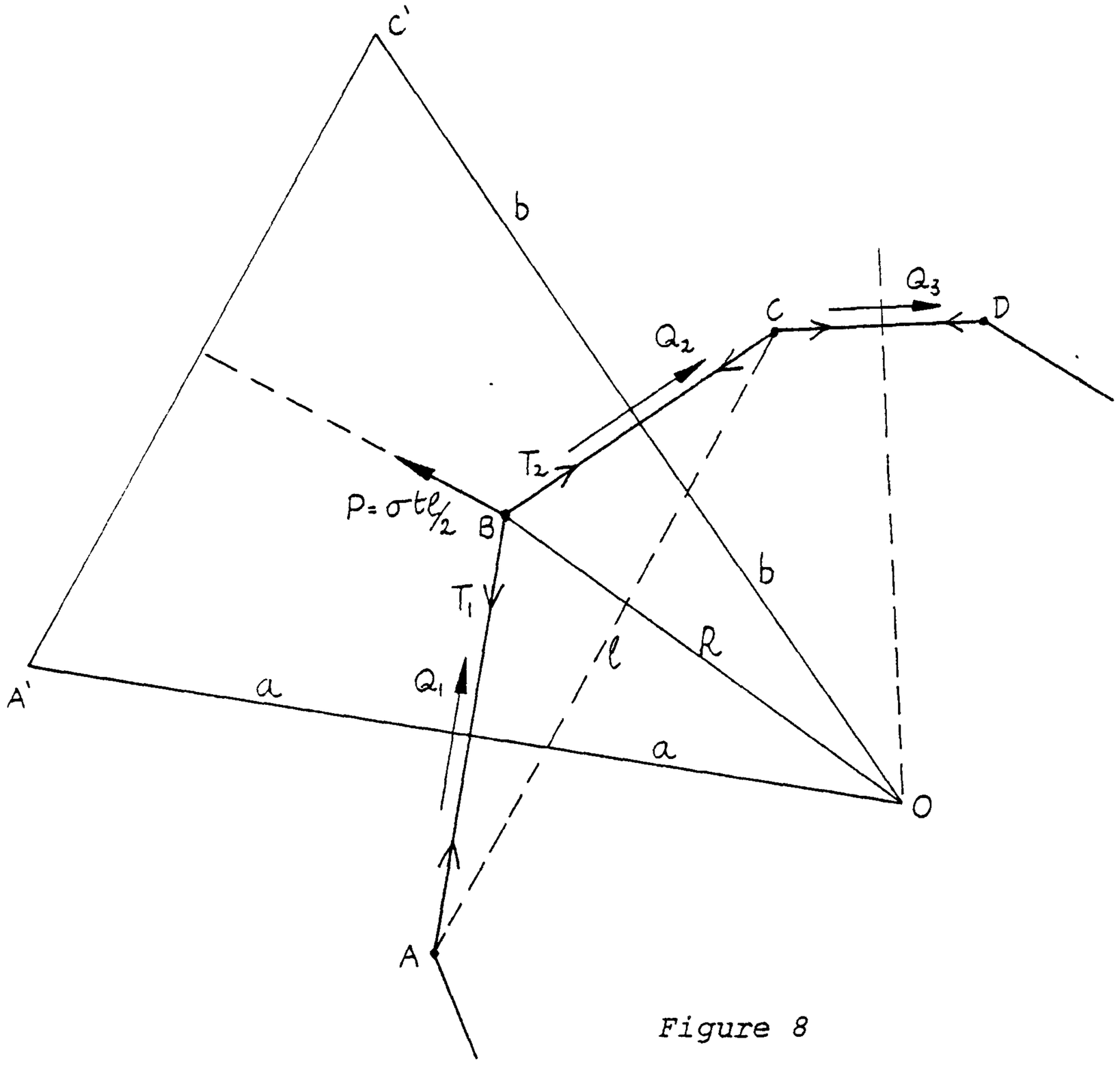


Figure 8

The resultant (P) of the nodal forces acting at B due to the membrane stress (σ) acts perpendicular to the chord AC and is equal to $\sigma t\ell/2$. Constructing perpendiculars A'O and C'O such that they bisect and are bisected by AB and BC respectively, it can be seen that A'C'O is a reciprocal diagram for the equilibrium of boundary forces T_1 and T_2 with the stress resultant P. Hence:

$$T_1 = a\sigma t; \quad T_2 = b\sigma t$$

Further, if a series of boundary links is considered, all nodes B, C, D etc. must lie on the same circular arc of radius R and centre O. For boundaries with a specified uniform tension or compression the length of all edge links AB, BC etc. must become identical for equilibrium; whilst for elastically controlled boundaries forces will vary slightly in accord with the above relations.

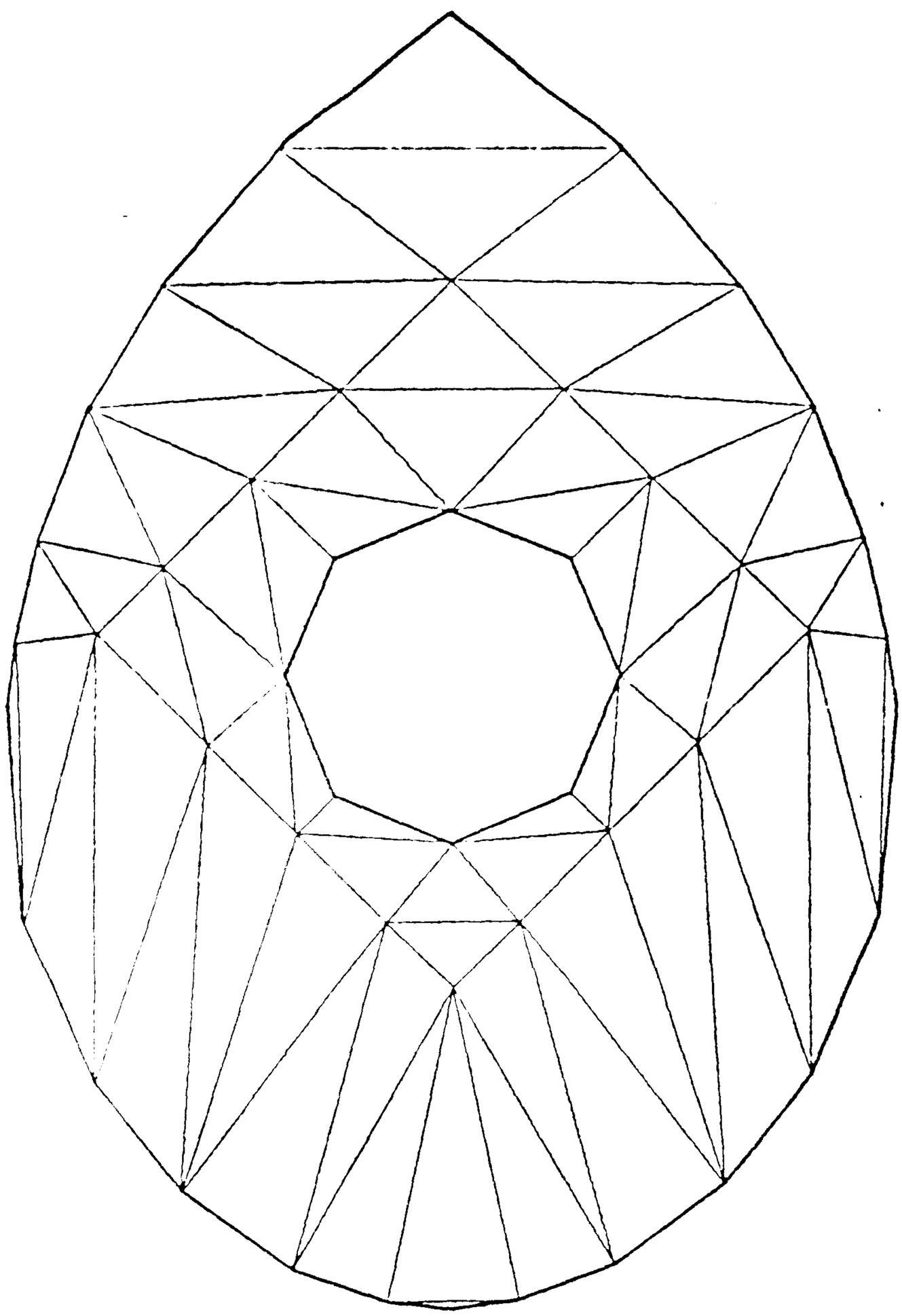


Figure 9

If traction forces Q are applied such that there is a force gradient in edge links, the radius of curvature may vary along the boundary. Figure 9 shows the result using a specified force

gradient of 500 N in each edge link but otherwise controlling the boundary elastically with EA values of -50kN. The solution shown has one fixed boundary point, though it is possible to derive a considerable variety of non-circular furnicular support curves (fig.10); including 'free' boundaries and combinations of tensile and compressive sections containing points of contraflexure at which concentrated traction forces are applied. In practical applications, for which spatial membranes would be required, distributed traction forces may be applied to the boundary by shear walls.

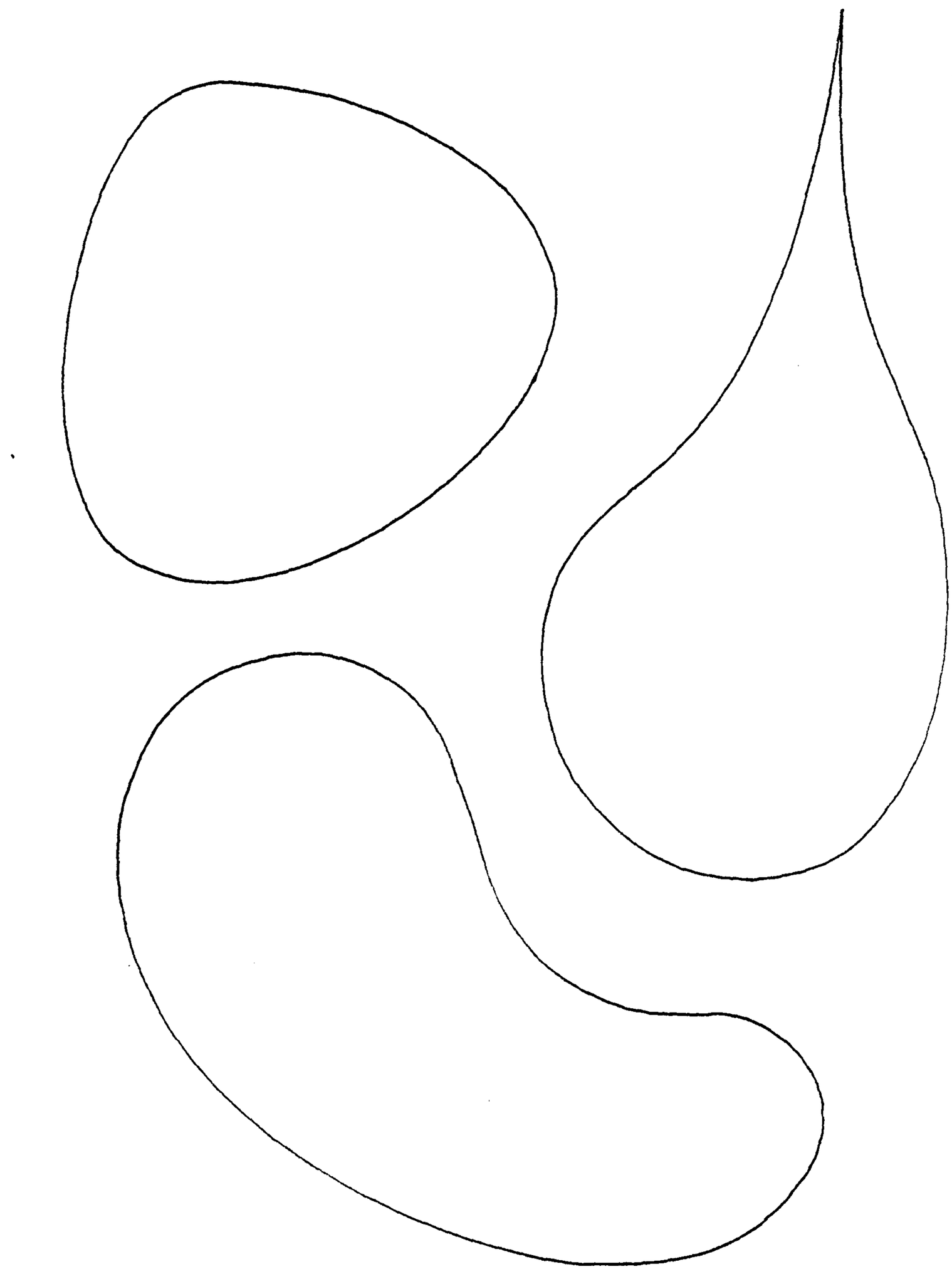


Figure 10

MINIMUM SURFACE SPATIAL MEMBRANES

The concepts outlined in the previous sections apply in a similar manner to doubly curved uniformly stressed membranes; the imposition of uniform stress giving rise to minimum surface solutions. Provided that curvature exists throughout the membrane the solution for a given subdivision and boundary conditions will either be damped to a unique result or oscillate with small deviations about a unique equilibrium position, but without decay due to viscous damping. The latter occurs when the required position of one or more nodes leads to a continuous process of inversion and restoration of particular elements. This situation, which has been termed quasi-instability, indicates that a local change in topology is required, but the overall solution is not invalidated.

The form of minimum surface membranes is dependent, for a given topology, solely on the boundaries and positions of support points, and an infinite family of surfaces can be generated from the same topology. Support nodes may either be fixed at their initial positions or be given specified displacements from these positions. Alternatively the magnitudes and directions of reactions may be specified. All nodes of the structure, including support nodes, are treated analytically as active nodes, and in order to provide restraints in one or more co-ordinate directions the corresponding mass components are assigned very large values. This is convenient when using interactive graphics to investigate a variety of support conditions; the fixing and releasing of supports being controlled by the assigned masses and loads applied to reposition them. The rate at which the structure changes may similarly be controlled by varying

the viscous damping and mass components, together with the elastic stiffnesses of edge links; and during this process the curvature of funicular boundaries may be adjusted by altering specified tensions or compressions in control links and any traction forces which may be applied. The use of such interactive controls is considered in Chapter 7 (ref. 4).

Using the previous initial subdivision, but with the length of all cable links made identical as shown in figure 11, a vertical load of 2300 N was applied to the inner cable at node P. The reaction in the horizontal plane at each of the edge nodes marked L and H was specified as 7000 N and the inclination between adjacent reactions was held constant at 60°. The mass components (0.2kg) in each co-ordinate direction were the same for all cable nodes except that the nodes marked L were assigned vertical mass components of 10^{10} kg to prevent only the motion in that direction.

The state of the structure after 120 iterations is shown in figures 12a and 12b. The membrane is almost stable, but the nodes marked A are oscillating with small amplitudes which are not decaying since the edge lines through these two points in fact contain collapsed triangular elements; this situation being expected because of the choice of initial topology. After a few more iterations the membrane elements adjacent to the inner cable links marked B invert and thereafter continue to oscillate in a state of quasi-instability. The system is neither unstable nor, in spite of the viscous damping, does it ever become completely stable without the necessary modifications to the topology. The effect of the oscillating nodes on the overall geometry is however extremely small:

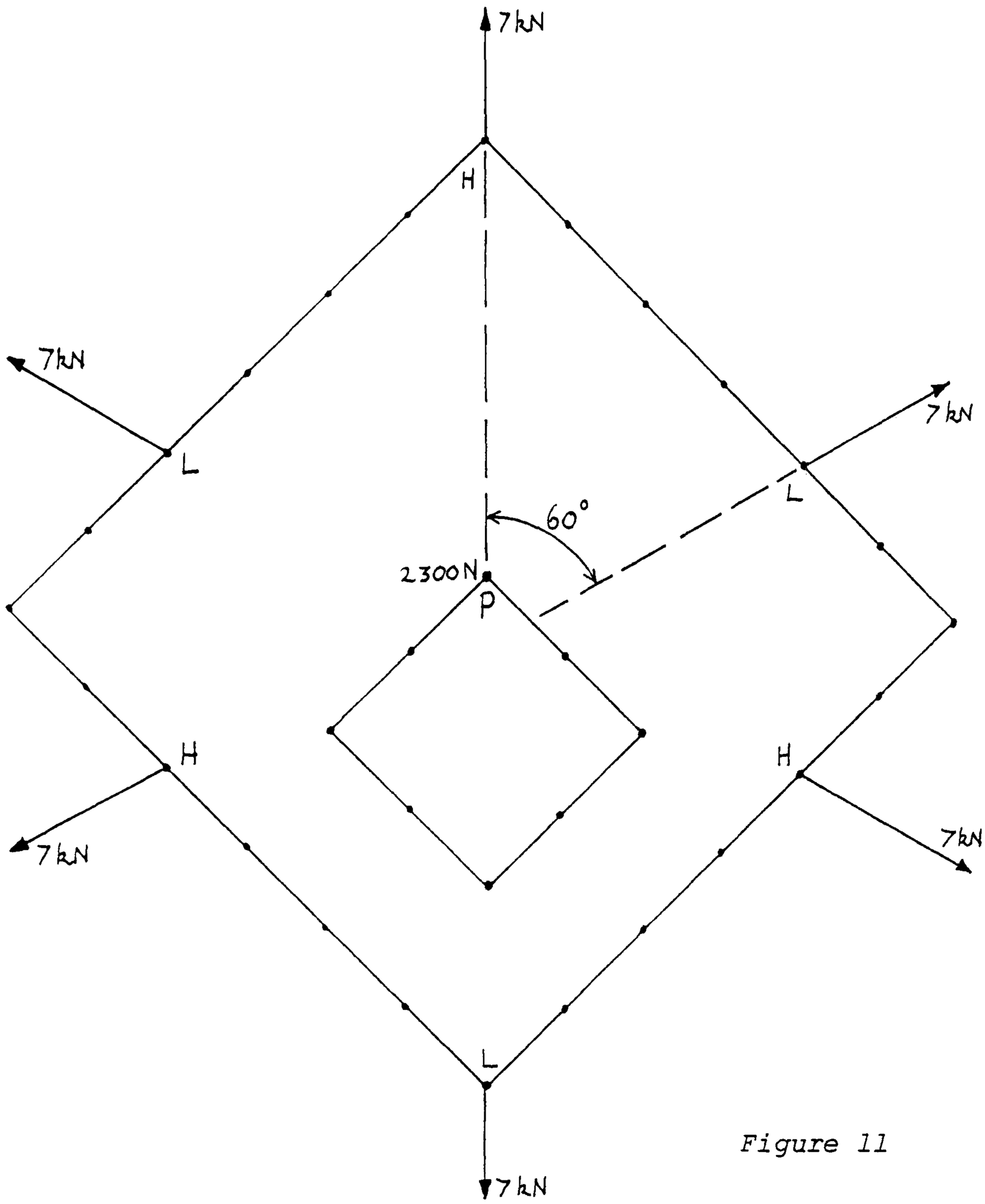


Figure 11

the situation after a further 1800 iterations is shown in figure 12c; similar conditions having been observed at intermediate stages. Anti-symmetric oscillation is apparent at B but not at A. The reason is that in the former case the motion of a surface node with a mass of only 0.02 kg is causing inversion, whilst in the latter case it is the motion of a less responsive edge node which is not stable. The quasi-instability which occurs in this structure can be eliminated either by refining the subdivision or by amending the topology. If for example the diagonals in the unstable areas are reversed, then with no increase in the number of nodes completely stable equilibrium is achieved.

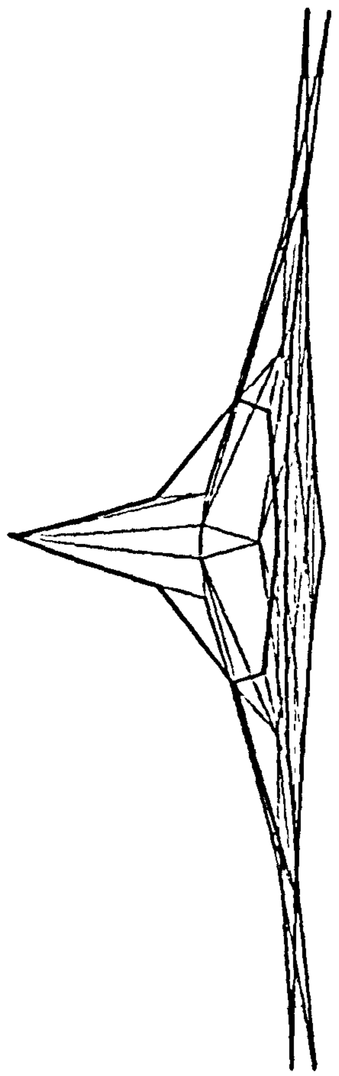


Figure 13a

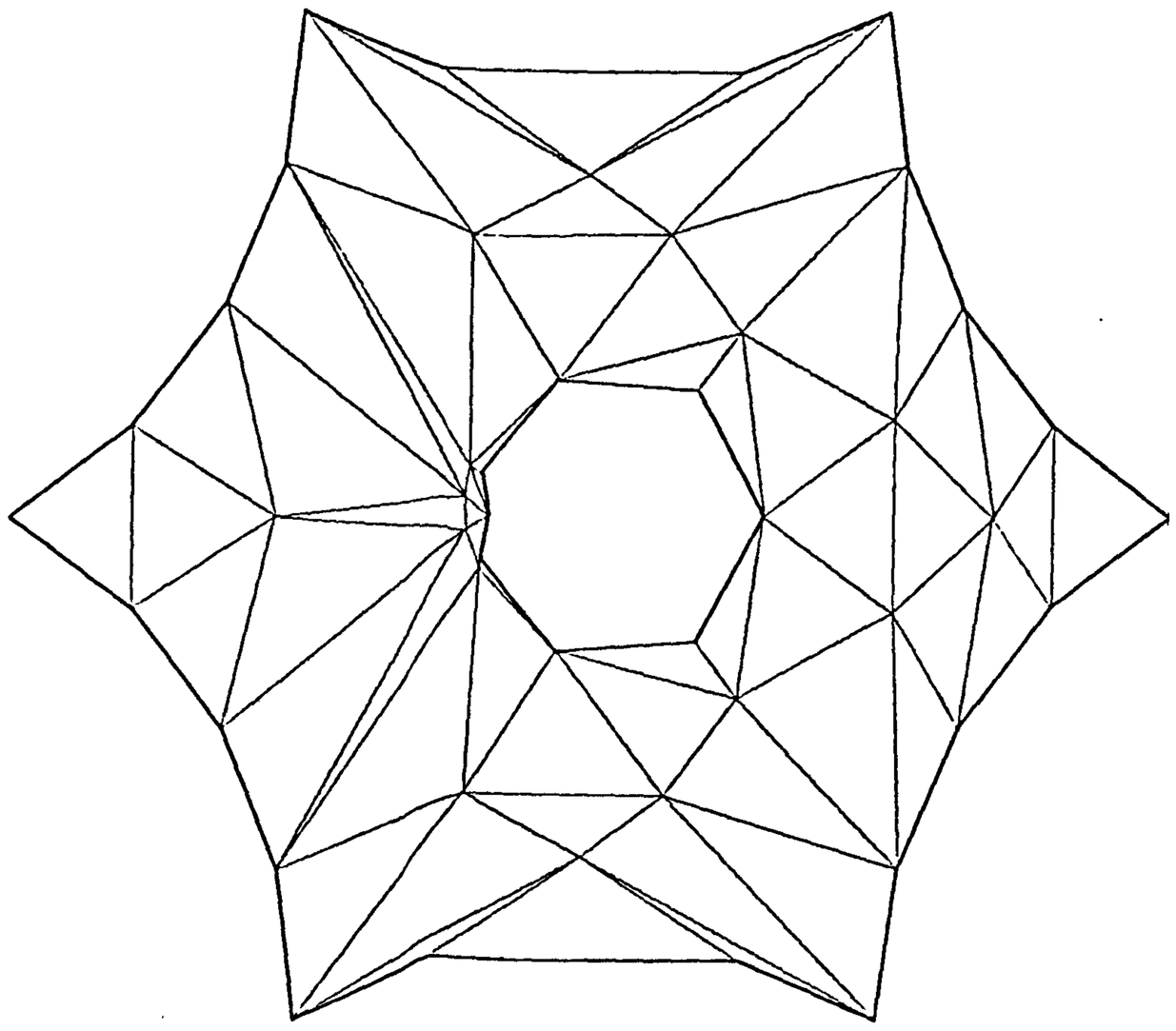


Figure 13b

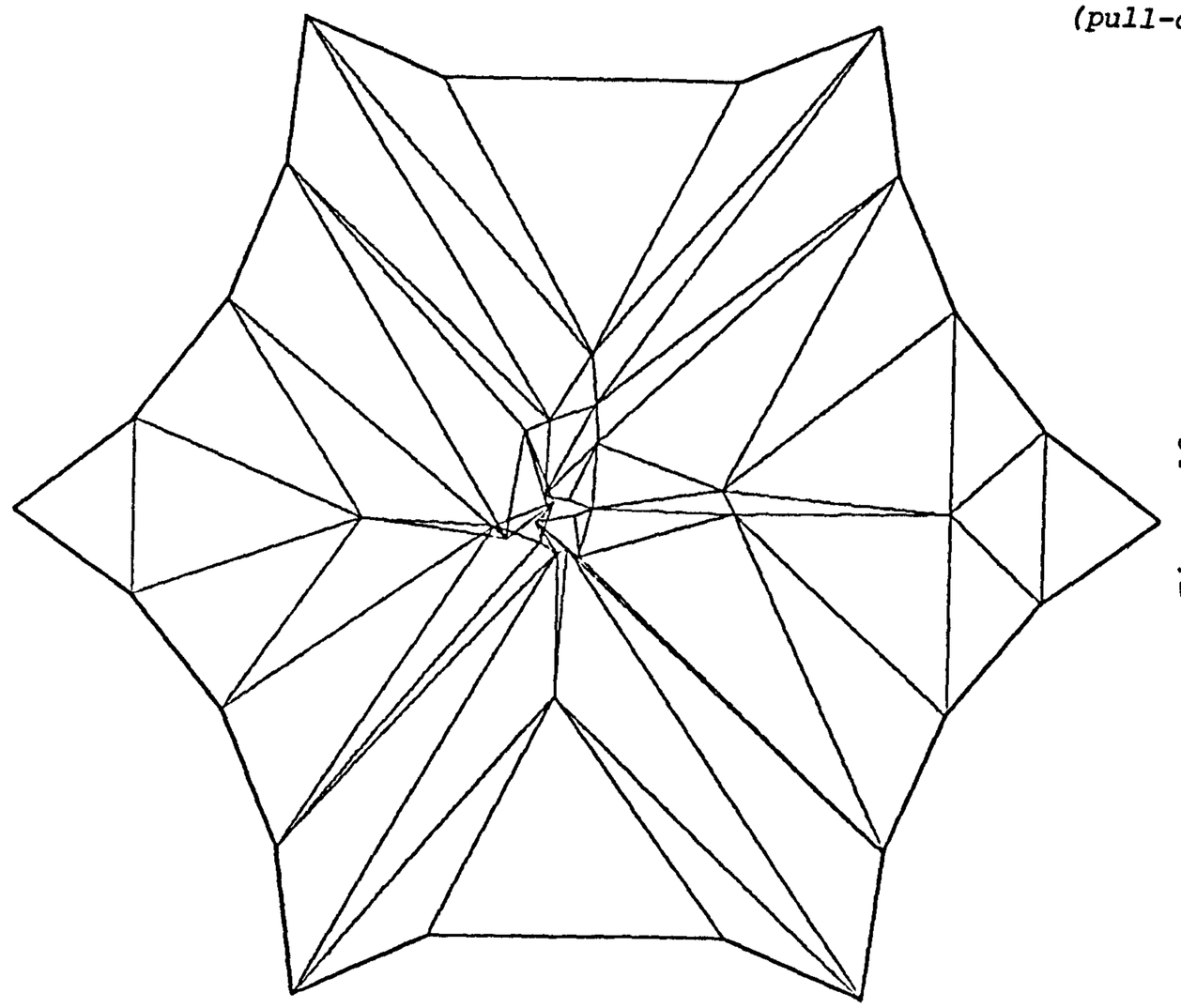


Figure 13c

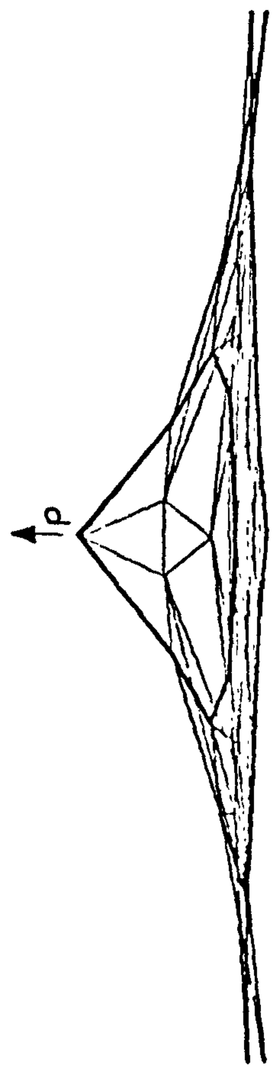


Figure 12a

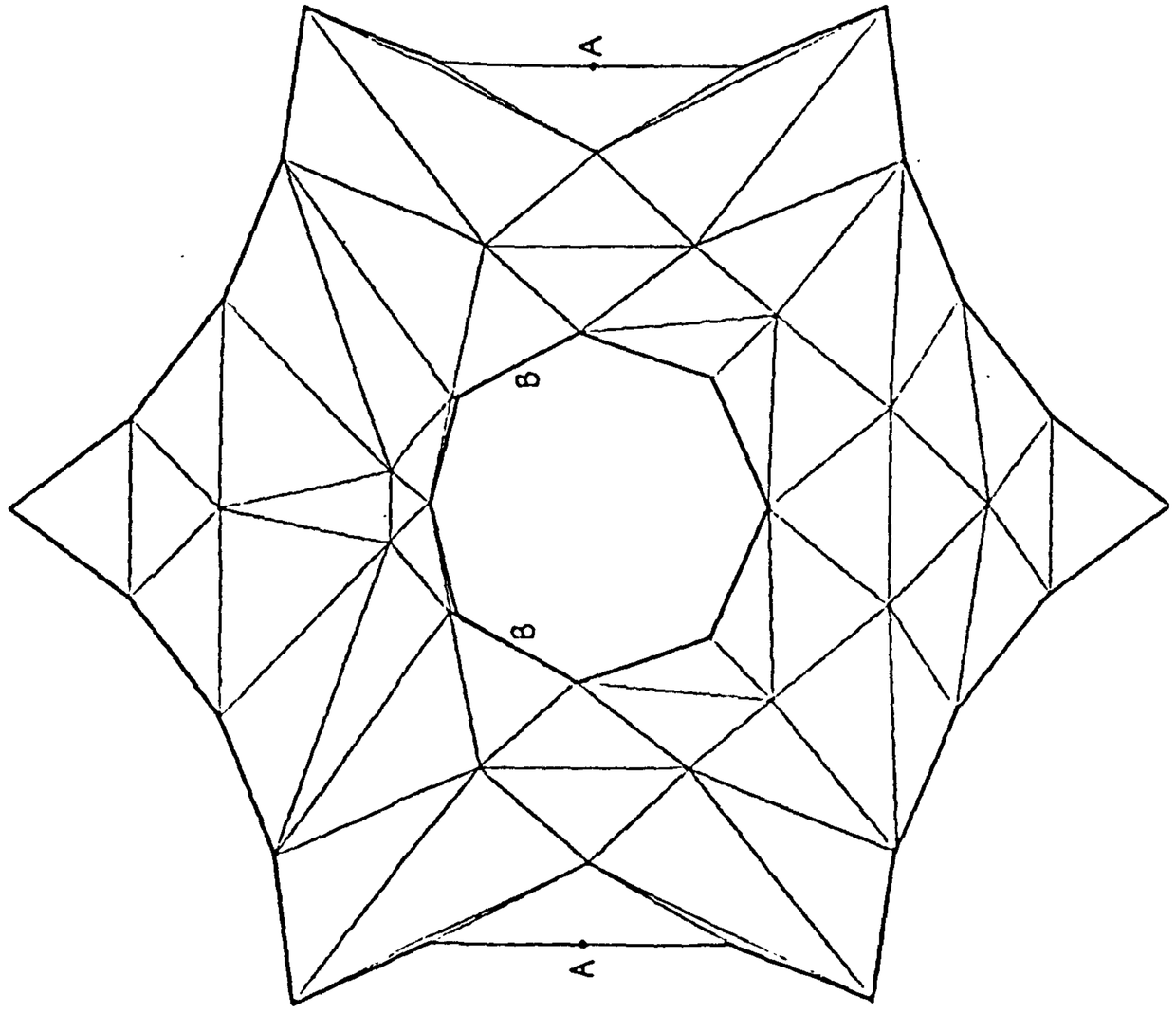


Figure 12b

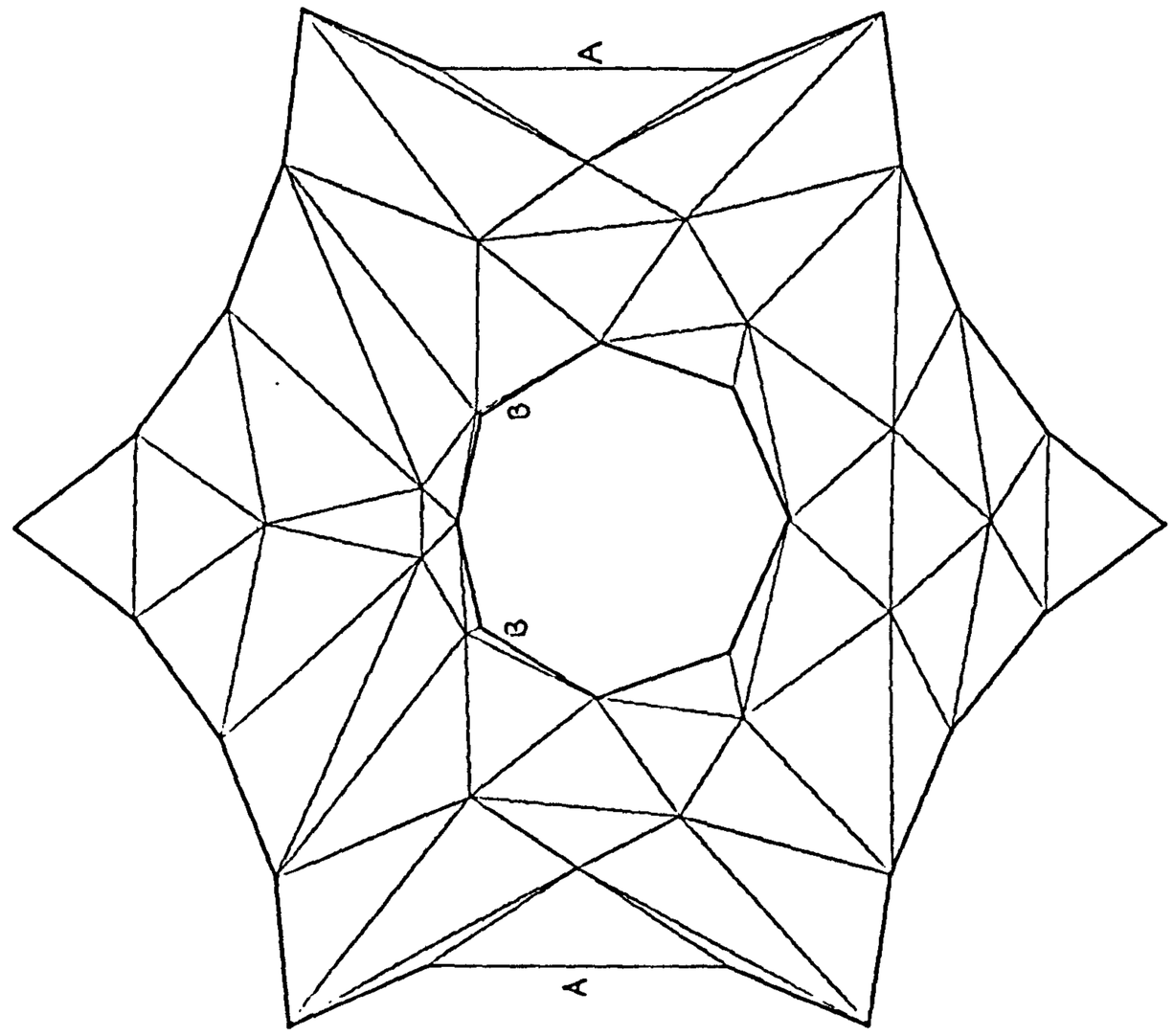


Figure 12c

And it will usually be the case that only such minor and self-evident amendments are required.

If the central load is increased to 2500 N the size of the loop is too small to sustain it. Figures 13a and 13b show the load accelerating prior to collapse in figure 13c. Collapse can be prevented by reducing the load or increasing the membrane tension. Alternatively the size of the inner tension loop can be increased by reducing the EA value of the links. The height of the loaded node is obviously a critical feature in such a membrane, and it may be advantageous to reduce its rate of deflection by increasing the nodal mass component, so that at all stages of its motion other nodes of the structure adapt relatively quickly to new equilibrium positions. It is of interest in relation to the possible use of interactive form-finding that even starting from the collapsed state, the correct topology and subsequent static equilibrium could be restored by taking the actions described.

In the case of the star shaped membrane example, with the topology used, quasi-instability will occur at A and B irrespective of the magnitude of the central load. For other membrane forms, particularly pneumatic structures, this condition appears only at a certain value of loading beyond which collapse will occur [3, 4].

An analysis for a membrane with compression boundaries and two loads applied to an inner tension loop was based on the topology shown, for half of the doubly symmetric structure, by the complete links in figure 14. Curvature varying from a minimum at x=0 to a

maximum at y=0 was imposed on the outer boundary be means of equal traction forces of 250N in each link; with average compressions being controlled elastically (EA = 50 kN). All nodes on the boundary were free to deflect with the exception of nodes R and R' at which vertical displacements were prevented. The results for two equal loads of 900 N applied at Q and Q' are shown in figures 15a and 15b. When the loads were increased to 1000 N quasi-instability occurred at nodes C and C'; and at 1150 N collapse occurred as shown in figure 15c. It is apparent that in this case, quasi-instability provided a forewarning of impending collapse.

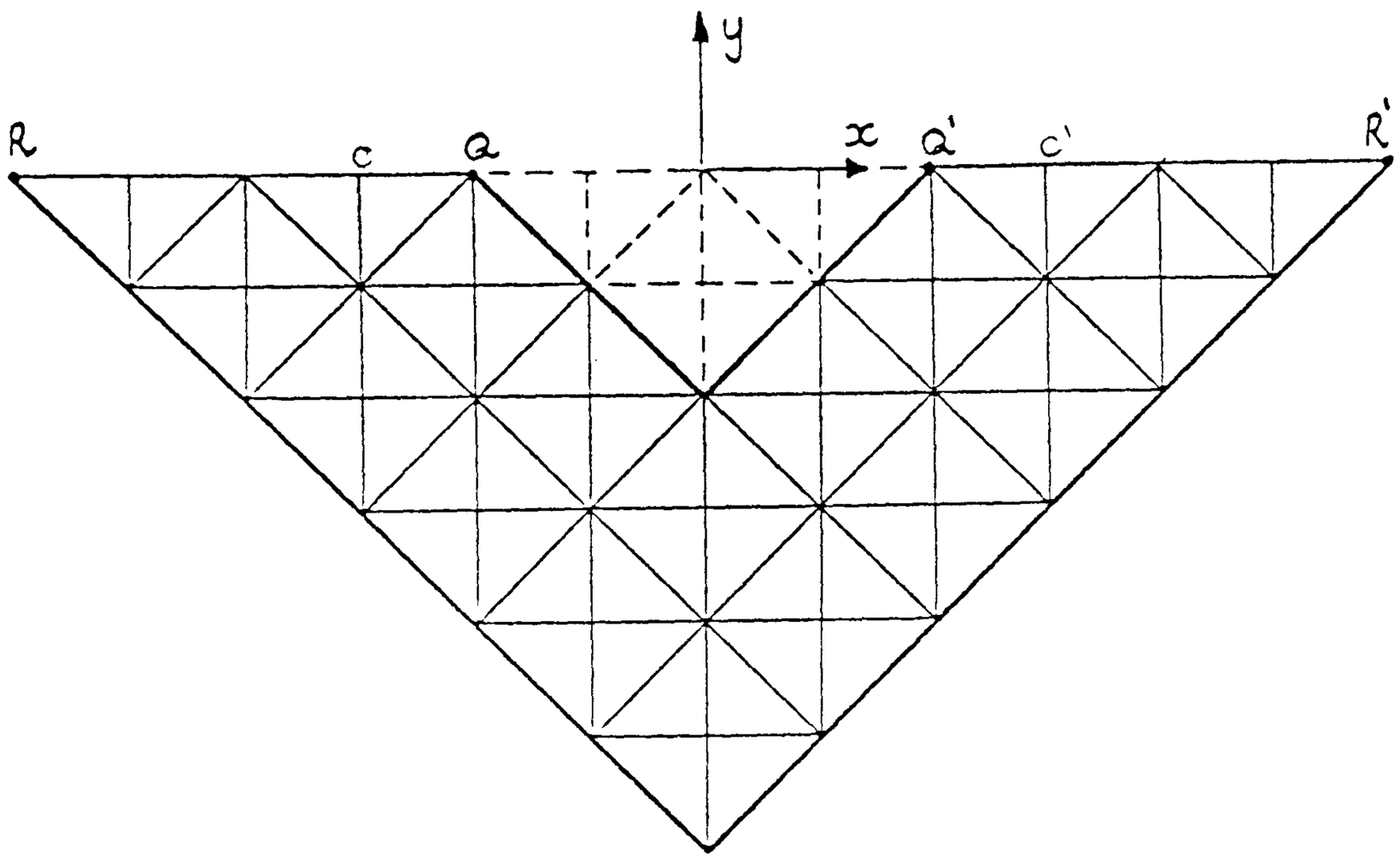


Figure 14

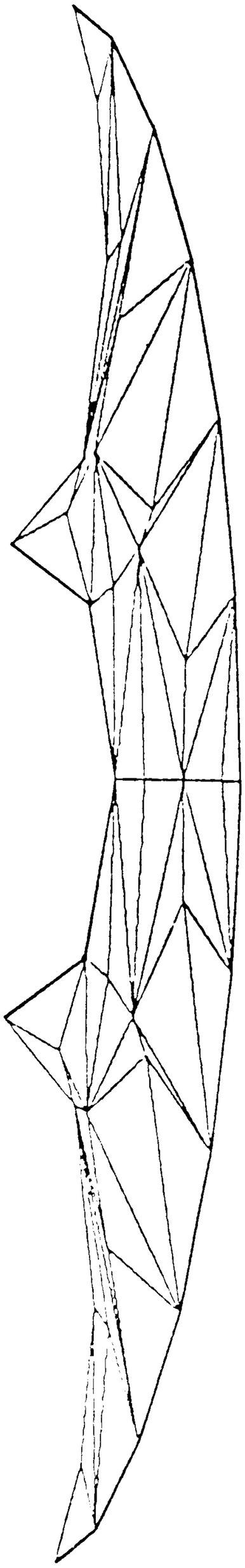


Figure 15a

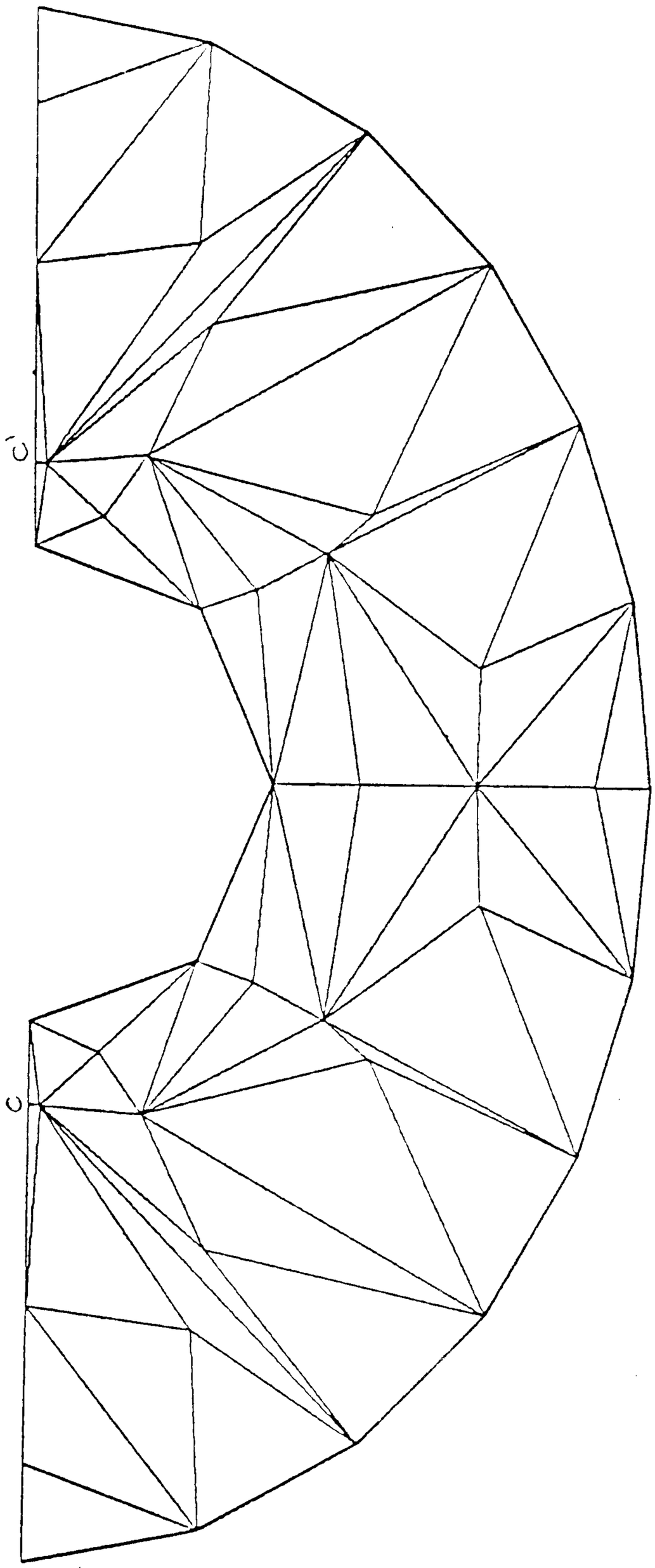


Figure 15b

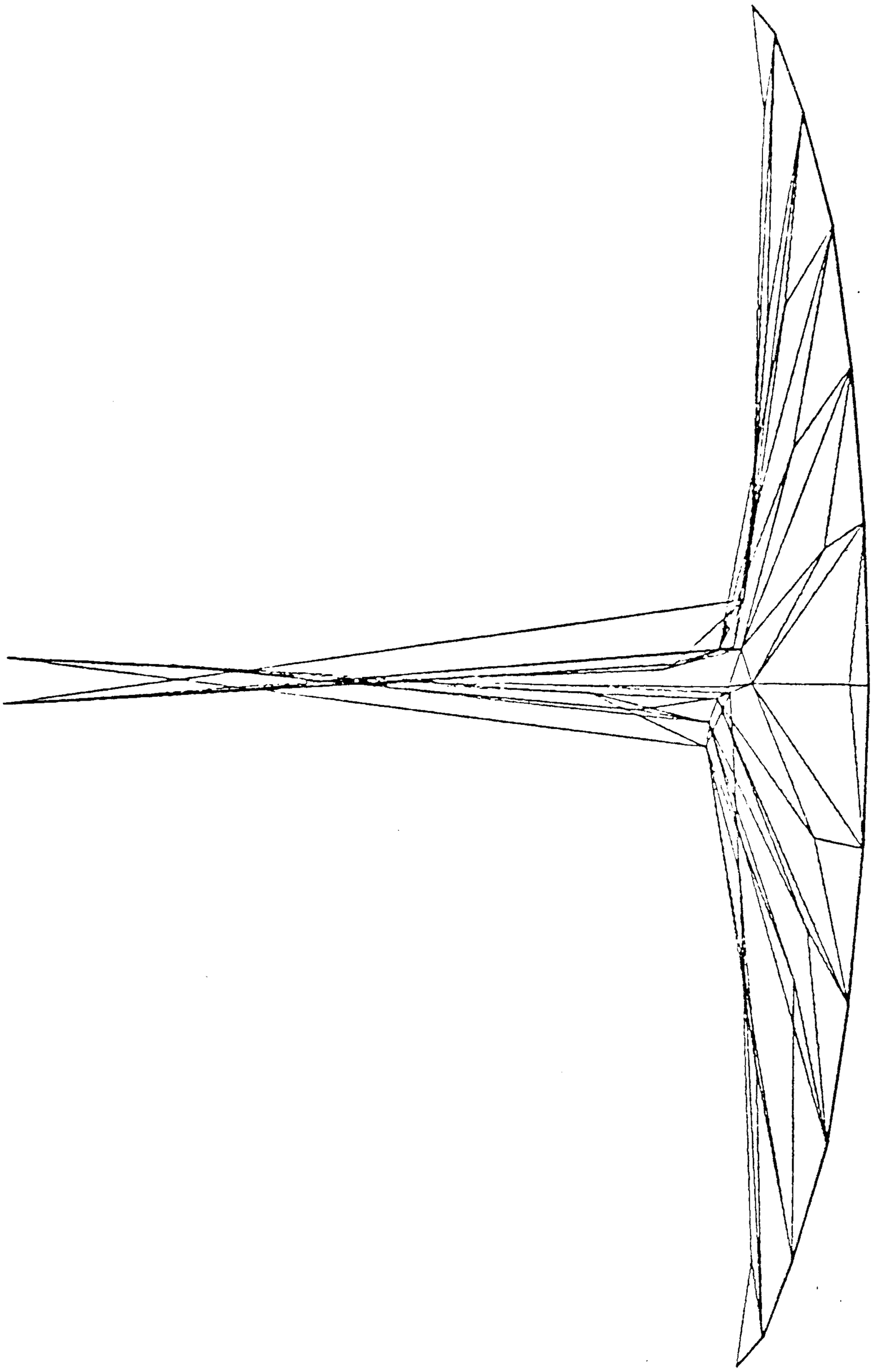


Figure 15c

PNEUMATIC STRUCTURES

Pressurised membranes may be derived by including in the analysis normal nodal forces proportional to the current areas of elements as they change in shape throughout the analysis. The structure shown in figures 16 was derived from the previous topology but with the central cut-out closed as shown by the dashed elements in figure 14. The membrane tensions of the outer and inner areas were 2500 N/m and 800 N/m respectively. And to enable this stress transition the inner cable was retained but the size of the loop was expanded by reducing to 2.5kN the EA values of the links. The outer boundaries were subject to traction forces and controlled elastically as in the previous membrane. The results shown are for an internal pressure of 1.6 kPa. The outer membrane is tending towards a cylindrical form in the central part whilst the inner membrane is tending to spherical with greater curvature.

CONCLUSION

Emphasis has been placed on the problem of instability which is an important physical limitation of uniform stress membranes. It has been shown that, even with a very coarse subdivision, results which are useful for preliminary stability investigations may be obtained. Whilst the practical application of such membranes is restricted, they provide a design guide for variable stress membranes and geodesic and uniform mesh cable networks [2]; each of which may in fact subsequently be analysed by similar procedures using a finer subdivision.

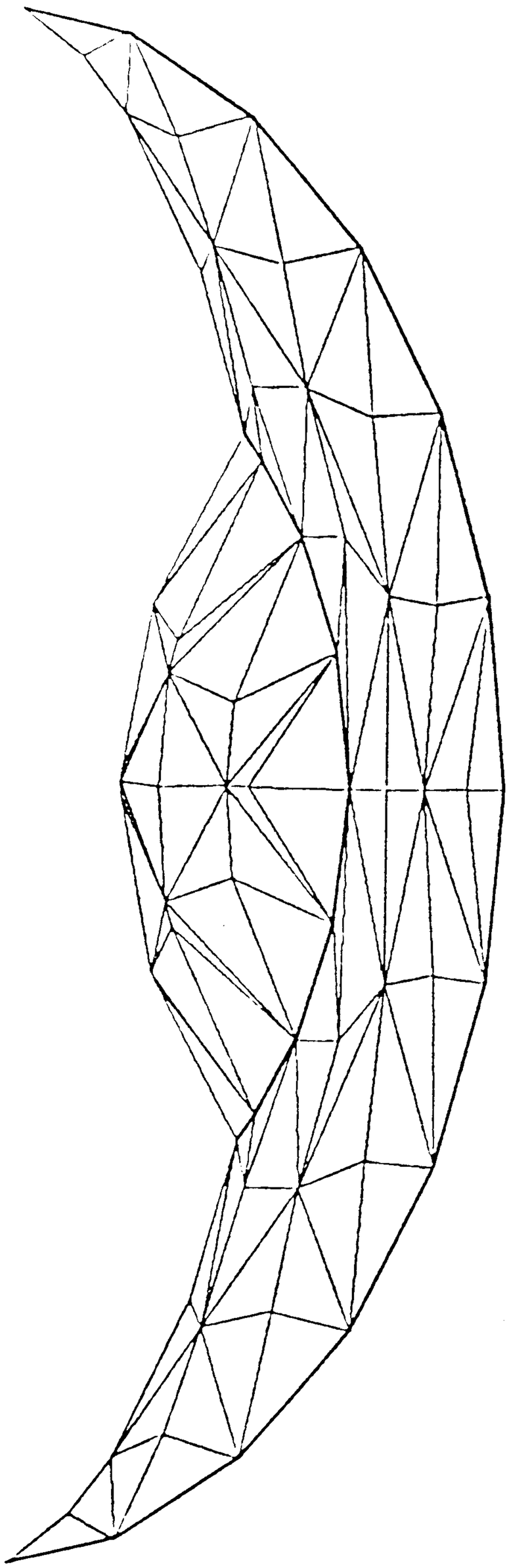


Figure 16a

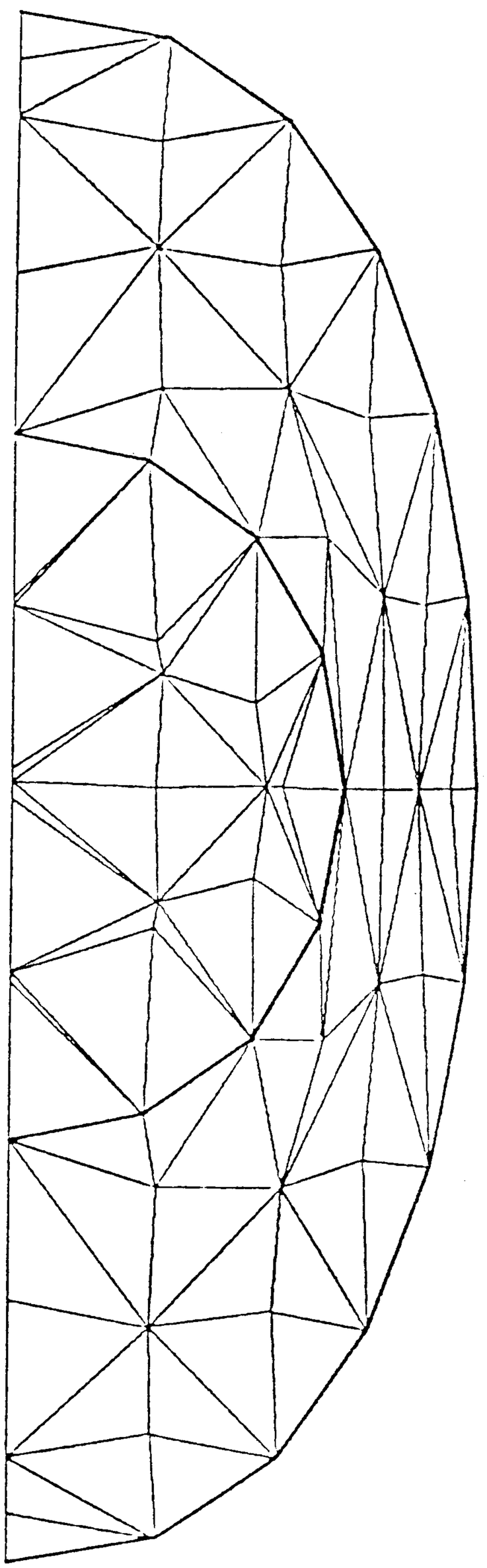


Figure 16b

Quasi-instability, of the type which occurred in the star membrane, that is independent of the magnitude of loading, is a consequence of the idealization into plane triangular elements. This might be avoided by the use of more complex curved elements; computing time would however be considerably increased by the accompanying transformations. To avoid this a process is required by which topology can be amended during, rather than subsequent to the analysis. Options available are: firstly automatic refinement of the mesh in areas where elements collapse; secondly to increase the mass at nodes which cause collapse so that, although complete convergence may not be obtained, variations are insignificant. The latter approach was demonstrated at the edges of the star membrane. Re-ordering of the topology, without mesh refinement, provides a third option (illustrated in appendix 4.1). In practice a combination of all these options would seem the ideal.

REFERENCES

(1) Clarke-Maxwell, J. 'On reciprocal figures, frames and diagrams of forces'. Proc. of the Royal Society, London (1864).

(2) Frei Otto 'Tensile Structures', MIT Press, (1967/69).

(3) Barnes, M.R. 'Applications of Dynamic Relaxation to the topological design and analysis of cable, membrane and pneumatic structures'. 2nd Int. Conf. on Space Structures, (Sept. 1975) Chapter 3.

(4) Barnes, M.R. 'Interactive graphical design of tension surface structures'. Int. Symposium on wide-span Surface-Structures, Stuttgart (April 1976) Chapter 7.

APPENDIX 4.1

DISTURBANCE OF PLANE MEMBRANE NODES

Figure 17b shows the initiation, after 20 iterations from the state in fig. 17a, of disturbances in the plane membrane caused by the movement of edge cables collapsing triangular elements (refer to fig. 3b in text). At 80 iterations, ill-conditioning of the expression for membrane link forces, due to the nodes of a triangle becoming co-linear, causes considerable displacement of one of the nodes as shown in fig. 17c. The triangle conditioning process given in the text, together with adequate damping, inhibits the occurence of such violent movements which could otherwise lead to complete divergence. In this particular case, although not conditioned, the correct topology was subsequently restored and convergence was obtained (fig.6 of the text).

ALTERATION OF TOPOLOGY

A normal load applied at point x of the planemembrane, with the topology shown by full lines in figure 17a, produces local quasi-instability as shown in figure 18a at triangles marked *. As in the case of the star membrane these local oscillations have an insignificant effect on the geometry of the structure and are due solely to the choice of topology. With the same number of nodes but some of the diagonals rearranged, as shown by the dashed lines in figure 17a, convergence without local oscillation is obtained (fig.19).

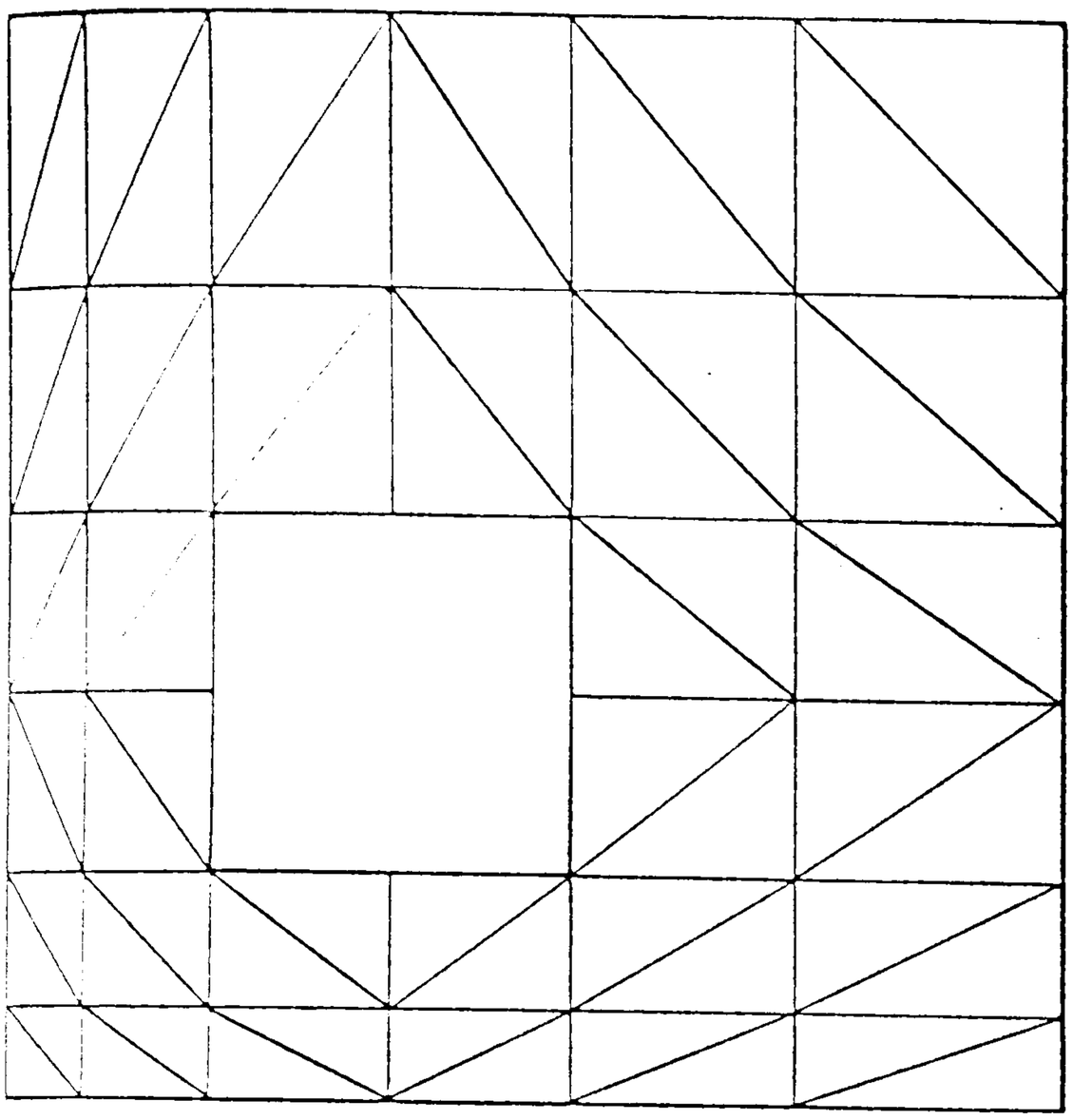


Figure 17a

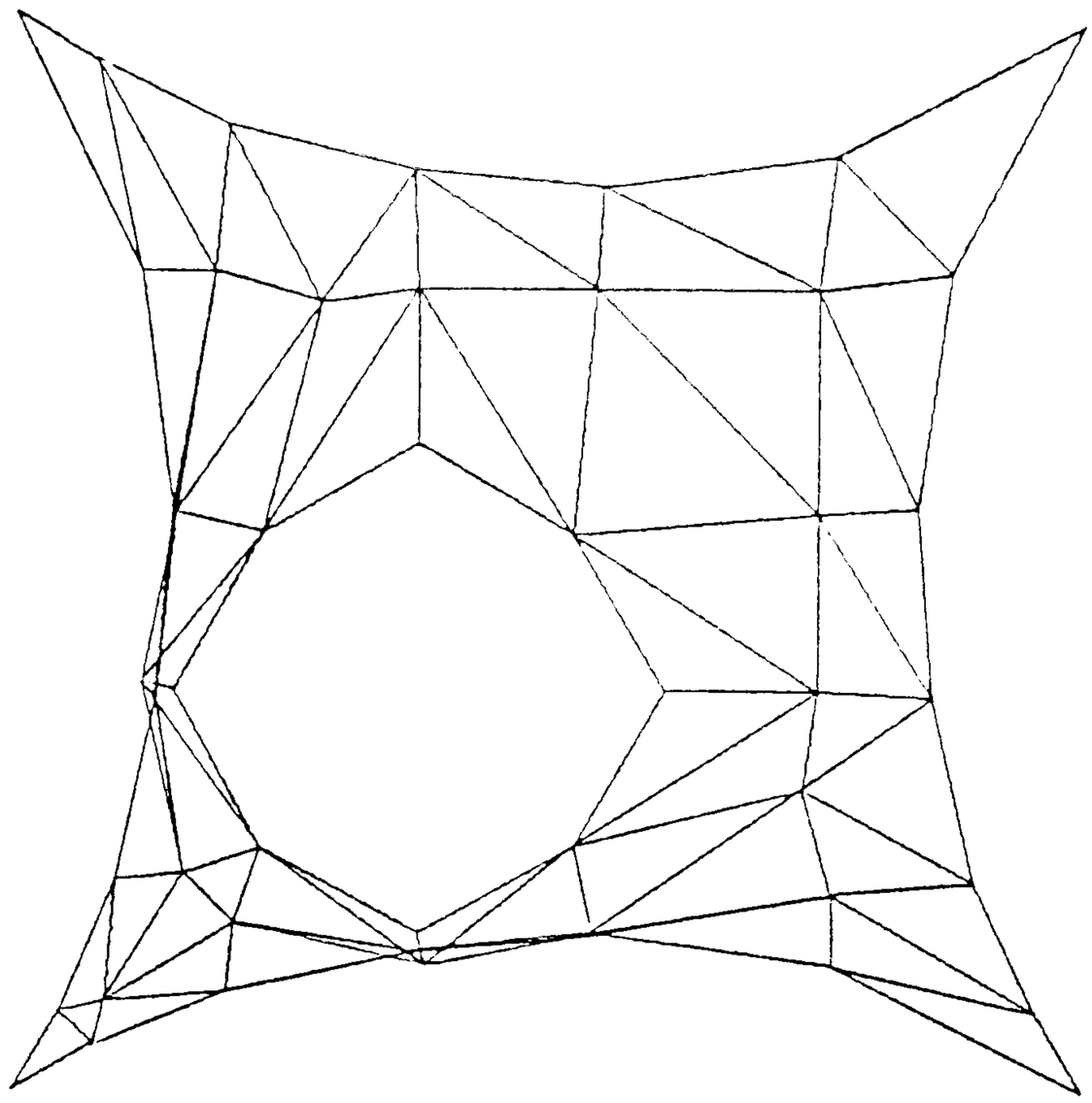


Figure 17b

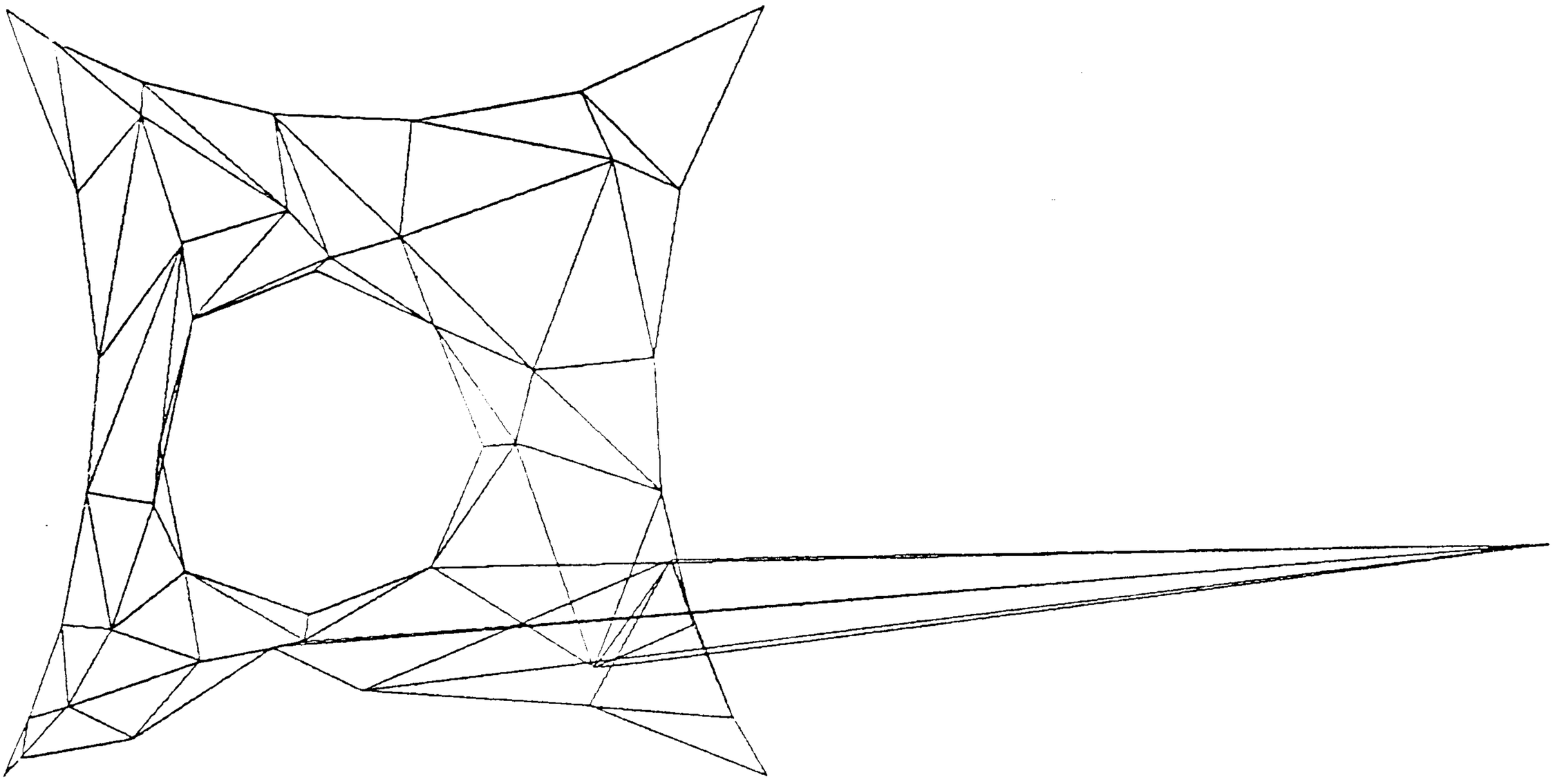


Figure 17c

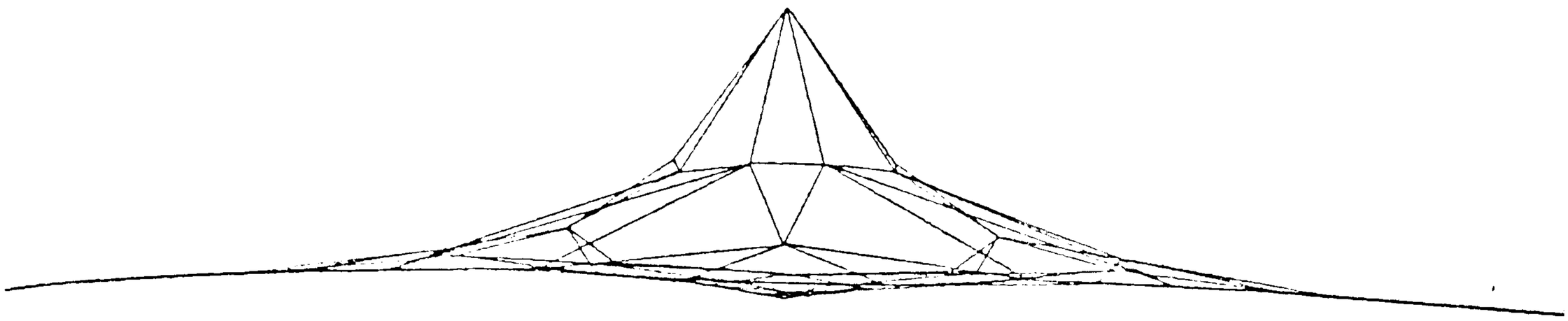


Figure 18b

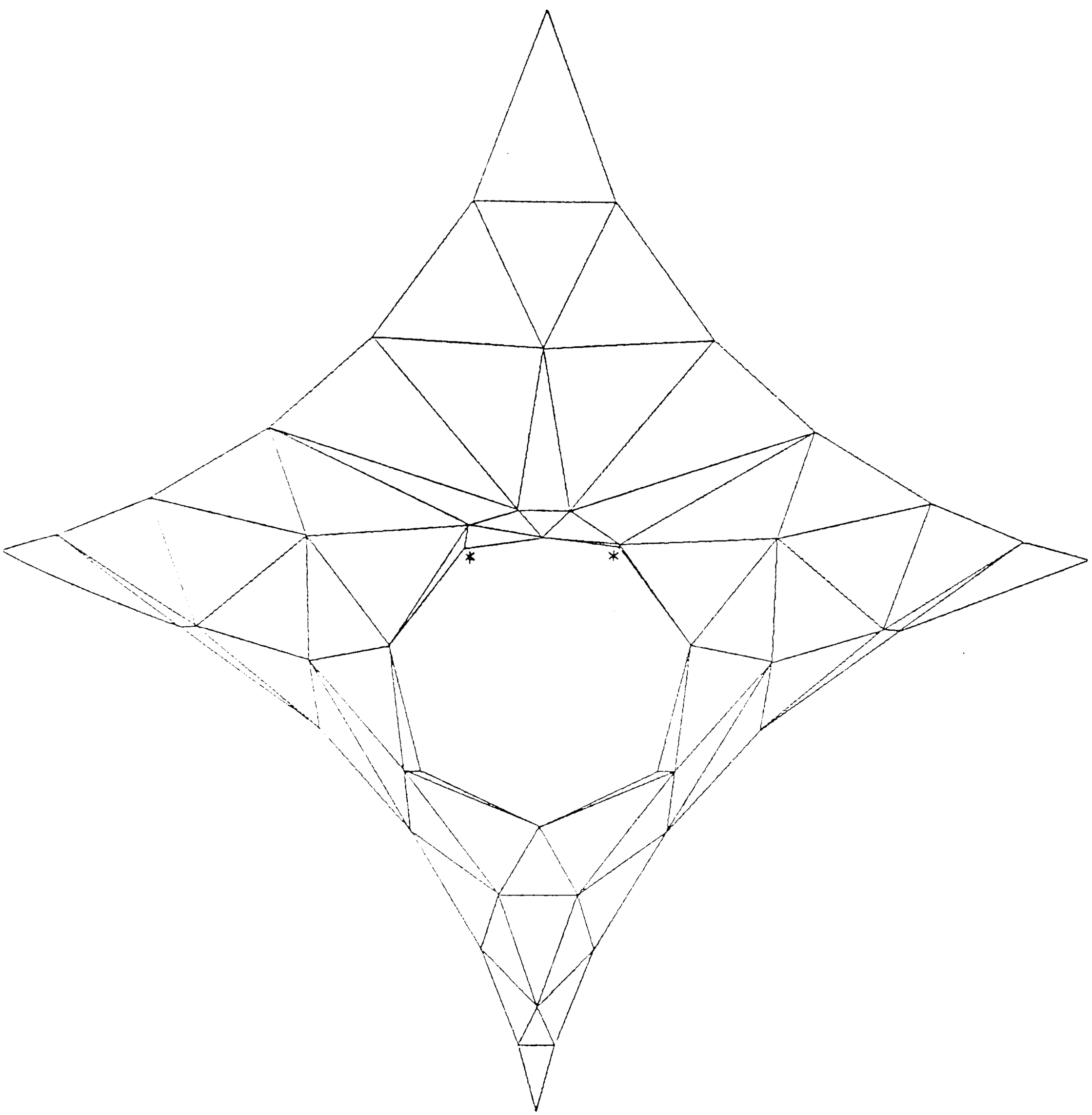


Figure 18a

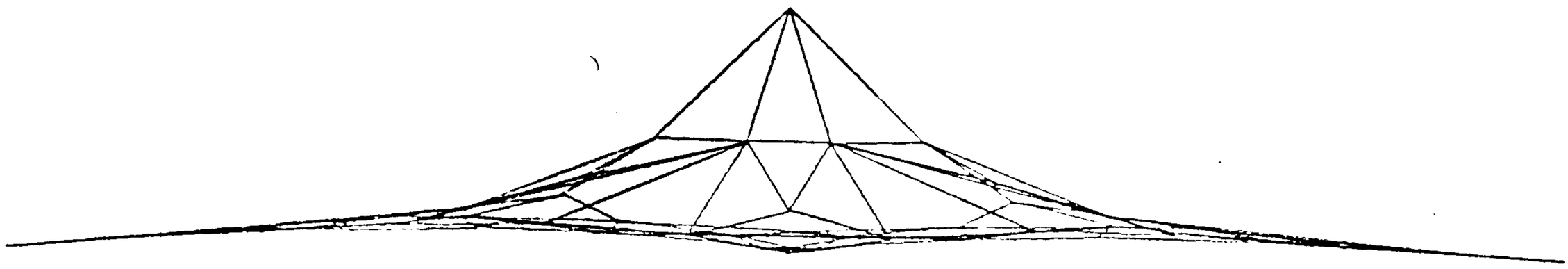


Figure 19b

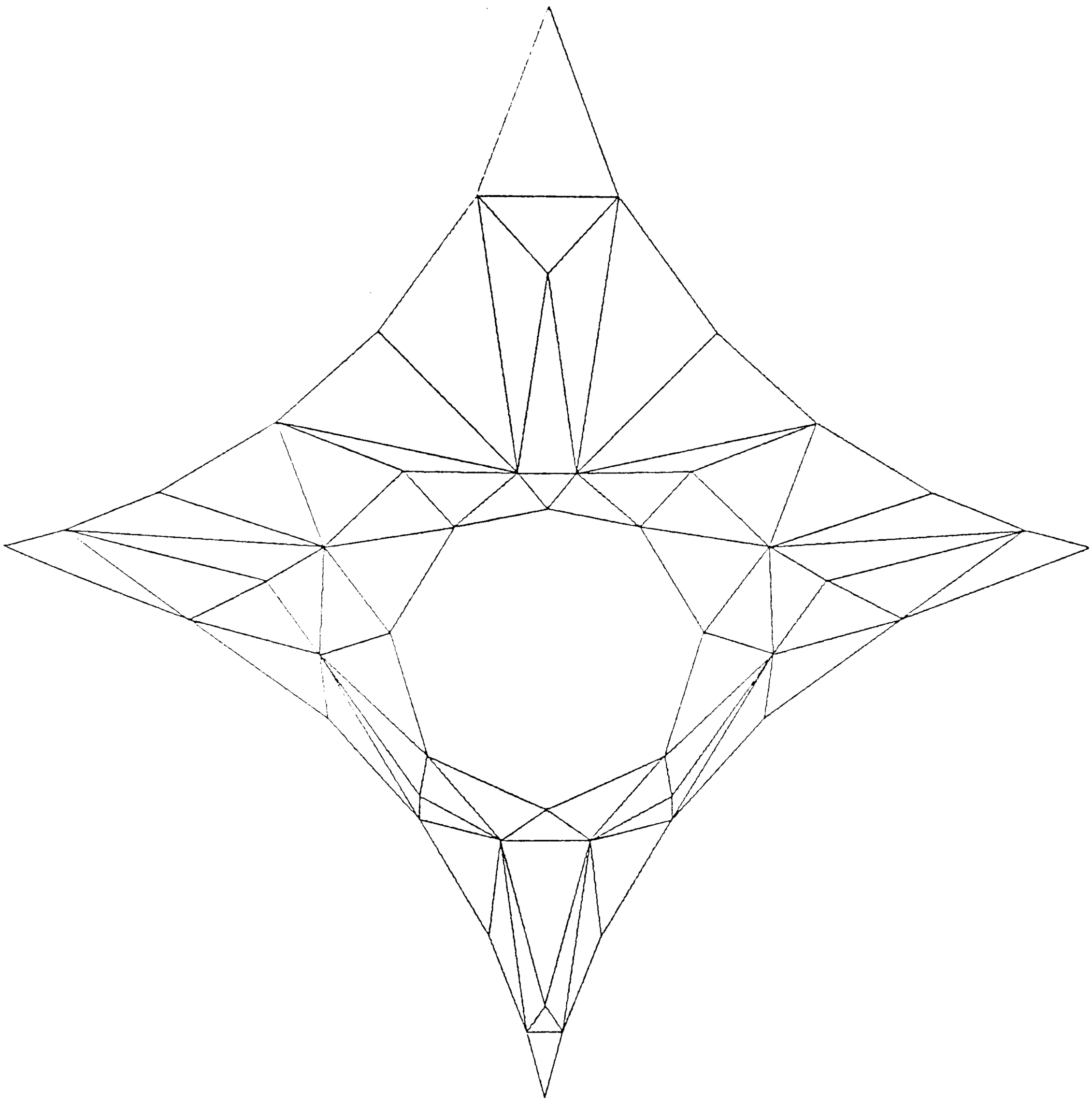


Figure 19a

CHAPTER 5

EXPLICIT DYNAMIC ANALYSIS OF TENSION STRUCTURES

SUMMARY

This chapter was presented as a paper at the International Conference on Wide Span Surface Structures (Stuttgart, April 1976). It outlines the analytical basis for the following chapters (6 and 7), also given as papers at the same conference. Although some aspects have previously been covered, the theory and computational procedure are generalized to include visco-elastic material behaviour in structures subject to buckling under dynamic loading. In pneumatic structures and space or network structures with reinforced plastic cladding such behaviour may provide important damping to the system.

STRUCTURAL AND TEMPORAL IDEALIZATION

The structure, whether continuous membrane or discrete cable system, is idealized into a set of nodes interconnected by straight links forming the edges of constant strain triangular elements and/or discrete constant strain cable lengths.

At each stage of an explicit dynamic analysis in which the simultaneous motions of the nodes, governed by Newton's second law, are traced step by step for small time increments Δt, displacement components and hence the elastic strains in all links may be determined purely in terms of the previous displacements, the residual nodal forces predicted from these displacements and, if the structural material is visco-elastic, the creep strains which have previously taken place. After the new displaced form has been determined, link forces and their resolved contributions to the next residual forces are calculated using the separate natural stiffness of elements. Provided computational procedures are properly organized, considerable savings in storage can thus be made compared with implicit schemes which require the transformation and assembly of element stiffnesses into an overall stiffness matrix. Accumulated geometrical errors which might otherwise occur when tracing, for many time steps, the transient response of highly non-linear structures are also more simply eliminated.

Oden [1] emphasises the importance in non-linear wave phenomena of the high frequency response, especially in the region of propogated discontinuities, and suggests that even when using an unconditionally stable implicit scheme the time step required

to retain higher frequencies is usually of the same order as that required for numerical stability of explicit schemes. Also, in addition to the formation of an overall stiffness matrix, consistent mass matrices involving a full inverse are advantageous in implicit schemes [1,2]. Krieg [3,4] has shown that for linear elasto-dynamic problems involving a square two-dimensional mesh the use of a diagonal mass matrix with an explicit central difference time-integration scheme provides the most practical means of computing a transient response, and further suggests that for equal work it produces a better overall frequency response in comparison with the best available implicit methods. The scheme outlined in the present paper is similar to the central difference scheme used by Krieg, save that an overall stiffness matrix is not operated on and for convenience an interlacing velocity formulation is used.

DYNAMIC ITERATION SCHEME

Newton's equation governing the motion of any node, i, in global co-ordinate direction x at time t is:

$$R_{ix}^{t} = m_{ix} \cdot \dot{V}_{ix}^{t} \qquad (1)$$

where R and V represent residual force and acceleration respectively; and for dynamic analyses the lumped nodal mass, m, will be a constant for each direction.

Velocity components at any instant may be expressed as a sine function:

$$V = a.Sin(q + \omega t) + C$$

where amplitude a, frequency ω, phase q, and datum C, are all variables (fig.1) and subscripts i,x have been omitted for convenience.

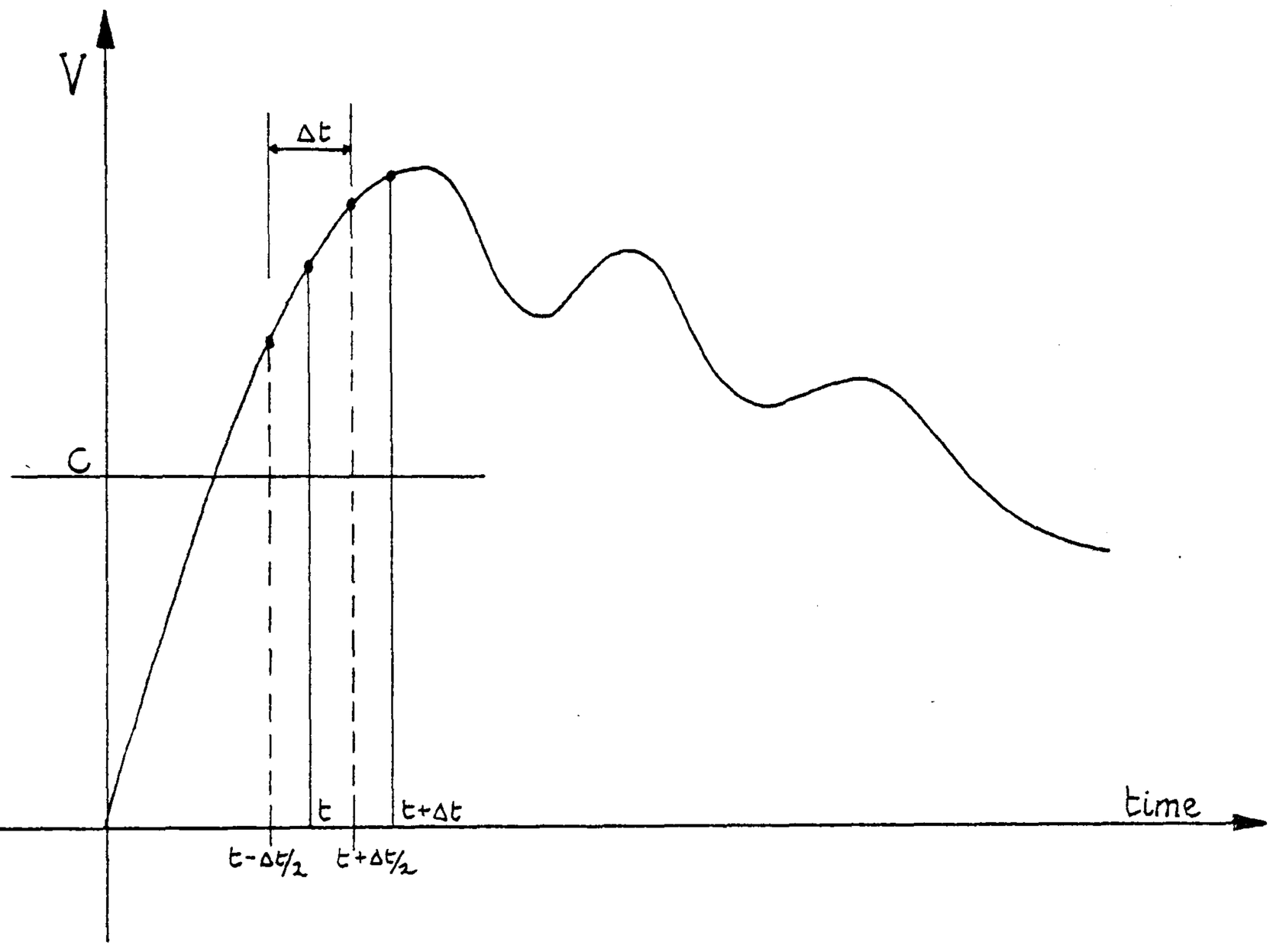


Figure 1

Considering a small interval of time, Δt, and assuming that ω is constant during this interval, the acceleration at mid-interval (time t) is:

$$\dot{V}^{t} = \frac{\omega(V^{t+\Delta t/2} - V^{t-\Delta t/2})}{2Sin(\omega\Delta t/2)} \qquad (2)$$

Unless the variation of ω for each degree of freedom can be traced during the analysis or the entire system vibrates with the same frequency, the procedure is simplified by imposing the condition

that $\omega \Delta t/2$ must be small. Equation (2) then approximates to:

$$V^{t} = \left(\frac{V^{t+\Delta t/2} - V^{t-\Delta t/2}}{\Delta t}\right) \tag{3}$$

Substituting in equation (1) gives the recurrence equation for velocities:

$$V_{ix}^{t+\Delta t/2} = \frac{\Delta t}{m_{ix}} . R_{ix}^{t} + V_{ix}^{t-\Delta t/2} \tag{4}$$

where the current residual force, R_{ix}^{t}, can be expressed in terms of V_{ix}^{t} and applied load P_{ix}^{t}, and the current elastic strains and position vectors of the structural elements connected to node i.

For small Δt:

$$\delta^{t+\Delta t} = \delta^{t} + \Delta t . V^{t+\Delta t/2} \tag{5}$$

whence the new link extensions and residual forces at $t+\Delta t$ may be determined. The process then continues with iteration between equations (4) and (5).

The interlacing scheme outlined, with velocities traced for times $\Delta t/2$, $3\Delta t/2$ ..... and displacements and forces for times 0, Δt, $2\Delta t$ ....., is equivalent to the central difference or lumped impulse procedure: ($\delta^{t+\Delta t} = 2\delta^{t} - \delta^{t-\Delta t} + \Delta t^{2} \ddot{\delta}^{t}$).

LINK AND NODAL FORCES

The tension in a cable or bar element at time t is:

$$T^{t} = T^{i} + K . \delta e^{t} \tag{6a}$$

where T^{i} is the initial tension (for elastic bar elements the

pretension) and K^t and δe^t are respectively the current stiffness and elastic extension from the initial (or pretension) state.

For a 'constant strain' triangular element the orthogonal strains may be expressed in terms of current side extensions (fig.2):

$$\begin{Bmatrix}\varepsilon_x\\ \varepsilon_y\\ \gamma_{xy}\end{Bmatrix}^t = \left[G\right]\begin{Bmatrix}\delta e_1\\ \delta e_2\\ \delta e_3\end{Bmatrix}^t \quad \text{or} \quad \left\{\varepsilon\right\}^t = \left[G\right]\left\{\delta e\right\}^t$$

whence the side tensions at time t are given by:

$$\begin{Bmatrix}T_1\\ T_2\\ T_3\end{Bmatrix}^t = \left[G^T\right]\begin{Bmatrix}\sigma_x\\ \sigma_y\\ \tau_{xy}\end{Bmatrix}^i + \left[G^T\right]\left[D\right]^t\left[G\right]\left\{\delta e\right\}^t \quad \text{or} \quad \left\{T\right\}^t = \left\{T\right\}^i + \left[K\right]^t\left\{\delta e\right\}^t \qquad (6b)$$

where $\left\{\sigma\right\}^i$ is the initial stress vector, $\left[D\right]^t$ is the elasticity matrix which in general depends on current stress level, and $\left[K\right]^t$ is the current 'natural' 3x3 stiffness matrix [5]. For convenience, in equation (6b) and subsequently, $\left[G^T\right]$ denotes the transpose of $\left[G\right]$ multiplied by the volume of the element.

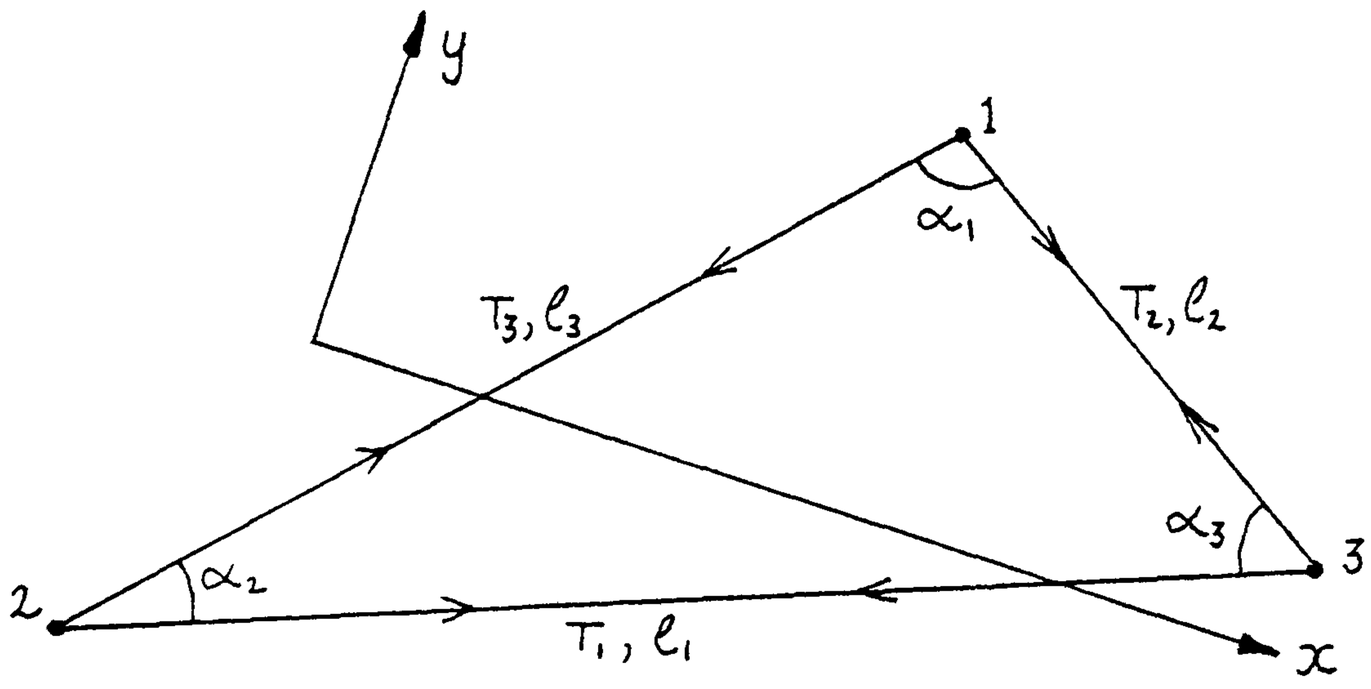


Figure 2

For the special case of uniform prestress, σ_o, the initial tension vector for membrane element links is given by:

$$\left\{T\right\}^{i} = \frac{\sigma_o h}{2} \begin{Bmatrix} \frac{\ell_1}{\tan\alpha_1} \\ \frac{\ell_2}{\tan\alpha_2} \\ \frac{\ell_3}{\tan\alpha_3} \end{Bmatrix} \tag{7}$$

where h is the membrane thickness.

Having obtained current membrane and/or cable tensions the contribution to the residual nodal forces by any link k joining nodes i and j is given by:

$$R^{t}_{ix} = R^{t}_{ix} + X^{t}_{jix} \left(T_k/\ell_k\right)^{t} \tag{8}$$

where X_{jix} denotes $(X_{jx} - X_{ix})$, the difference between nodal co-ordinates of the link in the x direction.

Additional contributions to the residual forces are due to:

a) concentrated applied static and dynamic loads, P^{t}_{ix}, which include also distributed gravitational loads lumped at the nodes.

b) distributed static and dynamic pressure loads, p^{t}, normal to the membrane elements which are the outward resultants of applied internal and external pressures; accounting also for perturbations in these pressures due to the kinetic energy of the mass of air moved by any membrane element (dp^{t}_{k}) and (for pneumatic structures) due to changes

in the internal volume caused by deformation of the whole structure at constant internal air mass and temperature (dp_p^t).

These perturbations are approximately:

$$dp_n^t = -\tfrac{1}{2} \rho_{air} (\bar{V}_n^t)^2 \qquad (9a)$$

$$dp_p^t = -\frac{\text{pneumatic pressure}.d(vol)}{(vol + d(vol))} \qquad (9b)$$

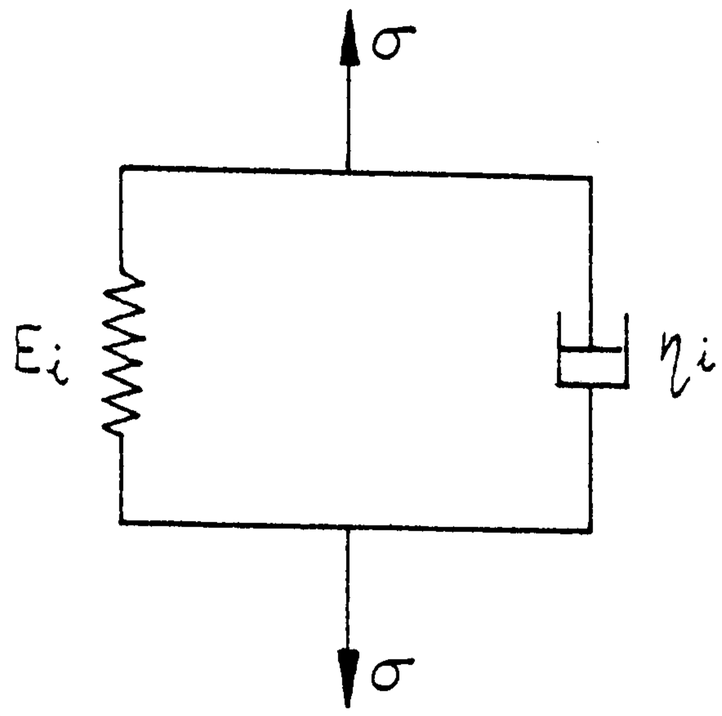
where A is the area of an element, $\bar{V}_n$ is the average normal velocity, and d(vol) is the change in volume from the state at which the pneumatic pressure and volume (vol) were previously set. The resolved forces (in x, y, z directions) at each node of a membrane element due to the resultant pressure are then given by:

$$P_x^t = \frac{p^t}{6} (X_{21y} \cdot X_{31z} - X_{31y} \cdot X_{21z}) \qquad (9c)$$

with P_y^t and P_z^t given by cyclic permutation of subscripts x,y,z. In the above equation, using a right-handed global co-ordinate system and element nodes numbered 1, 2, 3 anticlockwise, the normal vector is out of the plane (Appendix 5.1).

INCREMENTAL PROCEDURE ALLOWING FOR CREEP AND BUCKLING

It is assumed in the following that material properties are visco-elastic and can be represented by a series of Kelvin (Voigt) elements coupled with an elastic response [6].



$$\sigma = E_i . \varepsilon_c + \eta_i \dot{\varepsilon}_c$$

Figure 3

Considering uni-axial creep stress-strain relations characterized by a single Kelvin model (fig.3), the 'creep rate' may be written as:

$$\dot{\varepsilon}_c = a.\sigma - b.\varepsilon_c \qquad (10a)$$

For several Kelvin elements placed in series to represent more accurately the material properties:

$$\dot{\varepsilon}_c = \sum_{r=1,n} a_r . \sigma - \sum_{r=1,n} b_r . \varepsilon_c \qquad (10b)$$

where σ is the current stress level and ε_c is the accumulated creep strain.

The complexity of the model chosen will depend on the type of loading: for short-term dynamic loading a single element model may suffice, particularly if the main concern is a qualitative study of the vibration damping effect of visco-elastic membrane cladding; for long-term quasi-static creep investigations of pre-stressed structural membranes, for which wrinkling effects near boundaries are of interest, a more complex model will be necessary. In the present paper interest is centred on suddenly applied dynamic loading and only a single model is

considered. The procedure outlined however applies equally well to series models for long-term creep. Additionally, changes in the visco-elastic constants dependent on stress level may be conveniently accounted for.

In interlacing finite difference form equation (10a) can be written:

$$\left(\frac{\varepsilon_c^{t+n\Delta t/2} - \varepsilon^{t-n\Delta t/2}}{n\Delta t}\right) = a.\sigma^t - b\left(\frac{\varepsilon^{t+n\Delta t/2} + \varepsilon^{t-n\Delta t/2}}{2}\right) \qquad (11)$$

$$\text{hence } \varepsilon_c^{t+n\Delta t/2} = \frac{a.n.\Delta t.\sigma^t}{(1+b.n.\Delta t/2)} + \frac{(1 - b.n.\Delta t/2)}{(1 + b.n.\Delta t/2}\varepsilon_c^{t-n\Delta t/2} = a'\sigma^t + b'.\varepsilon_c^{t-n\Delta t/2} \qquad (12a)$$

This expression determines the level of creep strain ε_c appropriate to the mid-point of time intervals $n.\Delta t$, where n is an integer and Δt is the (smaller or equal) time interval used for the dynamic iteration scheme. These creep strains are then assumed to be lumped increments operative from the start of each interval $n\Delta t$ as 'initial' strains held constant to the end of the interval.

For membrane elements the vector of creep strains is given by:

$$\begin{Bmatrix} \varepsilon_{xc} \\ \varepsilon_{yc} \\ \gamma_{xyc} \end{Bmatrix}^{t+n\Delta t/2} = \{\varepsilon_c\}^{t+n\Delta t/2} = a'.[\psi]\{\sigma\}^t + b'.\{\varepsilon_c\}^{t-n\Delta t/2} \qquad (12b)$$

where, assuming that the material is isotropic and that creep is associated only with the deviatoric stress components, the poisson ratio is $\frac{1}{2}$ and matrix $[\psi]$ is:

$$[\psi] = \begin{bmatrix} 1 & -\frac{1}{2} & 0 \\ -\frac{1}{2} & 1 & 0 \\ 0 & 0 & 3 \end{bmatrix}$$

For short term dynamic loading, the effects of creep and buckling may be coupled by the computational process outlined on page 186 . The procedures shown relate to membrane elements, with bar elements being treated analogously.

The vector $\{e\}^t$ referred to in stage III(a) is the vector of total side extensions from the stress state $\{\sigma\}^i$ input at stage I; whereas $\{\delta e\}$, used in stage II for calculating link tensions from time $kn\Delta t$ to $(k+1)n\Delta t$, is the vector of extensions updated from time $kn\Delta t$. Accumulated errors due to roundoff and the difference approximations introduced in equations (12) may thus be reduced. If, however, the material constants are to vary as a continuous function of stress level, as opposed to on-off non-linearity due to buckling, the scheme must be modified so that stresses are checked on an incremental basis. The factor, n, governing the period at which creep strains are evaluated, may at the initial application of dynamic loads be conveniently set to a small value and subsequently increased (exponentially) as the analysis proceeds, on the assumption that errors introduced by the difference approximation for creep reduce as the amplitude of vibration decays with damping.

For long-term quasi-static creep analyses the dynamic iteration process at stage II must be made to approximately converge to a static equilibrium value by the use of fictitious viscous damping proportional to nodal velocities. This procedure is outlined in a subsequent section. For such long-term analyses the time interval associated with increments of creep strain will not then

I

For each element input $\{\sigma\}^i$ and visco-elastic and elastic constants appropriate to the initial stress level (Creep strains $\{\varepsilon_c\}$ to be measured from this datum)

Set initial force vector $\{T\}^i = [G^T]\{\sigma\}^i$

and natural stiffness $[K] = [G^T][D][G]$

$k=1$

II

Iterate simultaneously for n time intervals Δt using recurrence equations 4 and 5 and the expression for current link forces: $\{T\} = \{T\}^i + [K]\{\delta e\}$

$t = k.n.\Delta t$

III

For each element:

(a) Check stresses relative to chosen local axes

$$\{\sigma\}^t = \{\sigma\}^i + [D][G]\{e\}^t - [D]\{\varepsilon_c\}^{t-\frac{n\Delta t}{2}}$$

(b) Determine principal stresses $\{\sigma_p\}$ and inclination to x, y axes.

(c) If either principal stress $<$ limiting buckling stress set to zero and modify principal stress vector $\{\sigma_p'\}$

(d) Set modified elasticity matrix $[D_p']$ relative to principal axes (with elastic constants accounting for buckling), and transform to x, y axes:

$$[D'] = [C^T][D_p'][C]$$

(e) Set modified stresses $\{\sigma'\}^t = [C^T]\{\sigma_p'\}$; $\{\Delta\sigma'\}^t = \{\sigma'^t - \sigma^i\}$

(f) Set new creep strains: $\{\varepsilon_c\}^{t+\frac{n\Delta t}{2}} = a'[\psi]\{\Delta\sigma'\}^t + b'\{\varepsilon_c\}^{t-\frac{n\Delta t}{2}}$

(g) Set new Initial force vectors: $\{T\}^i = [G^T]\{\sigma'\}^t - [G^T][D']\{\varepsilon_c^{t+\frac{n\Delta t}{2}} - \varepsilon_c^{t-\frac{n\Delta t}{2}}\}$

(h) Set new natural stiffnesses $[K] = [G^T][D'][G]$

$k=k+1$

be equal to $n\Delta t$ but to a much greater time period since Δt, governed by stability criteria, is usually very small unless greatly increased by the device of high fictitious nodal masses. Non-linear visco-elastic materials in which properties depend continuously on stress level may be dealt with by returning at intervals to stage I.

CALIBRATION OF VISCO-ELASTIC CONSTANTS

For short term dynamic loading, interest is centred on the immediate elastic response and primary creep. For plastic coated voiles dynamically loaded this creep is high compared with the secondary quasi-static creep rate. If a strip of such material is subject to a suddenly applied constant load and dynamic deflections are recorded in a way which does not induce external friction to the system, a plot of strain vs. time is obtained which is typified by fig. 4.

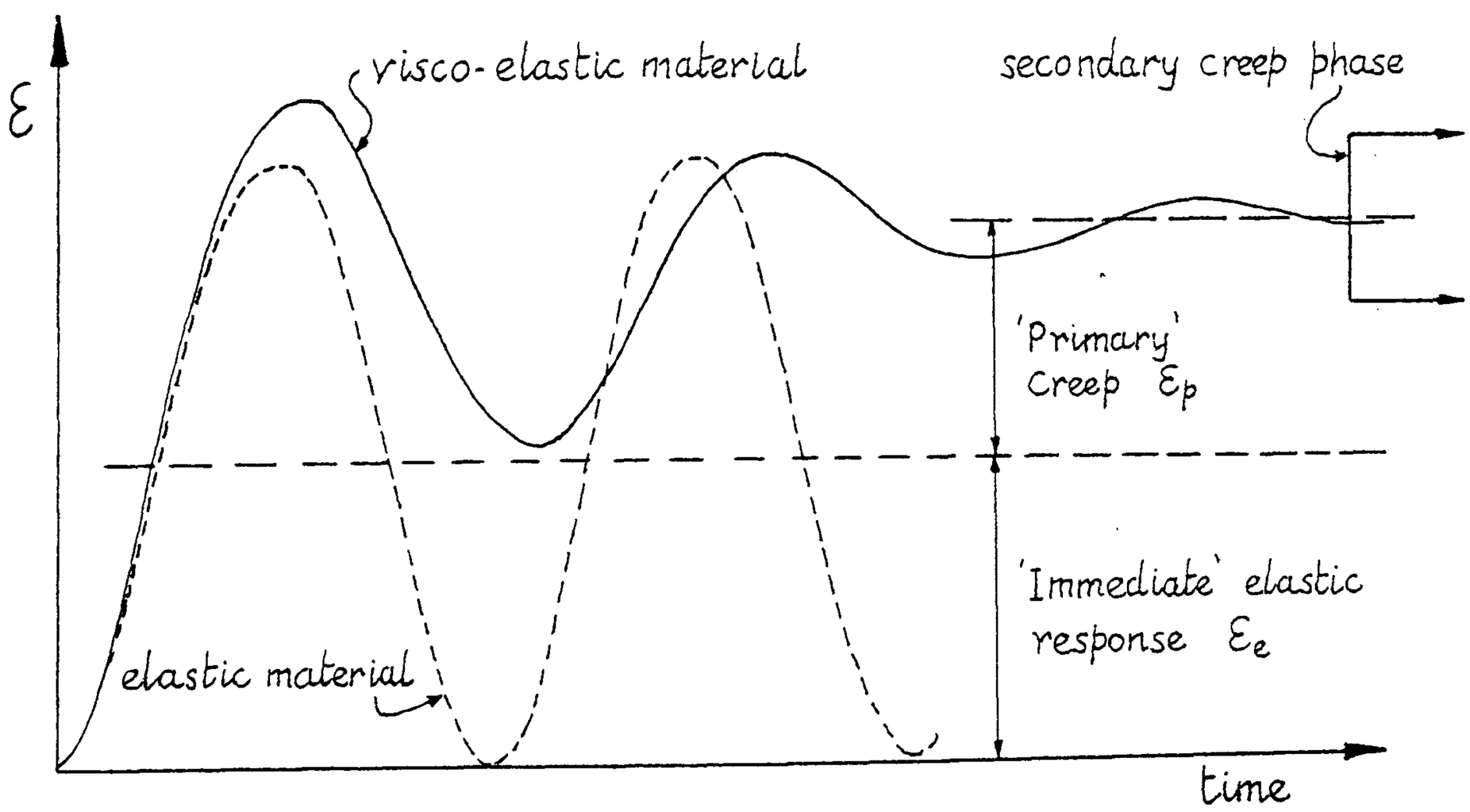


Figure 4

Restricting equation (12a) to the region termed primary creep stage, during which deflections are damped by the viscous property of the material, at the end of this stage:

$$\varepsilon_c^{t+n\Delta t/2} \triangleq \varepsilon_c^{t-n\Delta t/2} \triangleq \varepsilon_p$$

hence since σ is then constant: $b = \frac{a\sigma^t}{\varepsilon_p}$

Also the immediate elastic modulus is of the order, but greater than, $\frac{\sigma}{\varepsilon_e}$.

With these relations as guides, the material constants a, b and E may be determined by curve fitting a simple analysis to the experimental data.

Since in general the material 'constants' depend on stress level, calibration should be carried out as a perturbation from the expected initial stress. For the cladding of networks this may be zero, and for pneumatic structures it will be an approximately known value dependent on internal pressure.

The visco-elastic model and computational procedures outlined are highly simplified and require cross-calibration of the sort indicated to be effective. They do however allow at least a qualitative assessment of the effect of visco-elastic material damping on the vibratory behaviour of membranes and networks. The latter may more usefully be clad with sandwich panels. If 'constant moment' triangular elements (analogous to the membrane elements) are used the natural stiffness is

again 3x3 in terms of average side rotations. These rotations can be expressed in terms of normal nodal displacements of an element and the adjacent group of elements; the associated nodal forces being shears. Such sandwich elements can thus be incorporated into the basic iterative scheme with little modification or increase in storage requirements. An outline of the procedure is given in appendix 5.2.

DYNAMIC, STATIC AND FORM-FINDING ANALYSES

The critical time interval for numerical stability of the computations is given approximately by:

$$\sqrt{\frac{2m}{s}} < \Delta t_{crit} < \sqrt{\frac{4m}{s}} \qquad (13)$$

where m/s is the lowest ratio of mass to direct stiffness (relative to adjacent nodes) at any node of the structure [7]. In practice the lower value gives the closest estimate, and for surface or network structures the critical motion is tangential to the surface; stiffnesses normal to the surface being very much lower. Depending on the accuracy required of an analysis for dynamic stresses, the fineness of the structural idealization, and the importance of the highest frequency responses, the time interval chosen for such analyses may need to be much lower than that given by (13). The dominant frequencies of normal deflections however may be predicted accurately when using a value close to the critical time interval.

The numerical procedure may be used for static load analyses by imposing, in addition to any real damping, fictitious viscous damping proportional to nodal velocity components. The procedure is equivalent to Dynamic Relaxation [8,9] used in a separated finite element form.

The recurrence equation (4) for velocities may then be written as:

$$V_{ix}^{t+\Delta t/2} = A.\frac{\Delta t.R_{ix}^{t}}{m_{ix}} + B.V_{ix}^{t-\Delta t/2} \qquad (14)$$

where $A = \left(\frac{1}{1 + k\Delta t/2}\right)$; $B = \left(\frac{1 - k\Delta t/2}{1 + k\Delta t/2}\right)$

and k is the fictitious viscous nodal damping per unit mass. The vibratory behaviour of the nodes may in this way be rapidly damped to positions of static equilibrium. Ideally the motions of the structure should be just less than critically damped in order to obtain bounds to the true solution. The critical damping is given by $k = 4\Pi f$, where f is the frequency of vibration which may be obtained from a short trial run or adjusted during the analysis. Evidently, from (13) and (14) fictitious nodal masses m_{ix} which differ for each co-ordinate direction should also be used in order to optimise the convergence of the analysis. These matters are examined in relation to tension structures in ref. [10].

The procedure for static analysis can be extended to cope with the form-finding of uniform or variable stress membrane

and pneumatic structures, and isostatic, uniform-mesh or geodesic networks; the boundaries of which may be tension or compression funiculars with variable spatial curvature [10,11,12]. Control of the form may be effected dynamically, primarily by specifying in equations (6) the pre-stress or elastic stiffnesses of any element; and by the adjustment of link lengths and tractions, and reaction forces and positions.

Of major interest in the design of tension surface structures is the range of frequencies of free vibration to be expected throughout the structure under various conditions of static load and mass distribution. If the static analysis procedure is used with sub-critical damping and with real nodal mass components normal to the surface, these frequencies may be obtained as a useful by-product. It will often be the case that the frequencies of network surface structures involving degrees of mechanical freedom are very low, far-coupled and grouped within a narrow range such that beating phenomena may be observed. The use of structural cladding to triangulate the network across unbuckled diagonals may enable frequencies to be increased and the range dispersed. If the cladding is visco-elastic it may also have an important effect on the damping of unwanted vibrations. The main advantage of the type of analysis outlined in the paper is the consideration within a unified procedure of such design aspects from the stage of form-finding to final analysis and the ability to cope naturally with the occurrence of mechanisms and zero stiffness situations. It is appropriate that such structures should be treated as 'in motion', under all conditions, whether the loading is 'static' or dynamic.

REFERENCES

(1) Oden, J.T., Key, J.E., Fost, R.B., 'A Note on the non-linear dynamics of elastic membranes by the finite element method'. Computers and Structures, V.4.(1974), pp 445-452.

(2) Key, S.W., Belsinger, Z.E., 'The transient dynamic analysis of thin shells by the finite element method'. Proc. 3rd Conf. on Matrix Methods in Struct. Mechanic, Wright-Patterson Air Force Base, Ohio (1971).

(3) Krieg, R.D., Key, S.W., 'Transient shell response by numerical time integration'. Int.J. for Numerical Methods in Eng., V.7(1973) pp 273-286.

(4) Krieg, R.D.,'Unconditional stability in numerical time integration methods', J. Appl. Mech. V.40E.n.2 (1973) pp 417-421

(5) Argyris, J.H., 'Recent advances in matrix methods of structural analysis', Progress in Aeronautical Sciences V.4. London (1963).

(6) Zienkiewicz, O.C., Watson, M., King, I.P., 'A numerical method of visco-elastic stress analysis', Int.J.Mech.Sci. V.10 (1968) pp 807-827.

(7) Barnes, M.R., 'Dynamic relaxation analysis of cable networks', Int.Conf. on Tension Structures, London (April 1974) Chapter 2

(8) Day, A.S., 'An introduction of dynamic relaxation', Engineer, 219 (1965), pp 218-221

(9) Otter, J.R.H., 'Computations for pre-stressed concrete reactor pressure vessels using dynamic relaxation'.

(10) Barnes, M.R., 'Applications of dynamic relaxation to the topological design and analysis of cable, membrane and pneumatic structures', 2nd Int. Conf. on Space Structures, Guildford, (1975) Chapter 4

(11) Barnes, M.R., 'Form-finding of minimum surface membranes', World Congress on Structures for space enclosures, I.A.S.S., Montreal (July 1976) Chapter 5

(12) Barnes, M.R., 'Interactive graphical design of tension surface structures', Int. Symp. on wide-span surface structures, Stuttgart (April 1976) Chapter 8

APPENDIX 5.1

NORMAL PRESSURE VECTOR

For the triangular element in figure 5, the vector of side ①, V_{12}, is:

$$V_{12} = \begin{Bmatrix} x_2 - x_1 \\ y_2 - y_1 \\ z_2 - z_1 \end{Bmatrix} = \begin{Bmatrix} x_{21} \\ y_{21} \\ z_{21} \end{Bmatrix}$$ Similarly for V_{13}

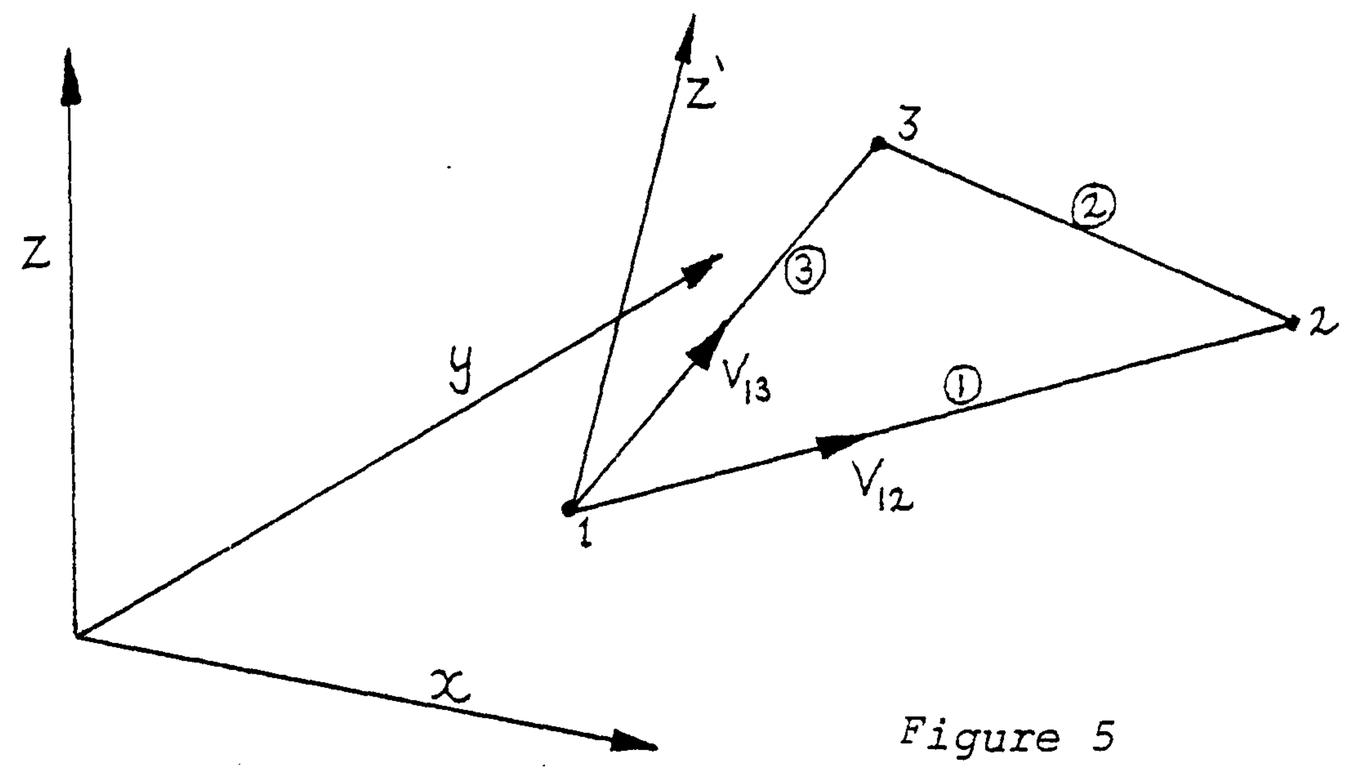


Figure 5

The vector z` normal to the plane of the element is given by the vector cross product of two sides[13], thus:

$$V_{z'} = V_{12} \times V_{13} = \det \begin{vmatrix} 1 & 1 & 1 \\ x_{21} & y_{21} & z_{21} \\ x_{31} & y_{31} & z_{31} \end{vmatrix}$$

$$= (y_{21} \cdot z_{31} - y_{31} \cdot z_{21}) - (x_{21} \cdot z_{31} - x_{31} \cdot z_{21}) + (x_{21} \cdot y_{31} - x_{31} \cdot y_{21})$$

As a vector $V_{z'} = \begin{Bmatrix} y_{21} \cdot z_{31} - y_{31} \cdot z_{21} \\ z_{21} \cdot x_{31} - z_{31} \cdot x_{21} \\ x_{21} \cdot y_{31} - x_{31} \cdot y_{21} \end{Bmatrix} = \begin{Bmatrix} A \\ B \\ C \end{Bmatrix}$ (15)

$(A^2 + B^2 + C^2)^{1/2} = 2\Delta$ where Δ is the area of the triangle.

The normal direction cosines are thus:

$$\begin{Bmatrix} \lambda_{z'x} \\ \lambda_{z'y} \\ \lambda_{z'z} \end{Bmatrix} = \frac{1}{2\Delta} \begin{Bmatrix} A \\ B \\ C \end{Bmatrix} \qquad (16)$$

For a distributed load p per unit area acting normal to the element, the equivalent load at each node is $p\Delta/3$. Hence, using the direction cosines, the resolved components at each node are:

$$P_x = \frac{p}{6} A \; ; \quad P_y = \frac{p}{6} B \; ; \quad P_z = \frac{p}{6} C \qquad (17)$$

For right-handed global co-ordinate system, the normal vector is out of the plane as shown in the figure. Thus internal pressure is +ve if the element is viewed externally.

From a programing point of view it is convenient to number the links of the structure and assign vector directions to these links by specifying the node numbers at end 1 and end 2 respectively. The sides of each triangle, in anticlockwise order, are then defined by the appropriate link numbers (which may also coincide with cable or bar elements). Noting that the signs of A, B and C are unaltered if the vectors of sides 1 and 3 are both reversed, the nodal force components may be set from the vector data of side links 1 and 3, irrespective of the vector directions, provided the sign of p is changed if end 1 of ① coincides with end 2 of ③ or vice versa.

REFERENCE

(13) O.C. Zienkiewicz, 'The finite element method in Engineering Science'. McGraw Hill, 1973.

APPENDIX 5.2

CONSTANT MOMENT HOMOGENEOUS OR SANDWICH PLATE ELEMENT

The purpose of the procedure outlined below is to suggest a method for the incorporation of panel cladding elements in which bending moments normal to the plane may be significant. The final derivation should allow such elements in the dynamic relaxation process without increasing the degrees of freedom to include rotations. Thus translational displacements remain the only ones to be considered. This is made possible because of the separation of equilibrium and compatibility in the DR iterative process. Curvatures and hence moments acting across element sides at any stage are determined from the normal nodal displacements of adjacent elements, and the moments are then transformed to equivalent nodal shear forces. The procedure might be simply extended to the case of sandwich construction with thin external elastic panels enclosing a shear medium. The formulation suggested, however, has not been checked by analytical trials.

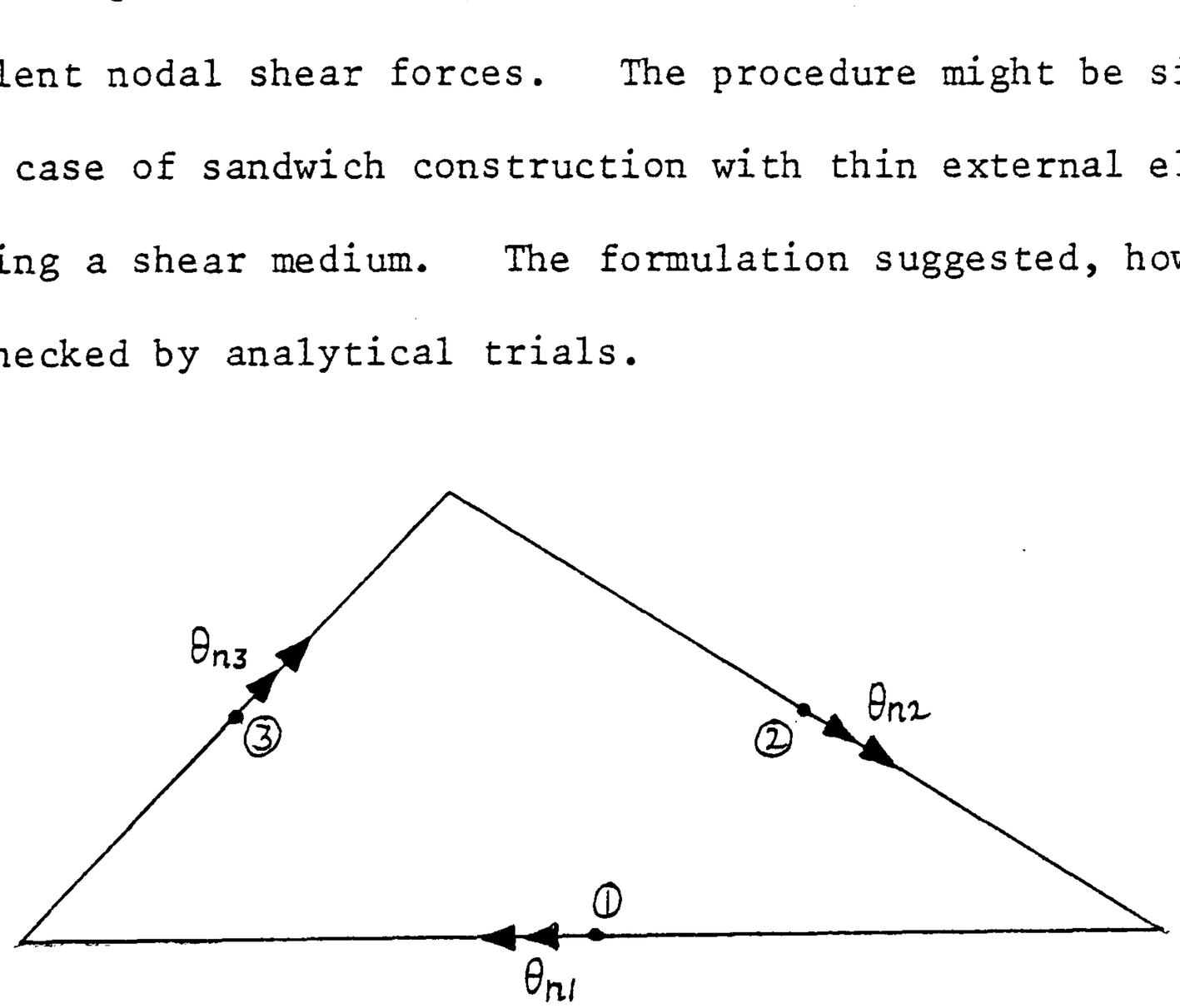


Figure 6

Consider a triangular bending element with mid-side nodes (fig. 6). The element displacements to be initially considered are the normal rotations at these points, and these are to be regarded as average

side rotations (Θ_n). Thus top, bottom and intermediate planes of the triangle have sides which remain straight lines after deformation. Under these conditions, in order that the displacement parameters should be independent, a uniform normal rotation of one side should produce no rotation at the mid-points of the other two sides (fig.7). Thus the average normal rotations of these sides are zero.

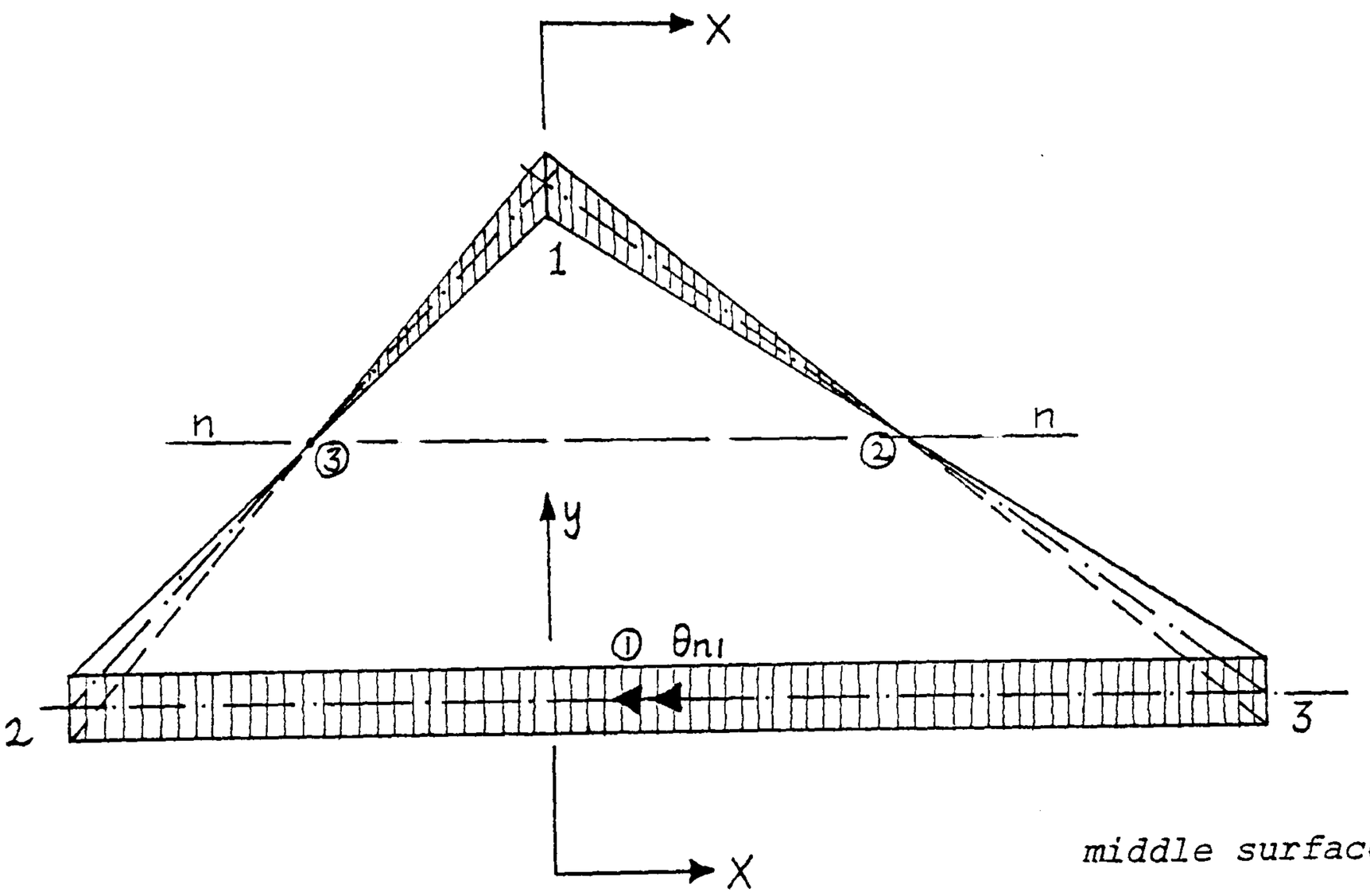


Figure 7 Plan View

Section XX may be viewed in two ways (figs. 8a,b):

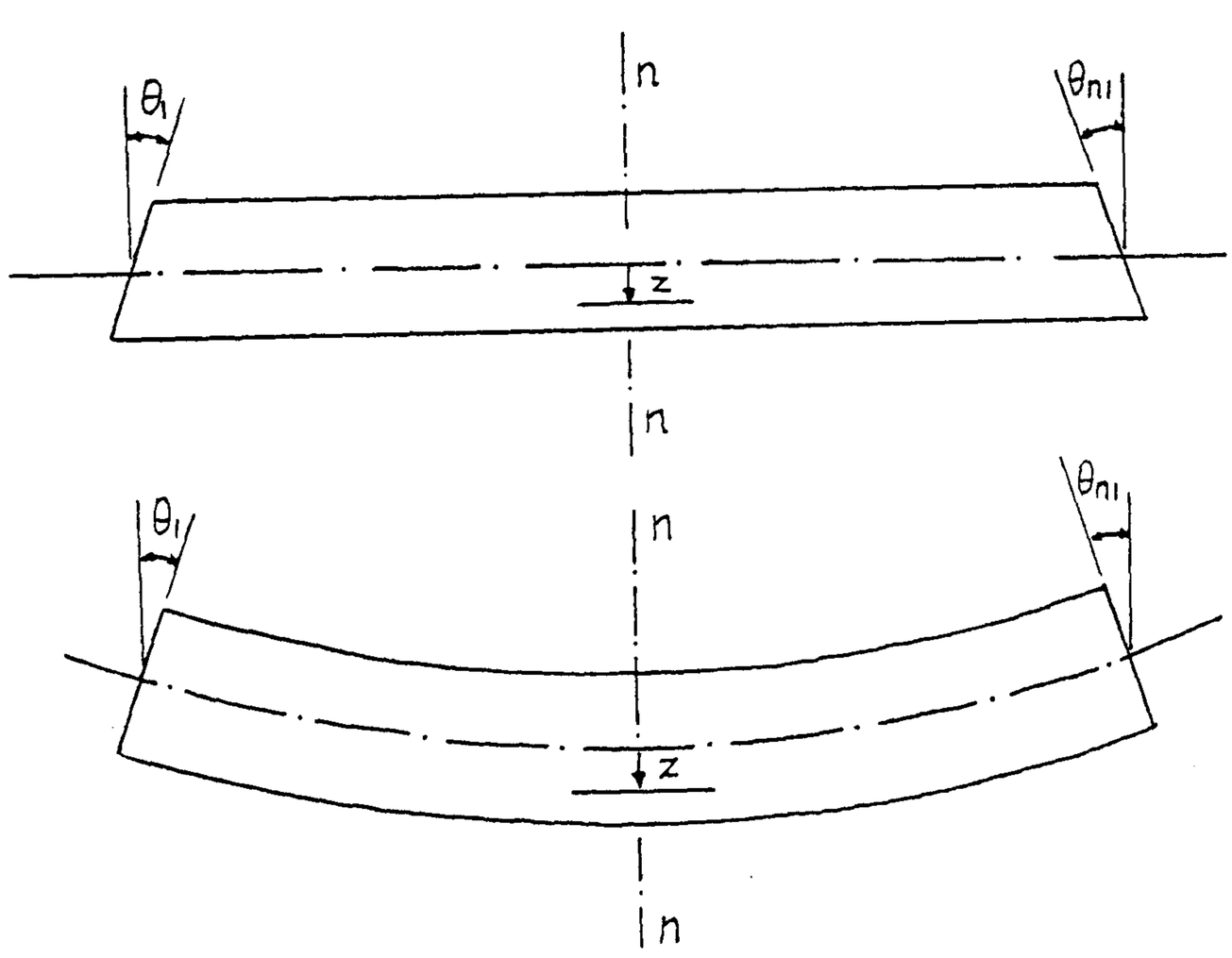


Figure 8a

Figure 8b

In either case the normal nn remains normal to the middle surface, and if the curvature in 8b is constant ($= \frac{2\theta_{nl}}{S}$), the strain in direction y, at any depth z from the neutral surface, is identical for the two cases and $\theta_1 = \theta_{nl}$. The derivation of moment stiffness relations can be based on either case, but the first (8a) is appropriate for present purposes and may also be extended to sandwich elements. The second case is considered by Morley[14] who assumes a quadratic normal displacement function to derive a 6x6 stiffness matrix for a constant moment element with mid-side moments and apex shear forces as the generalized element forces. The object of the present derivation is to derive 3x3 relative stiffness relations with only apex shears as the forces. In contrast to Morley's formulation, however, the Kirchoff plate conditions are satisfied only approximately.

Direct Strains in the Element

Consider two adjacent, initially co-planar, elements which have been deformed in a manner compatible with figure 8a:

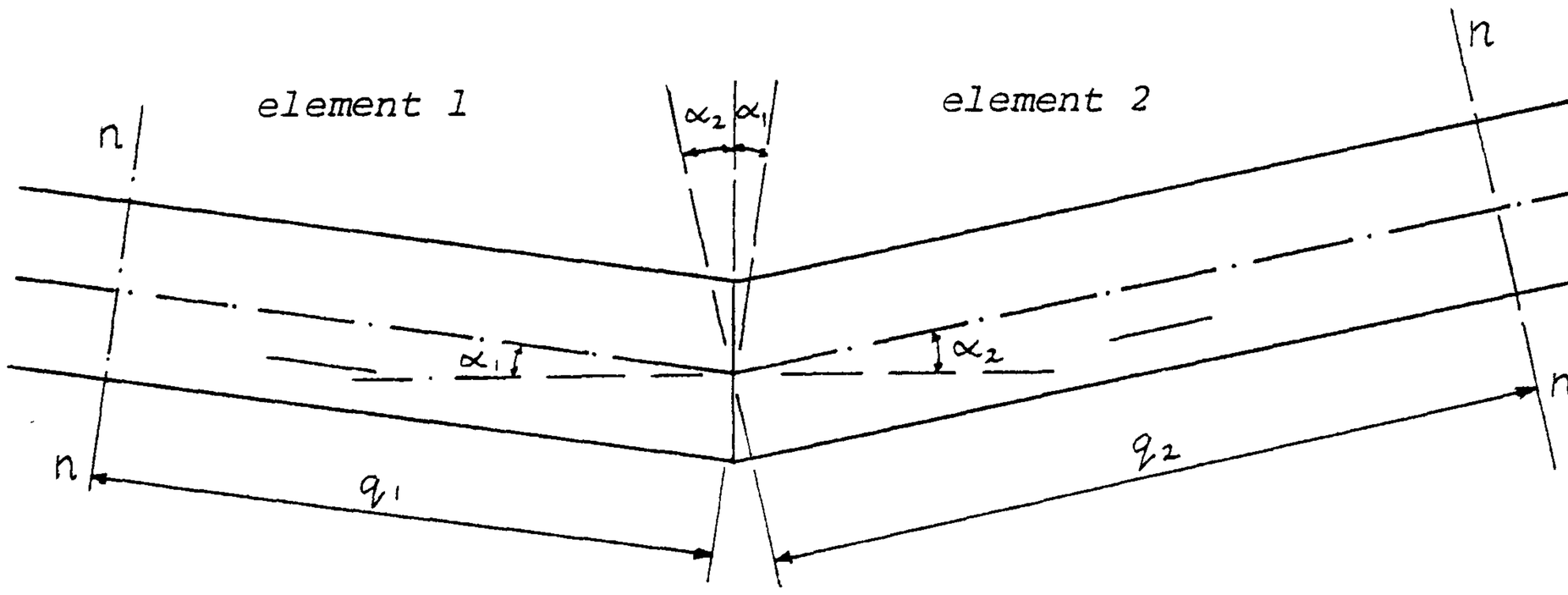


Figure 9

If the deformation angle between the two elements is:

$$\theta = \alpha_1 + \alpha_2$$

Then, assuming the direct strain normal to the boundary is continuous across the boundary, the strain ε at any depth z is given by:

$$\varepsilon = \frac{\Theta . z}{(q_1 + q_2)}$$

where q_1 and q_2 are the distances from the junction to the undistorted normals nn.

Hence, if A_1 and A_2 are the areas of the two triangular elements and ℓ is the length of the junction:

$$\varepsilon = \frac{\Theta . \ell . z}{(A_1 + A_2)} = \Theta . \rho . z \qquad (18)$$

At any stage in an iterative analysis the deformation angles (Θ) between adjacent elements can be set for each link using the normal vectors of the elements which are obtained from the current nodal co-ordinates (see Appendix 5.1). Referring to figure 10, the angle Θ between the two elements is given by the scalar product of the normal vectors v_1 and v_2:

$$\text{Cos}\,\Theta = \frac{V_1 . V_2}{\ell_1 . \ell_2}$$

where $\ell_1 = 2A_1$ and $\ell_2 = 2A_2$

$$\text{Thus:} \quad \text{Cos}\,\Theta = \lambda_{z'x_1} . \lambda_{z'x_2} + \lambda_{z'y_1} . \lambda_{z'y_2} + \lambda_{z'z_1} . \lambda_{z'z_2} \qquad (19)$$

where the direction cosines (λ) have already been set to deal with distributed pressure loading (appendix 5.1) and will subsequently be needed to resolve the nodal shears into cartesian global components.

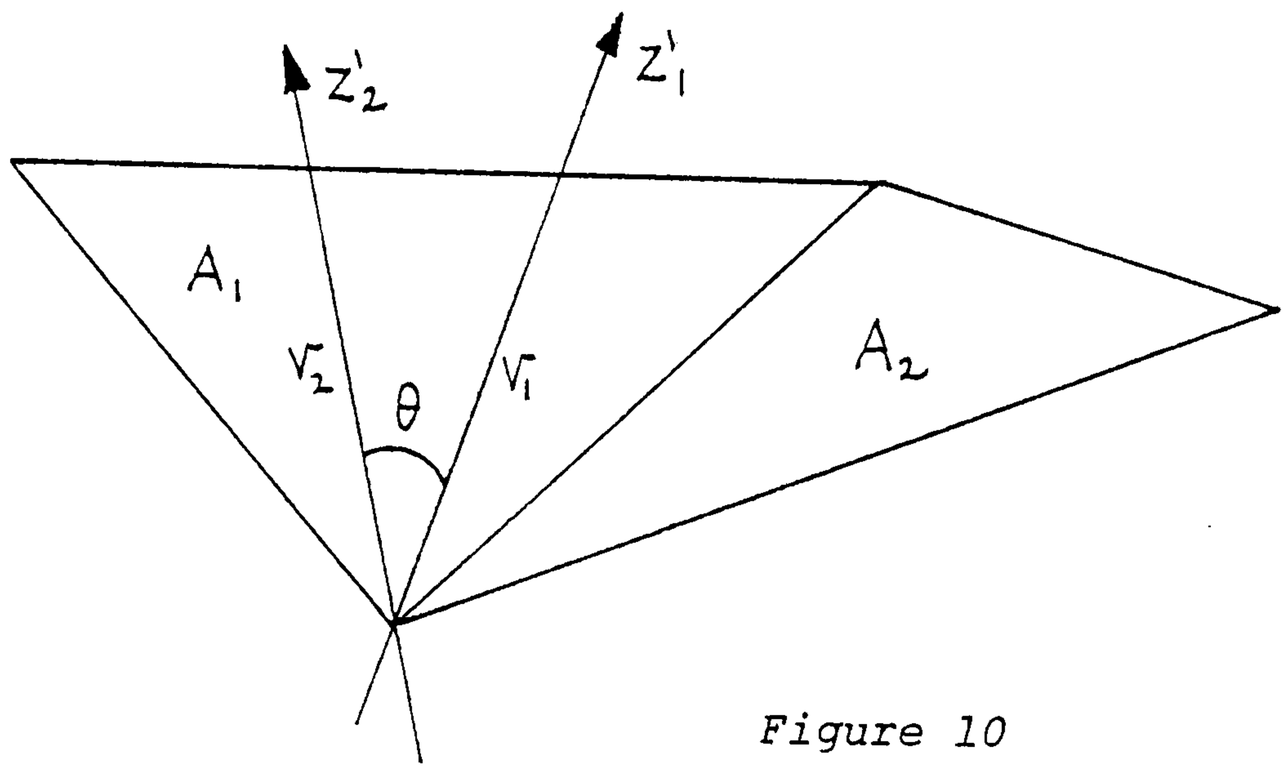


Figure 10

If the elements of the structure are not initially co-planar the difference between the current and initial discontinuity angles must be computed. Thus equation (18) becomes:

$$\varepsilon = z.\rho.(\Theta - \Theta_o) = z.\rho.\delta\Theta \qquad (20)$$

Referring again to figure 9, the normal rotation of the side for element 1 is:

$$\alpha_1 = \frac{q_1 \varepsilon}{z} = q_1.\rho.\delta\theta = \frac{A_1}{\ell}\rho\ \delta\theta = A_1\rho'\delta\theta$$

The vector or normal side rotations for any element is thus:

$$\{\Theta_n\} = \begin{Bmatrix}\Theta_{n1}\\ \Theta_{n2}\\ \Theta_{n3}\end{Bmatrix} = A\begin{bmatrix}\rho_1' & 0 & 0\\ 0 & \rho_2' & 0\\ 0 & 0 & \rho_3'\end{bmatrix}\begin{Bmatrix}\delta\Theta_1\\ \delta\Theta_2\\ \delta\Theta_3\end{Bmatrix} = [R]\{\delta\Theta\} \qquad (21)$$

and the vector or direct strains at depth z normal to the element sides (figure 11a) is:

$$\{\varepsilon\} = \begin{Bmatrix}\varepsilon_1\\ \varepsilon_2\\ \varepsilon_3\end{Bmatrix} = z\begin{Bmatrix}\rho_1.\delta\Theta_1\\ \rho_2.\delta\Theta_2\\ \rho_3.\delta\Theta_3\end{Bmatrix} = \frac{z}{A}\begin{bmatrix}\ell_1 & 0 & 0\\ 0 & \ell_2 & 0\\ 0 & 0 & \ell_3\end{bmatrix}\begin{Bmatrix}\Theta_{n1}\\ \Theta_{n2}\\ \Theta_{n3}\end{Bmatrix} = z[T]\{\Theta_n\} \qquad (22)$$

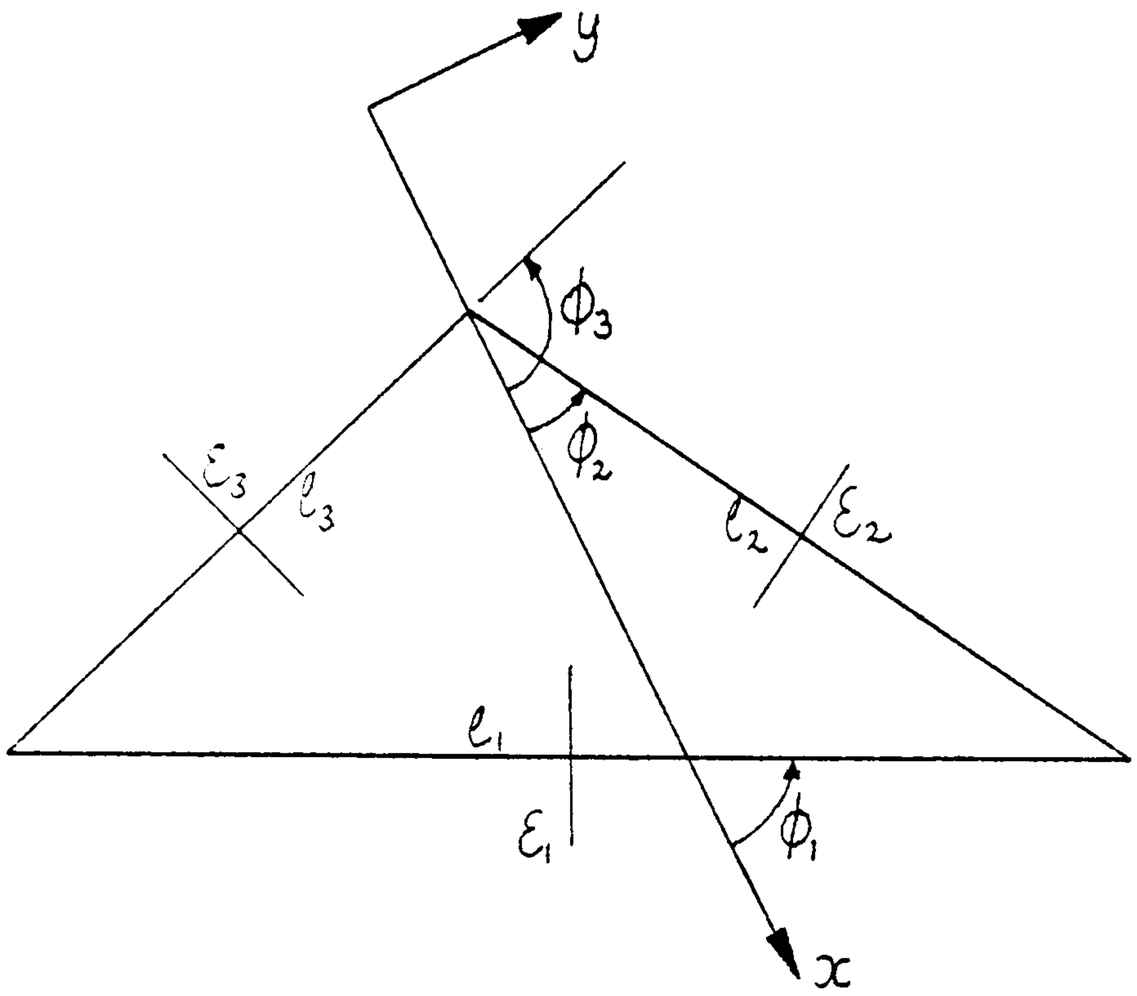


Figure 11a

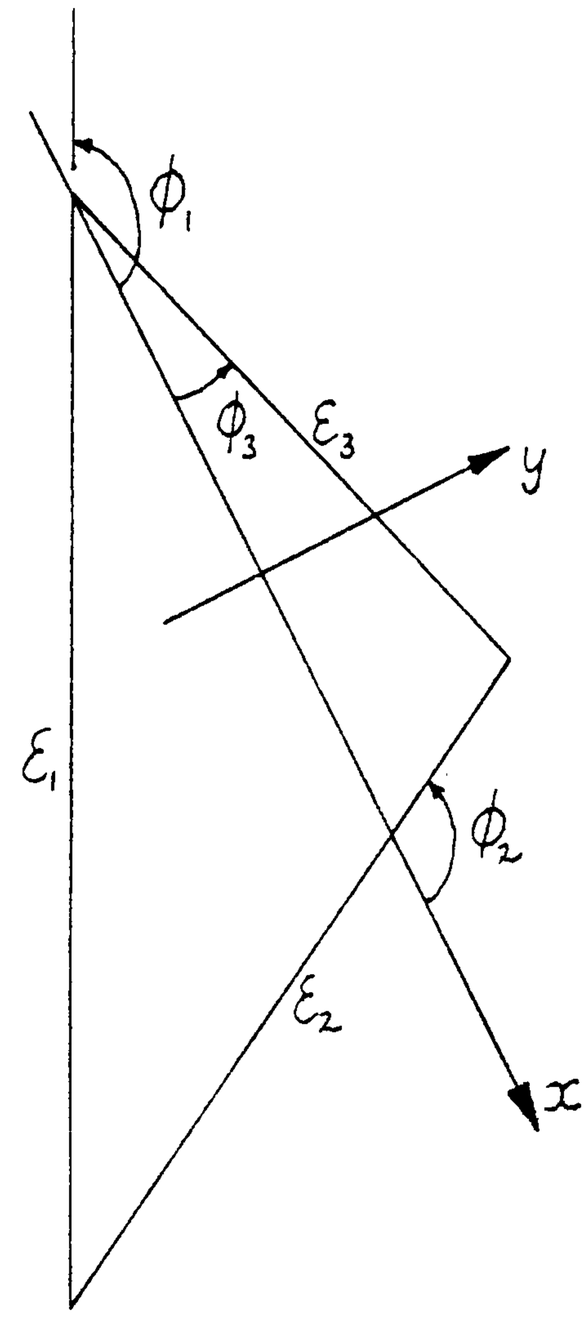


Figure 11b

The reciprocal diagram for these strains (constant throughout the plane at depth z) is shown in figure 11b, and the orthogonal strains may be expressed as:

$$\{\varepsilon_{xy}\} = \begin{Bmatrix}\varepsilon_x\\ \varepsilon_y\\ \gamma_{xy}\end{Bmatrix} = [G'] \begin{Bmatrix}\varepsilon_1\\ \varepsilon_2\\ \varepsilon_3\end{Bmatrix} = z\,.\,[G'][T]\{\theta_n\} \qquad (23)$$

where the terms in the matrix $[G']$ are given by the equations:

$$\frac{\varepsilon_x}{\begin{vmatrix} b_1 & c_1 & \varepsilon_1\\ b_2 & c_2 & \varepsilon_2\\ b_3 & c_3 & \varepsilon_3\end{vmatrix}} = \frac{-\varepsilon_y}{\begin{vmatrix} a_1 & c_1 & \varepsilon_1\\ a_2 & c_2 & \varepsilon_2\\ a_3 & c_3 & \varepsilon_3\end{vmatrix}} = \frac{\gamma_{xy}}{\begin{vmatrix} a_1 & b_1 & \varepsilon_1\\ a_2 & b_2 & \varepsilon_2\\ a_3 & b_3 & \varepsilon_3\end{vmatrix}} = \frac{1}{\begin{vmatrix} a_1 & b_1 & c_1\\ a_2 & b_2 & c_2\\ a_3 & b_3 & c_3\end{vmatrix}}$$

and $a_i = \cos^2\phi_i' = \sin^2\phi$, $b_i = \sin^2\phi_i' = \cos^2\phi_i$, $c_i = \sin\phi_i'\cos\phi_i' = -\cos\phi_i\sin\phi_i$

The stresses in the plane are:

$$\{\sigma_{xy}\} = \begin{Bmatrix}\sigma_x\\ \sigma_y\\ \tau_{xy}\end{Bmatrix} = \begin{bmatrix} d_{11} & d_{12} & 0\\ d_{21} & d_{22} & 0\\ 0 & 0 & d_{33}\end{bmatrix} \begin{Bmatrix}\varepsilon_x\\ \varepsilon_y\\ \gamma_{xy}\end{Bmatrix} = [D]\{\varepsilon_{xy}\} = z\,[D][G'][T]\{\theta_n\} \qquad (24)$$

where d_{ij} are orthotropic elastic constants.

equivalent nodal shears exerted by the element on the nodes are given by:

$$S_1 h = M_2 \cos\Theta_3 . M_3 \cos\Theta_2 - M_1$$

$$\therefore \quad S_1 = \frac{\ell_1}{2A}\left[M_2 \frac{(\ell_2^2 + \ell_1^2 - \ell_3^2)}{2\ell_1\ell_2} + M_3 \frac{(\ell_3^2 + \ell_1^2 - \ell_2^2)}{2\ell_1\ell_3} - M_1 \right]$$

where S_1 acts into the plane of the element.

Similarly for S_2 and S_3. Hence the vector of nodal shears is:

$$\begin{Bmatrix} S_1 \\ S_2 \\ S_3 \end{Bmatrix} = \{S\} = [H]\{M\} = [H][K]\{\Theta_n\}$$

where the terms in matrix $[H]$ are given by:

$$h_{ii} = -\ell_i/2A \; ; \quad h_{ij} = (\ell_i^2 + \ell_j^2 - \ell_k^2)/4A\ell_j$$

Finally, substituting from equation (21) for $\{\Theta_n\}$:

$$\{S\} = [H][K][R]\{\delta\Theta\} = [Q]\{\delta\Theta\} \qquad (27)$$

Provided gross straining of the middle surface due to in plane forces does not occur, the matrix $[Q]$ need be computed and stored once only for each element at the start of a DR analysis. If gross straining does occur $[Q]$ may be re-computed at infrequent intervals.

For a virtual deformation $\{\theta_n^*\}$ of the plate element, inducing corresponding virtual strains $\{\varepsilon_{xy}^*\} = z.[G'][T]\{\theta_n^*\}$ in a plane at depth z from the middle surface, the internal virtual work is given by the product of real stresses and virtual strains integrated throughout the volume of the element:

$$VW = A. \int_{-t/2}^{+t/2} \{\theta_n^*\}^T [T][G']^T [D][G][T]\{\theta_n\} z^2 dz \qquad (25)$$

The external virtual work is: $\{\theta_n^*\}^T \{M\}$

where $\{M\}$ is the vector of (total) moments acting across the element sides.

Equating the internal and external work, the relative stiffness relations are thus:

$$\{M\} = \left[\frac{At^3}{12}[T][G']^T[D][G'][T]\right]\{\theta_n\} = [K]\{\theta_n\} \qquad (26)$$

The moments $\{M\}$ are moments exerted on the element, +ve if they act in a sense causing tensile strains on the lower surface.

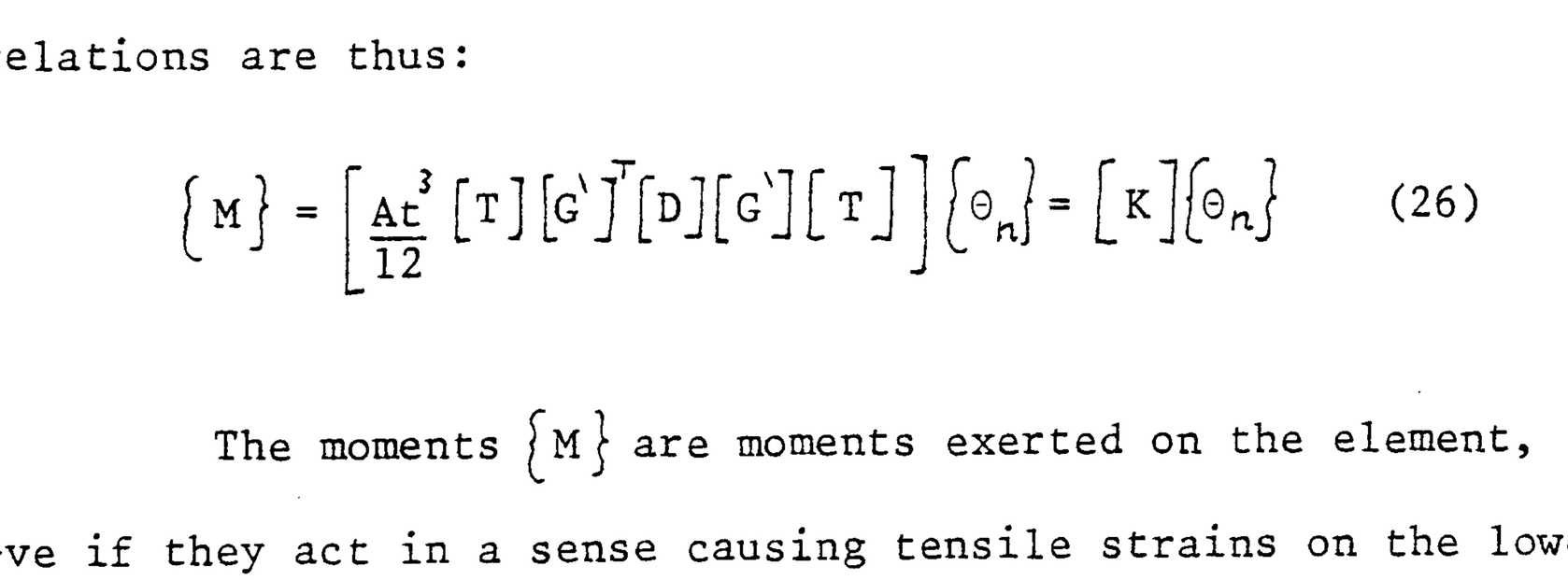


Figure 12

Referring to figure 12, taking moments about side ① : the

Relations (27) should, in principle, enable a DR analysis to be carried out using only translational displacements and lumped masses at the nodes of the structure (as opposed to deflections and rotations, and consistent mass matrices). The saving in computing time and storage should thus be considerable. Similar concepts might be applied in the case of "constant moment" beam elements. The derivation given might also be modified to account for sandwich cladding. In this case the virtual work expression (25) would have to account instead for discrete external panels and, if significant, the virtual work done by shearing of the fill material.

REFERENCE

(14) L.S.D. Morley, 'The constant-moment plate-bending element', Journal of Strain Analysis, Vol.6, no.1, 1971.

CHAPTER 6

AN INVESTIGATION OF VIBRATION DECAY IN A MODEL PNEUMATIC DOME

SUMMARY

The chapter forms an experimental correlation with the previous one (referenced [1] in the present text). It considers the suitability of a simple Kelvin model for visco-elastic dynamic behaviour by comparing the observed decay of deflections in a pneumatic dome subject to a suddenly applied load with those calculated using a central difference numerical integration scheme.

MODEL DOME CONSTRUCTION AND TESTING

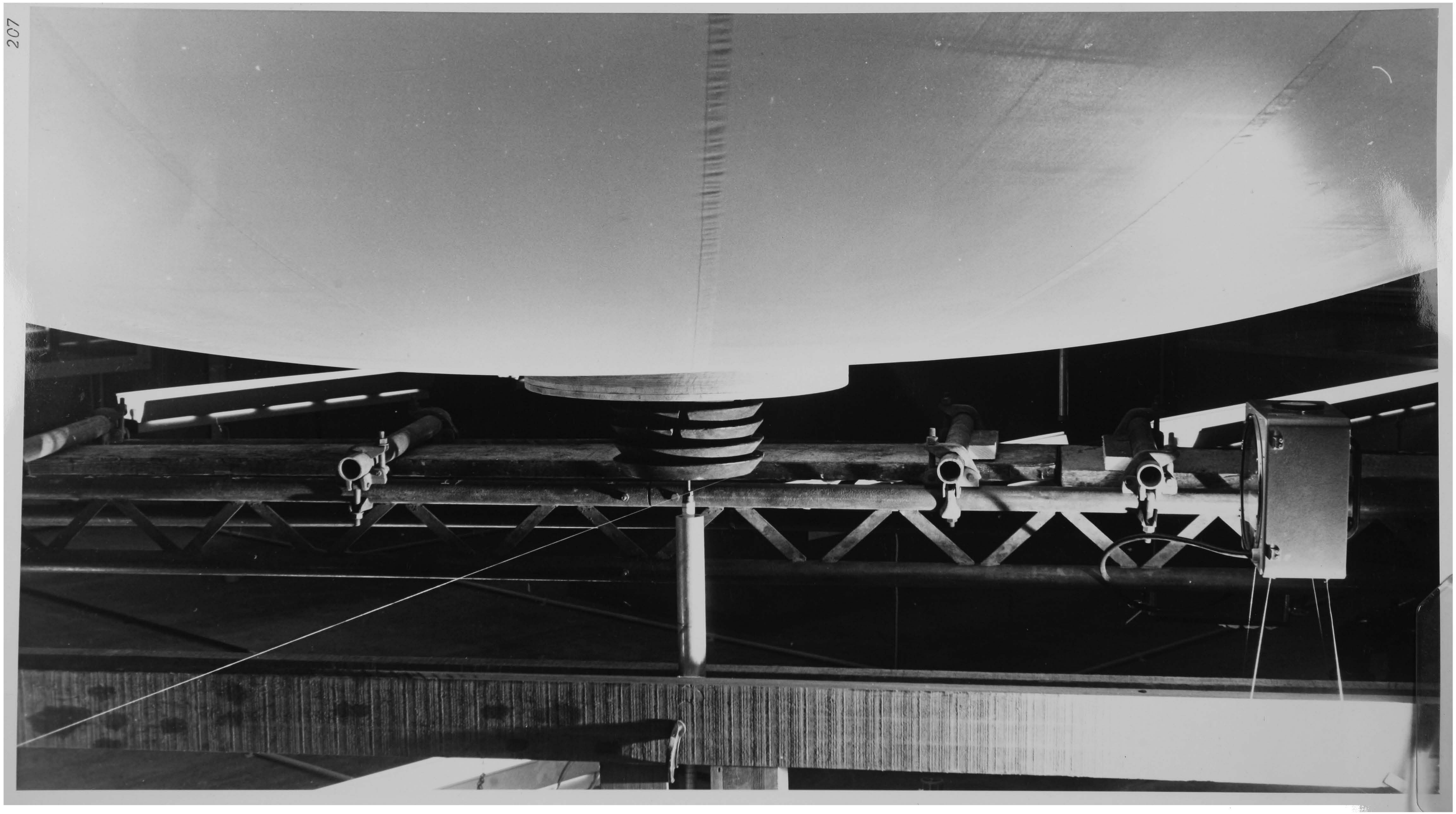
The model dome, a general view of which is shown in figure 1, had a base diameter of 4.74m and a crown height of approximately 0.9m when prestressed by internal pressure. The dome was assembled from twenty segments closed at the crown by a circular capping of 0.58m diameter. The membrane material was P.V.C. coated terylene voile approximatey 0.2mm thick, and the segments were cut so that the weave was aligned with the weaker weft direction parallel with hoop contours. The cutting template for the segments was shaped to give as closely as possible a spherical diameter of 7.0m for zero membrane stress; the segments being lap jointed with Bostik adhesive over a former of the correct curvature. The dome was sealed to the support base by double sided tape which enabled initial adjustment, and the base was bevelled so that this joint was subject to shear rather than peeling (fig.2).

The dome was prestressed by an internal pressure of 150 Pa. inducing an average membrane tension in the region of 260 N/m. After creep deformations had approached a terminal value under the prestress condition, a central 0.58m diameter ring load of 1000 N was suddenly applied to the dome by cutting a supporting cable which had previously been adjusted so that the ring was just touching the dome. Dynamic deflections were then traced by means of a 16mm cine camera (at 64 frames per second) sighted on to a fixed marker and a vertical scale attached to the loading platten (fig. 1b).



206

Figure 1



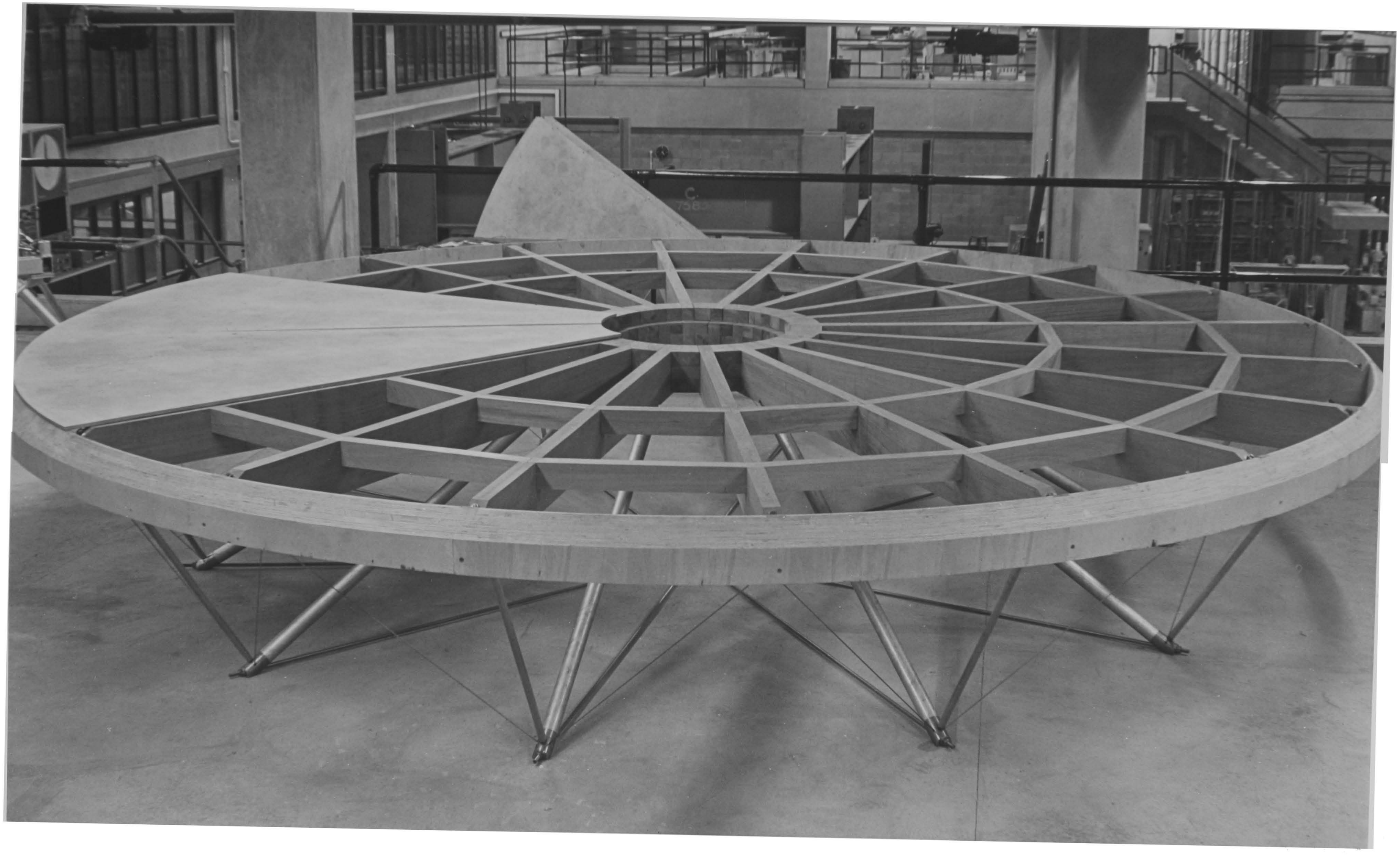


Figure 2

CALIBRATION OF MATERIAL CONSTANTS

The membrane material was such that the stiffness and strength in the warp direction of the weave was considerably greater than that in the weft direction and the shearing stiffness was negligible. The dynamic moduli and visco-elastic constants for each direction were calibrated by applying a sudden load to two identical strips cut from the material. The strips were suspended (figure 3) with a dead load of 25 N applied to induce membrane tension of approximately half the sum of the average tensions in the dome structure under prestress and loaded steady state conditions.

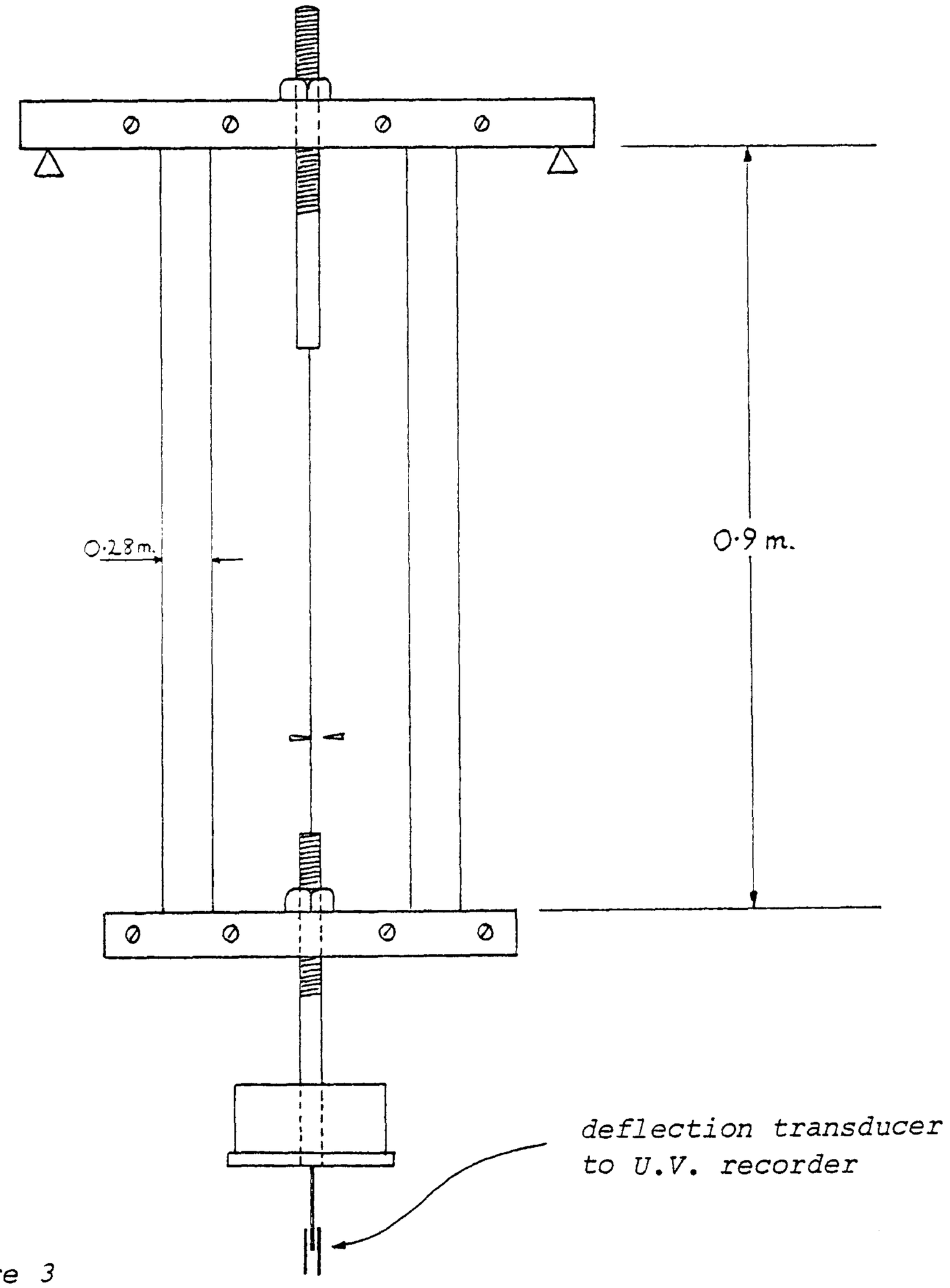


Figure 3

Deflections under the load could be recorded by means of a frictionless transducer coupled to an ultra violet recorder. The strips were allowed to creep for two hours under the dead loading and an additional load of 8 N was then applied but relaxed by tensioning a fine central wire so that the deflection returned to the dead load value. The full load was then suddenly applied by cutting the wire in such a way that no lateral disturbance was caused and the transducer core was at all times freely suspended in the coil housing.

The results for weft and warp directions are shown in figures 4 and 5 respectively. Because of the comparatively small creep in the warp direction, material constants (determined by trial analyses using the procedure outlined [1]) can be found which closely simulate the test results. In the weft direction, however, the three constants have been chosen to comply with the first peak deflection, the rate of decay, and the 'quasi-static' terminal deflection. In the intermediate stages the results are as good as can be expected bearing in mind the crudeness of the single Kelvin model for creep. Although the creep after one second continued at a fairly high rate, if allowance had been made for this the error in intermediate deflection values would have been even greater, and without the use of a more sophisticated creep model it was thought that the trace shown was the best that could be obtained.

For each calibration test the analysis was carried out using three different structural idealizations:

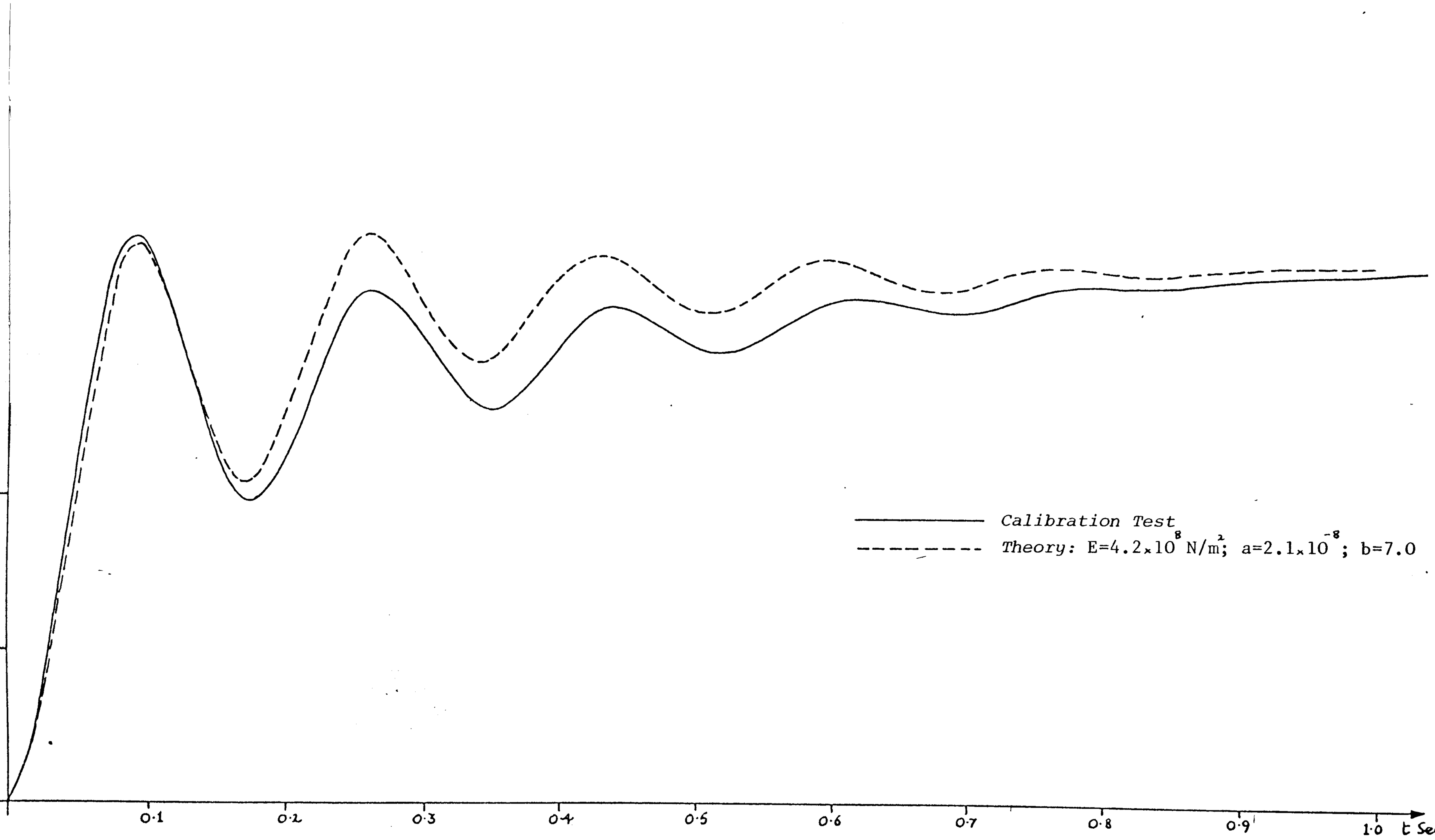


Figure 4 *Calibration Analysis for Weft Direction*

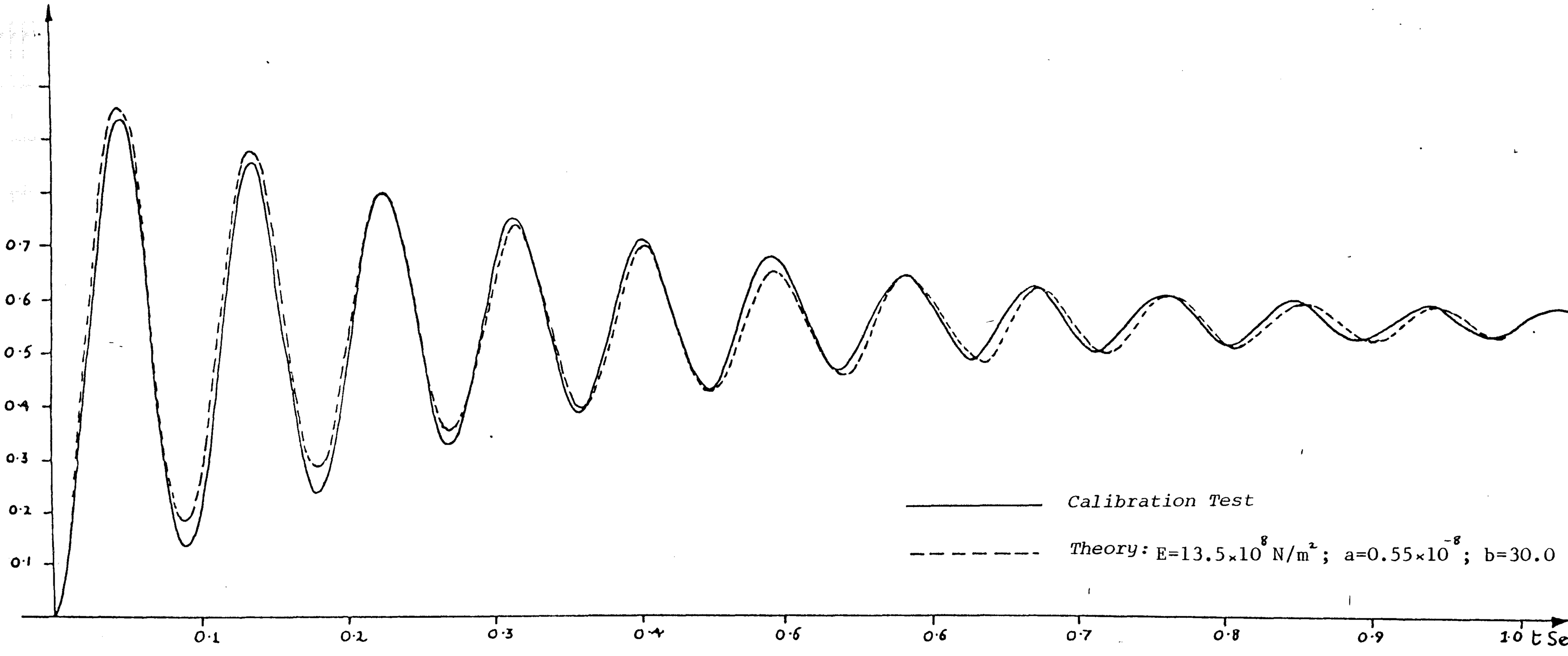


Figure 5 Calibration Analysis for Warp Direction

(i) as a single bar element with a time interval of 10% of the critical time interval.

(ii) as six bar elements with intermediate nodal masses of 2% of the end load mass and $\Delta t = 0.5\ \Delta t_{crit}$

(iii) as eighteen triangular membrane elements with intermediate nodal masses of 1% of the end load mass and $\Delta t = 0.5\ \Delta t_{crit}$

In each case creep strains were incremented at every time interval (n = 1 in Eq.(11) of [1]), and for case (ii) a second analysis was run using n = 5. The results were all found to plot on practically the same theoretical curves shown in figures 4 and 5. Using a single bar element with a time interval of 40% Δt_{crit} however, the error becomes signigicant. For illustrative purposes, hand calculations for the first two peaks of this case are given in Appendix 6.1 and the full trace for the weft direction is compared with figure 4.

The calibration tests described are of limited validity since, because of the mechanics of the weave, material properties in either direction will depend on the stress level in the other direction. A more realistic calibration might have been obtained by testing pressurized cylinders of the material but it would have been more difficult to obtain a trace of dynamic deflections without lateral disturbance and consequent friction in the transducer. The drawbacks of the strip test are to some extent aleviated by the fact that it was a short term test and the dynamic load was only 32% of the steady static load.

ANALYSIS OF THE DOME

The shape of the dome in the prestress condition was first determined with a segment of the structure (figure 6) idealized into orthotropic membrane elements possessing the calibrated visco-elastic constants, and using fictitious nodal damping (as outlined in [1]) so that convergence from the unstressed state to the stressed equilibrium condition was overdamped. The assumptions were thus made that the full pressure was rapidly applied to the membrane and that the ratios of modulus and visco-elastic constants in the warp direction to their values in the weft direction for long-term creep were the same as the ratios for short-term creep. The magnitudes of creep are of course not the same, but it is the ratios of material constants and rate of pressurization which, together with the specified unstressed geometry, are the main determinants of prestressed shape and subsequent behaviour under loading. The assumption of constant ratios of the material properties and rapid stressing is somewhat vague but unfortunately the rate of pressurization was not accurately recorded, and the use of thin strips of material for calibration would have been very inadequate for the determination of long term material constants.

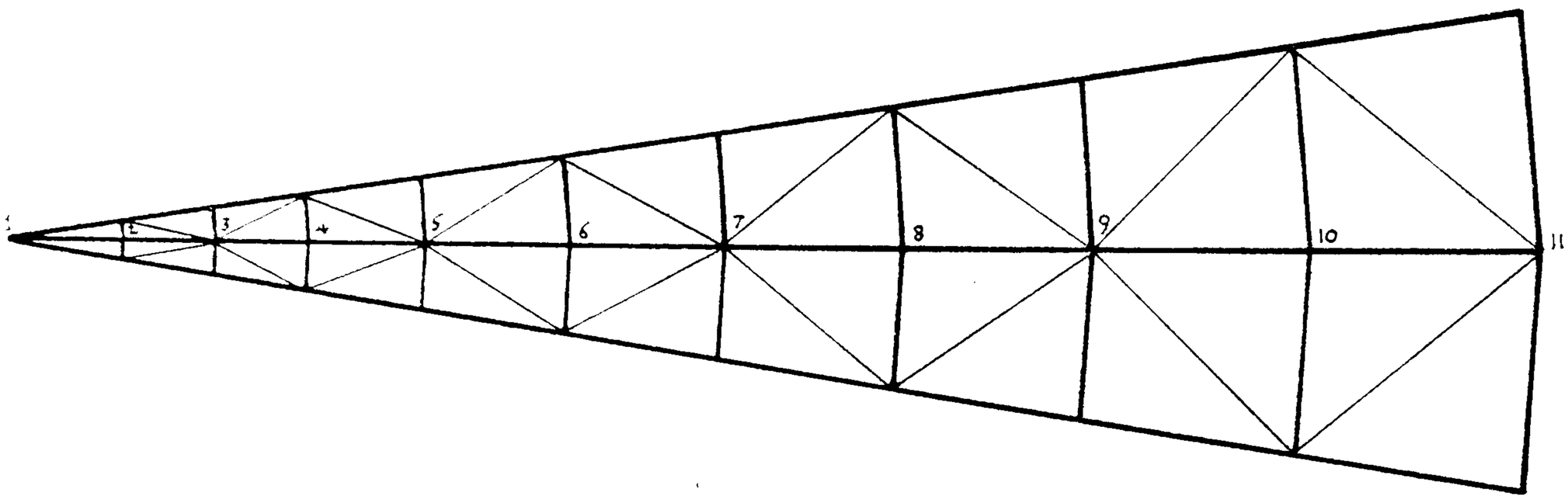


Figure 6

Because of the very low shear stiffness and the symmetry of loading the structure was subsequently idealized into orthogonal strips of material aligned with the warp and weft directions (as shown by the thick lines in figure 6), resulting in a reduction in computation time of about 50%. The strips were assigned EA values and initial tensions based on effective widths and the structure was re-analysed to obtain a stable and compatible prestress shape. The analysis for the 1000 N dynamic load was then carried out assuming nodal masses varying linearly from 0.008 kg at node 1 to 0.044 kg at node 10 apart from node 3 with a mass of 2.484 kg corresponding to the proportional segment load of 25 N reduced by the sum of the masses at nodes 1 to 5. The time interval used was 60% of the critical time interval based on these masses. The numerical stability of the entire system is highly dependent on the frequency at which pressure changes are calculated. The pressure P^i at any stage i of the analysis, assuming isothermal

contraction (or approximately also for adiabatic), is given by:

$$p^i = p^{i-1}\left(\frac{V^{i-1}}{V^{i-1}+dV}\right)$$

where $dV = \sum_{\text{all nodes } n}\sum_{x=1,3} q_{nx}\cdot(\delta^i_{nx} - \delta^{i-1}_{nx})$

and $\{\delta_n\}$, $\{q_n\}$ are respectively the deflection and unit pressure (or resolved area) vectors at node n; the latter being given by equation (9c) in [1] with p^t set to unity.

Depending on the relative 'stiffness' of the air and membrane the pressure changes may need to be calculated at closer intervals than creep increments or buckling checks. For the test model subject to a heavy dynamic load this was so, and the most efficient computational procedure was to reset the unit pressure vectors at the same stages (every 20 time intervals) as creep increments and buckling checks but, using these vectors, to determine pressure at every time increment using current nodal velocity components for the deflection increments ($\delta = V.\Delta t$).

The results of the analysis, compared with the experimental trace, are shown in figure 7, the maximum dynamic deflections in figure 8; and the membrane tensions and internal pressures for the three conditions: prestress, maximum dynamic and final steady state, are given in the top, middle and bottom segments respectively of figure 9.

In order to assess the likely maximum error in the assumption made regarding the ratios of long term to short term material constants and the rate of prestressing of the structure, a subsidiary form-finding analysis was carried out using long term "effective" moduli corresponding to the assumption of a very slow

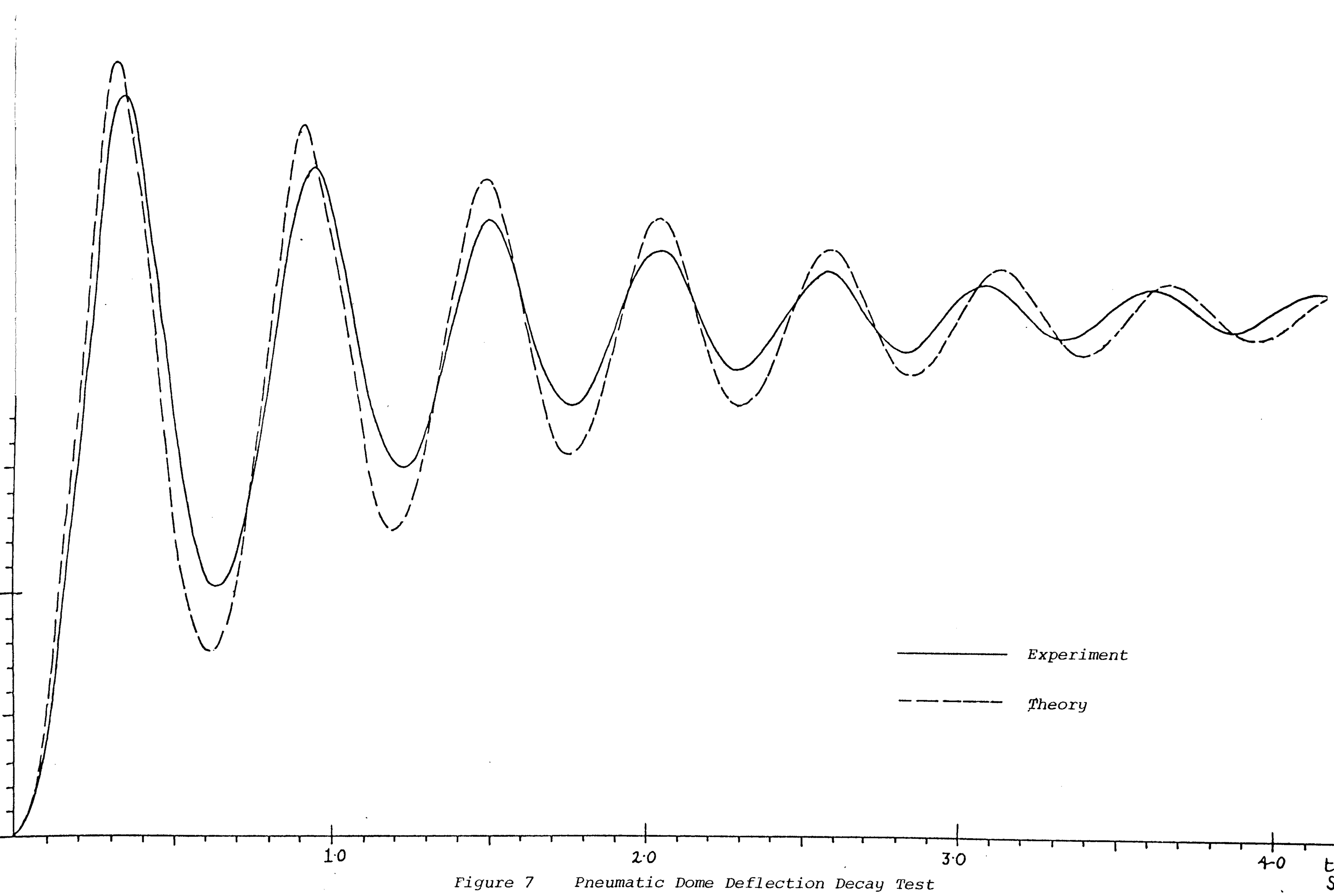


Figure 7 Pneumatic Dome Deflection Decay Test

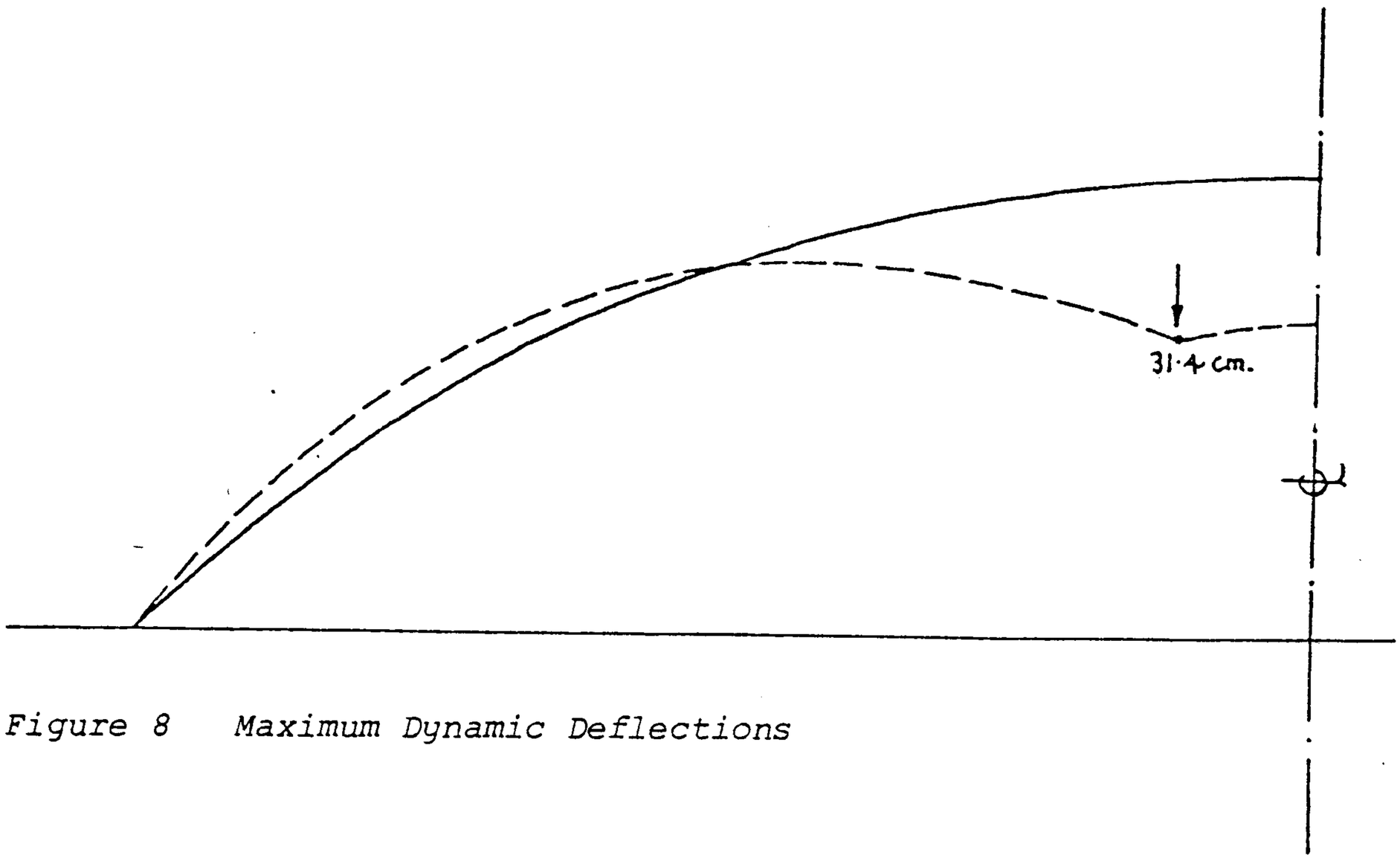


Figure 8 Maximum Dynamic Deflections

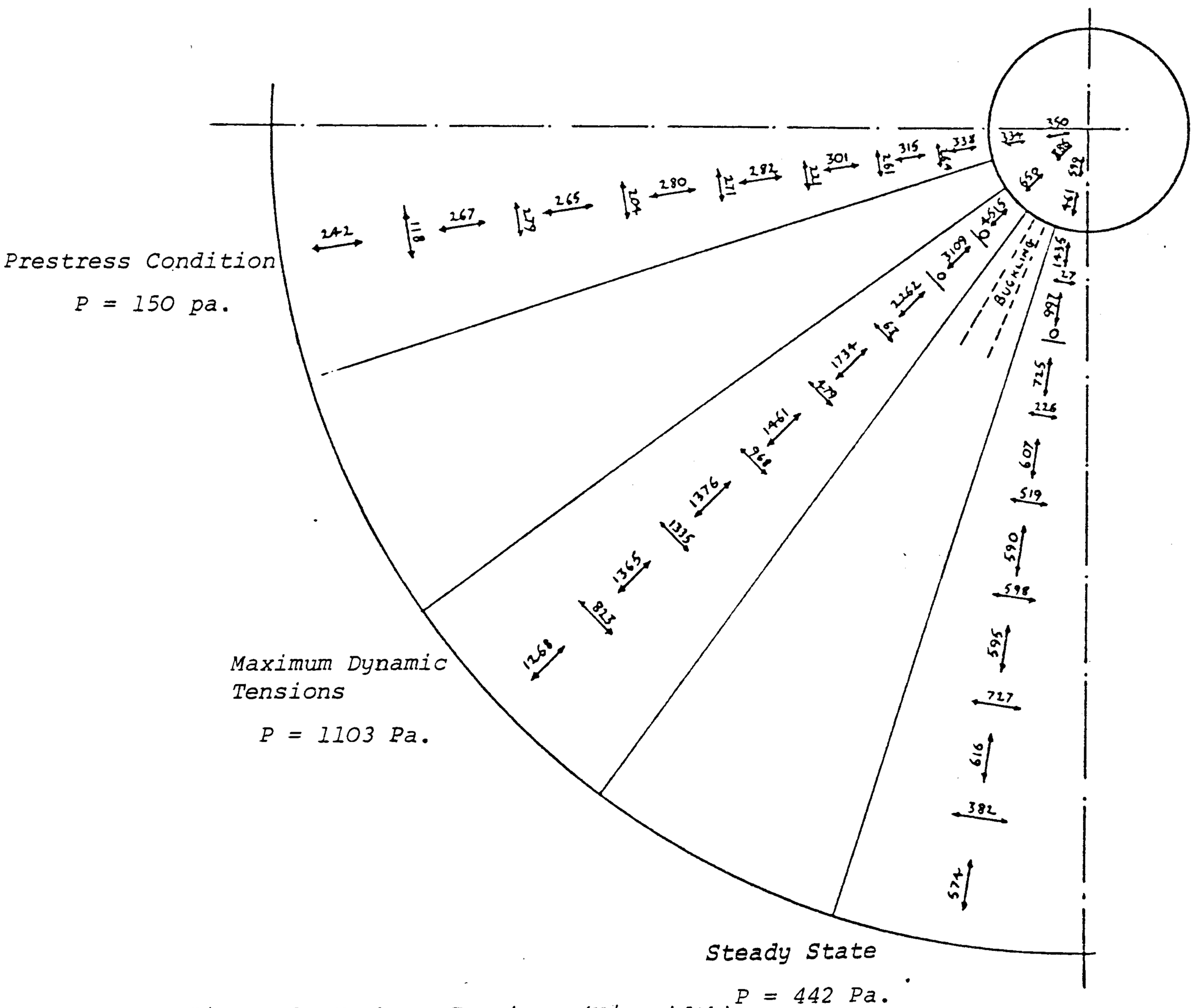


Figure 9 Membrane Tensions (N/m width)

rate of pressurization; in this case, the visco-elastic constants being set at zero. A dynamic load analysis was subsequently carried out based on this initial form and it was found that the peak and terminal deflections reduced by approximately 11%, and the average period by 3.7%.

CONCLUSIONS AND FUTURE WORK

Bearing in mind the limitations of the calibration test and the use of a single Kelvin model the results obtained are quite good, with frequencies, the rate of decay and the terminal deflection well simulated by the analysis. Although in the early and intermediate stages there is a considerable discrepancy in the degree of damping, this should be viewed in relation to the fact that maximum dynamic stresses were thirteen times the maximum prestress values with a corresponding increase in internal pressure of 735%; yet the creep and vibration decay behaviour were calibrated from an initial stress value mid-way between the prestress and terminal averages in the test structure with a dynamic load of only 32% of the dead load. For more realistic loading the visco-elasic model chosen should provide a good indication of damping and enable a simple numerical procedure to be used which is capable of handling quite large structural systems.

Calibration results for the weft direction visco-elastic constants are least satisfactory, and for materials exhibiting even greater rates of creep it may be necessary to use a series model to represent the behaviour. This does not appreciably increase computational effort, though curve fitting the calibration

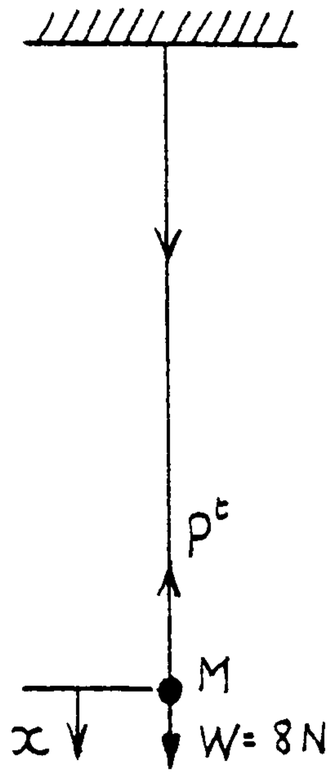
tests is more difficult. In the warp direction, which shows comparatively little creep, the results are excellent and one may speculate that the analysis could be used to model the dynamic behaviour of structures employing materials exhibiting little creep but significant vibration damping such as 'Kevlar' 29 or 49. When creep is insignificant the ratio a/b tends to zero; by increasing the Young's Modulus, however, the effective elastic strain becomes less than the total strain and constants may be chosen to adequately model the rate of vibration decay. Cable networks employing such materials, and a cable reinforced pneumatic dome with a geodesic membrane cutting pattern are subsequently to be investigated. For the latter the membrane will be unreinforced P.V.C. and a series model will be used to simulate creep, with more careful attention paid to the rate of pressurization.

REFERENCE:

(1) Chapter 5.

APPENDIX 6.1

CALIBRATION ANALYSIS FOR SINGLE VISCO-ELASTIC ELEMENT



Total area of strips = 2 x 28 x 0.02 = 11.2mm

Length = 900mm

Dead load = 25 N

Suddenly applied load W = 8N

Elastic & Visco-elastic constants:

E = 420 N/mm)
b = 7 sec) (Trial values)

$$a = b.\varepsilon p/\sigma$$

where σ = increase in stress due to W = 8/11.2 = 0.7143 N/mm

and εp = Total strain (measured from cal.test) - Elastic strain

= 0.0039 - 0.7143/420 = 0.0022

hence a = 0.021 mm /(N.sec)

Elastic stiffness S = EA/L = 420 x 11.2/900 = 5.2267 N/mm

Nodal Mass M = 33/9.81 kN

Critical time interval = $\sqrt{\frac{4M}{S}}$ 0.05 Sec.
(for one end fixed)

Use Δt = 0.02 Sec.

From equation (12a) in Chapter 5, the projected creep relation with n = 1 is:

$$\varepsilon_c^{t+\Delta t/2} = \frac{a.\Delta t.\sigma^t}{(1+b\Delta t/2)} + \frac{(1 - b\Delta t/2).}{(1 + b\Delta t/2)}\ \varepsilon_c^{t-\Delta t/2}$$

and corresponding to the flow chart in Chapter 5 at stage IIIa:

$$\sigma^t = \frac{S}{A}\ (x^t - x_c^{t-\Delta t/2})$$

Hence $x_c^{t+\Delta t/2} = L.\varepsilon_c^{t+\Delta t/2}$ gives:

$$x_c^{t+\Delta t/2} = 0.1649x^t + 0.7043x_c^{t-\Delta t/2} \quad \text{mm (1)}$$

The new residual force $R^t = W - p'^t$, where p'^t corresponds to stages

III g and h in the flow chart. Hence:

$$R^{t} = 8 - 5.2267\ (x^{t} - x_c^{t+\Delta t/2}\ )\ N \qquad (2)$$

From equation (4) in Chapter 5, the mid-interval nodal velocity is then:

$$V^{t+\Delta t/2} = V^{t-\Delta t/2} + \frac{\Delta t}{M}.R^{t}.10^{3} = V^{t-\Delta t/2} + 5.9455R^{t}\ \text{mm/sec} \qquad (3)$$

and hence the new deflection is:

$$x^{t+\Delta t} = x^{t} + \Delta t V^{t+\Delta t/2} \qquad (4)$$

At the start of the analysis the velocity at $\Delta t/2$ is given by:

$$V^{\Delta t/2} = \frac{1}{2}.\frac{\Delta t}{M}.W = 237818\ \text{mm/sec}$$

and $x_c^{\Delta t/2}$ is assumed zero.

The iterative analysis thus proceeds using equations $4 \rightarrow 1 \rightarrow 2 \rightarrow 3$ and back to 4 for the next cycle. The calibration analysis for this case ($\Delta t = 0.4\Delta t_{crit}$) is set out in table 1 up to the first maximum and minimum deflections. The complete trace for one second duration is shown in figure 10 compared with the calibration test and the trace computed using a single element but $\Delta t = 0.1\ \Delta t_{crit}$.

TIME	x	x	R	V
0	0	0	(W=8)	23.7818
0.02	0.4756	0.0784	5.9238	59.0018
0.04	1.6557	0.3282	1.0616	65.3137
0.06	2.9619	0.7194	-3.7208	43.1918
0.08	3.8258	1.1374	-6.0512	7.2148
0.10	3.9701	1.4556	-5.1424	-23.3590
0.12	3.5029	1.6027	-1.9319	-34.8452
0.14	2.8060	1.5913	1.6514	-25.0266
0.16	2.3055	1.5009	3.7946	- 2.4659
0.18	2.2561	1.4290	3.6768	19.3944
.	.	.	.	.
.	.	.	.	.

Table 1

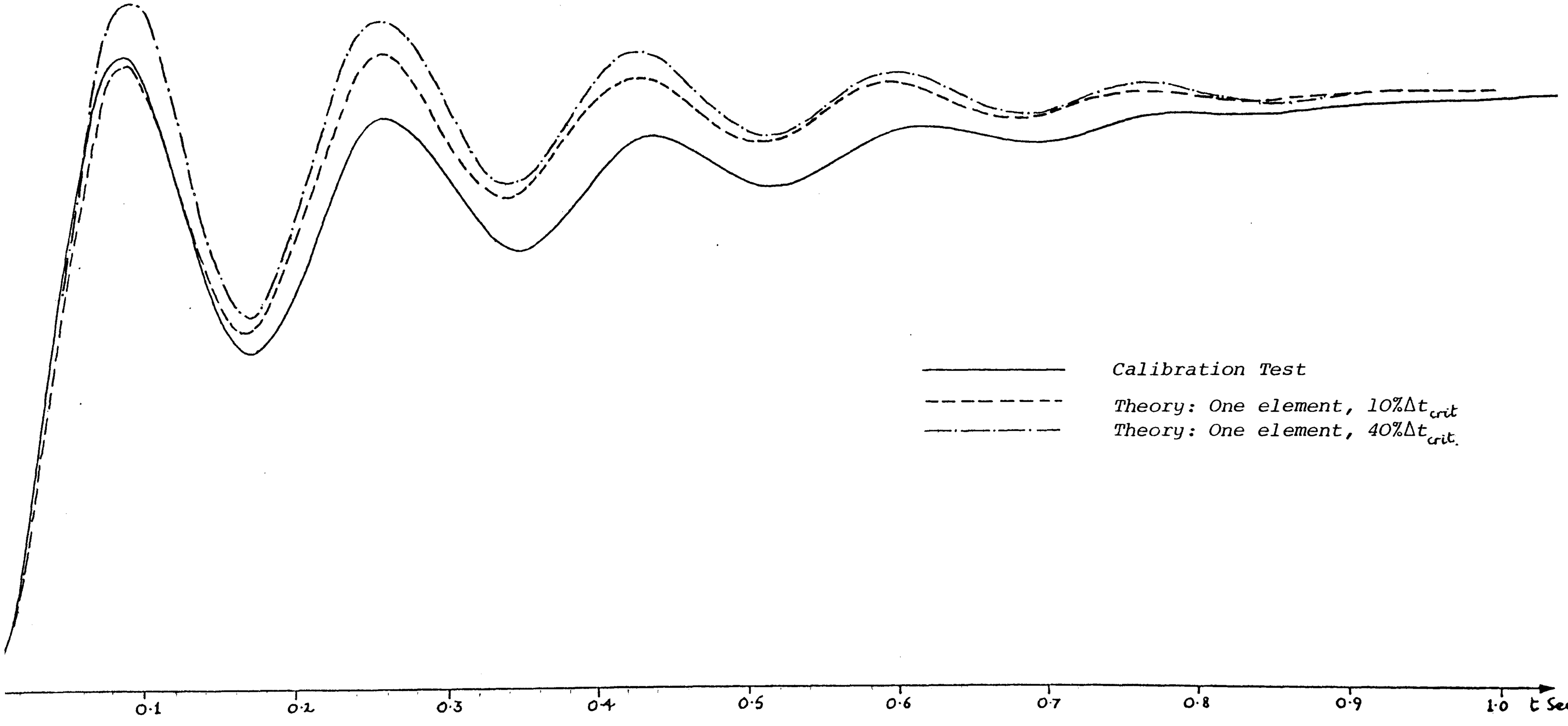

Calibration Test
Theory: One element, 10%Δt crit
Theory: One element, 40%Δt crit.
0·1
0·2
0·3
0·4
0·5
0·6
0·7
0·8
0·9
1·0
t Secs.

Figure 10

CHAPTER 7

INTERACTIVE GRAPHICAL DESIGN OF TENSION SURFACE STRUCTURES

SUMMARY

The chapter describes the Interactive use and control of Dynamic Relaxation for the form-finding of uniform or variable stress membranes and geodesic cable networks. The boundaries to the surface structures may be derived as tensile or compressive funicular curves, and may in addition have traction forces applied by boundary shear walls or network walls which considerably increase the variety of possible forms.

Initial convergence of the technique is rapid and provided sub-critical damping is used, damped oscillation about the equilibrium position provides an early signal for necessary design modifications such as the alteration of reaction forces or positions, control tensions or compressions, membrane stresses and boundary traction forces.

The paper represents a fairly direct extension of procedures given in chapter 4. In contrast, however, to previous examples of form-finding, the present applications indicate clearly the instructive benefits to be gained from interactive design.

BASIS FOR INTERACTIVE FORM-FINDING BY DYNAMIC RELAXATION

The numerical procedure is a special application of the general method set out in chapter 5 [ref.1] ; DR being discussed in the final section of that chapter. Nodal displacements at any time (t) may be expressed (using equations 5 & 13 of [1]) in terms of previous displacements and nodal forces (at $t-\Delta t$). New nodal forces may then be expressed in terms of these displacements, and hence the iteration proceeds.

The force exerted on any node by an adjoining cable link, in the direction of the link may be expressed as:

$$F^t = K_o(L^t - L_o) + T_o \pm Q_o \qquad (1)$$

where L^t is the current link length and L_o, K_o, T_o, and Q_o are respectively the specified slack length, elastic stiffness, pre-tension and traction force along the link; L^t and the resolved components of F^t being determined from current nodal displacements. In order to derive compression funicular boundaries, edge links are given either negative K_o or negative T_o values and residual forces at edge nodes are reversed at each stage in the analysis.

For a triangular membrane element subject to a specified uniform tensile stress resultant, $\sigma_o h$, the force at node i directed perpendicular to the opposite side, i, is given by:

$$F_i^t = \sigma_o h L_i^t/2 \qquad (2)$$

(an alternative expression in terms of edge tensions is given by eq. (7) of [1]).

The acceleration of any node is inversely proportional to the mass, and the applied viscous damping is taken as proportional to the mass. Thus during the form-finding process the rate of change in the various parts of a structure can be controlled by the mass components. Also the entire assembly of nodes is treated as 'active' with support points being fixed or released by the use or not of very large masses. The main controls on form-finding are however the adjustment of membrane tensions (σ_o in 2), and the parameters L_o, K_o, T_o and Q_o in equation (1). These may all be adjusted dynamically so that the process of form-finding is one of continuous change without the necessity to return to some initial state.

The application of the method to various types of tension surface structures is illustrated in the following sections; the forms considered all being based on the topology shown in figure 1. Although, in fact, all of the structures have three or six axes of symmetry, in order to show more clearly certain types of instability or quasi-instability which may occur, but be dispelled, during interactive form-finding of such structures, the analyses were based on the assumption of symmetry about XX only; symmetry being imposed by the use of large mass components in the y direction. For the sake of simplicity a very coarse subdivision has been used and specific data for the structures considered has been put in appendix 7.1.

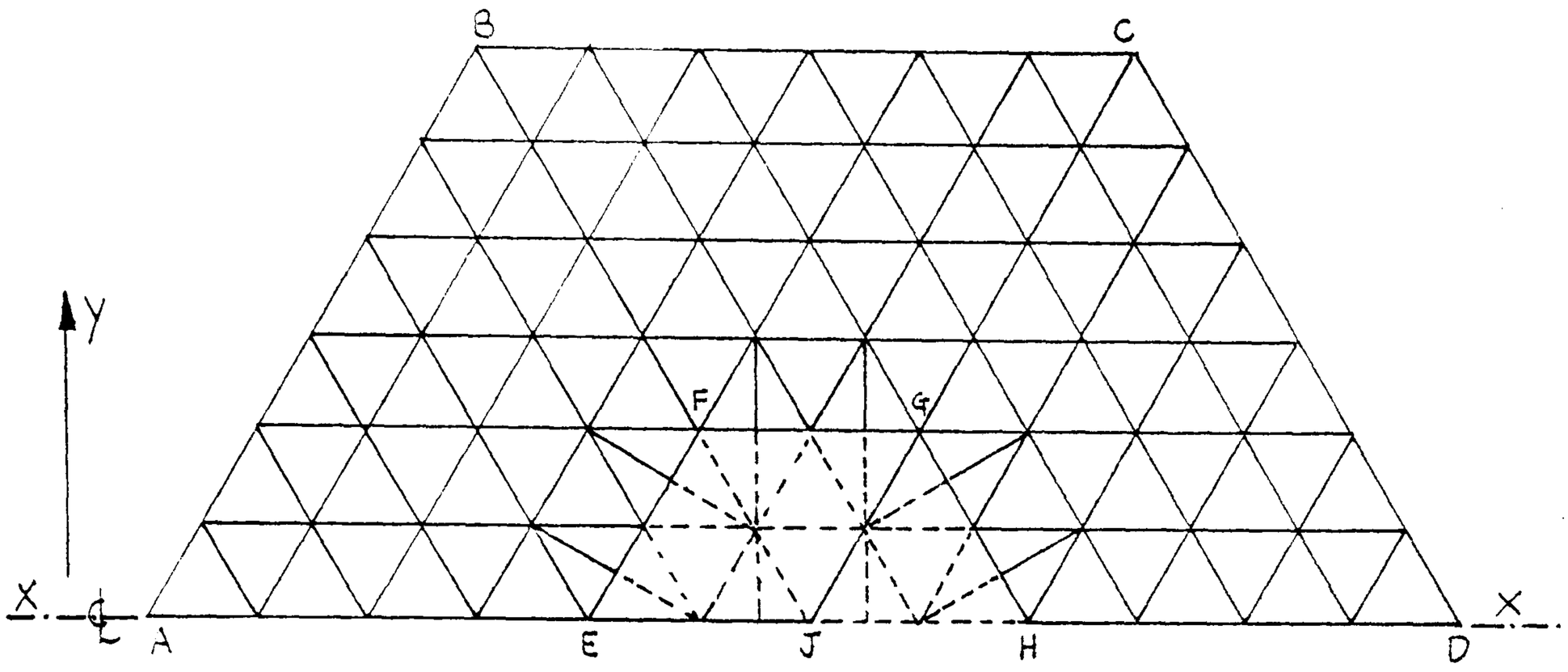


Figure 1

UNIFORM STRESS MEMBRANES

For the generation of the structure shown in figures 2a & b nodes A and C were fixed and an upward load was applied at J. The initially plane membrane was subdivided into triangular elements, shown by the full lines in fig.1, with a specified uniform stress. The membrane was supported by links EJ and GJ and bounded internally by cable loops, and externally by compression funiculars; the boundaries being controlled elastically with $+K_o$ and $-K_o$ values respectively, and T_o values set to zero in both cases. Uniform traction forces were applied along the outer boundary links (as indicated by the arrows in fig. 2a), together with downward loads which varied linearly from zero at the low points (A,C) to a maximum at the high points (B,D).

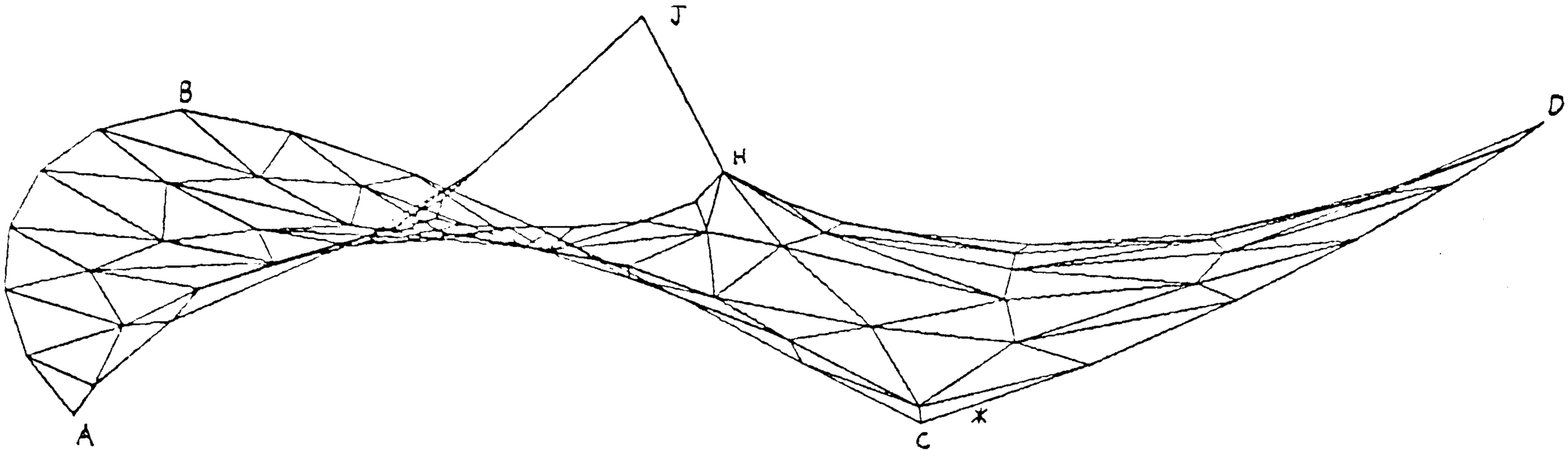


Figure 2b

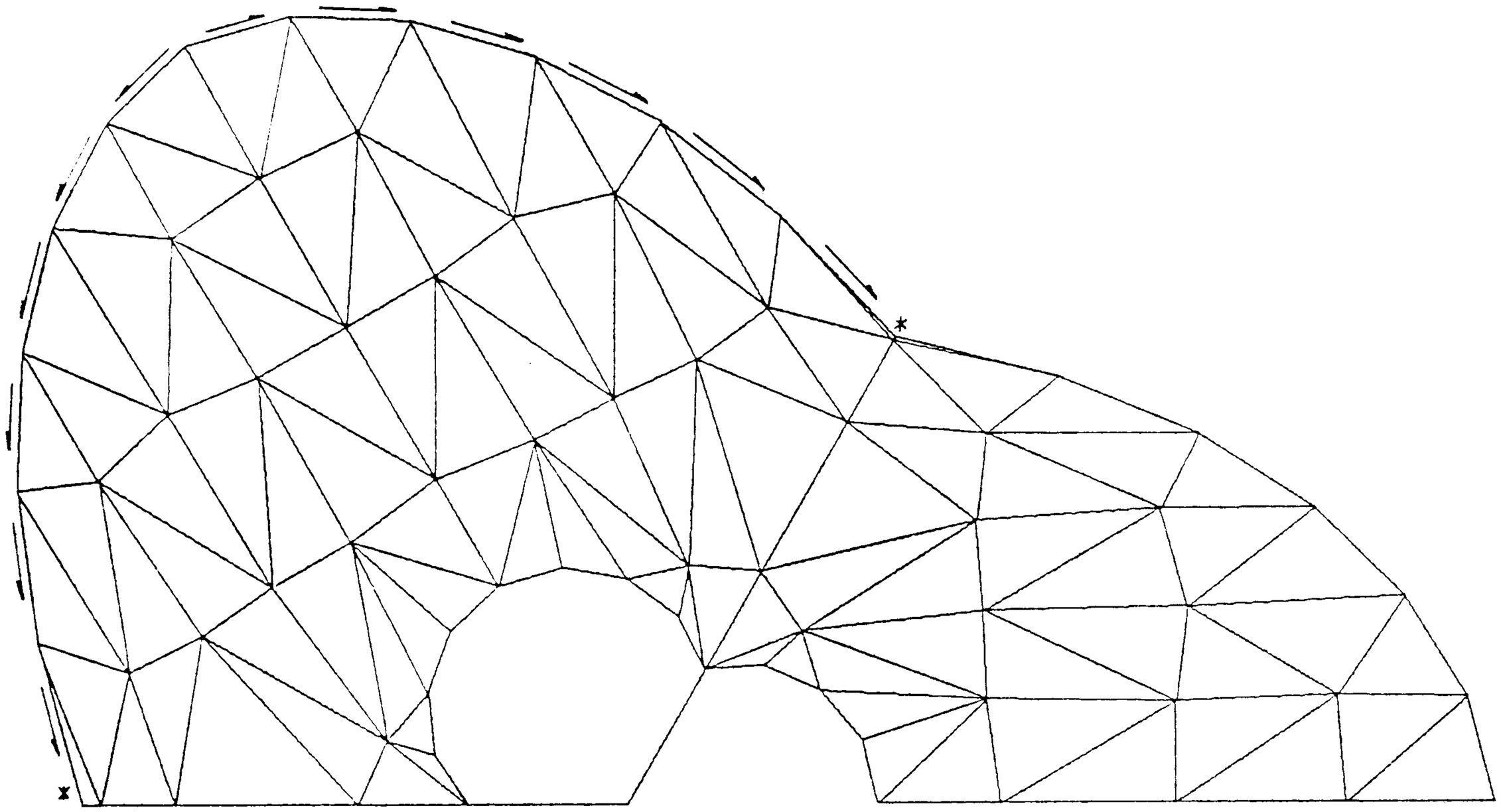


Figure 2a

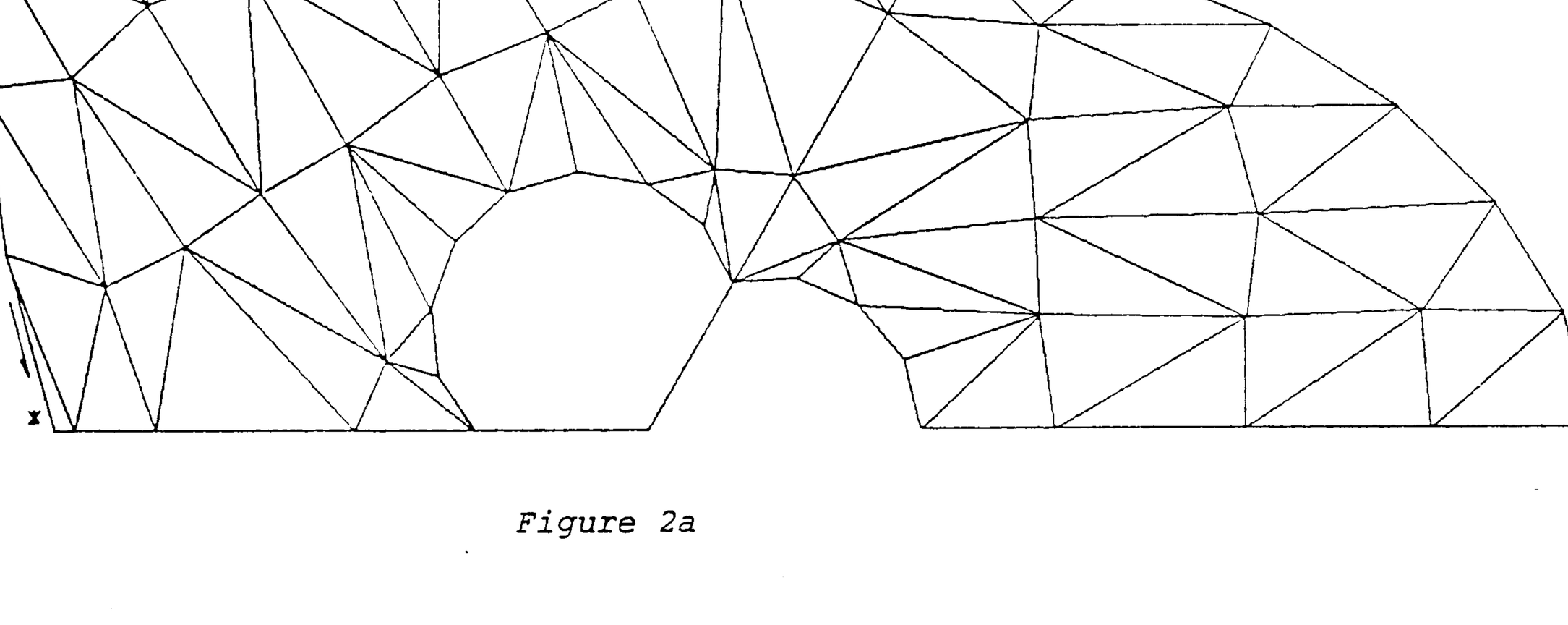


Figure 3

Whilst the overall form is obtained quite rapidly, the system never fully converges due to the successive collapse and expansion of the triangles marked * at the low points which cause slight oscillating lack of symmetry. The effect on other nodes of the membrane is very small and this state is termed quasi-instability. It may be dispelled by increasing considerably the mass of the node which is causing intermittent inversion of an element [2]. Alternatively, as in this case, it may indicate that the system is physically only just stable. For the structure shown, complete convergence may be obtained by taking any of the following actions.

a) increasing traction forces to decrease the discontinuity of boundary slopes at the low points

b) increasing $|K_o|$ values of the boundary links

c) reducing the central upward load

d) increasing the downward loads on the boundary nodes or altering the distribution

The effect of (d), when the total boundary load is increased by 40%, is to increase the edge curvature and the height of the high points (B,D) thus making the membrane more cylindrical near the low points. The system then becomes stable and symmetrical as shown by the plan view of fig. 4 (left-hand lobe).

With these increased boundary loads, if the central load is increased by 20% the effect is shown in the elevation of fig.3. Quasi-instability then develops due to inversion of the

inner triangles marked *; the effect on the variation in height at J being $\pm$0.1%. If the load is further increased, collapse will occur with contraction of the inner loops and upward acceleration of the load at J; and to restore stability, without reduction of the load, the K_o values of the inner loops may be reduced thus increasing their size (alternatively the membrane stress may be increased).

It is of value, in considering membrane reinforcement or the design of equivalent cable networks, to examine principal stress trajectories due to the application of a small uniform pressure normal to the surface. Figure 4 shows, in the right-hand half lobe, the principal tensile trajectories obtained by assigning elastic stiffness to the membrane elements and analysing the structure for normal pressure by the method in ref.[1]. Whilst the approximate trajectories would in this case be known intuitively, for more complex support systems they might not. Considering the coarseness of the subdivision and the type of elements used, the results are surprisingly good and can be obtained with very short computer runs. One aspect in favour of using 'constant strain' elements for such a loading condition is that stress gradients throughout the minimum surface membrane are very small.

CABLE NETWORKS

The ideal network, at least for the condition of uniform pressure loading, is the 'isostatic' network in which cables follow principal stress (and radii) trajectories over the surface with

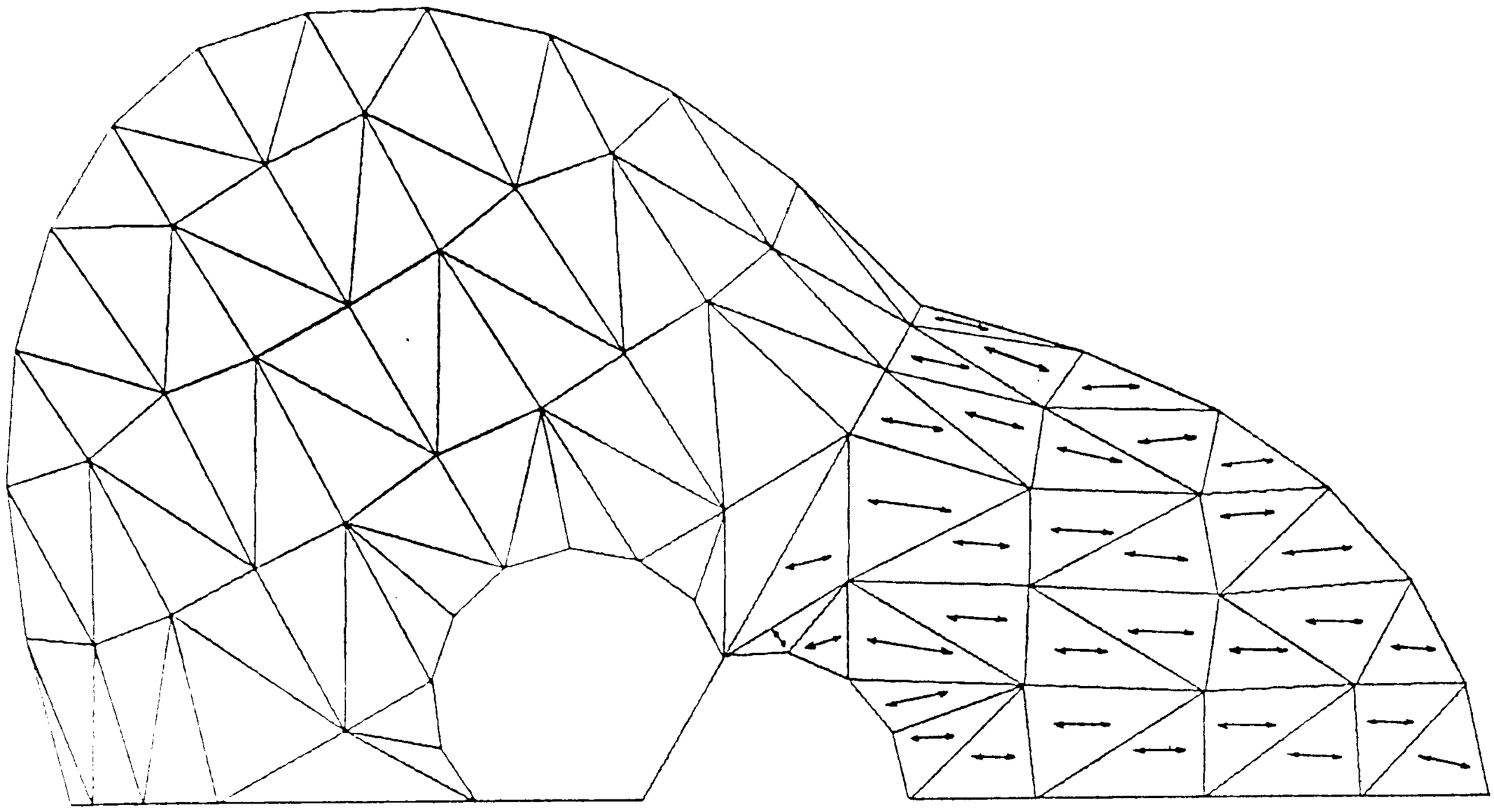


Figure 4

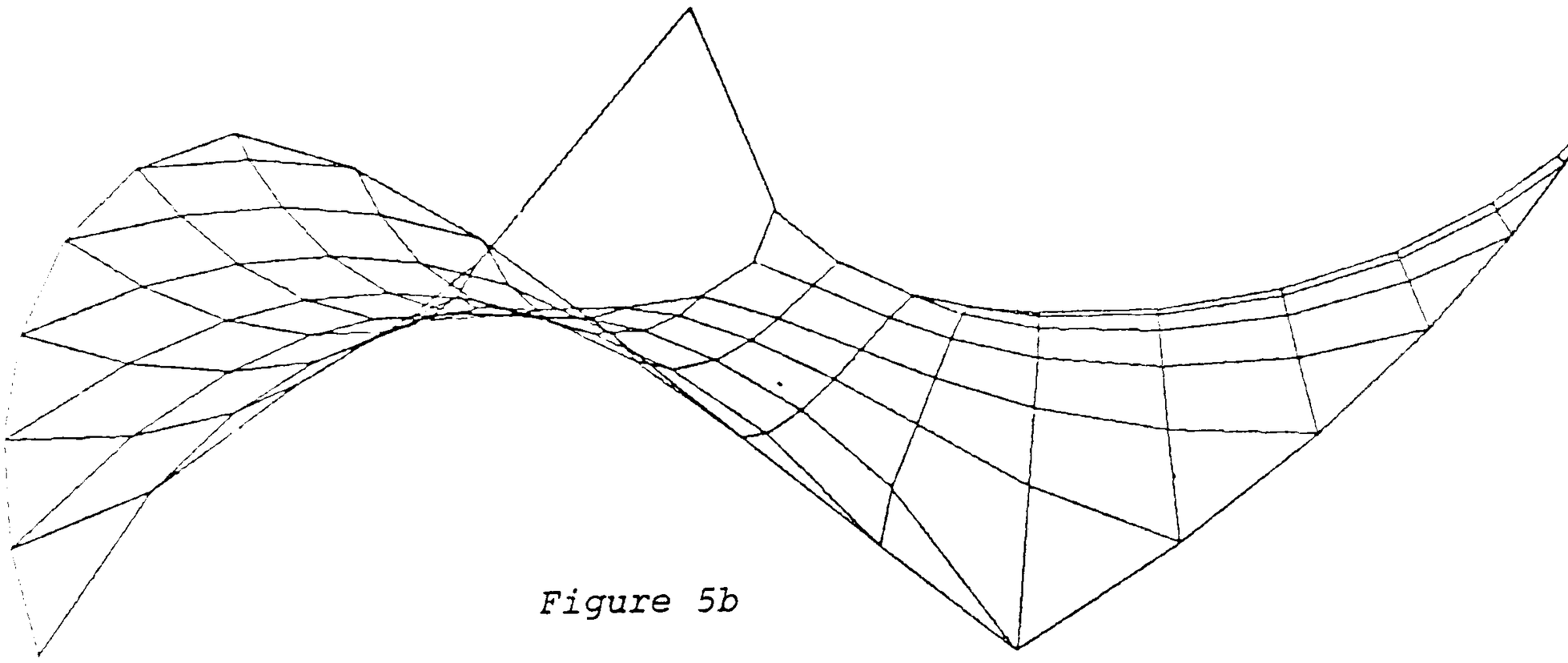


Figure 5b

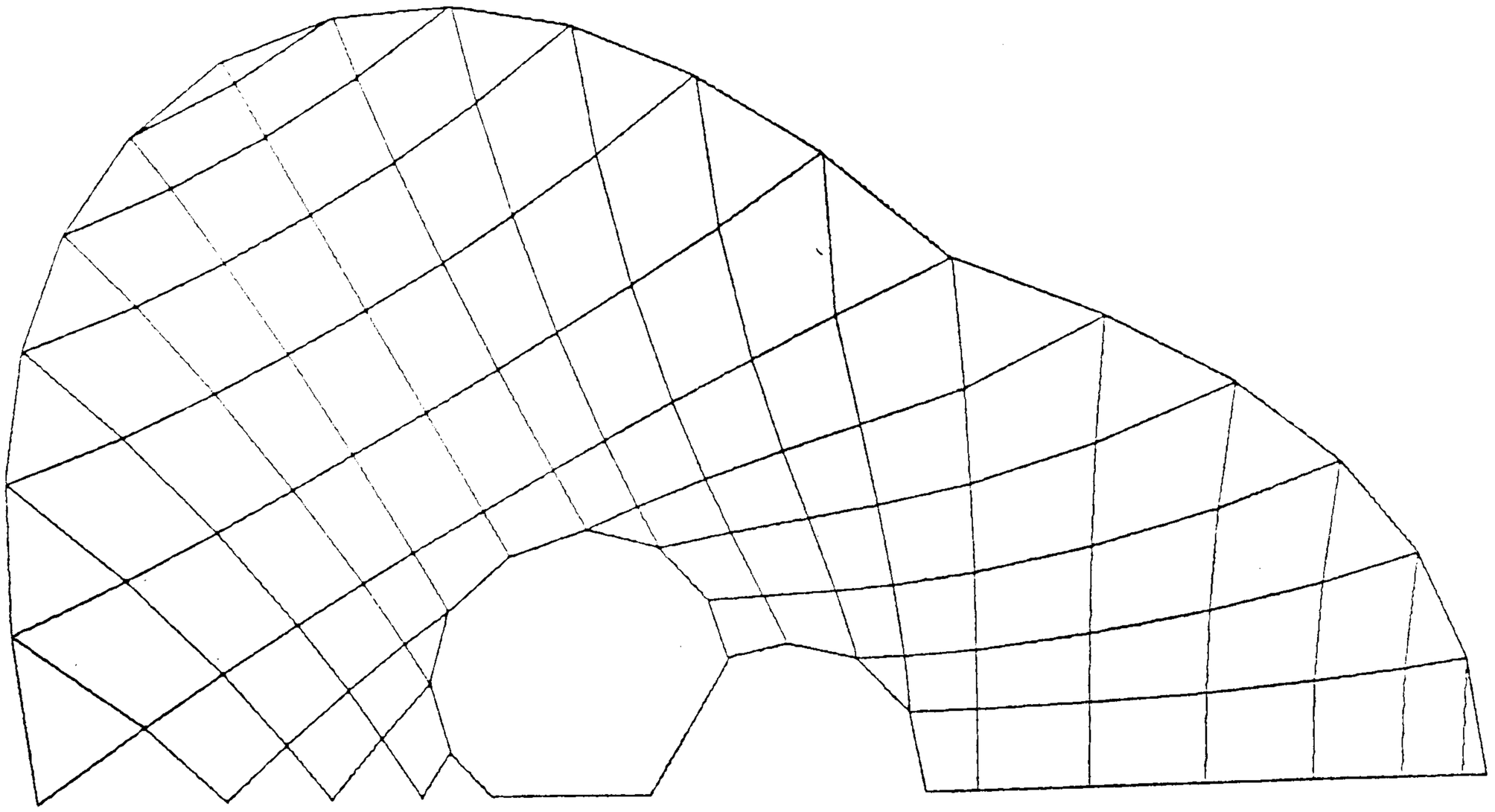


Figure 5a

spacing inversely proportional to the intensity of stress in a substitute membrane surface. For practical reasons nets are usually either of uniform mesh or geodesic construction, but the pattern of principal stresses may provide a guide for efficient cable arrangements.

Geodesic networks, in which the cables follow paths of minimum distance over the surface, may be derived by setting, for each cable link, the value of K_o to zero and thus holding the tensions of cables constant at a specified value of T_o throughout their lengths. Figures 5a and b show a geodesic network, derived in this way, with the same boundary and loading parameters used to derive the membrane in fig. 3, but with the ratio of cable tension/spacing approximately equivalent to the membrane tension.

With nearly optimum parameters of mass components, damping constant and time step convergence of deflections to an accuracy within 0.001% (passing through the first maxima and minima) was obtained after 150 iterations. If the fictitious nodal masses used at surface node points are reduced, numerical instability occurs at the most closely spaced of these nodes as shown in fig. 6 (for a structure with lower applied boundary loads). The type of instability developed is interesting in that it does not greatly affect other nodes or the overall form. This is because for geodesics with imposed constant tensions (and for uniform stress membranes) the stiffness is 'geometric' and reduces with increasing deflection in contrast to elastically controlled structures for which the numerical analysis becomes entirely unstable with an over-critical time interval.

For uniform mesh networks the form is controlled elastically using real stiffnesses and L_o values, but in some links it may be appropriate to specify T_o values to obtain a more even distribution of tensions and curvatures. Physically this corresponds to the use of turnbuckles during erection.

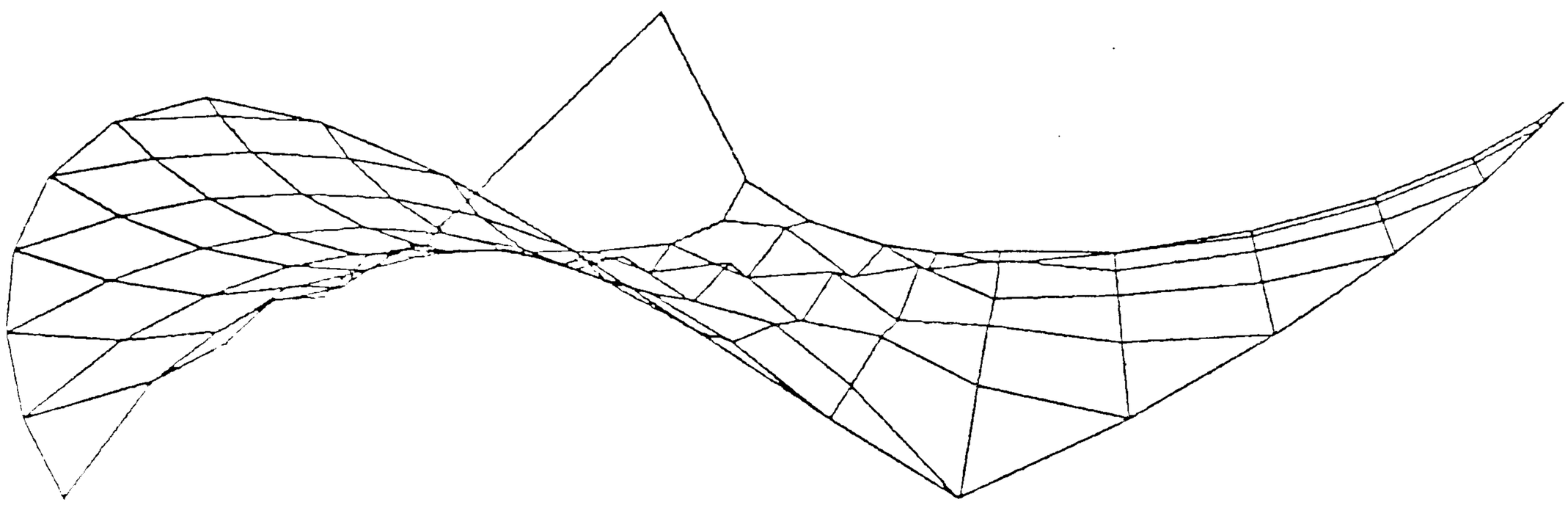


Figure 6

VARIABLE STRESS MEMBRANES

The curvatures, and thus the resistance to dynamic deformations, in uniform stress minimum surface membranes are restricted by stability criteria or the permissible size of support loops. If membrane elements within the surface are coupled with cable links along their edges, which may physically correspond with reinforcement, variable stress membranes may be derived which permit an increased variety of forms [3].

It is often permissible to couple uniform stress membrane elements with cable links for which T_o values are specified (and K_o set to zero). In some cases however this may create an unstable system, or one which is difficult to control numerically. For this reason it is preferable to specify the K_o and L_o values of cable links, and adjust them during the numerical process to obtain the form required. The links should preferably be initially overstiff and subsequently relaxed to a viable solution, otherwise the system may suffer at an early stage the physical instability effects which occur in uniform stress membranes. Even if the system does collapse however, it may still be restored by adjusting the control parameters; though this will entail increased computing time.

Figures 7 show the development of snap through buckling when the plane membrane of figure 1 was subject to an increasing load at the centre applied through four struts. The early stages of deformation are shown in the elevation 7a. The membrane was fixed at supports ABC and D and bounded internally and externally by edge cables. Radial cables joining AE, BF, CG, DH provided reinforcement to the membrane to permit an increased central height compared with that of a uniform stress membrane by effectively increasing the radial tension component. The membrane was otherwise uniformly stressed. The radial cables were elastically controlled; though a valid solution could have been obtained by specifying uniform tensions.

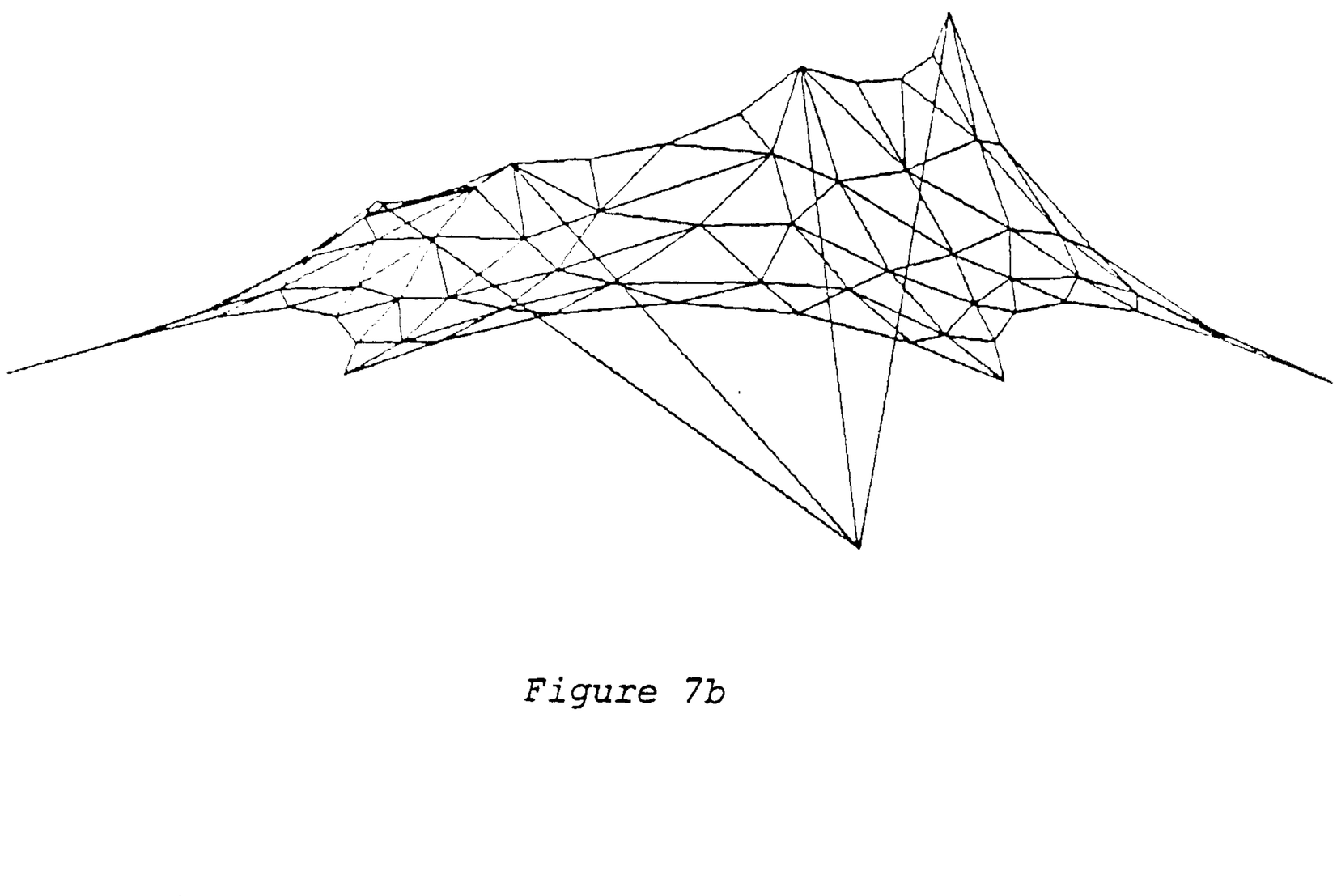


Figure 7b

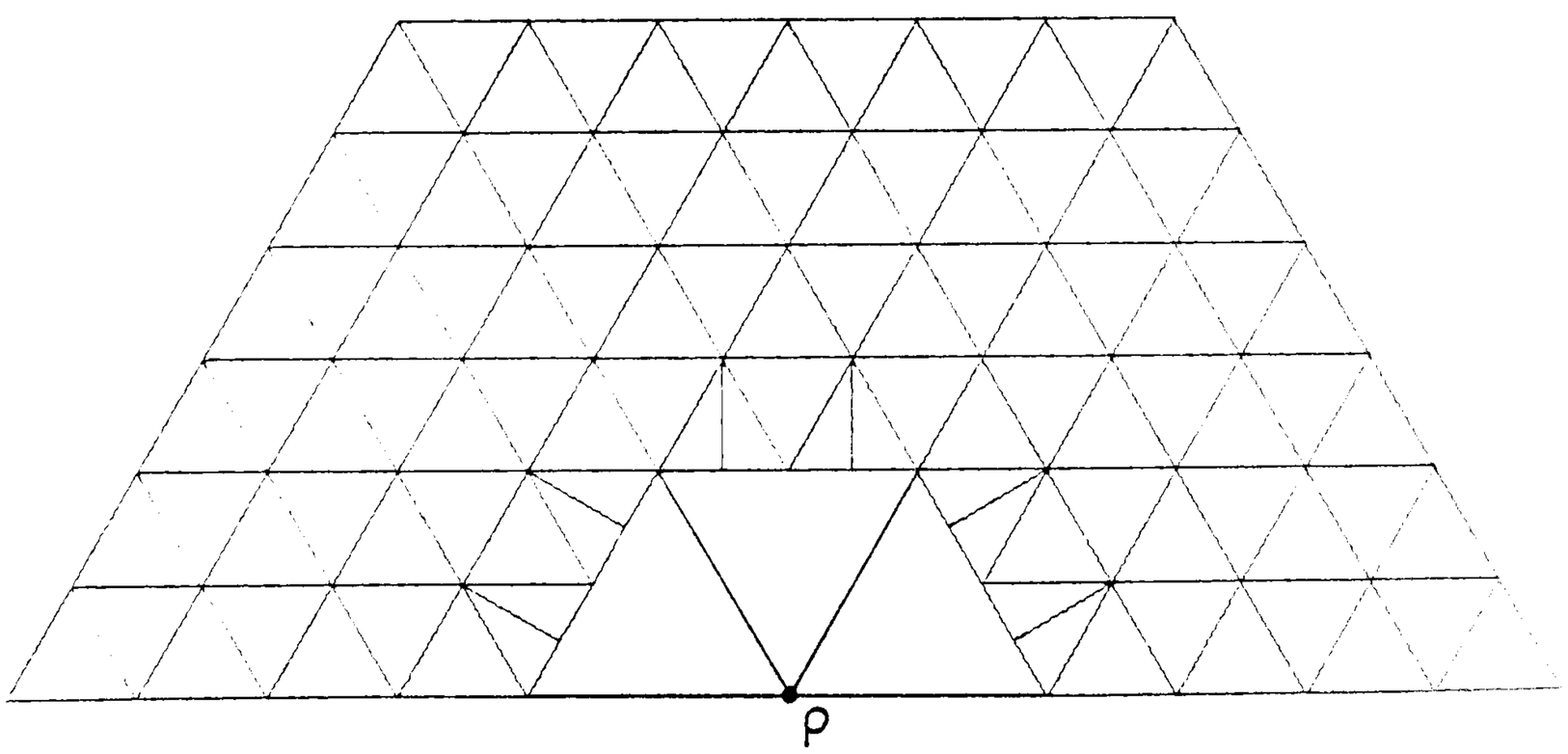


Figure 7a

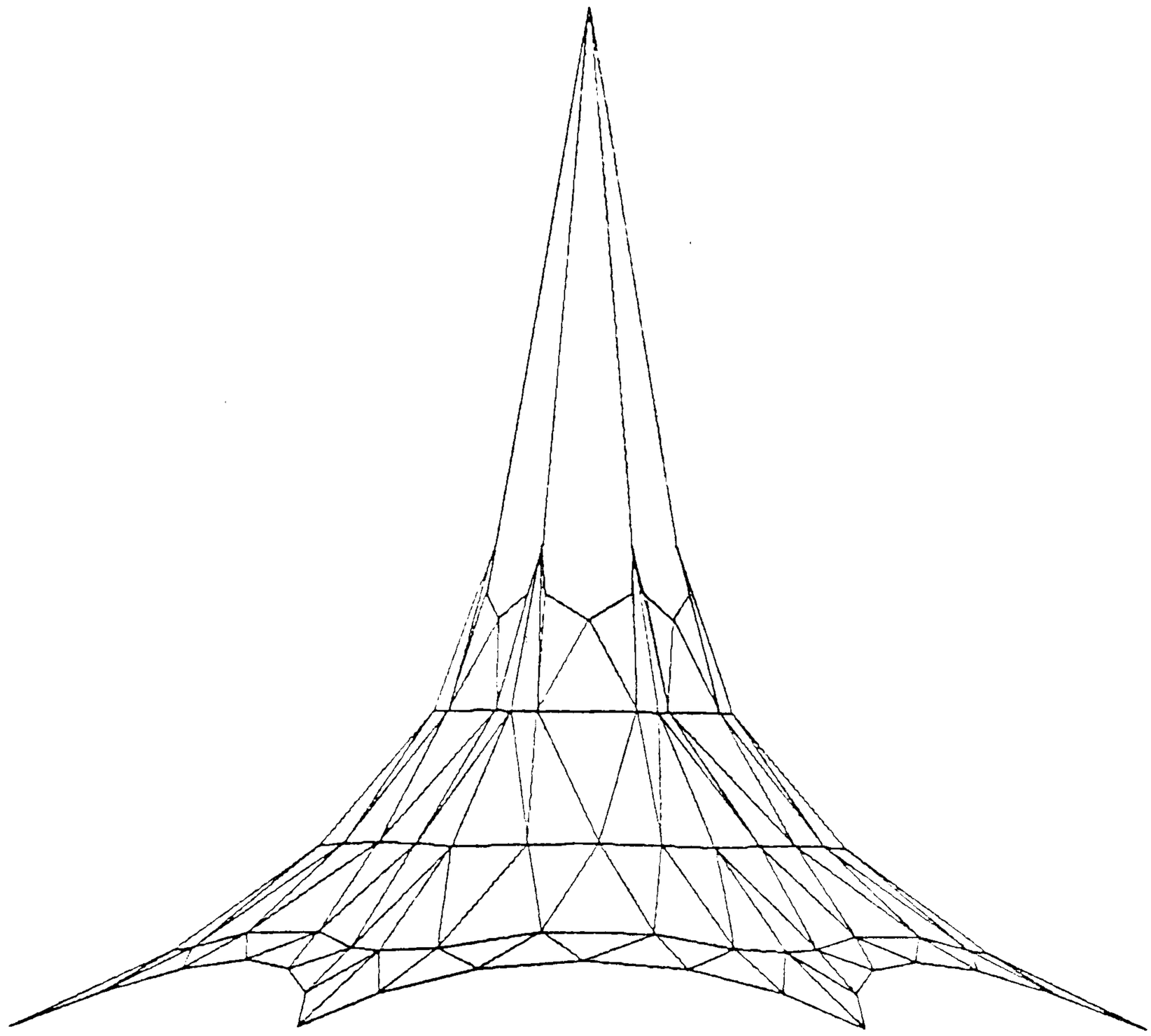


Figure 7d

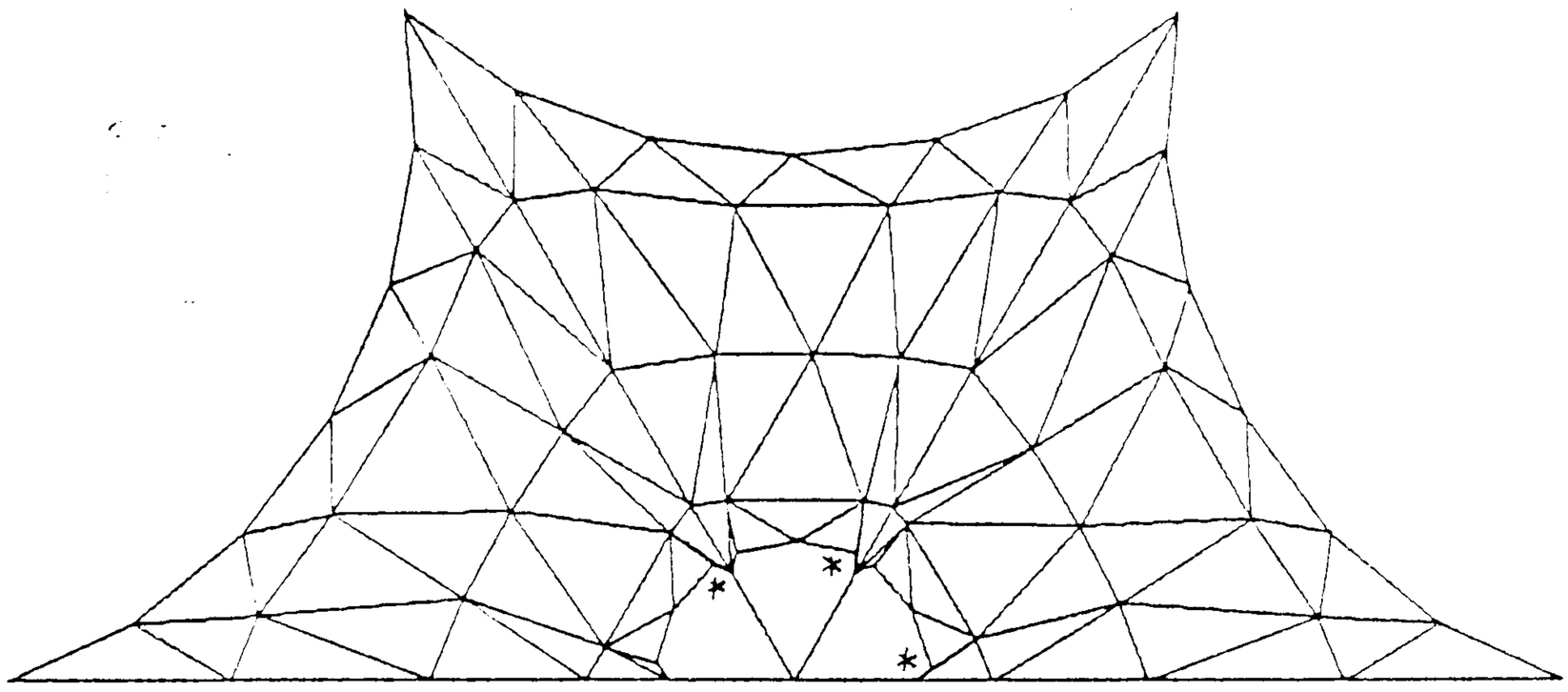


Figure 7c

In figure 7b the load P has been doubled and instability is occuring because the stiffness of the inner loop cable is too low and the load P was not constrained to deflect purely along the vertical centre line. After the struts have snapped through, if the load is held constant, the system becomes stable and symmetrical. Finally, with further increase of the load (figs. 7c and d) quasi-instability occurs at the centre nodes marked *. This is a result of the topology chosen and the type of elements used, but can be eliminated by increasing the mass at these nodes resulting in a topological reduction. Alternatively, the element subdivision in this area may be refined. The inversion of the system at stage 7b could have been prevented by assigning large horizontal mass components to the loaded node; either initially, or as soon as lack of symmetry became apparent.

The use of closed zones delineated by cable contours permits variation of the membrane stress σ_o, from zone to zone, in addition to the variation in effective membrane tensions due to the cable reinforcement [3]. The pneumatic structure shown in figures 8a and b, generated from the complete topology in fig.1, possesses five stress zones. The specified membrane stress resultants were varied linearly from S_1 to a minimum $S_5 = S_1/3$, and the elastic stiffnesses of cable hoops between zones were all set to $K_o = +11S$. The base boundary was determined as a compression funicular controlled elastically with negative K_o values. Only the vertical fictitious mass components of this boundary were set at very large quantities, thus the boundary was free to expand or contract laterally.

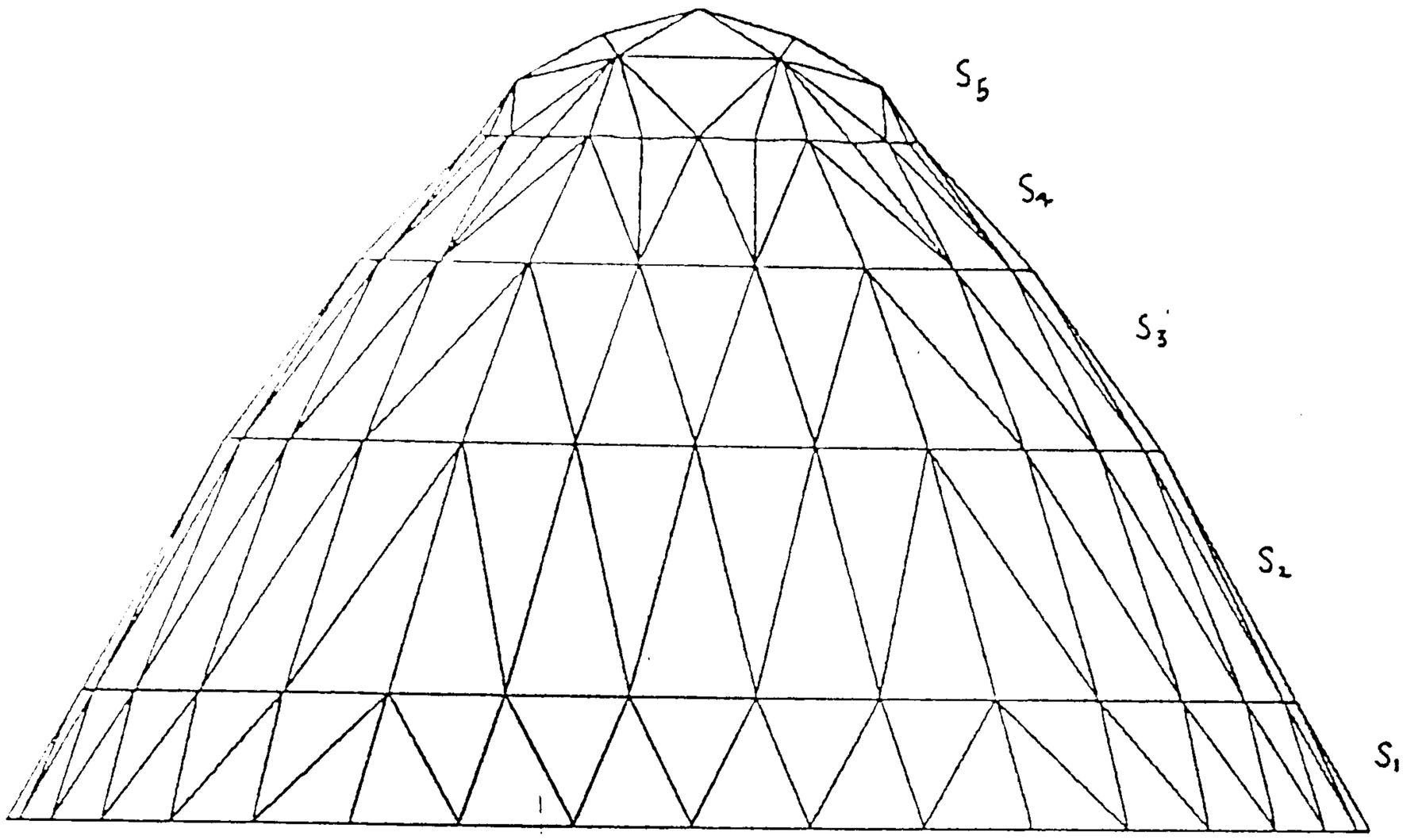


Figure 8b

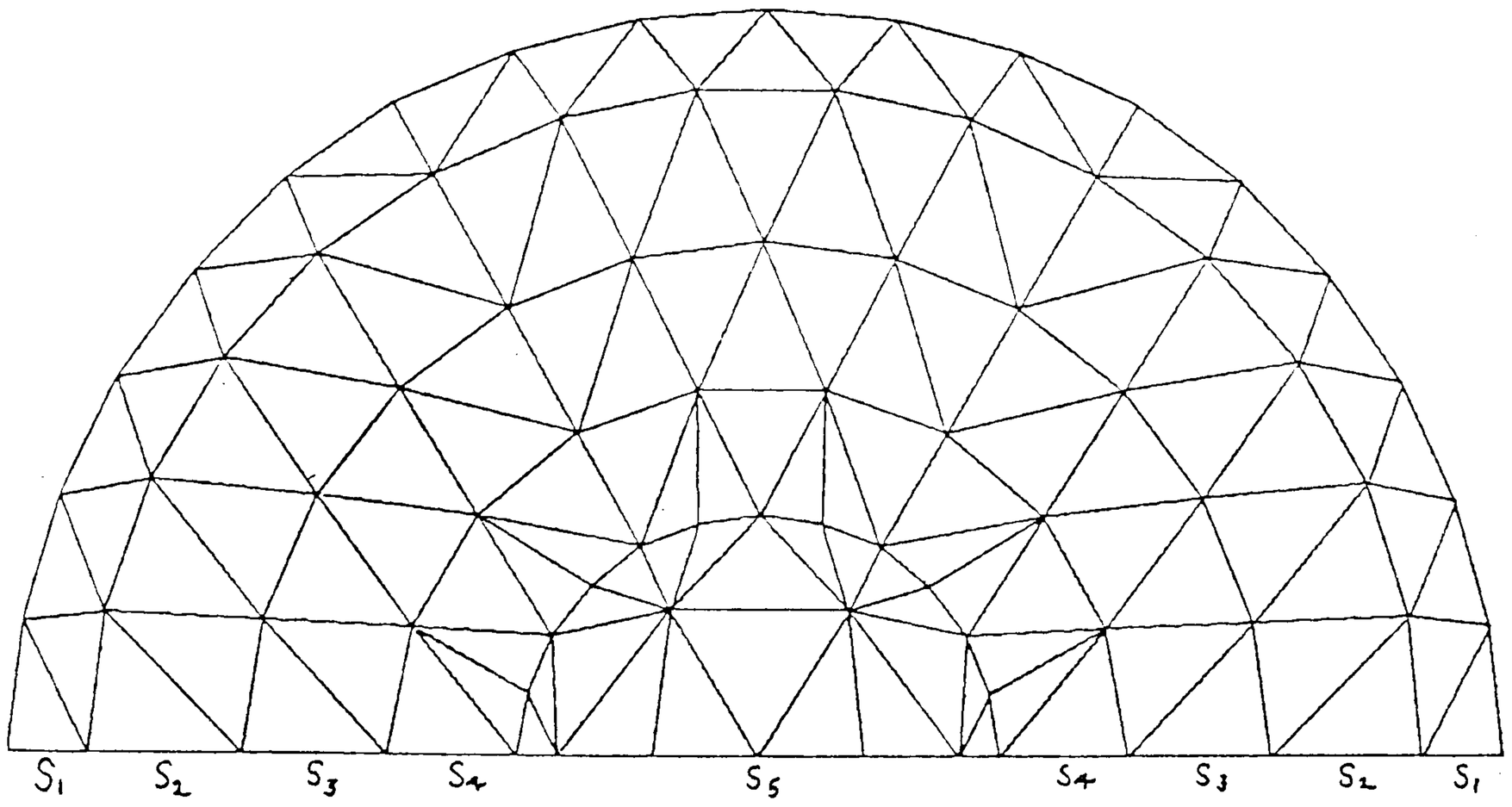


Figure 8a

The shape of the membrane may be controlled by varying K_o values of the hoops and the membrane stresses.

The structure illustrated in fig. 8 is rotationally symmetric but asymmetrical shapes (fig. 9) may also be derived. And by assigning to all other links K_o values which may be varied during form-finding, an infinite degree of control on the shape is obtained since all nodes of the structure are then elastically triangulated.

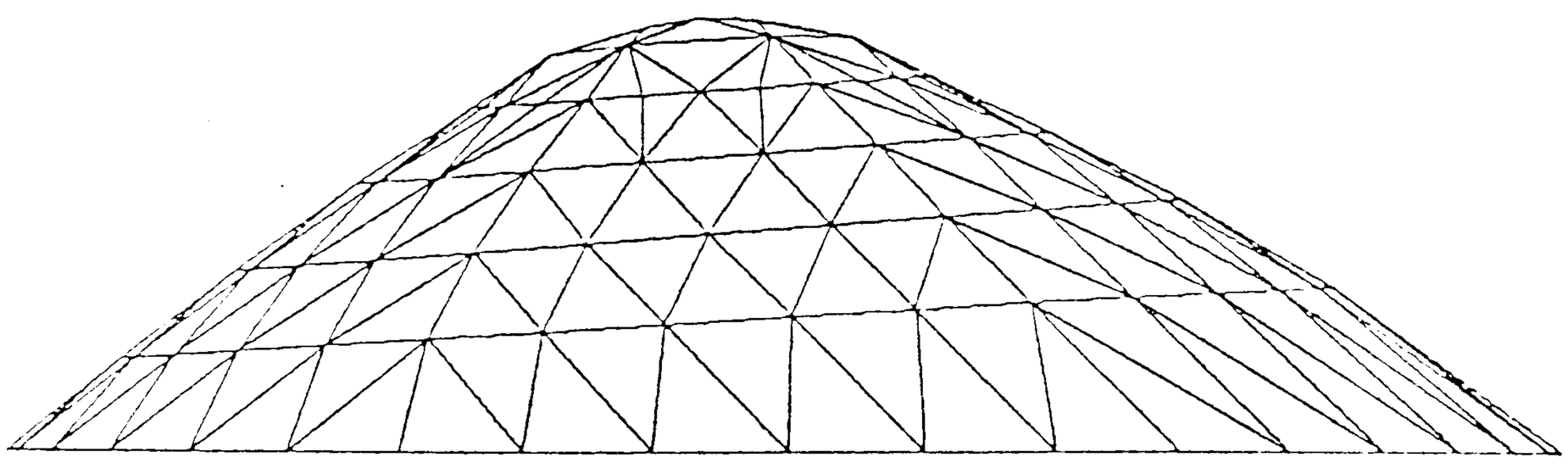


Figure 9

CONCLUSION

The main advantage of dynamic relaxation as an interactive form-finding techniqueis that it simulates a viable physical process, and the dynamic trace of deformed states aids investigation of tension systems in much the same way as model studies. Whilst the techniques described cannot replace model studies from the point of view of appreciation of design aesthetic,

they may complement the physical understanding and extend the range of investigation. The simulation, for example, of structures with combinations of tensile and compressive funicular boundaries, perhaps with traction forces, might be experimentally difficult, particularly if a family of such forms is to be investigated. The process also has a rapid initial convergence so that an early signal for necessary design changes is obtained, enabling trial investigations to be carried out economically. Furthermore, a very important design aspect of tension structures is their dynamic behaviour. Dynamic relaxation allows this to be considered at the formative design stage, provided of course that light damping and realistic values of stiffness and mass are substituted in place of the fictitious values used to accelerate the form-finding process.

Another advantage of the step-by-step trace of behaviour is the ability to cope with zero stiffness situations in highly non-linear situations involving instability or collapse, and more particularly the ability to restore stable topology even after the onset of collapse. The text illustrates, for certain examples, how interactive control enables understanding of physical behaviour so that necessary design changes can be made to achieve convergence. The instructive stages of failure for some additional examples are shown in appendix 7.2.

Although the number of iterations required for convergence is large when compared with matrix iteration techniques, the operations are extremely simple. In terms of equivalent CDC processor time, the 150 iterations for convergence of the geodesic net, with 320 degrees of freedom, requires 4 seconds. Membranes

or pneumatics with the same number of nodes require approximately double the time per iteration. Convergence times for tension surface structures are however greatly dependent on how closely the boundary and other controls require the surface to approach a state which is physically inadmissible. When investigating structures near this state, convergence is usually slow.

REFERENCES

(1) Barnes, M.R., 'Explicit dynamic analysis of tension structures', Int. Symp. on Wide-span Surface Structures, Stuttgart, (April 1976) Chapter 5

(2) Barnes, M.R., 'Form-finding of minimum surface membranes', World Congress on Structures for Space Enclosures, Montreal (July 1976) Chapter 4

(3) Frei Otto, 'Tensile Structures', M.I.T. Press, (1967/69).

APPENDIX 7.1

STRUCTURE PROPERTIES

The parameters used for the examples in the text are given below. The structures are referred to by figure numbers.

2. Central load 2 kN

   Boundary load 1.3 kN per lobe

   Boundary traction 2.5 kN/m

   Membrane tension 2.5 kN/m

   Central loop cable links $K_o = \frac{50}{3}$ kN/m

   Boundary cable links $K_o = \frac{-100}{3}$ kN/m

4. Same as 2 but

   Boundary load 1.8 kN per lobe

3. Same as 4 but

   Central load 2.4 kN

5. Geodesic Net: same as 3 but

   all surface cable tensions 600 N

7. Membrane tension 2.5 kN/m

   Radial cable links $K_o = \frac{25}{3}$ kN/m

   Central loop cable links $K_o = \frac{100}{3}$ kN/m

   Boundary cable links = $\frac{250}{3}$ kN/m

   Central load: Stage (a) 3kN; (b) 6kN; (c) 9kN

8. Pneumatic pressure 3 kPa

   Membrane Tension $S_1 = 3$ kN/m

   Hoop cable links $K_o = \frac{100}{3}$ kN/m, except centre hoop $K_o = \frac{200}{3}$ kN/m

   Boundary cable links $K_o = \frac{-250}{3}$ kN/m

APPENDIX 7.2

The plane membrane of fig. 1 (text), fixed at points ABC and D, and with cables connecting the inner loop points EFG and H to J, was subject to a normal load at J. The outer boundaries were assigned -ve K_o values (compression contours) and the specified membrane stresses were varied linearly from a maximum S_1 in the outer zone to a minimum S_4 in the centre; the stress differences being resisted (as in the pneumatic structure) by elastically controlled tension cable hoops T_1, T_2, T_3 (fig. 10a). Due to the low stress in zone 4 collapse started to occur with the inner loop gathering to the centre (fig. 10b). The stress gradients were then decreased and convergence was obtained with the tension hoops forming circular arcs lying in horizontal planes as shown in figure 10c; the surface being anticlastic.

With the problem reversed so that $S_4 > S_3 > S_2 > S_1$ necessitating compression hoops C_1, C_2, C_3 for equilibrium, form-finding commences in a satisfactory way (figs. 11a & b) but subsequently becomes unstable (fig. 11c) with the compression hoops eventually displacing alternately above and below the horizontal plane containing supports. With elastically controlled tension radials (AE, BF etc.) employed in an attempt to restrain the displacements of the compression hoops, divergence occurs as shown in figure 11d. The failure states indicate that in order to stabilize the system it is necessary to impose the condition that all vertical ordinates in any hoop must be identical. And that to achieve convergence to a system with synclastic curvature

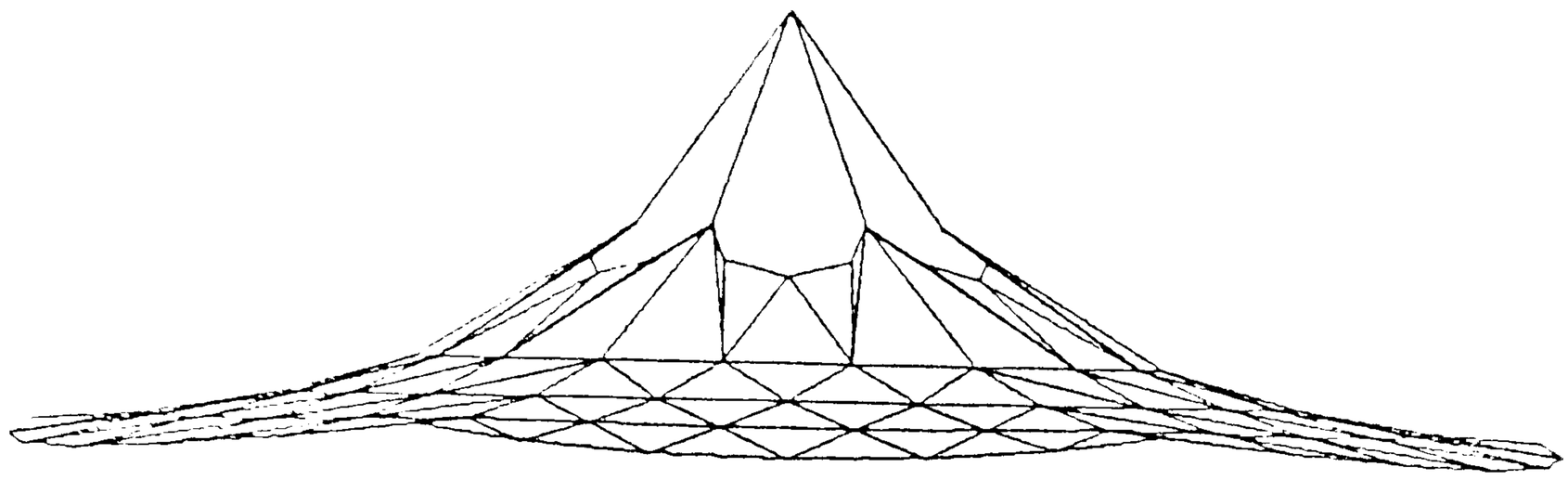


Figure 10c

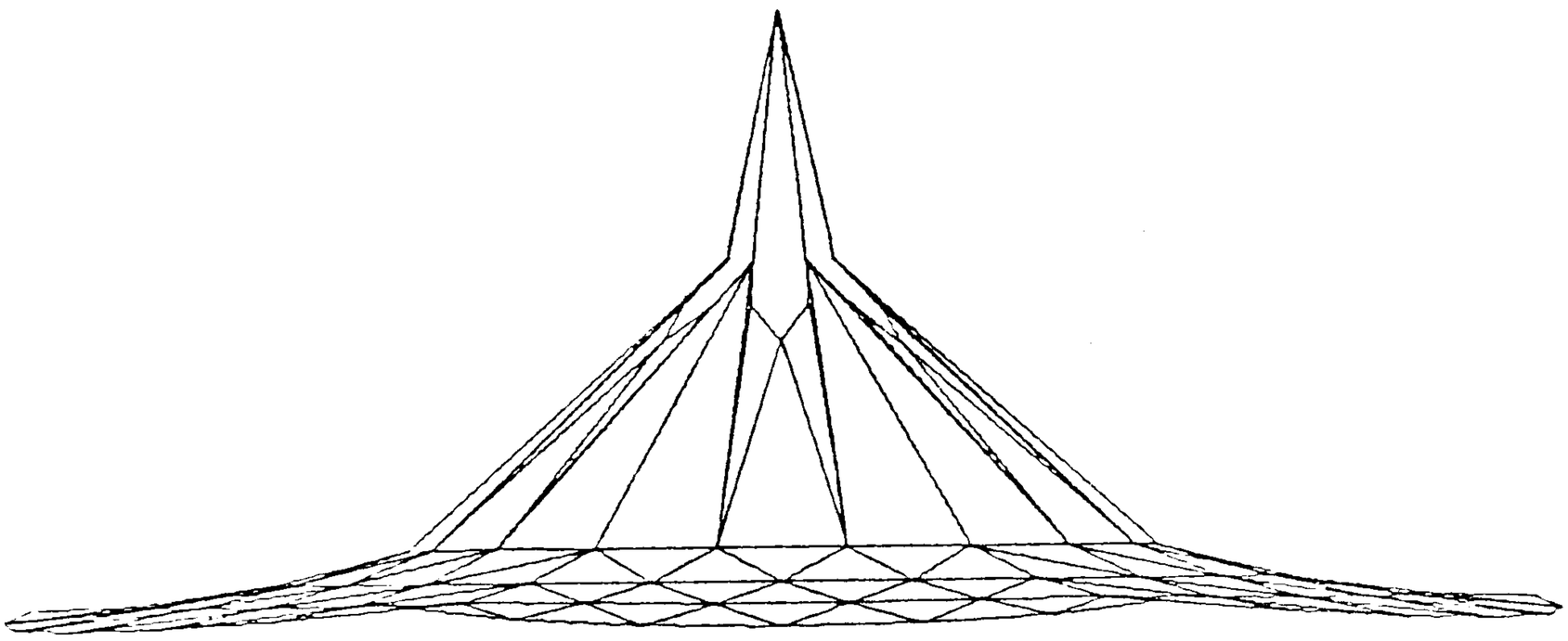


Figure 10b

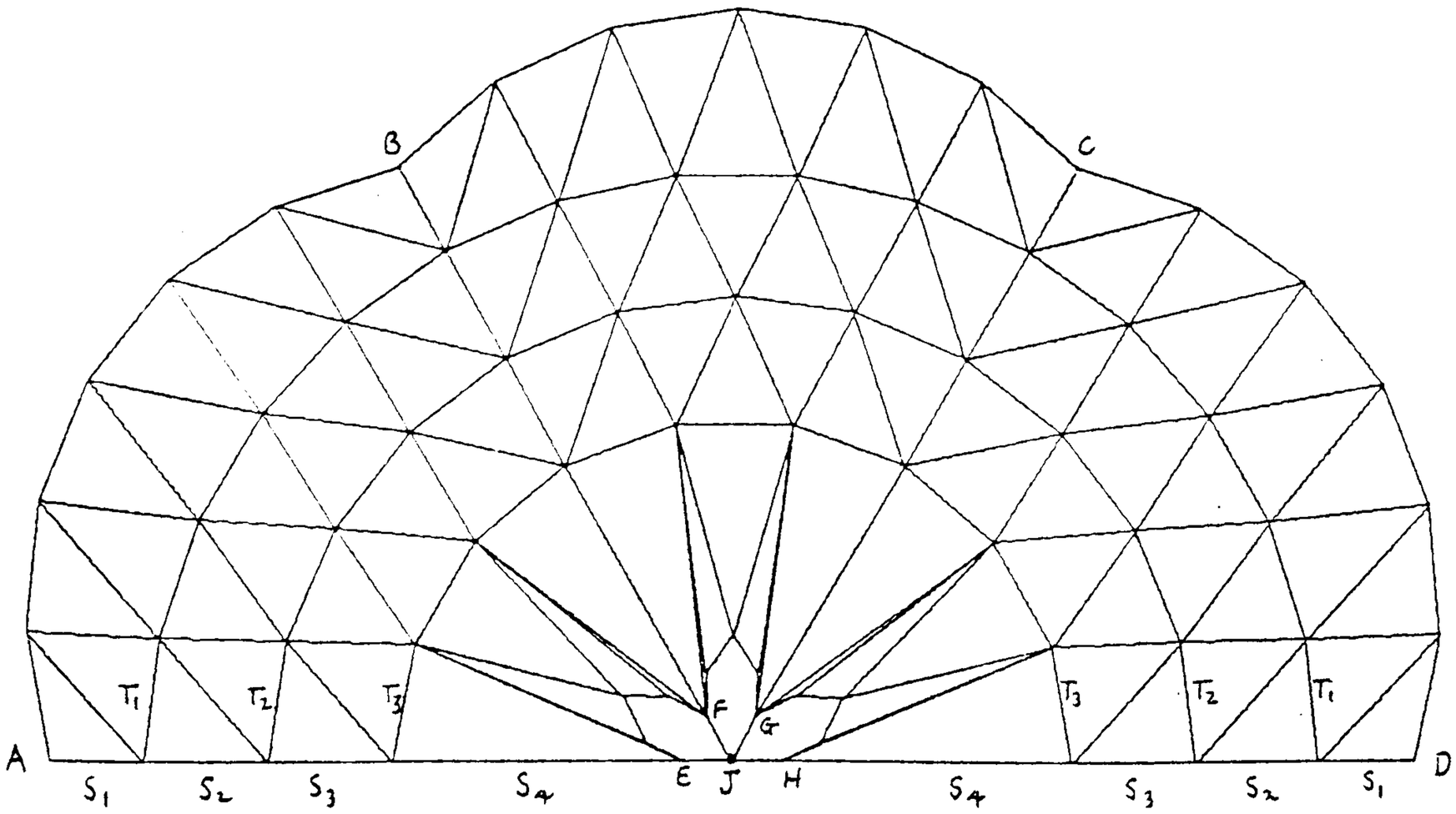


Figure 10a

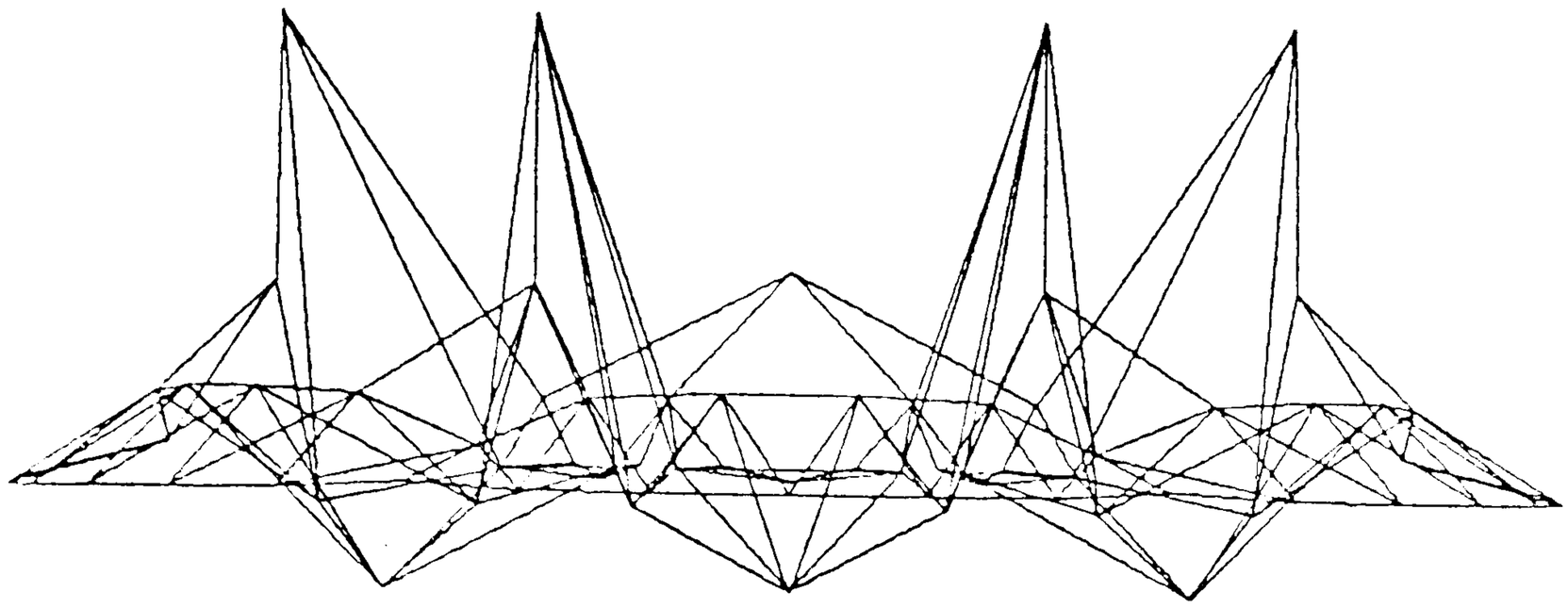


Figure 11d

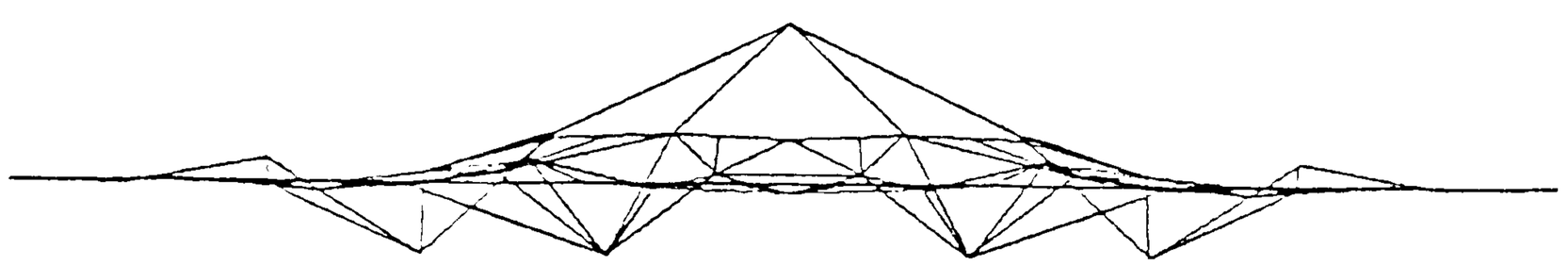


Figure 11c

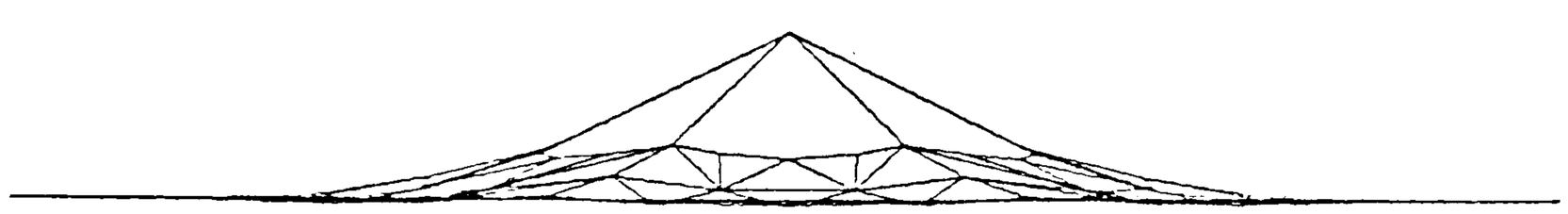


Figure 11b

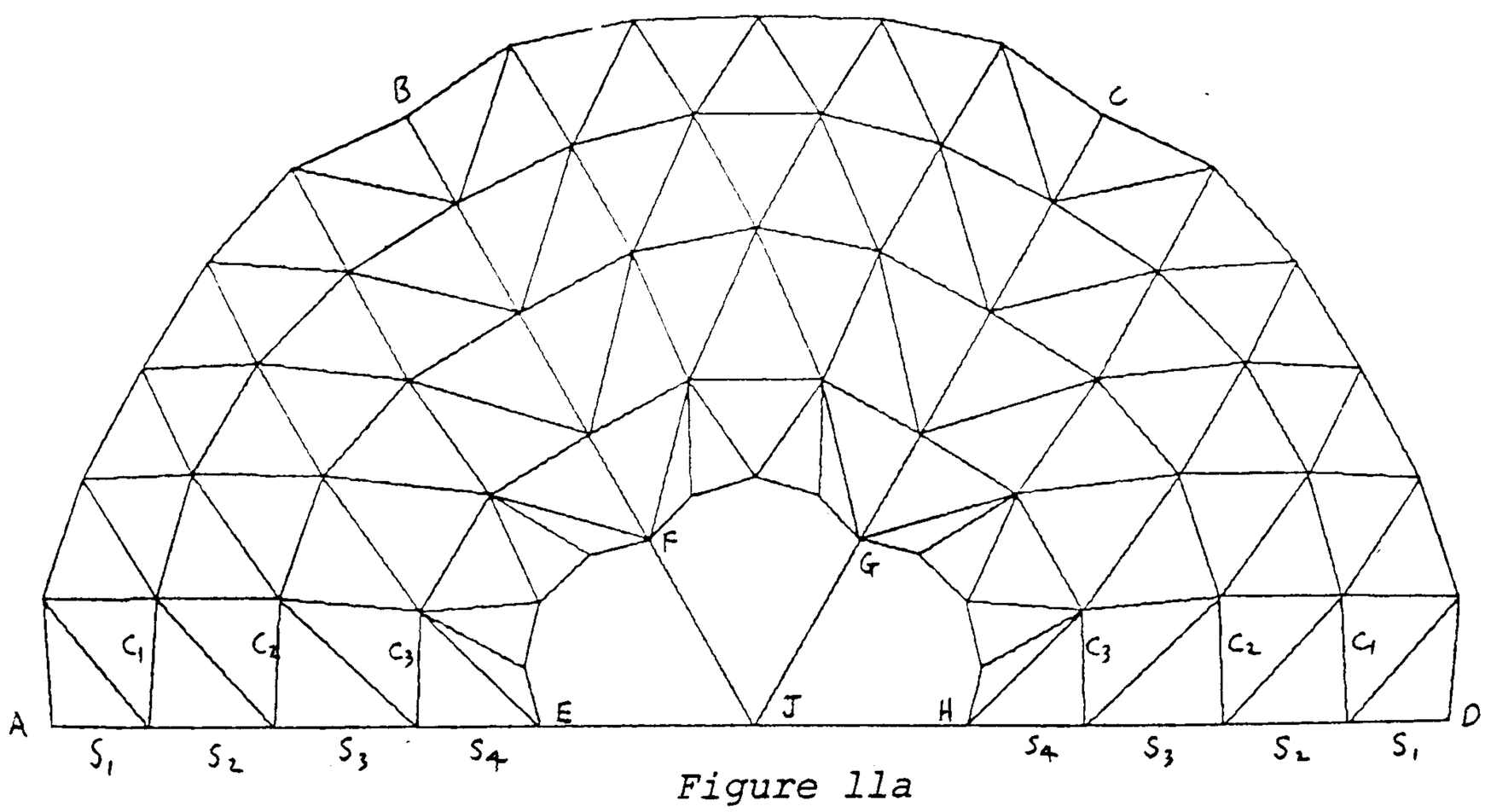


Figure 11a

(as required by the stress gradients) the bearing hoops should preferably be controlled by specifying, and adjusting interactively, their magnitudes of compression as opposed to elastic control.

The necessity for interactive form-finding of the type proposed is also emphasised by the following example (fig. 12a). This was an attempt to obtain a variable stress pneumatic dome (of the type considered in the text - fig.8) with a very steep gradient at the base. Thus the elastic stiffnesses of the tension hoops were reduced to enable expansion of the dome. Because the system was allowed to expand too far however, the lowest and most highly stressed zone of triangular membrane elements became vertical and consequently the lowest tension hoop could no longer sustain the specified stress difference between the adjacent zones. Figure 12a shows the state of the structure just after this had occurred; and in order to restore a viable structure the stresses must be equalized at this stage and large horizontal mass components must be assigned to the base boundary nodes if and until the diameter of the lowest tension hoop exceeds that of the boundary. When this occurs the base boundary becomes tensile and the sign of the elastic stiffness must accordingly be changed. The base node mass components may then be reduced again to allow continued motion to a final equilibrium position.

If the above actions are not taken, the system rapidly proceeds from stage 12a to 12b. Stages beyond 12a are no longer instructive and ultimately complete divergence occurs. The value of dynamic relaxation form-finding is that it gives an

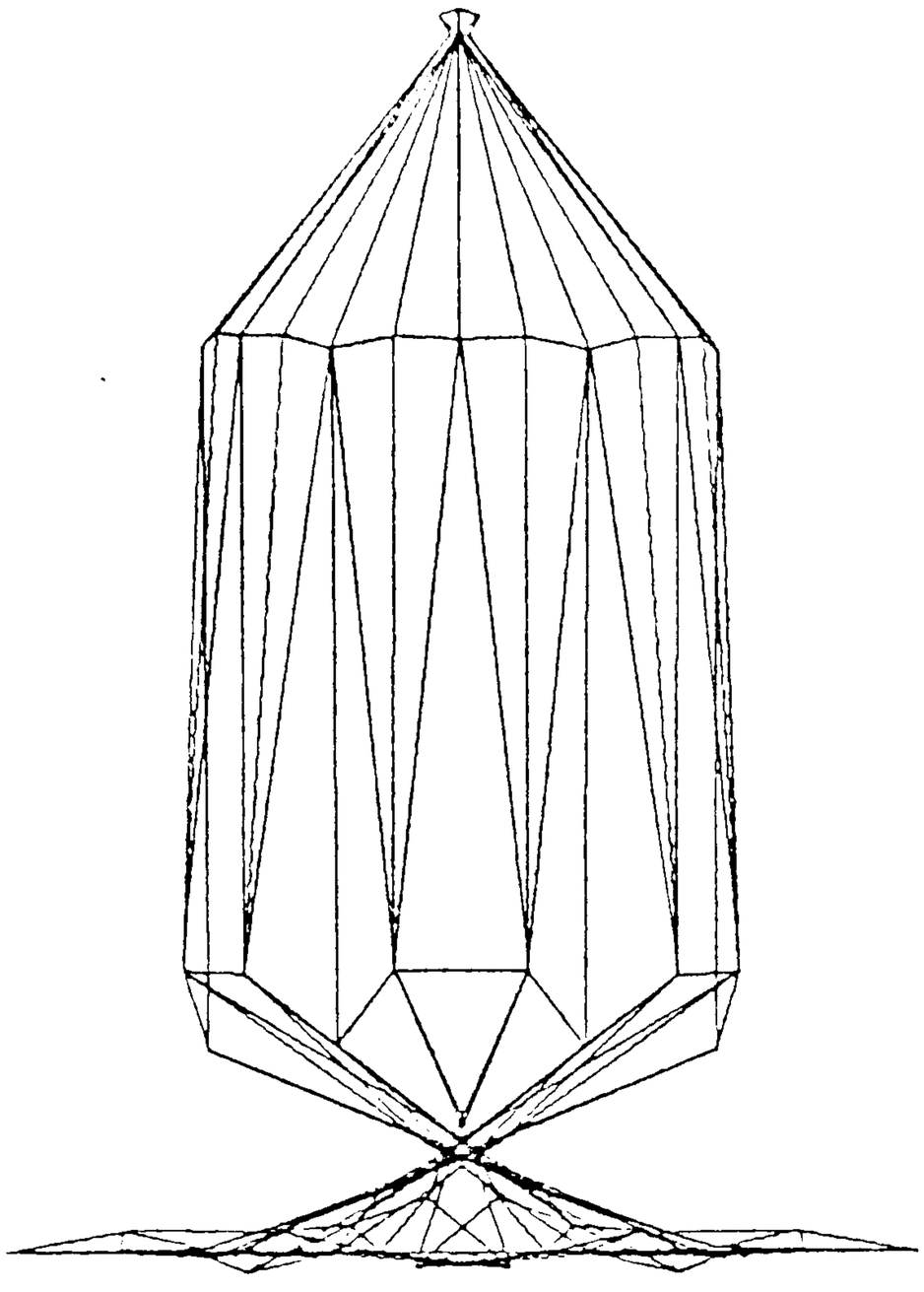


Figure 12b

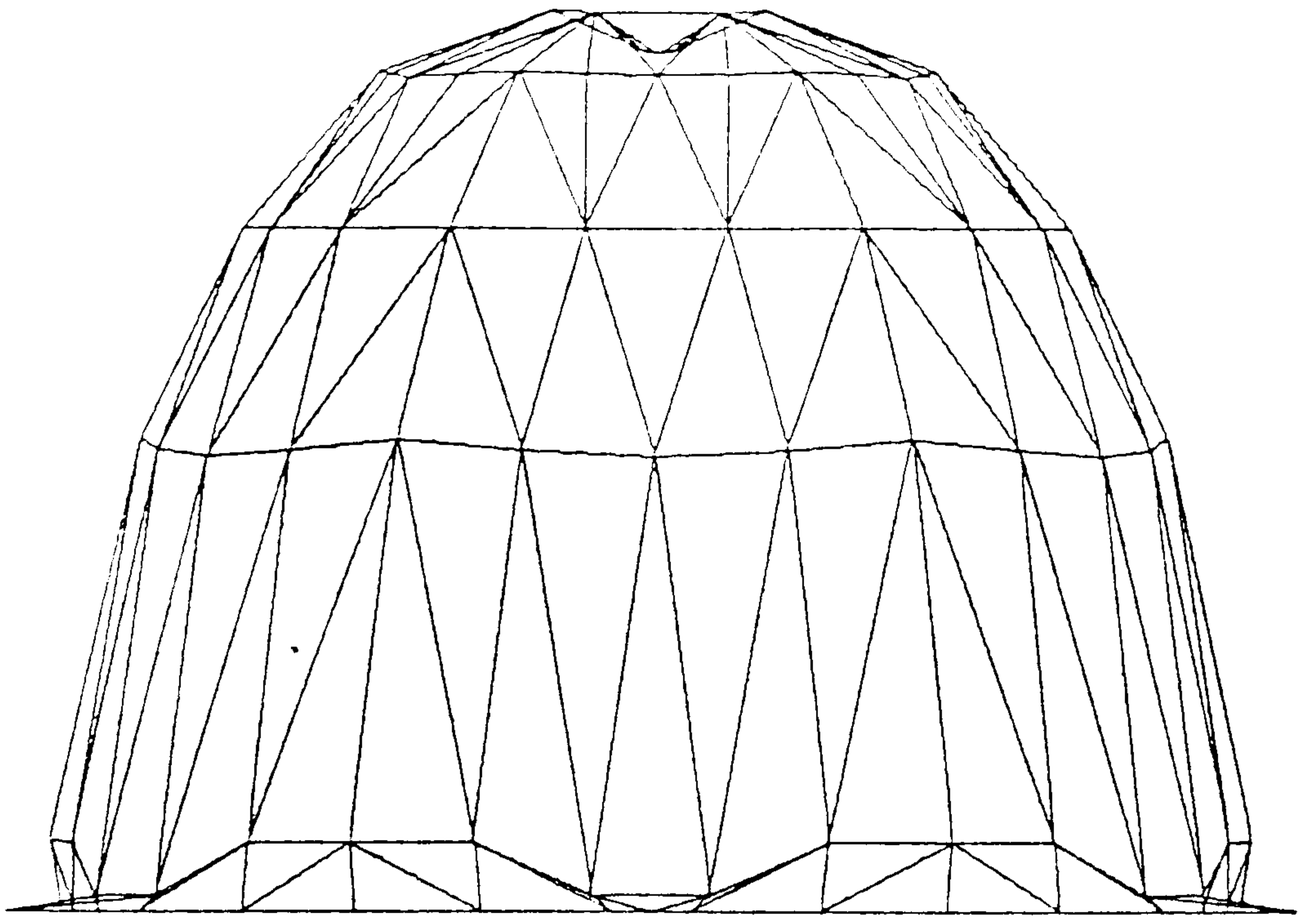


Figure 12a

indication, at the right stage, of the physical reasons for impending failure. In contrast, matrix methods based on Newton-Raphson iteration would merely indicate numerical divergence irrespective of whether they produce graphical output. It is the dynamic trace of physical behaviour and interactive control which enables the proper control conditions to be realised and applied.

CHAPTER 8

OPTIMIZATION OF SPACE TRUSS FORM

SUMMARY

The dynamic relaxation process is extended to cater for the optimization of the form of space trusses subject to a single loading condition. Using a modular 'ground structure' with generally defined external boundaries containing all possible alternative structures which comply with the modular grid, member sizes are continuously modified during the process until the structure obtained complies with criteria for a least-weight optimum. Physically, the process of adaptation is such that, as loads are taken up and transmitted to supports, members which do most work are increased in size and those that do least are decreased; respectively increasing or reducing their subsequent capacity to do work. In the limit, the majority of members have reduced to zero area and may be deleted whilst the remainder, forming the optimum, are stable in size and configuration.

A procedure suitable for the form-finding and member sizing of space structure building systems is then outlined which takes into account variable loading and general deflection constraints. This entails an interactive design mode in which at any stage a preferred structural policy is indicated, but allows the Architect or Engineer freedom of functional design.

The paper was presented as a lecture at the IASS Congress on Structures for Space Enclosure, Montreal, July 1976, and examples subsequently incorporated in a paper at the Conference on Slender Structures,London, Sept. 1977 (reference 20).

APPROACHES TO STRUCTURAL OPTIMIZATION

The classical approach to the optimization of structural form developed by Maxwell[1] (1854) and Michell[2] (1904) is based on a direct physical approach. Precise results may be obtained but, up to the present, only for relatively few cases[3-7]. Solutions for these "Michell" structures are dependent on the initial specification of appropriate principal strain fields, and do not account for constructional or architectural constraints such as the use of modular member sizes, standardized joints and the possible intrusion of functional space into the domain of the structure.

The more recently developed mathematical-programming techniques for structural optimization,[7-16] developed originally for tactical decision making, permit a variety of practical constraints. These abstract mathematical techniques have been applied to two broad categories of structural optimization: (a) the ideal form-finding of truss, space and shell structures, and (b) the optimal sizing of members in statically indeterminate structures with a specified layout but subject to a variety of loading cases with constraints on deflections, stresses and minimum member sizes. Either of these classes of application may require large amounts of computing time and core store for relatively simple structural systems. In 1966, for example, Richards and Chan[5] reported on the shape optimization by Linear-programming of a space-truss generated from a 'ground-structure' with only 59 degrees of freedom,subject to 360 inequality constraints,which required one of the largest computers then available[7]. For reasons of economy, in dealing with stress constrained problems in class (b), some researchers[16-20] have concentrated on the study of "fully-stressed

design" techniques. In general, these consist of the iterative factoring of member sizes with subsequent re-analysis leading to a design in which each member is subject to its limiting stress under at least one of the specified load conditions. This is possible provided the number of load conditions is greater than or equal to the ratio of members to degrees of freedom[19]. Although the analytical statement of the goal of minimum weight is absent from the procedure, it has been found that structural proportions are obtained which, if not optimum, are very close to the ideal[18-20]. Furthermore, mathematical-programming techniques also suffer from a similar uncertainty since, although leading to an optimum, there may be no assurance that this is a global rather than local optimum[16-20]. Analogous procedures, also restricted to structures with a fixed geometry, termed "optimality-criterion-based" design, have permitted an extension of the re-analysis methods to cope with multiple design constraints on deflectionsas well as stresses[21-23].

The techniques of linear-programming were introduced in 1964 to the problem of form-finding by Dorn, Gomory and Greenberg[10], and in parallel work by Hemp[7]. They approached the topological and geometrical design of structures by arranging a rectangular gridwork of possible node points to cover the design space, and allowing for the interconnection of all nodes with truss elements to form a "ground structure" of possible members. Neglecting buckling effects and the possibility of prestressing and assuming all members have the same elastic modulus then, for a single load case, the optimum structure is fully stressed and must be statically determinate, otherwise, except in special circumstances, the strains

throughout the structure could not be compatible. Hence, treating the member forces as the design variables (> number of joint equilibrium equations), the techniques of linear programming were used to select from the complete set of admissible (statically determinate) structures that which had the least weight; termed the "basic optimal structure", and containing as many bars as degrees of freedom (= number of independent equilibrium equations). The zero force members and unnecessary joints were then deleted to yield the final "reduced optimal structure" consistent with stability.

For multiple load conditions a minimum weight structure may be statically indeterminate and is not necessarily fully stressed[17]. Thus component weights may not in general be taken as proportional to member forces and a non-linear programming algorithm is required for optimization. Dobbs and Felton[11] tackled this problem using iterative displacement analysis of an initially complete ground truss structure with member areas modified through the use of a steepest descent-alternate mode algorithm. After a series of design cycles (each cycle consisting of a complete steepest descent and side-step move, controlled for each member by the greatest stress induced by any loading condition), bars which were found to have areas approaching zero were deleted in order to avoid the occurrence of ill-conditioning or violation of the constraint of non-negative member areas; such members not subsequently being permitted to re-enter the design process. Whilst there is no rigorous guarantee that some of the deleted members might not in fact be components of a global optimum, results obtained by the process

have been good. The deletion of members in this manner has not been applicable to cases in which buckling is accounted for since, when the area of a compression member is reduced to a small value, the buckling stress becomes critical and the area must then be increased.

Majid and Elliott[12] extended the non-linear approach to include deflection constraints and utilized theorems of structural variation in a direct, rather than iterative, re-analysis procedure. In doing so, because of the potentially large number of member force coefficient vectors and consequent core store requirements, it was found advantageous to examine a number of candidate reduced ground structures rather than a single fully connected structure. A possible advantage of their approach is that the influence, throughout the structure, of changes in any particular member are predicted and convergence to the optimum solution may thus be more stable.

All of the foregoing mathematical-programming design techniques are complex and rather abstract in formulation, and entail products of computing time and core store very much greater than the standard methods of structural analysis. The possibility of ill-conditioning may be a problem in matrix methods of re-analysis in which member properties are changing and in certain cases reducing to zero stiffness. And, for the formative design of complete space-structures (assuming the availability of very large computers), this difficulty is likely to increase with the size of stiffness matrix. The optimization method proposed in subsequent sections also utilizes the concept of a changing ground

structure but is based on a "Dynamic Relaxation" procedure in which equilibrium and compatibility considerations are separated[24-26]. The method allows a very considerable reduction in core store requirements and, since at any stage the deflections and rates of deflection of nodes are controlled by dynamic equations of motion, the possibility of ill-conditioning may be precluded by suitable control of the fictitious nodal mass components which govern accelerations.

It was previously noted that, in contrast to mathematical-programming techniques, the design of Michell structures is accomplished by a direct physical approach. In a restricted sense, the same is true of the dynamic relaxation procedure which entails a gradual reduction in stiffness of members which do least work with a corresponding increase in those that do most work as the complete ground structure takes up and transmits the loads to specified supports; convergence of the dynamic analysis to a static solution being achieved by the use of high fictitious viscous damping. Since justification of optimality of the process may be regarded as a corollary of the Michell proof with directional constraints, for the sake of completeness the Maxwell-Michell theory is restated below.

THEORY OF MICHELL STRUCTURES

Consider a pin-jointed framework contained within domain of space D. If the structure is in equilibrium with specified applied loads and reactions X_j, Y_j, Z_j at nodes j with co-ordinates x_j, y_j, z_j then, considering a uniform virtual dilation strain, ε,

of space D, by the principle of virtual work:

$$\sum_{\substack{\text{all tension}\\ \text{members } p}} F_p.L_p.\varepsilon - \sum_{\substack{\text{all compression}\\ \text{members } q}} F_q.L_q.\varepsilon = \sum\left[X_j.x_j.\varepsilon + Y_j.y_j.\varepsilon + Z_j.z_j.\varepsilon\right] \qquad (1)$$

where F_p, F_q denote absolute values of tensile or compressive force respectively, and corresponding member lengths are denoted by L_p, L_q.

The term on the right-hand side is independent of the choice of origin and is constant provided the structure has no redundant reactions or that statically admissible reactions are specified. Thus for all such frameworks in D:

$$\sum F_p.L_p - \sum F_q.L_q = C \qquad (2)$$

If the greatest allowable tensile stress is P and the greatest compressive stress Q, the volume of material in a given fully stressed frame is:

$$V = \sum L_p.\frac{F_p}{P} + L_q.\frac{F_q}{Q} \qquad (3)$$

For that framework in which V is least:

$$2PQ.V + (P-Q).C \quad \text{is also least}$$

Thus $$2PQ\left[\sum L_p.\frac{F_p}{P} + \sum L_q.\frac{F_q}{Q}\right] + (P-Q)\left[\sum L_p.F_p - \sum L_q.F_q\right]$$

$$= (P+Q)\left[\sum L_p.F_p + \sum L_q.F_q\right] \text{ is least}$$

or $$\sum L.|F| \text{ is least} \qquad (4)$$

Consider now a general type of imposed deformation such that the limits of strain in space D are $\pm\varepsilon$, and the virtual strain

of a typical member of a trial framework, A, within D, is e. The virtual work done by the specified applied loads (constant for any such framework) is given by:

$$\delta W = \sum e.L.F \qquad (5)$$

where $-\varepsilon \leqslant e \leqslant \varepsilon$ and F may be of different sign to e.

Hence:

$$\delta W = \sum e.L.F \not\geqslant \sum |e|.\ L.\ |F| \not\geqslant \varepsilon.\sum L.\ |F|$$

Thus for frame A: $\sum L_A . |F_A| \not< \frac{\delta W}{\varepsilon}$

If, however, a particular framework, M, can be found such that for any member $e = \overset{+}{-}\varepsilon$ and the signs of F and e correspond then:

$$\sum L_M . |F_M| = \frac{\delta W}{\varepsilon} \qquad (6)$$

hence $\sum L_M . |F_M|$ is a minimum and consequently the volume of frame M is also minimum.

In order that a virtual deformation of the domain of space D occupied by frame M can exist such that the virtual strains are $+\varepsilon$ and $-\varepsilon$ along the tension and compression members respectively, and that nowhere within D is the strain greater, the members of the frame must coincide with the mutually orthogonal principal trajectories of a virtual strain field compatible in sign with the member forces. A well known example of such a framework is the "Michell cantilever" formed from two sets of equiangular spirals (fig.1). Since the domain of space of the strain field can extend to infinity the structural form represents an absolute optimum.

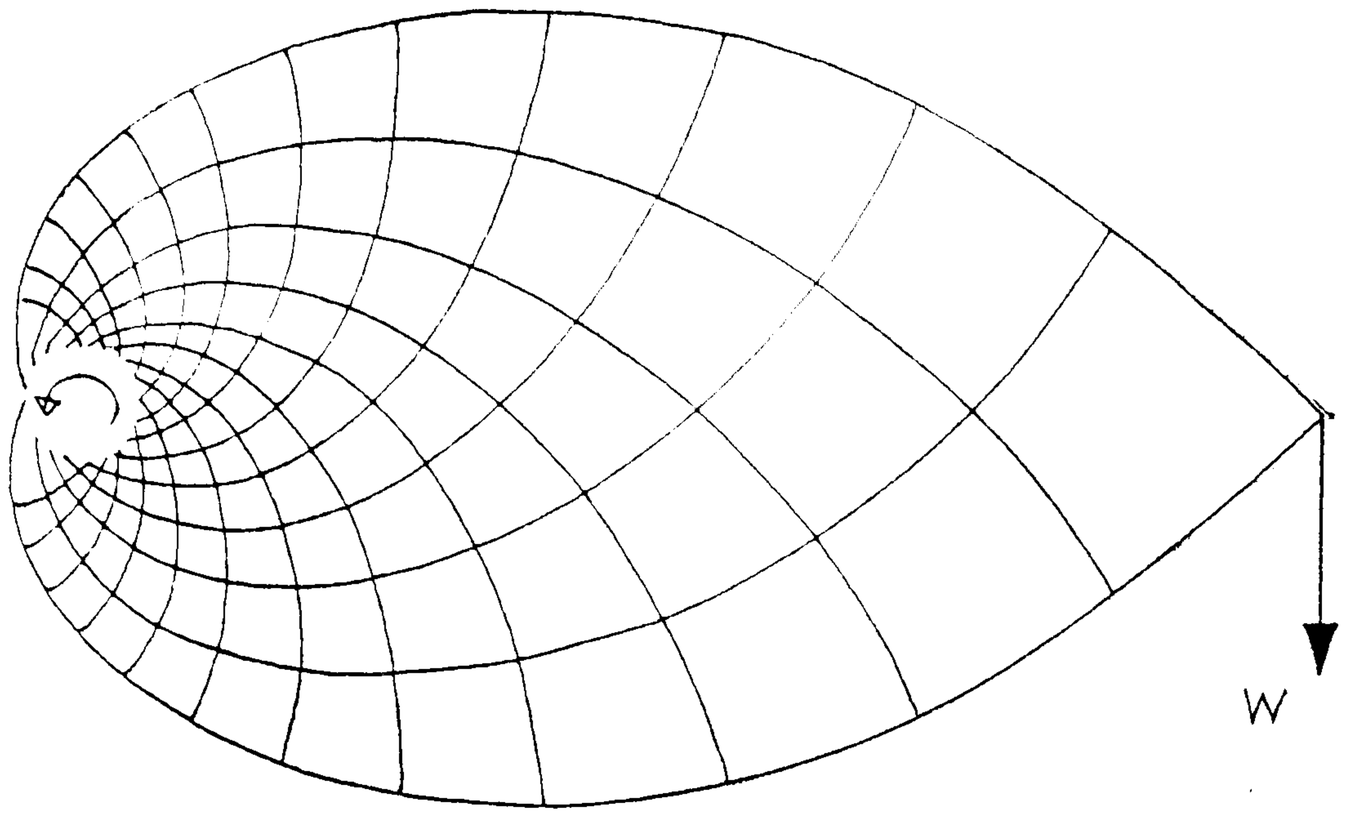


Figure 1

OPTIMUM MODULAR SPACE TRUSSES

Michell forms represent both an aesthetic ideal and a standard with which a prospective space or plane truss design may be compared. Unfortunately, however, they suffer from two main practical drawbacks:

(i) that it is necessary to specify a priori a feasible virtual strain field which, particularly for three dimensional space structures, limits the range of application, and

(ii) that member lengths, areas and jointing are non-standardised.

The first of these drawbacks might be partially countered by analysing, initially, a continuous elastic medium in a restricted domain of space enclosing the loading and supports. The principal stress trajectories so obtained then indicate the required orientation of potential members in the space truss. The second drawback, however, still applies.

A more general, modularly constrained, approach to the ideal form-finding of space structures subject to a single average design loading might be expressed as: Determine the most economical structure using a building system consisting of a particular type of space node connector allowing for the junction of many potential members, and sets of discrete member sizes which comply in length with the space filling capabilities allowed by the nodes. Functional demands must limit the domain of space which may be occupied by a potential structure, and internal regions may also be precluded.

Neglecting for the present the restriction of discrete member areas, the necessary and sufficient conditions for a least weight solution to this constrained problem are:

(1) The stresses in all the members due to the applied loading are either P (tension) or Q (compression).

(2) The framework must permit a virtual displacement of all its possible nodes which produces a strain of $+\varepsilon$ in its tension members, a strain of $-\varepsilon$ in its compression members, and no strain outside these limits in any segment along which a potential member could lie.

OPTIMIZATION BY DYNAMIC RELAXATION

Selection of a least-weight structural form from a large set of possibilites may be achieved without the use of mathematical programming to minimize a weight function if the analysis procedure leads to a direct physical solution which complies with the foregoing conditions.

Consider a completely connected ground structure (fig.3) in which member areas may change continuously such that at each stage in the growth of a structure, as loads (W) are taken up and transmitted to supports(S), the areas are adjusted by a function which tends to make them proportional to the current ratio of their own strain magnitude, $|e_c|$, to that in a particular member, $|\varepsilon_c|$, which is known to participate in the optimum solution (fig.2). If $|e_c|$ exceeds $|\varepsilon_c|$ the member area, A_c, is increased and conversely if $|e_c| < |\varepsilon_c|$ the area is reduced. Thus, since the work done by any member is $E.L.\int A_c . e_c . de_c$, members which do most work increase or retain their stiffness(EA_c/L) and those that do least are made less stiff.

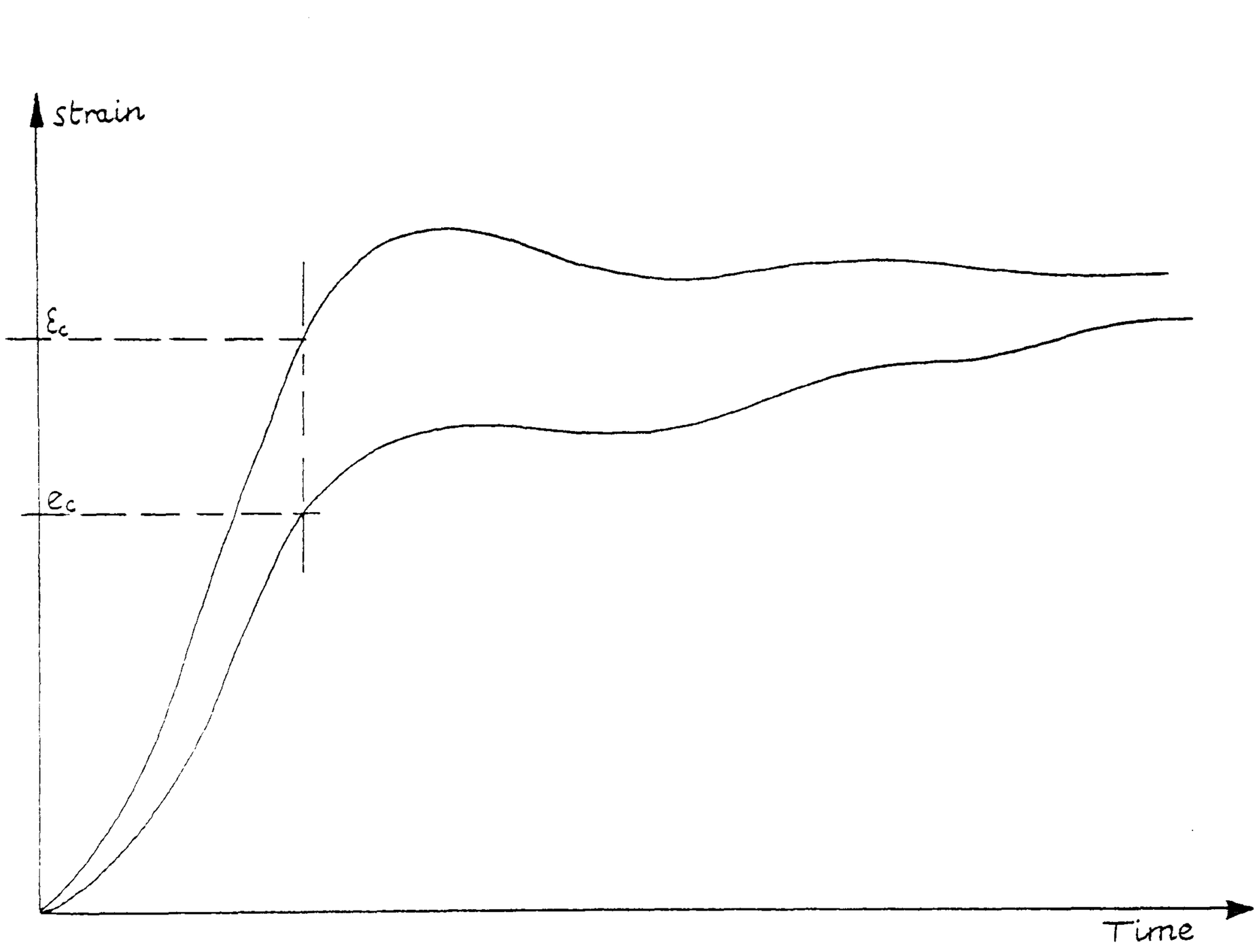


Figure 2

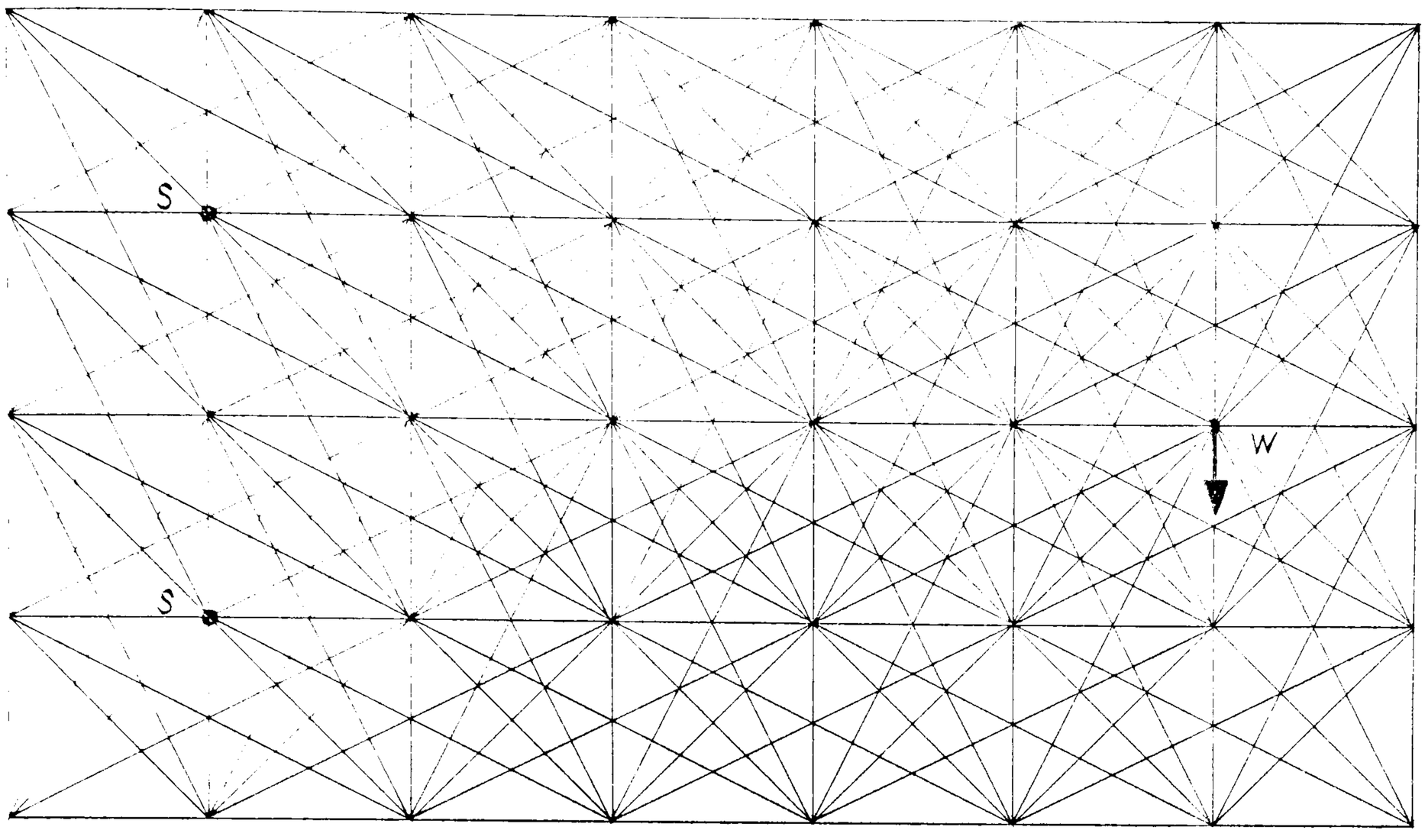


Figure 3

If the fully connected topology of the ground structure is retained at all stages, a converged solution to the above procedure is impossible to obtain since this would imply $|e_c| = |\varepsilon_c|$ in all members; yet node displacements, and hence all strains, are uniquely determined by any reduced combination of bars which make the frame simply stiff. Strains cannot therefore be of equal magnitude and compatible if the modulus E is the same for all members. Alternatively, if the weakest members are successively deleted from the ground structure, there may be no guarantee that a converged solution complies with condition (2). This problem can be avoided by retaining the complete topology and recording stiffness modifications until, after a sufficient number of iterations, a state is reached in which the component areas of a reduced set of bars forming a determinate solution are constant or slightly increasing, and all other members of the ground structure

have areas which tend to zero and are decreasing. Provided the analysis yields monotonic convergence then, by condition (2) and ultimately excluding bars of very low stiffness, the solution gives an optimum structural form.

Since the reduced optimum structure is determinate the actual stresses can be adjusted to any required values consistent with security. In particular, member areas may be amended to give tensile stresses = P and compressive stresses = Q<P. The form-finding analysis yields, in effect, a virtual strain field which gives the optimum layout. The constant, E, is a fictitious elastic modulus which must be sufficiently high to preclude gross deformation of the ground structure geometry and, to obtain actual deflections, the reduced optimum structure must be re-analysed using the real values of member areas and elastic modulus. In a later section it is shown, however, that form-finding and analysis may coincide, with the real areas and elastic modulii being dynamically adjusted to achieve a secure stress state and acceptable deflections during the form-finding process.

To enable a solution by Dynamic Relaxation, three stabilizing conditions should be observed:

(a) Convergence to the static solution should be heavily damped (fig.2).

(b) The changes in stiffness should lag behind the corresponding rates of change in strain.

(c) The (fictitious) mass component at each node in each co-ordinate direction should, at all stages, be made proportional to the corresponding direct stiffness component.

Since a constant time interval, Δt, is used throughout the explicit "dynamic" analysis, condition (c) is necessary in order that all nodes should have the same relative response and the same critical time interval governing numerical stability:

The critical time interval for motion in the x direction at any node i is given by[24]:

$$\Delta t_{crit} = \sqrt{\frac{2M_{ix}}{S_{ix}}} \tag{7}$$

M_{ix} is the mass component, and S_{ix} is the direct stiffness component given by:

$$S_{ix} = \sum_{\text{all bars m at i}} \left(\frac{EA}{L}\right)_m \cdot \left(\frac{DX}{L}\right)_m^2 \tag{8}$$

where, for bar m, $(EA/L)_m$ and $(DX/L)_m$ are respectively the axial stiffness and x direction cosine.

Hence, if the critical time interval is to remain identical for each deflection component throughout the ground structure and the time interval used in the analysis is to be 90% of Δt_{crit}, the required mass components at any stage are given by the relation:

$$\left(M_{ix}\right)_{c+1} = \left(\frac{\Delta t}{0.9}\right)^2 \cdot \left(\frac{S_{ix}}{2}\right)_c \tag{9}$$

Similarly for the y and z mass components and all other nodes.

The external subscripts denote that the mass components for stage c+1 may be set using the stiffness values at stage c. This simplifies computation and is satisfactory provided $\Delta t \neq \Delta t_{crit}$.

To comply with condition (b) member areas may be adjusted according to the relation:

$$\left(A\right)_{C+1} = \frac{(A)_C}{2}\left[1 + \frac{|e_c|}{|\varepsilon_c|}\right] \qquad (10)$$

For members which participate in the optimum solution the cross sectional areas thus become approximately converged when $|e_c| \rightarrow |\varepsilon_c|$= Constant. For bars which remain unstrained the areas reduce exponentially from stage to stage, whilst other bars which are strained, but do not belong to the final optimum, reduce at a slower rate.

TEST CASES

The application of the form-finding process is illustrated in the following simple examples which are all plane trusses subject to a single load cantilevered from two hinge supports.

1. Five Bay Sparse Ground Structure

The ground structure, loading and supports are shown in figure 4. The EA values of members were all set to 1500 N, and the grid points were spaced at 1m centres. The time interval used in all analyses was 0.01 sec, and nodal mass components were adjusted according to eq. (9) to give $\Delta t = 0.9\ \Delta t_{crit}$.

Initially, an undamped trial run without modifying member areas gave a fundamental frequency of 0.28, which yields an estimate for the critical damping per unit mass of:

$$K = 4\Pi f \triangleq 4$$

A form-finding analysis was subsequently carried out using a damping factor of 8 and modifying member areas, according to eq. (10), after every 10 time increments. The tensile strain in the member marked 'C' was used as the control value, ε_c; the area of this member being held constant throughout. After fifteen stages of modification (equivalent to ½ sec C.D.C. processing time) the pattern of most efficient members had become clear: the EA values of members indicated by a full line were all stable or increasing and lay in the range 1000 → 4500 N; EA values of the dashed members were in the range 300 → 800 N and decreasing; and all other members had values less than 300 N (half of which were less than 10 N). After ninety stages the full members all had EA values greater than 1490 N, and the remainder were less than 8 N (with 70% less than 0.01 N). At a later stage the analysis became unstable, possibly due to the fact that damping at each node was dynamically adjusted to be proportional to the mass components. The statically determinate optimum structure had, however, become apparent well before this stage was reached.

With the same number of time intervals (10) between each modification stage the analysis was convergent with damping factors down to 4. Below this value the analysis diverged. When, however, the number of time intervals per stage was increased to 25, the analysis was stable with a damping factor of 1.5. At the other extreme, with only two time intervals between modifications, the analysis quickly diverged even with damping as high as K = 15. A more efficient procedure would probably be to use a

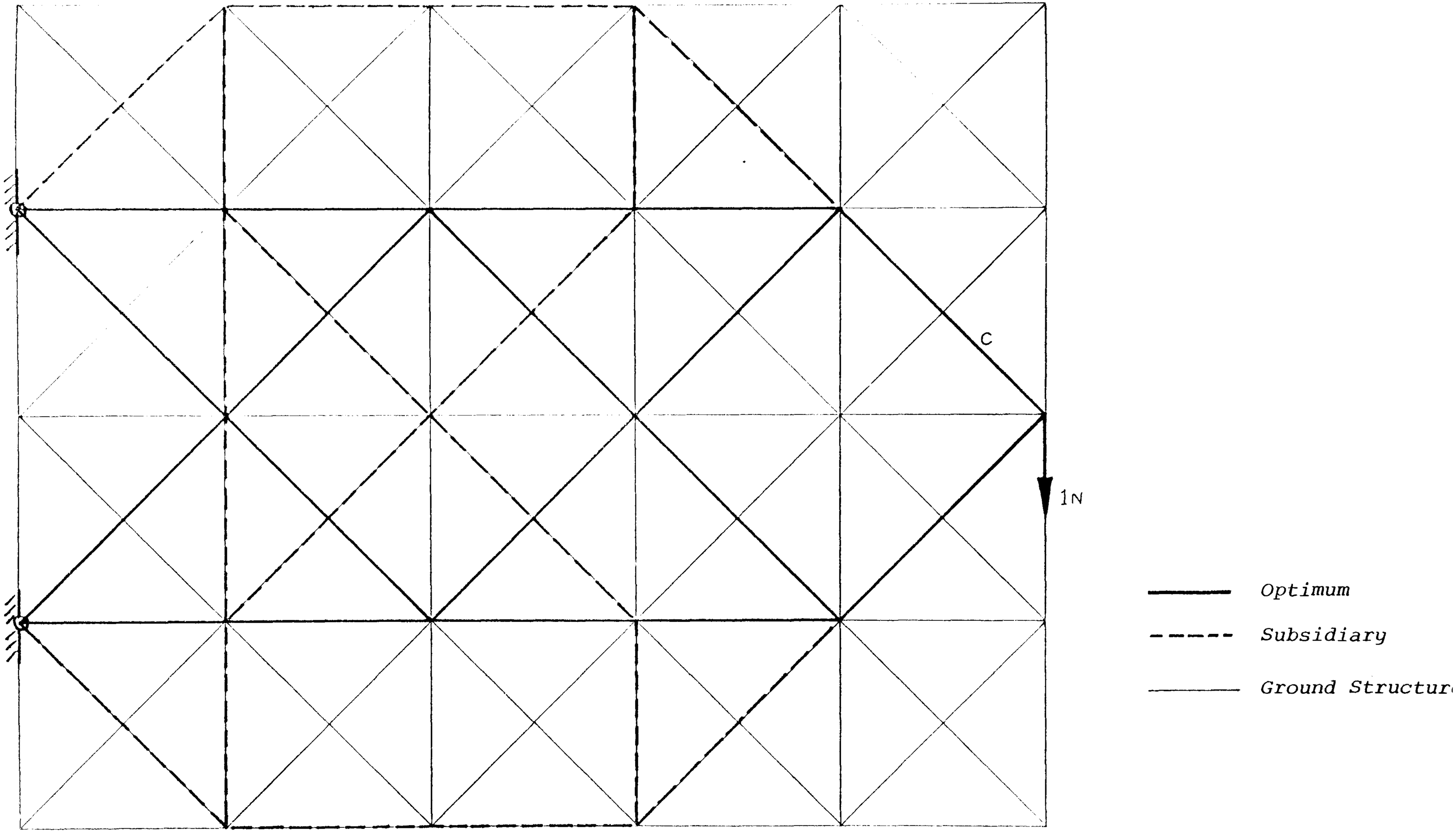


Figure 4

large number of time intervals between modifications in the early stages, with comparatively few at later stages. Although the damping factor should be in the region of the critical value, provided it is sufficiently high to ensure stability, the actual value does not appear to have a significant effect on convergence rate. Convergence of the test structure, using 10 time intervals per stage, was almost identical for all damping factors ranging from 5 to 15.

2. Five Bay Extended Ground Structure

The more extensively coupled ground structure shown in figure 5 was analysed using again a time interval of 0.01 sec and initial EA values of 1500 N. A preliminary undamped and unmodified analysis gave an estimate for the critical damping factor of 13.

Using a damping factor of 10 and modifying areas at every 10 time intervals, the state of the structure after 50 stages of modification is shown by the full, dashed and dotted lines in the figure, which correspond respectively to EA values >3000 N, >1000 N, and >300 N. For the remaining 115 members of the ground structure the EA values were less than 200 N, 81 of which were less than 0.5 N. After 100 stages the EA values of the full-line members, forming the optimum structure, were in the range $15000 \rightarrow 30000$ N, with all others less than 2000 N. The maximum values subsequently increased to 60000 N and thereafter the analysis became ill-conditioned.

It is of interest to note that the optimum structure

became clearly defined even though the control link, with EA held constant at 1500 N, did not in fact belong to the solution. It was thought that the rate of convergence might be improved by using the average of the strain magnitudes in all members as the control strain. It was found, however, that the analysis quickly diverged.

The structure obtained is a global optimum for the ground structure used. It provides a useful test of the form-finding procedure partly because the control link is eventually excluded, and also because it yields a weight reduction of less than 5% compared with the previously generated structure and several other possible structures which might perhaps have been obtained as local optima.

3. Seven Bay Extended Ground Structure

The ground structure shown in figure 6, with two additional bays, was analysed using the same time interval, damping factor and number of time intervals between modifications as for the previous structure. The optimum structure obtained is shown by the full-line members.

After 70 modification stages the EA values of members were:

a) for the full-line members: $>$ 400 N and stable or increasing

b) for other members: $<$ 400 N and decreasing

At 100 stages the corresponding values were:

a) $>$ 400 N and stable or increasing

b) $<$ 300 N and decreasing

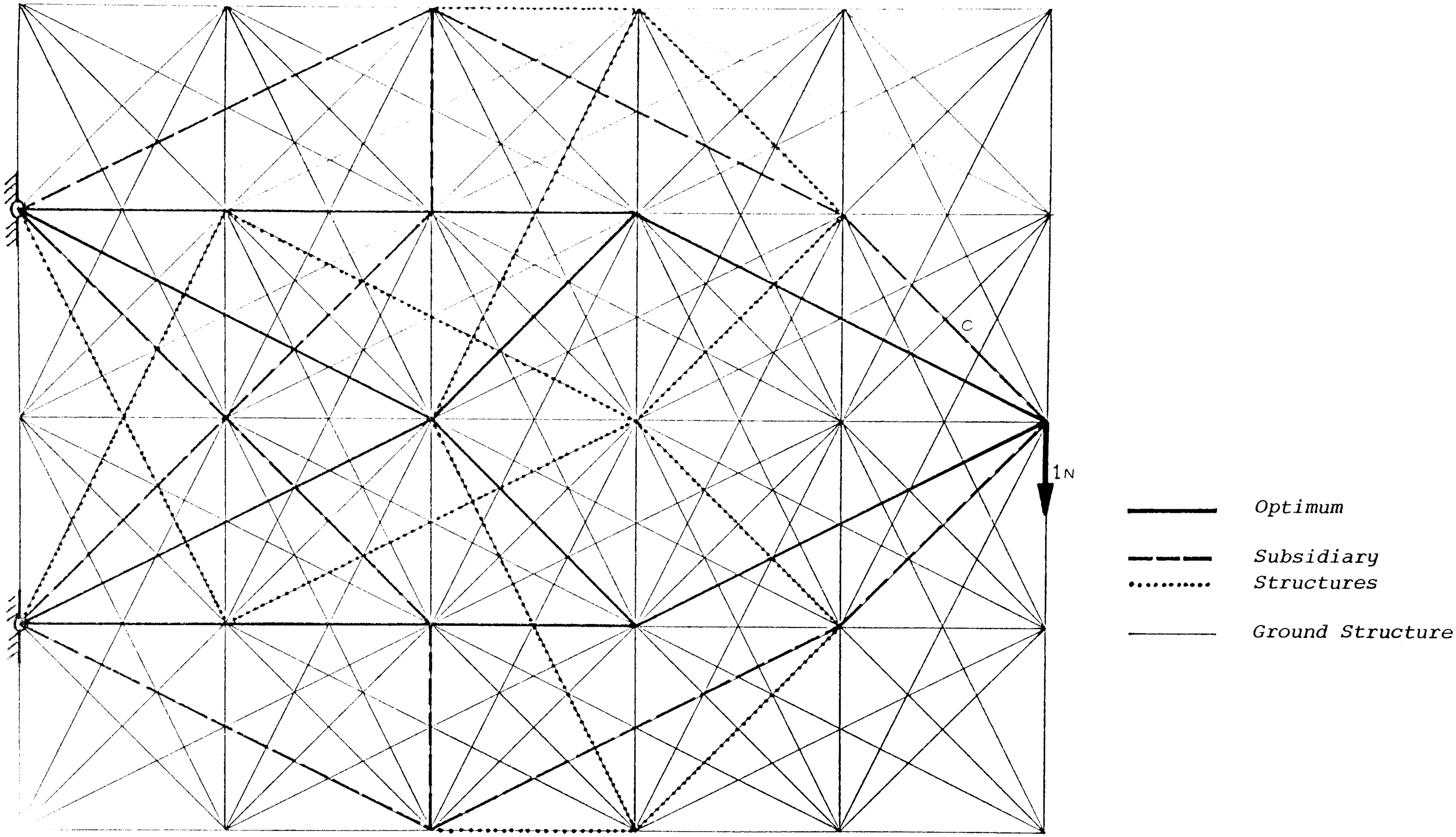


Figure 5

and at 130 stages:

a) $>$ 400 N and stable or increasing

b) $<$ 200 N and decreasing.

The only exceptions to this classification were the members shown dotted which, whilst not complying with categories (a), had EA values which were slowly increasing. The reason for this is that there are several statically determinate structures of equal optimum weight. For example, excluding the dotted members a, b and c, the full-line structure shown has a sum of products of member forces and lengths of 34.67 Nm. If members a and c, and the full members d and e are excluded, but members b are inserted, the resulting structure has the same value of $\sum|F|.L$. Several other determinate combinations of equal weight are possible.

Convergence of the analysis was comparatively slow because, in addition to the several optima of equal weight, numerous other possible structures have weights of less than 2% in excess of the optimum, and consequently their component members have areas which decrease slowly. The time required for 70 stages, at which the optimum could be obtained, was equivalent to 6 secs C.D.C. processing time. By examining trends, however, a good indication could be obtained before this stage. It should also be pointed out that the foregoing studies represent merely a preliminary investigation of the method, and no attempt has been made to increase computational efficiency or to examine more rapid modifying procedures than that given by equation (10).

If one imposes the restriction that members may only cross at the grid node points, a structure which is close to the

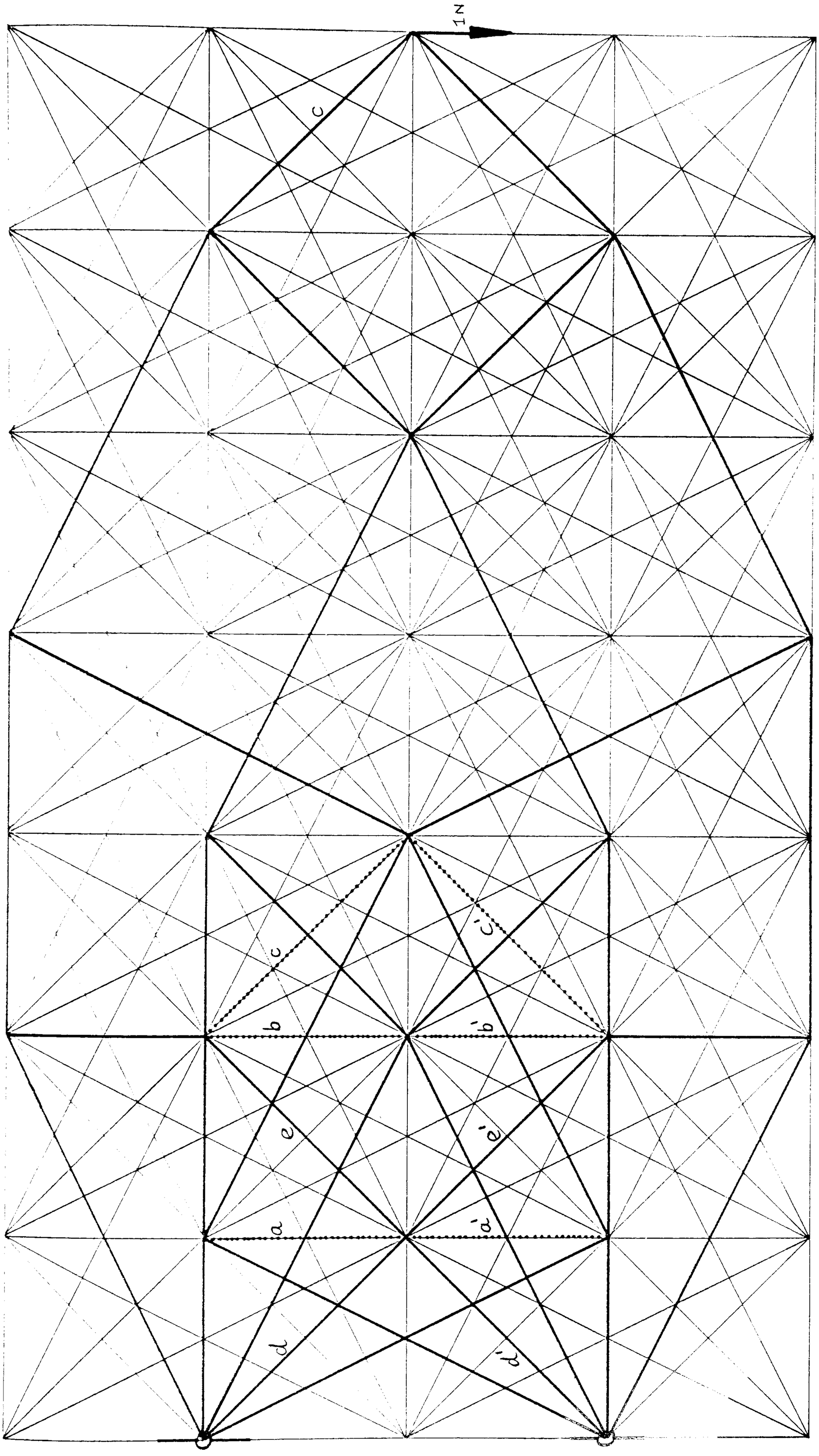


Figure 6

optimum, with $\sum|F|.L.$ = 35.3 N.m., is shown in figure (7). From an engineering point of view this is a simpler and more practical structure, but to incorporate automatic checks for this condition would complicate considerably the form-finding process. For the main application envisaged, however, which concerns three dimensional space structures, this problem would not arise.

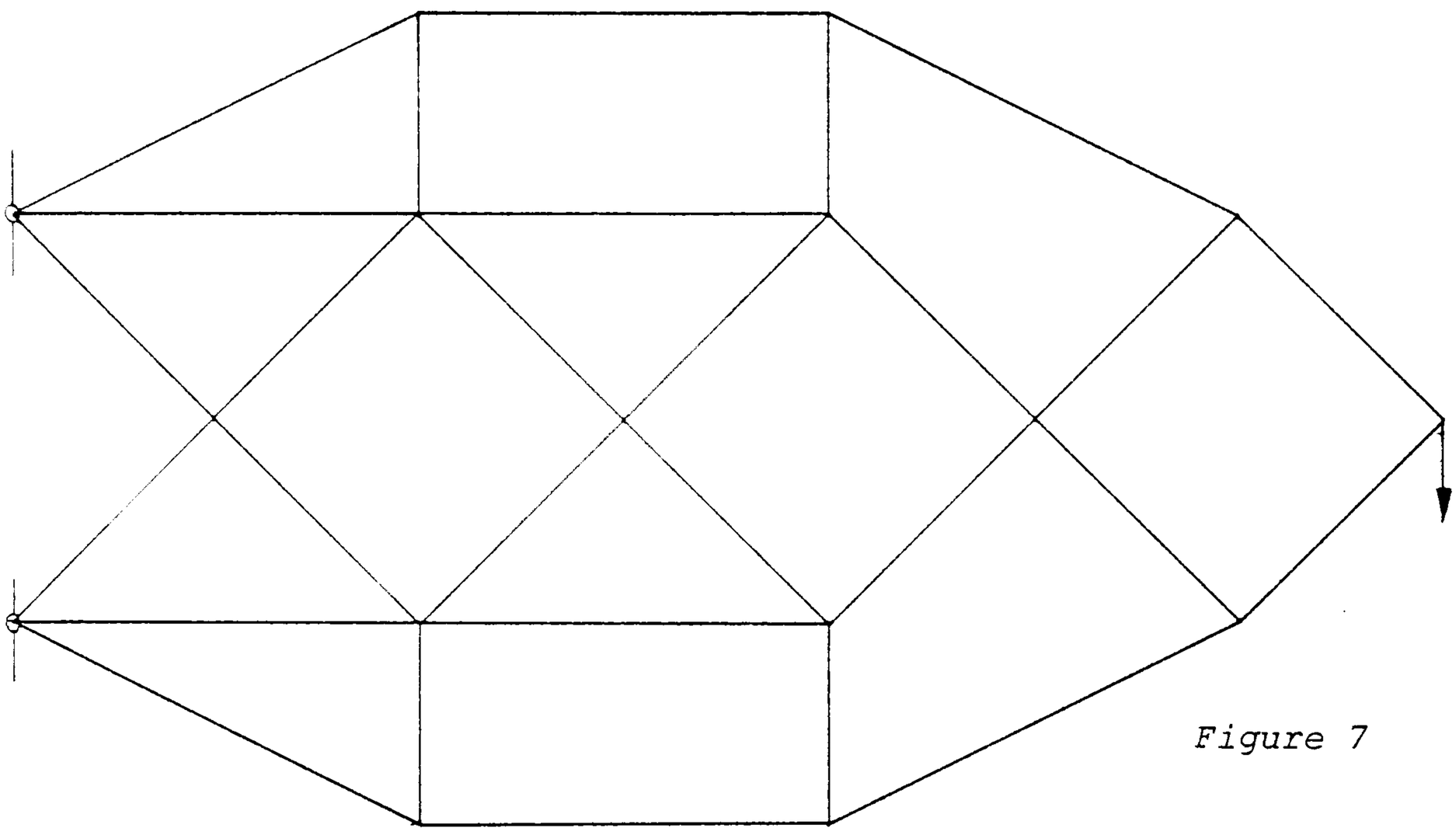


Figure 7

A POLICY FOR INTERACTIVE FORM-FINDING AND ANALYSIS

For complex three dimensional space structures with various internal regions subject to adaptable functional use, and such that the structural system forms an entire building (see for example Gabriel[27] and Pearce[28], to which figures 8-11 relate), the required design procedures represent in many respects the antithesis of conventional building design. Although termed a "structuralist" approach to Architecture,

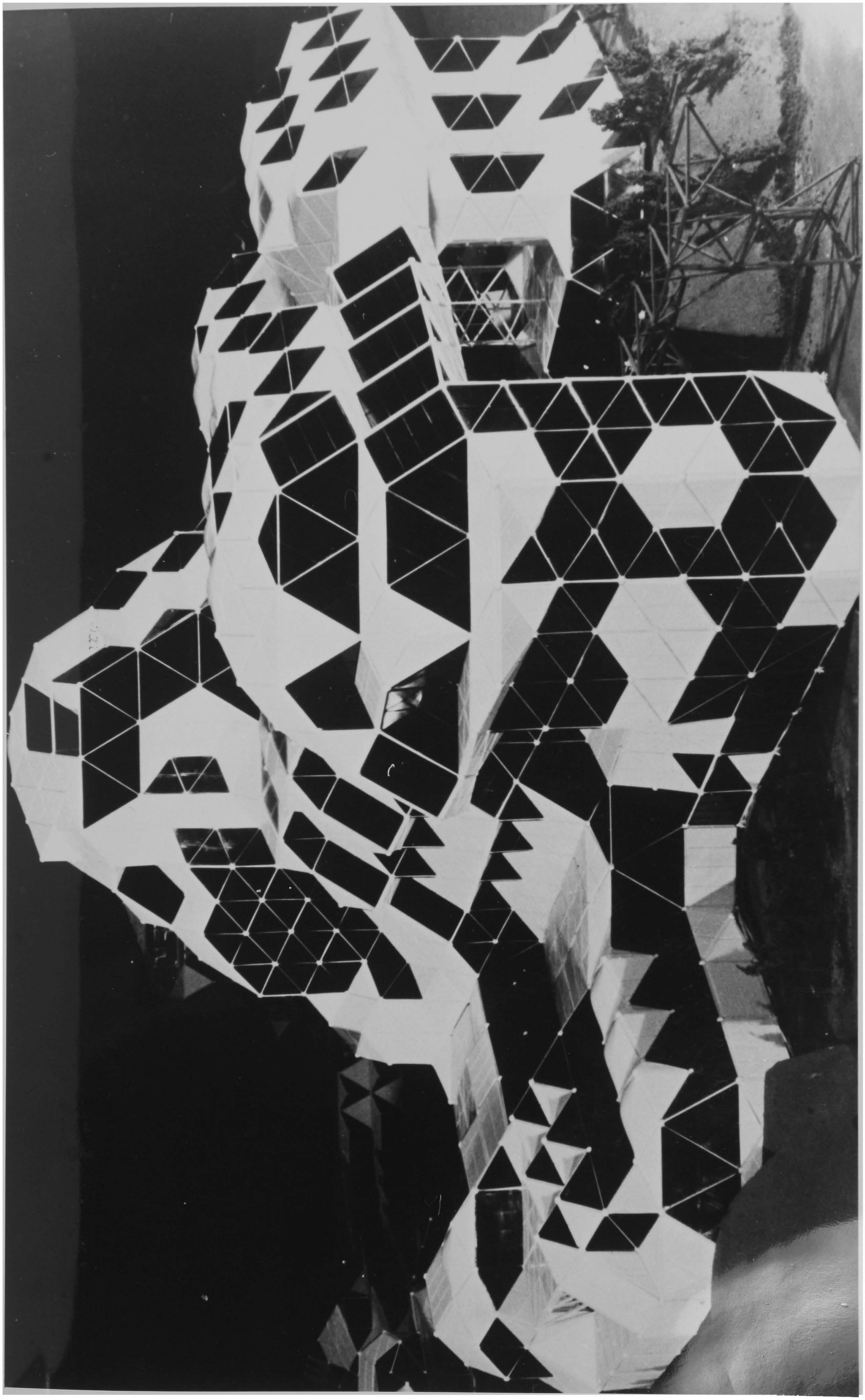


Figure 8 Eight Storey Building based on 26 way space node system (by Pearce[27])

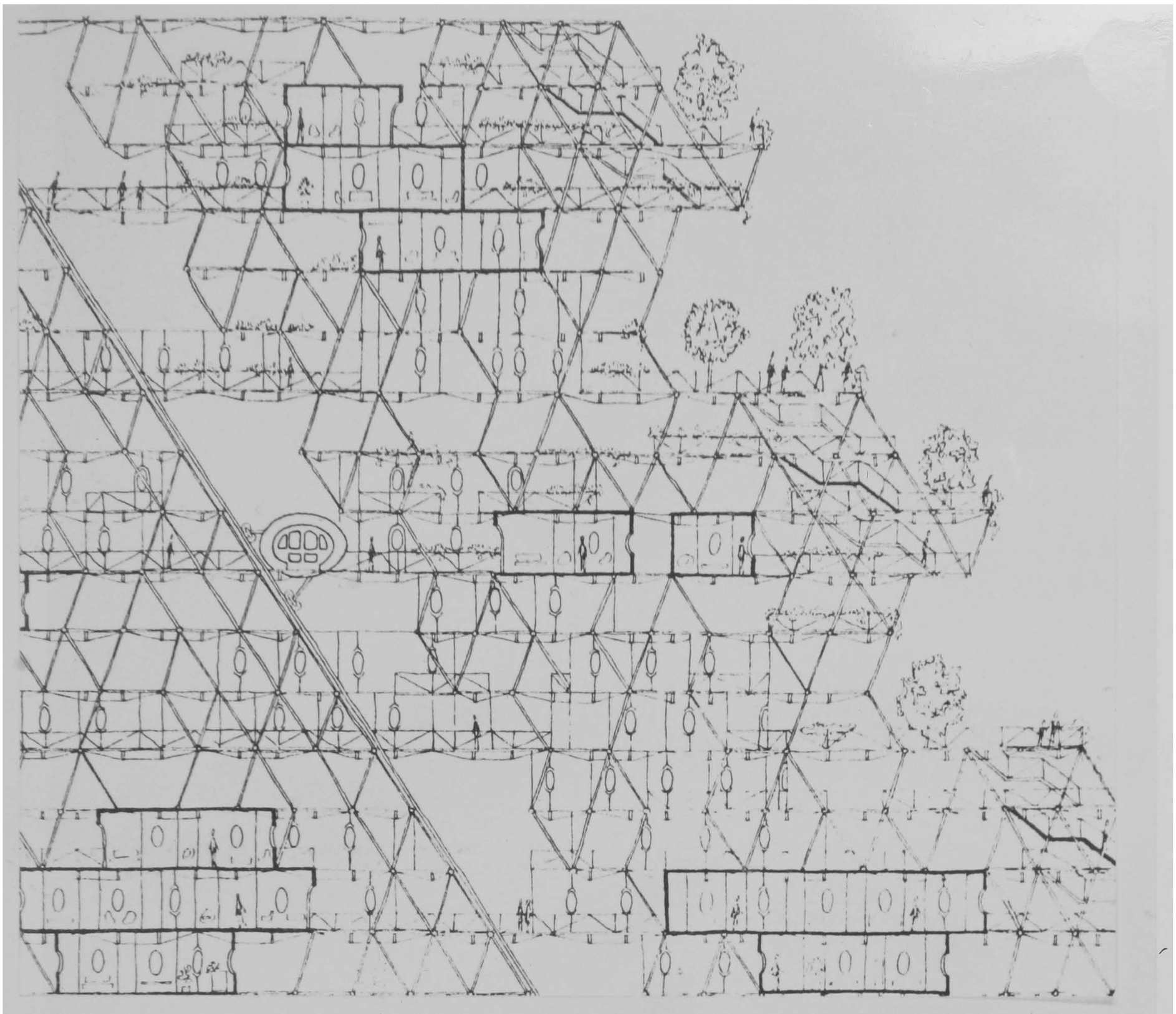


Figure 9 "Three-dimensional suberb" (by Gabriel[28])

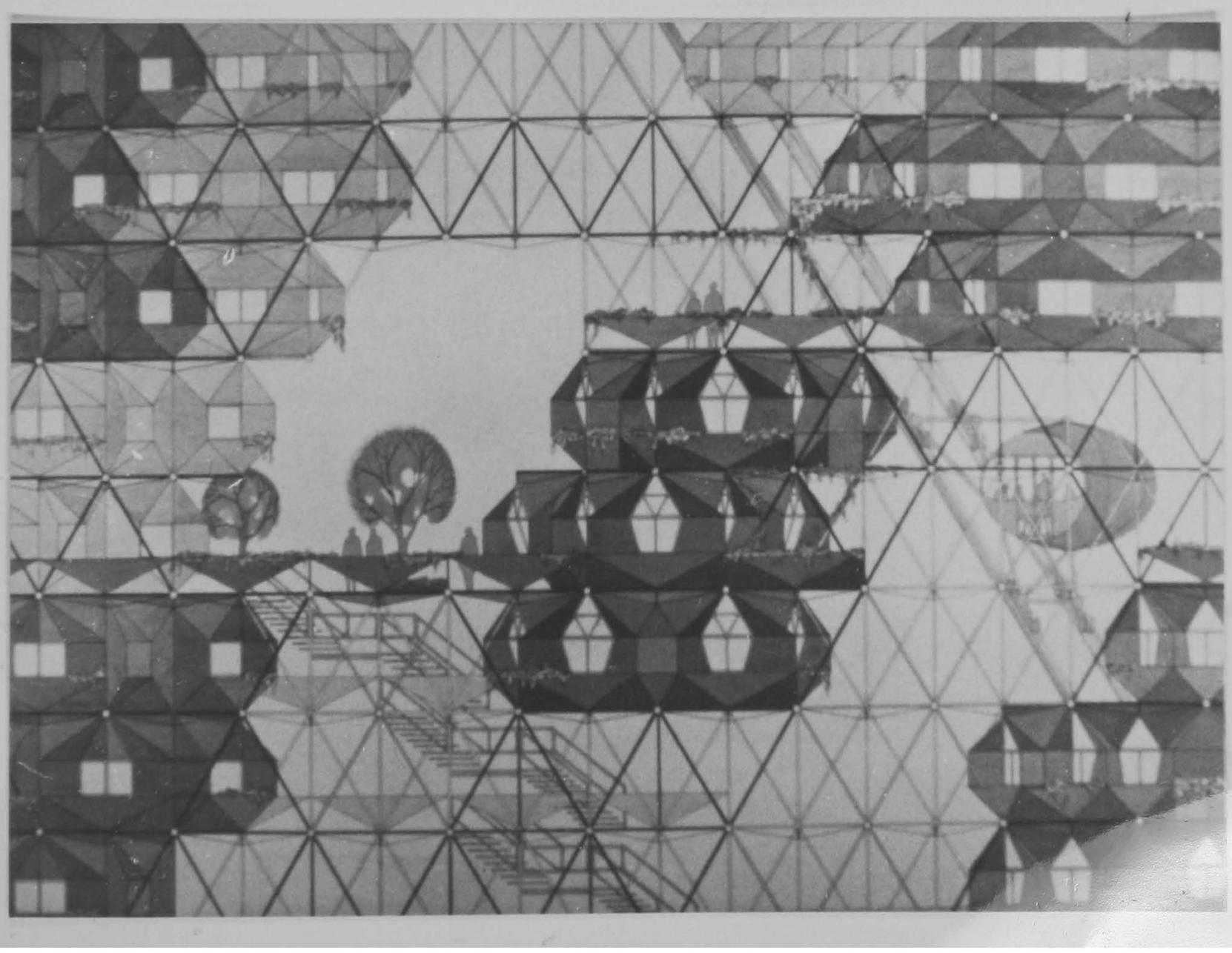


Figure 10

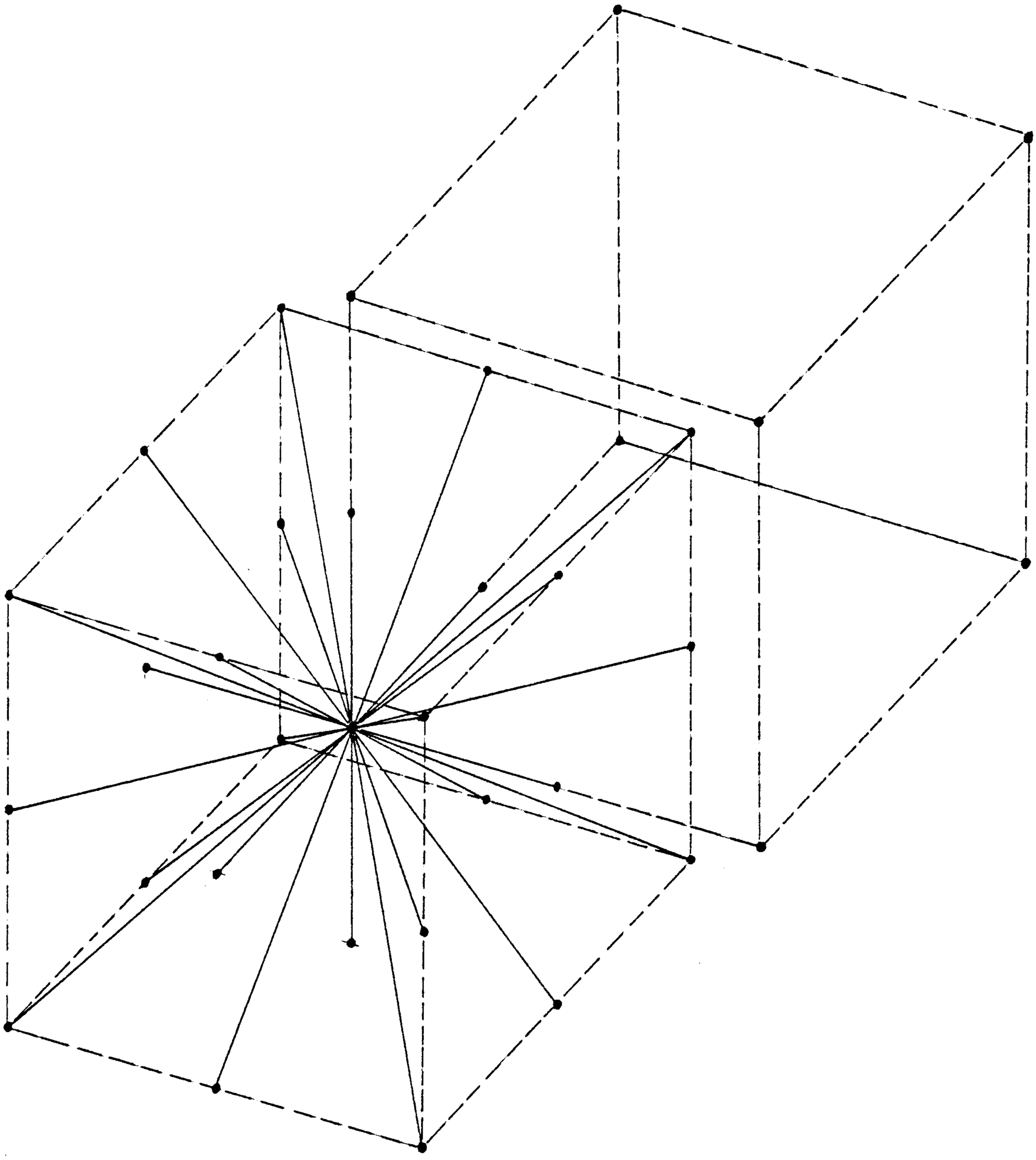


Figure 11 *26 Way Space Node Connector used for the design in figure 8.*

The modular grid is based on a set of interlacing cubes; the most dense arrangement of members being obtained with fully connected nodes at each corner and centroid. In practical applications the nodes would be comparatively sparsely connected, but the system allows considerable freedom of

provided the panel or "boxed-shell" system for the design of functional spaces is based on the same modular grid as a space structure imagined to fill the entire domain enveloping the functional design and potential support points, considerable freedom of spatial planning and design is allowed. The potential structure may be partially incorporated within the functional spaces or entirely precluded from these and perhaps other regions required for early expansion or adaptation. The abstract specification for the structural design, as opposed to subsequent analytical performance checks, is thus merely a permissible external domain, feasible support points, and partially or fully precluded internal regions. The loading may only be estimated as a maximum bound to internal loads allowing for functional adaptation, together with a set of maximum external load variations. Limits would be placed on maximum deflections (both in a general sense and at particular points), permissible stresses, and maximum and minimum member sizes of a discrete set.

The application, in an automatic mode, of the form-finding procedure previously given, would be wholly inappropriate for the problem set. To allow for functional adaptation and bridging action in the event of local catastrophe, the structural system should be highly redundant, yet the previous procedure, excluding the possible contribution of panel elements, yields a statically determinate form with member areas subsequently sized to comply with the stress limits. One feature of the process, however, is the gradual approach to the optimum, with sectional areas of the least effective members being most rapidly reduced

whilst the remainder are amended more gradually. Throughout the intermediate stages a graded preference of members, in hyperstatic layouts,is indicated. This suggests a policy for interactive design.

If the form-finding process is terminated at a statically indeterminate stage it is preferable that the continuous sizing of member areas should, at each stage, account for the differing stress limits for tensile and compressive members in order that areas may tend to bear correct ratios complying with real strains. It is also preferable that some control may be exerted, in a general sense, on the magnitude of deflections.

Referring to the Michell proof, if in addition to the general virtual deformation with strain limits of $\pm\varepsilon$ a uniform virtual dilation is superposed, equation (5) becomes:

$$\delta W = \sum e.LF + C \qquad (11)$$

where, from equations (1) and (2), C is identical for all of the candidate structures. The limits of virtual strain may thus alternatively be $+\varepsilon^{+}$ and $-\varepsilon^{-}$ where $\varepsilon^{+} \neq \varepsilon^{-}$. Consequently, as a corollary to the optimal condition (2) (P.259), the virtual strain system may be regarded as identical with the actual strains (P/E and Q/E) when a minimum weight design is achieved. The elastic modulus, E, is in this case the real value, and the relation for modifying member areas (Eq. 10) becomes:

$$(A)_{C+1} = \frac{(A)_C}{2}\left[1 + K.\frac{|e_c|}{|\varepsilon_c|}\right] \qquad (12)$$

where, if the control member is a tensile bar, k = 1 for tension members, but for compression members K = Q/P.

The above modified criteria give an optimum solution only at convergence of the form-finding process, yet the design will be fixed before this determinate stage is reached. The salient factor, however, is that the process now tends at each stage towards this solution with approximately correct ratios of member areas and, though terminated to give a hyperstatic form, should yield an efficient structure. In keeping with this practical approximation, and to increase computational efficiency, it is appropriate to delete bars during the process when it becomes clear that they are of low structural efficiency. Architecturally, the decision on which bars to delete will depend also on considerations of symmetry and possible amendments to the functional design. The form-finding process should thus ideally be used in an interactive mode to indicate a preferred structural policy which may only be partially followed, and the course of which might be constantly amended by ideas concerning the functional design.

Use of the real elastic modulus enables an estimate and control of service deflections to be obtained during form-finding. If deflections are tending, in a general sense, to be too high, the loads may be proportionally increased until the sum of products of these increased fictitious loads and the required deflections is equal to the sum of products of the real loads and deflections caused by the fictitious loads. The modified areas will then tend to the required deflection constrained design values. If particular deflections are to be constrained additional fictitious loads may be applied at the relevant points, but this device may then yield only a qualitative guide.

At an advanced stage in the process, potential members might be classified in three groups:

a) Bars which evidently play an important role and have areas (and forces) which are stable, increasing or decreasing slowly.

b) Bars which have currently significant, but reducing, forces.

c) Bars which have almost zero forces (or which have already been deleted).

At this stage all of bars (c) might be deleted, with the areas of bars (a) subsequently held constant. Bars of type (b), which form a large group, must then be selected for deletion or inclusion in the final design. Assuming a wide choice remains after a partial selection on the basis of functional design, a final choice might be made by considering the effects of external load variations. By noting which of the variable members increase in area as each load is applied, an indication may be obtained of which members should preferably be retained.

CONCLUSION

It is evident from the foregoing discussion that coincidence of form-finding and preliminary analysis, accounting for deflections and variations in loading, might only be achieved when the dynamic relaxation process is used in a fully interactive mode. The main

purpose of the process is to enable selection of an efficient structural form from a large set of possibilities within an amorphous boundary, and the distribution of member areas obtained provides only a crude estimate of design values. To account for more precise deflection constraints and loading conditions, final sizing of members might be achieved using a fully stressed design or analogous optimality criteria approach; with subsequent detailed analyses being required to check stability, dynamic response and the effects of local failures. And these detailed analyses would be required for each functional state.

The problem of form-finding of large space structures which allow for adaptable internal use and possible structural modification and extension does not lend itself to precise mathematical optimization. Specific loading cases cannot be defined and, at best, only maximum general bounds can be specified. The proposed procedure may, however, enable an efficient and rational approach to the design of such structures whilst allowing architectural freedom.

An extended investigation of form-finding and member sizing of modular space systems subject to variable loading is being carried out by Topping (197). Solutions will be compared with those obtained by fully stressed design methods and linear and non-linear programming.

REFERENCES

(1) Maxwell, J.C., 'Scientific Papers', Vol.2, p.175, 1869.

(2) Michell, A.G.M., 'The limits of economy of material in framed structures', Phil. Mag. Series 6, 8, 589-597, 1904.

(3) Hemp, W., 'Theory of structural design', Report 214, AGARD, Oct. 1958.

(4) Cox, H., 'The design of structures of least weight', Pergamon, Oxford, 1965.

(5) Richards, D.M., Chan, H.S.Y., 'Developments in the theory of Michell optimum structures', AGARD report 543, April 1966.

(6) Parkes, E.W., 'Braced frameworks', Commonwealth and Int. Library, 1965.

(7) Hemp, W.S., 'Studies in the theory of Michell structures', Int. Congress of Applied Mechanics, Munich, 1964.

(8) Livesley, R.H., 'The automatic design of structural frames', Quart. J. Mech. Appl. Math., 9, Part 3, 1956.

(9) Schmit, L, 'Structural design by systematic synthesis', Proc. of ASCE 2nd Conf. on Electronic Computation, Pittsburgh, Pa., 1960

(10) Dorn, W.S., Gomory, R.E., Greenberg, H.J., 'Automatic design of optimal structures', J. de Mechanique, Vol. 3 N.I., Mars 1964.

(11) Dobbs, M.W., Felton, L.P., "Optimization of truss geometry", Proc. ASCE, J. Struct. Div., ST 10, Oct. 1969.

(12) Majid, K.I., Elliott, D.W.C., "Topological design of pin-jointed structures by non-linear programming", Proc. I.C.E., V. 55 pp. 129-149, March 1973.

(13) Porter-Goff, R.F.D., 'Decision theory and the shape of structures', J.R. Aeronaut. Soc., 70(Mar.) 448-452, 1966.

(14) Palmer, A.C., 'Optimum structure design by dynamic programming', J. Struct. Div. ASCE, ST8 (Aug) 1887-1906, 1968.

(15) Templeman, A.B., 'Structural design for minimum cost using the method of geometric programming', Paper No. 7295, Proc. I.C.E., 1970.

(16) Gallagher, R.H., Zienkiewicz O.C. (editors), 'Optimum structural design - theory and applications', J.Wiley, London, 1973.

(17) Schmidt, L.C., 'Fully stressed design of elastic redundant trusses under alternative loading systems', Australian J. of Appl. Sc., 9, 337-348, 1958.

(18) Melosh, R.J., 'Structural analysis, frailty evaluation and design Vol. 1. safer theoretical basis', AFFDL TR 70-15, Vol.1, July, 1970.

(19) Patnaik, S., Dayaratnam, P., 'Behaviour and design of pin-connected structures', Int. J. Num. Methods Engrg., 2, 577-595, 1970.

(20) Razani, R., 'The behaviour of the fully-stressed design of structures and its relationship to a minimum weight design', AIAA J., e, Dec. 2262-2268, 1965.

(21) Barnett, R.L., Herrmann, P.C., "High perforance structures", NASA CR-1038, May 1968.

(22) Prager, W. 'Conditions for structural optimality', Computers and Structures, Vol. 2, pp 833-340, 1972

(23) Gellatly, R.A., Berke, L., 'Optimality-criterion-based Algorithms', Int. symposium on Optimization of Structural Design, Swansea, Jan. 1972 (see ref. 16).

(24) Barnes, M.R., 'Dynamic relaxation analysis of cable networks', Int. Conf. on Tension Structures, London, April 1974. [Chapter 2]

(25) Barnes, M.R., 'Applications of dynamic relaxation to the topological design and analysis of cable, membrane and pneumatic structures', 2nd Int. Conf. on Space Structures, Surrey, Sept. 1975. [Chapter 3.]

(26) Barnes, M.R. 'Interactive graphical design of tension surface structures', Int. Symposium on Wide-Span Surface Structures, Stuttgart, April, 1976. [Chapter 7.]

(27) Gabriel, J.F., 'Living in a space frame', 2nd Int. Conf. on Space Structures, Surrey, Sept. 1975.

(28) Pearce, P., 'A minimum inventory/maximum diversity building system', 2nd Int. Conf. on Space Structures, Surrey, Sept. 1975.

CHAPTER 9

CONCLUSIONS

A summary is given of the main advantages of dynamic relaxation for the design of tension structures, based principally on the concluding remarks of the papers forming this thesis. Particular emphasis is placed on the value of the method as a basis for interactive design, and lines of current research are indicated.

The conceptual design of tension surface structures is frequently based on physical modelling techniques using shear free fabric membranes. This allows a close collaboration between Architects and Engineers at the formative design stage, since alteration of support points and surface and edge curvatures can be carried out with the model providing a visual and tactile means for communicating ideas between the different members of the design team. Following photogrammetric measurements of fabric models, numerical analyses are normally carried out in three distinct stages using separate suites of programs for form-finding (and the determination of cutting and jointing patterns), static analysis, and dynamic analysis. The first of these has traditionally been the most difficult owing to gross changes in shape from the approximate measurements, the need to incorporate practical constraints on tensions and mesh lengths, and the occurrence of zero stiffness situations during the form-finding analysis (Appendix B).

A major advantage of the dynamic relaxation/central difference integration process is that it provides a unified method for all stages of design and analysis. Coupled with the small computer storage requirements this makes the process ideal as a computational basis for interactive design, enabling both rapid initial checks and accurate final analyses. Trial forms might be searched with alterations being made to boundary conditions, tension distributions and surface curvatures, and the same program used to check the effects of various static and dynamic loadings; forms being subsequently amended if necessary. Whilst at the present time available interactive facilities

would limit the process to comparatively small structures, the projected development of such facilities makes likely their greater use for complex design problems. This does not imply the demise of approximate physical modelling techniques, but rather that the two may be run in parallel. The physical model enables an aesthetic appreciation of the design and provides a means of specifiying a topology from which analysis may commence. The dynamic relaxation process, however, because it copes naturally with the occurrence of zero stiffness situations, is not subject to the possibility of ill-conditioning and thus requires less accurate model measurements than might otherwise be the case. The dynamic trace itself is also of value in providing a visual understanding of behaviour. Thus the examination of trends in the development of stresses and deformations can provide an early signal for necessary design changes without the need to obtain fully converged solutions. Furthermore the analytical process enables investigation of designs which may be difficult to model or check with alternative analyses, such as the support of networks on momentless compression arches, or the simulation of neutrally stable states such as impending collapse of membrane surfaces due to inadequate prestress or distribution of support loads into the membrane (chapters 4 and 7).

The explicit nature of the DR analysis, with equilibrium and compatibility conditions effectively separated, yields a number of advantages, compared with implicit matrix methods, in addition to those referred to above concerning storage and solution stability. In form-finding of network or funicular mesh systems, alteration of the

topology, with the introduction or deletion of nodes and links, is often necessary in the vicinity of boundaries as edge curves are amended during the form-finding process. Similarly, refinement of the mesh in these areas may be necessary to obtain sufficiently accurate results. The explicit formulation of the DR process makes this possible, and thus allows less accurate initial geometric and topological data from physical models. Alternatively it enables a true search of possible forms and topologies which is not permitted by other methods without re-setting the analytical problem (Appendix B). In relation to such alterations of topology the "kinetic" damping process referred to in Appendices D and D.1 is valuable since it enables sudden localized changes to be made during the analysis without propogating radical disturbances through the system as a whole. The process provides an automatic means of optimizing the DR analysis when used with mass components adjusted to give identical critical time intervals for each degree of freedom. In certain situations, with complex support conditions to networks or funicular grids in which additional links may be inserted to give local triangulation, it is possible that non-unique solutions may be obtained with compression in some links due to incorrect initial assumptions concerning unstressed lengths (Appendix D.1). Dynamic relaxation yields such solutions without the occurrence of singularity in the system of equations and modifications, if required, can also be made without fully re-setting the analysis.

For static analyses of path dependent problems involving both material and geometric non-linearities incremental loading techniques are necessary for all types of analysis (Appendix A). With suitably

high damping, however, a DR analysis might permit much larger load increments since the process itself ensures gradual transmission of the loads to the structure. In cases where the only source of material non-linearity is cable slackening or membrane buckling, it is certainly possible to apply the full load from the start provided that elastic properties are checked and re-set at sufficiently frequent intervals (chapter 3). For dynamic analyses the explicit formulation is again of value for dealing with on/off buckling (Appendix 3.2) and the effects of visco-elastic material damping and pneumatic stiffening and damping (Chapters 5 and 6). In each of these cases the use of implicit dynamic analyses would be considerably less efficient; and it is possible that the advantage which such methods have for problems with smaller non-linearities, namely the use of a larger time interval and the filtering out of high frequency response components, would be negated if, in applying explicit central difference integration, fictitious mass components were used for non-dominant degrees of freedom (appendix C).

The majority of applications of DR in this thesis have concerned structural mechanisms for which the pretension (and dead load) forces are in funicular equilibrium. The pretensioning in effect imposes a dominant internal force distribution to ensure stability under live load variations and the resulting forms express a natural aesthetic and reflect clearly their structural function. For triangulated space structures, however, the determination of shape and the satisfaction of engineering design requirements are not so closely coupled; their forms not being dependent on initially imposed force distributions. Computer aided design of such systems has therefore traditionally relied on mathematical programming techniques for minimizing weight (or cost) by

adjusting member areas for a given geometry. Alternatively, if the geometry and topology are allowed to vary, the use of such automatic techniques may place severe constraints on freedom of architectural design and, for multiple loading and deflection constraints, may result in irregular structures. In contrast, the approach using dynamic relaxation outlined in chapter 8 yields a structural policy with a graded preference of members for a dominant design loading and variations from this load. The preferred policy may change continuously with alterations in functional design, space constraints and support conditions, and this allows potentially much greater freedom for architectural design of modular systems when used in an interactive mode.

The contrast made above, between fully automatic minimization methods and a method which allows functional and intuitive design decisions to be made, investigated and changed during the process, has a parallel also in the opposing approaches to the design of tension structures. On the one hand the Architect may specify a preferred structural shape following the completion of model studies, and the structural analyst may then use an optimization method (appendix B, P. 337) to fit that shape whilst attempting to comply with bounds on constructional and equilibrium constraints. Thereafter the design is checked by a series of separate analyses and the process repeated if necessary. Interactive methods, however, allow a direct approach to shape fitting complying with engineering needs which may change as the design progresses (P. 343) or, alternatively, a continuous search for the design yielding analytical checks and conceptual ideas to the designer. Whilst this is not necessarily dependent on a specific type of analysis, dynamic relaxation does provide a physically ideal and economic basis for such a process.

APPENDIX A

REVIEW OF METHODS FOR THE STATIC ANALYSIS OF TENSION STRUCTURES

The principal methods for discrete non-linear analysis of tension structures are reviewed in the following classifications:

A. IMPLICIT ANALYSES

(1) Iterative Methods: Newton-Raphson (Tangent stiffness); Modified Newton-Raphson; Secant stiffness; Accelerated constant stiffness iteration

(2) Incremental methods: Euler; Mid-point slope; Extrapolation; Self-correcting methods

B. EXPLICIT ANALYSES

(1) Minimization methods: Steepest descent; Relaxed steepest descent; Conjugate gradient method; Scaled conjugate gradients

(2) Relaxation methods: Point-Jacobi; Gauss-Seidel; SOR; DR - (see also Appendix D)

Continuum Analysis of Tension Systems

The development of methods of analysis for tension structures began in about 1960 (11, 165). Much of the early work was based on approximating cable structures as continuous membranes without shear rigidity. Schleyer (166) derived non-linear integro-differential equations for the static analysis of nets whose sets of cables projected as straight lines on a plane, and for analysis of counterstressed double layer systems under two dimensional loading assuming the spreaders formed a continuous inextensible diaphragm. In both cases the equations were transformed into finite difference equations for iterative solution. Mollmann (123) further developed the continuous approach, and also derived Levy type analytical solutions for hypar networks which provided simple approximate formula for special cases of static loading (125). The shear-free membrane approach has also been applied to form-finding (86, 123), linearized free vibration analysis (125,168), and non-linear dynamic analysis (160).

The main advantage of analytical solutions lies in providing simple approximate analyses for preliminary design. Analyses of tension structures as discrete systems have, however, generally been preferred since they are more suited to automatic computation for all types of nets and boundary conditions with non-linear effects fully accounted for. For this reason, only the commonly used discrete methods are considered in the following review.

Discrete Analysis

The majority of published methods for the discrete non-linear static analysis of tension structures can be classified into three principal groups:

(1) Iterative methods

(2) Incremental methods

(3) Minimization methods

The first two groups have been most widely applied as implicit methods using matrix formulations for the overall stiffness (or tangent stiffness) of the structure. Minimization methods, however, are usually formulated as direct or explicit methods in which corrected displacements are computed using the previous displacement vector and the gradient of this vector. Since the gradient vector is derived by means other than inversion or reduction of an overall stiffness matrix, the storage requirements are considerably less than for the implicit methods. The classical point methods of iteration form a further class of explicit methods but have rarely been applied to tension systems; possibly because they may be less stable than implicit iterative methods when large deformations are involved.

For the analysis of tension systems involving, or assumed to involve, only geometric non-inearity, any of the methods listed will yield a unique solution provided that all members remain in tension (39, 123). The first two methods additionally require either that the stiffness matrix does not become singular or that proper controls are applied to limit the deflections in any

increment or iterative step (78). For systems involving both geometric and material non-linearities, however, the problem becomes path dependent and an incremental method, or a combination of incremental and iterative or minimization methods, must be applied to ensure convergence to a unique solution (29).

The following text reviews the available methods after a simplified consideration of the tangent stiffness properties for individual elements. This is given only for cable links but the concepts apply equally to membrane elements; the purpose being to illustrate the component parts of the large displacement tangent stiffness and the difference between small strain and large strain formulations. The review given here is restricted mainly to published analyses for tension systems, although parallel developments have taken place in the more general field of non-linear finite element analysis, of which some of the more important review contributions are noted in Appendix E.

Element Tangent Stiffness Relations

Consider the two bar symmetrical system shown in figure 1:

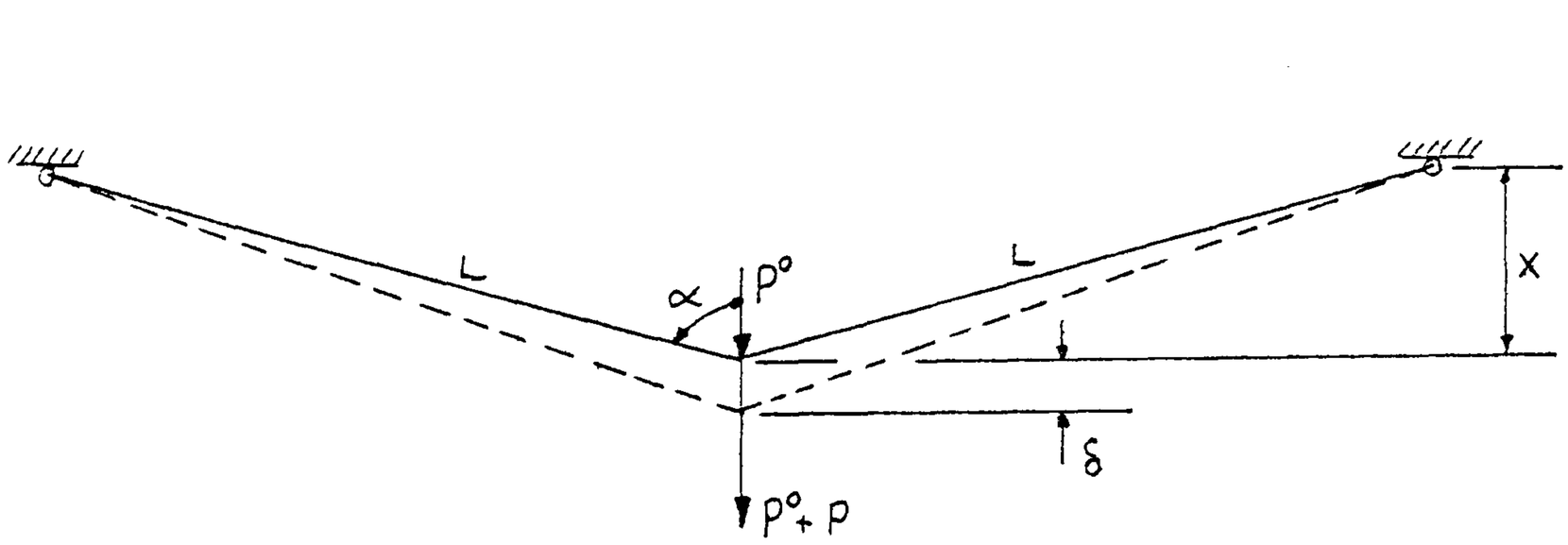


Figure 1

In the initial state the tension in the members is T due to the action of loads P°, and for equilibrium:

$$\frac{P^\circ}{X} = \frac{2T}{L} \qquad \text{or} \qquad P^\circ = 2T \cos\alpha \tag{1}$$

An additional load P causes a deflection δ and an increase in tension $\Delta T = \delta.\cos\alpha.EA/L_o$, where L_o is the slack length of the links. Assuming small strain linear elastic behaviour with δ negligible compared with X, then for equilibrium:

$$\frac{P^\circ + P}{X} = 2\left(\frac{T + \Delta T}{L}\right) = \frac{2}{L}\left[T + \frac{EA}{L_o}.\delta \cos\alpha\right] \tag{2}$$

Subtracting (1) from (2):

$$P = 2.\delta\left[\frac{EA}{L_o}\cos^2\alpha\right]$$

The term in square brackets is the direct vertical component of linear elastic stiffness for each member.

If changes in the geometry of the system and large strains are accounted for, the equilibrium condition is:

$$\left(\frac{P^\circ + P}{X + \delta}\right) = 2\left(\frac{T + \Delta T}{L + e}\right) \quad \text{where } e = \text{link extension} \tag{3}$$

Expanding, and subtracting (1) gives:

$$P(L + e) = 2T.\delta - P^\circ.e + \frac{2EA}{L_o}.\delta \cos\alpha\,(X + \delta)$$

Substituting $P^\circ.e = 2T\,\delta\cos^2\alpha$ and neglecting terms in δ^2:

$$P(L + e) = 2\delta\left[T(1-\cos^2\alpha) + \frac{EA.}{L_o} X\cos\alpha\right]$$

Neglecting now the term P.e, the stiffness relations are obtained as:

$$P = 2.\delta\left[\frac{EA}{L_o}\,\mathrm{Cos}^2\alpha + \frac{T}{L}\,(1-\mathrm{Cos}^2\alpha)\right] \qquad (4)$$

The vertical stiffness component is here composed of two parts: the elastic stiffness, and the "geometric" stiffness $T(1-\mathrm{Cos}^2\alpha)/L$, where L is the member length in the initial prestress condition or, when considering incremental loading and tangent stiffnesses, the length in the previous displaced state; $\mathrm{Cos}\,\alpha$ also being referred to this state.

If the term $P^{\circ}.e$ is also considered negligible (or alternatively e in equation (3) is neglected), the "small strain" stiffness relations become:

$$P = 2\delta\left[\frac{EA}{L_o}\,\mathrm{Cos}^2\alpha + \frac{T}{L}\right] \qquad (5)$$

It can be seen from the above formulations that when P is small compared with P°, for example when using an incremental solution method or Newton-Raphson iteration (21), equation (4) caters for the development of large strains and displacements more effectively than (5).

Generalizing equation (4) to three dimensions, the stiffness relations for an individual member take the form:

$$\{P\} = [K]\{\delta\} = ([K_E] + [K_G])\{\delta\}$$

where $\{P\}$ is a vector of six nodal forces and $\{\delta\}$ the corresponding vector of translational displacements in the x, y and z directions at both end nodes. The elastic and geometric stiffnesses take the form:

$$[K_E] = \begin{bmatrix} k'_E & -k'_E \\ -k'_E & k'_E \end{bmatrix} \qquad [K_G] = \begin{bmatrix} k'_G & -k'_G \\ -k'_G & k'_G \end{bmatrix}$$

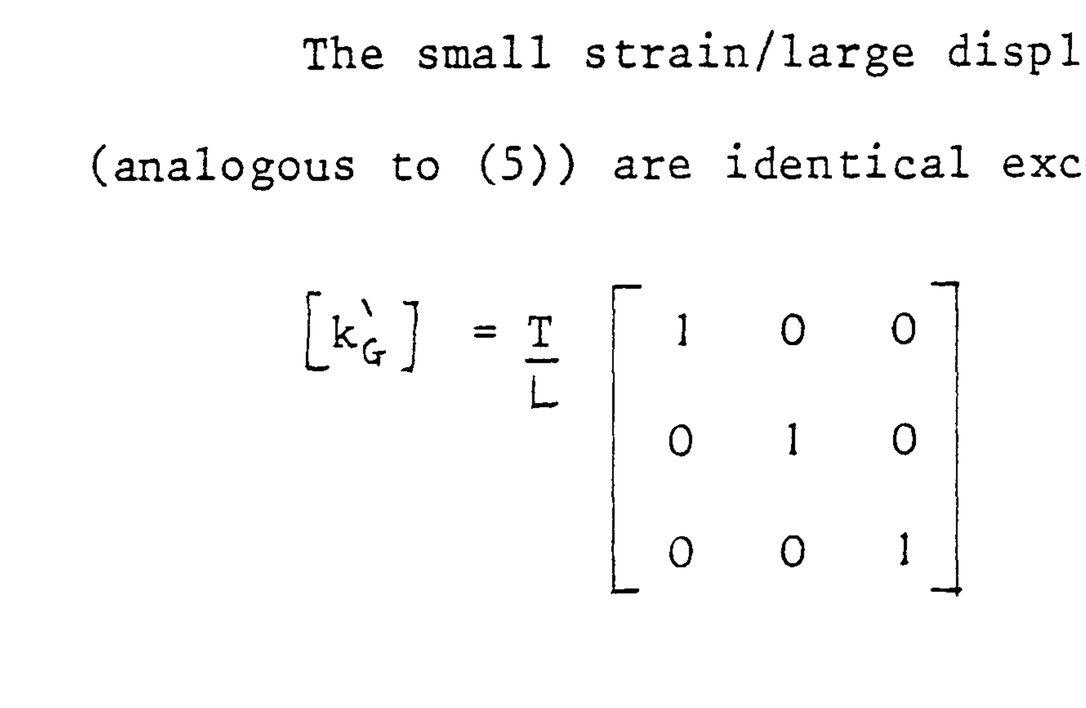
where $[k'_E] = \frac{EA}{L_o} \begin{bmatrix} \ell^2 & \ell m & \ell n \\ \ell m & m^2 & mn \\ \ell n & mn & n^2 \end{bmatrix}$ (6a) and $[k'_G] = \frac{T}{L} \begin{bmatrix} (1-\ell^2) & -\ell m & -\ell n \\ -\ell m & (1-m^2) & -mn \\ -\ell n & -mn & (1-n^2) \end{bmatrix}$ (6b)

ℓ, m and n being the direction cosines of the member w.r.t. the x, y and z global axes.

The small strain/large displacement stiffness relations (analogous to (5)) are identical except that k'_G takes the form:

$$[k'_G] = \frac{T}{L} \begin{bmatrix} 1 & 0 & 0 \\ 0 & 1 & 0 \\ 0 & 0 & 1 \end{bmatrix} \qquad (7)$$

Summation Form of Equilibrium Equations



notation:

δ_i ~displacement in x_i direction

i,j~subscripts for 3 co-od. axes

$\sum_m$ ~sum for all members m joining a to adjacent nodes b

In the initial state of the prestressed assembly, the condition of equilibrium at any joint, a, in the x_i direction is:

$$\sum_m (T.\frac{DX_i}{L_m})_m = P_i^\circ \qquad (8)$$

where T_m, L_m are the tension and length of member m joining node a to adjacent node b in the prestressed state, and $DX_{im} = (X_{ia} - X_{ib})$, the difference in co-ordinates in the x_i direction.

Under additional loading, P_i, the equilibrium condition becomes:

$$\sum_m \left\{(T + \Delta T)\frac{(DX_i + D\delta_i)}{(L + e)}\right\}_m = P_i^\circ + P_i = P_{Ti} \qquad (9)$$

where $D\delta_{im} = (\delta_{ia} - \delta_{ib})$

$(L + e)_m^2 = \sum_{i=1,3} (DX_i + D\delta_i)_m^2$ Expanding this, subtracting $L_m^2 = \sum_i DX_{im}^2$, and neglecting second order terms:

$$e_m = \sum_i (D\delta_i . \frac{DX_i}{L})_m \qquad (10a)$$

$$\Delta T_m = (\frac{EA}{L_o})_m \sum_i (D\delta_i . \frac{DX_i}{L})_m \qquad (10b)$$

The new direction cosine term in equation (9) can be approximated in the following way:

$$\left[\frac{DX_i + D\delta_i}{L + e}\right]_m = \left[\frac{DX_i/L + D\delta_i/L}{1 + e/L}\right]_m \simeq \left(\frac{DX_i}{L} + \frac{D\delta_i}{L} - \frac{DX_i}{L}.\frac{e}{L}\right)_m$$

Substituting in (9), subtracting (8), and neglecting second order terms:

$$\sum_m \left\{ \Delta T . \frac{DX_i}{L} + T\left(\frac{D\delta_i}{L} - \frac{DX_i}{L} . \frac{e}{L} \right) \right\}_m = P_i$$

Substituting for ΔT and ΔL from equations (10):

$$\sum_m \left\{ \frac{EA}{L} . \frac{DX_i}{L} \sum_j \left(D\delta_j . \frac{DX_j}{L} \right) + \frac{T}{L} \left[D\delta_i - \frac{DX_i}{L} \sum_j (D\delta_j . \frac{DX_j}{L}) \right] \right\}_m = P_i \quad (11)$$

In matrix form, for all joints and all directions:

$$\left[K_o \right] \left\{ \delta \right\} = \left\{ P \right\} \quad (12)$$

where $\left[K_o \right]$ is the overall stiffness matrix and terms T, DX and L in $\left[K_o \right]$ are referred to the prestress state.

Or for incremental loading:

$$\left[K_T \right] \left\{ \Delta\delta \right\} = \left\{ \Delta P \right\} \quad (13)$$

where $\left[K_T \right]$ is the tangent stiffness and T, DX and L terms in $\left[K_T \right]$ are referred to the previous displaced state.

The equilibrium conditions given in equation (11), corresponding with the stiffness relations given in (6a and b), were first derived by Siev (169). Turner et.al. (181) previously used a geometrically non-linear formulation for truss and triangular plane stress elements with geometric stiffness analogous to equation (7).

IMPLICIT ANALYSES

Iterative Methods of Analysis

The most widely used and stable iterative analysis for geometrically non-linear problems is the Newton-Raphson method, which has been applied to form-finding and static analysis of tension structures by Siev (169), Argyris (6), Knudson (95), Haug (78,79) and many other researchers (see notes in Appendix E). In the initial step of the process the full load is applied and displacements $\{\delta\}$ are calculated using equation (12). The out-of-balance or "residual" nodal forces in this displaced state are determined from equation (9) as:

$$R_i = P_{Ti} - \sum_m \left\{ (T+\Delta T) \left(\frac{DX_i + D\delta_i}{L + e} \right) \right\}_m \qquad (14)$$

Tangent stiffness relations are then reset using the displacements and tensions calculated in the initial step; and deflection increments resulting from the application of the residuals as load increments are determined using equation (13):

$$[K_T]\{\Delta\delta\} = \{R\} \qquad (15)$$

$$\text{new} \quad \{\delta\} = \{\delta\} + \{\Delta\delta\} \qquad (16)$$

The process is repeated using (14)→(16) until convergence is obtained. Diagramatically the procedure is illustrated in figures 3a and 3b respectively for a "stiffening" and "softening"

single degree of freedom system; the former being most representative of tension structures. Because of the poor conditioning of such structures, referred to in Chapter 1, a Gaussian elimination procedure should preferably be used in solving equations (15).

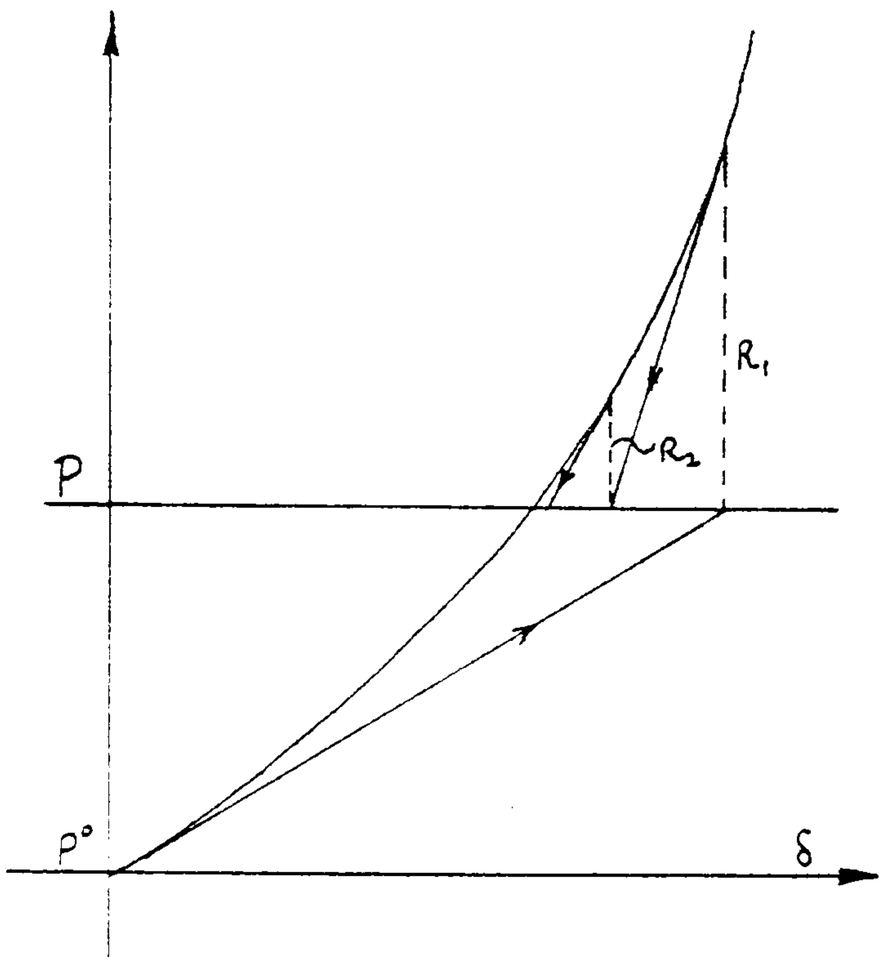


Figure 3a

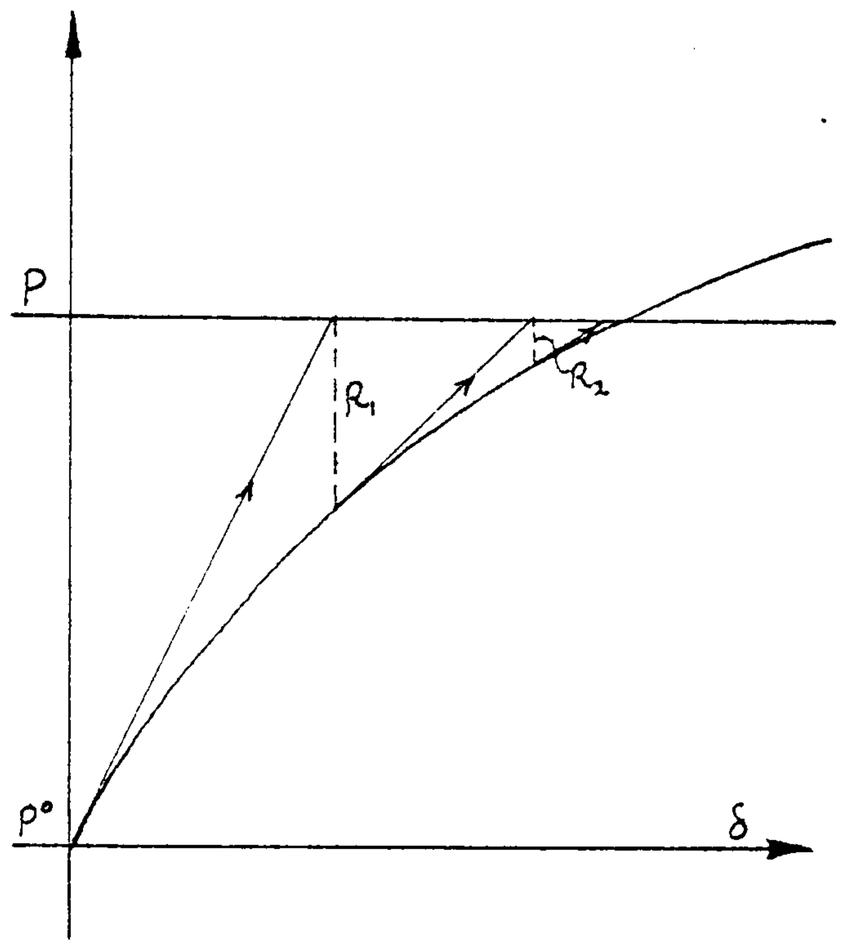


Figure 3b

A drawback of the Newton-Raphson method is that the tangent stiffness matrix has to be reset and solved at each stage. For this reason, when dealing with structures which are not highly non-linear a "Modified Newton-Raphson" method, in which the stiffness is held constant throughout, is generally more efficient (64,170). The degree of non-linearity of tension structural mechanisms is such that they will often fall outside the scope of this method; though Mollmann (124), Krishna (105) and others (21,65) have applied it with some

success by making adjustments either to the form of the initial geometric stiffness or to the residual load vector. And for triangulated systems it will usually be the method of choice. The process takes the same form as the Newton-Raphson method except that the initial stiffness is inverted and held constant throughout. Thus equation (15) becomes:

$$\{\Delta\delta\} = [K_o]^{-1} \cdot \{R\} \tag{17a}$$

Or, in total displacement form:

$$\{\delta\} = [K_o]^{-1} \cdot \{P + R\} \tag{17b}$$

The process (17a) for stiffening and softening systems is represented in figures 4a and 4b respectively. An alternative to using the initial value of the stiffness matrix throughout the process is to re-set it intervals with a number of constant stiffness iterations within each interval.

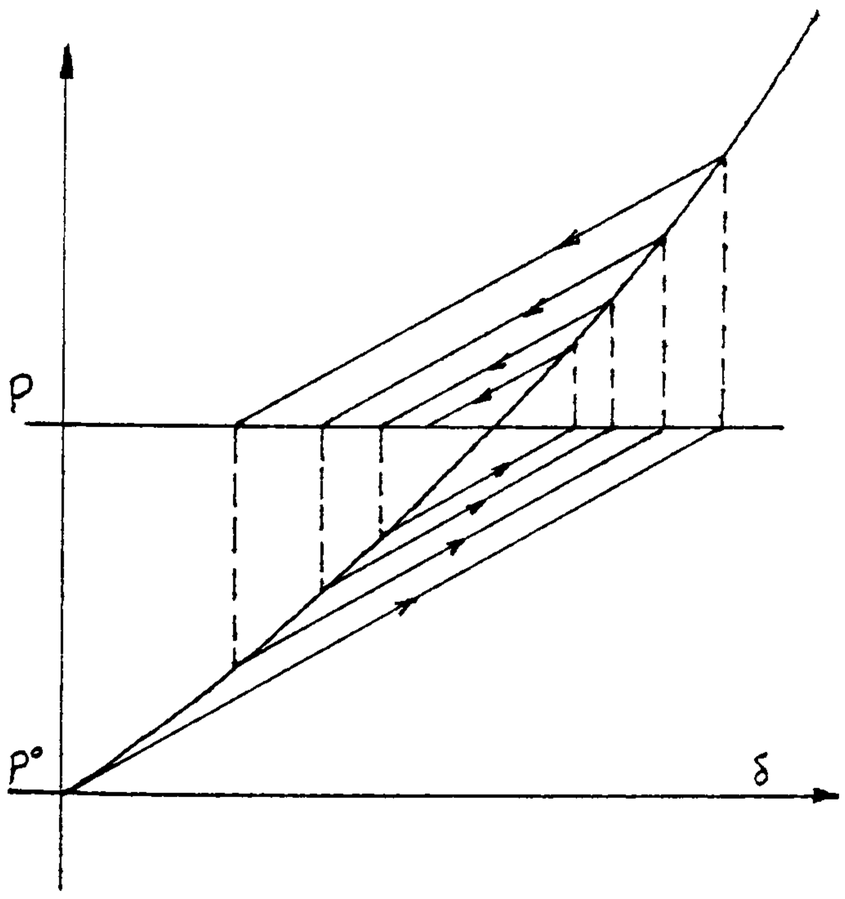


Figure 4a

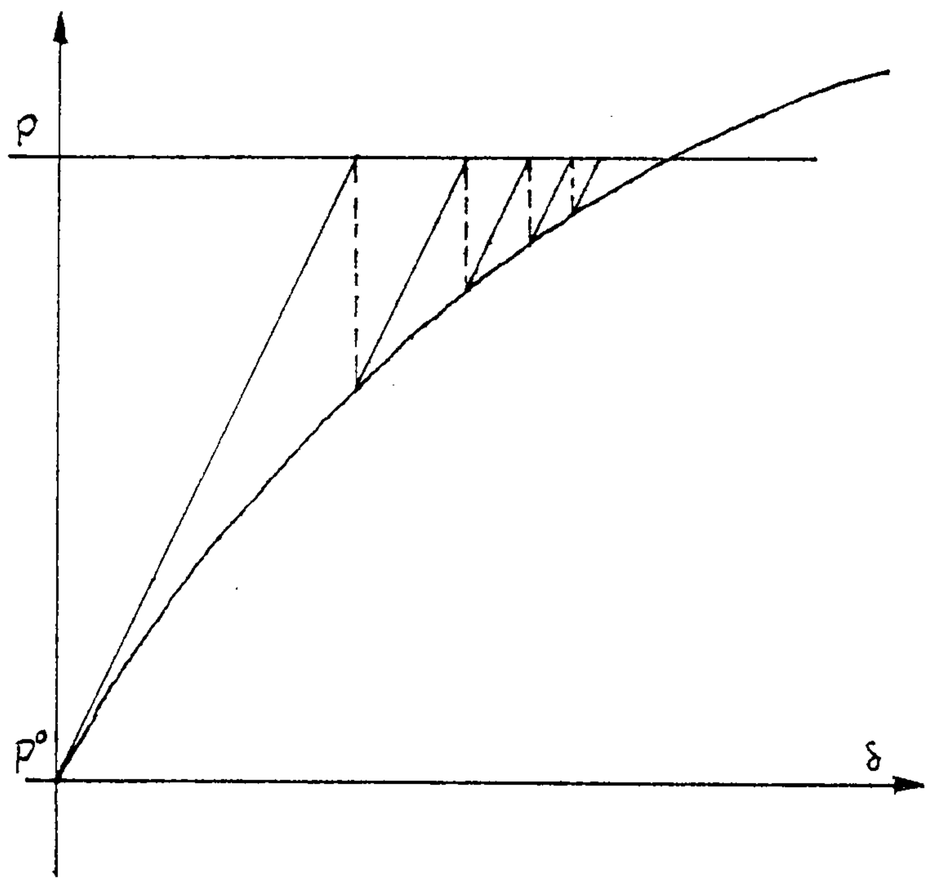


Figure 4b

It can be seen from figure 4b that for a geometrically softening system, such as an arch structure, the process should

always converge. And though convergence is less rapid than for the standard Newton-Raphson method, computationally the process may be more efficient provided the system is not grossly non-linear. For a stiffening system, however, if the initial out-of-balance is too large the analysis may diverge as shown in figure 5.

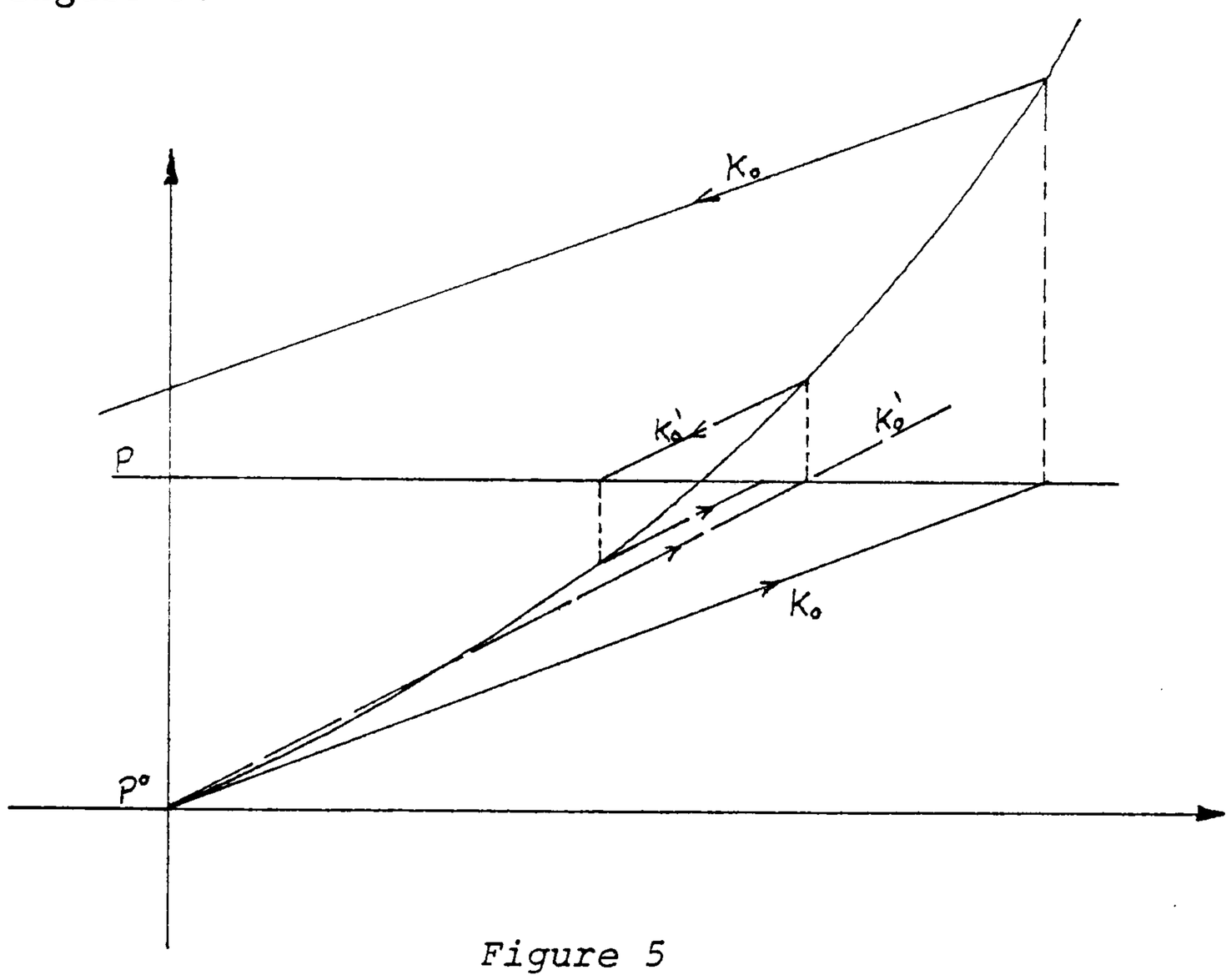


Figure 5

Mollmann and Mortensen (124) found that for prestressed networks the method converged for small applied loads but diverged when the loads were larger; and the latter generally occurred for loads below the normal design levels. To overcome this problem they suggested that, instead of using the pretension T^o to set the geometric stiffness (equation 6b or 11), the stiffness could be artificially increased by using a value of $T = T^o + \Delta T'$, where $\Delta T'$ is the estimated change in tension under the loading considered. In conjunction with an amended

expression for the residual forces, this was found to give convergence in the majority of cases for network problems.

In total displacement form, the Modified Newton-Raphson process is illustrated in figure 6, where $\overline{R}^i$ stands for the absolute value of the residual force at the ith iteration.

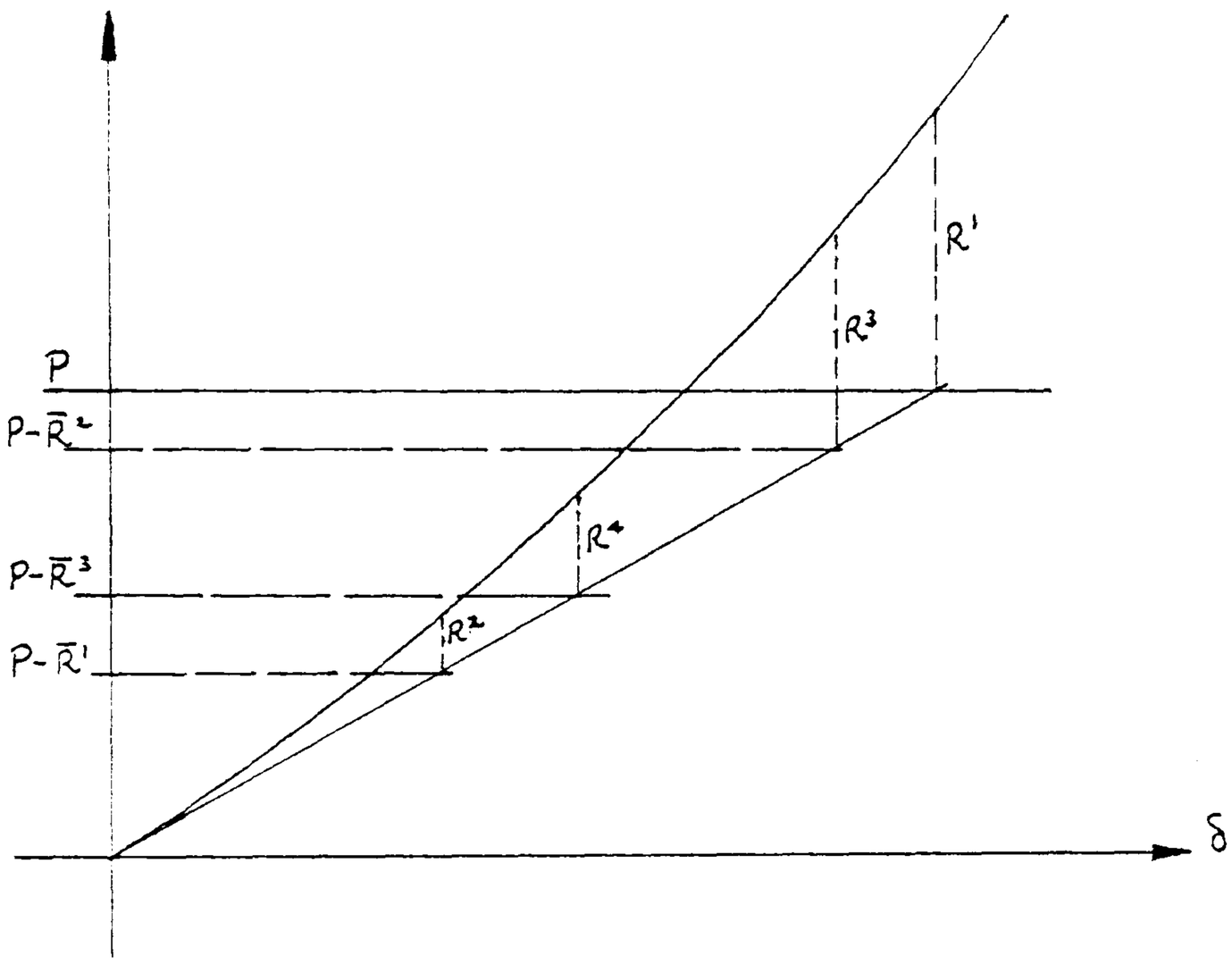


Figure 6

It can be seen that the value of R in successive iterations oscillates about the correct value. Krishna (105) found that very much more rapid convergence could be obtained by using the iteration formula:

$$\{\delta\}^{i+1} = [K_o]^{-1} \{ P + (R^i + R^{i-1})/2 \} \qquad (18)$$

The expression for modified residuals used by Mollmann and Mortensen was similar to the above except that only the third order components of the residuals were halved.

Another form of total displacement iterative procedure, applied to cable and truss structures by Baron and Venkatesan (21), is the Secant stiffness method (figure 7) in which the geometric stiffness is re-set in each iteration. Provided cable properties do not alter, the elastic component of the total stiffness is held constant, otherwise the process will diverge.

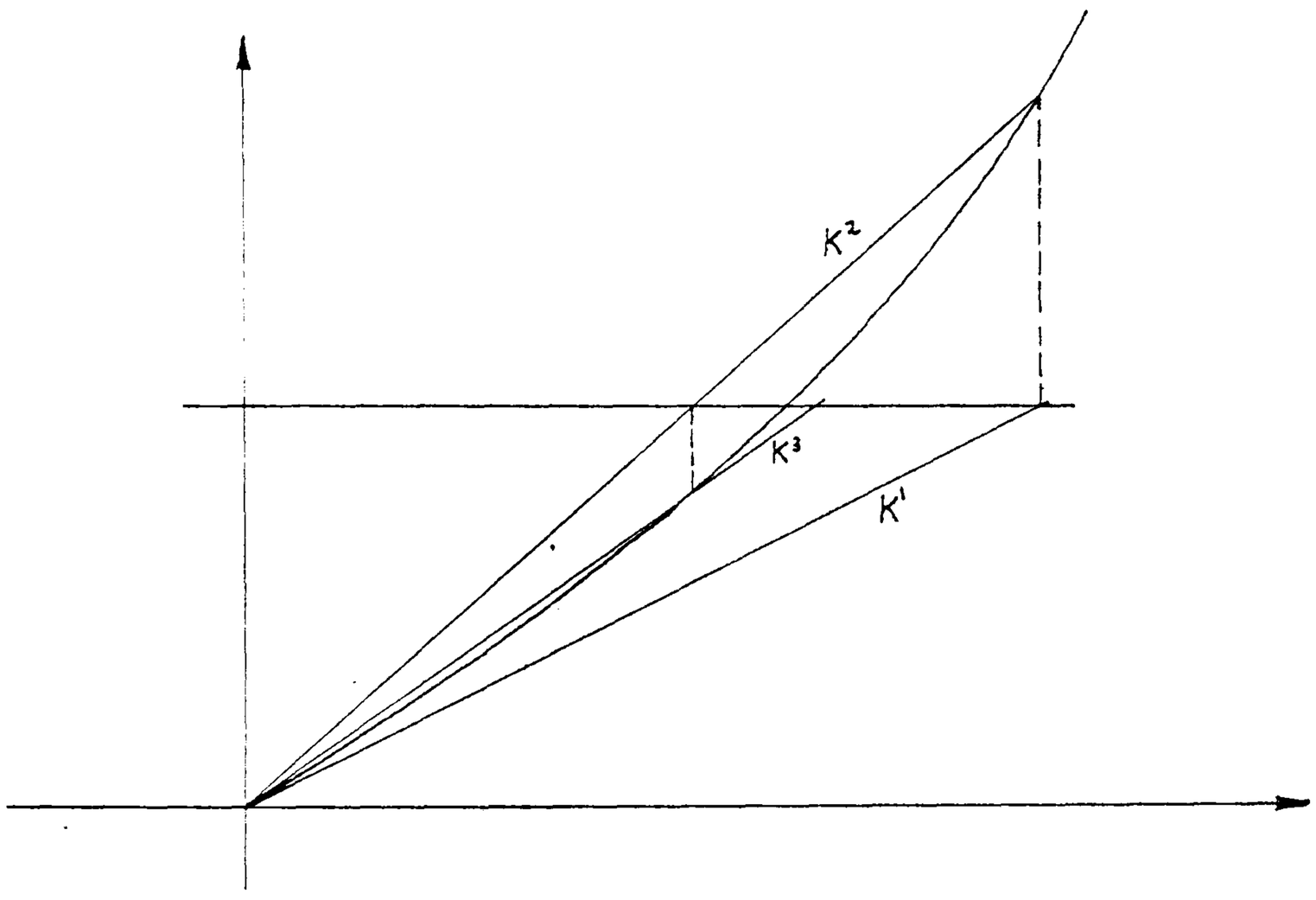


Figure 7

Whilst convergence is slower and computationally less efficient than for the Newton-Raphson process, the method has the advantage that, provided convergence is in fact obtained and the system is such that a unique solution exists, slackening of cable elements may be accounted for. It has been suggested by several authors that this may be accomplished by setting to zero in equation (11) the EA and T values of any cables that become slack when re-setting the overall stiffness. In fact, however, this does

not account for the proportion of work done by such cables before slackening occurs. The change in tension from the prestress state T° is:

$$\Delta T = s(EA + T^{\circ}) \text{ where } s = \text{strain}$$

But if $(T^{\circ} + \Delta T) < 0$ the strain magnitude based on nodal displacements is greater than $T/(EA + T^{\circ})$. To allow for slackening of cables in the iterative procedure it is thus necessary to use "equivalent" EA values which satisfy both equilibrium of forces and compatibility of deformations:

$$EA' = -T^{\circ}(1+1/S) \qquad (19)$$

where S is the compressive (-ve) strain based on nodal displacements.

An efficient means of dealing with practical problems in which slackening may occur in only a few of the cable elements is probably to combine the Secant and Modified Newton-Raphson methods. Thus stiffness matrices are re-set, using equivalent EA values given by (19), only when slack cables are encountered, and otherwise the iteration proceeds according to equation (18) or the alternative used by Mollmann and Mortensen (124). This approach is the basis of the method referenced in appendix 2.3 of Chapter 2 which was compared in computational efficiency with Dynamic Relaxation.

Nayak and Zienkiewicz (134) proposed a technqiue, termed the "alpha-constant stiffness method", by which the Modified Newton-Raphson iteration could be accelerated or "over-relaxed":

Let $\{\Delta\delta\}^i$ be the vector of displacement increments at the i.th iteration calculated by equation (17b), and assume that an improved value is given by:

$$\{\Delta\delta'\}^i = [\alpha]^i \{\Delta\delta\}^i \qquad (20)$$

where $[\alpha]^i$ is an unknown diagonal matrix of coefficients.

A measure of the degree of non-linearity at any stage is given by the difference between the initial and tangent stiffnesses:

$$[K_c] = [K_o] - [K_T]$$

Defining $\{\Delta\delta'\}^i$ as the correct change in displacements corresponding to residuals $\{R\}^{i-1}$ then approximately:

$$[K_T] \cdot \{\Delta\delta'\}^i = ([K_o] - [K_c])\{\Delta\delta'\}^i = \{R\}^{i-1}$$

Premultiplying by $[K_o]^{-1}$ and using (17b) and (20):

$$[\alpha]^i\{\Delta\delta\}^i - [K_o]^{-1} \cdot [K_c]\{\Delta\delta'\}^i = [K_o]^{-1}\{R\}^{i-1} = \{\Delta\delta\}^i$$

Assuming $\{\Delta\delta'\}^i = [\alpha]^{i-1}\{\Delta\delta\}^i \qquad (21)$

then: $([\alpha]^i - [I])\{\Delta\delta\}^i = \{\Delta u\}^i \qquad (22)$

where $\{\Delta u\}^i = [K_o]^{-1}[K_c][\alpha]^{i-1}\{\Delta\delta\}^i$, representing approximately the influence on displacements of the non-linear residual force contribution $[K_c]\{\Delta\delta'\}^i$.

From (22) the k th diagonal term of $[\alpha]^i$ is thus given by:

$$\alpha_k^i = \frac{\Delta U_k^i}{\Delta \delta_k^i} + 1$$

with the restriction that when $\delta\Delta_k^i \to 0, \alpha_k^i = 1$

In reference (134) a computational procedure based on the above accelerating process was outlined for softening structures and was found to result in considerably increased effeciency. This and similar accelerating procedures (29) have not to the author's knowledge been applied to tension structures and, comparing figures 4a and 4b, it seems probable that the approximation made in (21) could not be applied to stiffening systems. A possible revision to the process for such systems may be to use the approximation: $\{\Delta\delta'\}^i = [\alpha]^{i-2}\{\Delta\delta\}^i$, but it would seem safer not to use over-relaxing factors in matrix iteration analyses of tension structures.

Summarizing, the general recurrence equation for all matrix iteration schemes may be expressed in the form:

$$\{\delta\}^{i+1} = \{\delta\}^i + [\alpha]^i[K^i]^{-1} \cdot (\{P\} - [\beta]^i[K_s^i]\{\delta\}^i) \qquad (23)$$

where $[K_s]$ is the secant stiffness, and the term in brackets represents the residual force. When $[\alpha]^i = [I]$:

a) $[K]^i = [K_T]^i$ gives the Newton-Raphson method

b) $[K]^i = [K_o]$ gives Modified Newton-Raphson

c) $[K]^i = [K_S]^i$ gives the Secant stiffness method.

Incremental Solution Methods

For structures which are subject to both material and geometric non-inearity the solution is path-dependent and an analysis with loads applied in small increments must be used; $[K_T]$ in equation (13) being a function of the current configuration and possibly also the entire strain history.

Incremental methods can be divided into two groups:

(1) Purely incremental with equilibrium conditions generally not satisfied exactly and the solution tending to drift from the true deformation path (figure 8).

(2) Incremental with equilibrium corrections within each load increment, or as following corrections, termed "self-correcting" methods.

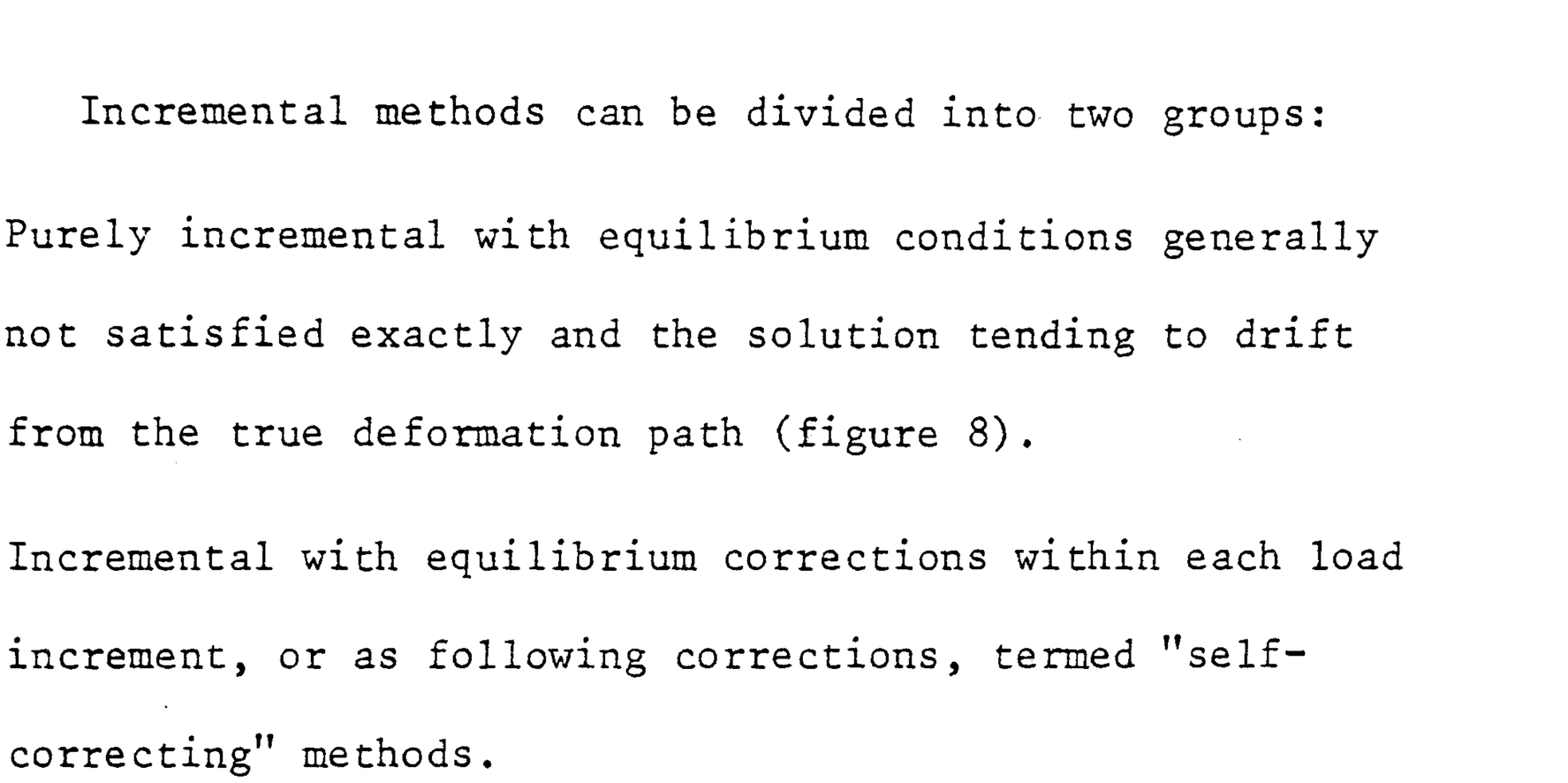


Figure 8

The simplest purely incremental method is the Euler method (85,181) which, although widely used, tends to drift rapidly from the true solution. Improved results, at the expense of additional

computations, can be obtained by taking $[K_T]$ near the mid-point of each increment, corresponding to a second order Runge-Kutta procedure (85, 7, 72). Bergan and Soreide (29) suggest a method for automatic computation of the size of load increment which uses large increments in linear regions but smaller increments with increasing non-linearity. This is achieved by fitting a parabola through the current and previous displacement values with slope equal to the current slope. The curve is then extrapolated and the load step determined by assigning a maximum truncation error between displacements given by a constant slope and those given by the extrapolated curve for the same load level; a maximum bound to the size of step being fixed for parts of the curve which are almost linear.

The simplest self-correcting method is to add the current force residuals to the next load increment (29,54,150). This corresponds to one cycle of Newton-Raphson iteration followed by a simple Euler increment in which the same gradient is used as for the iteration. Improved accuracy is obtained by carrying out several iterations for each level of loading (72,89,91). The tangent stiffness may either be held constant during iterations within each load step or may be re-set at each iteration; the latter corresponding with the Newton-Raphson procedure. A flow chart for a program (55) which encompases the primary incremental and iterative methods is shown in figure 9. The four alternative solution procedures shown are:

(1) Incremental

(2) Incremental & correction for out-of-balance loads from previous increment

(3) Newton-Raphson iteration

(4) Modified Newton-Raphson

In addition, (2) may be combined with (3) or (4) for several equilibrium iterations within each load increment. The choice of solution method will depend on the type of problem: For structures subject to large geometric and material non-linearities, such as flexible two-way networks with non-linear cable properties, (2) with (4) may be essential. Whereas if only material non-linearities without discontinuities are involved then (2) alone may be adequate. The preferred solution method will also depend on the level of loading and the idealization of material properties. An iteration method might be applied to account for a significant proportion of the total load up to which the structural elements behave elastically, and an incremental method applied for the remaining inelastic region.

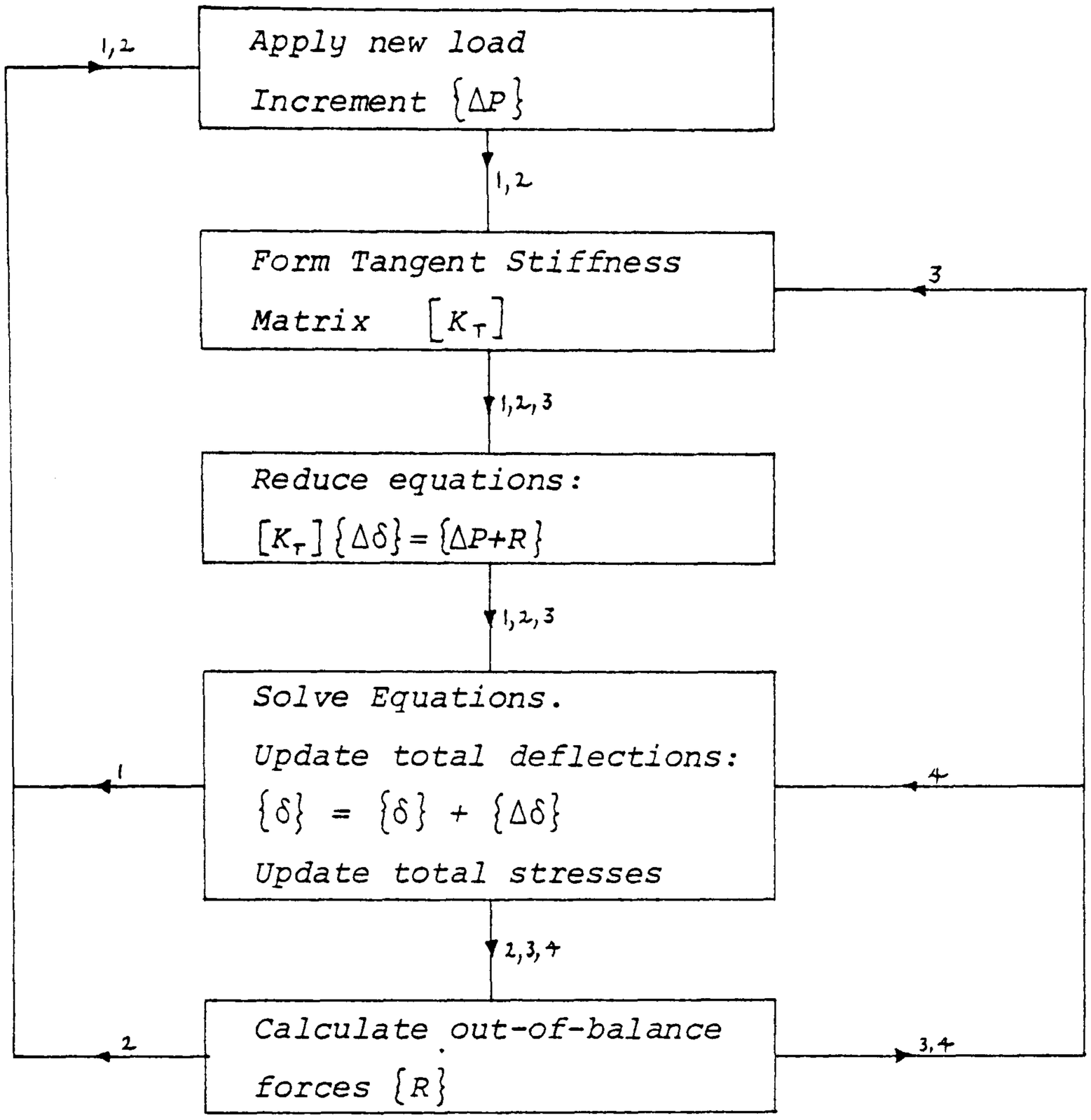


Figure 9

Accelerated convergence of Incremental solution methods may be obtained by basing the value of tangent stiffness in any step not on the slope at the beginning of the increment but on its estimated value at the mid-point of the increment. This may be achieved either by extrapolation of previously calculated deflections when re-setting the stiffness (176), or by iteration in each step to use an averaged value of tangent stiffness (7).

Johnson and Brotton (92) and Millar et.al. (121), using an incremental method for the analysis of space frames, estimated

initial deflection values for the fourth and all subsequent increments by extrapolating the three previous converged displacement vectors, and then iterated within each step using the constant tangent stiffness so calculated. Greenberg (72), for inelastic analysis of cable structures upto failure, used a scheme which averaged the main diagonal stiffness coefficients, k_{ii}, to correct the deflections at each cycle. The process is summarized in the following sequence:

1. Form $[K_T]$ based on current conditions and save k_{ii} terms.

2. Apply load increment ΔP and solve for linearized deflections and tensions.

3. Compute modulus of elasticity for individual members based on stresses from 2.

4. Form k'_{ii} coefficients based on new geometry and moduli.

5. Revise deflections: $\delta_i = \frac{k'_{ii} + k_{ii}}{2k'_{ii}} \times \delta_i$

6. Determine unbalanced loads using revised geometry and return to 1.

7. Repeat 1-6 until unbalance is negligible

8. Add another increment of load if member strains are all less than ultimate and return to 1.

9. Repeat 1-8 until ultimate load is reached.

In step 3, the moduli were calculated assuming a continuous exponential function to represent the inelastic portion of the stress/strain curve for steel cables. The function used conformed to manufacturers specifications and it was found that for typical cable networks the ultimate load could be 50% higher than that calculated assuming constant elastic moduli. Jonatowski (91) used a similar function for the entire stress/strain curve and applied standard Newton-Raphson iteration to achieve equilibrium in each load increment.

EXPLICIT ANALYSES

Minimization Methods

With minimization methods the physical problem is stated as that of finding a stationary value of the total potential energy function:

$$W = U + V \tag{24}$$

where U is the strain energy $U(\delta)$, and V is the potential energy, $\{\delta\}^T.\{P\}$, with the applied loads $\{P\}$ assumed independent of displacements $\{\delta\}$.

Direct minimization techniques, such as random search, make use of the objective function, W only. They have been applied with varying success to non-linear structural problems (115, 116), though they are not generally competitive with the

gradient methods of minimization:

A necessary condition for a minimum of W is that

$$\frac{\partial W}{\partial \delta_1} = \frac{\partial W}{\partial \delta_2} = \ldots\ldots \frac{\partial W}{\partial \delta_n} = 0$$

A solution is possible by searching along a set direction in n-dimensional space until the minimum in that particular direction is found; by changing direction and continuing the process, provided the energy surface is convex, the global minimum may eventually be located. The procedure is therefore iterative using the general equation:

$$\{\delta\}^{k+1} = \{\delta\}^{k} + S^{k}.\{V\}^{k} \qquad (25)$$

where $\{V\}^{k}$ is the gradient vector and S^{k} is a scalar "step-length" representing an incremental distance in that direction. Since the analysis procedure is explicit, it has the major advantage that an overall matrix system of equations does not have to be set and solved, and thus storage requirements for computations are considerably reduced.

Various first or second order gradient methods are available for determining the direction of search, $\{V\}$, and the minimum along a particular direction is located at each stage of iteration by representing the objective function as a polynomial and determining S to minimize the function. The simplest first order gradient method is the method of steepest descent, but the

orthogonality property of the search directions may result in severe convergence difficulties. These may be partially overcome by using relaxed steepest descent or conjugate gradient minimization. Second order optimization techniques utilize the second derivative of the objective function. The most widely used of these is the Newton-Raphson procedure which is essentially a deflected gradient technique in which the step in each new direction is determined by using the minimum of the approximating quadratic. The application of this process to tension structures subject to distributed cable loads is described by Burley and Harvey (45). Other than this application, however, nearly all minimization analyses of tension structures have been based on first order gradient methods. These have been principally developed and applied by H.A. Buchholdt, and the following account is based on his work (references 37-43).

Method of Steepest Descent

The derivative of the total potential with respect to a displacement, δ_i, at any node, a, in the i direction, is equal to the unbalanced force in that direction which, from equation (14), is given by:

$$g_i = \frac{\partial W}{\partial \delta_i} = P_{Ti} - \sum_m \left\{ (T^\circ + \Delta T) \frac{(DX_i + D\delta_i)}{(L + e)} \right\}_m \qquad (26)$$

where, as before, the summation applies to all links m joining node a to adjacent nodes b, and:

$$DX_{im} = X_{ia} - X_{ib}\,; \qquad D\delta_{im} = \delta_{ia} - \delta_{ib}$$

The complete set of unbalanced forces $\{g\}$ has for the displacement vector $\{\delta\}$ the direction of greatest decrease in the total potential, and in the steepest descent method the gradient vector $\{v\}$ is taken equal to this residual force vector or to the normalized vector (37).

The total potential can be expressed as a fourth order polynomial in the step-length S:

$$W = C_1 S^4 + C_2 S^3 + C_3 S^2 + C_4 S + C_5 \qquad (27)$$

For a minimum: $$\frac{\partial W}{\partial S} = 4C_1 S^3 + 3C_2 S^2 + 2C_3 S + C_4 = 0 \qquad (28)$$

The smallest positive root of this equation gives the required minimum of the total potential along the vector $\{v\}$ at any stage.

The strain energy in any link, m, may be expressed as:

$$U_m = \int T_m . de_m = \int \left(T^\circ + \frac{EA}{L_\circ}.e\right)_m de_m = T^\circ_m . e_m + \frac{EA}{2L_{\circ m}}.e_m^2 \qquad (29)$$

Neglecting second order terms, from Appendix 2.2 of Chapter 2:

$$e_m = \sum_i \left\{ \frac{(2DX_i + D\delta_i)}{2L} . D\delta_i \right\}_m \qquad (30)$$

and, from equation (24), at iteration (k + 1) the difference in end displacements, $D\delta_{im}$, of a link, m, is given by:

$$D\delta_{im}^{k+1} = D\delta_{im}^{k} + S^k . V_{im}^k \qquad (31)$$

Substituting (31) in (30) gives e_m in the form:

$$e_m = \frac{1}{L_m}(a_1 + a_2 S + a_3 S^2) \qquad (32)$$

where L_m is the current link length.

From equations (24) and (29) the total potential energy at iteration (k+1) is:

$$W^{k+1} = \sum U - \{P_T\}^T \cdot \{\delta\}^{k+1}$$

$$= \sum_{m=1}^{M} (T_m^o . e_m + \frac{EA}{2L_{om}} . e_m^2) - \{P_T\}^T \cdot \{\delta\}^k - \{P_T\}^T \cdot \{S.v\}^k \qquad (33)$$

Substituting for e_m from (32) and equating coefficients of S, S^2 etc. in (33) and (27) gives $C_1 \rightarrow C_5$, from which S^k may be obtained by solving equation (28). The next improved displacement vector $\{\delta\}^{k+1}$ is then given by equation (25), and the procedure is repeated until the out-of-balance forces are negligible.

Conceptually, the magnitude of any step-length is determined by the point at which the steepest descent vector grazes a contour of the energy surface, and each subsequent step is orthogonal to the previous one. A sufficient condition for convergence is that the energy surface is convex throughout; containing no saddle points or local minima. Buchholdt et.al. (39) show that, for tension structures, this condition is satisfied provided all elements remain in tension. The condition, however, is not a necessary one and it is possible for some members to go temporarily into compression during the descent process. In form-finding applications this could perhaps lead to convergence difficulties.

Relaxed Steepest Descent

The steepest descent path is not a continuous orthogonal trajectory to the energy surface contours but, as explained above, takes a zig-zag convergence path. In many cases this leads to slow convergence and an improvement is possible by reducing the calculated step-length to λS. It has been found that a value of λ between 0.3 and 0.9 can reduce the number of iterations to between 5% and 25% of those required using the full step-length (39).

Method of Conjugate Gradients

In the method of conjugate gradients the step-length is calculated as previously but the descent vector $\{v\}$ in equation (25) is given by (38):

$$\{v\}^{k+1} = \{g\}^{k+1} + \frac{\|g^{k+1}\|^2}{\|g^k\|^2} \cdot \{v\}^k \qquad (34)$$

where $\|g\|^2 = \{g\}^T \cdot \{g\}$

The first descent vector (or first few) is taken in the direction of steepest descent. Thereafter, the previous descent vector is given some weighting in choosing the current vector, which is dependent on the squared ratio of the euclidean norms of the residual forces. Graphically, for a structure with only two degrees of freedom δ_1 and δ_2, the procedure is illustrated in figure 10 (from ref. 41).

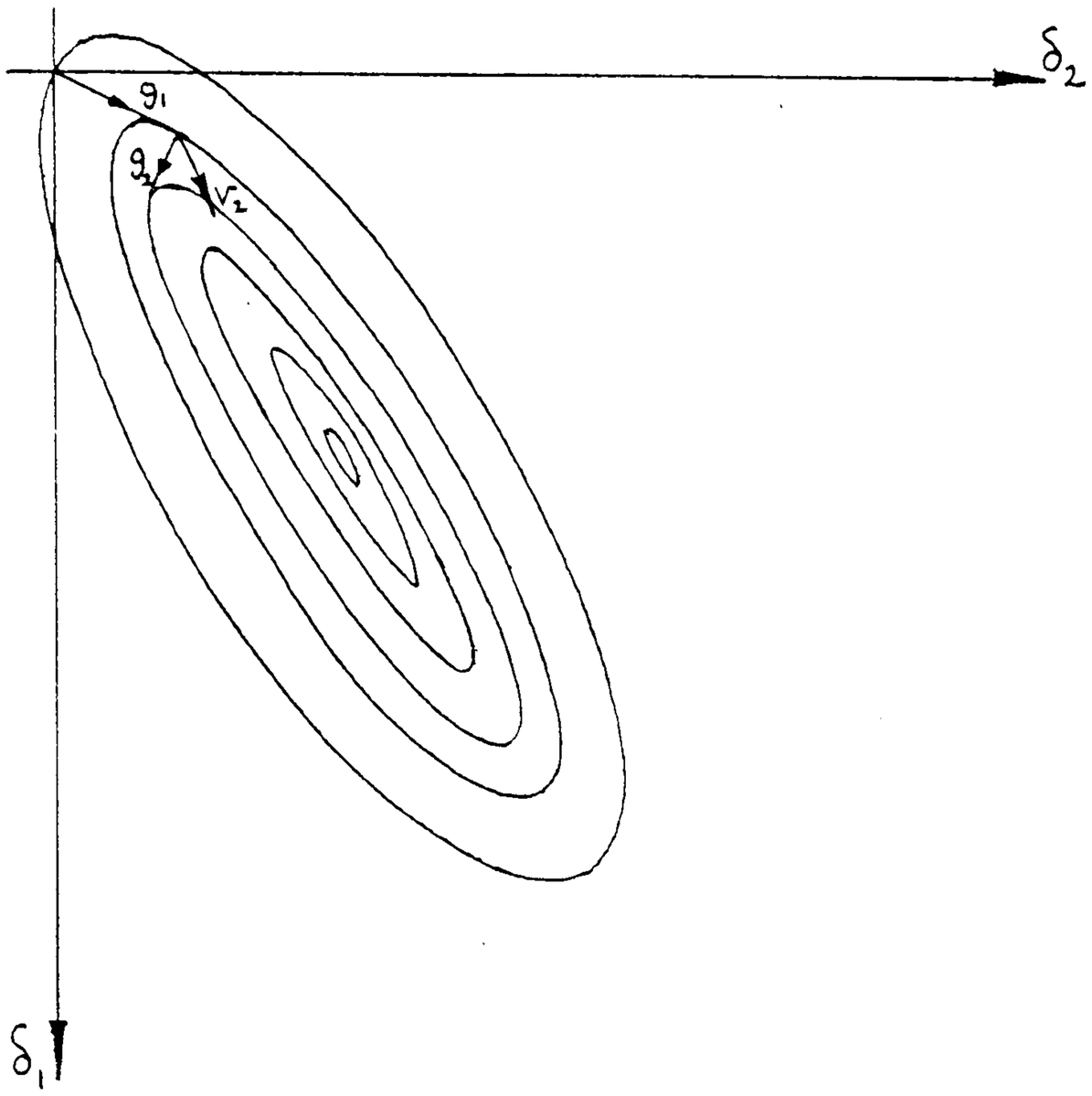


Figure 10

Scaling and Transformation of Energy Surface

The convergence rate of the conjugate gradient method, whilst considerably better than that of steepest descent, depends on the ratio of the highest to lowest eigenvalues, or condition number, of the associated stiffness matrix. For a two degree of freedom system (fig.10), the condition number is proportional to the squares of the axes forming the elliptic contours of the energy surface. For a large condition number the ellipses are very narrow and convergence is slow. The condition number is a measure of the ill-conditioning of the system of equations, and in cable structures, particularly structural mechanisms with fairly stiff boundaries, this can be a common problem due to large variations in the stiffness coefficients.

In Dynamic Relaxation, ill-conditioning is partially remedied by choosing fictitious masses proportional to corresponding direct stiffness coefficients so that the critical time interval for the numerical integraltion process is optimum at each node (see text and Appendix D for further discussion of conditioning). In the conjugate gradient method the ill-conditioning can be analogously remedied by transforming the contour lines to widen the total potential energy valleys (41). This is achieved by replacing the actual displacement vector $\{\delta\}$ with a scaled vector $\{u\}$ such that:

$$\{\delta\} = [H]\{u\} \tag{35}$$

where $[H]$ is square and referred to as a "scaling" matrix.

The total potential energy can be expressed in matrix form (not required computationally) as:

$$W = \tfrac{1}{2}\{\delta\}^T[K_T]\{\delta\} - \{P_T\}^T\{\delta\}$$

Substituting for $\{\delta\}$ from (35):

$$W = \tfrac{1}{2}\{u\}^T[K_T']\{u\} - \{P_T\}^T[H]\{u\}$$

and the transformed gradient vector is:

$$\{g'\} = \left\{\frac{\partial W}{\partial u}\right\} = [K_T']\{u\} - \{P_T\}^T[H] \tag{36}$$

where $[K_T'] = [H]^T[K_T][H]$

Equilibrium is achieved when $\|g'\| = 0$ and the real displacements are then given by equation (35).

The eigenvalues of $\left[K_T^{\backprime}\right]$ would be approximately equal, with ideal conditioning of equations (36), if $\left[H\right]$ could be chosen to make $\left[K_T^{\backprime}\right]$ symmetric with all elements on the leading diagonal approximately unity and off diagonal terms tending to zero. In practice this is not possible but considerable benefit can be gained if a diagonal matrix $\left[H\right]$ is chosen such that:

$$h_{ii} = \left(\frac{1}{k_{ii}}\right)^{1/2}$$

Buchholdt et.al. (41) applied the above method to cable systems with comparatively stiff boundary structures and found it to converge more quickly, using less storage, than the Newton-Raphson method. It was also compared with scaled and relaxed methods of steepest descent and the conjugate gradient method without conditioning and in all cases was found to be considerably more efficient.

Explicit Relaxation Methods

The three basic explicit iterative methods are Point-Jacobi, Gauss-Seidel, and Successive Over-Relaxation (182,114). For descriptive convenience the recursion equations appropriate to each method are most simply expressed in matrix notation though, as in the previous section, all of the methods can be applied as direct iterative solutions of un-coupled or semi-coupled equations, and thus applied conveniently to non-linear analyses.

The aim of the methods is to solve a set of linearized or incrementally linearized equations of the form:

$$\left[K_T\right]\left\{\delta\right\} = \left\{P\right\} \tag{37}$$

The stiffness matrix $\left[K_T\right]$ may be expressed in the form:

$$\left[K_T\right] = \left[L + D + U\right]$$

where $\left[D\right]$ is the main diagonal of $\left[K_T\right]$, and $\left[L\right]$ and $\left[U\right]$ are respectively the remaining lower and upper triangular portions of $\left[K_T\right]$. Unifying the diagonal coefficients of (37):

$$\left[D\right]^{-1}\left[K_T\right]\left\{\delta\right\} = \left[D\right]^{-1}\left\{P\right\}$$

$$\text{or} \quad \left[K_T'\right]\left\{\delta\right\} = \left\{P'\right\} \qquad \text{where } \left[K_T'\right] = \left[L' + I + U'\right]$$

In the Point-Jacobi method the iteration is begun by assuming the unknown vector $\left\{\delta\right\}$ to be equal to the diagonal of $\left[K_T'\right]$. This vector is then used to compute a new estimate of $\left\{\delta\right\}$ using the recurrence equation:

$$\left\{\delta\right\}^{k+1} = \left\{P'\right\} - \left[L' + U'\right]\left\{\delta\right\}^{k}$$

$$\therefore \quad \left\{\delta^{k+1} - \delta^{k}\right\} = \left\{P'\right\} - \left[K_T'\right]\left\{\delta\right\}^{k}$$

$$\text{or} \quad \left\{\Delta\delta\right\}^{k+1} = \left\{R'\right\}^{k} \tag{38}$$

where $\left\{\Delta\delta\right\}$ is the correction vector and $\left\{R'\right\}$ is the residual vector.

In the Gauss-Seidel method the most recently computed components of $\{\delta\}^{k+1}$ are utilized in computing subsequent components of this vector. The recurrence equation can be written in the form:

$$\{\delta\}^{k+1} = \left[1+L'\right]^{-1} \cdot \left(\{P'\} - \left[U'\right]\{\delta\}^{k}\right)$$

$$\text{or} \qquad \{\Delta\delta\}^{k+1} = \left[1+L'\right]^{-1} \cdot \{R'\}^{k} \tag{39}$$

Accelerating factors, β, can be used in either the simultaneous (Point-Jacobi) or successive (Gauss-Seidel) relaxation methods. Thus in the former case one obtains the Extrapolated Gauss method:

$$\{\Delta\delta\}^{k+1} = \beta \{R'\}^{k} \tag{40}$$

and when the Gauss-Seidel iteration is accelerated one obtains the method of Successive Over-Relaxation:

$$\{\Delta\delta\}^{k+1} = \beta\left[1+\beta L'\right]^{-1} \cdot \{R'\}^{k} \tag{41}$$

This latter method, with $1<\beta<2$, has the fastest rate of convergence (appendix D).

Any of the above iterative methods can be performed either in a semi-uncoupled form with main diagonal submatrix operations node by node, or in a form in which each degree of freedom is treated as uncoupled; both schemes reducing considerably the required storage compared with overall matrix formulations, and being computationally most suitable for non-linear problems.

The Successive Over-Relaxation (SOR) method, for example can be expressed in the following semi-uncoupled form:

At node i (with n degrees of freedom) the relaxation equation is:

$$\{\delta_i\}^{k+1} = \{\delta_i\}^{k} + \beta \left[k_i^c\right]^{-1} \{R_i^c\} \qquad (42)$$

where $\{\delta_i\}$ is the vector of n displacement components at node i, and $\left[k_i^c\right]$ and $\{R_i^c\}$ are respectively the nxn tangent stiffness submatrix and the nx1 residual load vector, each calculated using current co-ordinates of i and adjacent nodes j (with some of the latter co-ordinates being current to iteration k+1). In this form the over-relaxation process is successive node to node, but simultaneous for the component deflections at each node. An alternative fully uncoupled form may be expressed as:

$$\{\delta_i\}^{k+1} = \{\delta_i\}^{k} + \beta\left[\frac{1}{k_{di}}\right]^c \{R_i^c\} \qquad (43)$$

where $\left[1/k_{di}\right]^c$ is a diagonal matrix consisting only of the n reciprocals of the current direct tangent stiffness components.

The procedure in (43) avoids the need for inverting an n x n submatrix at each node and stage, and may also be computationally advantageous for cable or membrane structures in which it is possible that $\left[k_i^c\right]$ may become singular at some stage of this process. Convergence difficulties, however, might arise and it seems probable that the relaxation factor β would have to be reduced. It is not possible for the components k_{di} to

become negative, though due to a combination of cable slackening and co-planar elements they may become zero, giving rise to infinite deflection increments. To avoid this, conditional deflection controls are necessary or, alternatively, small additional fictitious stiffnesses might be used which are gradually relaxed to zero at later stages of an analysis when the structure is near a unique equilibrium state.

The above processes have not to the author's knowledge been used for the analysis of tension structures, though a similar technique, termed Non-linear Over-relaxation, has been used by Perrone and Kao (148) for solving non-linear problems involving large deflections of thin-walled tubes and spherical cap membranes.

Dynamic Relaxation may also be regarded as an uncoupled simultaneous iterative procedure for which the recurrence relation for any component deflection takes the form:

$$\delta^{k+1} = \delta^{k} + \alpha(\delta^{k}-\delta^{k-1}) + \gamma.R^{k}$$

where the factors α and γ are chosen to optimize the convergence. It has the major advantage that in highly non-linear problems the occurrence of transient zero stiffness situations is not accompanied by infinite deflection increments. A comparison of the convergence rate of DR with those of the basic iterative procedures is given in appendix D.

Any of the iterative methods may also be stated in the form of a minimization problem:

$$\{\delta\}^{k+1} = \{\delta\}^{k} + S.\{V\}^{k}$$

Apart from DR, however, the step-length S may be unbounded.

A comparative study of dynamic relaxation with the majority of the methods reviewed in the present appendix, applied to prestressed structural mechanisms, is being carried out by Papadrakakis (196).

APPENDIX B

REVIEW OF METHODS FOR FORM-FINDING OF NETS AND MEMBRANES

The following review is concerned mainly with methods for the form-finding of surface networks. The majority of the non-linear analyses considered are, however, equally applicable to general prestressed cable and membrane systems. As in the previous appendix, the review is restricted to systems idealized into discrete elements and, since many of the procedures considered in appendix A may be used for form-finding when based on data provided by accurate physical models, emphasis is placed in the present appendix on those techniques which do not necessarily require such close initial estimates of geometry and tensions.

LINEAR SOLUTIONS

Orthogonal Nets

The first analytical treatments of the problem of form-finding of cable networks were published by Bandel (11), Siev and Eidelman (170), and Dean and Ugarte (63). The analysis of Siev and Eidelman assumed the network to be orthogonal in plan, with known horizontal mesh spacing and boundary co-ordinates, and the heights of all interior nodes were obtained by solving one system of linear equations. For such networks the horizontal component of tension, T_h, is constant along all links of any cable, and the equation of equilibrium at any node, i, connected by links, m, to adjacent nodes j is:

$$\sum_m \left(\frac{T_h}{l_h}\right)_m .(Z_i - Z_j) = P_{zi} \qquad (1)$$

where P_{zi} is the self-weight load, Z_i, Z_j denote vertical ordinates, and l_h is the horizontal spacing between i and j.

In matrix notation the complete set of equilibrium equations is:

$$[H]\{Z\} = \{P_z'\} \qquad (2)$$

where $[H]$ is square and $\{P_z'\}$ denotes that the known boundary components (HZ_b/l_h) have been transferred to the R.H.S. to modify the load vector.

For a network in which the cables project orthogonally onto a plane, $x'y'$, inclined to the horizontal, the self-weight loads are resolved into components parallel and perpendicular to

$x'y'$ and equations of equilibrium perpendicular to this plane are set, as before, but with the horizontal force components H mofified along each cable by the summed self-weight traction loads. For networks with edge cables, both the boundary and surface co-ordinates must be determined by a non-linear analysis with iteration between the network and edge curve analyses; the latter involving two degrees of freedom at each node on the assumption that the horizontal spacing between the cables of each set is specified. This procedure was given by the author in reference (12) and was found to converge rapidly.

Dean and Ugarte (63) obtained closed form trigonometric series solutions for initially flat, doubly, triply or quadruply threaded nets, with a regular projected pattern, subject to single point loads or to uniform loading. Buchanan and Akin (36) later extended this approach to the form-finding of networks with elevated and spatially curved boundaries. The analysis, termed the reflection method, consisted of defining the spatial boundary to lie inside a larger initially plane net. By applying the trigonometric series solution for single loads to all boundary points, together with the series solution for uniform loading which accounted for self weight, the deflections of the boundary points were made to correspond with the specified elevations. The procedure has the advantage, compared with Siev's method, that the set of simultaneous equations to be solved is equal in number only to the number of boundary nodes rather than the number of interior nodes. It is not,

however, as general; being restricted to networks with regular projected mesh spacing. For curved boundaries it is necessary to interpolate between mesh points for the required boundary elevations and thus the order of the system of equations may be doubled. The method is also restricted to cases where all boundary positions are specified and, even with an iterative formulation, would be difficult to apply to nets with cable boundaries.

General Nets

A development of the procedure given by Siev and Eidelman, accounting for three degrees of freedom at each node and termed the Linear Force-densities method, was proposed by Linkwitz and Schek (110) to enable a rapid search of feasible forms for general networks:

For a system with M members (or branches) and N nodes, of which N are variable with co-ordinates denoted X_1, X_2, X_3 and N are fixed with co-ordinates X_{f1}, X_{f2}, X_{f3}, the vectors of co-ordinate differences for the complete set of branches may be expressed in matrix form as:

$$\{dX_i\} = [C]\{X_i\} + [C_f]\{X_{fi}\} \qquad (3)$$

where $[C]$ and $[C_f]$ are submatrices, relating respectively to the variable and fixed nodes, of the partitioned branch/node matrix $[C \mid C_f]$ in which the components are defined by:

$$c(i,j) \quad \left.\begin{array}{l} = +1 \text{ when } i = \text{node } 1 \\ -1 \text{ when } i = \text{node } 2 \end{array}\right\} \text{ of branch } j$$
$$0 \text{ elsewhere}$$

If the member forces are denoted by the vector $\{T\}$ and the lengths by $\{l\}$, or an MxM diagonal matrix $[L]$, the tension coefficients, or "force-densities", of the members are:

$$\{q\} = [L]^{-1}\{T\}$$

The set of 3N equilibrium equations is thus:

$$[C]^T[DX_i]\{q\} = \{P_{xi}\} \qquad (4a)$$

$$\text{or } [C]^T[Q]\{dX_i\} = \{P_{xi}\} \qquad i = 1:3 \qquad (4b)$$

where $[DX_i]$ and $[Q]$ are diagonal matrices corresponding with the vectors $\{dX_i\}$ and $\{q\}$.

Substituting (3) in (4b):

$$[H]\{X_i\} = \{P_{xi}\} - [H_f]\{X_{fi}\} = \{P'_{xi}\} \qquad (5)$$

where $[H] = [C]^T[Q][C]$ and $[H_f] = [C]^T[Q][C_f]$

Provided all $q>0$ then $[H]$ is positive definite and a variety of possible nets may be investigated simultaneously for different values of $\{X_{fi}\}$ by solving the linear equations (5) with simultaneous reduction of multiple R.H.S. vectors for each set of values $\{q\}$:

$$[H]\{X_1, X_2, X_3\} = \{V\}$$

where $\{V\}$ is a set of 3J vectors of order N, where J is the number of different boundary arrangements to be investigated simultaneously.

The above linear method permits an economic search of feasible forms and has been found to yield nets which are reasonably regular when all force-densities are identical (74). This procedure, however, gives only an approximate design guide since the nets so obtained are not constructionally practicable. The same drawback applies to all other linear form-finding methods, and to obtain either uniform mesh or geodesic networks a non-linear analysis must be used. The linear methods nevertheless enable preliminary investigation and can yield initial data for precise form-finding. In the case of the force-densities method the analysis may also be extended to account for non-linear constraints on member lengths and/or tensions. For continuity this is outlined at the start of the following section, though chronologically it is one of the more recent form-finding methods.

NON-LINEAR FORM-FINDING

Constrained Force Densitites Method

The method starts from the linear solution using estimated force-densities $\{q^{\circ}\}$. Additional constraints on member lengths and/or tensions are then introduced which take the general form:

$$g_1(X,Y,Z,q) = 0$$

$$g_2(X,Y,Z,q) = 0$$

.
.
.

$$g_t(X,Y,Z,q) = 0$$

Since from (5) the co-ordinates are functions of the force-densities, the t constraints may be rewritten as dependent on force-densities alone:

$$\{g^*(q)\} = 0$$

These constraint equations are non-linear and must be solved iteratively:

$$\{q^1\} = \{q^\circ\} + \{\Delta q\} \text{ subject to } \{g^*(q^1)\} = 0$$

Alternatively, linearizing the solution steps:

$$\{g^*(q^\circ)\} + \left[\frac{\partial g^*(q^\circ)}{\partial q}\right]\{\Delta q\} = 0$$

$$\text{or } [G]^T\{\Delta q\} = \{r\} \qquad (6)$$

where $[G]^T$ is a t x M matrix

Since, for many applications, the number of conditions, t, is less than M, equations (6) have (M-t) linearly independent solutions. A single solution is sought by minimization; for example, using the least squares principle:

$$\{\Delta q\}^T \cdot \{\Delta q\} \rightarrow \min$$

Alternatively, Schek (162) suggests the use of a damped system instead of equations (6):

$$\left[G \right]^{T} \left\{ \Delta q \right\} = \left[A \right] \left\{ r \right\} \qquad (7)$$

where $\left[A \right]$ is a diagonal matrix of damping factors, a. The associated minimum principle is:

$$\left\{ \Delta q \right\}^{T} \cdot \left\{ \Delta q \right\} + \left\{ 1-a \right\}^{T} \left[W \right] \left\{ 1-a \right\} \rightarrow \min$$

where $\left[W \right]$ is a diagonal weighting matrix.

The Lagrange factors, f, are obtained by solution of the txt system:

$\left[S \right] \left\{ f \right\} = \left\{ r \right\}$ where $\left[S \right] = \left[G \right]^{T} \left[G \right]$ in case (6), or $\left[S \right] = \left[G \right]^{T} \left[G \right] + \left[W \right]^{-1} \left[R^{2} \right]$ in case (7); $\left[R \right]$ being a diagonal matrix corresponding with $\left\{ r \right\}$.

Hence: $\left\{ f \right\} = \left[S \right]^{-1} \left\{ r \right\}$ and $\left\{ \Delta q \right\} = \left[G \right] \left\{ f \right\}$

For the next iteration q° is set to $q^{\circ} + \Delta q$ and the procedure repeated from (6) or (7) until $\left\{ g^{*}(q^{\circ}) \right\} = 0$ within given tolerances.

Schek gives expressions for the components $\partial g^{*}/\partial q$ of $\left[G \right]$ (in terms of $\left[C \right]$, $\left[D \right]$ and $\left[DX_{i} \right]$) for the three cases:

(1) specified member lengths under loading

(2) specified slack lengths

(3) specified member tensions

Thus enabling form-finding of grid-shells, uniform mesh nets or geodesic nets when, respectively, the lengths or tensions of the members are held constant.

Newton-Raphson Iteration

The most frequently used implicit form-finding methods have been based on Newton-Raphson (N-R) iteration,with incremental loading or imposed displacement stages when required deformations from the initially specified state are large (3,8, 78,95).

Haug (78) estimates initial shapes from sketches,and the net shapes and distribution of forces are then refined by appropriate operations involving prestressing and length changes after each solution of the overall system of equations. For strongly non-linear cases the basic N-R process may diverge, or converge only slowly, and in such cases the loads are applied in steps and approximate equilibrium after each increment obtained with a few N-R iterations; a larger number of iterations being used in the final step to achieve the required accuracy. To avoid ill-conditioning during the analysis a maximum allowable value for the displacement increment at any node may be specified. If this is exceeded, the computed increments are all scaled down proportionally until the maximum increment is equal to the maximum allowable value.

Whereas for typical non-linear static load analyses of networks Newton-Raphson iteration can be expected to give results of sufficient accuracy after about 10 iterations, in form-finding applications the rate of convergence is considerably slower. Haug quotes figures of 15 cycles of iteration for network systems with a fairly accurate initial estimate of geometry, but upto 33 cycles

for funicular nets (grid-shells) because of their greater degree of kinematic freedom and deformation from the initial state. For a similar reason the analysis of a retractable net required 30 cycles of iteration for each stage of retraction (78). The same procedure was applied by Haug and Powell (79) to the analysis and form-finding of membrane structures using linear displacement warped quadrilateral elements with an isoparametric formulation. With buckling (or wrinkling) ignored the static load analyses converged in a minimum of 5 cycles; the figure being lower than that for networks because of the effective triangulation of the structure. For form-finding of uniform stress membranes, however, an accuracy of 1% was obtained only after 30 cycles and, whilst this figure is sufficient for preliminary design, a greater degree of accuracy would be required for the purpose of defining cutting patterns.

Estimates of initial geometry based on architectural sketches entail very large out-of-balance forces with compression induced in many of the elements. As a consequence many iterations are required for convergence and there is possibly the danger of obtaining a non-unique solution. The same problems may also occur when initial data is based on measurements of small scale physical models. To avoid these difficulties Angelopoulos (3) and Argyris et. al. (8) suggested the use of a computer "model" with flexible linear elastic elements to simulate the physical modelling process. Starting with an initially flat uniform mesh net an approximate equilibrium configuration is obtained by deflecting the support nodes to their final positions in stages. The tangent stiffness for any increment is set from the geometry and tensions obtained from the previous stage, with slack (or compressed) cables encountered during

the process being ignored and later restored if strains revert to tensile. In the final stages N-R iteration is used to obtain a solution in accurate equilibrium. The resulting cable forces are for the most part too large with an irregular distribution, and to obtain forces which more closely correspond with required values it is necessary to transform the slack lengths according to the following relation:

$$L_o = \frac{L_o' + \Delta L'}{1 + T_D/EA} \qquad (8)$$

where T_D is the desired prestress, L_o' and $\Delta L'$ refer to the model lengths and increments, and the elastic properties (EA) in the "model" and actual structures are assumed the same.

Following the above transformation, the structure is no longer in equilibrium and thus the iterative solution procedure must be repeated. This yields a structure in which the tensions and surface curvatures are close to the design values, but because of the transformation in (8) the equivalent slack mesh is no longer uniform. Thus a final stage is required in which, by use of spline interpolation and mesh generation procedures developed by Knudson and Nagy (98), a uniform mesh network is generated on the surface. Using the previously determined prestress distribution this net is then analysed by N-R iteration to obtain an equilibrium state.

For the design of the Munich stadium Argyris and Scharpf (6) used cubic interpolation functions to smoothe data from a

physical model and generated on this smoothed surface an equal mesh net. N-R iteration was then used to obtain the equilibrium configuration and, to ensure approximately correct prestress levels, the tension in one end link of each cable was held constant during the process. To accelerate convergence it was found advantageous to use fictitious (reduced) EA values for the edge cables with the slack lengths of edge links adjusted at the end of each iteration to yield equivalently correct EA values. At the same time the connection points of the network to the edge cables could also be adjusted to comply best with a uniform mesh projection.

Optimization Techniques

As indicated by the foregoing discussion, shape finding methods must produce a qualitative prestress distribution as well as the geometry, and in this case the design problem may be more effectively posed as one of optimization. For a restricted class of networks (orthogonal), knudson and Scordelis (97) outline a least squares approach which seeks to achieve a desired surface geometry whilst at the same time satisfying the requirements of maximum and minimum cable forces in the network under various live loading conditions:

For a shallow network with orthogonal projected cable lines, the equations of vertical equilibrium (1) can either be

expressed as the linear system (2) with known tension coefficients but unknown vertical ordinates:

$$\left[H \right]\left\{ Z \right\} = \left\{ P_z^{\backprime} \right\}$$

or, if the vertical ordinates and projected cable spacings are specified, as an overdetermined set of equations for the horizontal tension components:

$$\left[B \right]\left\{ T_h \right\} = \left\{ P_z^{\backprime} \right\} \qquad (9)$$

Since in (9) there are more equations than unknowns, in general there will be no unique solution which satisfies all the equations. It is, however, possible to determine a vector $\left\{ T_h \right\}$, using the least squares technique, which makes the sum of the squares of the residual vector:

$$\left\{ R \right\} = \left[B \right]\left\{ T_h \right\} - \left\{ P_z^{\backprime} \right\}$$

a minimum with respect to the horizontal tension components:

$$\frac{\partial (R^T . R)}{\partial (T_h)} = 0$$

This minimization results in the set of equations:

$$\left[B \right]^T \left[B \right]\left\{ T_h \right\} = \left[B \right]^T \left\{ P_z^{\backprime} \right\} \qquad (10)$$

Equations (10) are symmetric positive definite and may be solved for the unknowns $\left\{ T_h \right\}$. It may be found, however, that the solution, referred to as the natural least squares solution, yields

some values of T_h which are less than zero. In this case the most negative value(s) can be specified as positive. The system of equations (10) may then be reduced by transferring the specified products to the R.H.S. and re-solving for the reduced set of unknowns $\{T_h'\}$. The specification of horizontal tension components need not, however, be restricted to only a few cables. Since cables running in one direction do not mutually intersect, it is possible to independently specify all tension components in either the hanging or prestressing set of cables. In particular, the approximate cable forces required to sustain an assumed worst loading case can be found subject to constraints either on the maximum tensions in one set of cables or minimum tensions in the other set.

The least squares procedure only yields the set of horizontal cable forces which approximately produces the set of specified interior nodal elevations; vertical equilibrium not being satisfied except in a qualitative overall sense. It is thus necessary to carry out a separate analysis to determine the true equilibrium configuration after the horizontal tension components have been found. If these forces have been obtained for the prestress state using only self weight components in the loading vector, the equilibrium configuration can be found by solving the linear equations (2). If, however, the approximate cable forces have been obtained for an assumed worst loading condition, the prestress configuration must be determined by releasing the loads in

excess of dead weight and applying a Newton-Raphson iterative analysis. In this case, unless deflections are small, the proposed surface shape will be complied with qualitatively only in the loaded state.

The least squares procedure has been extended by Ohyama and Kawamata (139) and by Namita and Nakanishi (133) to include nets for which the plan projection is not necessarily orthogonal and in which load components in each co-ordinate direction are accounted for; the necessary system of equations being 3n in number, where n is the number of surface nodes. The general formulation is simplified by Ohyama and Kawamata to the case of orthogonal nets in which the horizontal components of load are sustained purely by independent variations in horizontal components of tension along each set of cables, and the objective quantity of the minimization is confined to the vertical components of unbalanced loads. Thus the variables determined in the first (least squares) stage are still the horizontal tension components at one end of each cable. In reference (133), however, the full set of equations is used, with the minimization expressed as:

$$\left[B_{Co}\right]^{T}\left[B_{Co}\right]\left\{T\right\} = \left[B_{Co}\right]^{T}\left\{P'\right\} \qquad (11)$$

where $\left[B_{Co}\right]$ denotes the complete direction cosine matrix, and $\left\{P'\right\}$ is the vector of nodal loads (modified to account for boundary conditions) in all co-ordinate directions.

Values of $\{T\}=\{T_o\}$ so obtained are then used as initial tensions for a finite deformation (N-R) elastic analysis which yields an equilibrium state with some changes of tensions $\{T\}=\{T_1\}$ and joint co-ordinates $[B_c]=[B_{c1}]$. The finite deformation analysis is then repeated with initial tensions set to $\{T_1\}$ and the shape restored as given by $[B_{co}]$. The process is repeated until $\{T_n \rightarrow T_{n-1}\}$ and $[B_c]=[B_{cn}]$. If, at this stage, any tensions are found to be negative they are re-set as positive and the finite deformation analysis is repeated, again with the initial shape restored to $[B_{co}]$.

None of the above least squares procedures ensures that a resulting equilibrating surface is the closest approximation which may be obtained to an originally proposed one (based usually on model measurements), because the optimization is made not for the surface shape with the given external loads but for the load distribution under the assumed surface shape. Nevertheless, a solution obtained in such a way does reflect the mechanical characteristics inherent in a proposed surface. The drawback of the methods is that the prestress distribution obtained can be rather random with large variations in tension components, and the slack lengths of the mesh will not be regular. The application of the methods is also restricted to structures with specified boundaries. Edge cables would for example couple the tension components of the network, and approximating the vertical equilibrium of the surface in addition to satisfying boundary equilibrium would be difficult.

A constrained and weighted optimization analysis has been proposed by Nakanishi and Namita (132) which seeks an overall compromise between a prescribed shape and force distribution and

the shape and forces which satisfy statical equilibrium. The objective function to be minimized takes the form:

$$R = \left\| \left[W_a\right]\left\{X-X_s\right\} \right\|^2 + \left\| \left[W_e\right]\left\{q-q_s\right\} \right\|^2 \qquad (12)$$

where $\{X\}$ is a vector of all nodal co-ordinates in the equilibrium state, $\{X_s\}$ is the proposed shape, $\{q\}$ and $\{q_s\}$ are the equilibrating and proposed tension coefficients, and $[W_a]$ and $[W_e]$ are respectively diagonal weighting matrices for the shape and force distributions.

The equilibrium co-ordinates are given by equation (5):

$$[H]\{X_i\} = \{P'_{xi}\} \qquad i = 1,2,3$$

and, since $[H]$ depends solely on the tension coefficients, q, equation (12) has only the vector $\{q\}$ as independent variables. Thus, the optimization problem is to calculate $\{q\}$ which minimizes the objective function R subject to the constraint that all $q>0$.

The method has the advantage that section properties of the members need not be given in advance, and members may be designed with suitable safety factors after the shape finding. In practical computations, however, q_s values are given by the prescribed tensions, T_s, divided by lengths, L_s, corresponding with the proposed shape. When equilibrium is finally achieved the actual tensions are given by $T_s.L/L_s$, where L are the final member lengths. In the above form, the optimization process does not therefore yield solutions which can correspond either with

geodesic or uniform mesh networks. To achieve this it would be necessary to apply additional constraints on tension coefficients.

Direct Shape Fitting

With least squares or alternative optimization procedures, large amounts of computing time and storage are required and there is insufficient scope for engineering intuition during these automatic processes. An alternative approach using dynamic relaxation may enable an equivalent fitting of model shapes which does not suffer these drawbacks:

With all nodes of the model accurately measured and a crude estimate made of the tension or strain distributions, a D.R. (or N-R) analysis can be carried out to obtain the redistributed equilibrium geometry and tensions. If the cable links (or membrane elements) are very flexible the resulting tension distributions may be smoothe but the shape will not comply well with the specified one. If, however, the links are very stiff, movements from the intended shape will only entail essential rigid modes but the tension distribution will be very irregular (as with least squares). A compromise in stiffnesses might be used or, if the shape must be fitted as accurately as possible, the process could be repeated iteratively using stiff links and returning at each stage to the specified initial geometry with starting tensions adjusted according to experience gained from previous stages. In essence this process corresponds with the method of Namita and Nakanishi (133) but may allow more realistic engineering control. Ideally, specified link stiffnesses (EA/L) should be fairly uniform for better numerical conditioning (see appendix D), and the process should benefit from the use of interactive facilities with continuous adjustments.

APPENDIX C

NON-LINEAR DYNAMIC ANALYSES

Although tension structures have always been recognised as particularly sensitive to dynamic loading, in contrast to methods for non-linear static analysis, where publications parallel and in many cases precede developments in more general finite element applications, there is a comparative dearth of published work concerning dynamic analyses for tension systems. For this reason the following review, though centred on tension structures, refers also to non-linear finite element formulations applied to the dynamic behaviour of other types of structure.

Dynamic analyses applicable to tension structures may be conveniently reviewed under the following classifications:

1. Modal Superposition Methods
2. Implicit Numerical Integration:
   a) Finite differences in space and time
   b) Finite difference temporal and finite element spatial idelaizations
   c) Finite elements in space and time
3. Explicit Integration Methods (with the same subdivisions as in 2.)

The suitability of each class of method depends on the degree of geometric and material non-linearity involved in the structural response and on the frequency of the fluctuating load component and its magnitude in comparison with the mean load component. Thus, for example, modal superposition methods may be most efficient when the frequency spectrum of the fluctuating component of load tends to excite only the lower natural modes of the structure and the mean load component is comparatively high or the degree of structural non-linearity is small. Implicit step-by-step integration methods may, however, be more efficient when the structural non-linearity is significant but mass, damping and stiffness coefficient matrices are symmetric. And explicit integration methods may be necessary when non-linearities, particularly on/off non-linearities such as cable or membrane slackening, are severe; when the applied loading tends to excite the higher natural modes; and when the structure interacts strongly with the surrounding environment such as, for example, in pneumatic

structures in which internal pressure variations, visco-elastic and pneumatic damping, and added mass effects of the surrounding air may be significant.

MODAL SUPERPOSITION ANALYSES

Although oscillations of cable networks and shear free membranes are non-linear, as a first approximation it is often assumed that oscillations due to buffeting wind loads are linear about the quasi-static equilibrium configuration defined by the mean component of wind loading, and that wind-structure interaction is not significant (96,90,123,178).

With the above assumptions, Knudson (96), has outlined and compared both deterministic and non-deterministic analyses for wind induced vibrations of typical cable networks. In both approaches the wind velocity, V, is divided into a mean component, $\bar{V}$, and a randomly fluctuating component v. The total pressure at any instant of time is given by:

$$P(x,y,z,t) = \tfrac{1}{2}\rho C_p(x,y,z)\left[\bar{V}(x,y,z) + v(x,y,z,t)\right]^2$$

where ρ is the air mass density and C_p is the normal wind pressure coefficient.

The mean pressure component is:

$$\bar{P}(x,y,z) = \tfrac{1}{2}\rho C_p(x,y,z)\bar{V}^2(x,y,z)$$

which may be added to dead and live loads to form a quasi-static load vector R with the equilibrium position found by non-linear iteration.

The fluctuating component is then given by:

$$P(t) = P(x,y,z,t) = \tfrac{1}{2}\rho C_p(x,y,z)\Big[2V(x,y,z).v(x,y,z,t) + v^2(x,y,z,t)\Big] \qquad (1)$$

And, assuming linear oscillations take place about the equilibrium position, the differential equation of motion is:

$$[M]\{\ddot{\delta}\} + [C]\{\dot{\delta}\} + [K]\{\delta\} = \{P(t)\} \qquad (2)$$

where $[M]$, $[C]$ and $[K]$ are respectively the mass, damping and stiffness matrices (w.r.t. the mean displaced position).

For free, undamped, vibrations: $[M]\{\ddot{\delta}\} + [K]\{\delta\} = \{0\}$

and substituting $\{\delta\} = \{\phi\}\mathrm{Sin}\omega t$ gives: $[K]\{\phi\} = \omega^2[M]\{\phi\}$ (3)

where, for any natural frequency ω_n, $\{\phi_n\}$ is the associated mode shape eigenvector. The use of a diagonal, as opposed to consistent, mass matrix simplifies this eigenvalue analysis.

By the mode superposition technique, the displacement vector $\{\delta\}$ in equation (2) is expressed as a linear combination of the modes of vibration:

$$\{\delta\} = [\psi]\{A\}$$

where $[\psi]$ is a square matrix formed as an array of successive mode shape vectors and $\{A\}$ represents the vector of modal amplitudes. Equation (2) thus becomes:

$$[M][\psi]\{A\} + [C][\psi]\{A\} + [K][\psi]\{A\} = \{P(t)\}$$

Premultiplying by the transpose of an arbitrary modal vector $\{\phi_n\}^T$ and using the orthogonality properties:

$$\{\phi_n\}^T[M]\{\phi_m\} = \{\phi_n\}^T[C]\{\phi_m\} = \{\phi_n\}^T[K]\{\phi_m\} = 0 \text{ for } m \neq n \quad (4)$$

results in a single uncoupled equation of motion for the nth mode of the system:

$$M_n^* . \ddot{A}_n + C_n^* . \dot{A}_n + K_n^* . A_n = P_n^*(t) \quad (5)$$

where $M_n^* = \{\phi_n\}^T[M]\{\phi_n\}$; $C_n^* = \{\phi_n\}^T[C]\{\phi_n\} = 2\varepsilon_n w_n M_n^*$;

$$K_n^* = \{\phi_n\}^T[K]\{\phi_n\} = \omega_n^2 M_n^* ; \quad P_n^*(t) = \{\phi_n\}^T\{P(t)\}$$

and ε_n and ω_n are the nth modal damping ratio and natural frequency. The inclusion of $[C]$ in the orthogonality relations assumes that coupling produced by damping is negligible. This is so if Rayleigh damping is assumed:

$$[C] = a_1[M] + a_2[K] \quad (6)$$

Though more complex forms of (6), which satisfy the orthogonality relations, can be formed by adding product terms:

$$a_3[K][M]^{-1}[K] \quad \text{or} \quad a_4[M][K]^{-1}[M]$$

When $[C]$ does not satisfy the orthogonality conditions the modal superposition method may sometimes be used by neglecting, in the product $[\psi]^T[C][\psi]$, the off-diagonal terms [199].

Equations (5) can be solved exactly using the Duhamel integral or, alternatively, by numerical integration; and because the periods of vibration for each natural mode are known it is possible to choose a time step for each integration which ensures the required accuracy. The most time consuming part of the analysis is the solution of the eigenvalue problem; but if the higher modes are known not to participate significantly in the response it may be sufficiently accurate to include only the lowest eigenvalues and vectors (53). For tension surface structures, however, mode shapes are complicated and it is necessary to include many modes to determine the response (96); in particular, all of the dominant modes normal to the surface which, because of the lightweight of such structures, are highly dependent on any temporary loads. Condensation of the degrees of freedom of a system before evaluation of eigenvectors is appropriate and Franchi and Scirocco (67) use this procedure for the analysis of plane cable trusses.

For the deterministic analysis of wind response the loading may be based on Taylor's hypothesis that the velocity fluctuations recorded at a point travel unchanged in the direction of the mean wind at mean velocity (96). To represent the wind therefore, a wind record is assumed to be incident upon the structure as a plane wave and is moved across the structure as a series of strips with the different velocities indicated by the wind record. An improved represention of the wind is obtained by dividing the structure into

several strips parallel to the mean wind direction, with each strip having its own wind record assumed to obey the Taylor hypothesis (99). A single record represents only one out of an ensemble of records, and thus deterministic response should be regarded mainly as a qualitative description of the expected peak response. An alternative approach to the problem of wind response is a non-deterministic analysis in which the wind is characterized spatially in terms of its velocity spectrum, and by use of the techniques of random vibrations the expected peak response is obtained (96). For such an analysis, however, $v^2(x,y,z,t)$ in equation (1) is ignored in order to make the forcing function linear.

The modal superposition method assumes that the behaviour of the structure is linear with the mass, damping and stiffness matrices constant. Provided displacements are not very large, the errors introduced by this assumption may be less significant than those due to uncertainty concerning wind loading and damping effects. Modjahedi and Shore (122) investigated the non-linear steady state response of cable networks by means of a fourth order perturbation method and found that tensions and deflections differed considerably from those predicted by linearized modal superposition analysis. The systems investigated, however, were very flexible and the forcing function was simple harmonic with large amplitude.

If it is assumed that mode shapes during non-linear displacements are described adequately by the eigenvectors $\{\phi\}$,

equation (5) may still be used if the stiffness (and mass) matrices are amended to account for deformations at adequate stages during the numerical integration. This process can be economic provided the response behaviour can be represented using a reduced number of eigenvectors (53). But because of their lightweight and flexibility tension structures can interact comparatively strongly with their surrounding environments which introduces a further source of non-linearity. Thus, for example, the forcing function P(t) may itself be dependent on modally coupled accelerations, velocities and displacements due to added mass effects, pneumatic damping and internal air pressure stiffening (89,90,195). This, together with the non-constant tangent stiffness of the system due to geometric and material non-linearities, makes necessary the use of direct numerical integration of the complete system of equations, either in coupled form by implicit matrix methods or by de-coupled, but simultaneous, explicit integration.

IMPLICIT NUMERICAL INTEGRATION METHODS

General dynamic response analyses for non-linear systems, using step-by-step numerical integration procedures, may be carried out by dividing the time history into a sequence of finite time increments and computing response at the end of any increment in terms of the initial conditions and the loading during the increment. Differences in the methods available depend on the assumptions made concerning the variations of displacements, velocities and

accelerations during the increments; and the methods may be appraised on the bases of stability, amplitude decay or attenuation, phase shift and economy of the integration procedure. The methods which have been most widely reported are the Hubolt (84), Newmark β(135), Central difference (184) and Wilson θ(186) methods; of which the first three are probably the most well established. These methods are outlined in the following sections and comparisons of accuracy, together with variants of the methods, are subsequently discussed.

Hubolt Integration Method

In the Hubolt scheme (184), expressions for velocities and accelerations are derived by fitting a cubic through the current and three previous displaced states. Thus if Δt denotes the time step and subscript i refers to increment number:

$$\{\dot{\delta}_{t_i+\Delta t}\} = \{\dot{\delta}_{i+1}\} = \frac{1}{6\Delta t}(11\{\delta_{i+1}\} - 18\{\delta_i\} + 9\{\delta_{i-1}\} - 2\{\delta_{i-2}\}) \quad (7a)$$

$$\{\ddot{\delta}_{i+1}\} = \frac{1}{\Delta t^2}(2\{\delta_{i+1}\} - 5\{\delta_i\} + 4\{\delta_{i-1}\} - \{\delta_{i-2}\}) \quad (7b)$$

Substituting in the equations of motion at time $(t_i + \Delta t)$:

$$[M]\{\ddot{\delta}_{i+1}\} + [C]\{\dot{\delta}_{i+1}\} + [K]\{\delta_{i+1}\} = \{F(t_{i+1})\} \quad (8)$$

gives the following recurrence equations for displacements:

$$(2[M] + \frac{11}{6}\Delta t[C] + \Delta t^2[K])\{\delta_{i+1}\} = (5[M] + 3\Delta t[C])\{\delta_i\} - (4[M] + \frac{3\Delta t}{2}[C])\{\delta_{i-1}\}$$
$$+ ([M] + \Delta t[C])\{\delta_{i-2}\} + \Delta t^2\{F(t_{i+1})\} \quad (9)$$

where $[M]$, $[C]$ and $[K]$ are the current mass, damping and tangent stiffness matrices at time t_{i+1}.

To start the Hubolt time stepping process, at t = 0:

$$\{\dot{\delta}_o\} = \frac{1}{6\Delta t}(2\{\delta_1\} + 3\{\delta_o\} - 6\{\delta_{-1}\} + \{\delta_{-2}\})$$

and $$\{\ddot{\delta}_o\} = \frac{1}{\Delta t^2}(\{\delta_1\} - 2\{\delta_o\} + \{\delta_{-1}\})$$

Non-Linear Effects

Since the tangent stiffness itself depends on $\{\delta_{i+1}\}$, for precise results, iteration by Newton-Raphson (89) or Modified Newton-Raphson (53) techniques is required within each time step; though since the time interval is small the latter procedure should normally be adequate with the stiffness being evaluated at the beginning of the interval (t_i), or at less frequent intervals than every time step when non-linearities are not large (120). An alternative, suggested by Stricklin (175), is to expand the R.H.S of (8) in a first order Taylor series about the previous time increment. Thus if $\{F(t,\delta)\}$ denotes all the non-linear terms in (8) as well as the forcing function vector then:

$$\{F(t,\delta)_{i+1}\} = \{F(t,\delta)_i\} + \Delta t \frac{\partial}{\partial t}\{F(t,\delta)_i\}$$

hence, using a first order backward difference expression to approximate the derivative:

$$[M_i]\{\ddot{\delta}_{i+1}\} + [C_i]\{\dot{\delta}_{i+1}\} + [K_i]\{\delta_{i+1}\} = 2\{F(t,\delta)_i\} - \{F(t,\delta)_{i-1}\} \qquad (10)$$

Use of (10) corresponds to linear extrapolation of the loads at the two previous increments. The advantage of the method is that no iteration is required for the non-linear solution, though smaller time steps are required compared with the methods using equilibrium iterations.

Newmark β Method

In the Newmark family of step-by-step methods two free parameters, γ and β, are introduced to indicate the effect of the acceleration at the end of a time interval on the relations for velocity and displacements during that interval:

$$\{\dot{\delta}_{i+1}\} = \{\dot{\delta}_i\} + (1-\gamma)\Delta t\{\ddot{\delta}_i\} + \gamma\Delta t\{\ddot{\delta}_{i+1}\} \qquad (11a)$$

$$\{\delta_{i+1}\} = \{\delta_i\} + \Delta t\{\dot{\delta}_i\} + (\tfrac{1}{2}-\beta)\Delta t^2\{\ddot{\delta}_i\} + \beta\Delta t^2\{\ddot{\delta}_{i+1}\} \qquad (11b)$$

If $\gamma > \frac{1}{2}$ spurious damping is introduced proportional to $(\gamma-\frac{1}{2})$, and with $\gamma < \frac{1}{2}$ negative damping is introduced which involves self excited vibrations arising solely from the numerical procedure. Thus γ is nearly always chosen as $\frac{1}{2}$, though an exception is a procedure described by Nagarajan and Popov (131) in which $\gamma = 0.5 + \delta$ and $\beta > 0.25(1+\delta)$. This scheme preserves unconditional stability (for linear systems) and the effect of $\gamma > \frac{1}{2}$ is to suppress undesirable higher mode contributions when time steps are large. The advantage of this is debatable (see later section), particularly in view of the fact that more widely verified techniques, such as the Hubolt method, have the same effect.

The most common forms of the Newmark β method, with $\gamma = \frac{1}{2}$, are:

$\beta = 1/4$ which corresponds to a uniform acceleration equal to the mean of the initial and final values. For linear systems this is unconditionally stable (i.e. numerical instability does not occur with large time steps)

$\beta = 1/6$ which corresponds to a linear variation of acceleration in the time step.

$\beta = 1/8$ which corresponds to a step function representing the acceleration, with a constant value equal to the initial acceleration in the first half of the time step, and a constant value equal to the final for the second half.

The latter two methods are only conditionally stable, though the linear acceleration method has the advantage of generally greatest accuracy.

Substituting equations (11) in (7), evaluated at three successive times t_{i+1}, t_i and t_{i-1}, gives the following recurrence relations:

$$\left([M]+\frac{\Delta t}{2}[C]+\beta\Delta t^2[K]\right)\{\delta_{i+1}\} = \left(2[M]-\Delta t^2(1-2\beta)[K]\right)\{\delta_i\}$$
$$-\left([M]-\frac{\Delta t}{2}[C]+\beta\Delta t^2[K]\right)\{\delta_{i-1}\} + \Delta t^2\Big(\beta\{F(t_{i+1})\}$$
$$+(1-2\beta)\{F(t_i)\} + \beta\{F(t_{i-1})\}\Big) \qquad (12)$$

Here again $[M]$, $[C]$ and $[K]$ are current to time t_{i+1}, and iterative or extrapolation methods are needed to cope with non-linearities as outlined previously.

Wilson-Farhoomand Θ Method

The linear acceleration method, corresponding to $\gamma = \frac{1}{2}$, $\beta = 1/6$ in the Newmark method, was modified by Wilson (186) to generate an unconditionally stable step-by-step algorithm for linear systems. A linear variation of acceleration was assumed over an interval $\tau = 2\Delta t$, and the solution at a time $t + \Delta t$ was then obtained using kinematic relations originating from the linear acceleration assumption. The disadvantage of the method was that it possessed inherent damping considerably greater than that required to suppress the spurious higher mode frequencies of discreteized systems. Farhoomand (131) further extended the method by assuming $\tau = \Theta\Delta t$, where Θ must be chosen with regard to the stability and accuracy of the integration. It has been shown by Bathe and Wilson (23) that Θ must be greater than 1.37 for unconditional stability of linear systems and that, although strong damping of the higher modes is retained, integration accuracy of the lower modes is much improved by an optimal choice of Θ. The Wilson Θ method has been applied by Argyris et al. (9) to the analysis of tension systems and compared with their own method of Finite Element in Time, which is considered in a subsequent section.

Central Difference Method

In the central difference method the expressions for velocities and accelerations at time t_i are:

$$\{\dot{\delta}_i\} = \frac{1}{2\Delta t}(\{\delta_{i+1}\} - \{\delta_{i-1}\}) \tag{13a}$$

$$\{\ddot{\delta}_i\} = \frac{1}{\Delta t^2}(\{\delta_{i+1}\} - 2\{\delta_i\} + \{\delta_{i-1}\}) \tag{13b}$$

Substituting these expressions into the equation of dynamic equilibrium (8), but written for time t_i, gives the recurrence relations:

$$([M]+2\Delta t[C])\{\delta_{i+1}\} = (2[M]-\Delta t^2[K])\{\delta_i\}$$

$$+ (\frac{\Delta t}{2}[C]-[M])\{\delta_{i-1}\} + \{F(t_i)\} \tag{14}$$

In this case, $[M]$, $[C]$ and $[K]$ are current to time t_i and thus no iteration within each time step is required to cope with non-linear effects. For this reason the method is termed "explicit". To achieve the same accuracy as the implicit methods, however, a smaller time step is required and for stability of the process the value of this is governed by the highest natural frequency of the system (107).

Finite Elements in Time

All of the previous methods make use of a finite difference temporal idealization, together with either a finite difference or finite element spatial idealisation in forming the coefficient matrices $[M]$, $[C]$, $[K]$; usually the latter. The concept of finite time elements was introduced by Fried (69) who assumed that displacements during any time step varied as a cubic function of the displacements and velocities at the beginning and end of the increment. For linear systems this enabled a number of time steps, n, to be interconnected within multiple steps resulting in a system

of $2n \times N_d$ linear equations for the displacements and velocities: $\delta_i, \dot{\delta}_i, \delta_{i+1}, \dot{\delta}_{i+1} \ldots\ldots \delta_{n-1}, \dot{\delta}_{n-1}$, where N_d is the total number of degrees of freedom. This enabled more accurate results but entailed very large computer storage requirements and was thus inefficient. Fried therefore recommended that a stepwise solution process should be used, which had the further advantage that non-linear problems could be analysed using iteration within each step. Argyris et al. (7,9) extended this concept by assuming the inertia forces, $\{R\} = [M]\{\ddot{\delta}\}$, to vary cubically within each time step as functions of their values and derivatives at the beginning and end of the increment. The necessary relations are:

$$\{\dot{\delta}_{i+1}\} = \{\dot{\delta}_i\} + \frac{\Delta t}{12}[M]^{-1}\left(6\{R_i\} + \Delta t\{\dot{R}_i\} + 6\{R_{i+1}\} - \Delta t\{\dot{R}_{i+1}\}\right) \tag{15a}$$

$$\{\delta_{i+1}\} = \{\delta_i\} + \Delta t\{\dot{\delta}_i\} + \frac{\Delta t^2}{60}[M]^{-1}\left(21\{R_i\} + 3\Delta t\{\dot{R}_i\} + 9\{R_{i+1}\} - 2\Delta t\{\dot{R}_{i+1}\}\right) \tag{15b}$$

where: $$\{R_{i+1}\} = -\{R_{si}\} - [\bar{K}]\{\Delta\delta\} - [C]\{\dot{\delta}_{i+1}\} + \{F(t_{i+1})\} \tag{16}$$

and $$\{\dot{R}_{i+1}\} = -[K_{i+1}]\{\dot{\delta}_{i+1}\} - [C]\{\ddot{\delta}_{i+1}\} + \{\dot{F}(t_{i+1})\} \tag{17}$$

where $\{R_{si}\}$ is the internal elastic restoring force at time t_i, and $\{R_{i+1}\}$ and $\{\dot{R}_{i+1}\}$ are preferably assembled elementwise to avoid storage of the global matrices $[C]$ and $[K]$. In (16) $[\bar{K}]$ is the average stiffness for the increment $[K_i + K_{i+1}]/2$.

Equations (15) cannot be solved directly since they are dependent on the inertial force and its derivative at t_{i+1}. Hence an iterative solution for each time step is necessary:

starting from the state at t_i it is assumed that $\{\dot{R}_{i+1}\}=\{\dot{R}_i\}$ and $\{R_{i+1}\}=\{R_i\}+\Delta t\{\dot{R}_i\}$ as a first approximation. This enables $\{\delta_{i+1}\}$, $\{\dot{\delta}_{i+1}\}$ and $\{\Delta\delta\}$ to be calculated from equations (15). Whence $\{R_{i+1}\}$ (a second estimate) may be evaluated from (16), and $\{\dot{R}_{i+1}\}$ from (17) using $\{\ddot{\delta}_{i+1}\} = [M]^{-1}\{R_{i+1}\}$. The procedure is repeated until the results converge, with the end values of one time increment becoming the initial values of the next. The mass matrix may be assumed constant during the complete time sequence, in which case after initial inversion no further matrix inversions are required in the iterative loops. Using the above procedure for the analysis of cable networks, Knudson (99) found that for stability the time step should be less than about half of the smallest period of the system.

Loading and Coefficient Matrices

With numerical integration of the complete system of non-linear equations the loading at any time must be defined explicitly. Non-deterministic loading may, however, be partly accounted for by generating a time series for a typical load model that corresponds with a specified power spectral density (44). Numerical integration then accounts for the structure response. The damping matrix $[C]$ may be derived either as a linear combination of the stiffness and mass matrices (53) or, more conveniently in practice, from modal damping ratios (187). With implicit methods it is difficult to form damping matrices based on the fundamental properties of the structural material, and it is customary, therefore, to establish damping properties by comparison with damping observed in similar structures. Usually effective damping ratios are measured in several modes of vibration and assumed similar to the system being analysed.

If both the mass amd damping matrices are diagonal (as opposed to consistent) then the central difference method (Eq.14) and the method of finite elements in time (Eq. 15) can be handled as direct explicit methods without the need to form or store any of the coeffecient matrices. This does not in fact preclude the use of internal damping due to visco-elastic effects since strain rates may be approximated either by an Euler (117) or central difference formulation (17). These and other direct methods are reviewed in the following section.

EXPLICIT DIRECT INTEGRATION

Central Difference Method

The most convenient direct form of the central difference method is identical to the interlacing D.R. procedure outlined in the main text, with nodal forces compounded using natural stiffness of the structural elements in separated form. The use of such a scheme, with velocities calculated at the mid-points of time intervals, also readily permits the inclusion of real material damping due to visco-elastic behaviour as outlined in Chapter 5 (17). Similar schemes, though without damping and the use of natural stiffnesses, have been given by Witmer et al. (188) and Pian et al. (149) for the analysis of circular rings and beams using a finite difference spatial idealization, by Oden et al. (138) and Benzley and Key (28) for the analysis of non-linear membranes idealised respectively into constant strain and cubic curvilinear

isoparametric elements, and by Krieg and Key (103) for the investigation of transient shell response. Belytschko et al. (26,27) use a fully direct central difference integration scheme for the analysis of a very large soil/structure interaction problem with explosive loading, idealized as a mesh of plane finite elements. They incorporate Coulomb friction effects for sliding interfaces and artificial viscous damping to reduce spurious oscillations of high frequency components. The latter damping is expressed as a proportion of critical for the highest modes and introduced through element stress rates. The convected co-ordinate system which they use for generating element stiffnesses (for beam, triangular and rectangular elements) permits gross deformations though, in contrast to the use of natural stiffnesses (17), is restricted to the case of small strains.

Higher Order Methods

The central difference method corresponds to a lumped impulse procedure (30), with constant acceleration during a time step equal to the initial value. Chaudhury, Brotton and Merchant (52) use an interlacing version of the Newmark linear acceleration method ($\beta = {}^{1}/_{6}$):

With linear accelerations assumed in the interval $t - {}^{\Delta t}/_{2}$ to $t + {}^{\Delta 2}/_{2}$ velocities are calculated at these mid-intervals and displacements and accelerations at the end t, $t + \Delta t$.... The scheme is then approximated to give an explicit method:

1. Calculate $\{\dot{\delta}\}_{t+\Delta t/2} = \{\dot{\delta}\}_{t-\Delta t/2} + \Delta t\{\ddot{\delta}\}_t$

2. Evaluate member forces and residuals $\{R\}$ at $t+\Delta t$ using the approximation:

$$\{\delta\}_{t+\Delta t} = \{\delta\}_t + \Delta t\{\dot{\delta}\}_{t+\Delta t/2}$$

$t=t+\Delta t$

3. Calculate $\{\ddot{\delta}\}_{t+\Delta t}$ from $[M]\{\ddot{\delta}\}_{t+\Delta t} = \{F\}-\{R\}-[C]\{\dot{\delta}\}_{t+\Delta t}$

with approximation: $\{\dot{\delta}\}_{t+\Delta t} = \{\dot{\delta}\}_t + \frac{\Delta t}{2}\{\ddot{\delta}\}_t$

4. Calculate $\{\delta\}_{t+\Delta t} = \{\delta\}_t + \Delta t\{\dot{\delta}\}_{t+\Delta t/2} - \frac{\Delta t^2}{24}\{\ddot{\delta}_t - \ddot{\delta}_{t+\Delta t}\}$

The difference between the above scheme and the velocity formulated central difference process is essentially step (4). It may be noted that the approximation in (3) affects only the damping force and that the approximation in (2) is not cumulative since $\{\delta\}_{t+\Delta t}$ is recalculated at step (4). The method was applied in reference (52) to non-linear dynamic analysis and, with high viscous damping, to obtain the static solution of a portal frame problem. It was compared with the Newmark implicit integration method and considered to be more efficient.

Harztman and Hutchinson (77) investigating the transient analysis of plane structures subject to material and geometric non-linearity used the following 3rd order algorithm:

$\{\ddot{\delta}\}_t = (\{F\}_t - \{R\}_t)/m$ (lumped masses and therefore no mass matrix inversion)

$$\{\dot{\delta}\}_t = \{\dot{\delta}\}_{t-\Delta t} + \frac{\Delta t}{12}\left[5\{\delta\}_t + 8\{\ddot{\delta}\}_{t-\Delta t} - \{\ddot{\delta}\}_{t-2\Delta t}\right]$$

$$\{\delta\}_{t+\Delta t} = \{\delta\}_t + \Delta t\{\dot{\delta}\}_t + \frac{\Delta t}{6}\left[4\{\ddot{\delta}\}_t - \{\ddot{\delta}\}_{t-\Delta t}\right]$$

$$\{\Delta\delta\}_t = \{\delta\}_{t+\Delta t} - \{\delta\}_t$$

Hence incremental and total strains

Hence incremental and total stresses

Hence internal forces $\{R\}_{t+\Delta t}$

For calculating element stiffnesses and hence nodal forces they used a convected co-ordinate system which allowed for the development of fairly large plastic strains; the elastic and plastic strain increments being updated in parallel and assumed to be additive.

Fu (70) developed a self starting explicit integration method with a 4th order (global) truncation error. The method was applied to obtain both transient and damped static solutions for a pressurized cylindrical shell. Numerous other integration methods exist, such as the Runge-kutta methods and the Adams, Milne and Moulton predictor-corrector methods (85). All of these fourth or fifth order methods however, whilst more accurate than the 2nd order central difference procedure, require a smaller time step for stability and involve more complex computations.

Euler Methods

Because of its simplicity when applied to direct integration of structural problems, particularly when dealing with creep and plasticity effects, a number of researchers have preferred a first

order Euler extrapolation technique. Koenig and Davids (100,101) describe such a process for the transient analysis of internally damped, shear corrected, beams and plates; and also derive non-linear static solutions using viscous damping. Malone and Connors (117) generalized this procedure, for the anlaysis of finite element plane stress/plane strain problems, to account for creep and plasticity effects. With equations of dynamic equilibrium in the form:

$$[M]\{\ddot{\delta}\} = \{F_\varepsilon\} - \{F_I\}$$

internal forces, $\{F_I\}$, are computed using characteristic matrices for each element which give strains and strain rates in terms of nodal displacements and velocities, and nodal forces in terms of generalized stress quantities derived from elastic strain components. The computation procedure takes the following form:

Initialization: Form characteristic element matrices

Loop on Time

Loop on Elements

Kinematics: Compute element strains and strain rates

Material: Compute element stresses using appropriate constitutive relation

Equilibrium: Form internal force vectors and system internal force vector

Integration: Form accelerations and extrapolate to velocities and displacements at next time increment

The above technique was applied to the transient response of an earth dam subject to ground accelerations, with damping accounted for by means of a three element visco-elastic model. A model was also given for Coulomb damping (117).

A more accurate iterative Euler scheme (predictor-corrector) was used by Myklestad and Lawrence (130) for transient beam response calculations: Accelerations at a time t were assumed constant and integrated over the time interval to obtain a first estimate of displacements and velocities at time $t + \Delta t$. The moments and shears calculated from these displacements then gave a first estimate of accelerations at time $t + \Delta t$, and an improved estimate of displacements was obtained using the average of accelerations at t and $t + \Delta t$. Iteration was continued until no significant change in results was observed and the resulting quantities were then used as initial values for integration over the next time step.

Of the available explicit methods the central difference process has been most widely applied and lies, in terms of accuracy and complexity, between the simple Euler method and the higher order of predictor-corrector methods. It has also been shown by Krieg (102) to have the highest stable time step.

COMPARATIVE STUDIES OF INTEGRATION METHODS

For the transient analysis of simple cable structures subject to gross deformation, Argyris et al. (9) have compared the Wilson θ

method with their method of finite time elements with cubic acceleration formulated as both a direct and a matrix method. A fourth order Runge-Kutta explicit integration scheme was used as the basis for comparison; the latter method, with a very small time interval, being assumed exact. The methods were tested for plane network strucutres in which cables could slacken and compared with the same network with compression allowed in the links so that no buckling occurred. With buckling, smaller time intervals were necessary and the Wilson θ method (unconditionally stable for linear problems) became unstable with a sufficiently high time interval. At the same interval the direct integration method and the matrix method were stable; the former being considerably more accurate than the latter. Without buckling, however, the Wilson method was stable for time steps of 3 x the maximum value at which the direct integration method became unstable. There was, in this case, considerable period elongation such that after only $4\frac{1}{2}$ periods of vibration the system was exactly opposite in phase to the exact solution.

Other than the above study, which demonstrates the limitations, when applied to non-linear problems, of methods traditionally assumed unconditionally stable, there have been no reported stability and accuracy comparisons of different integration schemes applied to tension structures. A large number of comparisons have, however, been carried out for other non-linear systems idealized into finite elements; particularly in relation to dynamic buckling of a spherical shell cap subject to geometric and/or material non-linearity (24,175, 131,120). Stricklin et al. (175) examined the Hubolt and Newmark

mean acceleration methods (both unconditionally stable for linear problems), and found that with sufficiently high time intervals both methods became unstable; though the Hubolt method was stable for time intervals 3 x the maximum stable values for the Newmark method. The Hubolt method, however, exhibited considerable amplitude decay and the instability was caused largely by the load extrapolation technique used. Bathe et al. (24) examining the same problem with the Wilson θ and Newmark methods found that both approaches required equilibrium iterations at each time step to avoid large errors or instability. McNamara and Marcal (120) used the Hubolt scheme cast in incremental form with following load correction terms to account for the lack of balance at the beginning of a time step. Controls were introduced to avoid the generation of the stiffness matrix at every time step and thus uncouple the physical modelling from the smaller time step required for numerical accuracy. They found that this scheme, with reassembly every five time steps and load corrections at every step, was stable for time intervals 6 x the critical value for central difference integration, and that, for the same accuracy, the scheme allowed time steps an order of magnitude greater than the Hubolt scheme with load extrapolation and a total displacement finite element formulation.

Computational Efficiency

Concerning the efficiency and accuracy of the various integration schemes, opinions differ; particularly on the question of the relative merits of implicit and explicit methods. Wu and Witmer (191) investigating the response of impulsively loaded beams

undergoing elastic-plastic material behaviour compared the central difference explicit method with the Hubolt and Newmark mean acceleration implicit methods. Reliable results by the central difference method were obtained using a time interval 99% of the critical value, and results of similar accuracy were obtained by the Newmark and Hubolt methods with time intervals respectively two and four times this value. With higher time intervals the results using implicit methods degraded badly. They concluded that, despite its contamination by artificial viscosity, the Hubolt method was probably most efficient. For a similar problem, however, Weeks (184), using large but stable and identical time steps for all three methods, considered that the Hubolt method was too damped to be of any value. Results obtained by the central difference and Newmark methods were both acceptable, though the former exhibited artificial attenuation and the latter some phase shift. With large time steps all of the methods were found to be unstable when using load extrapolation, and although the implicit methods became stable if equilibrium iterations were applied they were computationally more efficient with smaller time steps and extrapolation. Weeks concluded that the central difference method was most efficient for such problems. Park (147) also compared the Hubolt and Newmark mean acceleration methods for non-linear problems and found that whilst the former was unconditionally stable, the latter was not. In order to counteract the artificial viscosity in the Hubolt method he introduced a modification which induced negative damping. The generality of this process is, however, questionable.

For the analysis of flexible membrane structures, Oden et al. (138) suggest that the advantage of unconditional stability in some implicit methods is overshadowed by the need to solve a complete set of simultaneous equations at each step, and that the time step required for accurate modelling is usually as small as that required for numerical stability of explicit schemes. Krieg and Key (103) compare the accuracy of explicit central difference integration with a family of implicit schemes for modelling the frequency response of membrane and bending deformations. For equal computational work the central difference process with lumped masses is shown to be more efficient than the best available implicit scheme. Johnson and Grief (93) consider a wider class of problems and conclude that the central difference process is most efficient when the response varies rapidly, whereas the Hubolt method is more efficient for slowly varying response. For tension structures involving gross deformation, and where the state may change significantly from one time step to another due to cable slackening or membrane buckling, it thus appears that explicit methods are likely to be most efficient.

Artificial Viscosity and Structural Idealization

The maximum time step in conditionally stable methods is governed by the highest frequency of the system, which in turn may be dependent on the use of a fine mesh idealization in localized areas, yet the overall dynamic response may be governed largely by the lower dominant modes of the system. Unconditionally stable implicit methods generally allow higher time intervals but in doing so may filter out the high frequency responses. Associated with this filtering out effect is an artificial damping of the system which

results in amplitude decay and period elongation. This occurs for example in the Hubolt and Wilson θ methods. In the Newmark method with β = 1/4 period elongation occurs but without amplitude decay. The high frequency responses in the latter case are not filtered out and large errors may occur in their associated periods.

Bathe and Wilson (23) and Nagarajan and Popov (131) suggest that the filtering out of the high frequency response from a solution may be beneficial since it allows one to obtain, with a relatively large time step, a total system solution in which the low mode response is accurately observed. In this case numerical integration methods for non-linear systems are quite equivalent to a mode superposition analysis (for linearized systems) in which only the lowest modes of the system are considered.

In view of the above considerations it would seem appropriate to use fictitious masses in explicit integration methods such that higher time intervals may be used whilst retaining true mass components associated with the more flexible degrees of freedom of the system. Thus the dominant frequencies should be preserved and, in effect, the procedure should have an effect equivalent to the methods of reduction for modal superposition analyses. For tension surface structures such as spatially curved networks or membranes this would entail the use of a variable co-ordinate system with one axis always normal to the surface. Mass components associated with the normal direction would then take their true values, with the other components being chosen to satisfy stability for a time step governed by the highest frequency normal to the surface.

APPENDIX D

REVIEW OF DYNAMIC RELAXATION AS AN ITERATIVE METHOD AND THE CHOICE OF OPTIMUM ITERATION PARAMETERS

The development of DR is reviewed and compared analytically with other iterative methods. Techniques for selecting the optimum mass and damping coefficients are discussed, and the continuous alteration of these parameters in highly non-linear problems is considered.

The concept of Dynamic Relaxation as an explicit solution technique for the static behaviour of structures originated from an analogy drawn by A.S. Day with tidal flow computations he had previously carried out with J.R.H. Otter (140). Equations of fluid motion and continuity were replaced respectively by equations of damped structural motion and the constitutive equations of elasticity in separated form; the latter being permitted by the use of a central difference formulation. The non-linear static solution of structural problems was then regarded as the limiting equilibrium condition of heavily damped structural vibrations. Newmark (135) had previously commented on the possibility of obtaining static solutions in this way, but his suggested use of an implicit integration scheme put the technique at a disadvantage compared with the standard matrix methods for non-linear structural analysis and DR in explicit form (114). In the earliest applications of DR (141,60), stress increments were determined from velocities and it was possible for small round-off errors to accumulate. Subsequently the method was amended so that stresses were calculated at each stage from the total displacements, thus precluding these errors (143).

The most common form of DR, using both a spatial and temporal finite difference idealization, has been applied to a variety of linear elastic problems including, at an early stage, pressure vessels (141), cylindrical arch dams (143), thin plates

(61, 156), thin shells (49) and orthotropic sandwich plates (22). Non-linear material effects were first included by Holland (83) who examined local stresses in prestressed concrete end blocks up to cracking of the concrete. Large deflection behaviour of plates under in-plane transverse loads has been examined by Rushton (157,158) using both stress function and displacement solutions, again cast in finite difference form.

Finite element spatial idealizations of DR have been less widely used, though Day included an illustration for linear plane frames in his original paper (60). Lynch, Kelsey and Saxe (114) applied DR to two dimensional finite element analyses using constant strain triangular elements and an overall stiffness matrix formulation. Brew and Brotton (34) used the method for the analysis of plane frames subject to large deflections, elastic instability and plasticity. Their formulation employed separated equations of equilibrium and compatibility (or motion) and did not require the formation of an overall stiffness matrix.

The first application to tension structures with geometrically non-linear behaviour was published by Day and Bunce (62). They described the analysis of an initially plane, unstressed, rectangular cable net subject to a central point load, and emphasised particularly the advantages of the method in dealing with zero stiffness situations which in implicit analyses would lead to a singular stiffness matrix. The application of DR to form-finding and the analysis of spatial networks and membranes was reported on by the author (13). And subsequent papers on the subject form the main chapters of this thesis.

Assessment of DR as an Iterative Method

Theoretical assessments of DR as a simultaneous method, the choice of optimum iteration parameters relating to time interval, mass components and damping factor, and comparisons of convergence rate with previously developed standard iterative methods, have been given by a number of authors. For the most part these assessments have been restricted to finite difference spatial idealizations of linear elastic structures with particular types of mesh and governing equations.

Otter, Cassell and Hobbs (143), using a finite difference idealization, considered the progress of the calculations as a wave which must outrun the wave corresponding to the physical problem and used an expression for the critical time step given by Forsythe and Wasow (66). If C denotes the faster velocity of either the pressure or shear wave, which depends on the elastic constants and mass density of the structural material, the critical time step is given by:

$$\Delta t < \frac{1}{C}\left[\left(\frac{1}{\Delta x_1}\right)^2 + .. + \left(\frac{1}{\Delta x_m}\right)^2\right]^{-1/2}$$

where Δx_1 .. Δx_m are respective mesh lengths in co-ordinate directions 1 .. m.

In the same paper, assuming an exponential function for the damped wave equations, the following expression for the optimum convergence rate of DR was obtained:

$$\lambda = \frac{2-K'_{cr}/2}{2+K'_{cr}/2}$$

where λ is the ratio of successive error vectors and K'_{cr} is as defined in the text of this thesis, with the subscript cr denoting critical damping in the fundamental mode; the latter being derived by trial runs.

Dynamic Relaxation was shown to be equivalent to the Frankel or second order Richardson iteration (68), and a comparison of the above convergence rate with those for the three basic iterative methods, namely the Jacobi, Gauss-Seidel and Successive Over-Relaxation iterative methods, was also given for the particular case of the two-dimensional Laplace equation in finite difference form. It was concluded that SOR has a faster convergence rate for linear problems of this type, but that DR had alternative advantages in its capacity to deal with complex problems through the simplification of boundary conditions resulting from the use of separated equations. In the discussion of the paper (143) Welch and Postlthwaite suggested the use of fictitious densities or mass components such that the time interval was the same proportion of the critical value for each degree of freedom; this having the effect of better conditioning the system of equations. This was later investigated by Rushton (157) and Cassell (50) and has subsequently been used in the majority of applications.

Further comparisons of DR with the basic iterative methods using finite difference formulations have been given by Wood (143 , 189), Otter (142) and Cassell et al (49,51). Cassell (50) also gives a comparison of DR with the Frankel iteration scheme to obtain optimum parameters. A similar comparison, in finite element form, is given in a subsequent section. Hodgkins shows that DR is similar to the Chebyshev semi-iterative method provided that mass components are adjusted so that they are proportional to the direct stiffness components. The Chebyshev iteration incorporates a variable "damping" which starts at zero and is increased progressively to a steady value in order to optimize convergence, and Hodgkins suggests that the rate of convergence of DR might analogously be increased by using non-linear damping or internal damping. (The latter aspect is considered in Chapter 5, though there it is the real material damping). Hussey (143) and Wood (190) also compare DR with a degenerate Chebyshev iteration, and the latter shows that DR has a faster rate of convergence by a factor of $\sqrt{2}$ for well triangulated structures. This comparison assumed the use of fictitious mass components equal to the corresponding row sum of moduli of elements of the stiffness matrix, and damping and time interval optimized as in the Frankel iteration scheme in terms of the maximum and minimum eigenvalues (see following section).

The determinations of critical time steps have in general been based on similar considerations to those originally given by Otter, including cases where stability is governed by flexural waves (157). Essentially, the time step is dependent on both the highest and lowest eigenvalues of the system, but in cases where these values differ considerably, which is normally so with finite difference formulations, this reduces to the physical heuristic of the progress of calculations outrunning the physical wave, for which simple expressions are available.

The determination of the critical damping factor is a more difficult task since it entails the prior determination of the lowest natural frequency of the system. For structures which are not grossly non-linear a standard eigenvalue analysis may be carried out and, since only the lowest frequency is required, this may be achieved with reasonable economy (30). Most investigators, however, have based the estimate of K_{crit} on inspection of the deflection output obtained from an undamped or lightly damped trial run. Rushton (156) suggests tracing the total kinetic energy of the system which has the advantage that the first peak may be obtained in approximately $\frac{1}{4}$ of the fundamental period, as opposed to $\frac{1}{2}$ the period required for deflections. In either case, however, the traces obtained may be somewhat irregular and require several periods to enable a reasonable estimate of the lowest frequency component. An alternative to this simple inspection process is to decompose the traces at one or more nodes by fourier analysis (114).

This was shown in Appendix 2.1 to provide an accurate value and does not require much computation. Furthermore it gives an estimate for other dominant frequencies which, particularly for tension systems and lightweight dynamically responsive structures in general is necessary design information.

Comparisons of DR with other iterative methods using a finite element spatial idealization have been given by Lynch, Kelsey and Saxe (114) and Brew and Brotton (34). In both cases a more general assessment than other finite difference comparisons is given since the problem is posed in matrix form as the solution to a set of linear equations, with the iteration scheme analysed by considering displacement error vectors. For linear systems it was concluded by both groups that SOR had a convergence rate twice that of DR. The theoretical assessment was not extended to non-linear systems though on the basis of numerical comparisons for such problems Brew and Brotton suggest that DR is more stable with greater control on the path to solution. They also investigated DR used in successive form, as opposed to the standard simultaneous form, and found the method to be as fast as SOR; though the advantage of greater stability of the process would presumably not then apply (35).

DR solutions for linear plane frames were also compared by Brew and Brotton with a direct stiffness solution and the latter was found to be two or three times more efficient; though strict comparison was not viable since the stiffness program was developed to a more sophisticated level. For non-linear frames a matrix iteration scheme with incremental loading (121), again more highly developed than the DR program, was found to be more efficient for

small non-linearities but less efficient when the non-linearities became more pronounced. Mass components in the DR process were taken as proportional to the corresponding leading diagonal of the stiffness matrix, and for non-linear sway frames without cross-bracing the conditioning of the system of equations was further improved by the use of "block operations". For such frames the overall lateral stiffness is low, but for a chosen value of time step, fictitious masses in the sway direction would be governed by axial stiffness of the cross beams. Since this is high the mass components for lateral movement of the columns would also be high and thus the fundamental period and the necessary time for convergence to a solution would be increased. This problem was avoided by changing the variables such that the column sways were combined into one degree of freedom, and relative motions were accounted for as separate degrees of freedom with differing fictitious masses associated with them. Mathematically this corresponds to changing the co-ordinates of the system to something more nearly approaching normal co-ordinates. A similar problem which occurs in some double layer tension systems with stiff spreaders or short ties was indicated in Chapter 3 and solved using fictitious stiffnesses and a force transfer process. Whilst this provided a general approach independent of member orientation it suffered from the need for the calculations to be critically damped.

Lynch et. al. gave a very comprehensive comparison of DR in finite element matrix form with the basic iterative methods.

A comparison of the standard explicit central difference form of DR with an implicit form was also given and the latter was shown to be less efficient. The explicit form was then applied to a series of plane stress problems with cut-outs using simple triangular finite elements. A major feature of their investigation, referred to in a subsequent section, was the use of an on-going alteration of the iteration parameters.

Both of the investigations of DR in finite element form referred to above obtained optimum iteration parameters (relating to time interval and damping factor) each of which were functions of the maximum and minimum eigenvalues, implying the need for prior or on-going determination of these values for efficient convergence. The simpler criterion for the time interval derived in Chapter 2 (14) by considering relative nodal velocities in the limiting condition is, however, direct and has been found to be accurate. In the following two sections this approach is correlated with the optimum parameters for the Frankel iteration, and a direct, or non-matrix, derivation of convergence rate.

Choice of Optimum Iteration Parameters by Comparison with the Frankel Iteration

From Chapter (2) Equation (3a), adjusted to account for fictitious masses at each node in each co-ordinate direction:

$$V_{xi}^{t+\Delta t/2} = A'_{xi} . R^{t} + B' . V_{xi}^{t-\Delta t/2}$$

where $A'_{xi} = \dfrac{\Delta t}{M_{xi}(1+K'/2)}$; $B' = \dfrac{1-K'/2}{1+K'/2}$

Multiplying by Δt gives a recurrence equation for displacement increments:

$$\Delta\delta_t^{t+\Delta t} = \frac{\Delta t}{M(1+K'/2)} \cdot R^t + \frac{(1-K'/2)}{(1+K'/2)} \cdot \Delta\delta_{t-\Delta t}^{t} \qquad (1)$$

where suffixes xi have been omitted for convenience.

Equation (1) has been defined as dynamic iteration by Otter et al. (143). It was first proposed as a recursion formula by Frankel (68) with the optimum form of the iteration given by

$$\Delta\delta_n^{n+1} = \left[\frac{2}{\sqrt{a}+\sqrt{b}}\right]^2 \cdot R^n + \left[\frac{\sqrt{a}-\sqrt{b}}{\sqrt{a}+\sqrt{b}}\right]^2 \cdot \Delta\delta_{n-1}^{n} \qquad (2)$$

Comparing (1) and (2) gives:

$$\frac{\Delta t^2}{M} = \frac{4}{a+b} \qquad (3) \qquad \text{and } K' = \frac{4\sqrt{ab}}{a+b} \qquad (4)$$

where a and b are respectively the numerical values of the smallest and largest eigenvalues of the stiffness matrix of the structure being considered.

An upper bound for b may be determined by Gershgorin's theorem (50) provided the stiffness matrix is symmetric with a dominant leading diagonal:

$$b < b_G = \max_{j=1,n} i \; \Sigma |S_{ij}|$$

where S_{ij} are all the elements in row i of the stiffness matrix, and the largest numerical sum (for any i) is taken.

If all other masses, M_k, are adjusted so that:

$$\frac{M_k}{\Sigma|S_{kj}|} = \frac{Mi}{b_G} = \frac{M}{\Sigma|S|}$$

and the structure is such that $a + b < b_G$ with $a \ll b$, which will often be the case, then (3) gives

$$\Delta t < \sqrt{\frac{4M}{\Sigma |S|}} \qquad (5)$$

This may be compared with the criteria derived directly in Chapter (2):

$$\sqrt{\frac{2M}{S}} < \Delta t_{crit} < \sqrt{\frac{4M}{S}} \qquad (6)$$

Here, however, S is the direct stiffness (or leading diagonal component) relative only to adjacent nodes, and when all mass/direct stiffness ratios are adjusted to be identical the lower bound, $\sqrt{2M/S}$, is the appropriate criterion. The drawback of (5) is that a lower bound to Δt_{crit} is not available, though for the majority of structures with dominant diagonal stiffness components the value of Δt given by (5) will lie between the limits of (6). For cable network and shallow membrane structures, however, this will usually not be so. Davidson (50), describing shell buckling analysis by DR, gives an "initial disturbance" process for calculating $\Delta t_{crit} = \sqrt{4M/S}$. This, however, fails when mass components are optimized.

An alternative expression for the critical time interval is:

$$\Delta t_{crit} = \frac{1}{\pi . f_{max}}$$

where f_{max} is the maximum frequency of vibration.

From (4) if $a \ll b$: $K' \doteq 4\sqrt{(a/b)}$

which, if all mass components are made proportional to the corresponding direct stiffness components, may be expressed as:

$$K' \doteq 4\frac{f_{min}}{f_{max}} \doteq 4\pi f_{min} \cdot \Delta t_{crit} \qquad (7)$$

This agrees with the optimum value of K' based on the dynamic heuristic of critically damping the fundamental mode. Rushton (156) shows that when this is so all other modes are adequately damped in converging to a solution.

Convergence Rate

The optimum assymptotic convergence rate of the DR iterative procedure may be examined in the following way, which corresponds with the direct derivation of the time interval criteria given in Chapter 2, without recourse to matrix eigenvalue analysis.

If the mass/stiffness ratios of all nodes of the structure in each co-ordinate direction are made identical, then the expression for relative velocities of adjacent nodes i and k in successive time intervals, as given by equation (16) in Chapter (2), may be multiplied by Δt to give corresponding relative deflection increments:

$$\Delta\delta_{xik}^{t+2\Delta t} - (B'+1).\Delta\delta_{xik}^{t+\Delta t} + B'.\Delta\delta_{xik}^{t} = -A'_{xi}.\Delta t(S_{xi}.2\Delta\delta_{xik}^{t+\Delta t})$$

where $\Delta\delta_{xik}^{t+\Delta t} = \Delta t.(V_{xi} - V_{xk})^{t+\Delta t/2} = (\delta_{xi}^{t+\Delta t} - \delta_{xi}^{t}) - (\delta_{xk}^{t+\Delta t} - \delta_{xk}^{t})$

$$\therefore \frac{1}{(B'+1)}\left[\frac{\Delta\delta_{xik}^{t+2\Delta t}}{\Delta\delta_{xik}^{t+\Delta t}} + B'.\frac{\Delta\delta_{xik}^{t}}{\Delta\delta_{xik}^{t+\Delta t}}\right] = 1 - 2\,\frac{A'_{xi}\,\Delta t.S_{xi}}{(B'+1)} \qquad (8)$$

$\frac{A'_{xi}}{(B'+1)} = \frac{\Delta t}{2M_{xi}}$, and since all $\frac{S_{xi}}{M_{xi}}$ are identical, the

optimum value of Δt is $\sqrt{2M_{xi}/S_{xi}}$. Equation (8) thus reduces to:

$$\left[\frac{\Delta\delta_{xik}^{t+2\Delta t}}{\Delta\delta_{xik}^{t+\Delta t}} + B'.\frac{\Delta\delta_{xik}^{t}}{\Delta\delta_{xik}^{t+\Delta t}}\right] = -(B'+1) \qquad (9)$$

The assymptotic convergence rate, λ, of the iteration is defined as the ratio of successive errors in deflections:

$$\lambda = \frac{\delta_{xi}^{t+\Delta t} - \delta_{xi}}{\delta_{xi}^{t} - \delta_{xi}} = \frac{\varepsilon_{xi}^{t+\Delta t}}{\varepsilon_{xi}^{t}} = \frac{\varepsilon_{xi}^{t+2\Delta t}}{\varepsilon_{xi}^{t+\Delta t}} \qquad \text{for all nodes i}$$

$$\text{or } \lambda^2 = \frac{\delta_{xi}^{t+2\Delta t} - \delta_{xi}}{\delta_{xi}^{t} - \delta_{xi}} \qquad (10)$$

where δ_{xi} is the true deflection.

The first term on the L.H.S. of equation (9) may be written:

$$\frac{\Delta\delta_{xik}^{t+2\Delta t}}{\Delta\delta_{xik}^{t+\Delta t}} = -\left[\frac{(\delta_{xik}^{t+2\Delta t} - \delta_{xik}^{t+\Delta t})}{(\delta_{xik}^{t} - \delta_{xik}^{t+\Delta t})}\right]$$

Since we are dealing with relative deflection changes in succesive time steps (the signs of which reverse in accordance with the derivation of the stability criteria in Chapter (2)) we may, for

the purpose of examining the eventual convergence rate, associate $\delta_{xik}^{t+\Delta t}$ with the true relative deflection,

$\delta_{xik} = (\delta_{xi} - \delta_{xk})$, which gives:

$$\frac{\Delta\delta_{xik}^{t+2\Delta t}}{\Delta\delta_{xik}^{t+\Delta t}} = -\left[\frac{(\delta_{xi}^{t+2\Delta t} - \delta xi) - (\delta_{xk}^{t+2\Delta t} - \delta_{xk})}{(\delta_{xi}^{t} - \delta_{xi}) - (\delta_{xk}^{t} - \delta_{xk})}\right]$$

Dividing the numerator and denominator by $(\delta_{xi}^{t} - \delta_{xi}) \times (\delta_{xk}^{t} - \delta_{xk})$ and using equation (10) gives:

$$\frac{\Delta\delta_{xik}^{t+2\Delta t}}{\Delta\delta_{xik}^{t+\Delta t}} = -\lambda^2$$

Similarly, the second term on the L.H.S. of equation (9) may be written as: $-B/\lambda^2$. The equationthus becomes:

$$\lambda^4 - \lambda^2 (B^{\prime}+1) + B^{\prime} = 0$$

The least positive root of this gives $\lambda = \sqrt{B^{\prime}}$. Thus the optimum convergence rate of the dynamic relaxation iteration is:

$$\lambda = \left(\frac{1-K^{\prime}/2}{1+K^{\prime}/2}\right)^{1/2} \qquad (11)$$

This derivation assumes that the process has been optimized using fictitious masses and a critical time interval. Taking also the optimum value of $K^{\prime}$ given by equation (7):

$$K^{\prime} = 4\,\frac{f_{min}}{f_{max}} = \frac{4}{\sqrt{N}}$$

where N is the conditioning number of the stiffness matrix $(\sqrt{b/a})$, we obtain:

$$\lambda_{opt.} \simeq \left(\frac{1-2/\sqrt{N}}{1+2/\sqrt{N}}\right)^{1/2} \simeq \left(\frac{\sqrt{N}-1}{\sqrt{N}+1}\right) \tag{12}$$

Lynch et. al. examined the convergence of dynamic relaxation in a mathematically more rigorous way by transforming the iterative process into a standard matrix eigenvalue problem for error vectors. In principle this type of convergence analysis takes the following form:

From Appendix (A), any of the iterative procedures may be expressed in the form:

$$\{\delta\}^{k+1} = \{\delta\}^{k} + [H](\{P'\} - [K']\{\delta\}^{k})$$

or: $$\{\delta\}^{k+1} = [H]\{P'\} + [M]\{\delta\}^{k} \tag{13}$$

Subtracting the true solution from equation (13) gives the relationship between successive error vectors:

$$\{\varepsilon\}^{k+1} = [M]\{\varepsilon\}^{k} \tag{14}$$

where $\{\varepsilon\}^{k} = \{\delta\}^{k} - \{\delta\}$ and $\{\delta\}$ is the true solution vector. Considering an error vector of such form that it is changed in magnitude only, by a factor λ, during each iterative step:

$$\{\varepsilon\}^{k+1} = \lambda\{\varepsilon\}^{k} \tag{15}$$

Thus from equations (14) and (15):

$$[\lambda[I] - [M]]\{\varepsilon\} = 0 \tag{16}$$

Then for convergence the modulus of all the eigenvalues of $[M]$ from (16) should be less than 1 and the iterative procedure is

optimized by choosing the accelerating parameters incorporated in $[M]$ such that $|\lambda_{min}| = |\lambda_{max}|$. The expressions for these accelerating factors and the convergence rates are then obtained in terms of the maximum and minimum eigenvalues of $[K']$.

The direct convergence analysis given previously contrasts with the above error vector approach in that it must be assumed a priori that fictitious mass components have been optimized and thus that all nodes are equally responsive with relative displacements out of phase; this same assumption having been made to obtain directly the stability criterion governing the choice of masses. The results given by Lynch are summarised in the following table:

Simultaneous Methods	Successive Methods
Point Jacobi $\lambda = \frac{N-1}{N+1}$	Gauss-Seidel $\lambda = \left(\frac{N-1}{N+1}\right)^2$
D.R. $\lambda = \frac{\sqrt{N}-1}{\sqrt{N}+1}$	S.O.R. $\lambda = \left(\frac{\sqrt{N}-1}{\sqrt{N}+1}\right)^2$

From this comparison, given for linear structures with tri-diagonal stiffness matrices, it can be seen that the reduction in the error vector accomplished in one cycle of the Successive Over-Relaxation method takes two cycles in the Dynamic Relaxation method.

The same relationship exists between Gauss-Seidel and Point Jacobi, though DR is faster than either of these methods. Lynch also obtained results for the optimum parameters of DR which agreed with those given in equations (3) and (4). Similar comparisons of DR with other iterative methods, as referred to previously, have been given by Otter, Wood and Cassell for finite difference formulations.

The foregoing sections on optimum parameters and convergence rate demonstrate that the dynamic heuristic for the iteration procedure is soundly based for all cases where N>>1. This will nearly always be the case though exceptions may occur when using approximate analyses in which only the dominant deflection components are considered. Summarising, for complete analysis of practical structures with a<<b, DR is optimized when fictitious mass components are chosen such that $M_{xi} = \Delta t^2 . S_{xi}/2$ for all x and i, and the damping factor is: $K' = 4\pi . \Delta t . f_{min}$

Automatic Adjustment of Mass and Damping Parameters

In the majority of applications of DR fictitious masses have been adjusted at the start of the analysis and held constant throughout. Whilst for most structures this is satisfactory, in highly non-linear problems with large changes in geometry or member stiffnesses it may be advantageous to alter the mass components as the analysis progresses. An example of this, in which

it is essential to do so, is given in Chapter 8 where the DR optimization process entails changing member areas. Continuous mass adjustment could also be of value in speeding the convergence of form-finding of tension or grid-shell structures.

Whilst adjustment of masses according to equation (6) for a given time interval entails little additional programming, estimating the lowest frequency or eigenvalue is more involved. Instead of seeking such an estimate, the parameters $A_\lambda^{\backprime}$ and $B^{\backprime}$ might be sought directly using the dynamic relaxation process itself to provide updated values as the analysis progresses. Referring to equation (12):

$$\lambda = \sqrt{B^{\backprime}}$$

and ultimately, after a sufficient number of iterations, this convergence rate may be expressed in terms of the incremental deflection vectors as:

$$\lambda = \frac{\{\Delta\delta\}_{n+1}}{\{\Delta\delta\}_n} = \frac{\{\delta\}^{t+\Delta t} - \{\delta\}^{t}}{\{\delta\}^{t} - \{\delta\}^{t-\Delta t}} \qquad (17)$$

Thus, assuming an on-going alteration of $B^{\backprime}$ an averaged estimate of this parameter (which is common for the entire structure) may be obtainable using the expression:

$$B^{\backprime} = \frac{1}{m} \sum_{j=k}^{j=k+m} \frac{\{\Delta\delta\}_{j+1}^{T} \cdot \{\Delta\delta\}_{j+1}}{\{\Delta\delta\}_{j}^{T} \cdot \{\Delta\delta\}_{j}} \qquad (18)$$

Estimating a value for λ^2 based on an average for the preceding (m+1) time steps (where m>1) should avoid the possibility of an

ill-conditioned estimate which might occur if only two successive time steps were used. Updated values for the nodal parameters A'_{xi} are then given by:

$$A'_{xi} = \frac{\Delta t}{2M_{xi}}(B' + 1) \tag{19}$$

Lynch et. al. (114) suggested the use of an on-going alteration of the iteration parameters (equivalent to A'_{xi} and B') based either on equation (17) or iterative determination of the minimum eigenvalue, and investigated the efficiency of the latter method on the basis of convergence rate with checks made at intervals during the analysis. Starting with a rough estimate for the damping, when a check on the curvatures of the deflection vector norms for each co-ordinate direction indicated that the process was overdamped, a change in parameters was made. Similarly, changes were made every time an alteration in the sign of a displacement norm indicated underdamped behaviour. Their analyses were for linear structures only, and conclusions were uncertain to the extent that large adjustments could take the parameters beyond their optimum values and give inferior convergence to that of analyses using constant parameters in the correct region. Also, no comparison was given on the basis of computational effort. The process did, however, allow automatic adjustment of the damping and generally improve the convergence rate in cases where a poor first estimate of the minimum eigenvalue (or damping) had been made.

For non-linear structures, with large changes in geometric or elastic stiffnesses, similar techniques could prove even more valuable but must be taken a stage further with simultaneous alteration of both the parameters $B^{\backprime}$ (and $A^{\backprime}_{xi}$) and the fictitious masses. The latter evidently directly affect the lowest natural frequency (or critical damping) and hence $B^{\backprime}$, in addition to the changes in this parameter necessitated by a poor initial estimate and alteration of the overall stiffness to deformation in the fundamental mode shape. Both parameters are also coupled in calculating the values of $A^{\backprime}_{xi}$ from equation (19).

In any of the methods considered for automatically determining $B^{\backprime}$ it is necessary to have some starting estimate of the fundamental frequency. Although the use of trial runs may at first appear analytically crude, it should be borne in mind that it is usual to carry out preliminary analyses during the course of the design of a structure which may be based on a fairly coarse element idealization. The fundamental frequency can thus be obtained at these stages and should not be altered significantly by the use of a fine idealization. Furthermore, knowledge of the fundamental frequency may be of value at early stages of design, and the progress in successive stages from a coarse to a fine idealization is useful for obtaining information concerning convergence and accuracy of the spatial idealization. In practise, therefore, estimating the critical damping of a structure involves computations which have other uses.

The additional computations involved in estimating the fundamental frequency may alternatively be eliminated for purely static analyses if use is made of a technique suggested by Cundall (56). He uses step function damping in which no viscous damping is applied but the kinetic energy of the system is followed. When a maximum in the total K.E. for the structure is reached all velocities are set to zero and the system restarted from this displaced state. For a linear system oscillating in only one mode this state of stress would be the desired solution. In practise, however, this process must be continued through several further peaks until the K.E. from all modes has been eliminated. The process is apparently very rapid: Cundall quotes only $\frac{1}{2}$ period required for sufficiently accurate results to some problems; evidently implying that velocities are zeroed at every local peak of the K.E. It also has the advantage that no trial runs are necessary to obtain critical damping. This is achieved automatically. The use of "kinetic damping" in form-finding applications has been investigated by Wakefield (198) who found that very large initial out-of-balance forces could be accommodated without the need for reduced stiffnesses which otherwise are required when using viscous damping. The two approaches are compared in the following sub-appendix which illustrates the form-finding of a funicular lattice shell carried out by the author for a design by Frei Otto.

APPENDIX D.1.

FORM-FINDING OF A LATTICE SHELL DOME

The following example is given for two reasons: firstly it is the only example of its type in the text and shows that for hanging network mechanisms form-finding computations by DR may be much lengthier than for prestressed systems of equivalent size; secondly it demonstrates the potential value of kinetic damping in dealing with large initital out-of-balance forces or changes in topology. The description is taken from reference (20).

The lattice shell dome was treated as a pin-jointed mechanism and a solution was obtained to the inverse problem of finding a tension funicular system with dead weight loads reversed in sign. The dome was supported internally on six branched 'tree' columns and externally on an elevated, lobed, boundary ring (sectional elevation - figure 8). The proposed structure is approximately 70m in diameter with a tubular steel hexagonal mesh in which the majority of members are 1.5m long. For preliminary form-finding a hanging chain model was constructed by Frei Otto at the Atelier Warmbronn, Stuttgart, and from photographs of the model the required mass components for the DR analysis were estimated. The structure was six fold rotationally symmetric and thus only a 1/12 segment with about 400 degrees of freedom was analysed. Plan and elevation of the initial geometrical data are

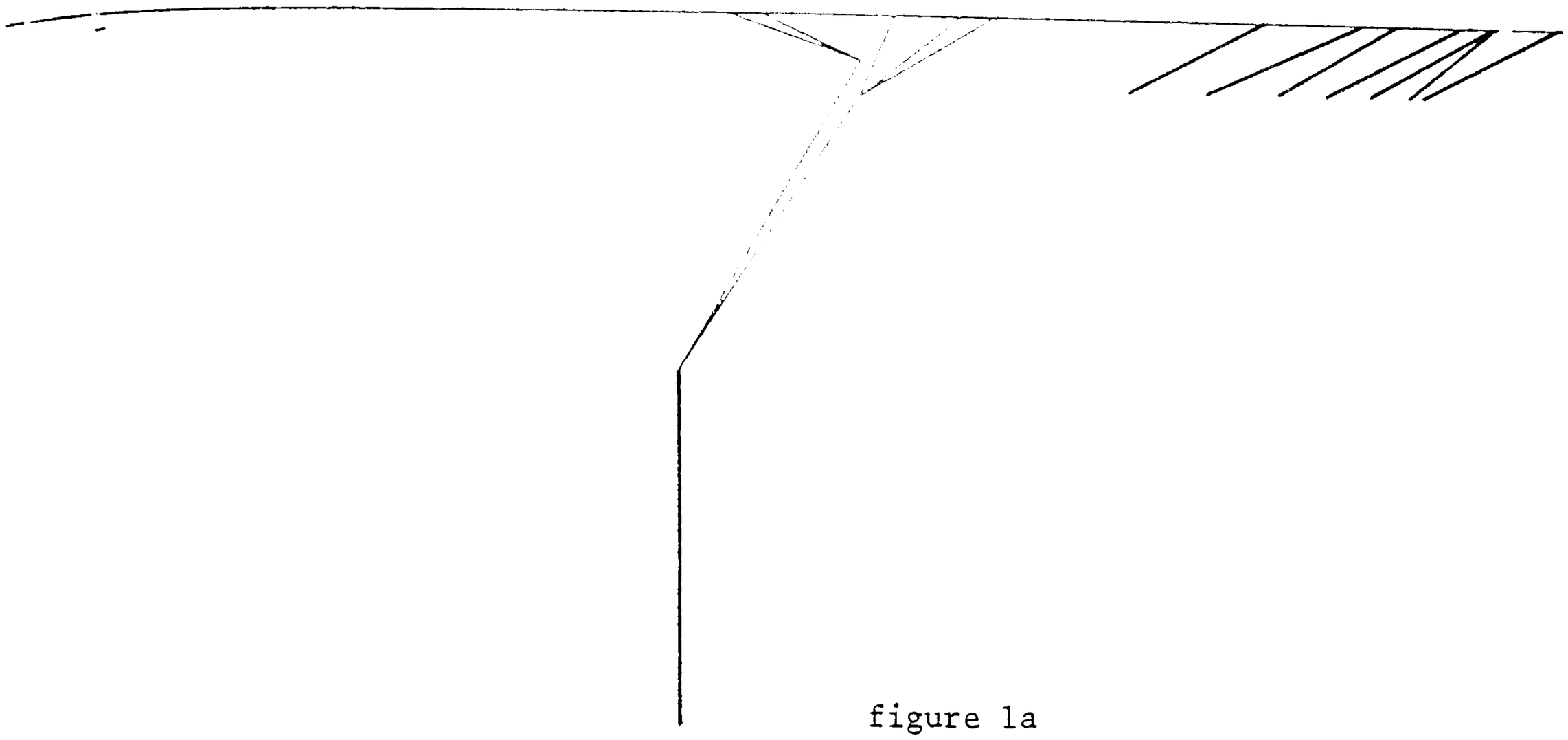


figure 1a

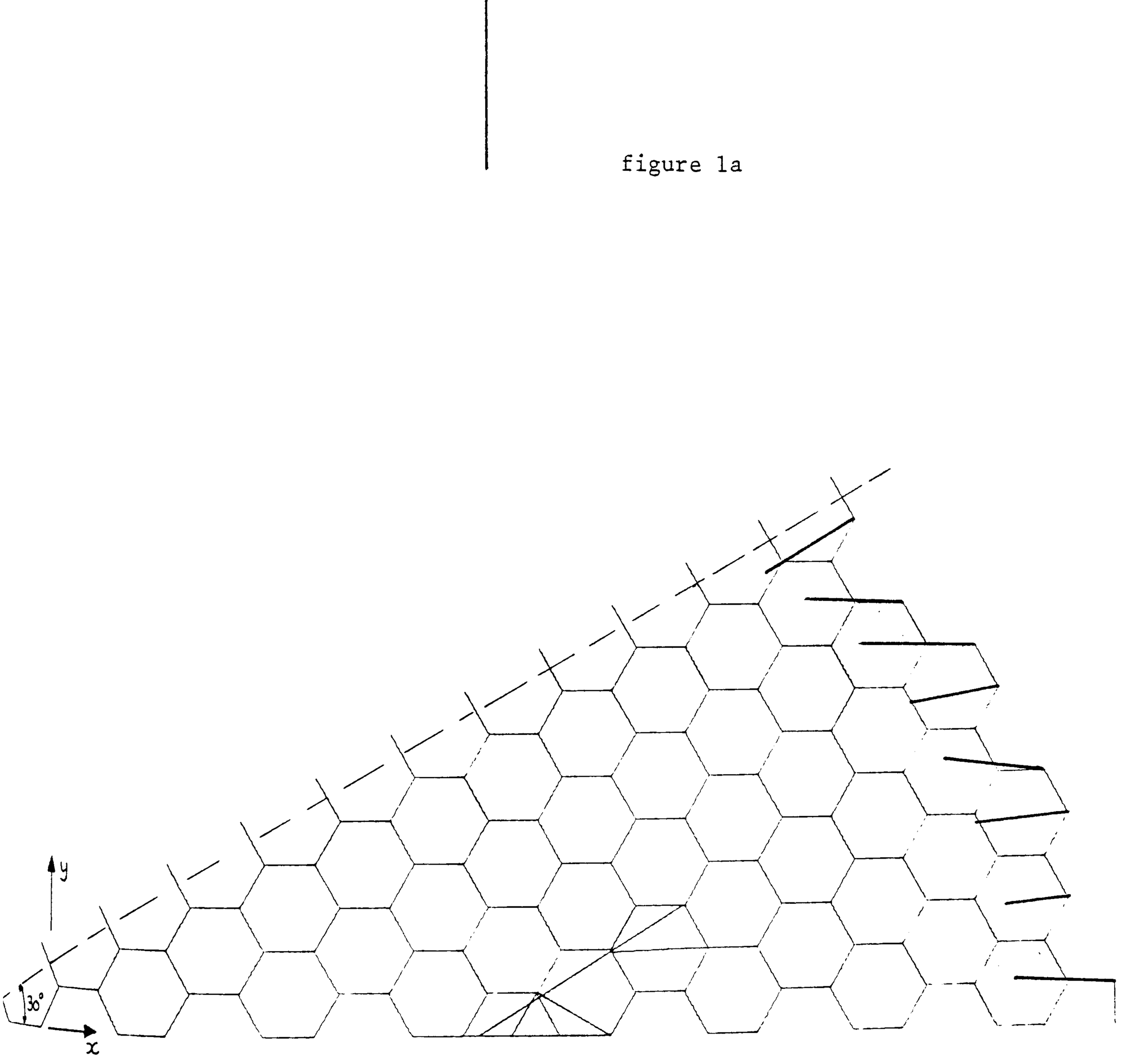


figure 1b

shown in figures 1a and b. Symmetry of the analysis was imposed by reflecting the co-ordinates of nodes adjacent to the 30° line at each stage, and by assigning very large y direction mass components at nodes lying along the x axis.

Viscous Damping Solution

The thicker lines in fig. 1 represent links (mainly connecting to specified boundary points) in which, to comply with the initially flat surface grid, the extensions from required lengths and the resulting out of balance forces, if based on correct EA values, are very large. To cope with this situation the areas of these members were reduced to 0.1% of their true values, and the analysis carried out in three stages:

(1) 0.1% EA in grossly extended links, with very light damping. Run for 1000 integration steps, after which a very approximate shape was obtained (see figure 2) with surface links becoming significantly strained.

(2) 3500 time steps with greater damping (but still expected to be sub-critical) and the EA values of boundary links increased from 0.1% so that they approached their true value asymptotically. The output from this gave an estimate of the critical damping and the final form.

(3) 2000 steps with true EA values and nearly critical damping.

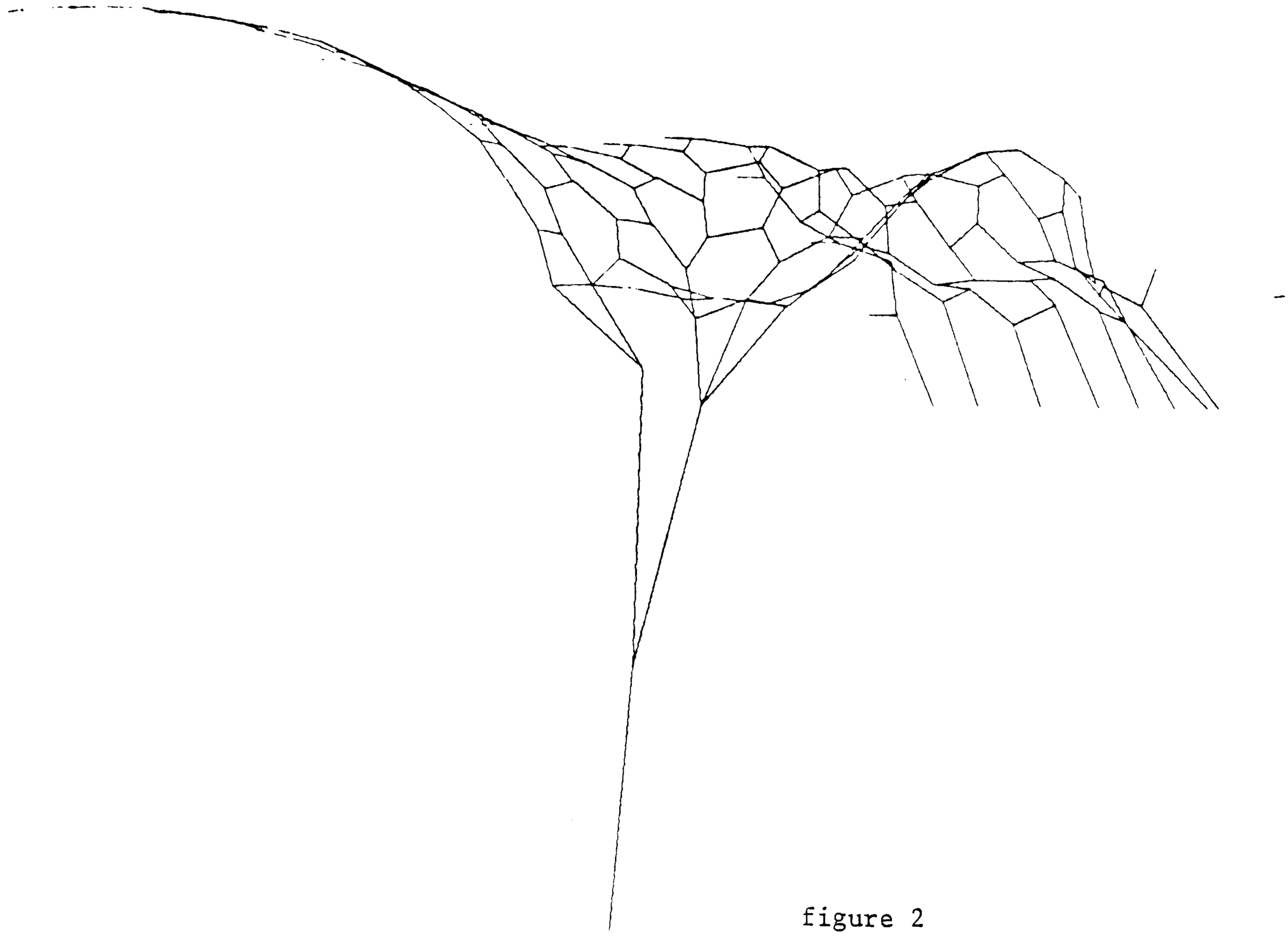


figure 2

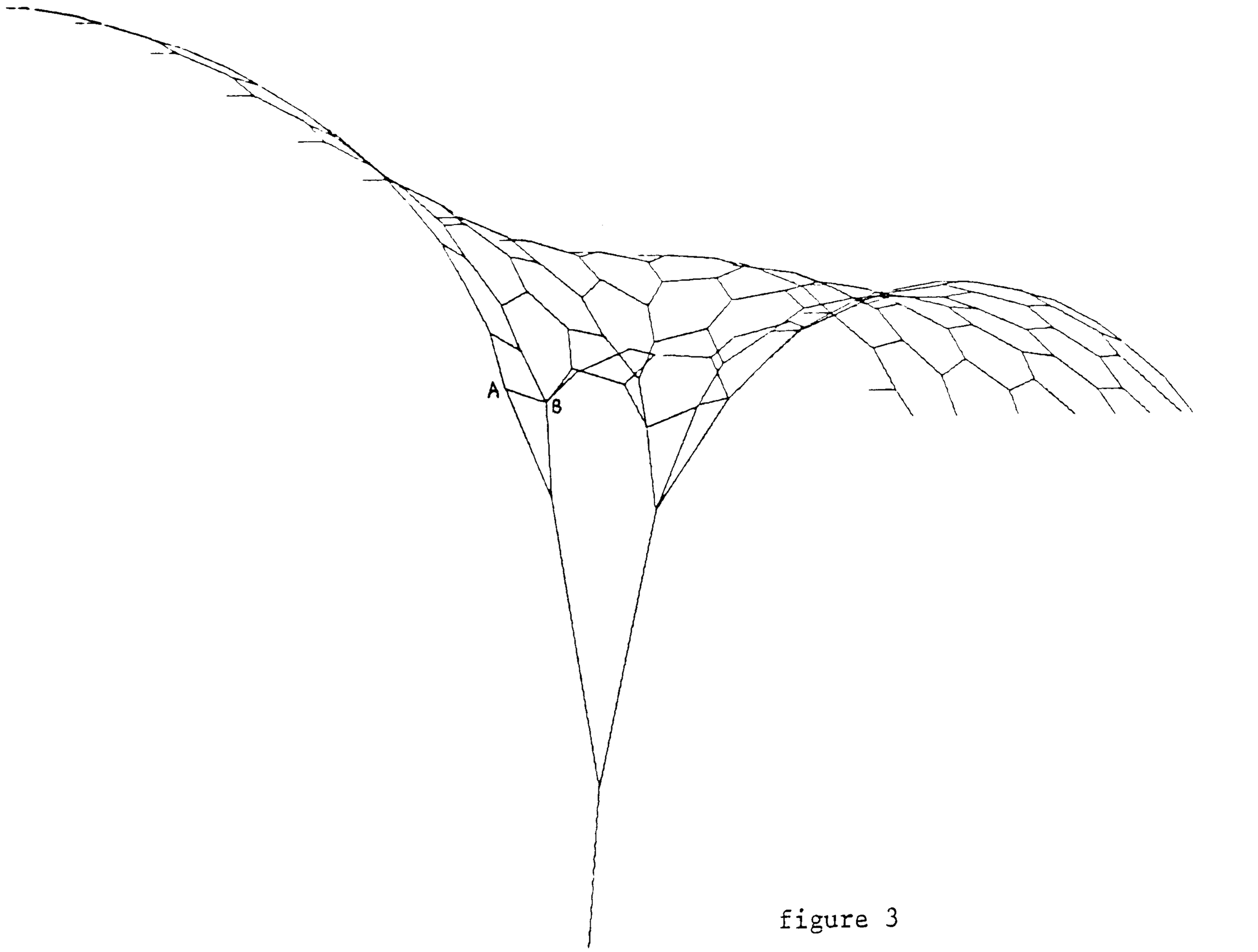


figure 3

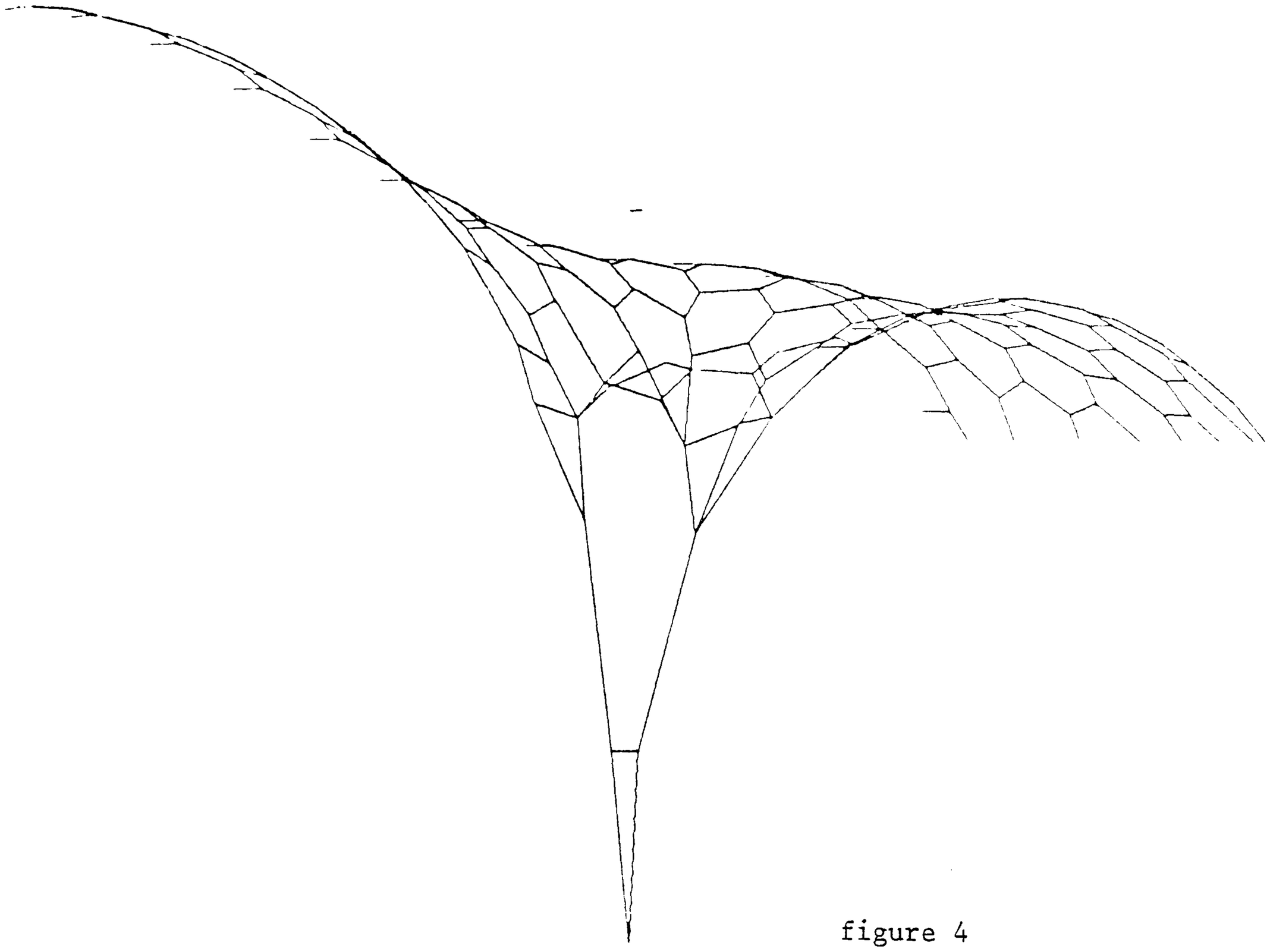


figure 4

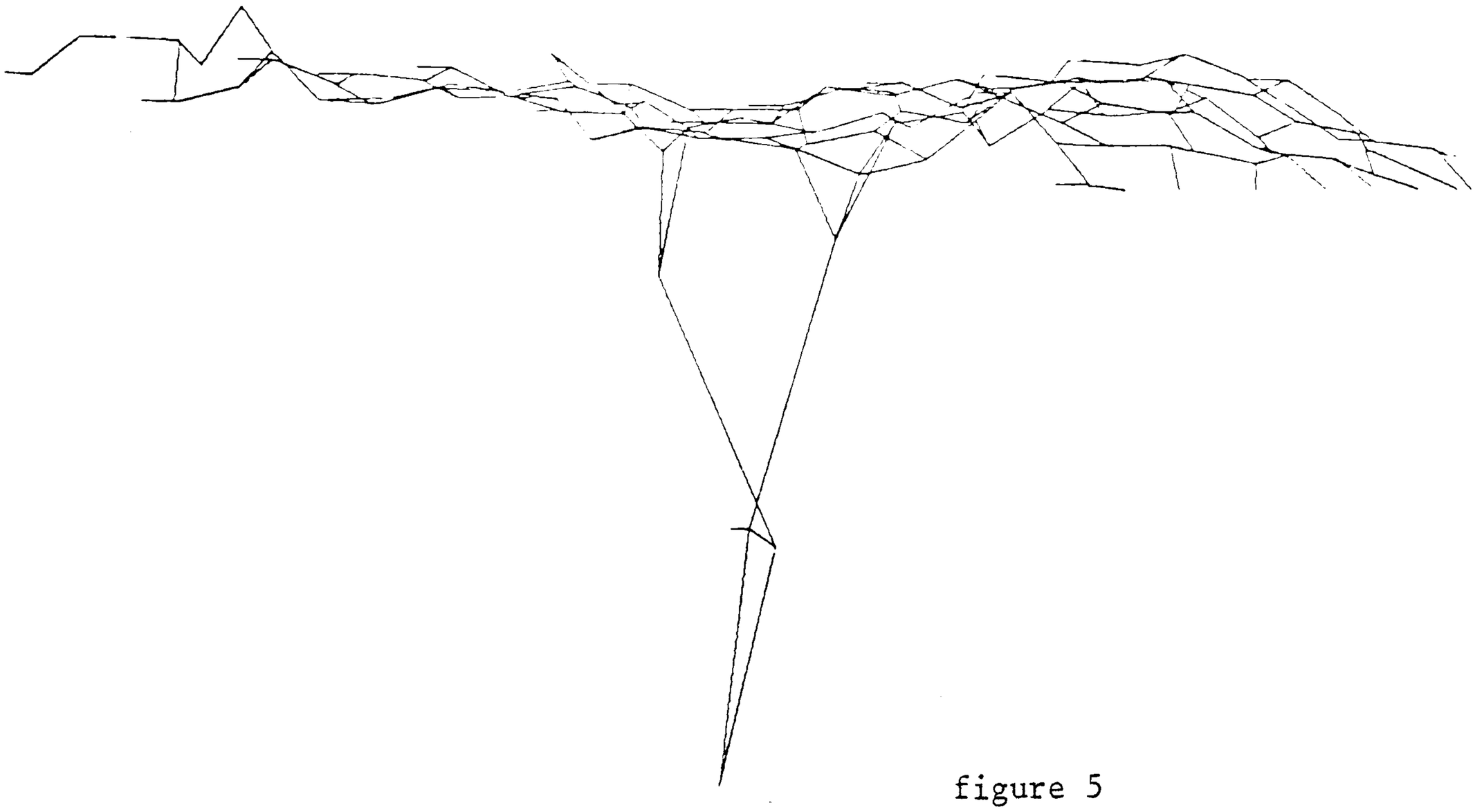


figure 5

The converged form of the structure after stage 3 is shown in figure 3. The solution is non-unique because the specified length for member AB is such that it is in compression, and point A may thus have an alternative position in the symmetry plan xz. Following further studies of the physical model the length of this and other members was altered and the topology of the tree support and the surface network above it rearranged.

Data for the new topology was based as far as possible on the previous converged form, as shown in figure 4, and the EA values of all members were reduced to between 0.1 and 10% of correct values in order to accommodate the large initial out-of-balance forces. In spite of this, very considerable disturbance of the network occurred. The situation after 1000 steps is shown in figure 5, and after 2000 steps (figure 6) the configuration is stable but the splay geometry at the tree support has become inverted with compression in the spacing links. This problem could have been avoided by restricting forces in the links to tension only, but in doing this numerous full mechanisms occur during the analysis and the time step has to be considerably reduced. In the final phase of the analysis the geometry at the tree spacing links was corrected and the problem was run through 5000 time steps with the slack lengths (L^o) of members adjusted at regular intervals so that the stressed lengths were equal to the specified values. The geometry obtained was accurate to 0.05mm and the residual forces to within 0.1% of the dead weight load at any node. The final form of the structural segment is shown in figure 7, and a sectional elevation of the complete structure in figure 8.

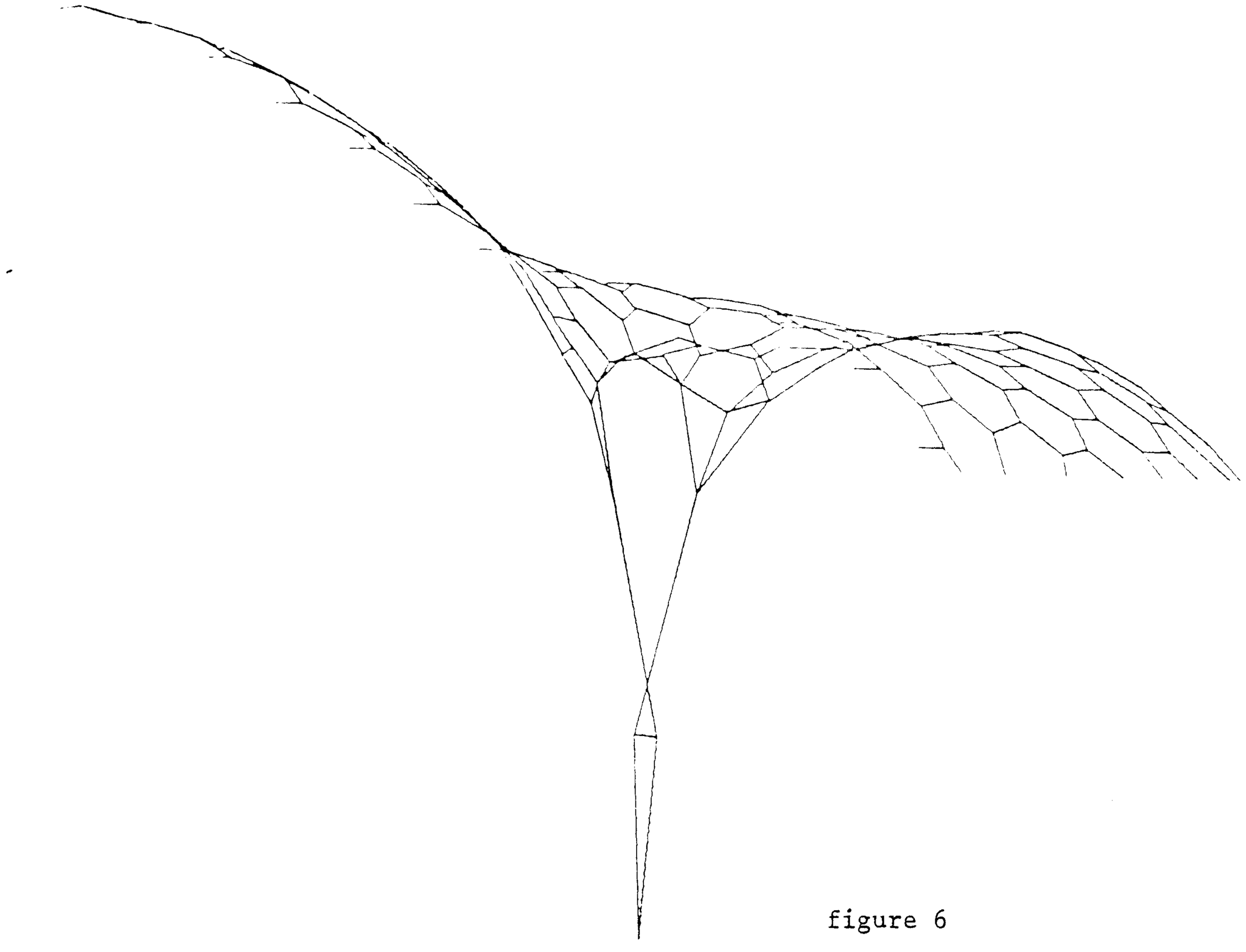


figure 6

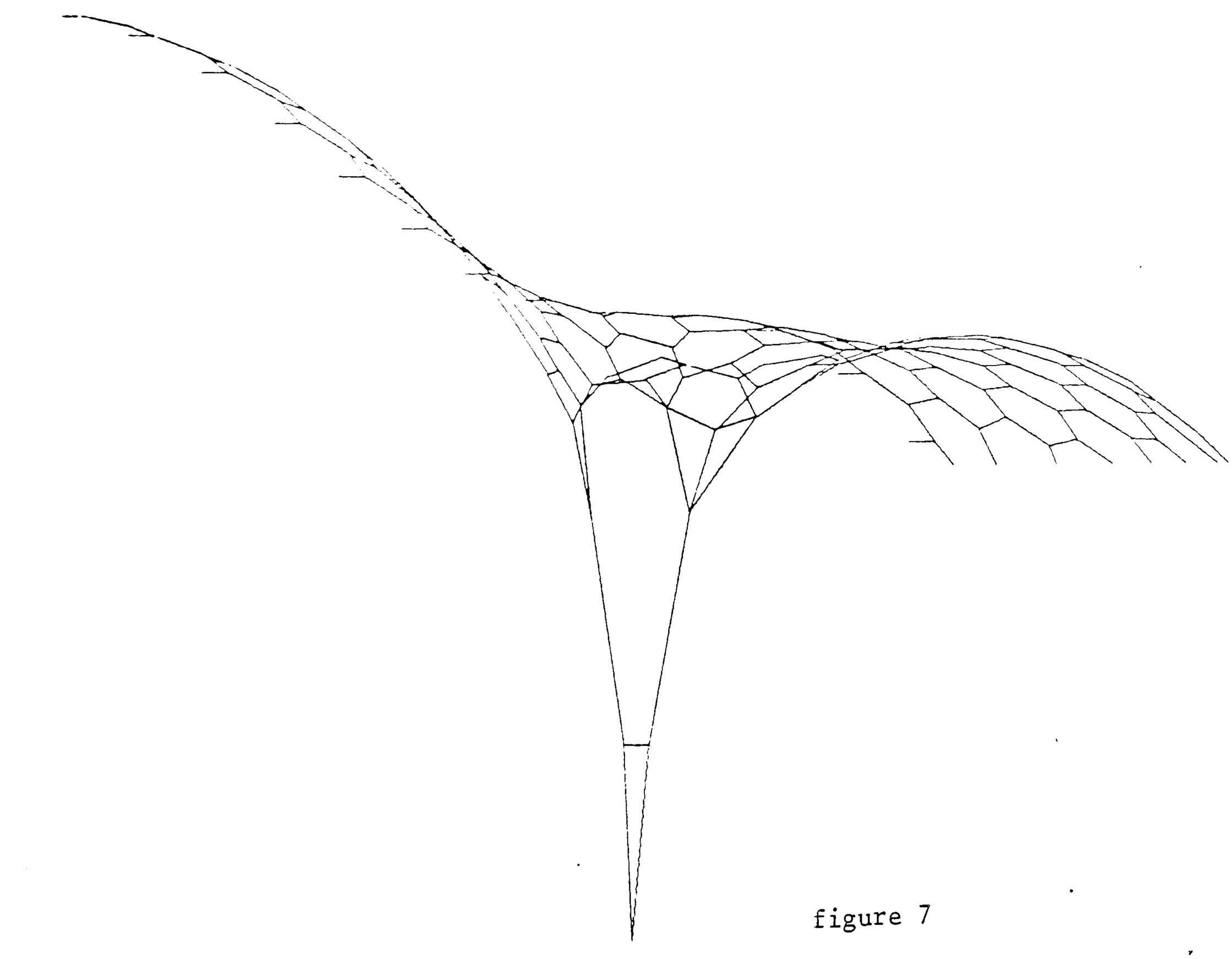


figure 7

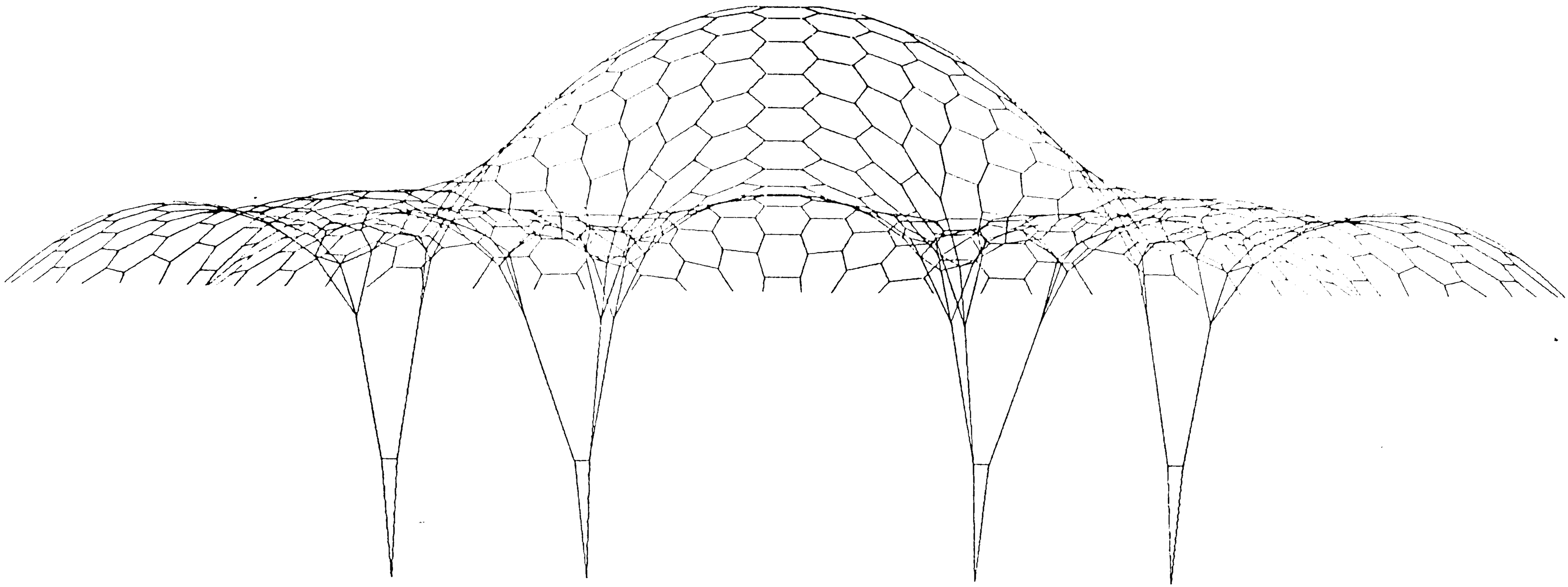


figure 8

It was evident during the analysis described that, because of the sensitivity of the structure to mechanical deformations and the very large initial out-of-balance forces, the form-finding process was considerably less efficient than for anticlastic tensioned networks of similar size. In consequence various means of increasing the efficiency of the DR analysis for this class of problem were subsequently investigated. These included the use of both close and far-coupled damping, updating the tensions in boundary links less frequently, the use of reduced EA values and effective slack lengths throughout the process, and a procedure termed "kinetic damping". The latter was found to be the most efficient method and this is examined in the following section.

Kinetic Damping

The analysis of the structure, irrespective of the magnitude of errors in the initial out-of-balance forces, was based throughout on true EA values and zero viscous damping; displacements of the system being controlled by re-setting velocity components to zero each time a peak in the total kinetic energy was attained.

With mass components approximately 50% greater than the critical values initial forms were obtained in about 2/3 of the computing time previously required with viscous damping to obtain the same state. This is mainly due to the fact that in the viscous damping process it is difficult to estimate the damping (because the system is an unconfined mechanism in early stages) and the rate at which EA values should be increased to ensure stability with efficiency. The main value of the kinetic damping process is that

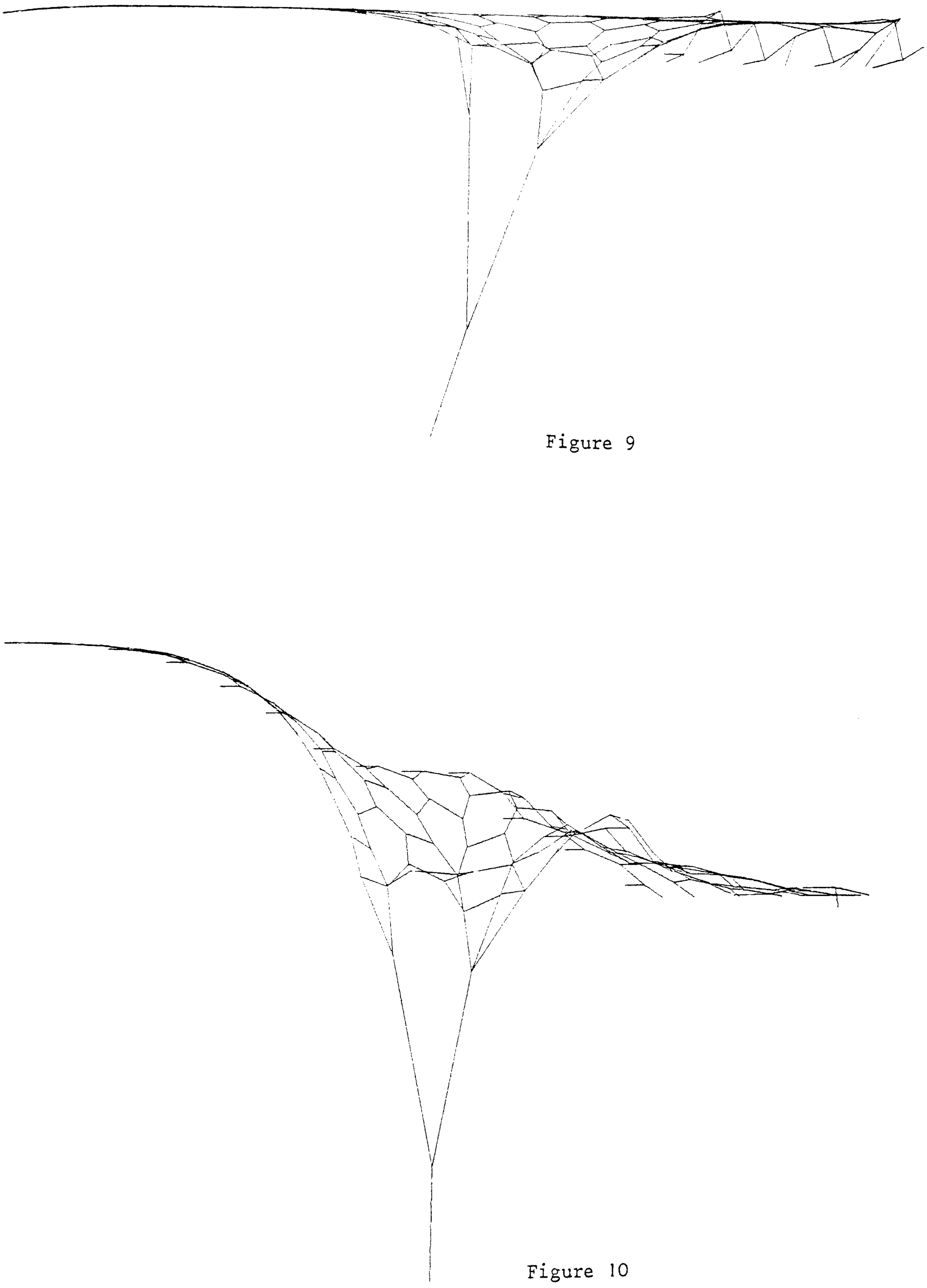


Figure 9

Figure 10

computations can proceed automatically without intermediate examination of convergence trends.

In operation, the major part of the net remains undisturbed whilst the large out-of-balance forces in boundary links or in areas adjacent to topology changes are dispersed with usually only about three iterations between velocity resets. After this stage large mechanical deformations in the surface net take place in a single reset stage involving many time increments. Thereafter the net jumps in fairly large deformation steps to its final position. Starting from the initially flat system shown in figure 1, the state of the structure after 112 velocity resets (350 time intervals) is shown in figure 9. At the next reset stage, but following a further 1800 time steps, the surface net has displaced to the position shown in fig. 10. Subsequent convergence to an accuracy equivalent to stage 3 of the viscous process was obtained after 118 resets involving a total of 4500 time steps. The effects of the sudden changes in topology, which, with viscous damping and reduced EA values propogated the disturbances shown in fig. 5, were confined to the immediate locality of the changes; though final convergence was no more rapid.

APPENDIX E

BIBLIOGRAPHY CONCERNING THE DESIGN AND ANALYSIS OF TENSION STRUCTURES

The references, with short notes, contained in this appendix relate to Chapter 1 and appendices A→D.

1. Abu-Sitta, S.H., Elashkar, I.D., "The dynamic response of tension roofs to turbulent wind", Int. Conf. on Tension Structures, London, 1974.

(Aero-elastic model tests of drum tension roof. First symmetric mode strongly dependent on wall openings. Analysis accounts for both stiffening effect of enclosed air and reduction of frequency due to attached air inertia. Gives added mass expression in terms of porosity of structure.)

2. Alwar, R.S., Rao, N.R. "Large elastic deformations of clamped skewed plates by dynamic relaxation", Computers and Structs., V.4, 381-398, 1974.

(Non linear behaviour of isotropic plates. Finite difference idealization with parameters chosen as in Rushton - refs 156 - 158.)

3. Angelopoulos, T., "Zur formfindung, statik und dynamik von vorgespannten netzwerk-konstruktionen", Dr. Ing. dissertation, University of Struttgart, 1977.

(General review and development of matrix methods of analysis of cable net structures at I.S.D., Stuttgart. Emphasis on Newton-Raphson formfinding from initially flat nets)

4. Argyris, J.H., Kelsey, S., Kamel, W.H., "Matrix methods of structural analysis: A precis of recent developments", Proc. 14th Meeting Structures and Materials Panel, AGARD, 1963

(Finite element matrix analysis with material non-linearities using initial strains process and constant stiffness matrix)

5. Argyris, J.H., Kelsey, S., Kamel, W.H., "Matrix methods of structural analysis", AGARDOGRAPH No. 72, Pergamon Press, N.Y., 1964.

(Generalized finite element analyses for large displacement - small strain problems using initial stress matrices)

6. Argyris, J.H., Scharpf, D.W. "Berechnung vorgespannter netzwerke", Bayr. Akad. der Wiss., Sonderdruck 4 der Sitzungsber, 1970. OR "Large deflection analysis of prestressed networks", J. Struct. Div., ASCE, 98, 1972.

(Formfinding of Munich athletics stadium: Approximate mathematical specification of surface from architectural data. Projection of uniform mesh on surface and iterative analysis by Newton-Raphson method)

7. Argyris, J.H., Chan, A.S.L., "Applications of finite elements in space and time", Ingenieur-Archiv 41, 1972.

(General finite-element formulation for geometrically and materially non-linear static and dynamic analyses. Static analysis by incremental procedure with iteration in each step to use averaged value of tangent stiffness. Dynamic analysis by numerical integration with cubic variation of accelerations. Displacements and velocities at end of an interval derived in terms of the inverse of the mass matrix and the inertial forces and their derivatives at beginning and end. Iteration used in each time step to obtain solution without solving large set of equations)

8. Argyris, J.H., Angelopoulos, T., Bichat, B., "A general method for the shape finding of lightweight tension structures", Int. Conf. on Tension Structures, London, 1974.

(Four stage formfinding process for uniform mesh cable networks: (]) very flexible flat net distorted incrementally to conform with specified support points (2) transformation to desired prestress distribution and re-analysis (3) Automatic equal mesh net generated on resulting surface (4) re-analysis using previous prestress to obtain final network)

9. Argyris, J.H., Dunne, P.C., Angelopoulos, T., "Dynamic analysis of tension roof structures", Int. Conf. on Tension Structures, London, April 1974.

(Finite elements in space and time method used in a direct iterative form for very large systems. Calculations performed element-wise without formation of overall stiffness matrix using iteration in each time step. Comparison with Wilson θ method for cable structures)

10. Asplund, S.O., "Force-method analysis of orthogonal cable nets", Int. Symp. on Wide Span Surface Structures, Stuttgart, 1976.

(Solves cable net by force method with horizontal cable tension increments, assumed constant along cables, as redundants. Numerical examples indicate sharp covergence. Applicable to shallow nets as approximate solution)

11. Bandel, H.K., "Das orthogonale seilnetz, hyperbolisch-parabolischer form unter vertikalen lastzustanden und temperatur-anderung", Der Bauingenieur, 394, Oct. 1959.

(First published paper on the analysis of cable networks. Approximate solution for orthogonal networks subject to vertical loads)

12. Barnes, M.R., "Prestressed cable networks", M.Sc. thesis, University of Manchester, 1966.

(Approximate force-method of analysis for networks accounting for vertical displacements only but including both horizontal and vertical forces. Newton type solution with horizontal components at one end of each cable as unknown. Sharp convergence cf. Asplund ref. 10)

13. Barnes, M.R., "Pretensioned cable networks", CONRAD, V.3, n.1, April 1971.

(Compares dynamic relaxation analysis and formfinding with results of model studies)

14. Barnes, M.R., "Dynamic relaxation analysis of tension networks", Int. Conf. on Tension Structures, London, April 1974.

(See Chapter 2)

15. Barnes, M.R., "Applications of dynamic relaxation to the design and analysis of cable, membrane and pneumatic structures", 2nd Int. Conf. on Space Structures, Guildford, September, 1975.

(Chapter 3)

16. Barnes, M.R., "Formfinding of minimum surface membranes", World Congress on Structures for Space Enclosure, Montreal, July 1976.

(Chapter 4)

17. Barnes, M.R., "Explicit dynamic analysis and model correlation of tension structures", Int. Symp. on Wide Span Surface Structures, Stuttgart, April 1976.

(Chapter 5)

18. Barnes, M.R., "An investigation of vibration decay in a model pneumatic dome", Int. Symp. on Wide Span Surface Structures, Stuttgart, April 1976.

(Chapter 6)

19. Barnes, M.R., "Interactive graphical design of tension surface structures" Int. Symp. on Wide Span Surface Structures, Stuttgart, April 1976.

(Chapter 7)

20. Barnes, M.R., Topping, B.H.V., Wakefield, D.S.,"Aspects of form-finding using dynamic relaxation", Int. Conf. on Slender Structures, London, September 1977.

(Comparison of optimisation procedure given in Chapter 8 with solutions by Linear Programming andfully-stressed design techniques. Application of DR to form-finding of lattice or grid-shells. Comparison of viscous and kinetic damping procedures.)

21. Baron, F., Venketesan, M.S., "Nonlinear analysis of cable and truss structures", J. Struct. Div., ASCE, V.97, n.ST2, 1971.

(Newton-Raphson, modified Newton-Raphson and Secant stiffness analyses. Derivation of tangent stiffness matrices from first principles)

22. Basu, A.K., Dawson, J.M., "Orthotropic sandwich plates", Int. J. Mech. Sci., 10, 1968.

(D.R. finite difference linear analysis)

23. Bathe, K.J., Wilson, E.L., "Stability and accuracy analysis of direct integration methods", Int. J. Earthquake Eng. and Struct. Dynamics, V.1, 1973.

(Examines amplitude decay and period elongation for differing time steps in the Hubolt, Wilson θ and Newmark β numerical integration methods applied to linear systems)

24. Bathe, K.J., Ramm, E., Wilson, E.L., "Finite element formulations for large deformation dynamic anlysis", Int. J. Num. Meth. in Eng., V.9, 1975.

(Examines Wilson and Newmark methods based on incremental and total displacement formulations. Both methods found to require equilibrium iterations in each time step)

25. Begēr, G., Machat, E., "Results of wind tunnel tests on some pneumatic structures", IASS Colloquium on Pneumatic structures, Stuttgart, 1967.

(Influence of deformations on pressure coefficients)

26. Belytschko, T., Hsieh, B.J., "Non-linear transient finite element analysis with convected co-ordinates", Int. J. for Num. Meth. in Eng., V.7, 1973.

(Convected co-ordinate procedure for large displacements, small strains and orthotropic plane problems with either constant strain triangular elements or cubic displacement beams. Uncoupled dynamic equations solved directly by explicit integration using Newmarks method with β = O (C.D.))

27. Belytschko, T., Chiapetta, R.L., Bartel, H.D., "Efficient large scale non-linear transient analysis by finite elements", Int. J. for Num. Meth. in Eng., V.10, 579, 1976.

(Convected co-ordinate direct integration scheme extended to include rectangular elements, sliding-debonding interfaces and artifical damping. Comparison of comuptational requirements with explicit and implicit methods using stiffness matrices. Application to large soil-structure interaction problem with explosive loading)

28. Benzley, S.E., Key, S.W., "Dynamic response of membranes with finite elements", J. Eng. Mech. Div., ASCE, June 1976.

(Use curvilinear cubic isoparametric elements to idealise the membrane, accounting for large deformations and strains. Numerical time integration by velocity formulated central difference scheme)

29. Bergan, P.G., Soreide, T., "A comparative study of different numerical solution techniques as applied to a non-linear structural problem", Comp. Meth. in Appl. Mech. and Eng., V.2, 1973.

(Classifies major numerical solution techniques in three groups: (]) Minimisation - unconstrained minimisation, 1st and 2nd order gradient methods (2) Iterative methods - secant or functional iteration, Newton-Raphson, Modified N-R, weighted N-R (3) Incremental-Euler and incremental with equilibrium iterations. Example examined in paper is simple truss/spring problem - shows three possible equilibrium positions. Different solutions obtained by different methods. Concludes need for incremental combined with direct or minimization methods to follow true path)

30. Biggs, J.M., "Introduction to Structural Dynamics", McGraw-Hill, 1964.

(Illustrative examples on the application of numerical methods)

31. Bird, W.W., "The development of pneumatic structures, past, present and future", Proc. IASS Int. Colloquium on Pneumatic Structures, Stuttgart, 1967.

(Design review)

32. Bogner, F.K., Mallett, R.H. Minich, M.D., Schmit, L.A., "Development and evaluation of energy search methods of non-linear structural analysis", AFFDL-TR-65-113, 1965.

(Direct minimisation of potential energy without explicitly forming stiffness matrix equations. Large displacement behaviour followed into past-buckling. Applied to shells)

3. Braga, F., Care, A., "Study on cable networks subject to loads however distributed", Int. Conf. on Tension Structures, London, April, 1974.

(Uses general F.E. non-linear analysis treating distributed loads as effective nodal loads and accounting for non-linearity of displacements in any cable segment with intermediate nodes with the additional degrees of freedom eliminated before assembly of overall matrix. Solution by N-R or incremental loading. Comparison with lumped load idealization shows small difference (1-3%) in deflections)

4. Brew, J.S., Brotton, D.M., "Non-linear structural analysis by dynamic relaxation", Int. J. Num. Meth. in Engng., V.3, 463-483, 1971.

(DR finite element solution of framed structures accounting for instability, member bowing and plasticity effects with stiffness matrices in unassembled form. Use of block operations for sway frames. Comparison with finite deflection matrix iteration method (ref. 121) shows DR advantageous for highly non-linear problems. Theoretical analysis for optimum convergence and iteration parameters given for linear problems on the basis of an eigenvalue analysis for error vectors)

5. Brew, J.S., "The application of dynamic relaxation to the solution of non-linear structural plane frames", M.Sc. Thesis, U.M.I.S.T., Manchester, 1968.

(As ref. 34 but applies DR in both simultaneous and successive forms. Considers SOR to be a special case of the latter with similar convergence rate)

6. Buchanan, G.R., Akin, J.E., "The deflection analysis of structural nets using the reflection method", Int. Conf. on Space Structures, Guildford, 1966.

(Analysis for formfinding of regular 2-3-or 4 way nets with cables in vertical planes. Boundaries defined as lying inside larger initially plane net, deformed to required elevations using closed form trigonometric analysis of Dean and Ugarte)

7. Buchholdt, H.A., "A non-linear deformation theory applied to two dimensional pretensioned cable assemblies", Proc. ICE., V.42, Jan.1969.

(Outlines steepest descent method for minimization of the total potential energy. Classification of cable systems as structural mechanisms)

8. Buchholdt, H.A., "Pretensioned cable girders", Proc. ICE., V.45, March, 1970.

(Conjugate gradient method for minimizing T.P.E. Comparison of load/deformation characteristics of braced cable girders with varying degrees of mechanical freedom)

9. Buchholdt, H.A., Davies, M., Hussey, M.J.L., "The analysis of cable nets", J. Inst. of Mathematics and its Applications, V.4, 1968.

(Show that total potential energy of a pin-jointed assemblage is a convex function of the joint displacements for all configurations in which members are in tension and that the equilibrium state is therefore stable and unique. Outline methods of steepest descent and relaxed steepest descent for minimizing T.P.E. of cable structures. The latter is shown to converge most rapidly)

40. Buchholdt, H.A., McMillan, B.R., "Iterative methods for the solution of pretensioned cable structures and pin-jointed assemblies having significant geometrical displacements", IASS Symp. on Tension Structures and Space Frames, Tokyo and Kyoto, 1971.

(Solutions of cable systems by minimizing T.P.E. using various gradient methods of optimization. Six different methods are compared: steepest descent, relaxed steepest descent, Runge-Kutta, Newton-Raphson, Conjugate gradients, and the Fletcher-Powell method. Conjugate gradient method found to be most efficient for cable nets and N-R method for cable beams, with the latter found to diverge in certain cases. For all methods the step length was determined by expressing T.P.E. as 4th order polynomial)

41. Buchholdt, H.A., Das, N.K., Al-Hilli, A.J., "A gradient method for the analysis of cable structures with flexible boundaries", Int. Conf. on Tension Structures, London, April 1974.

(Analysis of cable and boundary structures by scaled conjugate gradient method using weighting functions inversely proportional to leading diagonal stiffnesses. Comparison with scaled and relaxed methods of steepest descent)

42. Buchholdt, H.A., Dixon, R., "The design and analysis of the cable roof for Odsal Sports Centre", 2nd Int. Conf. on Space Structures, Guildford, 1975.

(Natural frequencies determined from linearized eigenvalue analysis. Comparison with frequency spectrum of wind energy)

43. Buchholdt, H.A., "The behaviour of saddle shaped nets with flexible boundaries", Int. Symp. on Wide Span Surface Structures, Stuttgart, 1976.

(Numerical investigation into the behaviour of circular saddle shaped cable net roofs considering variations in cable EA and pretension values, curvature of roof and stiffness of ring beam. Concludes that for lightness and economy, circular saddle shaped roofs should be designed with shallow curvatures, slender ring beams and high pretension in cables)

44. Burke, B.G., Tighe, J.T., "A time series model for dynamic behaviour of off-shore structures", Soc. of Petroleum Engineers J., V.253, 1972.

(Random sea model generates time series for velocities and accelerations which correspond to a sea condition with a specified power spectral density. Numerical integration then accounts for structure response allowing for hydrodynamic drag and relative water/structure motion in hydrodynamic force equation)

45. Burley, E., Harvey, R.C., "Behaviour of tension structures subjected to uniformly distributed cable loading", Int. Conf. on Tension Structures, London, April 1974.

(Derives expressions for total potential energy with distributed loads accounted for. Applies 2nd order Newton Raphson gradient method. Gives general description of minimization processes)

46. Bychawski, Z., "Large deflections of non-linear visco-elastic rotational membranes", IASS Symp. on Tension Structures and Space Frames, Tokyo and Kyoto, 1971.

and visco-elastic

47. "Cable-suspended roof construction - State of the art", J. Struct. Div., Proc. A.S.C.E., June 1971.

(Review paper)

48. "Computation and Analytical Methods Discussion", Int. Symp. on Wide Span Surface Structures, V.3, Stuttgart, 1976.

(Concerning generally poor convergence or divergence of solution methods for membranes. Possibility of non-unique solutions for membranes subject to buckling)

49. Cassell, A.C., Kinsey, P.J., Sefton, D.J., "Cylindrical shell analysis by dynamic relaxation", Proc. ICE., V.39, Jan. 1968.

(Interlacing grid finite-difference solution using full shell equations. Stability criteria for]-3 dimensional problems. Damping from trial run)

50. Cassell, A.C., "Shells of revolution under arbitrary loading and the use of fictitious densities in dynamic relaxation", Proc. ICE., V.45, 1970.

(Uses fictitious densities at each node adjusted to give $\Delta t = 1$ everywhere. Trial runs with trace of kinetic energy to obtain critical damping. Comparison of DR with Frankel iteration to derive optimum values of Δt and K in terms of max. and min. eigenvalues)

Discussion of ref. 50 , Proc. ICE, V.47, Nov., 1970.

(Davidson, J.H: Initial disturbance process for calculating critical time interval. Describes shell buckling analysis by DR)

51. Cassell, A.C., Hobbs, R.E., "Dynamic relaxation", Symp. on High Speed Computing of Elastic Structures, Liege, 1970 (Proc. Ed: B. Fraeijis de Veubeke, 1971).

(Review of development of DR. Comparison with Frankel iteration and convergence of other iterative methods. Use of fictitious densities proportional to row sum of moduli or stiffness coefficients. Damping estimated by trial runs on coarse mesh idealization)

52. Chaudhury, N.K., Brotton, D.M., Merchant, W., "A numerical method for dynamic analysis of structural frameworks", Int. J. Mech. Sci., V.8, 1966.

(Interlacing version of Newmark linear acceleration method. Velocities calculated at mid-points and displacements and accelerations at end points, with scheme then approximated to give an explicit method. Applied to non-linear analysis and to the damped static solution of a portal frame)

53. Clough, R.W., Bathe, K.J., "Finite element analysis of dynamic response", 2nd U.S. Japan Seminar on Matrix Methods of Structural Design, (U.A.H. Press), Aug. 1972.

Evaluation of explicit damping matrices as linear combination of mass and stiffness matrices. Survey of F.E. dynamic analyses. Modal superposition method, linear and non-linear, with reduced number of unknowns. Application of Wilson θ method)

54. Contro, R., Zavelani-Rossi, A., "Creep analysis of pretensioned cable systems", IASS Symp. on Tension Structures and Space Frames, Tokyo and Kyoto, 1971.

(Cables characterised by elastic-plastic-viscous constitutive law. Modulus, creep and yield stress known functions of temperature. Incremental solution process with plasticity accounted for in initial strain matrix)

55. Crisfield, M.A., "Collapse analysis of box-girder components using finite elements", Symp. Struct. Analysis, Non.linear Behaviour and Techniques, TRRL Report 164 UC, Dec., 1974.

(Generalised solution process for Incremental / N-R/Mod. N-R/ Incremental with equilibrium iterations)

56. Cundall, P.A., "Explicit finite-difference methods in geomechanics", Proc. E.F. Conf. Numerical Methods in Geomechanics, Blacksburg, Va., June, 1976.

(Dynamic relaxation and undamped central difference analyses of non-linear soil structure interaction problems. Includes creep effects, plastic flow, and treatment of discontinuities such as fractured rocks which are idealized as a system of rigid blocks. Step function damping in which K.E. of system is followed to max. and velocities set to zero with system restarted from this state. Process continued through several further peaks until K.E. of all modes eliminated)

57. Cundall, P.A., Voegele, M.D., Fairhurst, C., "Computerized design of rock slopes using interactive graphics for input and output of geometrical data", Proc. 16th. Symp. on Rock Mechanics, University of Minnesota, Minneapolis, 1975.

(Discrete block analysis examines effects of sliding, opening, rotation and interlocking of blocks with internal deformations assumed negligible. Use of interactive graphics procedure allows user to change parameters and idealization during the analysis)

58. Davids, N., Koenig, H.A., "Direct analysis of the flexural travelling waves in beams and plates", Eng. Mech. Bulletin, n.1, Sept., 1966.

(Direct (uncoupled) analysis of waves in beams and circular plates. Integration by Euler method with angular velocities of elements expressed in terms of end shears and moments and the rotational inertia of element, allowing large displacements)

59. Davidson, I., "The analysis of cracked structures", Transactions 3rd Int. Conf. on Struct. Mech. and Reactor Tech., V.3, 1975.

(D.R. finite difference analysis of crack propagation in reinforced structures capable of sustaining a cracked state. Loads applied incrementally with compatible cracked system established at each stage, and new boundary conditions (such as zero shear) applied at internal cracks. Idealized as rectangular mesh with zig-zag cracks along mesh lines. Each load increment treated as separate computer run. Empirical resetting of time interval and damping)

60. Day, A.S., "An Introduction to Dynamic Relaxation", The Engineer, Jan., 1965.

(Outlines DR with reference to a portal frame analysis using line bending elements and a plate bending problem with a finite difference idealization)

61 Day, A.S., "Analysis of plates by dynamic relaxation with special reference to boundary conditions", Symp. on Use of Electronic Digital Computers in Struct. Eng., University of Newcastle, July, 1966

(Finite-difference analysis of linear elastic plates)

62. Day, A.S., Bunce, J.W., "Analysis of cable networks", Civil Eng. and Public Wks. Rev., April, 1970.

(Application of DR to plane unstressed cable network subject to central concentrated load)

63. Dean, D.L., Ugarte, C.P., "Analysis of structural nets", Publs. Int. Assoc. Bridge Struct. Engng., 23, 71-90, 1963.

(Closed form trigonometric series solution for flat regular nets subject to single point loads or uniform loading)

64. Eras, G., Elze, H., "Zur berechnung und statisch vorteilhaften formgebung von seilnetzwerken", IASS Colloquium on Hanging Roofs, Paris, 1962 (North-Holland Publishing Co., N.Y., 1963).

(Modified Newton-Raphson (constant initial stiffness matrix) solution for cable networks.)

65. Filippa, C.A., "Finite element analysis of three-dimensional cable structures", Proc. Int. Conf. on Computational Methods in Non-linear Mechanics, Austin, Texas, Sept., 1974.

(Describes program system incorporating linear, quadratic or cubic displacement cable elements and associated consistent load vectors. Solution by Modified Newton Raphson)

66. Forsythe, G.E., Wasow, W.R., "Finite difference methods of partial differential equations", J. Wiley, 1960.

(General mathematical basis of various systems of iterative finite-difference analysis)

67. Franchi, A., Scirocco, F., "On the dynamics of plane pretensioned cable structures: theoretical and experimental research", Proc. IASS Symp. on Tension Structures and Space Frames, Tokyo and Kyoto, 1971.

(Static equilibrium by incremental process. Using displaced configuration and stiffness matrix calculates natural frequencies and normal modes assuming linear behaviour. Condensed degree of freedom analysis for dominant vertical motion only of a plane cable girder)

68. Frankel, S.P., "Convergence rates of iterative treatments of partial differential equations" Math. Tables Aids Computation, V.4, 65-75, 1950.

(Frankel iteration scheme - equivalent to DR)

69. Fried, I., "Finite element analysis of time-dependent phenomena", AIAA Journal, V.7., n.6, 1968.

(Introduces concept of finite time elements, assuming a cubic variation of displacements governed by the nodal values and derivatives at the end points of any time step. Enables a number of time steps, n, to be interconnected resulting in a system of 2n x Nd equations, where Nd is the number of degrees of freedom. Due to excessive store requirements a stepwise solution is more efficient)

70. Fu, C.C., "A method for the numerical integration of the equations of motion arising from a finite element analysis", J. Appl. Mech. ASME, Sept., 1970.

(Explicit numerical integration method with 5th order truncation error which is self-starting and requires small storage. Static solution for cylindrical shell obtained by damping)

71. Fung, Y.C., "Flutter", Handbook of Engineering Mechanics, Ed:W.Flugge, McGraw-Hill, 1962.

(Concepts concerning classical flutter of a structure in a uniform laminar flow)

72. Greenberg, D.P., "Inelastic analysis of suspension roof structures", J. Struct. Div., ASCE, V.96, n.ST5, May, 1970.

(Incremental solution scheme with displacement corrections using $U_i = U_i(K_{ii}\grave{} + K_{ii})/2.K_{ii}\grave{}$, where u_i predicted using [K] and $K_{ii}\grave{}$ is leading diagonal stiffness coefficient in displaced position. Equilibrium corrections by iteration. Inelastic portion of cable stress strain curves represented by exponential function. Numerical tests using manufacturer's specification for ultimate strains gives, for practical structures, 50 % higher ultimate load carrying capacity than elastic net based on linear stress strain curve)

73. Grieger, I., "Anwendung interaktiver computer-graphik fur den optimalen tragwerksentwurf", Int. Symp. on Wide Span Surface Structures, Stuttgart, 1976.

(Use of interactive graphical methods for coupled design and analysis of cable structures. Shape, prestress and other parameters can be controlled and modified in each step of design)

74. Gruendig, L., Schek, H.J., "Analytical formfinding and analysis of prestressed cable networks", Int. Conf. on Tension Structures, London, 1974.

(Application of linear force-densities method for approximate shape investigation. Subsequent non-linear analysis with constraints on member lengths or forces using a minimization technique to yield- a uniform mesh or geodesic network conforming Closely to chosen shape)

75. Haisler, W.E., Stricklin, J.A., Stebbins, F.J., "Development and evaluation of solution procedures for geometrically non-linear structural analysis by the direct stiffness method", AIAA/ASME 12th Structures, Struct. Dynamics and Materials Conf., Anaheim, California, 1971.

(Reviews non-linear finite element static analyses by Euler and self-correcting incremental procedures)

76. Hangleiter, U., "Problems of accuracy with prestressed cable-net structures", Int. Conf. on Tension Structures, London, 1974.

(Considers error sensitivity of cable networks, particularly of link forces near edge cables)

77. Hartzman, M., Hutchinson, J.R., "Non-linear dynamics of solids by the finite element method", Computers and Structures, V.2, 1972.

(Explicit transient analysis of isotropic plane strain structures subject to large deformations and strains. Use of lumped masses and local displacements resulting in uncoupled system of equations solved directly. Numerical integration by fourth order single step algorithm)

78. Haug, E., Powell, G.H., "Analytical shape finding of cable nets", IASS Symp. on Tension Structures and Space Frames, Tokyo and Kyoto, 1971.

(Shapes initially estimated from sketches, with equilibrium positions then found by Newton-Raphson iteration incorporating conditional controls on deflections to avoid singularities. Net shape and distribution of forces refined by appropriate operations involving prestressing and length changes)

79. Haug, E., Powell, G.H., "Finite element analysis of non-linear membrane structures", IASS Symp. on Tension Structures and Space Frames, Tokyo and Kyoto, 1971.

(Quadrilateral elements warped in space. Constitutive relations for isotropic or fibrous membranes. Solution by Newton-Raphson iteration. Applied to form-finding and analysis excluding wrinkling)

80. Haug, E., "Finite element analysis of pneumatic structures", Int. Symp. on Pneumatic Structures, Delft, 1972.

(Use of warped quadrilateral elements for modelling minimum surfaces. N-R solution of an isotropic membrane subject to hydrostatic pressure distribution, floating membranes and plate supports to rolling membranes)

81. Haug, E., "Remarks on unsymmetric coefficient matrices in implicit non-linear finite element membrane and cable analyses", Int. Symp. on Wide Span Surface Structures, Stuttgart, April, 1976.

(Newmark direct integration with N-R iteration in each time step. Shows mass, stiffness and damping matrices for highly non-linear structures which interact with environments can be unsymmetric (eg: directional anisotropy or drag effects, added mass effects, space dependent pressure magnitudes). Use of approximate matrices which are symmetric reduces computation but rate of convergence may be slower and some problems diverge. Decreased time step then necessary, or use of accurate coefficient matrices which doubles the computation. Explicit integration may be more efficient.

82. Hodgkins, W.R., "On the relation between dynamic relaxation and semi-iterative matrix methods", Numerische Mathematik, 9, 1967.

(DR, with mass components proportional to direct stiffness components, compared with Chebyshev semi-iterative method. Suggests DR rate of convergence might be improved by use of non-linear variable damping as in Chebyshev method)

83. Holland, J.A., "Dynamic relaxation applied to local effects", Conf. on Prestressed Concrete Pressure Vessels, ICE, London, 1967.

(Stress analysis of prestressed concrete end blocks up to cracking of concrete)

84. Hubolt, J.C., "A recurrence matrix solution for the dynamic response of elastic aircraft", J. Aeronaut. Sci., 17, 1950

(Implicit numerical integration scheme with velocities and accelerations derived by fitting a cubic through the current and three previous displaced states)

85. Isaacson, E., Keller, H.B., "Analysis of Numerical Methods", J. Wiley & Sons, 1966.

(General reference on numerical methods)

86. Ishii, K., Suzuki, T., "Shape of membrane structures", IASS Symp. on Tension Structures and Space Frames, Tokyo and Kyoto, 1971.

(Minimum surfaces expressed through non-linear differential equations which are approximated to finite difference equations to give numerical solutions. Curved boundaries dealt with by interpolation)

87. Ishii, K., "On developing of curved surfaces of pneumatic structures" Delft, 1972.

(Cutting patterns for membranes by developing geodesic lines on polygonal surfaces with triangular facets)

88. Jawerth, D., "Einige bauten mit vorgespannter hange konstruktion aus gegensinnig gekrummten seilen", IASS Colloquium on Hanging Roofs, Paris, 1962.

(Design review of various structures built with the Jawerth system)

89. Jensen, J.J. "An investigation of the static and dynamic behaviour of suspension structures", IASS Symp. on Tension Structures and Space Frames, Tokyo and Kyoto, 1971.

(Static analysis by incremental loading with equilibrium iterations. Dynamic analysis by implicit linear acceleration method with iteration in each time step)

90. Jensen, J.J., "Dynamics of tension roof structures", Int. Conf. on Tension Structures, London, 1974.

(Discussion of factors influencing the dynamic behaviour of cable and membrane structures. Representation of wind. Added mass effects of surrounding air. Structural, material and aerodynamic damping effects investigated by model studies)

91. Jonatowski, J.J., "Tensile roof structures: an inelastic analysis", Int. Conf. on Tension Structures, London, April 1974.

(Examines ultimate load behaviour using incremental analysis with N-R equilibrium iterations. Non-linear stress strain/strain law for cables with increasing stress, but linear for unloading elements - path dependent problems. Allows for cable slackening and ultimate load analysis)

92. Johnson, D., Brotton, D.M., "A finite deflection analysis for space structures", Int. Conf. on Space Structures, Guildford, 1966.

(N-R iteration for rigidly jointed and cable systems. Incremental failure analysis with equilibrium corrections by N-R at each step. If more than three increments taken, initial deflection values for fourth and all subsequent increments obtained by extrapolating three preceding displacement vectors)

93. Johnson, D.E., Grief, R., "Dynamic response of cylindrical shell: two numerical methods", AIAA Journal, V.4, n.3, 1965.

(Compares central difference and Hubolt integration schemes. C.D. found most efficient for rapidly varying response, and Hubolt for predicting slower responses)

94. Karrholm, G., Samuelsson, A., "Analysis of prestressed cable roof anchored in a space-curved ring beam", IABSE 9th Congress, Amsterdam, 1972.

(Uses linear flexibility matrix for ring beam translational displacements as preliminary to solution of net system. ie: net and boundary uncoupled in a similar manner to "deflection" analysis of suspension bridges)

95. Knudson, W.C., "Static and dynamic analysis of cable-net structures", Ph.D. dissertation, University of California, Berkeley, 1971.

(Form-finding, static and dynamic analyses. Static solutions by N-R iteration. Dynamic by modal superposition for fluctuating components of loading. Non-deterministic response analysis for wind loading)

96. Knudson, W.C., "Response of cable-net structures under dynamic loads", Proc. IASS Symp. on Tension Structures and Space Frames, Tokyo and Kyoto, 1971.

(N-R iteration for static equilibrium. Wind ($V = \bar{v} + v$) fluctuating component, v, dealt with by modal superposition. Integration of uncoupled equations by Newmark β method. Deterministic analysis regarded as qualitative description of expected peak response; non-deterministic approach based on theory of random vibrations more rational but assumes $2\bar{v}v >> v^2$ in order to make forcing function linear. Vibration characteristics for networks found to involve high frequency components and complex mode shapes. For deterministic analysis wind (v) is approximated as a plane wave incident on whole structure)

97. Knudson, W.C., Scordelis, A.C., "Cable forces for desired shapes in cable-net structures", IASS Symp. on Tension Structures and Space Frames, Tokyo and Kyoto, 1971.

(Applies least squares approach to obtain cable forces for desired shape with constraints on minimum forces under most severe loads. Then N-R iteration to obtain true equilibrium geometry allowing elastic changes. Applicable to orthogonal nets with horizontal tension components as initial unknowns)

98. Knudson, W.C., Nagy, D., "Spline interpolation and automatic generation of initial geometry for cable-net structures", Int. Conf. on Tension Structures, London, 1974.

(Interpolation and smoothing of discrete data from architectural models or sketches, and automatic generation of equal mesh net on resulting surface)

99. Knudson, W.C., "Some aspects of the response of cable nets to wind loadings", Int. Symp. on Wide Span Surface Structures, Stuttgart, April,1976.

(Deterministic non-linear analysis. Uses finite elements in space and time, representing inertia force, R, by cubic interpolation function in terms of R and $\dot{R}$ at end points of step. R and $\dot{R}$ assembled element wise, thus avoiding storage of global matrix, and dynamic equilibrium achieved by Jacobi iteration (with $\Delta t<0.3T_{min}$) Approximation of wind as plane wave is extended by dividing structure into strips with each strip having own wind record, by which more realistic representation is achieved (damping C = 0.3M + 0.0003K))

100. Koenig, H.A., Davids, N., "Dynamical finite element analysis for elastic waves in beams and plates", Int. J. Solids Structures, V.4, 1968.

(Direct analysis (see ref. 58) extended to include shear deformations)

101. Koenig, H.A., Davids, N., "The damped transient behaviour of finite beams and plates", Int. J. Num. Meth. in Engng., V.1, 1969.

(Incorporates nodal viscous damping in direct analysis procedure. Static solutions obtained with heavy damping)

102. Krieg, R.D., "Unconditional stability in numerical time integration methods", Proc. ASME, J. Appl. Mech., June 1973.

(Class of explicit time integration methods is defined and found to contain no unconditionally stable method, and no method with a larger time step than the central difference scheme)

103. Krieg, R.D., Key, S.W., "Transient shell response by numerical time integration", Int. J. for Num. Meth. in Engng., V.7, 1973.

(Compares the accuracy of explicit central difference integration with a family of implicit schemes for modelling the frequency response of membrane and bending deformations. For equal computational work the central difference scheme with lumped mass matrix is shown to be most efficient)

104. Krishna, P., Sparkes, S.R., "An influence coefficient method for pretensioned cable systems", Proc. ICE, V.41, Nov ., 1968.

(Approximate analysis of plane cable systems with vertical ties. Force method in which redundants are taken as forces in ties, and law of superposition assumed to apply in limited way)

105. Krishna, P., "Theoretical analysis of pretensioned cable networks", IASS Symp. on Tension Structures and Space Frames, Tokyo and Kyoto, 1971.

(N-R, Modified N-R and averaged residual N-R methods-illustrated graphically)

106. Krishna, P., Agravral, T.P., "Approximate analysis of cable structures", Int. Conf. on Tension Structures, London, 1974.

(Approximate analysis of plane girders and hypar networks treated as continuous systems. Kinematic non-linearity neglected and superposition admitted. Amenable to hand computations for few special load cases)

107. Leech, J.W., Hsu, P.T., Mack, E.W., "Stability of a finite difference method for solving matrix equations", J. AIAA, 3, 1965.

(Stability limit for central difference time integration with stiffness matrix equations: $\Delta t \leq 2/\omega max$)

108. Leonard, J.W., "State-of-the-art in inflatable shell research", J.Eng. Mech. Div., ASCE, V.100, n.EM1, Feb. 1974.

(Review of published papers)

109. Leonhardt, F., Schlaich, J., "Vorgespannte seilnetzkonstruktionen - das Olympiadach in Munchen", Der Stahlbau, H.2, 1973.

(Concerning detail design of the Munich Olympic Stadium)

110. Linkwitz, K., Schek, H.J., "Einige bemerkungen zur berechnung von vorgespannten seilnetzkonstruktionen", Ingenieur - Archiv., 40, 1971.

(Form-finding procedure by non-linear force-densitites method which minimizes simultaneously the quadratic deviations of shape and force distribution)

111. Linkwitz, K., "New methods for the determination of cutting pattern of prestressed cable nets and their application to the Olympic roofs Munchen", IASS Symp. on Tension Structures and Space Frames, Tokyo and Kyoto, 1971.

(Determination of cutting pattern for the Munich stadium and intermediate structures. Non-linear Force-densitites method)

112. Linkwitz, K., "Combined use of computation techniques and models for the process of form-finding for prestressed nets, grid shells and membranes", Int. Symp. on Wide Span Surface Structures, Stuttgart, 1976.

(Discusses the development of form-finding techniques, and the advantages at different design stages of the various methods)

113. Liudkovsky, I.M., "Optimum types of suspended roofs and their bearing contours", IASS Colloquium on Hanging Roofs, Paris, 1962.

(Comparison of deadweight and prestressed suspended shells. Form-finding of efficient momentless bearing contours for radial and orthogonal cable networks)

114. Lynch, R.D., Kelsey, S., Saxe, H.C., "The application of dynamic relaxation to the finite element method of structural analysis", Tech. Report No. THEMIS-UND- 68-1, University of Notre Dame, Sept., 1968.

(Investigates convergence rate and optimum parameters of the basic iterative methods and compares with DR as an iterative method (matrix eigenvalue analysis for error vectors). Considers use of a Newmark implicit integration scheme, which is unconditionally stable, for DR in place of C.D. explicit integration. Latter found more efficient. Application of DR to plane stress problems using finite elements with on-going alteration of iteration parameters)

115. Mallett, R.H. Schmidt, L.A., "Non-Linear structural analysis by energy search", J. Struct. Div., ASCE, V.93, n.ST3, 1967.

(Instability analysis of plates by minimization method. Difficulties arise due to local minima)

116. Mallett, R.H., Berke, L, "Automated method for the finite displacement analysis of three dimensional truss and frame assemblies", AFFDL-TR-102, 1966.

(Direct minimization applied to frameworks. Elementwise formulation)

117. Malone, D.W., Connors, J.J., "Transient dynamic response of linearly visco-elastic structures and continua", ASME/AIAA 10th Struct., Struct. Dyn. and Matls. Conf., New Orleans, 1969.

(Generalization of direct (non-matrix) analysis procedure accounting for material non-linearity and visco-elastic material damping in structures subject to small displacements. Numerical integration by Euler method)

118. Marcal, P.V., "Finite element analysis of combined problems of non-linear material and geometric behaviour", Proc. ASME Conf. on Comp. Approaches in Appl. Mech, Chicago, 1969.

(Review paper concerning material non-linearity: Initial strain or tangent modulus approaches; geometric non-linearity: Initial stress and initial displacement stiffness matrices included (coupled K_G matrix). Extends incremental stiffness procedure to non-linear material behaviour coupled with large displacements. Langrangian formulation for element functions and therefore restricted to small strains)

119. Martin, H.C., "Derivation of stiffness matrices for the analysis of large deflection and stability problems", Proc. 1st Conf. on Matrix Methods in Struct. Mech., AFFDL-TR-66-80, 1966.

(General derivation of intial stress (geometric) stiffness matrices with non-linear strain/displacement relations. Incremental loading)

120. McNamara, J.F., Marcal, P.V., "Incremental stiffness method for finite element analysis of the non-linear dynamic problem", Num. and Comp. Meth. in Struct. Mech., Academic Press, N.Y., 1973.

(Review of non-linear dynamic analysis by numerical integration. Application of Hubolt's method. Comparison of corrected and uncorrected incremental solutions for static and dynamic analyses. Examines numerical efficiency and size of increments or time intervals in relation to frequencies of reassembly of stiffness and residual load corrections)

121. Millar, M.A., Brotton, D.M., Merchant, W., "A computer method for the analysis of non-linear elastic plane frameworks", Int. Symp. on the use of Electronic Digital Computers in Struct. Eng., Newcastle, July 1966.

(Incremental and N-R iteration. Three preceding converged displacement vectors predict initial displacement for next in resetting stiffness matrix)

122. Modjtahedi, D., Shore, S., "The non-linear steady state response of flexible cable networks", IASS Symp. on Tension Structures and Space Frames, Tokyo and Kyoto, 1971.

(Establish non-linear equations of motion which include displacement terms of order four and below. Analysed by a perturbation method which allows steady state solutions for the case of simple harmonic forcing functions to be obtained. Tensions and deflections in a network found to differ significantly from those predicted by linearized modal superposition analysis)

123. Mollmann, H., "A Study in the Theory of Suspension Structures", Akademisk Forlag, 1965.

(Comprehensive treatment of the theory of tension structures as both discrete and continuous systems. Deals with formfinding, static non-linear analyses, and linearized dynamic analyses. In each case methods are outlined for both general nets and approximate orthogonal nets. Proof given to show uniqueness of solutions for cable nets in which all links of one set of cables remain intension)

124. Mollmann, H., Mortensen, P.L., "The analysis of prestressed suspended cable nets", Int. Conf. on Space Structures, Guildford, 1966.

(Modified Newton Raphson solution (constant stiffness) with K_G set assuming small strains but assumed final values of T used for T/ℓ terms. 5 iterations for convergence - Secant type solution i.e. total displacements used: $[K].\{\delta\} = \{P-C\}$)

125. Mollmann, H., "Analytical solutions for a cable net over a rectangular plan", IASS Symp. on Tension Structures and Space Frames, Tokyo and Kyoto, 1971.

(Linearized analytical solution derived for rectangular hyperbolic parabaloid cable nets. Expressions are derived for small vibration normal modes and frequencies. The normal modes are then used to derive Levy type series solutions for various cases of static loading)

126. Mollmann, H., "Analysis of prestressed cable systems supported by elastic boundary structures", Int. Conf. on Tension Structures, London, April 1974.

(Considers 2 methods for analysis of cable nets supported by elastic flexural boundaries:(1) Displacement analysis of complete structure $3^{\circ}F$ net, $6^{\circ}F$ boundaries. (2) Mixed method with horizontal components of cable tensions as extra unknowns but only vertical displacements of net. Both solved by N-R iteration. (2) has fewer unknowns but applies only to shallow orthogonal nets - Similar to Karrholm and Samuelsson)

127. Moriya, K., Uemura, M., "An analysis of the tension field after wrinkling in flat membrane structures", IASS Symp. on Tension Structures and Space Frames, Tokyo and Kyoto, 1971.

(F.E. analysis using triangular elements. Newton Raphson iteration. Young's modulus in compression direction gradually reduced)

128. Murray, D.W., Wilson, E.L., "Finite element large deflection analysis of plates", Proc. ASCE. J., Eng. Mech. Div., n.EM1, Feb. 1969.

(Investigate large deflections of plates using incremental & Mod. N-R for equilibrium in each increment. Noted that use of K_G not essential, but speeds convergence. - Cf Mollmann for networks - K_G essential)

129. Murray, T.M., Willems, N., "Analysis of inelastic suspension structures", J. Struct. Div., ASCE, V.97, n.ST2, Dec. 1971.

(Non-linear material properties - cf: Greenberg)

130. Myklestad, N.O., Lawrence, K.L., "Transient beam response calculations using Euler's method", Tech. Note, J. AIAA, V.5, n.2, 1967.

(Writes equations of motion for each mass#inertia point in terms of shears and moments to left and right of node. Moments and shears in turn expressed in terms of relative rotations and translations, allowing large displacements. Uses modified Euler integration with uncoupled (or direct) explicit integration. Iteration in each time step to use average accelerations)

131. Nagarajan, S., Popov, E.P., "Non-linear dynamic analysis of axisymmetric shells", Int. J. for Num. Meth. in Engng., V.9, 1975.

(Visco-plastic pseudo loads obtained by decomposition of stress increments into instantaneous elastic and delayed visco-plastic components. Linearized incremental equations of motion solved by Newmark numerical integration with equilibrium corrections at each time step. Geometric and material non-linearity)

132. Nakanishi, H., Namita, Y., "Shape determination of cable Structures by means of the methods for optimization problems", Int. Symp. on Wide Span Surface Structures, Stuttgart, 1976.

(Optimization procedure for obtaining the equilibrium state of cable structures subject to both configuration and member force constraints, with tension coefficients as independent variables. Maximum neighbourhood method applied to determine correction vectors, and optimum step length determined by approximating the objective function locally as a parabolic curve)

133. Namita, Y., Nakanishi, H., "A method of computation for determining the shape of cable structures", Int. Conf. on Tension Structures, London, 1974.

(Two stage least squares approach incorporating modification of member lengths in the secondary stage iterative equilibrium analysis to achieve more even force distribution in the network)

134. Nayak, G.C., Zienkiewicz, O.C., "Note on the 'alpha'-constant method for the analysis of non-linear problems" Int. J. for Num. Meth. in Engng., V.4, 1972.

(Uses modified N-R scheme to calculate $\Delta\{\delta\}^i = [K_o]^{-1}\{R\}^{i-1}$ *then corrects using* $\Delta\delta`^i = \alpha^i\Delta\delta^i$ *where* α^i *is a correction dependent on the current tangent stiffness matrix (uninverted). After initial inversion of* K_o *only simple matrix manipulation is required at each stage, For path dependent non-linear problems an incremental process is adopted in which improved* α *values calculated from previous increment are used to start the iteration)*

135. Newmark, N.M., "A method of computation for structural dynamics", J. Eng. Mech. Div., ASCE, V.85, n.EM3, 1959.

(Expresses velocity and displacement at the end of a time increment in terms of acceleration, velocity and displacement at beginning and acceleration at end of the increment. Two common forms: conditionally stable linear acceleration method; and unconditionally stable constant average acceleration method (implicit))

136. Oden, J.T., "Numerical formulation of non-linear elasticity problems", J. Struct. Div., ASCE., V.93, n.ST3, June 1967.

(Develops non-linear stiffness relations for geometrically and materially non-linear problems. Equations solved by incremental N-R method. Large strains and displacements)

137. Oden, J.T., Kubitza, W.K., " Numerical analysis of non-linear pneumatic structures", Proc. Int. Colloquium on Pneumatic Structures, IASS, Stuttgart, 1967.

(Reviews application of F.E. method to analysis of non-linear behaviour in elastic, elasto-plastic and viscoelastic pneumatic structures. Formulations for natural and synthetic rubbers; plastics and reinforced fabrics. Uses Voigt type element for viscoelastic formulation. Comments that procedure provides rational means for dealing with material damping. Elasto-plastic behaviour analysed through incremental process with step repeated if element found to go plastic during increment. Accuracy improved by choosing increments so that one element at most yields during increment)

138. Oden, J.T., Key, J.E., Fost, R.B., "A note on the analysis of non-linear dynamics of elastic membranes by the finite element method", Computers and Structures, V.4, 1974.

(Thin isotropic sheets of hyperelastic material idealized with constant strain triangular elements and lumped mass matrix. Examines wave phenomena in flat membrane using velocity formulated central difference scheme which is traced for a large number of time intervals)

139. Ohyama, H. Kawamata, S., "A problem of surface design for prestressed cable nets", IASS Symp. on Tension Structures and Space Frames, Tokyo and Kyoto, 1971.

(Two phase method of shape determination: (1) stress distribution for assumed surface shape and loading is approximated by least-squares (2) with stress distribution obtained, tension coefficients are fixed in all links and exact equilibrium determined by system of linear equations)

140. Otter, J.R.H., Day, A.S., "Tidal computations", The Engineer, Jan.1960.

(Finite difference solution for tidal flow equations in one and two dimensions)

141. Otter, J.R.H., "Computations for prestressed concrete reactor pressure vessels using dynamic relaxation", Nuclear Struct. Engng., 1, 61-75, 1965.

(Analysis of axi-symmetric thick-walled pressure vessel using DR infinite difference and incremental form)

142. Otter, J.R.H., "Dynamic relaxation compared with other iterative finite difference methods", Nuclear Eng. and Design, 3, 1966.

(Compares DR with classical explicit point methods of iterative analysis and outlines advantages of DR)

143. Otter, J.R.H., Cassell, A.C., Hobbs, R.E. "Dynamic Relaxation", Proc. ICE., 35, 633-656, Dec., 1966.

(Finite difference formulation for arch dams. DR shown to be equivalent to Frankel iteration and compared with Jacobi, Gauss-Seidel and SOR iteration methods for Laplace equation in two dimensions. Optimum convergence rate derived using exponential function for damped wave equations. SOR more rapid convergence but value of separated equations and simple boundary conditions in DR)

Discussion to "Dynamic Relaxation", Proc. ICE, 723-750, 1967.

(Welch, A.K., Postlethwaite, R.W: Use of fictitious densities Wood, W.L., Hussey, M.J.L: further comparison of DR with other iterative methods)

144. Otto, F., "The Hanging Roof" (in German), Ullstein Verlag, Berlin, 1954.

(Original work on the concepts of tension structures)

145. Otto, F., Trostel, R., "Tensile Structures Vol.I", MIT Press, Cambridge, Mass., 1967.

(Structural and architectural concepts of pneumatic and membrane structures)

146. Otto, F., Schleyer, F.K., "Tensile Structures Vol.II", MIT Press, Cambridge, Mass., 1969.

(Structural and architectural concepts of cable structures)

147. Park, K.C., "An improved stiffly stable method for direct integration of non-linear structural dynamic equations", Transactions ASME, June 1975.

(Investigates Newmark and Hubolt integration schemes for non-linear problems with gradual changes in material properties. Hubolt scheme found unconditionally stable but not Newmark. Introduces negative damping in Hubolt method to counteract artificial viscosity)

148. Perrone, N., Kao, R., "A general non-linear relaxation iteration technique for solving non-linear problems in mechanics", J.Appl. Mech., 38, Ser. E, n.2, June 1971.

(Successive Over Relaxation method used for solving large deflection problems)

149. Pian, T.H.H., Balmer, H.A., Bucciarelli, L.L., "Dynamic buckling of a circular ring constrained in a rigid circular surface", Int. Conf. on Dynamic Stability of Structures, Illinois, Ed: G. Herrmann, 1965.

(Elastic-plastic dynamic response of plane structure subject to dynamic snap-through buckling. Central difference numerical integration with finite difference/constant moment element idealization)

150. Poskitt, T.J., "Numerical solution of non-linear structures", J. Struct. Div., ASCE, ST4, Aug.1967.

(Uses incremental method to obtain approximate equilibrium then N-R iteration for final equilibrium. First stage - incremental - also accounts for cable slackening)

151. Purdy, D.M., Przemieniecki, I.S., "Influence of higher order terms in the large deflection analysis of frameworks", Proc. ASCE Conf. on Optimization and Non-linear problems, April 1968.

(Extend initial stress (geometric) matrix formulation to include previously neglected terms coupling quadratic and linear terms in strain-displacement expressions)

152. Rabinovitz, I.M., "Instantaneously rigid systems, their characteristics and the basis of their calculation", "Hangedacher", Weisbaden, Bauverlag, 1966.

(Shows that for prestressed systems straining must take place for finite deformations even though systems may be classified as structural mechanisms)

153. Reitmeier, G.F., Punnett, M.B., "Design developments in large span cabled structures", Int. Symp. on Pneumatic Structures, Delft, 1972.

(Design of tri-grid cable domes - membrane damping)

154. Rudolf, F., "A contribution to the design of air-supported structures", Proc. IASS Colloquium on Pneumatic Structures, Stuttgart, 1967.

(Discusses design aspects - loads, pressure changes etc.. Gives approximate formula for stresses and deformations of cylindrical and spherical membranes under pneumatic, snow and wind loads. Membrane treated as inextensible but mechanically deformable)

155. Ruhle, H., "Development of design and construction in pneumatic structures", IASS Colloquium on Pneumatic Structures, Stuttgart, 1967.

(Discusses inter-relation of form and loading. Static and dynamic pressure)

156. Rushton, K.R., "Dynamic relaxation solutions of elastic plate problems", J. Strain Analysis, V.3, n.1, 1968.

(Automatic determination of critical damping by checking number of iterations to first max. of kinetic energy. Analysis then repeated with damping and traced for two periods. Time interval by trial - reset to 0.8 previous value if instability occurs)

157. Rushton, K.R., "Large deflection analysis of variable thickness plates", Int. J. Mech. Sci. , 10, 1968.

(Non-linear finite difference solution by DR. Fictitious masses for in plane degrees of freedom)

158. Rushton, K.R. "DR solution for the large deflection of plates with specified boundary stresses", J. Strain Anal., V.4, n.2, 1969.

(As above. Separated equations allow simple boundary conditions)

159. Saafan, A.S., "Theoretical analysis of suspension roofs", J. Struct. Div., ASCE, V.96, n.ST2, Feb., 1970.

(N-R solution allowing for material non-linearity. 11→17 cycles for simple nets with non-linear properties. Solutions obtainable when not path dependent)

160. Sangster, K.G., Batchelor, B., "Non-linear dynamic analysis of 3-D cable networks", Proc. Int. Conf. on Comp. Meth. in Non-linear Mech., Austin, Texas, Sept. 1974.

(Method for determining the geometrically non-linear vibration frequencies of networks using shear free membrane theory. Solution by harmonic functions with frequency dependent on amplitudes)

161. Sayar, K.F., "On the statics of a tension roof structure", Int. Conf. on Tension Structures, London, 1974.

(Application of shear free membrane theory to geodesic net)

162. Schek, H.J., "The force density method for form-finding and computation of general networks", Comp. Meth. in Appl. Mech. and Eng., 3, 1974.

(Linear and non-linear force densities analysis for nets. Linear provides rapid search of approximate forms. Non-linear solution using least squares or damped least squares minimization for precise form-finding with constraints on member lengths or forces)

163. Schek, H.J., Grundig, L., Steidler, F., "Mathematische methoden der netzberechnung und begrundung des kraftdichtenansatzes", Int. Symp. on Wide Span Surface Structures, Stuttgart,1976.

(Use of conjugate gradient method of minimization for non-linear force densities analysis with constraints on lengths and forces)

164. Schlaich, J., "Lecture on cable structures", Int. Symp. on Wide Span Surface Structures, V.3, Stuttgart, 1976.

(General discussion of design factors affecting the cost of cable structures)

165. Schleyer, F.K., "Ueber die berechnung von seilnetzen", dissertation, University of Berlin, 1960.

(First treatment of cable structures as continuous systems)

166. Schleyer, F.K., "Die berechnung von seilnetzen", IASS Colloquium on Hanging Roofs, Paris, 1962.

(Finite difference solution for cable nets and trusses treated as continuous systems)

167. Shore, S., Bathish, G.N., "Membrane analysis of cable roofs", Int. Conf. on Space Structures, Guildford, 1966.

(Approximate analytic solution as continuous system)

168. Shore, S., Chaudhari, B., "Free vibrations of cable networks utilizing analogous membrane", Proc. Int. Assoc. for Bridge and Struct. Eng., 9th Congress, Amsterdam, 1972.

(Free vibrations of rectangular network treated as shear free membrane)

169. Siev, A., "A general analysis of prestressed nets", Publs. Int. Assoc. Bridge Struct., p.283-292 , 1963.

(First general analysis catering for large strains and displacements with equilibrium equations set in summation form. Modified N-R and N-R + incremental solutions for buckling analysis)

170. Siev, A., Eidelman, J., "Stress analysis of prestressed suspended roofs", J. Struct. Div., ASCE, ST4, Aug. 1964.

(Approximate analysis for orthogonal nets with vertical displacements as unknowns. Uses modified N-R scheme to account for non-linearity. Solutions converge only for light loads)

171. Siev, A., "Experimental study of flutter in suspended roofs", IASS Bulletin n.23, Sept. 1965.

(Examines the occurrence of flutter in a model hypar membrane at critical wind speeds. Air volume changes in closed structure inhibit flutter in fundamental mode)

172. Sofronie, R.A., "The response to wind of tension roof structures", Int. Conf. on Tension Structures, London 1974.

(Analytical classification of tension structures as large displacement low frequency oscillators)

173. Sofronie, R.A., "Aeroelastic analysis of wide-span surface structures", Int. Symp. on Wide Span Surface Structures, Stuttgart, 1976.

(Considers flutter in a rectangular open sided cable girder structure treated in similar manner to rigid wing with only bending and torsional degrees of freedom)

174. Stricklin, J.A., "Geometrically non-linear static and dynaic analysis of shells of revolution", Proc. IUTAM High Speed Computing of Elastic Struct., Liege, 1970.

(Modified N-R and incremental solution procedures for static analysis with first order Taylor expansion used to extrapolate out-of-balance residual forces. Brief review of implicit integration schemes for dynamic analysis)

175. Stricklin, J.A., Martinez, J.E., Tillerson, J.R., Hong, J.H., Haisler, W.E., "Non-linear dynamic analysis of shells of revolution by the matrix displacement method", AIAA Journal, V.9, n.4, April 1971.

(Geometric non-linearity. Various integration schemes examined with Hubolt's method found most suitable)

176. Stricklin, J.A., Haisler, W.E., "Formulations and solution procedures for non-linear structural analysis", Computers and structures, V.7, 1977.

(Review paper for F.E. non-linear methods - Statics and Dynamics)

177. Tezcan, S.S., Mahapatra, B.C., Mathew, C.I., "Tangent stiffness matrices for finite elements", Publs. IABSE, v.30/1, Aug. 1970.

(Small strains, large displacements. Newton Raphson iteration)

178. Tezcan, S.S., Cherry, S., Mahapatra, B.C., "Dynamic analysis of cable structures", Proc. IASS Symp. on Tension Structures and Space Frames, Tokyo and Kyoto, 1971.

(Equilibrium under static loads determined by N-R iteration using small strain tangent stiffness. Eigenvalue solution of linearized system for natural periods and mode shapes. Modal superposition technique and response spectrum analysis used for determining response to given excitation)

179. Thornton, C.H., Birnstiel, C., "Three dimensional suspension structures", J. Struct. Div., ASCE, v.93, n.ST2, April, 1967.

(Newton Raphson iteration, incremental loading)

180. Tsuboi, Y., Kawaguchi, M., "Design problems of suspension structure", IASS bulletin nos. 27, 28, 1966.

(Design of Tokyo Olympic swimming pool roof. Consideration of wind tunnel tests, proof tests on built structure, damping and stiffening effects, and construction problems)

181. Turner, M.J., Dill, E.H., Martin, H.C., Melosh, R.J., "Large deflection analysis of complex structures subject to heating and external loads", J. Aero. Space Sci., v.27, Feb. 1960.

(Tangent stiffness approach for small strains only. Initial stress (or geometric) stiffness matrices developed to account for effects of initial stress in truss and plane-stress assemblies)

182. Varga, R.S., "Matrix Iterative Analysis", Prentice-Hall, 1962.

(Basic iterative methods)

183. Vishwanath, T., Glockner, P.G., "Arbitrarily large deformations of flat circular membranes under external loads and inflation pressure", Int. Symp. on Pneumatic Structures, Delft, 1972.

(Non-Linear continuum equations written in terms of displacements for case of isotropic elastic membranes. Equations expressed in finite difference form and solved by N-R iteration. Accounts for changes in internal pressure, volume and temperature. Axisymmetric loading)

184. Weeks, G., "Temporal operators for non-linear structural dynamics problems", J. Eng. Mech. Div., ASCE, Oct. 1972.

(Compares Hubolt, Newmark and central difference numerical integration schemes for dynamic analyses with damping. Considers store, execution time, attenuation and viscosity for each method for various time intervals)

185. White, K., Happold, E., Dickson, M., "Notes on the theoretical costs of cable structures", Int. Conf. on Tension Structures,London, 1974.

(Costs of open, closed and dead weight cable systems compared with traditional structures for varying spans)

186. Wilson, E.L., "A computer program for the dynamic stress analysis of underground structures", Report SEL 68-1, University of California, Berkeley, 1968.

(Linear acceleration Newmark integration scheme modified to generate an unconditionally stable step-by-step algorithm for linear systems)

187. Wilson, E.L., Penzien, J., "Evaluation of orthogonal damping matrices", Int. J. Num. Meth. in Engng., v.4, n.1, Jan. 1972.

(Derivation of damping matrix from modal damping ratios)

188. Witmer, E.A., Balmer, H.A., Leech, J.W., Pian, T.H.H., "Large dynamic deformations of beams, rings, plates and shells", AIAA Journal, v.1, n.8, 1963.

(Finite difference analysis of axisymmetric shells subject to impulsive loading. Account taken of elastic-plastic or elastic-strain hardening behaviour, strain-rate, and large deflections. Numerical integration by explicit central difference)

189. Wood. W.L., "Comparison of dynamic relaxation with three other iterative methods", The Engineer, Nov., 1967.

(Unified comparison of DR with Jacobi, Gauss-Seidel and SOR iterative methods given on the basis of time dependent equations decaying to steady state solutions with appropriate choice of iteration parameters)

190. Wood, W.L., "Note on dynamic relaxation", Int. J. for Num. Meth. in Engng., V.3, 1971.

(Mass components equal to corresponding row sum of moduli of elements in the stiffness matrix, and damping and time interval optimized as in the Frankel iteration scheme. DR then shown to have a faster rate of convergence than the degenerate Chebyshev iteration method by a factor of 2 for well triangulated structures)

191. Wu, R.W.H., Witmer, E.A., "Non-linear transient response of structures by the spatial finite element method", AIAA Journal, V.11, n.8, 1973.

(Compares unconditionally stable Newmark and Hubolt integration methods with explicit central difference solution. Efficiency of lumped mass idealization. Artifical damping in stable methods. Formulation for all methods based on semi-direct procedure using linear extrapolation of generalized forces)

192. Yokoo, Y., Matsunaga, H., Yokoyama, H., "On the behaviour of wrinkled regions of pneumatic membranes in the form of a surface of revolution under symmetrical loading", IASS Symp. on Tension Structures and Space Frames, Tokyo and Kyoto, 1971.

(Membrane theory of shells applied to governing equations assuming inextensional deformations of membrane. Subdivides surface into unwrinkled regions and wrinkled regions in which tensile stresses exist only in the meridional directions. Imposes continuity conditions at junction to obtain solution)

193. Zetlin, L., "Elimination of flutter in suspension roofs", Proc. IASS Colloquium on Hanging Roofs, Paris, 1962.

(Discusses means of preventing mechanical vibrations of two layer cable girders)

194. Zienkiewicz, O.C., Valliappan, S., King, I.P., "Stress analysis of rock as a no tension material", Geotechnique, v.18, 1968.

(Modified N-R iteration using constant stiffness. Stresses in cracked elements relieved using load transfer process)

195. Zingali, A., "Remarks on the dynamic characteristics of a large net hanging roof structure", Int. Conf. on Tension Structures, London, 1974.

(Approximate design for the Palasport, Milan. Account taken of stiffening effect of internal air pressure due to deformation of roof in fundamental mode and damping effect of exponential decay of this pressure due to escape of air through openings. Added mass effects of air also included)

196. Papadrakakis, E,M., "Discrete statical analyses of structural mechanisms", Ph.D. thesis, to be submitted to The City University, London, Aug. 1978.

197. Topping, B.H.V., "Comparison of intuitive design philosophies with mathematical programming techniques", Ph.D. thesis, to be submitted to The City University, London, Aug. 1978.

198. Wakefield, D.S., "Pretensioned networks supported by compression arches", Ph.D. thesis, to be submitted to The City University, London, Aug. 1978.

199. Warburton, G.B., "Some recent advances in structural dynamics", Int. Conf. on Slender structures, The City University, London, Sept., 1977.

FORM-FINDING AND ANALYSIS

OF

TENSION SPACE STRUCTURES

BY

DYNAMIC RELAXATION

A thesis submitted on the basis of published papers by

Michael Robert Barnes for the degree of Doctor of Philosophy

The City University,
Department of Civil Engineering,
October, 1977.